UNIVERSITAT POLITÈCNICA DE VALÈNCIA
DEPARTAMENTO DE QUÍMICA
INSTITUTO UNIVERSITARIO MIXTO DE TECNOLOGÍA QUÍMICA
(UPV-CSIC)

DOCTORAL THESIS

Hydrogen-Abstraction, Energy Transfer and Exciplex Formation in Photoactive Systems Based on Bile Acids

Paula Miró Richart

Valencia, March 2016

Directors:
Prof. Miguel A. Miranda Alonso
Dra. M. Luisa Marín García

CERTIFICATION

Miguel Ángel Miranda Alonso, Full Professor of the Universitat Politècnica de València (UPV) and María Luisa Marín García, Associate Professor of the UPV,

CERTIFY that the Doctoral Thesis entitled "Hydrogen-Abstraction, Energy Transfer and Exciplex Formation in Photoactive Systems Based on Bile Acids" has been developed by Paula Miró Richart under their supervision in the Instituto Universitario Mixto de Tecnología Química (UPV-CSIC).

Prof. Miguel A. Miranda Alonso Dr. M. Luisa Marín García

A, Acceptor

BA, Bile acid

Bip, Biphenyl

BS, Bile salt

Bzp, Benzophenone

CA, Cholic acid

CAMe, Cholic acid methyl ester

Cbz, Carbazole

CDCA, Chenodeoxycholic acid

Ch, Cholesterol

CPD, Cyclobutane pyrimidine dimer

Cyt, Cytosine

Cyt<>Cyt, Cyclobutane cytosine dimer

D, Donor

DBU, 1,8-Diazabicyclo [5.4.0] undec-7-ene

DCA, Deoxycholic acid

DCC, *N,N*-Dicyclohexylcarbodiimide

DEAD, Diethyl azodicarboxylate

DIEA, Diisopropil ethyl amine

4-DMAP, 4-Dimethylaminopyridine

DMF, Dimethylformamide

DNA, Deoxyribonucleic acid

Dns, Dansyl

EDC, *N*-(3-Dimethylaminopropyl)-*N*-ethylcarbodiimide

ET, Energy transfer

F, Fluorescence

Gly, Glycine

HAT, Hydrogen atom transfer

HSDH, Hydroxysteroid dehydrogenase

IC, Internal conversion

ISC, Intersystem crossing

KP, *(S)*-Ketoprofen

KPMe, Ketoprofen methyl ester

KPMe-H$^{\cdot}$, Benzhydril radical of ketoprofen methyl ester

KP-OH, Reduced *(S)*-ketoprofen

LA, Litocholic acid

LFP, Laser flash photolysis

NaCA, Cholic acid sodium salt

NaCDCA, Chenodeoxycholic acid sodium salt

NaDCA, Deoxycholic acid sodium salt

NaLA, Litocholic acid sodium salt

NaUDCA, Ursodeoxycholic acid sodium salt

NEA, *(S)*-1-(1-Naphthyl)ethyl amine

Npt, Naphthalene

Npx, Naproxen

P, Phosporescence

PBA, 4-Phenylbenzyl alcohol

S_0, Ground state

S_1, Singlet excited state

Sens, Sensitizer

SSET, Singlet–singlet energy transfer

τ , Lifetime

T_1 or T, Triplet excited state

Tau, Taurine

TB, Through–bond

TB–TEX, Through–bond triplet exciplex

TBTU, *O*–(Benzotriazol–1–yl)–*N,N,N',N'*–tetramethyluronium tetrafluoroborate

Thd, Thymidine

THF, Tetrahydrofuran

Thy, Thymine

Thy<>Thy, Cyclobutane thymine dimer

TTET, Triplet–triplet energy transfer

UV–Vis, Ultraviolet–Visible

VR, Vibrational relaxation

Chapter 1: Introduction

1.1. Chemical structure of bile acids

Bile acids (BAs) are a family of amphiphilic water-soluble steroids that play a pivotal role in a high variety of physiological functions and are biosynthesised from cholesterol (Ch) in the hepatocytes of the liver.[1,2] Chemically they share a steroidal skeleton with an unusual *cis* fusion between rings A and B, two angular methyls, a short side chain ending in a carboxylic moiety and different number of hydroxyl groups on the α-face of the skeleton. These structural characteristics contribute to their facial amphiphilia, associated with a convex hydrophobic β-face and a concave and hydrophilic α-face (Figure 1.1).[3,4] The amphiphilic properties of BAs allow aggregation in aqueous solution by the interaction of the β-faces of the monomers at low concentrations (primary aggregates); further agglomeration as the concentration increases results in the formation of secondary aggregates.[5-7]

BAs can be classified into primary and secondary ones. Thus, primary BAs are directly synthesised from Ch and include cholic acid (CA) and chenodeoxycholic acid

(CDCA) while secondary BAs, synthesised from the corresponding primary analogs, are deoxycholic acid (DCA) and lithocholic acid (LA) (Figure 1.1). The hydrophobicity of BAs, reversely proportional to the number of hydroxyl groups, has also been associated with their potential toxicity.[3,4,8,9] Thus, LA with one hydroxyl group is highly hydrophobic and extremely toxic, while DCA or CDCA, with intermediate hydrophilicity show also intermediate toxicity. Accordingly, CA, the most hydrophilic one, is also the less toxic BA.

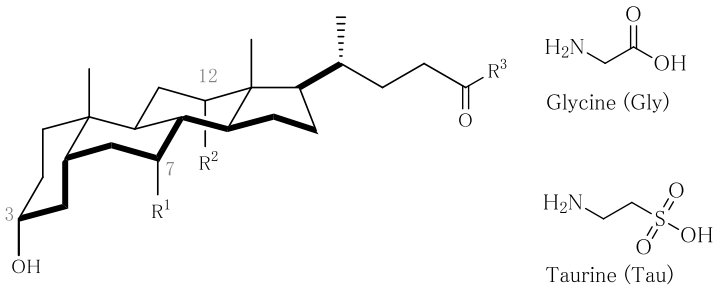

R^1=R^2=R^3=OH	Cholic Acid (CA)
R^1=R^3=OH; R^2=H	Chenodeoxycholic Acid (CDCA)
R^1=H; R^2=R^3=OH	Deoxycholic Acid (DCA)
R^1=R^2=H; R^3=OH	Litocholic Acid (LA)
R^1=R^2=OH; R^3=Gly	Glycocholic Acid (GlyCA)
R^1=R^2=OH; R^3=Tau	Taurocholic Acid (TauCA)
R^1=OH; R^2=H; R^3=Gly	Glycochenodeoxycholic Acid (GlyCDCA)
R^1=OH; R^2=H; R^3=Tau	Taurochenodeoxycholic Acid (TauCDCA)

Figure 1.1. Chemical structure of primary, secondary and conjugated BAs.

Primary BAs with pKa~5 are found in the organism mainly conjugated by a peptidic bond to either glycine (Gly) or taurine (Tau) amino acids. Gly conjugated BAs have lower pKa values (3.8-4.8) than the corresponding non-conjugated analogs and represent ~70 % of the bile, while Tau conjugation decreases the pKa below 2 and represents ~20% of the bile. Thus, the conjugation of BAs ensures their aqueous solubility along the whole intestinal tract.[3,10]

1.2. Biosynthesis of the bile acids

Primary BAs are biosynthesised in the hepatocites of the liver starting from Ch, a C27 sterol with a double bond between C5 and C6 and an isooctane side chain at the D ring. In the process, Ch exhibiting highly hydrophobicity is transformed into the BAs characterized by their amphiphilic properties and high solubility in water at physiological pHs. This complex biosynthetic process includes four main multienzymatic-mediated steps: i) 7-hydroxylation of Ch, ii) modification of the ring structure, iii) shortening of the lateral chain and iv) final conjugation with amino acids.

The enzyme 7α-hydroxylase, expressed only in the liver, catalyzes the hydroxylation of Ch along the initiation step of the biosynthetic route (Scheme 1.1, reaction i). Then, the ring structure modification begins with the oxidation of the 3β-position together with the isomerization of the double bond from the 5- to the 4-position mediated by 3β-hydroxy-C27-steroid reductase (Scheme 1.1, reaction ii). The obtained molecule is hydroxylated by the 12α-hydroxylase enzyme leading to the appropriate intermediate for the ultimate CA (Scheme 1.1, reaction iii) or remains unmodified in the route to CDCA. Both intermediates in parallel are subjected to the hydrogenation of the double bond in the A-ring by 3-oxosteroid-5β-reductase (Scheme 1.1, reaction iv). Finally, the reduction of the 3-oxo group to an alcohol with the α-configuration is achieved by 3α-hydroxysteroid dehydrogenase (Scheme 1.1, reaction v). Next, side chain oxidation is triggered by the performance of sterol-27-hydroxylase, which introduces a hydroxyl group that finally is oxidized to a carboxylic acid at carbon 27, leading to the 25-*R* isomer (Scheme 1.1, reaction vi). Next step is the activation of the side chain by conjugation with coenzyme A, catalyzed by coenzyme A-ligase (Scheme 1.1, reaction vii), then 2-methylacyl-coenzyme A racematase converts the 25-*R* isomers into 25-*S* isomers (Scheme 1.1, reaction viii), and acyl coenzyme A oxidase catalyzes dehydrogenation to obtain 24,25-*trans* unsaturated derivatives (Scheme 1.1, reaction ix). Hydration and oxidation at the C24 bond is mediated by a D-bifunctional protein (Scheme 1.1, reaction x). Then, the peroxisomal thiolase catalyzes cleavage of the C24-

C25 bond and allows for the synthesis of the primary BAs, CA and CDCA (Scheme 1.1, reaction xi). Primary BAs can be transformed into the conjugated Gly and Tau derivatives by an amide linkage to carbon 24.[11,12]

Secondary BAs are formed in the intestine by the action of anaerobic bacteria that are able to remove 7 α -hydroxyl group of the primary BAs. In this process, CA is converted to DCA, while CDCA results in the formation of LA (see Figure 1.1).[13]

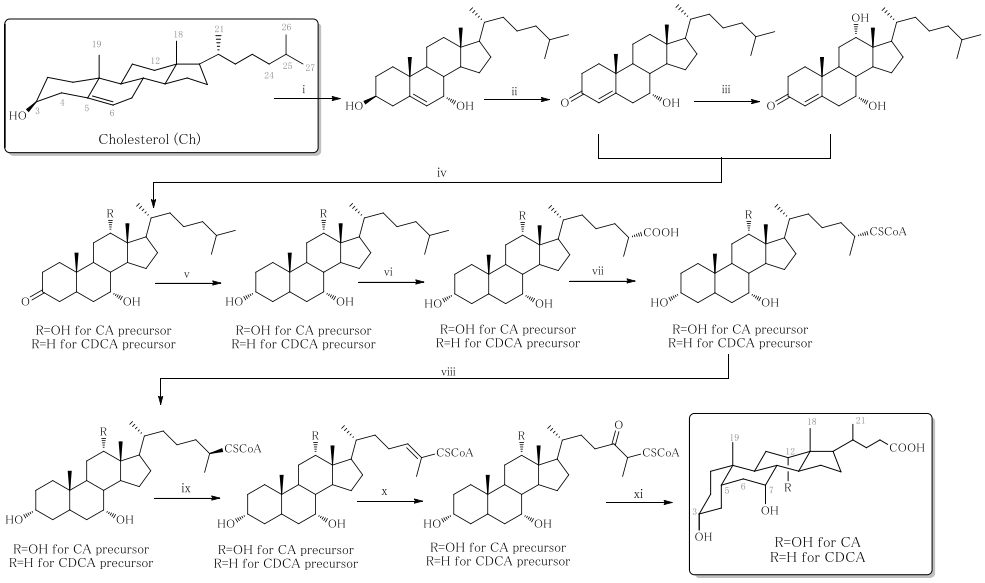

Scheme 1.1. Enzyme-mediated biosynthesis of primary BAs. The involved enzymes are: i) 7 α -hydrolase, ii) 3 β -hydroxy-C27-steroid reductase, iii) 12 α -hydroxylase, iv) 3-oxosteroid-5 β -reductase, v) 3 α -hydroxysteroid dehydrogenase, vi) sterol-27-hydroxylase, vii) coenzyme A-ligase, viii) 2-methylacyl-coenzyme A racematase, ix) acyl coenzyme A oxidase, x) D-bifunctional protein and xi) peroxisomal thiolase.

1.3. Enterohepatic circulation

The liver is a vital organ, which plays a major role in the synthesis of BAs. It is connected to two blood vessels: the hepatic artery and the portal vein. While the hepatic artery transports oxygen-rich blood from the aorta, the portal vein transports blood containing the digested nutrients obtained in the gastrointestinal tract.[14,15] The hepatocytes are the key functional cells of the liver, they constitute roughly ~80% of its mass and synthesize about 200-600 mg of primary BAs from Ch every day.[12] These just synthesized primary BAs, after conjugation with the amino acids Gly and Tau in the peroxysomes of the hepatocytes, and together with other substances such as lipids, Ch, pigments, proteins and mineral salts, constitute a mixture called bile. Bile is secreted from the liver to the hepatic conduct and travels to the gallbladder where it is stored. Upon each meal ingestion, the contractions of the gallbladder induce the drop of the bile into the lumen of the intestine, where BAs aid the solubilization of dietary lipids present in the cud. Once the lipids have been solubilized, BA are deconjugated by different anaerobic bacteria usually present along the gastrointestinal tract.[16] Then, most of the BAs are reabsorbed by the endothelial cells of the intestine using a Na^+-BA cotransporter which drives them to the portal blood circulation where they travel mostly linked to human serum albumin or, less commonly, to high density lipoproteins. As this portal blood supplies the liver, the BAs are reincorporated to the total hepatic bile pool after developing their function. However, a small part of BAs is not reabsorbed and passes through the big intestine and the colon, where bacterial transformation catalyzed by 7α-hydrolase leads to the secondary BAs, DCA and LA. These secondary BAs characterized by their lipophilicity can be passively reabsorbed by diffusion, reaching the liver again through the portal circulation.[12] BAs which are not absorbed are eliminated by the feces and their lack is supplied by the daily biosynthesis of new BAs in the liver (see Figure 1.2).

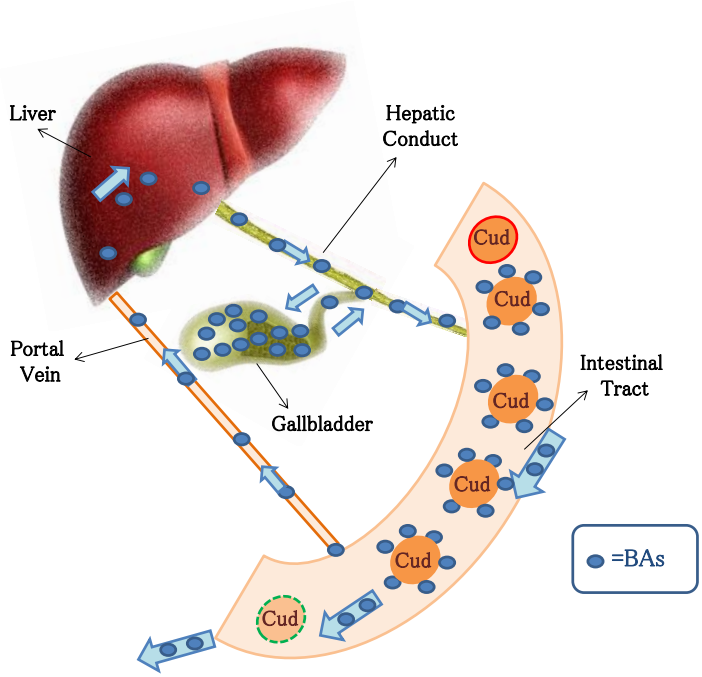

Figure 1.2. Schematic representation of the entereohepatic circulation of BAs.

Along the enterohepatic circulation, BAs play a relevant role in some physiological functions such as: i) emulsion and solubilization of dietary lipids making their digestion and absorption by the epithelial cells possible; ii) transport of these lipids through the intestinal tract and iii) elimination of the excess of Ch present in the organism.

The normal performance of the entereohepatic circulation can be altered by diseases such as cholestasis. Cholestatic liver disease is a particular type of hepatotoxicity consisting of the failure of bile outflow from the liver to the duodenum, causing intracellular accumulation of BAs and, as a consequence, membrane alterations, mitochondrial dysfunction and cellular necrosis.[17–19] It can be classified in: primary biliary cirrhosis (an intrahepatic cholestatic liver disease which destroys the bile duct, finally making an impact on the liver tissue) and primary sclerosing cholangitis (an extrahepatic

liver disease, which firstly affects the bile duct present outside the liver but over the time, it can also affect the liver tissue).[20]

1.4. Photophysics and photochemistry

1.4.1. Basic concepts

The Sun is an essential source of ultraviolet-visible (UV-Vis) light, which enables the life on the Earth. In fact, some physiological functions of living beings such as photosynthesis or formation of vitamin D are inconceivable without light. The ozone layer is able to block UVC below *ca.* 290 nm, but it does not prevent moderate penetration of UVB (290-320 nm) and to a higher extent, UVA (320-400 nm) and Vis light.

Molecular photochemistry is the discipline which studies chemical reactions induced by the absorption of UV-Vis light (200-800 nm). The first law of photochemistry or Grotthus-Draper law states that the development of a photochemical reaction requires the previous absorption of light by the reacting molecule. A chromophore is an atom or a group of atoms, which absorb light behaving as a unit; among the typical ones are organic functional groups such as olefins, aromatic rings, ketones or enones. The radiation absorbed by the chromophores of a molecule can induce photochemical and/or photophysical changes in it. Upon absorption of a photon, a molecule reaches an excited electronic state. Excited molecules are generally unstable and short-lived but they can be studied on the focus of the physical (photophysics) or chemical changes (photochemistry) they suffer.[21-24] These photophysical phenomena can be summarized in a Jablonsky diagram (see Figure 1.3).[25] When a molecule absorbs light, one electron is promoted from the highest occupied orbital (HOMO, HO) to the lowest unoccupied orbital (LUMO, LU). As the excited species tend to deactivate rapidly, they relax

following either radiative or non-radiative mechanisms. Radiative mechanisms such as fluorescence (F) or phosphorescence (P) imply the emission of light upon deactivation. Otherwise, non-radiative mechanisms include chemical reactions from the different excited states, but also thermal deactivation, namely internal conversion (IC) or intersystem crossing (ISC).

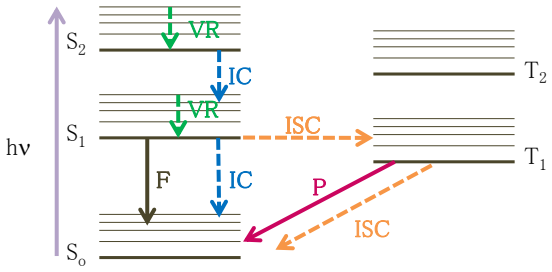

Figure 1.3. Jablonsky diagram.

More in detail, upon absorption of light (hν), a molecule can reach an upper singlet excited state, for instance S_2. Rapidly, the molecule deactivates from the upper vibrational levels of S_2 by vibrational relaxation (VR) and then the IC allows for the change of the electronic excited state to the first singlet excited state (S_1). Then, the molecule can deactivate by the spontaneous emission of a photon generating F or by the thermal deactivation IC, both of them to reach the ground state (S_0). Molecules in S_1 can also suffer spin conversion to the triplet excited state (T_1) by means of a forbidden transition denominated ISC (in this case $S \rightarrow T$). ISC involves an isoenergetic radiationless transition between two electronic states having different multiplicities often resulting in a vibrational excited molecular entity in the lower electronic state, which then decays to its lowest molecular vibrational level by VR. After that, from T_1 to the ground state S_0, a radiative transition denominated P or again an ISC deactivation can occur.[22,26,27]

The main difference between a photochemical and a thermal reaction is the amount of energy intervening in each case. While in a thermal activation only translational, rotational and vibrational degrees of freedom play a role, in a photochemical process the molecules suffer the transition from one electronic excited state to another one, involving an energetic change higher than the one suffered in a thermal reaction. The energy of the photons absorbed in the UV region ranges from 143 kcal mol^{-1} for photons of 200 nm to 87 kcal mol^{-1} for 350 nm. This interval of energy is enough to achieve the breaking of any bond from O-O (35 kcal mol^{-1}) to O-H (110 kcal mol^{-1}). Moreover, photochemical reactions allow for the selectivity of the excitation of the selected reactant using the correct emission source, while thermal activation affects the whole reaction pool.[28]

1.4.2. Specific photophysical and photochemical processes of interest in this Thesis

Among the photophysical and photochemical processes that can be explained in detail, some of them are of particular interest in this Thesis and deserve to be emphasized, in particular the photophysical process of energy transfer (ET). Furthermore, the basis of photochemical processes such as hydrogen-abstraction, Paternò-Büchi and 2+2 cycloaddition of alkenes will also be explained in detail along the following sections.

1.4.2.1. Energy transfer

In a thermodynamically favored ET process, an excited donor (D) deactivates to its ground state by transferring its energy to an acceptor (A). As a consequence, A reaches an electronic excited state. The common mechanisms to explain ET processes are the electron exchange or Dexter and the dipole-dipole interactions or Förster (Figure 1.4).

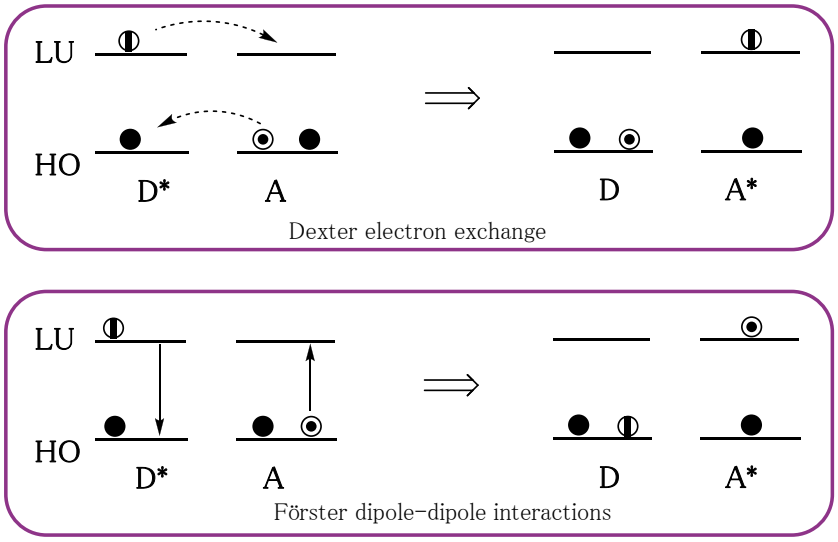

Figure 1.4. Schematic representation of the Dexter electron exchange (top) and the Förster dipole–dipole interactions (bottom) mechanisms for ET.

Dexter mechanism comprises the travelling of the electron from the LUMO (LU) of the excited D to the LU of A, while an electron from the HOMO (HO) of A travels to the HO of D. As a consequence, the excited D results in D in its ground state while A is converted to an excited A state (see Figure 1.4, top). For this electronic exchange, frontier molecular orbital overlap between D and A is required, so the process is highly distance–dependent and can be quantified by the Dexter equation (Eq. 1.1):[29]

$$k_{ET} = k\,J e^{-2R_{DA}/L} \qquad \text{Eq. 1.1}$$

Where k is the rate constant, J is the integral of the spectroscopic D–A overlap, R_{DA} is the distance between the D and the A and L is the van der Waals radii.

Sometimes, as a result of the D–A overlap, A and D form a bimolecular encounter complex of an excited D molecule and A in its ground state, called exciplex. An exciplex

is a charge-transfer entity formed by collision in the excited state, which present a differenced energy minimum.[30]

The Förster or dipole-dipole interactions to explain the ET process states the effect of an oscillating electric field which induces the promotion of one electron from the LU to the HO of the D and another one from the HO to the LU of A, so consecutively generating an excited A and a ground state D (see Figure 1.4, bottom). In this case, there is not any electron exchange, so the orbital overlap between the van der Waals radii is not needed. The rate constant of this process can be determined by means of the Förster equation (Eq. 1.2):[31]

$$k_{ET} = k\frac{\kappa^2 K_D^0}{R_{DA}^6} J(\varepsilon_A) \qquad \text{Eq. 1.2}$$

Where k is a constant in the experimental conditions, κ^2 is the interaction between dipoles, K_D^0 is the emission of the D, R_{DA} is the distance between D and A, and $J(\varepsilon_A)$ is the integral of the spectroscopic D-A overlap.

To discriminate which of the ET mechanisms is operating in a specific process, the modulation of the distance between a specific D-A pair is an alternative: while Förster ET can occur through distances up to 100 Å, Dexter ET requires orbital overlap and distances not higher than 10 Å. Other possibility is determination of the excited states involved in the ET process: while Förster ET only can happen in S-S ET (Figure 1.5), Dexter ET can happen either in S-S or T-T ET (Figure 1.6). More in detail, in the Förster mechanism, the dipole-dipole interactions produce the movement of an electron from the LU to the HO of the excited D simultaneously with the movement of an electron from the HO to the LU of the A, but each species conserve its own electrons and there is not electron exchange. That is why, if the excited D is a S, the spin conservation rules are obeyed when the electron from the LU drops to the HO of the D, but if the excited D is a T, the spin conservation rule is not obeyed, avoiding the explanation of an ET process through this mechanism (see Figure 1.5). However, if the ET process happens through a Dexter mechanism, an electron exchange between D and

A is produced, so it can occur independently of the nature of the excited D (see Figure 1.6).

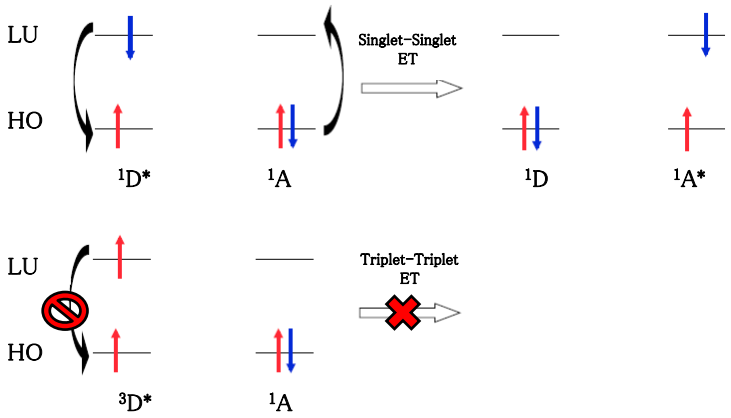

Figure 1.5. Schematic ET possibilities explained by a Förster mechanism. The blue and red arrows represent the spins while the black ones represent the movement of the electrons during the process.

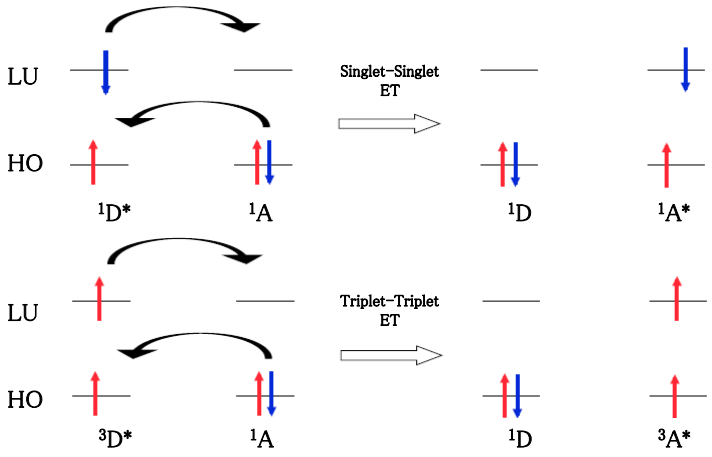

Figure 1.6. Schematic ET possibilities explained by a Dexter mechanism. The blue and red arrows represent the spins while the black ones represent the movement of the electrons during the process.

1.4.2.2. Photochemical hydrogen atom transfer

The chemistry of an excited species may differ from that of the ground-state species as a consequence of both, the excess of energy and the particular electronic arrangement of the excited species. Among the photochemical organic processes, hydrogen atom transfer (HAT) from a hydrogen donor to an excited carbonyl compound has been widely studied.[26,32,33] HAT has been described to occur generally to the electronic excited T_1 with $n\pi^*$ configuration of a carbonyl group, although it can also happen to a $n\pi^*$ S_1.

In a HAT reaction, the excited carbonyl, upon hydrogen-abstraction is converted to the corresponding ketyl radical. Then, the ketyl radical can: react with other radicals present in the medium to form new compounds, dimerize leading to pinacols or abstract hydrogen again leading to its reduced species (see Figure 1.7).

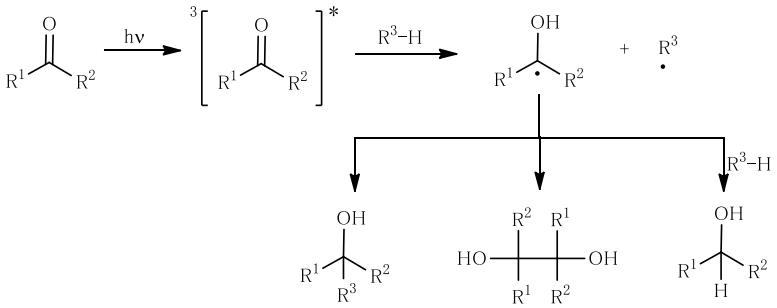

Figure 1.7. General pathways upon hydrogen atom transfer (HAT) reaction.

In general, the rate constants for HAT reactions from a triplet carbonyl are proportional to the energy of the excited state and reversely proportional to the dissociation energy of the X-H bond of the hydrogen donor. Giving specific examples, it means that biacetyl (E_T = 236 kJ mol^{-1}) will undergo a slower HAT than phenyl ketones

(E_T ~ 300 kJ mol^{-1}) and on the other side, isopropanol like C–H bonds (E_{C-H} ~ 380 kJ mol^{-1}) are more likely abstracted than O–H bonds (E_{O-H} ~ 442 kJ mol^{-1}).[27]

Recently, a mechanistic study on the HAT between benzophenone and a series of 1,4 dienes has been performed in our group.[34–36] Among the hydrogen donors, 1,4–cyclohexadiene, 1,4–dihydro–2–methylbenzoic acid, 1,4–dihydro–1,2–dimethylbenzoic acid and linoleic acid have been used. The involvement of HAT has been proven by LFP experiments, which allow for the detection of the triplet ketone and its ketyl radical, and from the study of the resulting photoproducts. As a conclusion, the involvement of HAT in lipid peroxidation has been established.

1.4.2.3. Photochemical 2+2 cycloaddition of alkenes

Formation of cyclobutanes can be achieved by the addition of an alkene in its ground state to another photoexcited alkene (photocycloaddition) or by dimerization of two identical alkenes, one of them previously excited (photodimerization).[37]

The mechanistic pathway of this reaction depends on the way in which the photoexcited species is generated. The direct excitation of an alkene may lead to its S_1, from which 2+2 cycloaddition can directly occur. Usually, this sort of reactivity happens when the alkenes absorb at long wavelengths and their S_1 is $\pi\,\pi^*$ (Figure 1.8, reaction i). However, the low yields achieved by direct excitation are sometimes due to the competitive dissipation of energy, producing side reactions such as *cis/trans* isomerization.[38] In the particular case of α,β-unsaturated carbonyl compounds, the S_1 usually with high ISC, yields efficiently T_1 which is $n\pi^*$, from where 2+2 cycloaddition occurs *via* 1,4–biradical intermediates (Figure 1.9, reaction ii).[39] A further possibility is to generate the T_1 excited state of the alkene by means of a sensitizer (Sens). Then, the cycloaddition occurs from the T_1 of the alkene (Figure 1.9, reaction iii).[40]

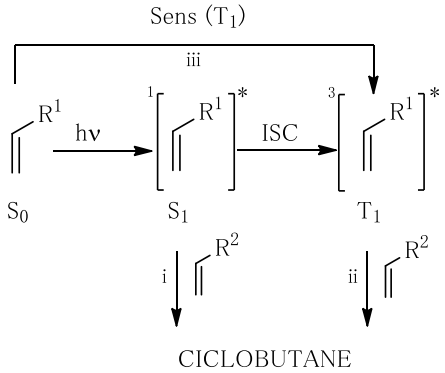

Figure 1.8. Different pathways for the 2+2 cycloaddition reaction between alkenes: i) 2+2 cycloaddition from the singlet excited state of an alkene; ii) 2+2 cycloaddition from the T_1 and iii) sensitized 2+2 cycloaddition.

The main interest of this reaction, from a synthetic point of view, is the formation of two C–C bonds and four stereogenic centers in a single step. Photocycloaddition has been used in the synthetic preparation of structures such as cubane,[41] being the key step for the formation of the cubane cage. 2+2 cycloaddition is known to generate the undesired cyclobutane pyrimidine dimers (CPDs) in living beings exposed to UV. In principle, they can be formed via direct absorption of UVB, which leads to a 2+2-cycloaddition from the S_1. However, the presence of chromophores in the media acting as Sens may lead to higher yield of photosensitized CPDs, causing damage even employing wavelengths at which pyrimidine units do not absorb. In the double-stranded DNA form, CPDs would result predominantly in the *cys-syn* form.[42] That lesion introduces conformational changes in the DNA structure, destroying the normal base-pairing double strand in that concrete area. Luckily, photolyases or nucleotide excision repair play a key role in CPDs reversion,[43] whereas unrepaired dimers may lead to skin cancer.

1.4.2.4. Photochemical 2+2 cycloaddition of carbonyls and alkenes: the Paternò-Büchi reaction

The Paternò-Büchi reaction is a photochemical 2+2 cycloaddition consisting of the formation of a 4-membered oxetane ring by the coupling of an excited carbonyl group and an alkene.[44,45]

The carbonyl group is the light absorbing chromophore, whose $n\pi^*$ S_1 or T_1, accessed by ISC, can be the electronic excited species involved in the photoreaction (see Figure 1.9). Carbonyl compounds usually exhibit absorption bands ranging from 280 to 350 nm, consequently enabling their excitation by means of UVA. Upon formation of the oxetane, its lack of absorption avoids the back reaction.[37]

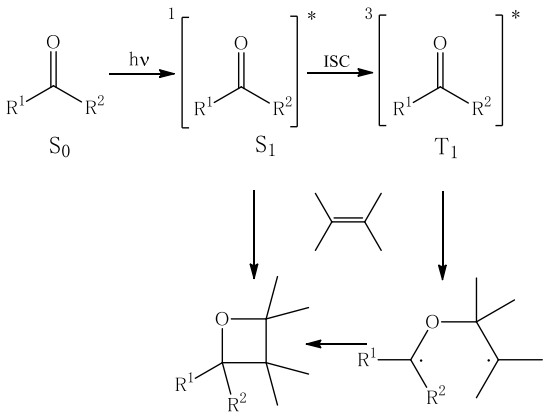

Figure 1.9. General pathway of a Paternò-Büchi reaction.

The involvement of 1,4-biradicals derived from carbonyl triplets was first spectroscopically studied in a benzophenone-diene Paternò-Büchi reaction where the biradical was detected with a time resolution of 25 ps and its maximum at 525 nm was clearly different from the one of the ketyl radical present in the same region.[46] Trapping of 1,4-biradicals derived from *p*-benzoquinone or benzophenone by quenchers such as molecular oxygen or sulfur dioxide, leading to the corresponding trioxides or sulfones

also acts as a proof of the formation of a biradical in this reaction.[47] However, the influence of the implied biradical in the regio- and stereochemistry of the Paternò-Büchi is not completely understood and that stereochemistry just can be estimated in some cases by defining the most stable potential biradical derived from the carbonyl.

The presence of different nucleobases with unsaturated functions together with exogenous xenobiotics such as benzophenone, submitted to the Sun irradiation seems to constitute an optimum scenario for the Paternò-Büchi reaction.[48-52] However, more often photosensitization of DNA gives mainly rise to CPDs by the 2+2 cicloaddition of alkenes in the organism.[48] That reaction, which implies an energy transfer from the Sens to the alkene, is favored in the body due to the diminishing of the T_1 energy of the nucleobases caused by the π-stacking and base pairing phenomena taking place in the DNA, which, for instance, decreases the T_1 energy of thymine from 310[53] when it is a free base to 267 kJ mol^{-1} in DNA.[40] Conversely, pyrimidine (6-4) pyrimidone photoproduct is also a DNA lesion which is thought to occur via a Paternò-Büchi reaction activated by direct irradiation of DNA. In this case, the cycloadduct is formed between the 4-carbonyl of one thymine and the C5-C6 unsaturated bond of an adjacent unit, leading to unstable oxetane intermediates, finally rearranging to generate pyrimidine (6-4) pyrimidone stable photoproducts (Scheme 1.2).[49,50,52,54]

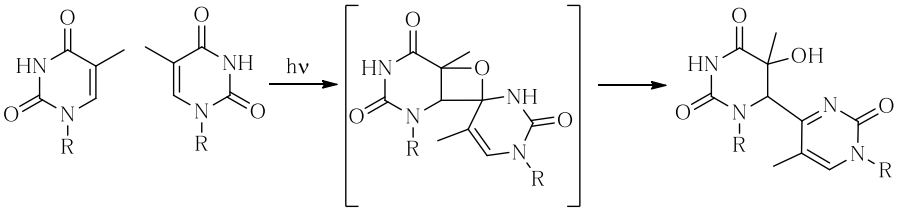

Scheme 1.2. UVB-induced pyrimidine (6-4) pyrimidine formation *via* a Paternò-Büchi reaction.

Moreover, synthesis of some organic interesting structures has been achieved by a Paternò-Büchi reaction. Among them, the antiviral nucleoside oxetanocin[4,55] whose

synthetic strategy begins with a Paternò-Büchi reaction, or the synthesis of the antibiotic oxetin,[56] in which the specific relative configuration of the oxetane substituents is achieved by means of this photochemical step (Scheme 1.3).

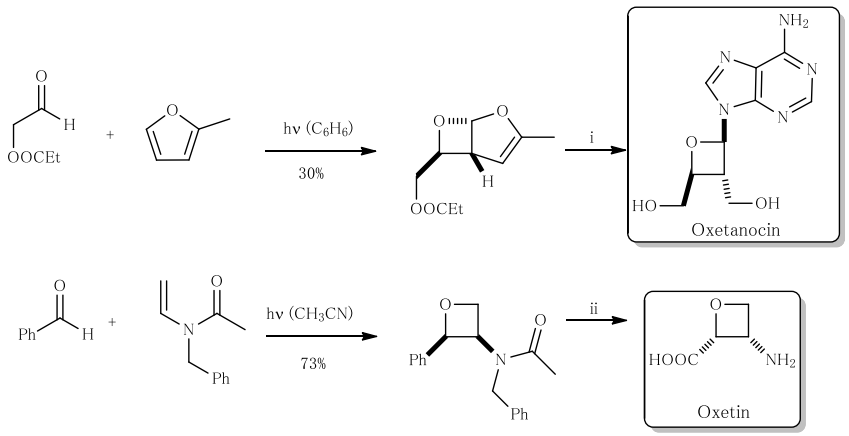

Scheme 1.3. Synthetic schemes to prepare oxetanocin (i) and oxetin (ii) via the Paternò-Büchi reaction.

1.5. Recent studies based on bile acids

The chemical structure of BAs is the key feature which enables the development of their previously described physiological functions. In fact, β-convex hydrophobic face and the α-concave and hydrophilic face in BAs result in their facial amphiphilia. This property justifies their tendency to form aggregates in aqueous solution as the concentration of BA increases. In fact, formation of aggregates is essential for lipid solubilisation and digestion along the intestinal tract.

The basis of the aggregation behaviour of BAs was firstly described by Small, based on the NMR broadening of the corresponding signals at the hydrophobic and hydrophilic faces.[5] He established the interaction of the hydrophobic faces of 2-10 monomers at low

BA concentrations (primary aggregates). Then, if the concentration increases, formation of secondary aggregates takes place.

Moreover, micellation of the sodium salts derived from BA, NaCA, NaCDCA, NaDCA and NaUDCA has been studied at different temperature ranges. The specific critical micellar concentration for each salt was established from the modifications in the emission intensities of pyrene with increasing concentrations of bile salts.[57]

More recently, aggregation behaviour of BAs has been investigated in our group based on the preparation of BAs derivatives, in particular of CA, upon covalent attachment of different fluorophores that act as fluorescence reporters. Hence, covalent attachment of Dansyl (Dns) to CA[58] produces minimal changes in the molecule, thus keeping unchanged its original physiological functions. Then, by replacing only 5% of the original BA with the marked one, the high fluorescence of Dns acts as a reporter of aggregation of NaCA.[7] Either from steady-state and time-resolved techniques, the modulation of fluorescent intensities or singlet lifetimes of Dns with increasing concentration of NaCA evidences three different behaviors: i) in solution, ii) forming primary aggregates or iii) forming secondary aggregates. Hence, it has been established that CA stays in solution until its concentration reaches 20 mM, primary aggregates are formed all along the mM concentration ranges having a maximum at 15 mM, while secondary aggregates begin to appear slowly from 10 mM.

The scope of that work has been extended to investigate the differences in the speciation diagrams for other bile acids such as GlyCA, TauCA, CDCA, GlyCDCA, DCA and UDCA using 3α-Dns CA as the fluorescent probe.[6]

The same fluorescent reporter has been used to probe the incorporation of CA and Ch within mixed micelles.[59] The formation of mixed micelles takes place by the interaction of BS with unilamellar vesicles of Ch and lecitine.[60,61] They are responsible for the solubilisation of Ch in the small intestine.[62] Linking chromophores such as Dns or naproxen (Npx) to the structures of CA or Ch and subsequent incorporation into mixed

micelles, has allowed for monitoring solubilization on the basis of different photophysical techniques such as fluorescence or laser flash photolysis. These techniques together with DLS and TEM have demonstrated the capability of mixed micelles to solubilize CA and Ch.

Fluorescent BA conjugates have also been used as reporters for monitoring the BA uptake by the hepatocytes by using flow cytometry. The fluorescent probes are submitted to flow cytometry kinetic assays in fresh suspensions of rat hepatocytes and are specifically taken up, suggesting the suitability of these molecules for the study of BA transport[58,63,64] Then, the usefulness of this technique has been demonstrated upon detection of compounds such as troglitazone, that affects in vitro BA uptake.[63]

Moreover, complexes between fluorescent CA derivatives and human serum albumin have provided a tool to investigate the binding behaviour of the BAs–proteins systems by means of photophysical techniques.[65]

Overall, BAs have demonstrated to be stereoselectively transformed into different fluorescent derivatives that have proven to be useful for monitoring aggregation behaviour, solubilisation of CA or Ch within mixed micelles, uptake by hepatocytes or binding to proteins. Therefore, the usefulness of a rigid scaffold, which allows the modulation of the separation distances between chromophores seems appropriate for investigating different photochemical reactions and photophysical processes. With this background, it seems interesting to use the complex architecture of BAs to further investigate other processes of interest, such as energy transfer through a rigid hydrocarbon skeleton or DNA photodamage related reactions, changing the relative distances between the reacting units.

Chapter 2: Objectives

The main goal of this Thesis is to use the architecture of bile acids to study different photophysical processes of interest such as hydrogen-abstraction, energy transfer or exciplex formation.

Firstly, bile acid derivatives have been designed and synthesized. Then the synthesized compounds or the unmodified bile acids have been employed to achieve the following specific objectives:

- To explore the radical-mediated dehydrogenation of bile acids using benzophenone triplet carbonyls for hydrogen atom transfer.
- To investigate through-bond triplet-triplet energy transfer and through-bond exciplex formation processes in synthesized donor-acceptor' systems based on bile acids.
- To demonstrate benzophenone photosensitized formation of thymine dimers through a novel mechanism involving delocalized triplet excited states.
- To evidence the generation of the triplet excited state of thymine upon photosensitized through-bond energy transfer from benzophenone.

- To generate direct or carbazole photosensitized thymine dimers susceptible to be repaired by inter- or intramolecular carbazole.

Chapter 3: Radical-Mediated Dehydrogenation of Bile Acids*

3.1. Introduction

Enzymes are key biomolecules in the reactions of biological systems. They are specialized proteins with great catalytic power, even higher than that of synthetic or inorganic catalysts. They are characterized by their high specificity to a certain substrate, their capability to accelerate specific chemical reactions and their performance in aqueous solutions under mild conditions of temperature and pH. Structurally, as most of them are proteins, they are constituted by linear chains of amino acids, with the exception of a small group of enzymes that are formed by RNA molecules.

Some of them are able to develop their functions by themselves, but others require an additional chemical unit called cofactor or coenzyme. The cofactor can be one or more inorganic ions such as Fe^{2+}, Mg^{2+}, Mn^{2+} or Zn^{2+}, while the coenzyme is an organic molecule.

*Reproduced in part from: P. Miro, M. L. Marin and M. A. Miranda, *Org. Biomol.Chem.*, 2016, **14**, 2679-2683 with the permission of the Royal Society of Chemistry

Enzymes are classified, and sometimes called according to the kind of reaction they catalyze. Moreover, their activity is due to the specific microenvironment in their active site, where the present amino acids can be bonded to a specific substrate in order to catalyze a chemical transformation.[66]

Enzyme-mediated bacterial transformations of bile acids (BAs) have recently attracted considerable interest in connection with diseases of the human gastrointestinal tract and, more specifically, colon cancer.[67] In addition, products obtained in the biotransformation of BAs by bacteria have been exploited in the commercial production of biologically active compounds.[68]

The microbial transformations of BAs include dehydrogenation of the α-OH groups at positions C-3, C-7 and/or C-12, which results in the oxidation to the corresponding oxo-derivatives in a reversible, regio- and stereoselective manner.[69] In general, these processes are driven by hydroxysteroid dehydrogenases (HSDHs) that belong to the oxydoreductase type enzymes and use the nicotinadenine cofactors NADPH/$NADP^+$ or NADH/NAD^+ together with an efficient recycling system, such as the pyruvate/lactate pair (Figure 3.1).[70] The potential of HSDHs as a tool to discover new lead compounds for the pharmaceutical industry has also been explored by means of combinatorial biocatalyzed approaches. This strategy has been effectively used to generate libraries of BA derivatives suitable for high-throughput biological screening.[68] An interesting application is the chemoenzymatic/ multienzymatic synthesis of ursodeoxycholic acid[71,72], used as a drug to dissolve cholesterol gallstones.[73]

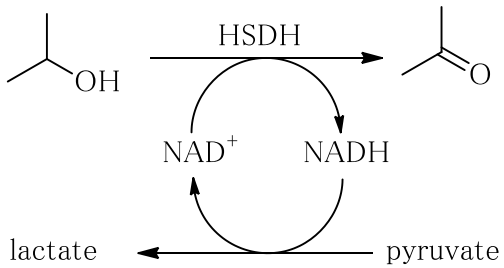

Figure 3.1. An example of hydroxysteroid dehydrogenases (HSDHs) performance.

With this background, the aim of the present chapter is to explore the potential of radical-mediated dehydrogenation of BAs as an artificial equivalent to the enzymatic action of HSDH. As this new approach is based on a different reaction mechanism, it could allow, after optimization, achieving complementary regio- and stereoselectivities that could expand the available synthetic toolbox. To prove the concept, carbonyl triplets, such as those of benzophenone (Bzp) derivatives (Figure 3.2), have been chosen because they can be efficiently generated upon selective UVA-excitation, and have reactive $n\pi^*$ electronic configuration. In fact, they are known to act as formal biradicals, mediating H-abstraction from allylic positions in polyunsaturated fatty acids[74,75] and cholesterol[35,36], a key step in type I lipid peroxidation.

In spite of the intensive efforts devoted to develop alcohol oxidation methodologies, the photochemical dehydrogenation for synthetic purposes remains almost unexplored, and the reported examples are basically restricted to benzyl alcohols.[76]

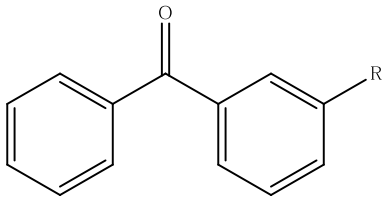

R=H Benzophenone (Bzp)
R=CH(CH_3)COOH Ketoprofen (KP)
R=CH(CH_3)$COOCH_3$ Ketoprofen methyl ester (KPMe)

Figure 3.2. Chemical structures of Bzp and Bzp-derivatives.

3.2. Results and discussion

A simplified picture of the radical-mediated approach to achieve dehydrogenation of BSs is shown in Figure 3.3. It involves generation of free radicals through hydrogen atom transfer (HAT) from BSs to triplet Bzp derivatives, ultimately leading to reduction of the Bzp chromophore concomitantly with formation of the oxo-analogs of the corresponding BSs. Accordingly, the direct reactivity of triplet Bzp with BSs will be evaluated by determining the kinetic rate constants using laser flash photolysis (LFP), and the overall reaction will be monitored through the disappearance of the typical Bzp absorption band at 260 nm. The outcome of the reaction will be assessed by isolation and full spectroscopic characterization of the dehydrogenated BS products.

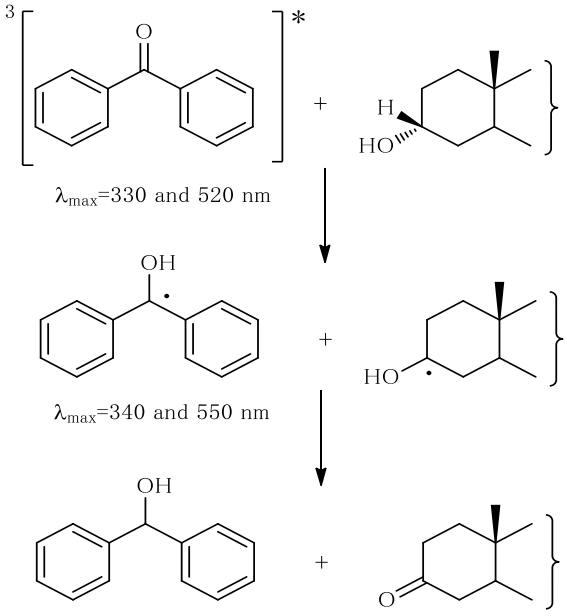

Figure 3.3. Mechanistic scheme of the radical-mediated dehydrogenation of the 3 α -position of a BS, triggered by a triplet carbonyl.

The generation and behavior of the triplet excited state of the Bzp chromophore in the presence of bile salts (BSs) was investigated by LFP. Thus, upon laser excitation (λ = 266 nm) of ketoprofen methyl ester (KPMe) in a deaerated saline aqueous solution ([NaCl] = 0.2 M), a transient absorption spectrum with two bands peaking at 330 and 520 nm, characteristic of the triplet excited state (^{3}KPMe*), was observed (Figure 3.4 left). However, when the spectrum was taken in the presence of BSs (NaCA, NaCDCA, NaDCA, NaLA or NaUDCA) a new transient signal with two maxima at 340 and 550 nm, characteristic of the benzhydryl radical (KPMe-H·) was observed in all cases as a proof of the HAT process (see Figure 3.4 right).

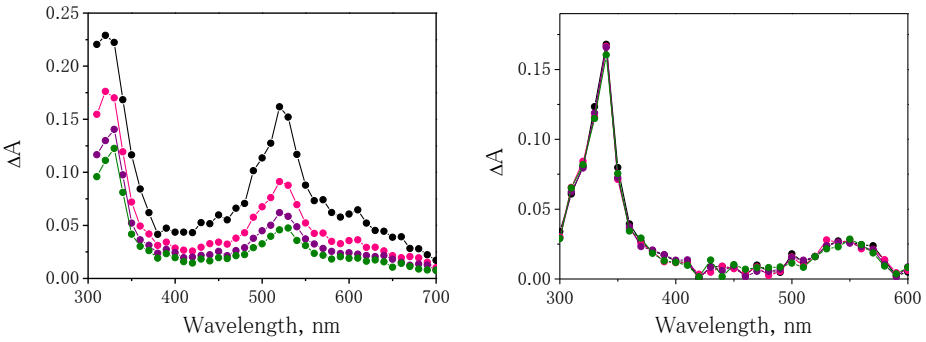

Figure 3.4. Transient absorption spectra (λ_{exc} = 266 nm) obtained from deaerated aqueous saline ([NaCl] = 0.2 M) solutions of KPMe (1 x 10^{-5} M). Left: in the absence of NaCA at 0.3 μs (black), 0.8 μs (red), 1.3 μs (purple) and 1.8 μs (green) after the laser pulse. Right: in the presence of NaCA (15 mM) at 1.8 μs (black), 4.3 μs (red), 9.3 μs (purple) and 14.4 μs (green) after the laser pulse.

To quantify the reactivity of ^{3}KPMe* with BSs, the quenching rate constants were determined. Hence, the triplet decay was monitored (λ = 520 nm) upon increasing BSs concentrations and, in fact, a progressive shortening was observed in all cases (see Figure 3.5). The reverse of the triplet lifetime was plotted *versus* BS concentrations, and the corresponding rate constant values were obtained from the slopes of the linear fittings (Figure 3.6 and Table 3.1).

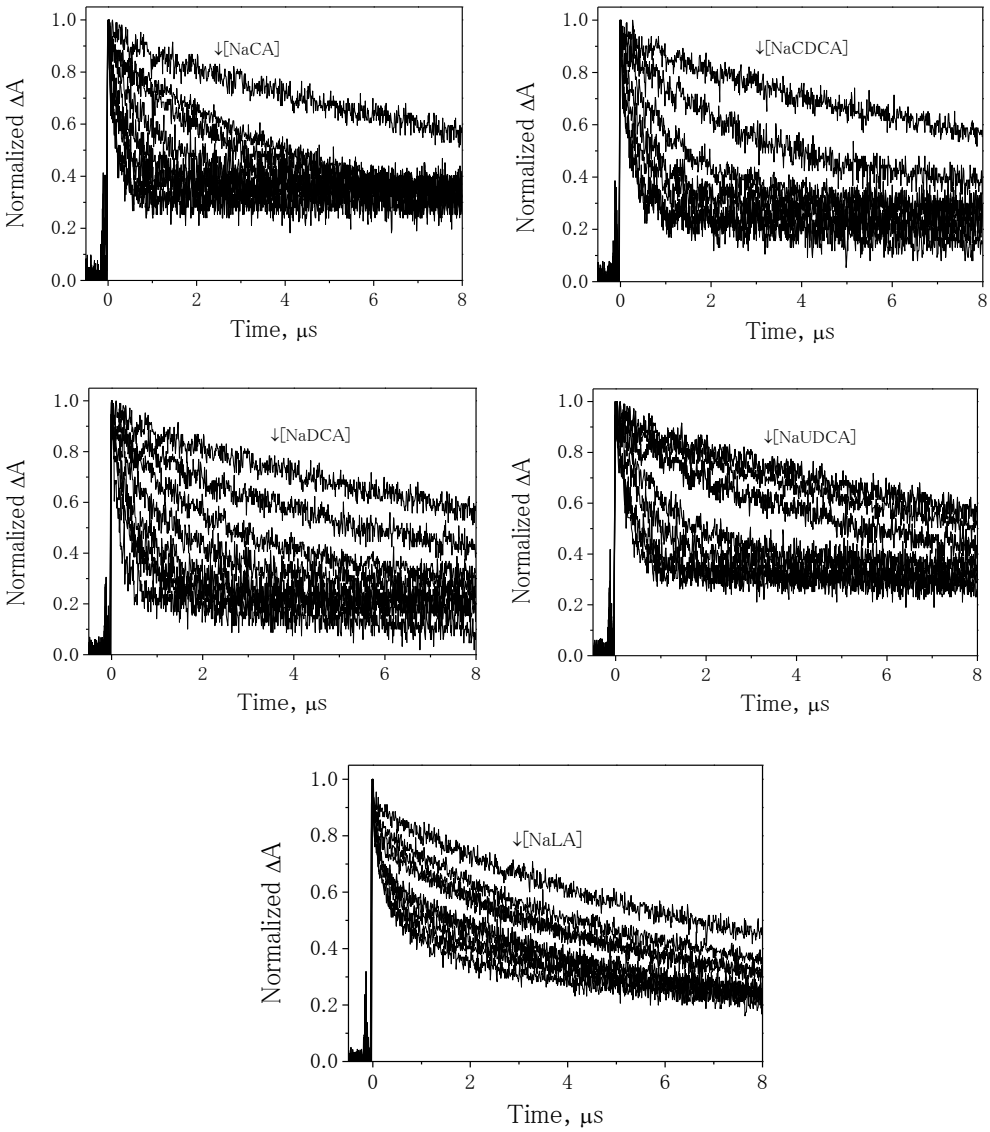

Figure 3.5. Kinetic traces recorded at 520 nm after laser flash irradiation (λ_{exc} = 266 nm) of deaerated aqueous solutions ([NaCl] = 0.2 M) of KPMe (1 x 10^{-5} M) in the presence of increasing concentrations of NaCA, NaCDCA, NaDCA and NaUDCA (0 - 17 mM) and NaLA (0 - 7.5 mM).

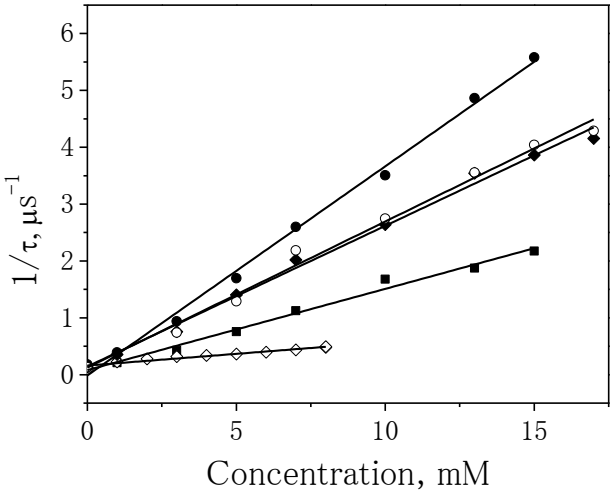

Figure 3.6. Stern-Volmer plots of the reciprocal KPMe triplet lifetime *versus* [NaCA] (●), [NaCDCA] (♦) [NaDCA] (■), [NaLA] (◊) and [NaUDCA] (○).

Table 3.1. Determined quenching rate constants for the reaction of ^{3}KPMe* with BSs.

BS	k_q (M^{-1} s^{-1})
NaCA	3.7 x 10^8
NaCDCA	2.5 x 10^8
NaDCA	1.4 x 10^8
NaLA	4.1 x 10^7
NaUDCA	2.6 x 10^8

In general, the observed reactivity of the HAT process follows the same trend as the number of CHOH moieties in the BS, thus indicating that the isopropanol-like methine hydrogens are indeed the most reactive sites. The regioselectivity of the reaction was evaluated by comparing the quenching rate constants obtained for NaCDCA, NaDCA and NaUDA, having the same number of CHOH moieties. The values found for NaCDCA and NaUDA having the two hydroxyl groups at C-3 and C-7 (either

on the α- or β- face), were similar; by contrast, a remarkably lower value was found for NaDCA whose hydroxyl groups are at C-3 and C-12. This indicates a lower reactivity of the hydrogen atom at C-12 than that of the one at C-7. Assuming an additive effect for the hydroxyl groups and comparing these values to the one obtained for NaLA, in which only the hydroxyl group at C-3 is present, the contribution of each position can be roughly calculated (see Table 3.2). The sum of each contribution can be successfully compared to the experimental constant for NaCA (k_q = 3.7 x 10^8 *versus* 3.5 x 10^8 $M^{-1}s^{-1}$ experimental and calculated, respectively). Therefore, the order of reactivity of the hydrogen atom is C-3<C-12<C-7.

Table 3.2. Evolution of the contribution of each hydroxyl group at different positions of the BS to the experimental global k_q.

BS	k_q (M^{-1} s^{-1})$_{exp}$	3 α contribution	7 α contribution	12 α contribution
NaCA	3.7 x 10^8	4.1 x 10^7	2.1 x 10^{8a}	9.9 x 10^{7b}
NaCDCA	2.5 x 10^8	4.1 x 10^7	2.1 x 10^{8a}	-
NaDCA	1.4 x 10^8	4.1 x 10^7	-	9.9 x 10^{7b}
NaLA	4.1 x 10^7	4.1 x 10^7	-	-

[a]Determined as k_q(NaCDCA)$_{exp}$-k_q(NaLA)$_{exp}$; [b]Determined as k_q(NaDCA)$_{exp}$-k_q(NaLA)$_{exp}$.

Next, the steady-state reactivity of KPMe with NaCA in solution was monitored by UV-spectrophotometry, following the characteristic KPMe band at 260 nm (Figure 3.7). As expected for a triplet-mediated reaction, the kinetics was much faster under N_2 than under O_2, supporting the role of the oxygen-quenchable ^{3}KPMe* in the dehydrogenation process.

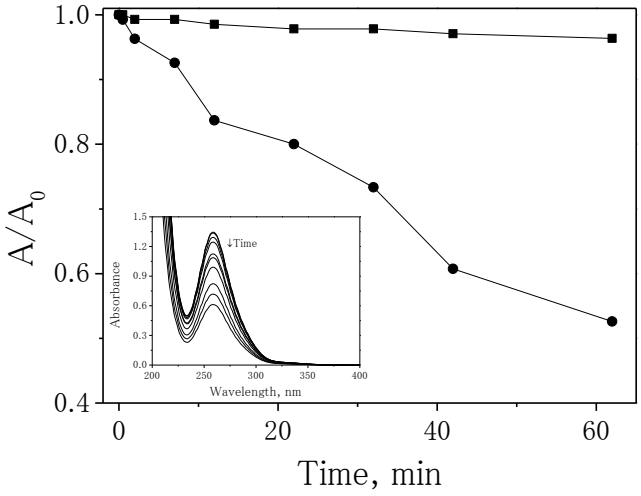

Figure 3.7. Relative absorbance measured at 260 nm *versus* irradiation time (λ_{irr} centered at 350 nm) in aqueous solutions ([NaCl] = 0.2 M) containing KPMe (8 x 10^{-5} M) and NaCA (1 x 10^{-2} M) under N_2 (●) or O_2 (■) atmosphere. Inset: UV-Vis spectra of KPMe (8 x 10^{-5} M) and NaCA (1 x 10^{-2} M) under N_2 at different irradiation times.

Next, the oxo-analogs of BSs arising from the HAT process were fully characterized for CA as the most appropriate example of BS, derivatized as methyl ester (CAMe) for practical purposes. For this purpose, an acetonitrile solution of CAMe and Bzp was irradiated (λ_{irr} centered at 350 nm) under N_2 atmosphere. The resulting crude photomixture was concentrated and purified by column chromatography yielding three products (Scheme 3.1). Their structural characterization was based on ^{1}H and ^{13}C NMR spectroscopy, including NOEDIFF experiments, combined with exact mass determination. The first eluted product (A) showed a loss of four amu in the MS, together with the appearance of two new ^{13}C signals at >210 ppm and the disappearance of two of the signals in the 65-75 ppm region, thus pointing to the oxidation of two out of the three hydroxyl groups. Moreover, the second (B) and third (C) eluted products showed a loss of two amu in the MS and the displacement of one ^{13}C signal from 65-75

ppm to >210 ppm; thus, the oxidation of one of the hydroxyl groups at C-3, C-7 or C-12 was inferred in those cases. To unequivocally characterize the three photoproducts, NOEDIFF experiments were performed, and the resulting spectra were thoroughly analyzed.

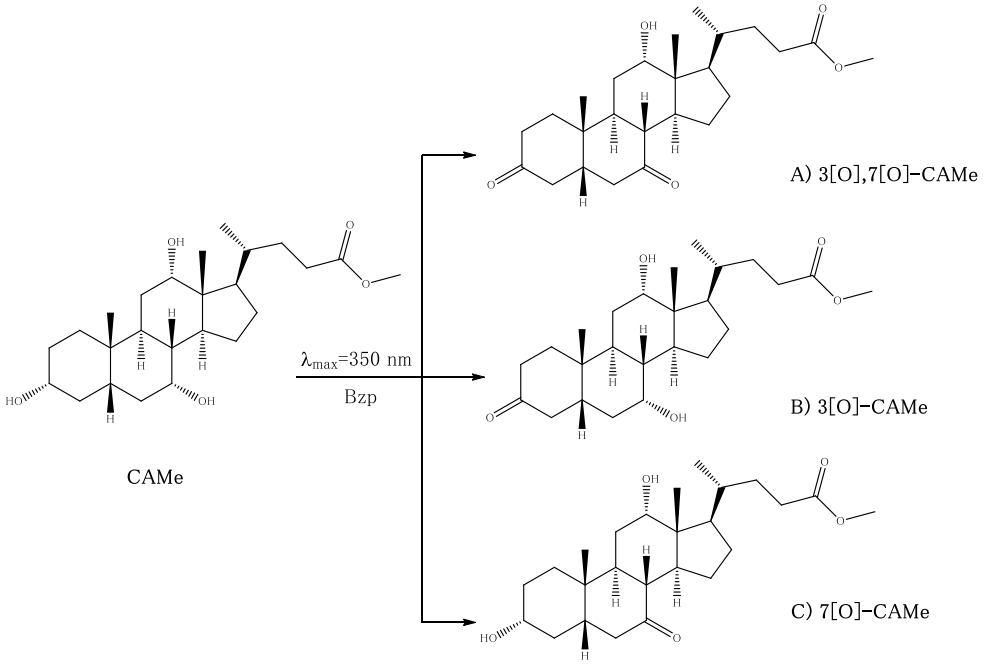

Scheme 3.1. Irradiation (λ_{irr} centered at 350 nm) of CAMe in the presence of Bzp in deaerated CH_3CN solution to obtain 3[O],7[O]-CAMe, (5%), 3[O]-CAMe, (7%) and 7[O]-CAMe, (21%).

Compound A was unambiguously assigned as the one resulting from the oxidation at C-3 and C-7 positions, 3[O],7[O]-CAMe. In fact, irradiation of proton at 4.06 ppm produced NOE effect on methyl groups at 0.98 (d) and 0.72 (s) ppm. This indicates that the proton at 4.06 ppm corresponds to 12β-H, and the methyls to 21-CH_3 and 19-CH_3. Furthermore, irradiation of methyl group at 1.28 ppm resulted in a NOE effect only on signal at 0.72 ppm, indicating that the former corresponds to 18-CH_3. Compound B was identified as arising from the oxidation at C-3, namely 3[O]-CAMe, based on the NOE enhancement on methyl groups at 0.97 (s and d) and on the proton at 4.03 ppm

upon irradiation of the methyl group at 0.72 ppm. From this result, the methyl group at 0.72 ppm can be assigned to 19-CH_3 and the singlet at 4.03 ppm to 12β-H. In fact, when the latter was irradiated, a NOE effect was found on 19-CH_3 (0.72 ppm) and 21-CH_3 (0.97 ppm, d), while irradiation of proton at 3.92 ppm did not result in any NOE effect on the methyl groups indicating that this signal corresponds to 7β-H. Finally, compound C was identified as the one resulting from oxidation at the C-7 position, namely 7[O]-CAMe, based on the NOE effect observed on methyls 21-CH_3 (d) and 19-CH_3 (s) upon irradiation on 12β-H (4.02 ppm). Interestingly, no product was found arising from oxidation at C-12.

After isolation and unequivocal characterization of the methyl esters, the three oxo-analogs were subjected to saponification and used to monitor the kinetics of the photooxidation of NaCA in deaerated aqueous solution ([NaCl] = 0.2 M), in the presence of KPMe, to mimic the conditions used in the LFP experiments. The kinetics of the photooxidation was monitored by UPLC-MS operating in negative ionization mode. The obtained results (see Table 3.3) indicate that again the main photoproducts arise from the oxidation at C-3 and/or C-7. Therefore photooxidation of CA from triplet KPMe resulted independent on the organic or aqueous media employed.

Table 3.3. Photoproduct evolution during the irradiation of NaCA with KPMe (λ_{max}=350 nm) monitored by UPLC-MS-MS.

		Kinetics (%) based on area			
Compound	Retention time (min)	t_{irr}=0h	t_{irr}=3h	t_{irr}= 9h	t_{irr}=12h
NaCA	10.67	100	71	60	60
Na 3[O]-CA	10.10	-	19	22	23
Na 7[O]-CA	8.28	-	10	10	10
Na 3[O],7[O]-CA	7.90	-	-	8	7

Although the rate constants determined by LFP could, in principle, appear inconsistent with the product distributions obtained in steady-state photolysis, the observed differences can be explained taking into account that the rate constants are associated with the initial step while the product distributions are the result of the global process that includes disproportionation or reversible HAT in the primary radical pair. Indeed, the long lifetime of KPMe-H$^{\cdot}$ supports that the subsequent processes occurring from these species are in the origin of the observed regioselectivity.

3.3. Conclusions

Dehydrogenation of bile salts at positions C-3 and/or C-7 has been achieved by a radical-mediated mechanism, as an alternative artificial equivalent to the enzymatic action of hydroxysteroid dehydrogenases. The triplet excited states of benzophenone derivatives, generated upon selective UVA-excitation, have proven to be appropriate radical precursors, which operate through hydrogen atom transfer from the methine CH-OH groups. As this new approach is based on a different reaction mechanism, it could allow, after optimization, achieving complementary regio- and stereoselectivities that could expand the available synthetic toolbox.

3.4. Experimental

3.4.1. Synthesis

KPMe and CAMe were prepared following standard procedures:

3.4.1.1. Synthesis of KPMe[77]

To a stirred solution of KP (0.500 g, 1.97 mmol) in 4 mL of MeOH, a catalytic amount of H_2SO_4 was added. The reaction was refluxed overnight, re-dissolved in EtOAc, washed with $NaHCO_3$, dried over $MgSO_4$ and concentrated under vacuum. The crude was purified by column chromatography (SiO_2, EtOAc:Hexane, 50:50) to give KPMe (0.516 g, 98%). ^{1}H NMR (300 MHz, $CDCl_3$): δ (ppm) 1.33 (d, J = 7.2 Hz, 3H, CH_3); 3.45 (s, 1H, OCH_3); 3.61 (q, J = 7.2 Hz, 1H, CH); 7.17-7.65 (m, 9H, arom). ^{13}C NMR (75 MHz, $CDCl_3$): δ (ppm) 196.1 (C), 174.3 (C), 140.7 (C), 137.7 (C), 137.3 (C), 132.4 (CH), 131.4 (CH), 129.9 (2xCH), 129.0 (CH), 128.9 (CH), 128.4 (CH), 128.2 (2xCH), 52.0 (CH_3), 45.1 (CH), 18.4 (CH_3); m/z found 291.0995, calculated for $C_{17}H_{16}O_3Na$ (MH^+) 291.0995.

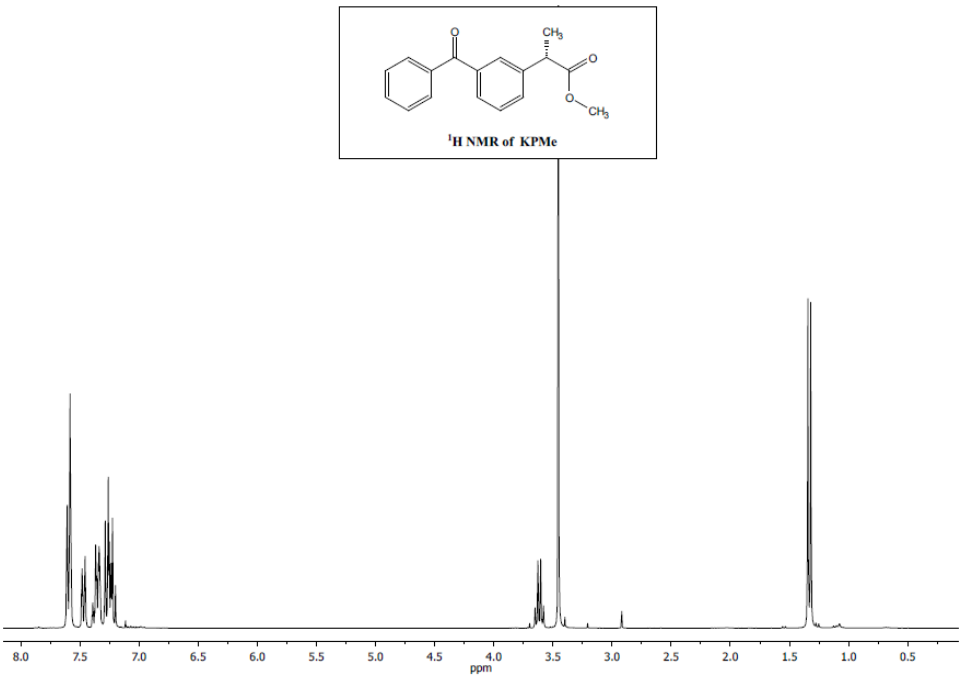
^{1}H NMR of KPMe
8.0
7.5
7.0
6.5
6.0
5.5
5.0
4.5
4.0
3.5
3.0
2.5
2.0
1.5
1.0
0.5
ppm

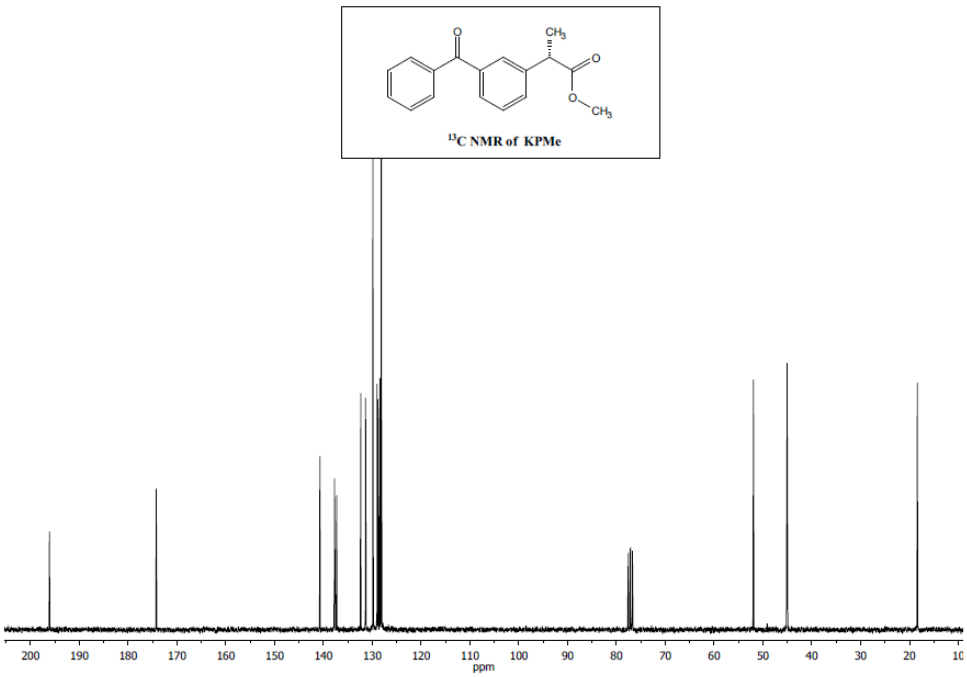
^{13}C NMR of KPMe
200
190
180
170
160
150
140
130
120
110
100
90
80
70
60
50
40
30
20
ppm

3.4.1.2. Synthesis of CAMe[78]

Briefly, to a stirred solution of CA (2 g, 4.9 mmol) in 10 mL of MeOH, 0.3 mL of HCl and 5 mL of dimetoxypropanone were added. The reaction was stirred overnight and then re-dissolved in EtOAc, washed with $NaHCO_3$ and brine and dried over $MgSO_4$. Concentration under vacuum gave CAMe (1.95 g, 94%). ^1H NMR (300 MHz, $CDCl_3$): δ (ppm) 0.69 (s, 3H, CH_3); 0.90 (s, 3H, CH_3); 0.98 (d, J = 6.3 Hz, 3H, 21-CH_3); 1.04-2.41 (complex signal, 24H); 3.46 (m, 1H, 3β-H); 3.66 (s, 3H, CH_3); 3.86 (*br* s, 1H, 7β-H); 3.98 (*br* s, 1H, 12β-H). ^{13}C NMR (75 MHz, $CDCl_3$): δ (ppm) 174.9 (C), 73.2 (CH), 72.0 (CH), 68.6 (CH), 51.6 (CH_3), 47.1 (CH), 46.5 (C), 41.7 (CH), 41.6 (CH), 39.6 (CH+CH_2), 35.4 (CH_2+CH), 34.9 (C), 34.8 (CH_2), 31.2 (CH_2), 31.0 (CH_2), 30.4 (CH_2), 28.3 (CH_2), 27.6 (CH_2), 26.5 (CH), 23.4 (CH_2), 22.6 (CH_3), 17.4 (CH_3), 12.6 (CH_3); m/z found 423.3122, calculated for $C_{25}H_{43}O_5$ (MH^+) 423.3110.

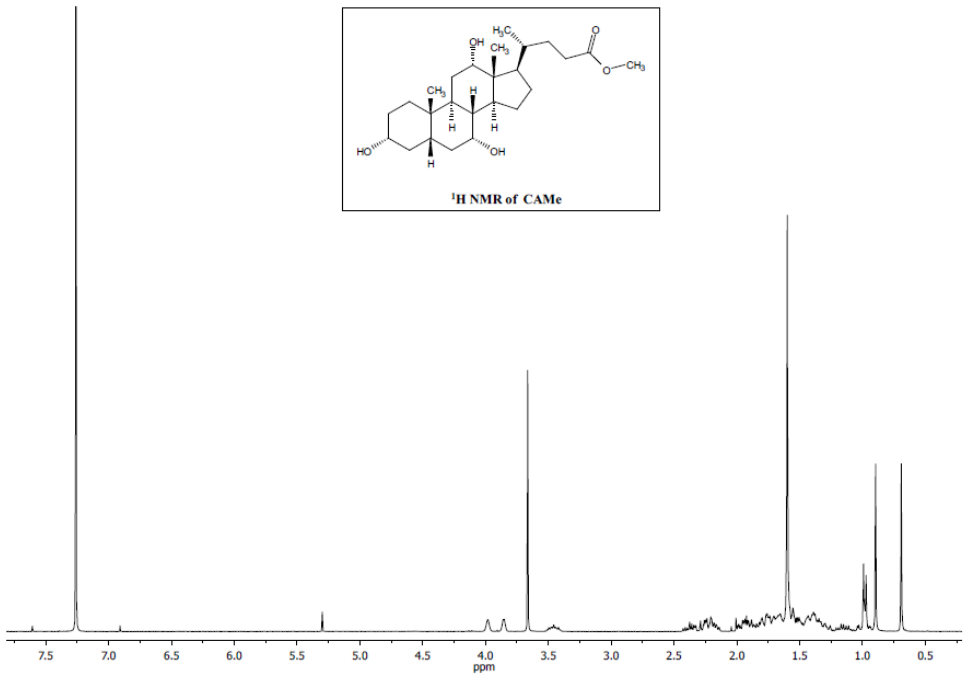
^{1}H NMR of CAMe
7.5
7.0
6.5
6.0
5.5
5.0
4.5
4.0
3.5
3.0
2.5
2.0
1.5
1.0
0.5
ppm

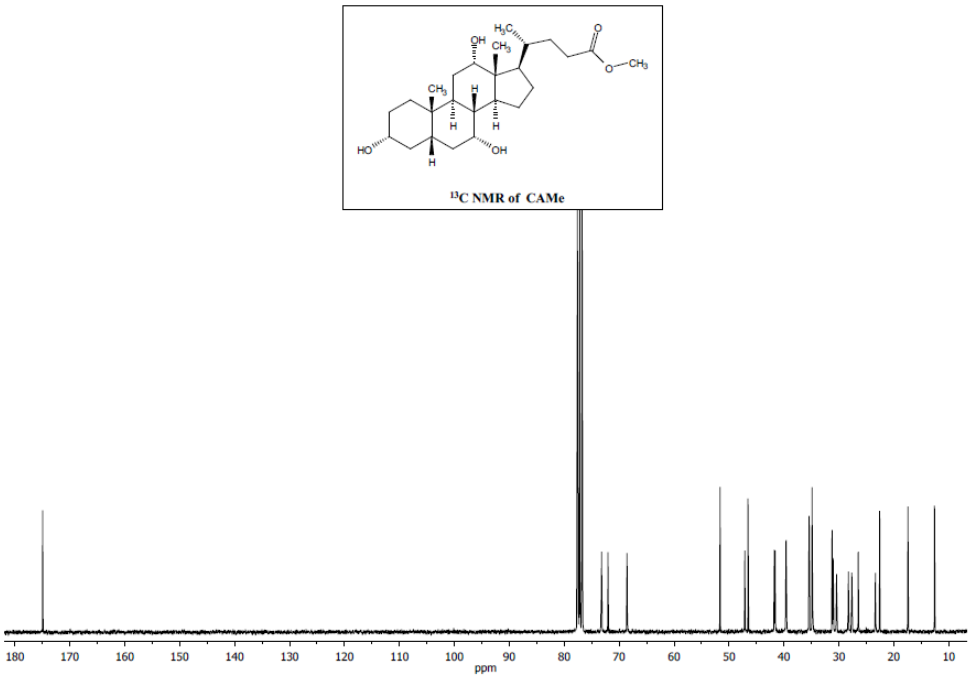
^{13}C NMR of CAMe
180
170
160
150
140
130
120
110
100
90
80
70
60
50
40
30
20
10
ppm

3.4.2. Preparative irradiation of CAMe in the presence of Bzp

A solution of CAMe (0.557 g, 1.37 mmol) and Bzp (0.250 g, 1.37 mmol) in CH_3CN (150 mL), placed in a Pyrex flask was purged with N_2 and irradiated in a 14-lamps photoreactor (λ_{max} = 350 nm) for six hours. Then, the solvent was concentrated under vacuum and the crude was purified by column chromatography (SiO_2, EtOAc:Hexane, 70:30) to yield **3[O],7[O]-CAMe** (0.0267 g, 5%), **3[O]-CAMe** (0.0406 g, 7%) and **7[O]-CAMe** (0.116 g, 21%). After isolation each photoproduct was repurified by reverse phase column chromatography before characterization (Li Chroprep RP-18, CH_3CN:H_2O, 60:40).

3.4.2.1. Characterization of 3[O],7[O]-CAMe

^{1}H NMR (300 MHz, $CDCl_3$): δ (ppm) 0.71 (s, 3H, 19-CH_3); 0.97 (d, J = 6.0 Hz, 3H, 21-CH_3); 1.14-2.53 (complex signal, 23H); 1.28 (s, 3H, 18-CH_3); 2.86 (dd, J = 13.2 and 4.8 Hz, 1H); 3.66 (s, 3H, CH_3O); 4.04 (*br* s, 1H, 12 β-H). ^{13}C NMR (75 MHz, $CDCl_3$): δ (ppm) 210.8 (C), 210.4 (C), 174.7 (C), 72.1 (CH), 51.7 (CH_3), 49.7 (CH), 47.8 (CH), 46.8 (CH), 46.7 (C), 45.1 (CH_2), 43.1 (CH_2), 40.8 (CH), 36.8 (CH_2), 36.2 (CH), 35.5 (CH_2), 35.0 (C+CH), 31.2 (CH_2), 31.0 (CH_2), 29.7 (CH_2), 27.7 (CH_2), 24.4 (CH_2), 22.4 (CH_3), 17.7 (CH_3), 13.1 (CH_3); m/z found 419.2813, calculated for $C_{25}H_{39}O_5$ (MH^+) 419.2797.

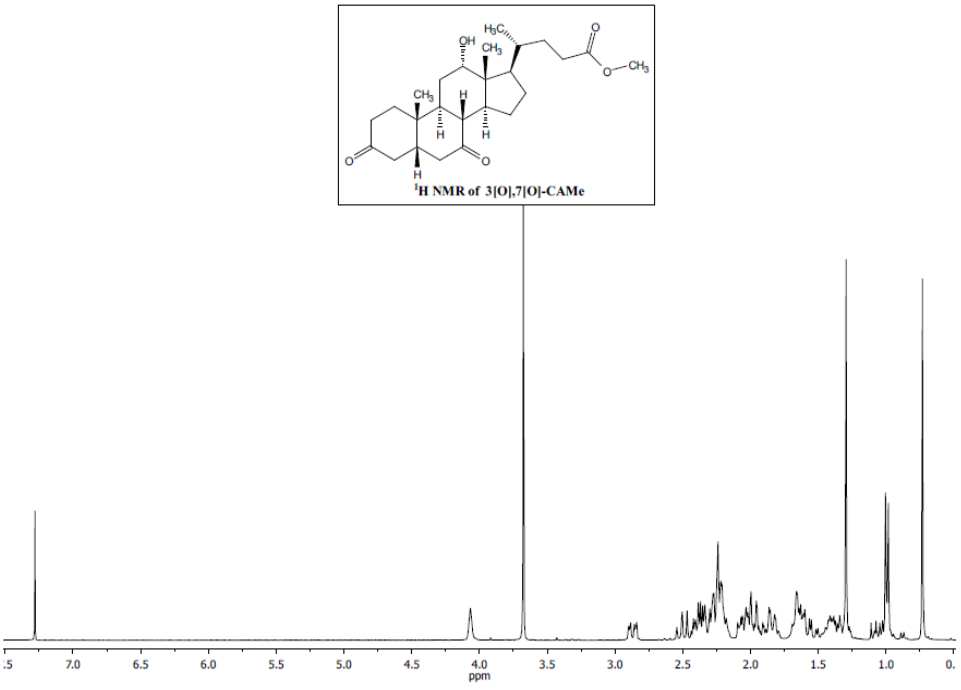

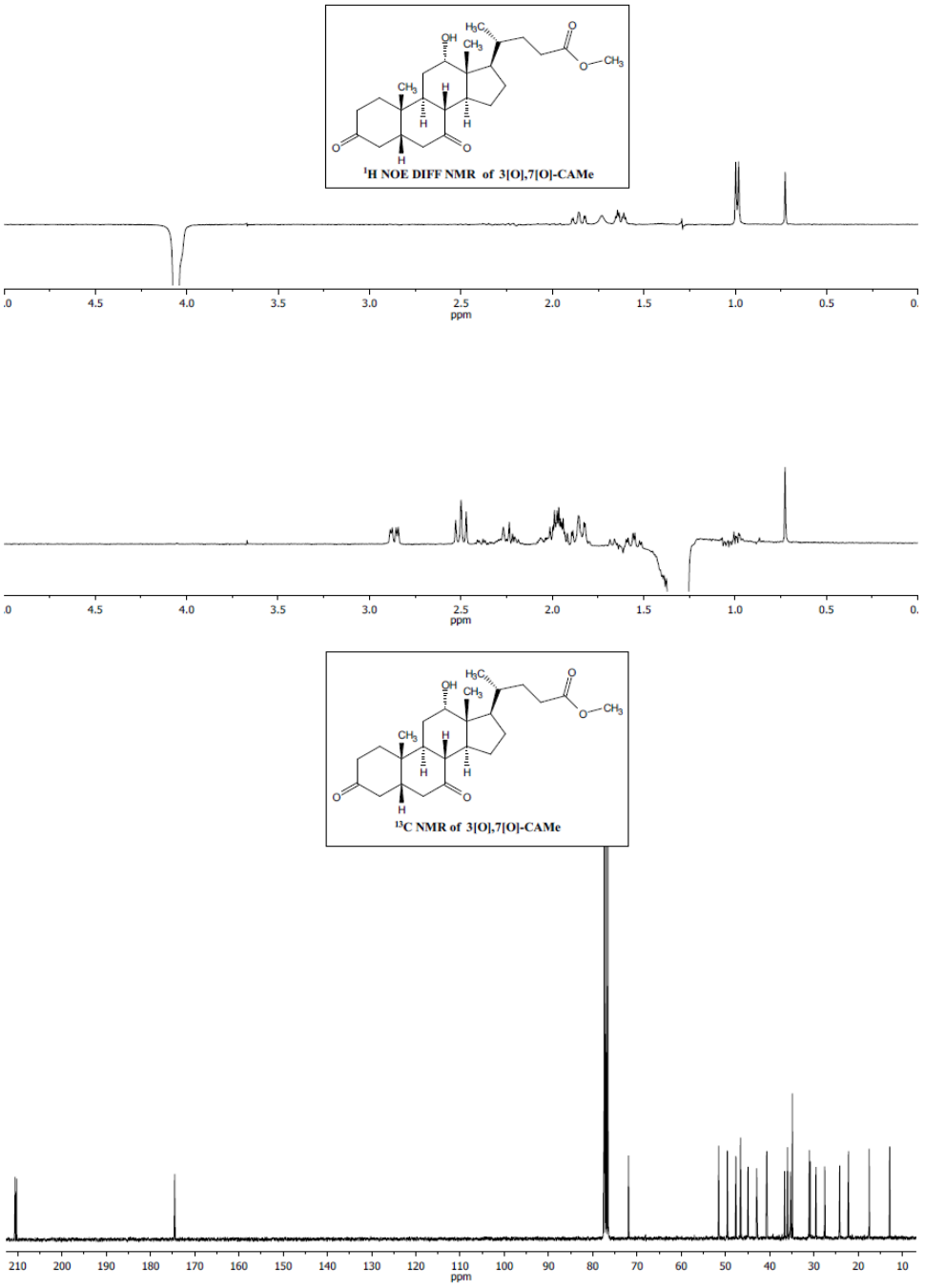
^{1}H NOE DIFF NMR of 3[O],7[O]-CAMe
ppm
^{13}C NMR of 3[O],7[O]-CAMe
ppm

3.4.2.2. Characterization of 3[O]-CAMe

^{1}H NMR (300 MHz, $CDCl_3$): δ (ppm) 0.72 (s, 3H, 19-CH_3); 0.97 (m, 6H, 21-CH_3+18-CH_3); 1.11-2.48 (complex signal, 23H); 3.39 (dd, *J* = 15.0 and 13.5 Hz, 1H); 3.66 (s, 3H, CH_3O); 3.91 (*br* s, 1H, 7β-H); 4.02 (*br* s, 1H, 12β-H). ^{13}C NMR (75 MHz, $CDCl_3$): δ (ppm) 213.3 (C), 174.9 (C), 73.0 (CH), 68.4 (CH), 51.7 (CH_3), 47.4 (CH), 46.8 (C), 45.7 (CH_2), 43.2 (CH), 42.0 (CH), 39.7 (CH), 37.0 (CH_2), 36.8 (CH_2), 35.3 (CH), 35.0 (C), 34.0 (CH_2), 31.2 (CH_2), 31.0 (CH_2), 28.8 (CH_2), 27.6 (CH_2), 27.4 (CH), 23.3 (CH_2), 21.8 (CH_3), 17.5 (CH_3), 12.7 (CH_3); m/z found 443.2756, calculated for $C_{25}H_{40}O_5Na$ (MNa^+) 443.2773.

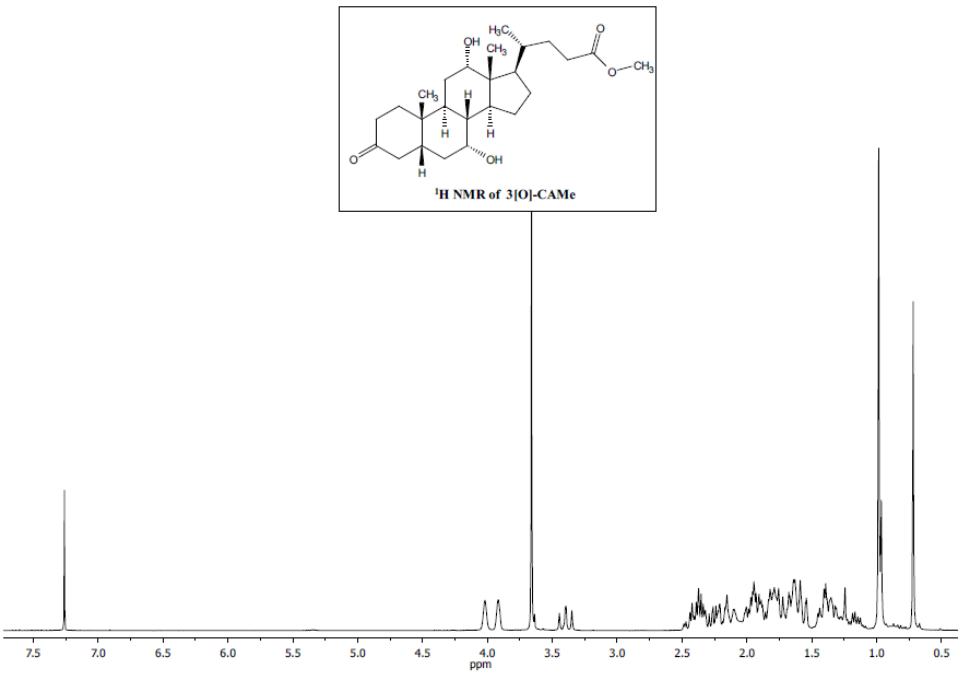

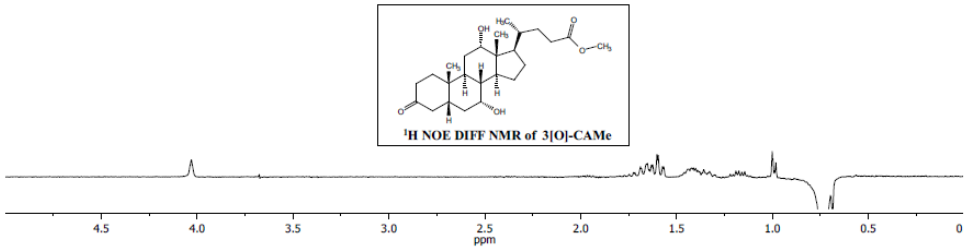
^{1}H NOE DIFF NMR of 3[O]-CAMe
4.5 4.0 3.5 3.0 2.5 2.0 1.5 1.0 0.5 0
ppm

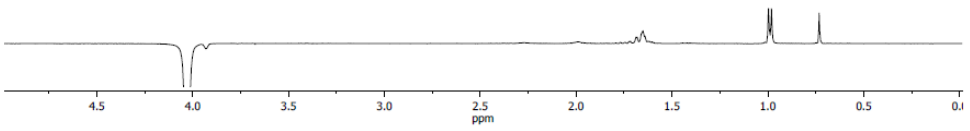
4.5 4.0 3.5 3.0 2.5 2.0 1.5 1.0 0.5
ppm

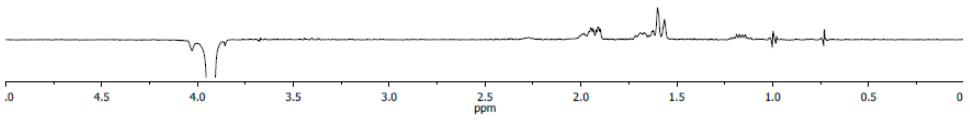
.0 4.5 4.0 3.5 3.0 2.5 2.0 1.5 1.0 0.5 0
ppm

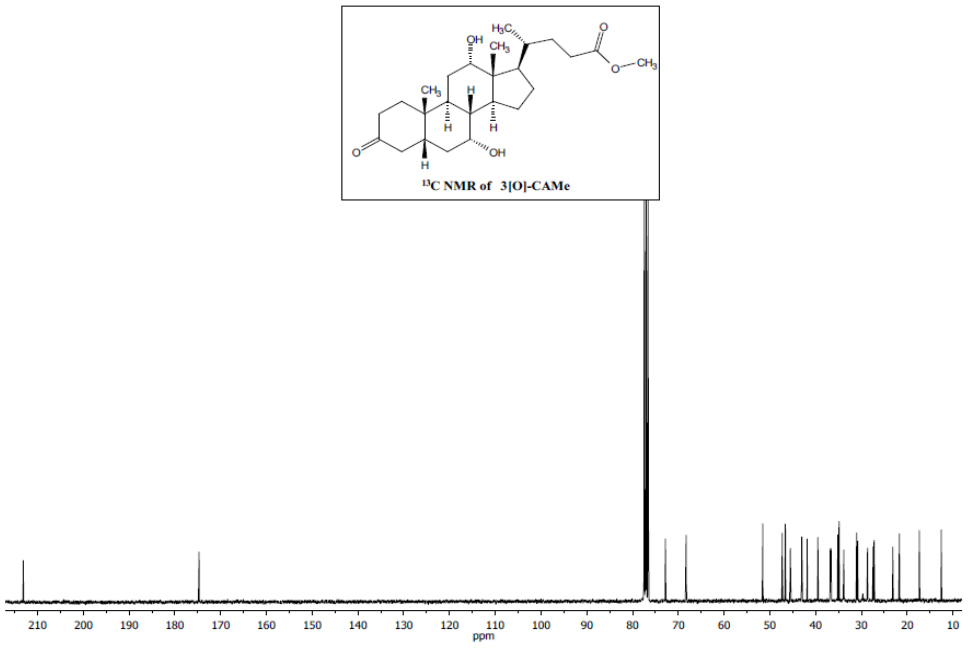
^{13}C NMR of 3[O]-CAMe
210 200 190 180 170 160 150 140 130 120 110 100 90 80 70 60 50 40 30 20 10
ppm

3.4.2.3. Characterization of 7[O]-CAMe

^{1}H NMR (300 MHz, $CDCl_3$): δ (ppm) 0.68 (s, 3H, 19-CH_3); 0.97 (d, J = 6.0 Hz, 3H, 21-CH_3); 1.10-2.42 (complex signal, 23H); 1.18 (s, 3H, 18-CH_3); 2.83 (dd, J = 12.4 and 6.4 Hz, 1H); 3.58 (m, 1H, 3 β -H); 3.66 (s, 3H, CH_3O); 4.01 (*br* s, 1H, 12 β -H). ^{13}C NMR (75 MHz, $CDCl_3$): δ (ppm) 211.5 (C), 174.7 (C), 72.2 (CH), 71.1 (CH), 51.7 (CH_3), 49.7 (CH), 46.7 (CH+C), 46.2 (CH), 45.5 (CH_2), 40.9 (CH), 37.6 (CH_2), 36.1 (CH), 35.1 (CH), 34.8 (C), 34.2 (CH_2), 31.2 (CH_2), 31.0 (CH_2), 30.0 (CH_2), 29.4 (CH_2), 27.7 (CH_2), 24.4 (CH_2), 23.0 (CH_3), 17.6 (CH_3), 13.0 (CH_3); m/z found 421.2962, calculated for $C_{25}H_{41}O_5$ (MH^+) 421.2954.

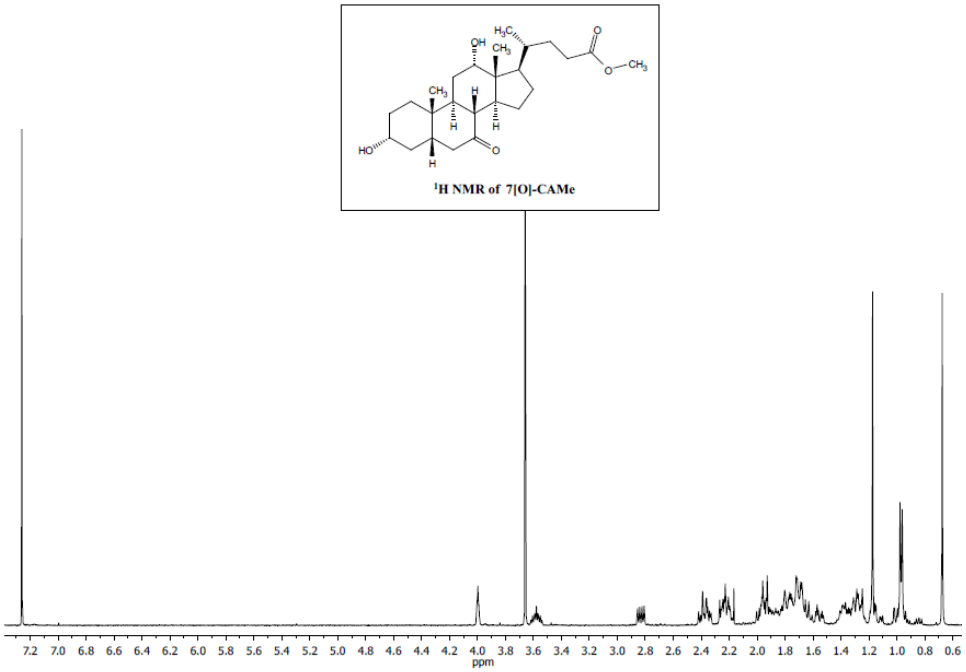

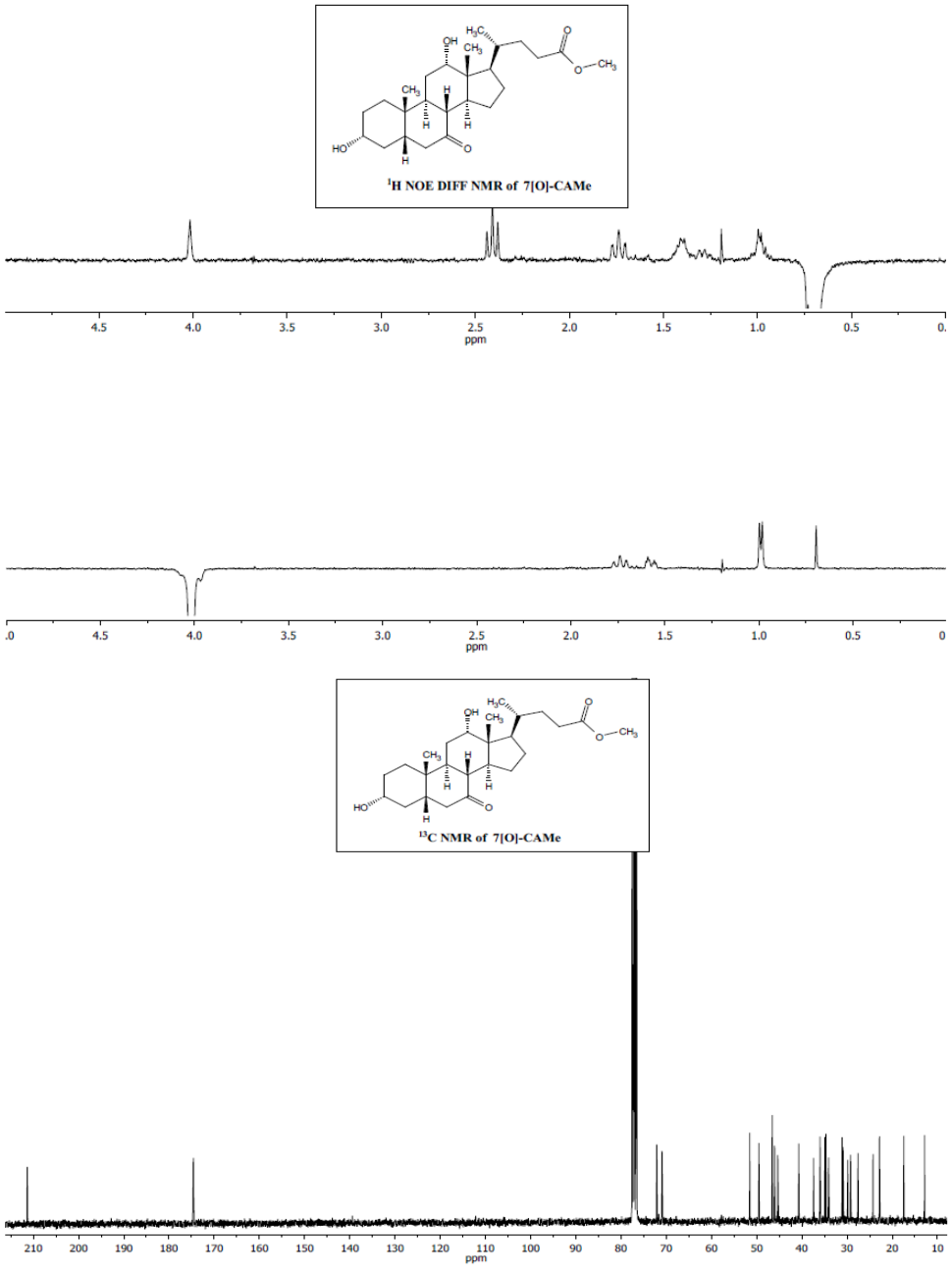
^{1}H NOE DIFF NMR of 7[O]-CAMe
4.5 4.0 3.5 3.0 2.5 2.0 1.5 1.0 0.5 0.
ppm
.0 4.5 4.0 3.5 3.0 2.5 2.0 1.5 1.0 0.5 0
ppm
^{13}C NMR of 7[O]-CAMe
210 200 190 180 170 160 150 140 130 120 110 100 90 80 70 60 50 40 30 20 10
ppm

3.4.3. Preparative irradiation of CA in the presence of KPMe

A solution of NaCA (0.215 g, 0.5 mmol) and KPMe (1.86 g, 0.5 mmol) in 100 mL of aqueous solution ([NaCl] = 0.2 M), placed in a Pyrex flask was purged with N_2 and irradiated in a photoreactor (λ_{max} = 350 nm) for twelve hours. The kinetics of the photoreaction was analyzed at different times by UPLC-MS-MS. The photoproducts in the crude were identified by comparison with isolated standards obtained upon saponification of 3[O],7[O]-CAMe, 3[O]-CAMe and 7[O]-CAMe in aqueous NaOH, 1M. Quantification was based on area integration.

Cuvete irradiations in water ([NaCl] = 0.2 M) at the concentration of 10 mM of NaCA with 1 x 10^{-5} M of KPMe were purged with O_2 or N_2 and followed by UV-Vis spectroscopy at different irradiation times.

3.5. Supplementary material

3.5.1. Instrumentation

Laser flash photolysis at 266 nm. Transient spectra were recorded at room temperature using N_2-purged aqueous solutions of 1 x 10^{-5} M of KPMe ([NaCl] = 0.2 M) and different concentrations of BSs.

Irradiations for the UV-Vis analysis. Irradiations were performed in the Luzchem photoreactor with lamps centred at 350 nm.

UPLC-MS-MS. The analysis was performed with isocratic elution of 60% CH_3CN and 40% water (containing 0.01% formic acid) as the mobile phase during 12 minutes followed by a gradient to reach 100% of MeOH. The injection volume was 1 μL. The ESI source was operated in negative ionization mode with the capillary voltage at 3.0 kV. The temperature of the source and desolvation was set at 120 °C and 500 °C, respectively.

3.6.3. Additional NMR spectra

3.6.3.1. KPMe

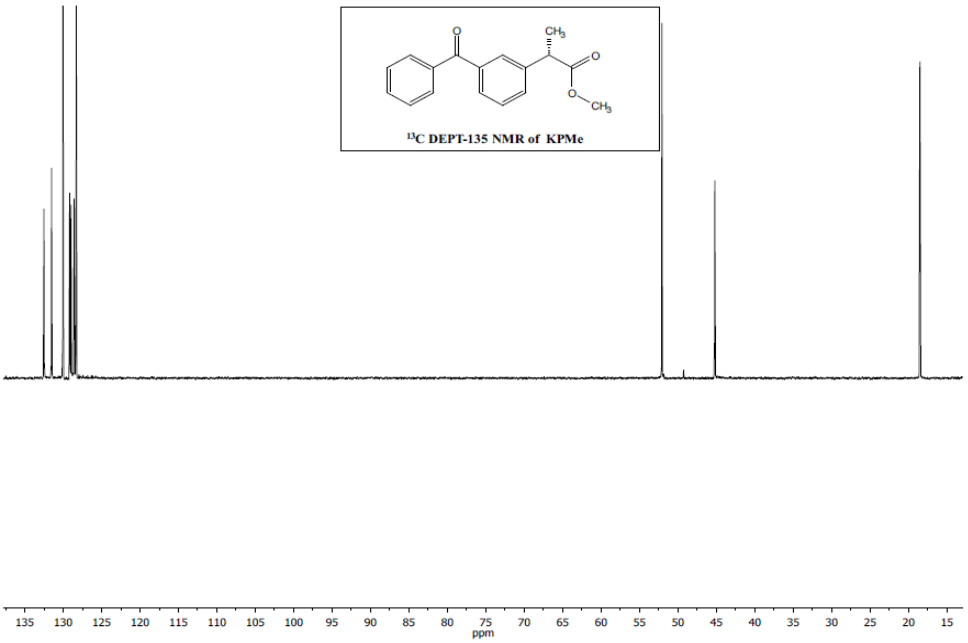

3.6.3.2. CAMe

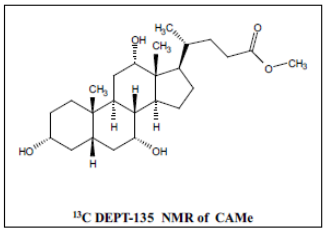

^{13}C DEPT-135 NMR of CAMe

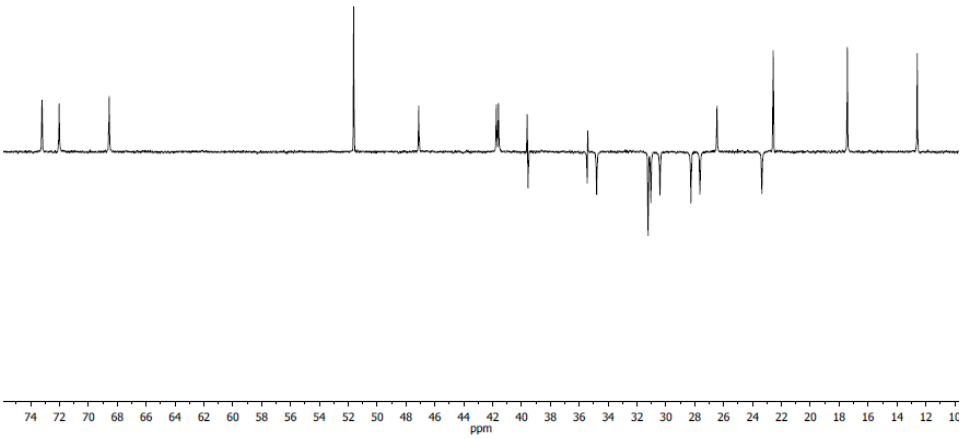

3.6.3.3. 7[O]-CAMe

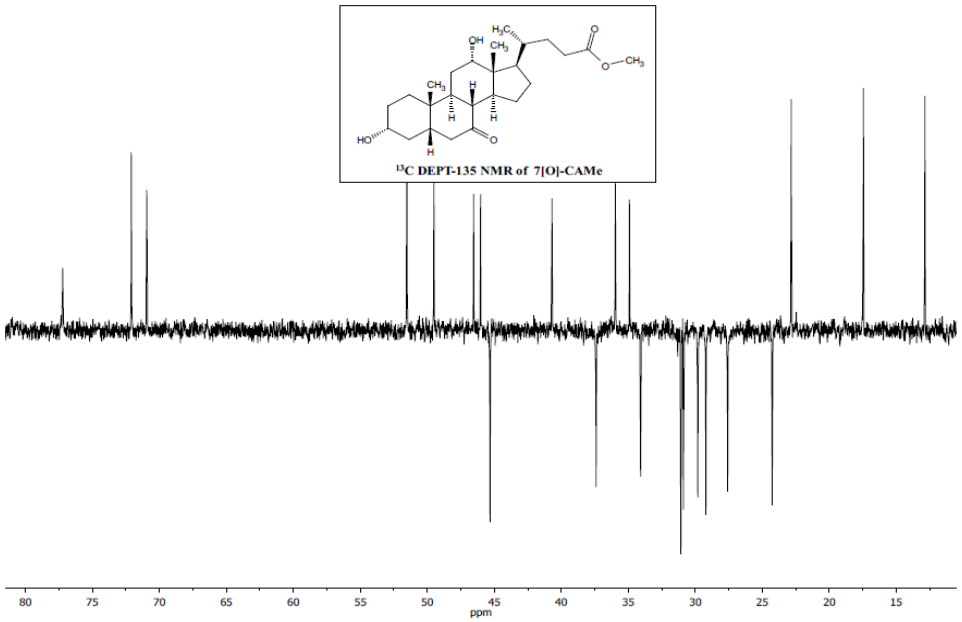
^{13}C DEPT-135 NMR of 7[O]-CAMe
80 75 70 65 60 55 50 45 40 35 30 25 20 15
ppm

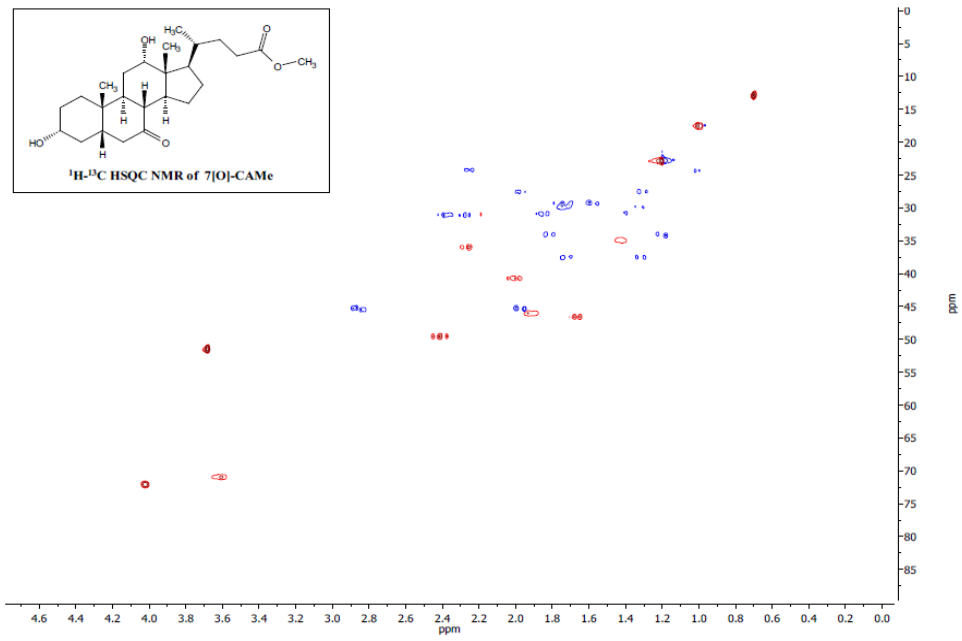
^{1}H-^{13}C HSQC NMR of 7[O]-CAMe
4.6 4.4 4.2 4.0 3.8 3.6 3.4 3.2 3.0 2.8 2.6 2.4 2.2 2.0 1.8 1.6 1.4 1.2 1.0 0.8 0.6 0.4 0.2 0.0
ppm
0 5 10 15 20 25 30 35 40 45 50 55 60 65 70 75 80 85
ppm

3.6.3.4. 3[O]-CAMe

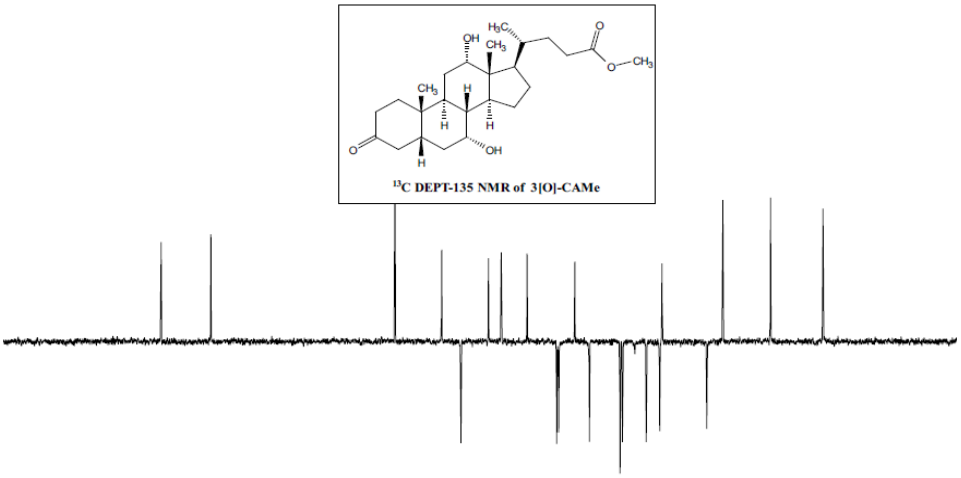

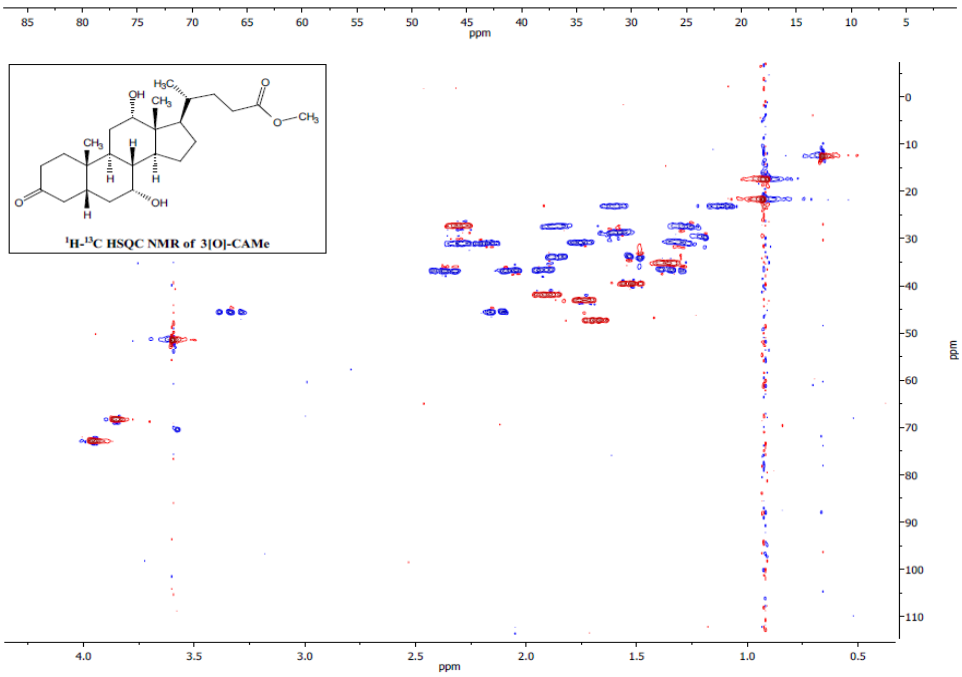

3.6.3.5. 3[O],7[O]-CAMe

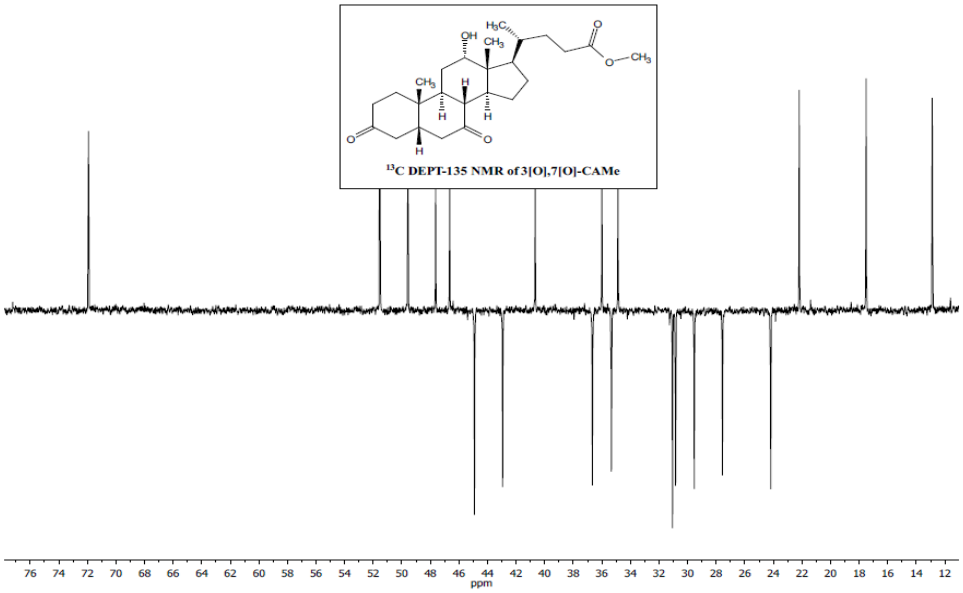

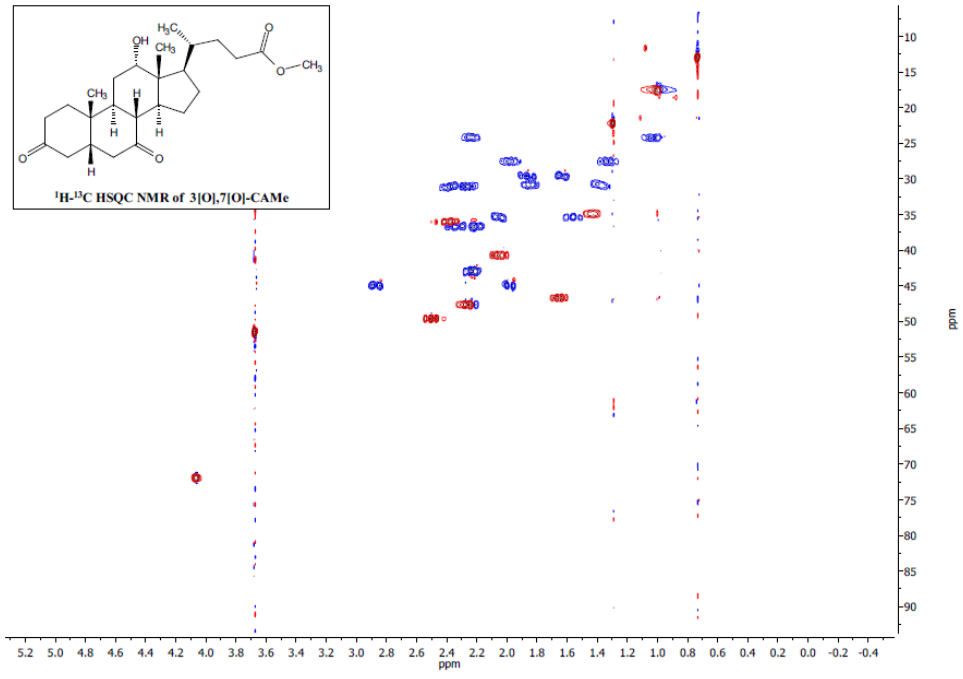

Chapter 4: Through-Bond Energy Transfer and Exciplex Formation Processes*

4.1. Introduction

In a thermodynamically favored energy transfer (ET) process, an excited donor (D) deactivates to its ground state by transferring its energy to an acceptor (A). As a consequence, A reaches an electronic excited state. The common mechanisms to explain ET processes are the electron exchange or Dexter and the dipole-dipole interactions or Förster. Regarding the Dexter mechanism, triplet-triplet ET (TTET) among two chromophores requires effective orbital overlap within the van der Waals radii of D and A chromophores.[29] Understanding the operating mechanisms of the intramolecular TTET in bichromophoric systems has been subject of intense research.[79-103] When D and A are linked by a spacer, TTET could proceed through-space or through-bond (TB) mechanisms depending on the nature of the bridge. In flexible bridge-linked D-A systems, a rapid conformational equilibrium leads to spatial arrangements, in which the two chromophores are close enough for orbital overlap within the lifetime of the D triplet, so that TTET happens through-space.[87,97,98,104-107]

*Reproduced in part from: P. Miro, I. Vayá, G. Sastre, M. C. Jiménez, M. L. Marin and M. A. Miranda, *Chem. Commun.*, 2016, **52**, 713-716 with permission from the Royal Society of Chemistry

Conversely, in the case of rigid saturated hydrocarbon bridges, where D and A distances are substantially longer than the sum of the van der Waals radii, TB mechanism is largely predominating.[84-86,92-96,108,109] In these systems, the observed TTET happening TB is facilitated by the σ and σ^* orbitals of the bridge and, in general, is strongly dependent on the conformations.[110-112] To explain the movement of an electron from the D to the A through an intervening rigid bridge when the wave functions of the D and the A are separated by distances higher than 10 Å, the following mechanism is used: it consists of the overlap of the LUMO (LU) of D with the σ^* of the nearest bond of the bridge (Figure 4.1). Consequently, this interaction propagates across the bridge until it is adjacent to the LU of the A, enabling an electron to travel from the LU of the D to the LU of the A. Simultaneously, the half-filled HOMO (HO) of the D overlaps with the σ of the nearest bond of the bridge and this interaction propagates until it rises the HO of the A, enabling an electron to travel from the HO of the A to the HO of the D.[110] Qualitatively, as the number of σ bonds separating the D and A increases, the occurrence of ET processes will decrease. In this context the rate constant for ET processes has been found to be exponentially dependent on the number of bonds separating D and A in a series with the same D and A chromophores.[80]

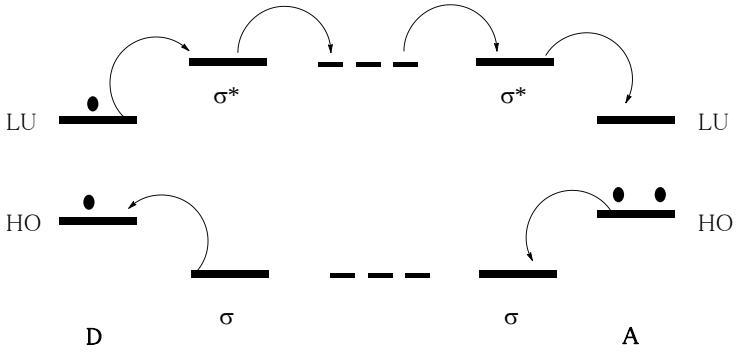

Figure 4.1. Through-bond energy transfer across the σ and σ^* orbitals of the bridge separating D and A.

Although this chapter will be focused on TTET, singlet-singlet energy transfer through-bond (TB-SSET) has also been reported. In such cases, the main contribution of TB-SSET by electron exchange through-bond over a dipole-dipole ET has been demonstrated by the modulation of the distance between D and A and its fitting to the Dexter equation (Eq. 1.1, Section 1.4.2.1) rather than the Förster equation (Eq. 1.2, Section 1.4.2.1).[113,114]

Moreover, further alterations have been reported for excited states deactivation. In fact, exciplex formation constitutes an alternative,[21] whose involvement has been reported in the intramolecular singlet quenching of flexible systems.[98,104,115-120] Interestingly, several examples have been reported, in which photoinduced et in D-A systems linked through a rigid bridge leads to 'exciplex' type fluorescence, more appropriately referred to as extended charge separated state.[114,121-126] Moreover, triplet exciplex formation has been investigated in flexible benzophenone (Bzp)/naphthalene (Npt) bichromophoric systems, in which decay of ^{3}Npt* occurs through intramolecular exciplex formation with ground state Bzp.[127-129]

However, the possibility of TB triplet exciplex (TB-TEX) formation in D-A systems linked through a rigid bridge has not been explored yet. Herein, this issue has been addressed by means of a novel approach based on a 'tandem' TB-TTET with subsequent formation of an extended TB-TEX from the triplet A, as illustrated in Figure 4.2.

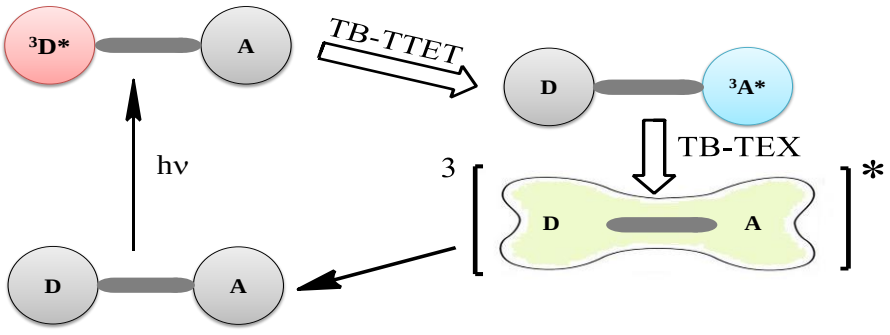

Figure 4.2. Sequential TB-TTET and TB-TEX in D-A linked through a rigid bridge system.

Hence, D-A systems including a rigid hydrocarbon skeleton provided by the natural lithocholic acid (LA) and the chromophores Bzp as a D and Npt or biphenyl (Bip) as A have been designed and synthesized (Figure 4.3). The selected chromophores fulfill the following requirements: i) selective excitation of Bzp is possible at 355 nm (see inset in Figure 4.19, in Section 4.7 of the Supplementary material); ii) the intersystem crossing quantum yield of Bzp is very high (*ca.* 1); iii) the triplet energies of Npt (60.9 kcal mol^{-1}) or Bip (65.4 kcal mol^{-1}) are lower than that of Bzp (68.6 kcal mol^{-1}),[27] thus the exergonicity of the ET process is guaranteed; iv) ^{3}Bzp* has phosphorescence emission as well as transient absorption bands different from ^{3}Npt* or ^{3}Bip*.

In the synthesized systems, D is attached at C-3 on the α or β face of the skeleton to analyze the influence of the stereochemistry on the kinetics of the processes.

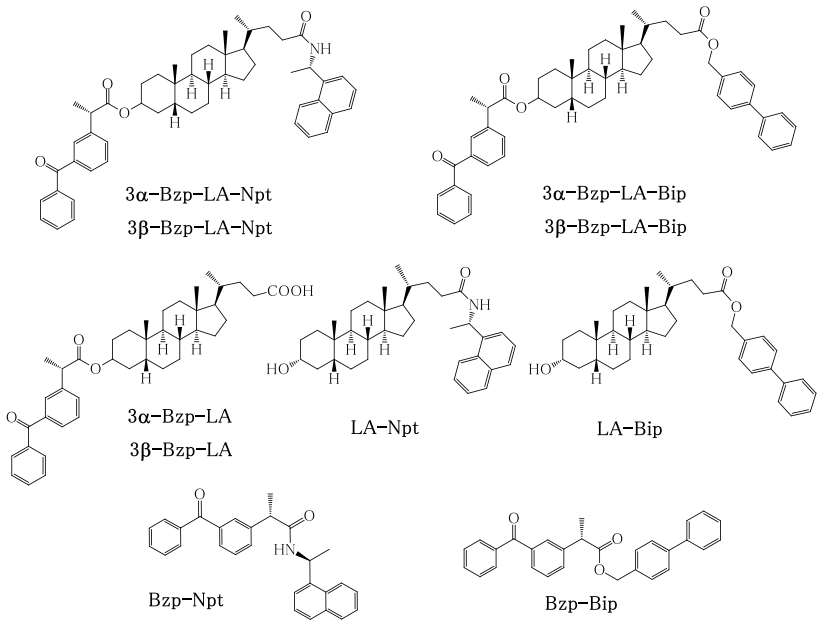

Figure 4.3. Chemical structures of the synthesized through-bond linked D-A systems (top row), control compounds (middle row) and direct dyads (bottom row).

4.2. Synthesis

Compounds **3α-Bzp-LA-Npt**, **3β-Bzp-LA-Npt**, **3α-Bzp-LA-Bip** and **3β-Bzp-LA-Bip** were obtained as shown in Scheme 4.1. Esterification between LA and (*S*)-ketoprofen (KP) afforded **3α-Bzp-LA** which was reacted with (*S*)-1-(1-naphthyl)ethylamine (NEA) to give **3α-Bzp-LA-Npt**. As a control, **LA-Npt** was obtained by direct reaction of LA with NEA. In parallel, LA was esterified with 4-phenylbenzylalcohol (PBA), to give **LA-Bip**. Subsequent derivatization with KP yielded **3α-Bzp-LA-Bip**. To obtain the compounds with 3β-configuration, LA was reacted with *p*-nitrobenzoic acid under Mitsunobu conditions,[130] to afford **3β-NBz-LA**, which was subsequently hydrolyzed and treated with KP to give **3β-Bzp-LA**. Final coupling of

3β-Bzp-LA with NEA or PBA allowed obtaining **3β-Bzp-LA-Npt** and **3β-Bzp-LA-Bip**, respectively.

To prepare **Bzp-Npt** and **Bzp-Bip** systems, where the two chromophores are directly connected (Figure 4.3), KP was esterified with NEA or PBA, respectively.

Synthetic procedures, NMR spectroscopic data and exact mass for the new compounds are detailed in the experimental section of this chapter. Further NMR experiments and experimental procedures can be found in the supplementary material of this chapter.

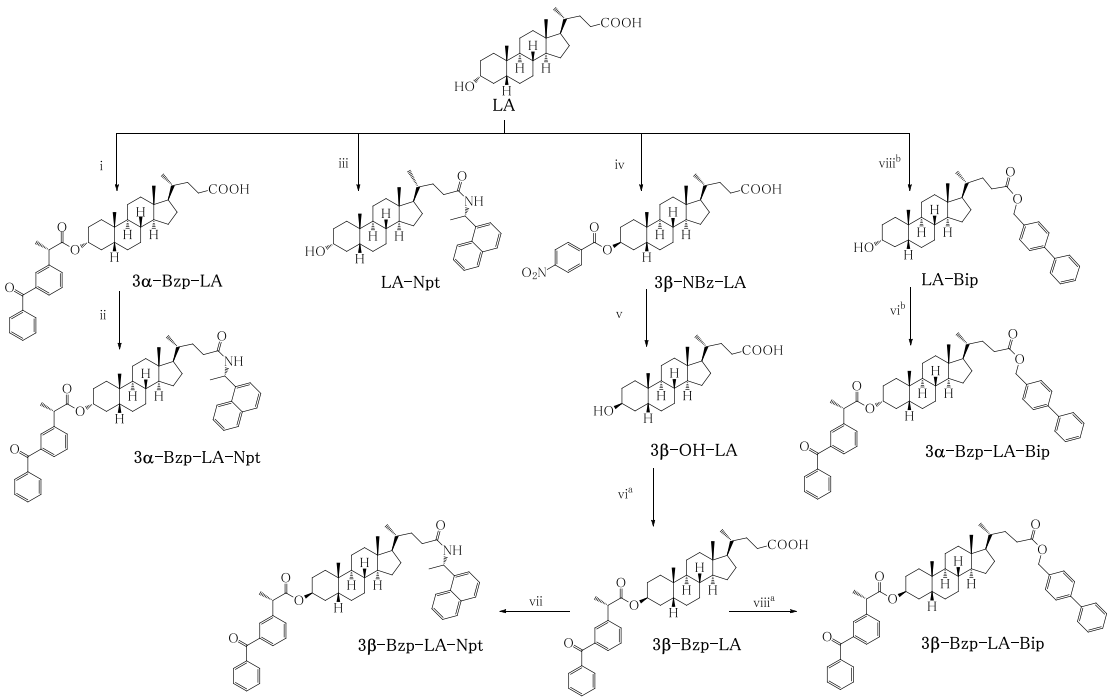

Scheme 4.1. Synthetic strategy to prepare **LA** derivatives incorporating **Bzp** at 3-position and **Npt** or **Bip** at the lateral chain. Reagents and conditions: (i) KP, DCC, 4-DMAP, C_5H_5N, (70%); (ii) NEA, EDC, CH_2Cl_2, (72%); (iii) NEA, EDC, toluene, (74%); (iv) 4-nitrobenzoic acid, Ph_3P, DEAD, THF, (87%); (v) KOH, THF, (82%); (vi) KP, TBTU, DIEA, DMF, [a](21%), [b](69%); (vii) NEA, TBTU, DIEA, DMF, (88%); (viii) PBA, TBTU, DIEA, DMF, [a](57%), [b](76%).

4.3. Results and discussion

The ultraviolet-visible (UV-Vis) absorption spectra of **3α- or 3β-Bzp-LA-Npt** and **3α- or 3β-Bzp-LA-Bip** matched with the sum of the absorption spectra of the isolated chromophores in 1:1 ratio at the same concentration **3α- or 3β-Bzp-LA** + **LA-Npt** or **3α- or 3β-LA** + **LA-Bip** (Figure 4.4); the same was true for equal concentrations of **Bzp-Npt** and **Bzp-Bip**, lacking the LA spacer. These observations indicate the absence of significant ground state interactions between the D and A units.

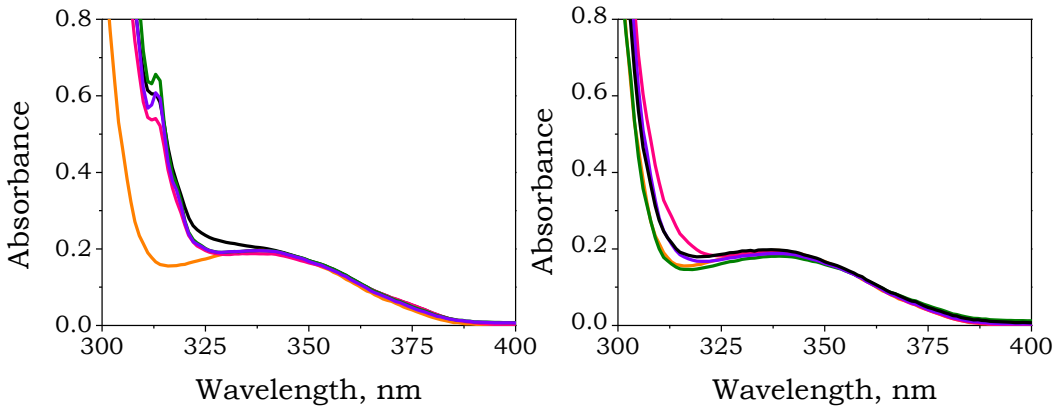

Figure 4.4. Left: UV-Vis absorption spectra of **3α-Bzp-LA-Npt** (red), **3β-Bzp-LA-Npt** (purple), **3α-Bzp-LA** (orange), **3α-Bzp-LA + LA-Npt** (black) and **Bzp-Npt** (green). Right: UV-Vis absorption spectra of **3α-Bzp-LA-Bip** (red), **3β-Bzp-LA-Bip** (purple), **3α-Bzp-LA** (orange), **3α-Bzp-LA + LA-Bip** (black) and **Bzp-Bip** (green).

The phosphorescence spectra of **3α-Bzp-LA-Npt** and **3β-Bzp-LA-Npt** in ethanol at 77 K upon Bzp excitation at 355 nm were coincident with that of **3α-Bzp-LA** (Figure 4.5), with maxima at 408, 441, 474, 511 and 559 nm, indicating that Bzp is the main chromophore exhibiting phosphorescence under these conditions, so TB-TTET is completely prevented in the matrix when the chromophores are separated by the LA spacer. By contrast, when Bzp and Npt were directly connected through an amide bond in **Bzp-Npt** the phosphorescence arose exclusively from the Npt moiety (maxima at 470, 504 and 540 nm), demonstrating that TTET within the D-A pair is associated with clear phosphorescence spectral changes. Therefore, the lack of TB-TTET in **3α-Bzp-LA-Npt** and **3β-Bzp-LA-Npt**. at 77 K may be due to the predominance of frozen inefficient conformations.

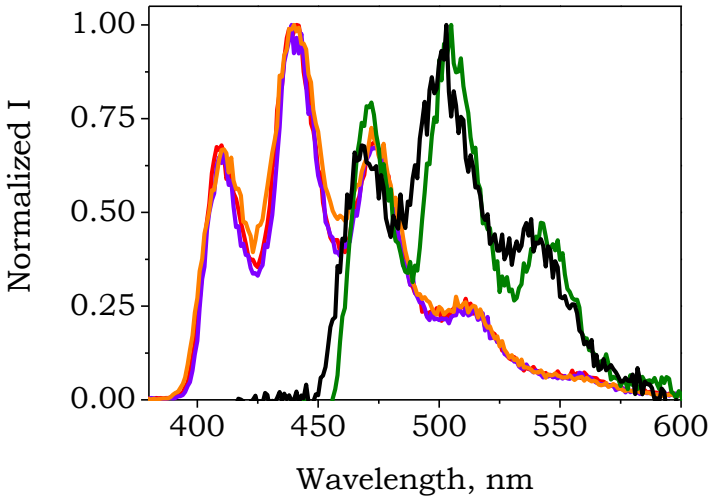

Figure 4.5. Normalized phosphorescence spectra of **3α-Bzp-LA-Npt** (red), **3β-Bzp-LA-Npt** (purple), **3α-Bzp-LA** (orange), **LA-Npt** (black), and **Bzp-Npt** (green) in ethanol matrix at 77 K. The excitation wavelength was 355 nm for all the systems except for **LA-Npt**, 266 nm.

To enhance the prospects of TB-TTET, the systems were investigated in solution at room temperature. Thus, LFP of **3α-Bzp-LA-Npt** with selective excitation of Bzp at 355 nm, gave rise to transient absorption spectra where contribution of the Bzp triplet excited state (^{3}Bzp*, λ_{max} *ca.* 530 nm) was almost negligible, yet ^{3}Npt* (λ_{max} = 420 nm) was the predominating species as early as 20 ns after the laser pulse (Figure 4.6, left). This indicates a very fast TB-TTET from Bzp to Npt in this system. A markedly different result was obtained for **3β-Bzp-LA-Npt** (Figure 4.6, right), where the 320 and 530 nm centered bands due to ^{3}Bzp* were clearly observed in the submicrosecond range. At longer delays, the ^{3}Bzp* contribution to the overall spectra decreased, with concomitant growth of ^{3}Npt* at 420 nm. Control experiments performed under the same conditions showed that an intermolecular 1:1 mixture of **3α-Bzp-LA** and **LA-Npt** exhibited after 200 ns the ^{3}Bzp* bands (Figure 4.7, left), which were not even detected

for the directly linked system **Bzp-Npt**, immediately after the laser pulse (Figure 4.7, right).

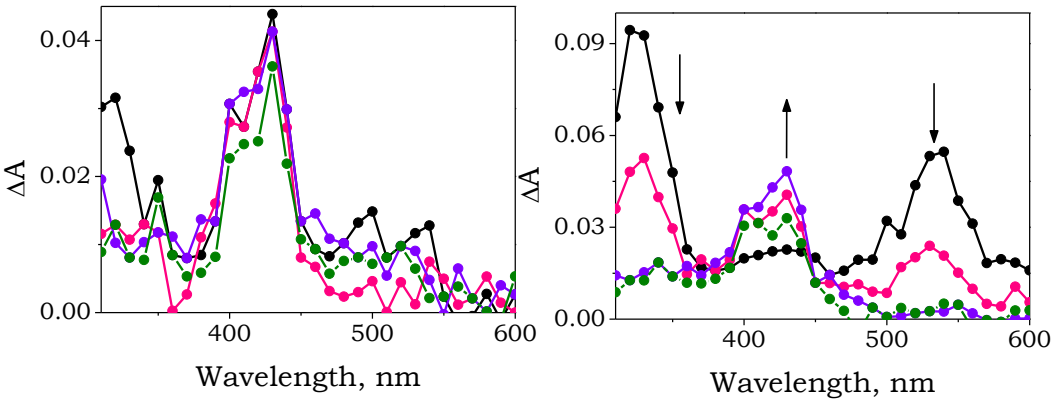

Figure 4.6. LFP (λ_{exc} = 355 nm, CH_2Cl_2, N_2, A_{355} = 0.2, 5 × 10^{-4} M) of left: **3α-Bzp-LA-Npt** and right: **3β-Bzp-LA-Npt**. Transient absorption spectra obtained 0.02 μs (black), 0.2 μs (red), 1 μs (purple) and 2 μs (green) after the laser pulse.

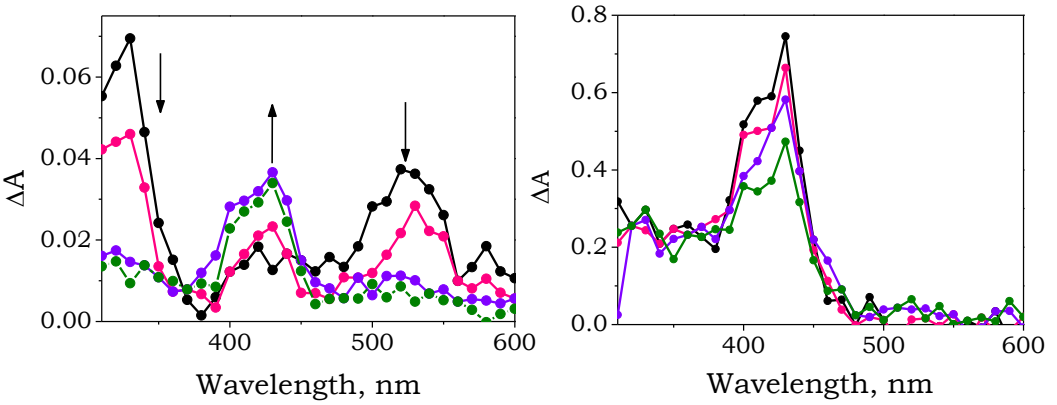

Figure 4.7. LFP transient absorption spectra (λ_{exc} = 355 nm, CH_2Cl_2, N_2, A_{355} = 0.2, 5 × 10^{-4} M) of left: **3α-Bzp-LA +LA-Npt** and right: **Bzp-Npt**. Transient absorption spectra obtained at 0.02 μs (black), 0.2 μs (red), 1.0 μs (purple) and 2.0 μs (green) after the laser pulse.

The TB-TTET process can be analyzed more accurately by looking at the kinetic traces monitored at 530 nm ($^3Bzp^*$). Thus, it can be clearly observed in Figure 4.8 left,

that the process occurs instantaneously in the case of **3α-Bzp-LA-Npt** and **Bzp-Npt** (mostly during the laser pulse), is slower for **3β-Bzp-LA-Npt** and takes even longer for the intermolecular situation (**3α-Bzp-LA** + **LA-Npt**). Accordingly, formation of ^{3}Npt* (monitored through the growth at 420 nm) was observed in the respective time window (Figure 4.8, right). The determined Bzp triplet lifetimes and TB-TTET rate constants are shown in Table 4.1.

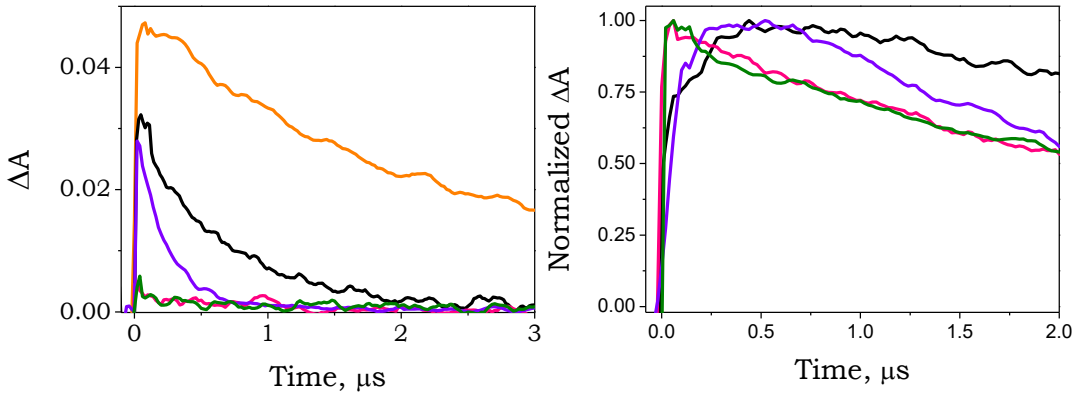

Figure 4.8. LFP (λ_{exc} = 355 nm, CH_2Cl_2, N_2, A_{355} = 0.2) of **3α-Bzp-LA-Npt** (red), **3β-Bzp-LA-Npt** (purple), **3α-Bzp-LA** (orange), **3α-Bzp-LA** +**LA-Npt** at 1:1 molar ratio (black) and **Bzp-Npt** (green). Traces monitored at left: 530 nm, right: 420 nm.

Table 4.1. Triplet lifetimes together with TTET and TEX rate constants for Bzp-Npt systems.

System[a]	τ (^{3}Bzp*)[b]	k (TTET)[c]	τ (^{3}Npt*)[b]	k (TEX)[c]
3α-Bzp-LA-Npt	< 0.06	> 1.5×10^7	3.18	1.1×10^5
3β-Bzp-LA-Npt	0.22	3.0×10^6	2.54	1.9×10^5
3α-Bzp-LA	2.37	N.A.	N.A.	N.A.
3α-Bzp-LA+LA-Npt[d]	0.65	N.A.	4.83	N.A.
Bzp-Npt[e]	< 0.01	>1.0×10^8	3.81	5.5×10^4

[a]In all cases, the concentration was 5×10^{-4} M; [b]Units: μs; [c]Units: s^{-1}, determined as: $1/\tau - 1/\tau_{(3\alpha\text{-Bzp-LA+LA-Npt})}$; [d]Each compound at 5×10^{-4} M concentration; [e]Control system for the corresponding through-space processes.

The decay of the 420 nm band should contain relevant information related to the possible involvement of an extended TB-TEX from ^{3}Npt*. The kinetic traces monitored at 420 nm are shown in Figure 4.8 right, and the ^{3}Npt* lifetimes, together with the TB-TEX rate constants, are given in Table 4.1. The observed changes in ^{3}Npt* lifetimes demonstrate that extended TB-TEX formation is an efficient deactivation pathway for ^{3}Npt* in the investigated linked systems **3α-Bzp-LA-Npt** and **3β-Bzp-LA-Npt**. The rate constant of this process was even higher than the described through-space exciplex formation in **Bzp-Npt**,[127-129] where the chromophores are directly linked. Interestingly, TB-TEX was faster for the β-epimer than for its α-analogue, in contrast to the tendency found in the TB-TTET.

In order to extend the scope of the concept, the Npt unit was replaced with Bip. The smaller Bzp/Bip triplet energy gap in **3α or 3β-Bzp-LA-Bip** was expected to result in a slower TTET process and therefore in a broader dynamic range.

The phosphorescence spectra of **3α-Bzp-LA-Bip** and **3β-Bzp-LA-Bip** in ethanol matrix (Figure 4.9), after selective excitation of Bzp at 355 nm, showed exclusively the typical ^{3}Bzp* emission with maxima at 408, 441, 474 and 511 nm, indicating that TB-TTET is again blocked in the frozen matrix, whereas **LA-Bip** has a markedly different emission with maxima at 434, 462 and 486 nm. With this D-A pair, even the directly connected system **Bzp-Bip** showed incomplete TTET, as revealed by its spectral fingerprint partially due to ^{3}Bzp* and partially due to ^{3}Bip*.

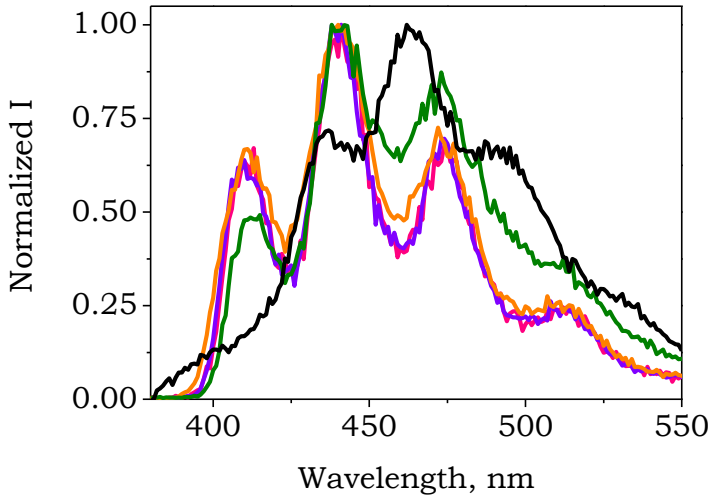

Figure 4.9. Normalized phosphorescence spectra of **3α-Bzp-LA-Bip** (red), **3β-Bzp-LA-Bip** (purple), **3α-Bzp-LA** (orange), **Bzp-Bip** (green) and **LA-Bip** (black) in ethanol matrix at 77 K. The excitation wavelength was 355 nm except for **LA-Bip**, 285 nm.

Furthermore, as in the case of the Npt analogs, the TB-TTET process was also investigated at room temperature (see Figure 4.10). Hence, excitation of the Bzp chromophore at 355 nm in **3α-Bzp-LA-Bip** showed a spectrum with no contribution of ^{3}Bzp* (λ_{max} *ca.* 530 nm) after 0.1 μs, while ^{3}Bip* (λ_{max} *ca.* 380 nm) is immediately formed after the laser pulse, demonstrating an efficient TB-TTET. Conversely, in the **3β-Bzp-LA-Bip** system, both species, ^{3}Bzp* and ^{3}Bip*, were observed at short times, although after longer delays, the typical bands of ^{3}Bzp* decreased simultaneously with an increase of the ^{3}Bip* band. This difference showed a slower TB-TTET in the system with β-configuration than in the system with α-configuration. Control experiments for the intermolecular 1:1 mixture of **3α-Bzp-LA** + **LA-Bip** (Figure 4.11, left) and the direct dyad **Bzp-Bip** (Figure 4.11, right) showed the typical bands of ^{3}Bzp* in the intermolecular mixture, while its contribution was negligible in the directly linked system.

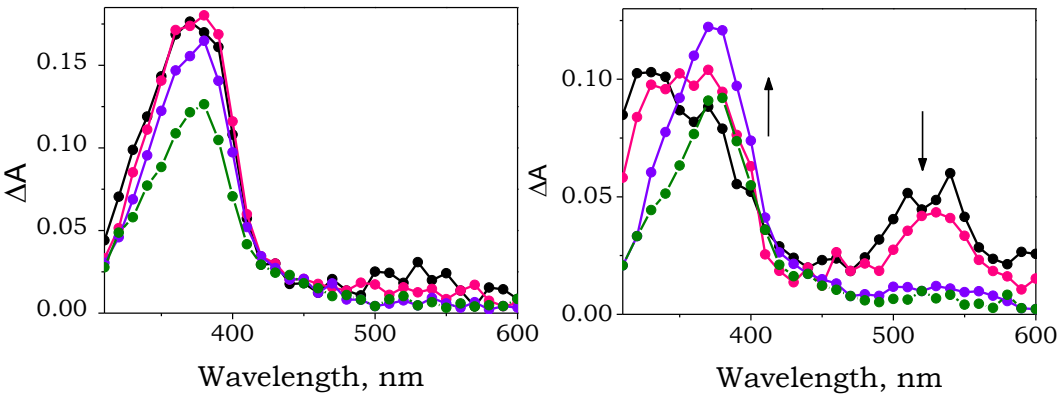

Figure 4.10. LFP (λ_{exc} = 355 nm, CH_2Cl_2, N_2, A_{355} = 0.2, 5 × 10^{-4} M) of left: **3α-Bzp-LA-Bip** and right: **3β-Bzp-LA-Bip**, obtained 0.1 μs (black), 0.2 μs (red), 1.0 μs (purple) and 2.0 μs (green) after the laser pulse.

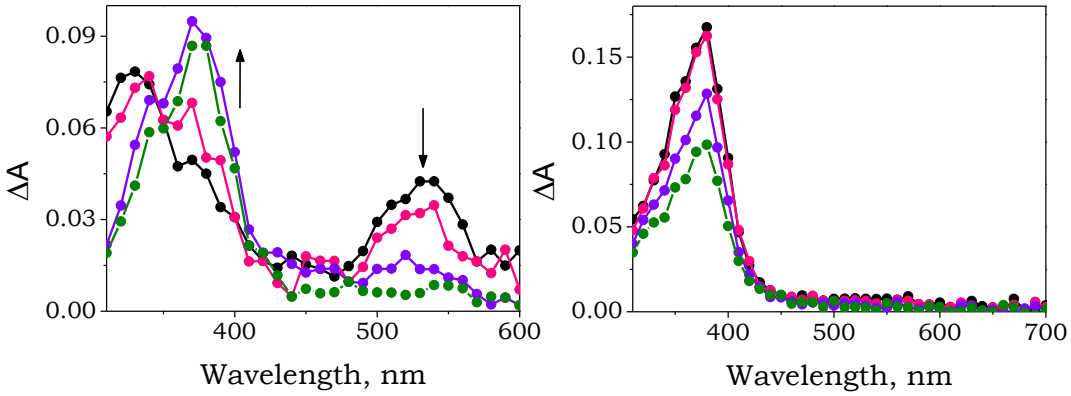

Figure 4.11. LFP transient absorption spectra (λ_{exc} = 355 nm, CH_2Cl_2, N_2, A_{355} = 0.2, 5 × 10^{-4} M) of left: **3α-Bzp-LA** + **LA-Bip** and right: **Bzp-Bip** obtained at 0.02 μs (black), 0.2 μs (red), 1.0 μs (purple) and 2.0 μs (green) after the laser pulse.

The main difference between the Npt systems (**3α-Bzp-LA-Npt** and **3β-Bzp-LA-Npt**) and the Bip systems (**3α-Bzp-LA-Bip** and **3β-Bzp-LA-Bip**) was found in the kinetics of $^3Bzp^*$ decay (Figure 4.12, left), which was slower for the Bip derivatives,

allowing for more accurate determination of the triplet lifetimes and rate constants (Table 4.2). The ^{3}Bzp* lifetime of the β-derivative **3β-Bzp-LA-Bip** was similar to that of the intermolecular **3β-Bzp-LA** + **LA-Bip** mixture, and *ca.* 5 times longer than that of the α-analog, **3α-Bzp-LA-Bip**; accordingly, the k (TB-TTET) values were found to differ by one order of magnitude. As expected, when the two chromophores were directly connected, **Bzp-Bip**, TTET took place within the laser pulse.

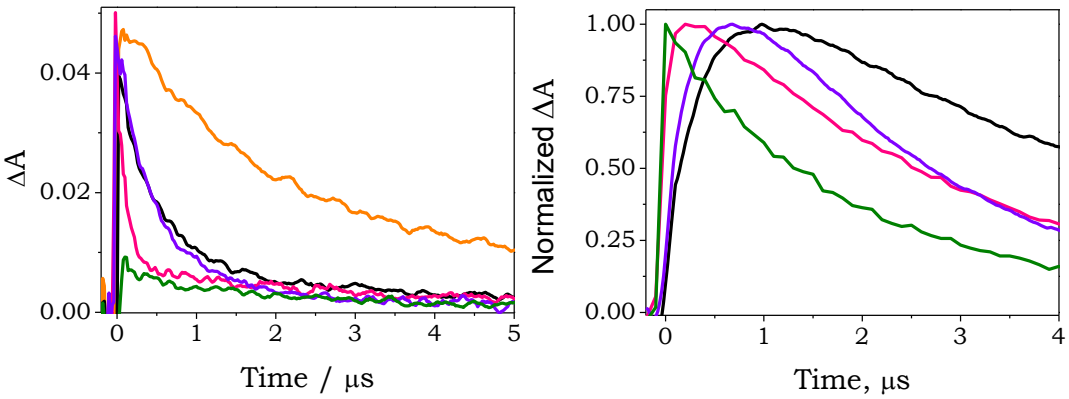

Figure 4.12. LFP (λ_{exc} = 355 nm, CH_2Cl_2, N_2, A_{355} = 0.2) of **3α-Bzp-LA-Bip** (red), **3β-Bzp-LA-Bip** (purple), **3α-Bzp-LA** (orange), **3α-Bzp-LA** + **LA-Bip** at 1:1 molar ratio (black) and **Bzp-Bip** (green). Traces monitored at left: 530 nm, right: 380 nm.

Moreover, analysis of the kinetic traces of the 380 nm band (Figure 4.12, right), allowed obtaining the ^{3}Bip* lifetimes and the TB-TEX rate constants (Table 4.2), providing information concerning the involvement of the extended TB-TEX from ^{3}Bip*. As a matter of fact, it can be observed that TB-TEX formation constitutes an efficient deactivation pathway for ^{3}Bip* in the LA-containing systems, **3α-Bzp-LA-Bip** and **3β-Bzp-LA-Bip**, with rate constants in the same order than that of the through space process, in **Bzp-Bip**. As stated before for **Bzp-LA-Npt**, TB-TEX was slightly faster for the β-derivative, **3β-Bzp-LA-Bip**, than for the α-isomer, **3α-Bzp-LA-Bip**.

Table 4.2. Triplet lifetimes together with TTET and TEX rate constants for Bzp-Bip systems

System[a]	$\tau(^3Bzp^*)$[b]	k (TTET)[c]	$\tau(^3Bip^*)$[b]	k (TEX)[c]
3α-Bzp-LA-Bip	0.12	6.8×10^6	2.96	1.2×10^5
3β-Bzp-LA-Bip	0.52	4.3×10^5	2.30	2.2×10^5
3α-Bzp-LA	2.37	N.A.	N.A.	N.A.
3α-Bzp-LA + LA-Bip[d]	0.67	N.A.	4.60	N.A.
Bzp-Bip[e]	< 0.02	> 4.8×10^7	1.91	3.1×10^5

[a] [a]In all cases, the concentration was 5×10^{-4} M; [b]Units: μs; [c]Units: s^{-1}, determined as: $1/\tau - 1/\tau_{(3\alpha\text{-Bzp-LA+LA-Bip})}$; [d]Each compound at 5×10^{-4} M concentration; [e]Control system for the corresponding through-space processes.

To ruled out the potential involvement of a through-space mechanism in the extended triplet exciplex formation, a collaboration with a researcher of the ITQ with expertise in molecular dynamics was undertaken. This enabled us to investigate the chromophore-chromophore distances, taking into account all types of interactions, including $\pi-\pi$ stacking. The obtained distribution of distances for **3α-Bzp-LA-Bip** and **3β-Bzp-LA-Bip** was centered at ca. 18 and 15 Å, respectively (Figure 4.13). Overall, conformations with chromophore-chromophore distances in the range [14-19] Å dominate the landscape with frequencies of 45.5 % (**3α-Bzp-LA-Bip**) and 49.3% (**3β-Bzp-LA-Bip**) of the total. Yet, conformations with intramolecular chromophore-chromophore distances < 10 Å, necessary for through-space mechanism, have frequencies lower than 2 % in both cases.

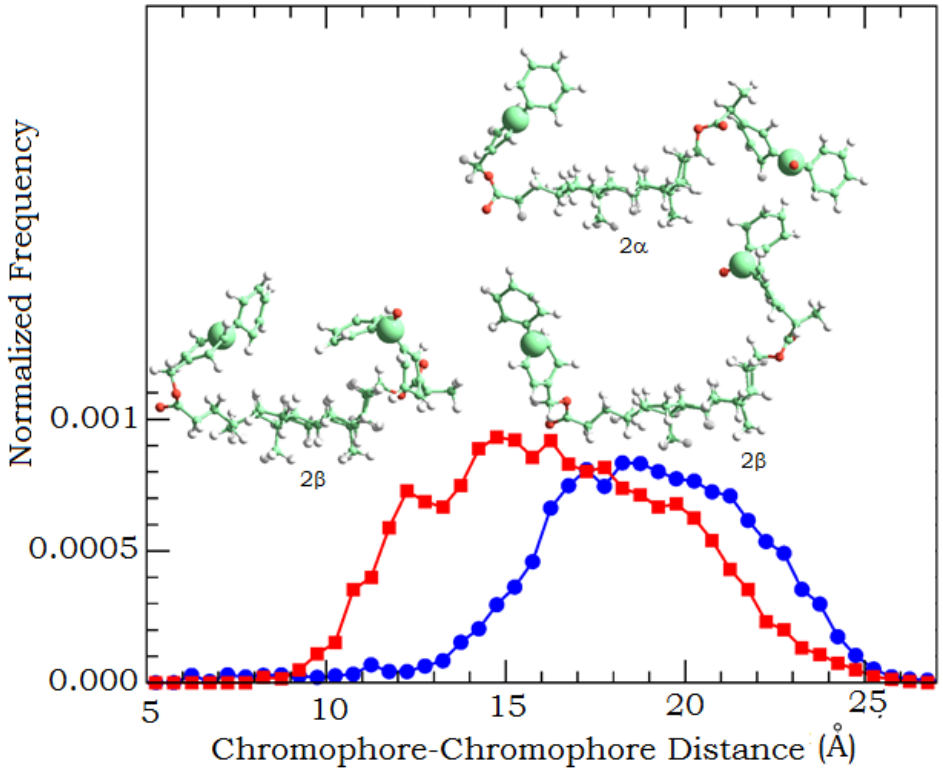

Figure 4.13. Conformational landscape of **3 α -Bzp-LA-Bip** (blue) and **3 β -Bzp-LA-Bip** (red), based on the intramolecular chromophore-chromophore distance in dichloromethane at 300 K. One representative example of **3 α -Bzp-LA-Bip** (top), with chromophore-chromophore distance 18 Å; and two conformations of **3 β -Bzp-LA-Bip** (bottom), with chromophore-chromophore distances of 11 (folded) and 15 (unfolded) Å are shown.

4.4. Conclusions

The involvement of extended through-bond triplet exciplex formation in Bzp/Npt and Bzp/Bip linked systems has been demonstrated by means of LFP in solution, at room temperature. Kinetic evidence supporting this concept has been obtained from the decay of the Npt or Bip triplets after population *via* TB-TTET from ^{3}Bzp*. All TB processes proceed across a rigid saturated bile acid scaffold and are strongly dependent on the relative spatial arrangement of the chromophores: while TB-TTET is faster in the systems with α-configuration either in Npt or Bip derivatives, TB-TEX for deactivation of the triplet acceptor is more marked in systems with β-configuration. TB-TTET has also been found to be dependent on the nature of the matrix: in frozen matrix TB-TTET process does not play any role either in Npt or Bip derivatives, while in solution TB-TTET is very efficient as revealed by LFP. Differences in the energy gap between D and A are in agreement with the different results found from the kinetic behavior.

4.5. Scope of the through-bond energy transfer process

4.5.1. Introduction

TB-TTET has been demonstrated to occur across the rigid LA system between Bzp as the D and Npt or Bip as the A. Moreover, extended TB-TEX formation constitutes an efficient channel for ^{3}Npt* or ^{3}Bip* deactivation.

To extend the scope of these processes, additional systems with the same scaffold have been prepared. Differences in the triplet-triplet energy gap between the D and the A and the influence of the nature of the D triplet in the overall ET process has been explored. The influence of the nature of the triplet of D has been studied by replacing the $n\pi^*$ ^{3}Bzp* present in the above studied systems with the $\pi\pi^*$ ^{3}Cbz* (carbazole triplet). In this context, the isoenergetic system containing Cbz (E_T=70.2 kcal mol^{-1}) as a

D and Thy (Thymine, E_T=74 kcal mol^{-1}) as A was investigated, as well as the analog with Cbz as D and Npt (E_T=60.9 kcal mol^{-1}) as the A (see Table 4.3 for a summary of the energies and the nature of the triplet excited states of the involved chromophores).

Table 4.3. Energies and nature of the triplet excited states of the involved chromophores.

Chromophore	Function	Triplet nature	Triplet energy (kcal mol^{-1})
Cbz	D	$\pi\ \pi^*$	70.2[22]
Bzp	D	$n\pi^*$	68.9[22]
Thy	A	$\pi\ \pi^*$	74[131]
Bip	A	$\pi\ \pi^*$	65.4[22]
Npt	A	$\pi\ \pi^*$	60.9[22]

The selected chromophores will allow: i) selective excitation of Cbz at 308 nm, where the A Thy does not absorb and the molar absorption of Npt is very low compared to that of Cbz (see Figure 4.19 in the Section 4.7. Supplementary material) and ii) selective detection of ^{3}Cbz* (max at 420 nm) in a region different from that of ^{3}Thy* (max at 360 nm). All the combinations led to the synthesis of the systems shown in Figure 4.14.

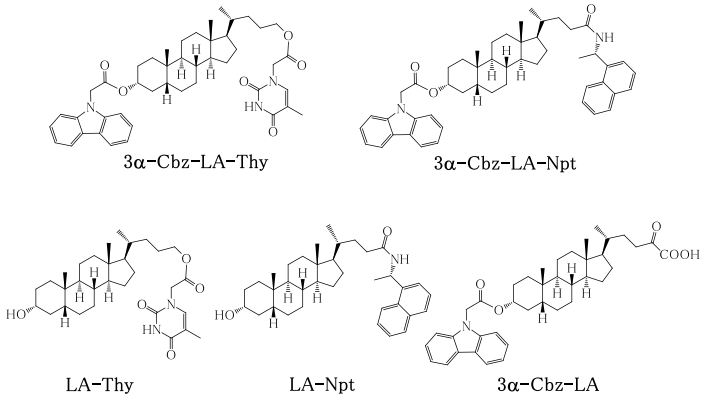

Figure 4.14. Chemical structures of the synthesized D-A systems (top row) and control compounds (bottom row).

4.5.2. Synthesis

Final compounds **3α-Cbz-LA-Thy** and **3α-Cbz-LA- Npt** were obtained as shown in Scheme 4.2. Briefly, LA was reduced with $LiAlH_4$, to give the corresponding alcohol. Subsequent derivatization with thymine 1-acetic acid (Thy-CH_2CO_2H), yielded **LA-Thy**. To obtain **3α-Cbz-LA-Thy**, **LA-Thy** was reacted with 9-carbazoleacetic acid. In parallel, esterification of LA with 9-carbazoleacetic acid gave **3α-Cbz-LA** which was subsequently reacted with NEA to give **3α-Cbz-LA-Npt**.

Synthetic procedures, NMR spectroscopic data and exact mass for the new compounds are detailed in the experimental section of this chapter. Further NMR experiments and experimental procedures can be found in the supplementary material of this chapter.

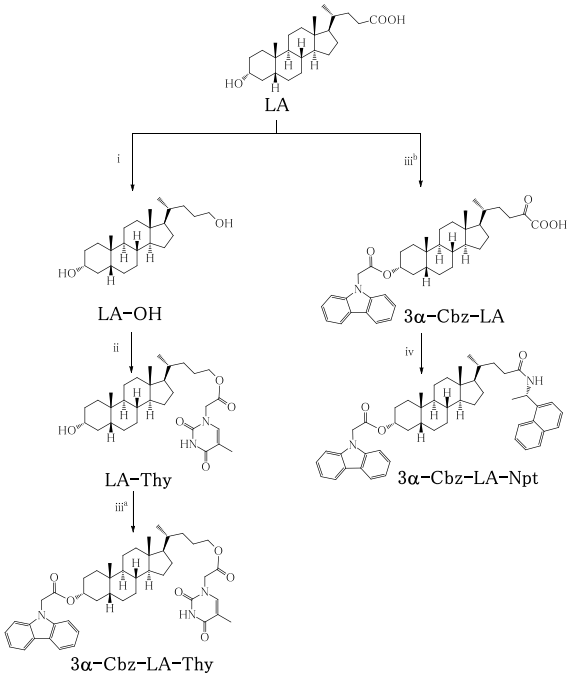

Scheme 4.2. Synthetic strategy to prepare **LA** derivatives incorporating **Cbz** at 3α-position and **Thy** or **Npt** at the lateral chain. Reagents and conditions: (i) $LiAlH_4$, THF, (88%); (ii) Thy-CH_2CO_2H, TBTU, DIEA, DMF, (36%); (iii) 9-carbazoleacetic acid, DIEA, TBTU, DMF, [a](86%), [b](46%); (iv) NEA, EDC, CH_2Cl_2, (43%).

4.5.3. Results and discussion

TB-TTET in these systems was investigated by LFP. Experiments were performed at room temperature in the **3α-Cbz-LA-Thy** system, where D and A triplets are nearly isoenergetic (^{3}Cbz* E_T=70.2 kcal mol^{-1} and ^{3}Thy*, E_T=74 kcal mol^{-1}), but D has a $\pi\pi^*$ configuration different from the $n\pi^*$ ^{3}Bzp*. Selective excitation of Cbz at 308 nm allows for the generation of the transient absorption spectra of **3α-Cbz-LA-Thy** (Figure 4.15, left). In this case, the typical band of the ^{3}Cbz* (λ_{max} *ca.* 420 nm) was observed. This spectrum was compared with that of the intermolecular 1:1 mixture **3α-Cbz-LA** + **LA-Thy** (Figure 4.15, right).

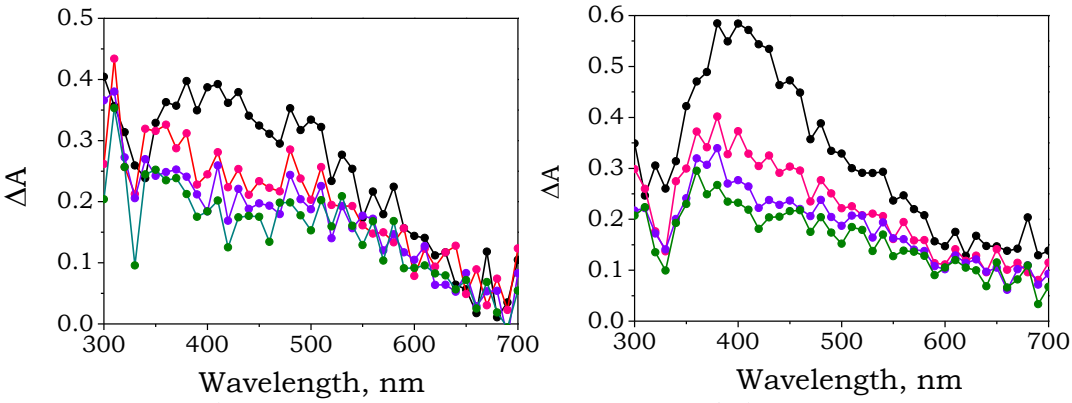

Figure 4.15. LFP (λ_{exc} = 308 nm, CH_2Cl_2, N_2, A_{355} = 0.2, 2.5 × 10^{-4} M) of left: **3α-Cbz-LA-Thy** and right: **3α-Cbz-LA** + **LA-Thy**. Transient absorption spectra obtained at 3.1 μs (black), 4.5 μs (red), 11.9 μs (purple) and 16.3 μs (green) after the laser pulse.

A lower intensity of the band at 420 nm was observed when comparing spectrum **3α-Cbz-La-Thy** to the one of the mixture **3α-Cbz-LA** + **LA-Thy** which may indicate a TB-TTET to ^{3}Thy*, although the typical ^{3}Thy* was not unequivocally inferred. Nevertheless, the decays of ^{3}Cbz* in the two systems were also analyzed in order to obtain further information about the potential TB-TTET process (Figure 4.16). The lifetime of ^{3}Cbz* in **3α-Cbz-LA** is higher than the ones determined for **3α-Cbz-LA-Thy** or the intermolecular mixture **3α-Cbz-LA** + **LA-Thy.** Since there were no

significant differences between the decays of **3α-Cbz-LA-Thy** and **3α-Cbz-LA** + **LA-Thy**, it appears that the quenching of ^{3}Cbz* is mainly intermolecular and the TB-TTET is not playing a role in this system.

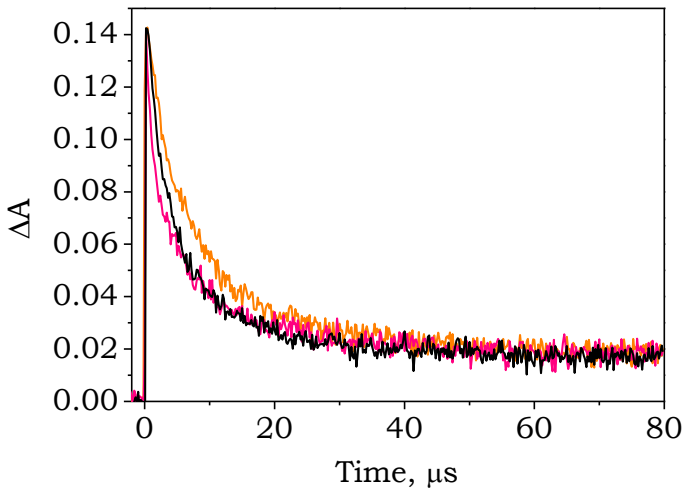

Figure 4.16. LFP (λ_{exc} = 308 nm, CH_2Cl_2, N_2, A_{355} = 0.2, 2.5 × 10^{-4} M) of **3α-Cbz-LA-Thy** (red), **3α-Cbz-LA** (orange) and **3α-Cbz-LA** + **LA-Thy** at 1:1 molar ratio (black). Decays monitored at 420 nm.

Table 4.4. Triplet lifetimes for Cbz-Thy systems

System[a]	τ(^{3}Cbz*)[b]
3α-Cbz-LA-Thy	6.27
3α-Cbz-LA	7.50
3α-Cbz-LA + **LA-Thy**[c]	6.27

[a]In all cases, the concentration was 2.5 × 10^{-4} M; [b]Units: μs; [c]Each compound at 2.5 × 10^{-4} M concentration.

To distinguish between the two factors that could be responsible for the lack of TB-TTET in the **3α-Cbz-LA-Thy** system, either the isoenergetic D and A triplets or

the $\pi\,\pi^*$ nature of ^{3}Cbz*, the **3α-Cbz-LA-Npt** was next investigated. Thus, selective excitation of Cbz at 308 nm led to the generation of the transient absorption spectra of **3α-Cbz-LA-Npt** and the intermolecular control **3α-Cbz-LA+LA-Npt** (Figure 4.17). In both cases, a band centered at 420 nm was observed that was not unequivocally associated to ^{3}Cbz* or ^{3}Npt* because both chromophores show their triplet bands in the same region (ε_{425nm}=14000 and $\varepsilon_{415\ nm}$=24500 M^{-1} cm^{-1} for ^{3}Cbz* and ^{3}Npt*, respectively).[22]

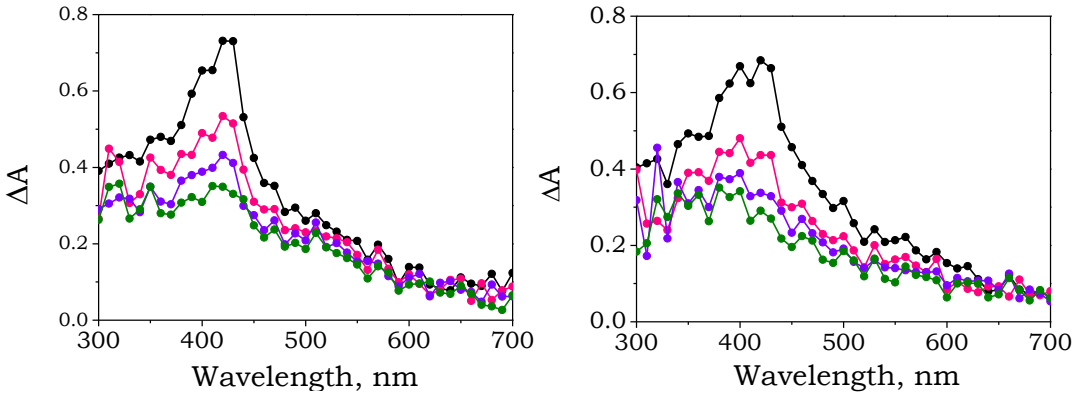

Figure 4.17. LFP (λ_{exc} = 308 nm, CH_2Cl_2, N_2, A_{355} = 0.2, 2.5 × 10^{-4} M) of left: **3α-Cbz-LA-Npt** and right: **3α-Cbz-LA** + **LA-Npt**. Transient absorption spectra obtained at 3.1 μs (black), 4.5 μs (red), 11.9 μs (purple) and 16.3 μs (green) after the laser pulse.

Nevertheless, analysis of the decays provided more information about the occurrence of the TB-TTET process. Therefore, the triplet lifetimes monitored at 420 nm in the **3α-Cbz-LA-Npt** system were compared to the intermolecular mixture **3α-Cbz-LA** +**LA-Npt**, the control **3α-Cbz-LA** and **LA-Npt** (Figure 4.18). The triplet lifetimes of **3α-Cbz-LA** and **LA-Npt** monitored at 420 nm were obviously different because of the different transient triplets responsible for each decay. Accordingly, the triplet lifetime of the intermolecular **3α-Cbz-LA** +**LA-Npt** mixture was coincident with that of **3α-Cbz-LA**, while the triplet lifetime of **3α-Cbz-LA-Npt** was similar to that of **LA-Npt**. The obtained values indicate that the main triplet species present in the

intermolecular **3α-Cbz-LA** +**LA-Npt** mixture was ^{3}Cbz*, while the main species present in **3α-Cbz-LA-Npt** was ^{3}Npt*. This clearly points to quenching of the ^{3}Cbz* by a TB-TTET process.

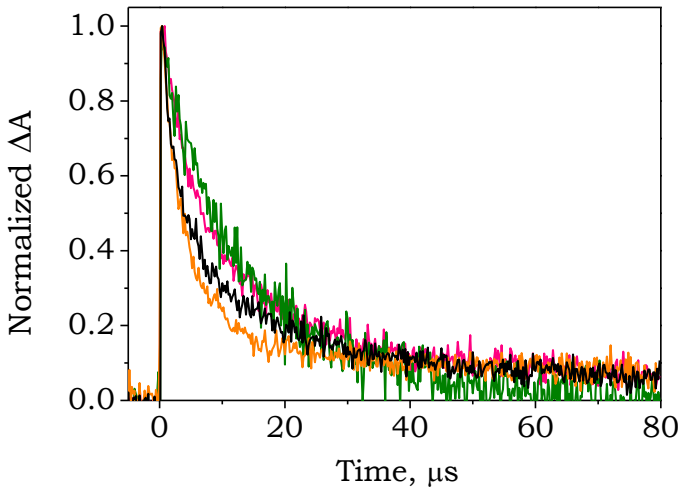

Figure 4.18. LFP (λ_{exc} = 308 nm, CH_2Cl_2, N_2, A_{308} = 0.2, 2.5 × 10^{-4} M) of **3α-Cbz-LA-Npt** (red), **3α-Cbz-LA** (orange), **3α-Cbz-LA** + **LA-Npt** at 1:1 molar ratio (black) and **LA-Npt** (green). Decays monitored at 420 nm.

Table 4.5. Triplet lifetimes for Cbz-Npt systems

System[a]	$\tau_{420\ nm}$ [b]
3α-Cbz-LA-Npt	10.73
3α-Cbz-LA	7.50
3α-Cbz-LA + **LA-Npt**[c]	8.45
LA-Npt	13.83

[a]The concentration was 2.5 × 10^{-4} M in all cases except of 7.8 × 10^{-4} M for **LA-Npt**; [b]Units: μs; [c]Each compound at 2.5 × 10^{-4} M concentration.

4.5.4. Conclusions

Further insight into the TB-TTET has demonstrated that the triplet-triplet energy gap is the main factor that controls the efficiency of the process, while the nature of the triplet of the donor does not seem to play a role. In fact, Bzp/Npt and Bzp /Bip systems, where the energy gap between the donor and the acceptor is higher than in the isoenergetic systems Bzp/Thy or Cbz/Thy, show more efficient energy transfer. The Cbz/Npt system, where the energy gap between the donor and the acceptor is also considerable, does not give unambiguous information about the energy transfer process due to the overlap between the triplet of the Cbz and Npt in the same spectral region.

4.6. Experimental

4.6.1. Synthesis and characterization

4.6.2.1. Synthesis of 3α-Bzp-LA

To a solution of KP (0.203 g, 0.8 mmol) in CH_2Cl_2 (10 mL), DCC (0.207 g, 0.85 mmol) and 4-DMAP (catalytic amount) were added as solids. The reaction was stirred while **LA** (0.301 g, 0.8 mmol) in 5 mL of CH_2Cl_2 was added dropwise. After 24 h, the crude product was washed with diluted $NaHCO_3$, HCl 1 M and brine. Final purification by preparative layer chromatography (SiO_2 Merck 60 PF254, EtOAc:Hexane, 80:20) followed by recrystallization gave **3α-Bzp-LA** (0.343 g, 70%). ^{1}H NMR (400 MHz, CD_3OD): δ (ppm) 0.64 (s, 3H, CH_3); 0.65 (s, 3H, CH_3); 0.77-2.43 (complex signal, 28H); 0.91 (d, J = 6.3 Hz, 3H, CH_3); 1.51 (d, J = 7.2 Hz, 3H, KP-CH_3); 3.75 (q, J = 7.2 Hz, 1H, KP-CH); 4.72 (m, 1H, 3β-H); 7.40-7.84 (m, 9H, arom). ^{13}C NMR (100 MHz, CD_3OD): δ (ppm) 196.8 (C), 179.3 (C), 173.9 (C), 141.3 (C), 138.0 (C), 137.7 (C), 132.6 (CH), 131.6 (CH), 130.2 (2xCH), 129.4 (CH), 129.0 (CH), 128.7 (CH), 128.4 (2xCH), 74.2 (CH), 56.7 (CH), 56.2 (CH), 45.8 (CH), 42.9 (C), 42.1 (CH), 40.6 (CH),

40.3 (CH_2), 36.0 (CH), 35.5 (CH), 35.2 (CH_2), 34.7 (C), 32.4 (CH_2), 31.9 (CH_2), 31.2 (CH_2), 31.0 (CH_2), 28.3 (CH_2), 27.2 (CH_2), 26.5 (CH_2), 24.3 (CH_2), 23.5 (CH_3), 21.0 (CH_2), 18.8 (CH_3), 18.4 (CH_3), 12.2 (CH_3); m/z found 613.3893, calculated for $C_{40}H_{53}O_5$ (MH^+) 613.3896.

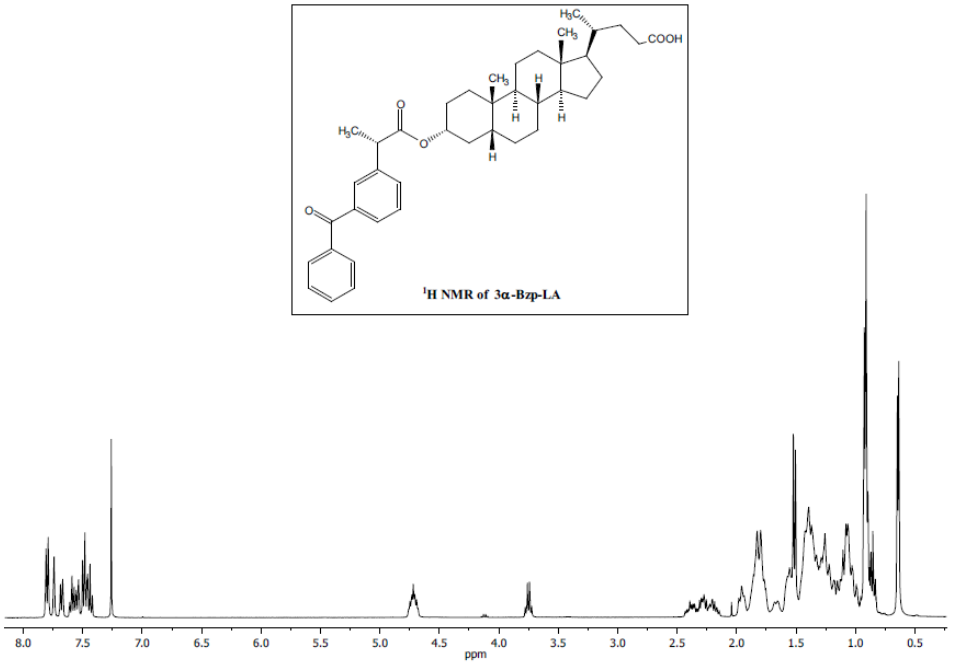
COOH
^{1}H NMR of 3α-Bzp-LA
8.0 7.5 7.0 6.5 6.0 5.5 5.0 4.5 4.0 3.5 3.0 2.5 2.0 1.5 1.0 0.5
ppm

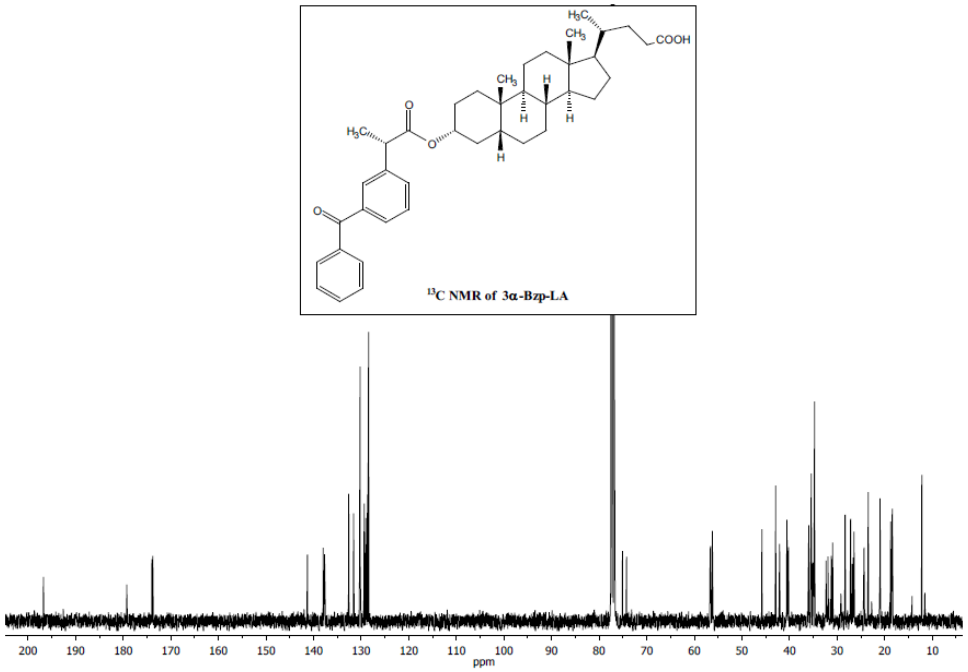
COOH
^{13}C NMR of 3α-Bzp-LA
200 190 180 170 160 150 140 130 120 110 100 90 80 70 60 50 40 30 20 10
ppm

4.6.2.2. Synthesis of 3α-Bzp-LA-Npt

To a solution of **3α-Bzp-LA** (0.140 g, 0.23 mmol) in CH_2Cl_2 (10 mL) containing EDC (0.048 g, 0.25 mmol), a solution of NEA (0.058 g, 0.23 mmol) in CH_2Cl_2 (2 mL) was added dropwise. The mixture was stirred overnight at rt and then the solvent was evaporated under vacuum; the crude product was dissolved in CH_2Cl_2 and washed with diluted $NaHCO_3$, HCl 1 M and brine. Final purification by preparative layer chromatography (SiO_2 Merck 60 PF254, CH_2Cl_2:EtOAc, 80:20) followed by recrystallization gave **3α-Bzp-LA-Npt** (0.127 g, 72%). ^{1}H NMR (400 MHz, $CDCl_3$): δ (ppm) 0.59 (s, 3H, CH_3); 0.78-2.26 (complex signal, 28H); 0.86 (d, *J* = 6.0 Hz, 3H, 21-CH_3); 0.91 (s, 3H, CH_3); 1.51 (d, *J* = 6.8 Hz, 3H, KP-CH_3); 1.66 (d, *J* = 6.8 Hz, 3H, NEA-CH_3); 3.74 (q, *J* = 6.8 Hz, 1H, KP-CH); 4.72 (m, 1H, 3β-H); 5.63 (d, *J* = 8.0 Hz, 1H, NEA-NH); 5.93 (m, 1H, NEA-CH); 7.39-7.90 (m, 15H, arom); 8.09 (d, *J* = 8.4 Hz, 1H, arom). ^{13}C NMR (100 MHz, $CDCl_3$): δ (ppm) 196.7 (C), 173.8 (C), 172.5 (C), 141.3 (C), 138.5 (C), 138.0 (C), 137.7 (C), 134.1 (C), 132.6 (CH), 131.6 (CH), 131.3 (C), 130.2 (2xCH), 129.4 (CH), 129.0 (CH), 128.9 (CH), 128.7 (CH), 128.5 (CH), 128.4 (2xCH), 126.7 (CH), 126.1 (CH), 125.3 (CH), 123.7 (CH), 122.7 (CH), 75.1 (CH), 56.6 (CH), 56.2 (CH), 45.9 (CH), 44.6 (CH), 42.9 (C), 42.1 (CH), 40.6 (CH), 40.2 (CH_2), 35.9 (CH), 35.6 (CH), 35.1 (CH_2), 34.7 (C), 33.9 (CH_2), 32.1 (CH_2), 31.9 (CH_2), 28.4 (CH_2), 27.2 (CH_2), 26.6 (CH_2), 26.4 (CH_2), 24.3 (CH_2), 23.5 (CH_3), 21.0 (CH_2), 20.7 (CH_3), 18.8 (CH_3), 18.5 (CH_3), 12.2 (CH_3); m/z found 766.4835, calculated for $C_{52}H_{64}O_4$ (MH^+) 766.4799.

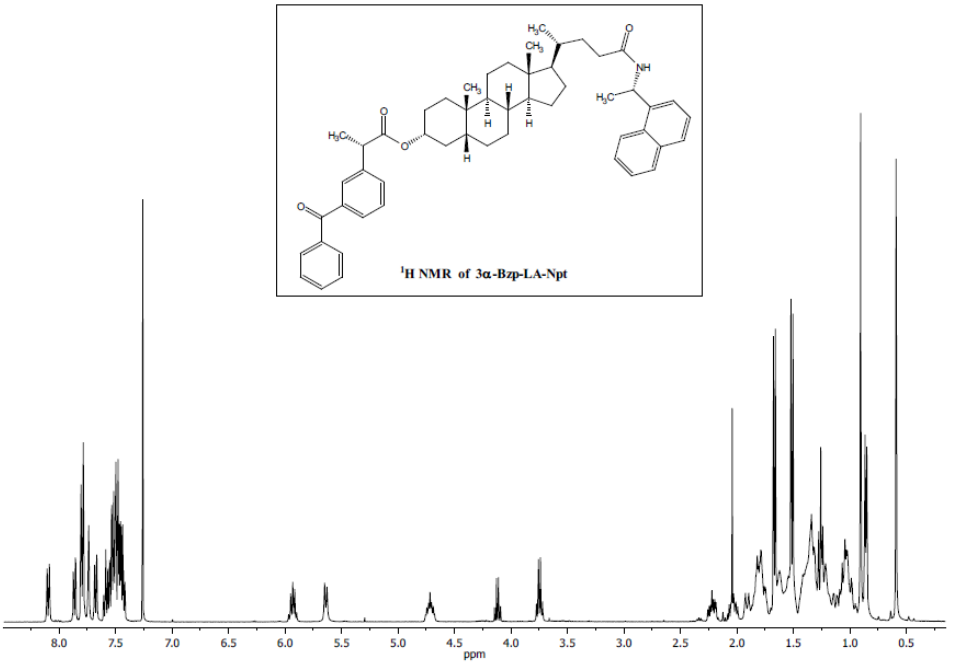
^{1}H NMR of 3α-Bzp-LA-Npt
8.0
7.5
7.0
6.5
6.0
5.5
5.0
4.5
4.0
3.5
3.0
2.5
2.0
1.5
1.0
0.5
ppm

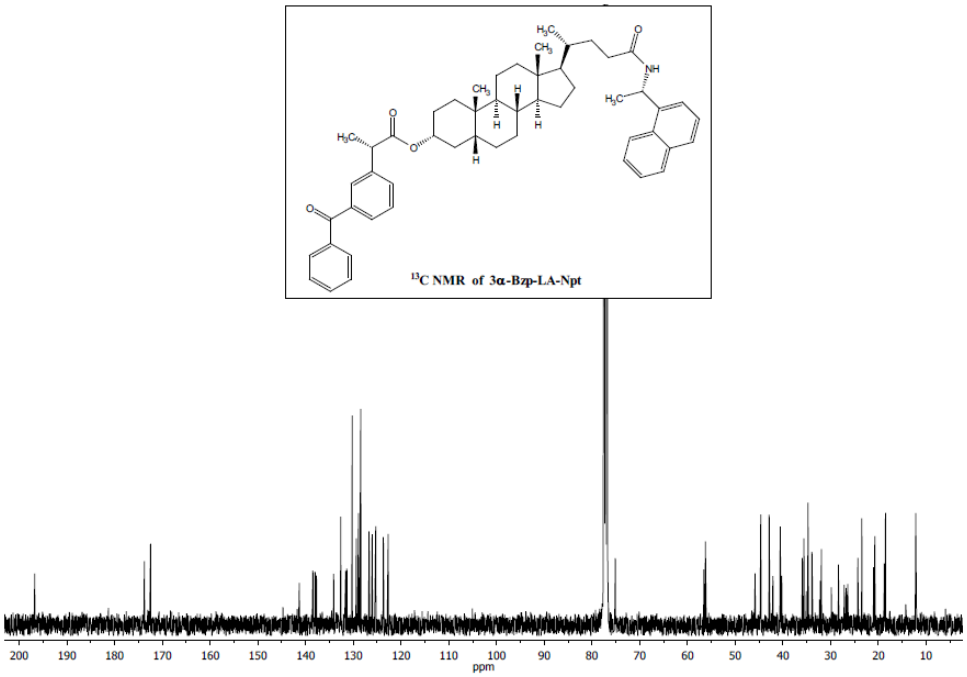
^{13}C NMR of 3α-Bzp-LA-Npt
200
190
180
170
160
150
140
130
120
110
100
90
80
70
60
50
40
30
20
10
ppm

4.6.2.3. Synthesis of LA-Npt

To a solution of **LA** (0.338 g, 0.9 mmol) in anhydrous toluene (10 mL) containing EDC (0.182 g, 0.95 mmol), a solution of NEA (0.154 g, 0.9 mmol) in anhydrous toluene (5 mL) was added dropwise. The reaction was stirred overnight at rt. Then the solvent was concentrated under vacuum; the crude product was dissolved in EtOAc and washed consecutively with diluted $NaHCO_3$, HCl 1 M and brine. Purification by preparative layer chromatography (SiO_2 Merck 60 PF254, EtOAc:MeOH, 95:5) followed by recrystallization gave **LA-Npt** (0.350 g, 74%). ^{1}H NMR (400 MHz, $CDCl_3$): δ (ppm) 0.60 (s, 3H, CH_3); 0.64 (s, 3H, CH_3); 0.80-2.08 (complex signal, 24H); 0.86 (d, J = 6.4 Hz, 3H, 21-CH_3); 1.67 (d, J = 6.8 Hz, 3H, NEA-CH_3); 2.15-2.30 (m, 2H, CH_2); 2.33-2.45 (m, 2H, CH_2); 3.62 (m, 1H, 3β-H); 5.63 (d, J = 8.0 Hz, 1H, NEA-NH); 5.93 (m, 1H, NEA-CH); 7.38-7.57 (m, 4H, arom); 7.75-7.89 (m, 2H, arom); 8.09 (d, J = 8.4 Hz, 1H, arom). ^{13}C NMR (100 MHz, CD_3OD): δ (ppm) 172.6 (C), 138.4 (C), 134.1 (C), 131.3 (C), 128.9 (CH), 128.5 (CH), 126.7 (CH), 126.0 (CH), 125.3 (CH), 123.7 (CH), 122.7 (CH), 72.1 (CH), 56.6 (CH), 56.2 (CH), 44.7 (CH), 42.9 (C), 42.2 (CH), 40.6 (CH), 40.3 (CH_2), 36.6 (CH_2), 36.0 (CH), 35.6 (CH), 35.5 (CH_2), 34.7 (C), 33.9 (CH_2), 31.9 (CH_2), 31.0 (CH_2), 30.7 (CH_2), 28.4 (CH_2), 27.3 (CH_2), 26.6 (CH_2), 24.4 (CH_2), 23.5 (CH_3), 21.0 (CH_2), 20.7 (CH_3), 18.5 (CH_3), 12.2 (CH_3); m/z found 530.3998, calculated for $C_{36}H_{52}NO_2$ (MH^+) 530.3989.

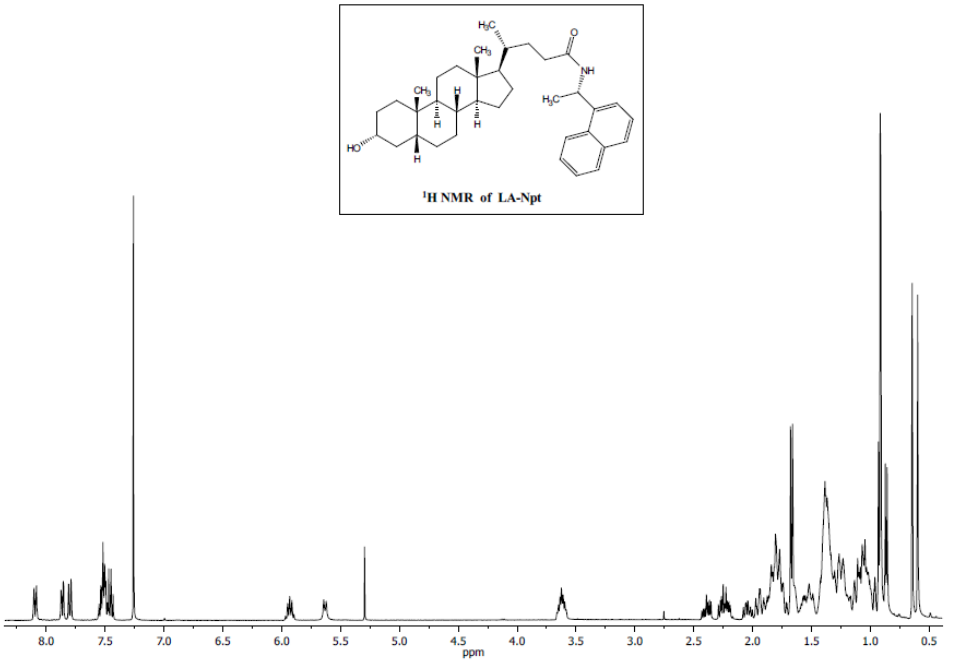
^{1}H NMR of LA-Npt
8.0
7.5
7.0
6.5
6.0
5.5
5.0
4.5
4.0
3.5
3.0
2.5
2.0
1.5
1.0
0.5
ppm

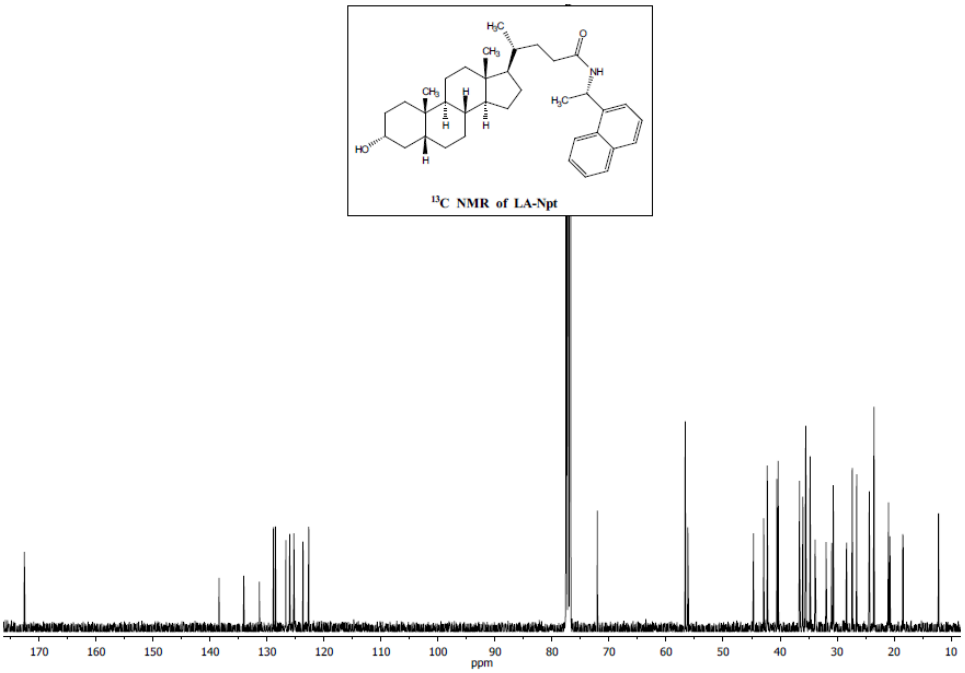
^{13}C NMR of LA-Npt
170
160
150
140
130
120
110
100
90
80
70
60
50
40
30
20
10
ppm

4.6.2.4. Synthesis of 3β-NBz-LA

To a stirred solution of **LA** (0.500 g, 1.33 mmol), 4-nitrobenzoic acid (0.266 g, 1.59 mmol) and Ph_3P (0.418 g, 1.59 mmol) in anhydrous THF (5 mL) at 0 ºC, DEAD 40% (0.625 mL, 1.59 mmol) was added dropwise, and then the reaction mixture was allowed to react overnight at rt. Afterwards, it was poured into brine and extracted with CH_2Cl_2; the combined organic layers were washed with brine, dried over $MgSO_4$ and concentrated under reduced pressure. Purification by column chromatography (SiO_2, EtOAc:Hexane:CH_3COOH, 10:90:1) gave **3β-NBz-LA** as a colorless solid (0.614 g, 87%). ^{1}H NMR (300 MHz, $CDCl_3$): δ (ppm) 0.67 (s, 3H, CH_3); 0.85-2.13 (complex signal, 26H); 0.93 (d, *J* = 6.3 Hz, 3H, 21-CH_3); 1.02 (s, 3H, CH_3); 2.33 (m, 2H, CH_2); 5.38 (*br* s, 1H, 3α-H); 8.16-8.33 (m, 4H, arom). ^{13}C NMR (75 MHz, $CDCl_3$): δ (ppm) 180.2 (C), 164.2 (C), 150.6 (C), 136.7 (C), 130.7 (2xCH), 123.7 (2xCH), 73.0 (CH), 56.7 (CH), 56.1 (CH), 42.9 (C), 40.3 (CH_2), 40.1 (CH), 37.9 (CH), 35.8 (CH), 35.5 (CH), 35.2 (C), 31.2 (CH_2), 31.1 (CH_2), 30.9 (CH_2), 30.8 (CH_2), 28.3 (CH_2), 26.6 (CH_2), 26.3 (CH_2), 25.3 (CH_2), 24.3 (CH_2), 24.2 (CH_3), 21.3 (CH_2), 18.4 (CH_3), 12.2 (CH_3); m/z found 524.3012, calculated for $C_{31}H_{42}NO_6$ ($M-H^+$) 524.3012.

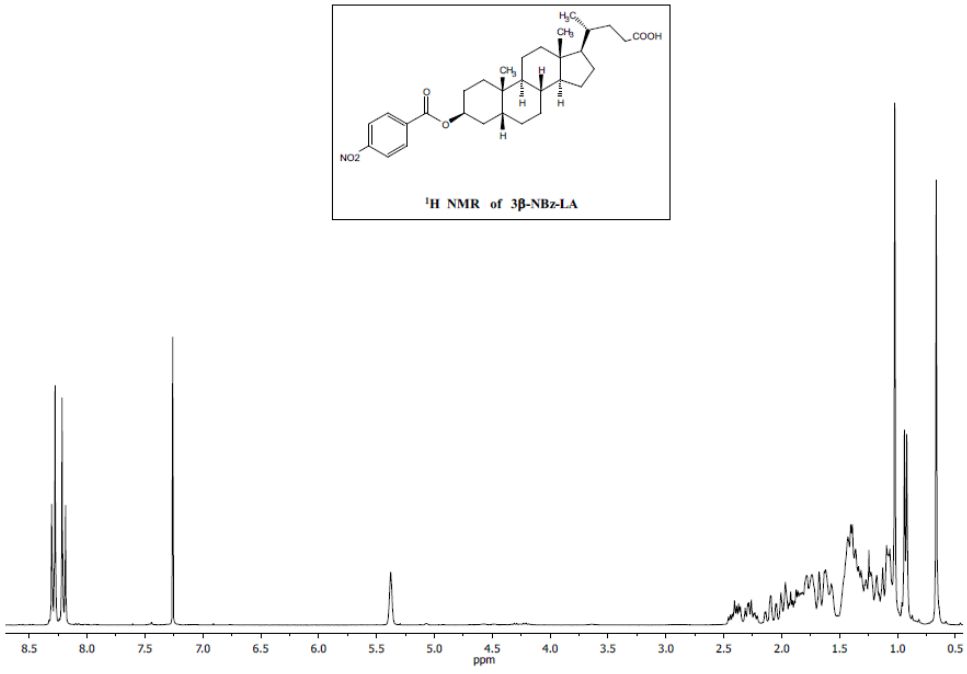
COOH
NO2
^{1}H NMR of 3β-NBz-LA
8.5 8.0 7.5 7.0 6.5 6.0 5.5 5.0 4.5 4.0 3.5 3.0 2.5 2.0 1.5 1.0 0.5
ppm

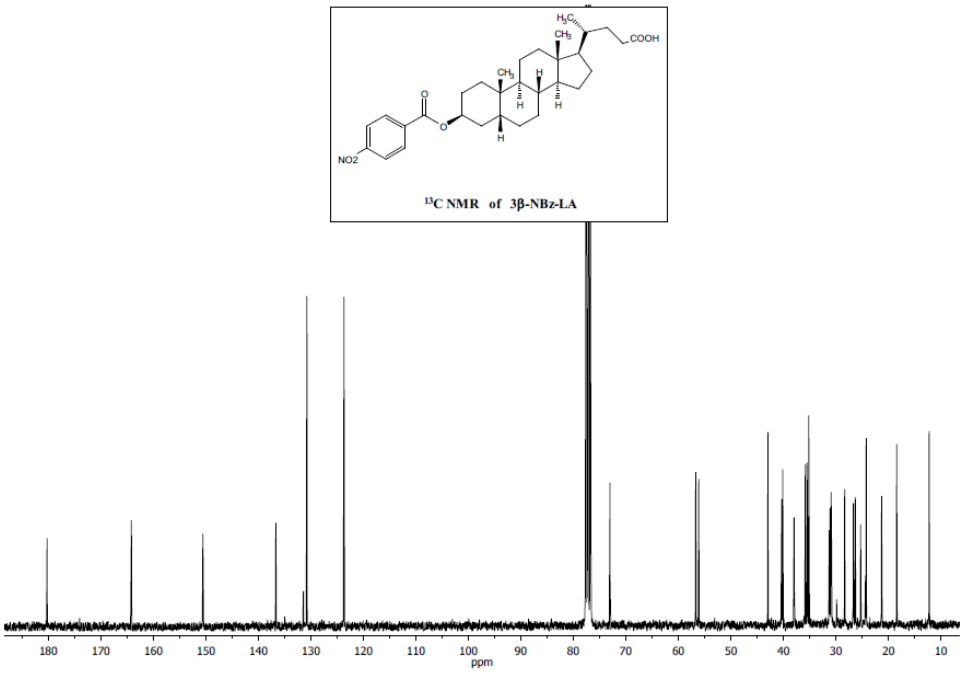
COOH
NO2
^{13}C NMR of 3β-NBz-LA
180 170 160 150 140 130 120 110 100 90 80 70 60 50 40 30 20 10
ppm

4.6.2.5. Synthesis of 3β-OH-LA

A stirred solution of **3β-NBz-LA** (0.386 g, 0.73 mmol) in THF (4 mL) was treated with 7.3 mL of KOH 1M in MeOH and then the reaction mixture was allowed to react overnight at rt. Afterwards, it was poured into HCl 1M and extracted with CH_2Cl_2; the combined organic layers were washed with brine, dried over $MgSO_4$ and concentrated under reduced pressure. Purification by column chromatography (Li Chroprep RP-18, CH_3CN:H_2O, 90:10) gave **3β-OH-LA** as a colorless solid (0.227 g, 82%). ^{1}H NMR (300 MHz, CD_3OD): δ (ppm) 0.71 (s, 3H, CH_3); 0.96 (d, *J* = 6.6 Hz, 3H, 21-CH_3); 0.98 (s, 3H, CH_3); 1.05-2.05 (complex signal, 26H); 2.27 (m, 2H, CH_2); 4.04 (*br* s, 1H, 3α-H). ^{13}C NMR (75 MHz, CD_3OD): δ (ppm) 178.1 (C), 67.8 (CH), 58.0 (CH), 57.5 (CH), 43.9 (C), 41.6 (CH_2), 41.1 (CH), 37.8 (CH), 37.1 (CH), 36.7 (CH), 36.2 (C), 34.4 (CH_2), 32.3 (CH_2), 32.0 (CH_2), 31.0 (CH_2), 29.2 (CH_2), 28.5 (CH_2), 27.9 (CH_2), 27.5 (CH_2), 25.3 (CH_2), 24.5 (CH_3), 22.2 (CH_2), 18.8 (CH_3), 12.6 (CH_3); m/z found 375.2896, calculated for $C_{24}H_{39}O_3$ ($M-H^+$) 375.2899.

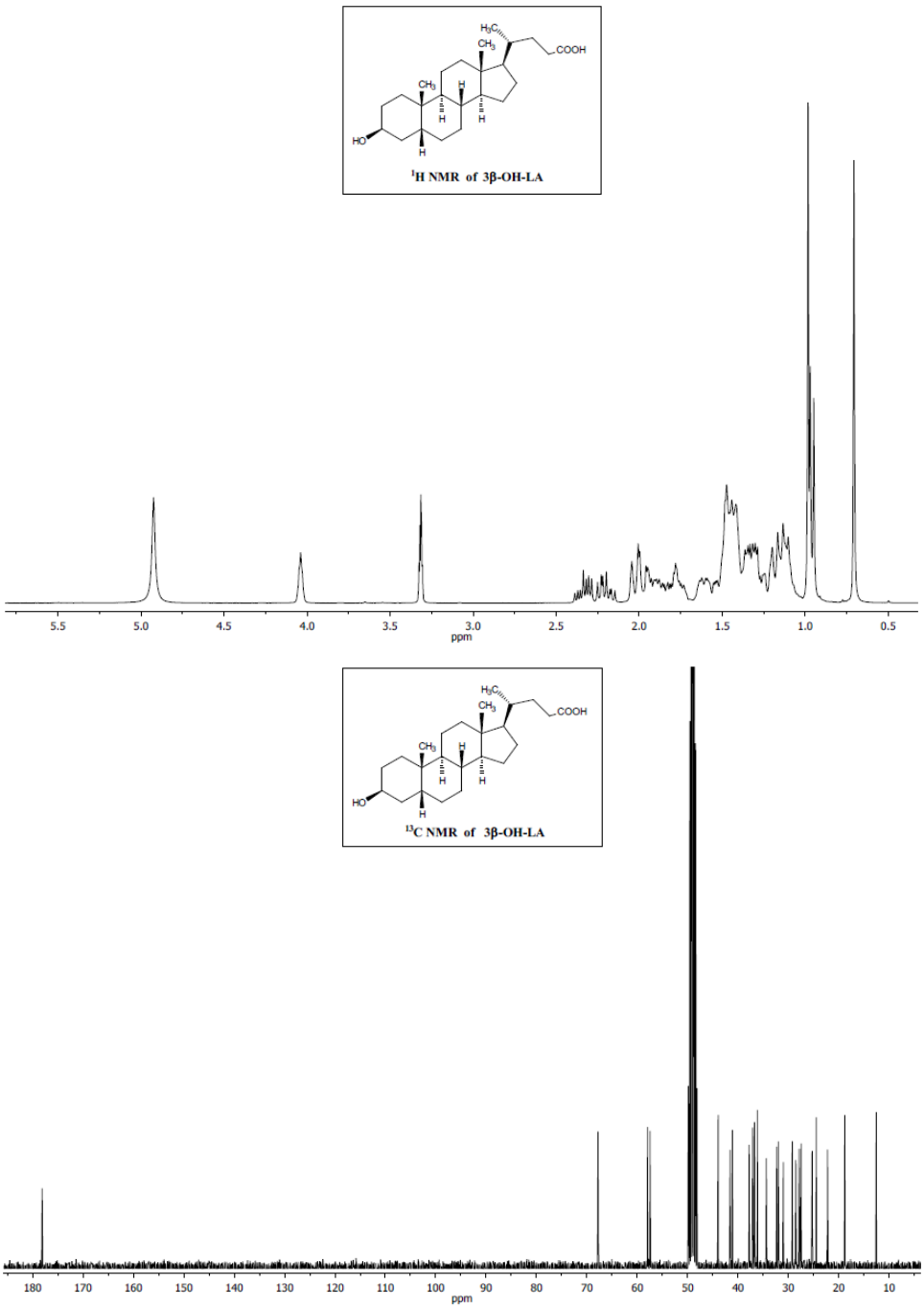
^{1}H NMR of 3β-OH-LA
5.5
5.0
4.5
4.0
3.5
3.0
2.5
2.0
1.5
1.0
0.5
ppm
^{13}C NMR of 3β-OH-LA
180
170
160
150
140
130
120
110
100
90
80
70
60
50
40
30
20
10
ppm

4.6.2.6. Synthesis of 3β-Bzp-LA

To a stirred solution of **3β-OH-LA** (0.163 g, 0.36 mmol), TBTU (0.174 g, 0.54 mmol) and KP (0.139 g, 0.54 mmol) in DMF (5 mL), DIEA (0.19 mL, 1.08 mmol) was added dropwise and then the reaction mixture was allowed to react overnight at rt. Afterwards, it was poured into brine and extracted with CH_2Cl_2; the combined organic layers were washed with brine, dried over $MgSO_4$ and concentrated under reduced pressure. Purification by column chromatography (Li Chroprep RP-18, CH_3CN:H_2O, 80:20) gave **3β-Bzp-LA** as a colorless oil (0.057 g, 21%). ^{1}H NMR (300 MHz, CD_3OD): δ (ppm) 0.65 (s, 3H, CH_3); 0.68-2.02 (complex signal, 26H); 0.79 (s, 3H, CH_3); 0.91 (d, *J* = 6.3 Hz, 3H, 21-CH_3); 1.50 (d, *J* = 6.9 Hz, 3H, KP-CH_3); 2.24 (m, 2H, CH_2); 3.85 (q, *J* = 6.9 Hz, 1H, KP-CH); 5.00 (*br* s, 1H, 3α-H); 7.43-7.85 (m, 9H, arom). ^{13}C NMR (75 MHz, CD_3OD): δ (ppm) 198.0 (C), 178.1 (C), 174.9 (C), 143.0 (C), 139.1 (C), 138.7 (C), 133.9 (CH), 133.0 (CH), 131.0 (2xCH), 130.2 (CH), 129.9 (CH), 129.7 (CH), 129.5 (2xCH), 72.8 (CH), 57.8 (CH), 57.4 (CH), 46.9 (CH), 43.9 (C), 41.4 (CH_2), 41.0 (CH), 38.7 (CH), 37.0 (CH), 36.7 (CH), 35.8 (C), 32.3 (CH_2), 32.0 (CH_2), 31.7 (CH_2), 31.3 (CH_2), 29.2 (CH_2), 27.6 (CH_2), 27.2 (CH_2), 25.9 (CH_2), 25.2 (CH_2), 24.4 (CH_3), 22.2 (CH_2), 18.8 (CH_3), 18.2 (CH_3), 12.5 (CH_3); m/z found 613.3918, calculated for $C_{40}H_{53}O_5$ (MH^+) 613.3993.

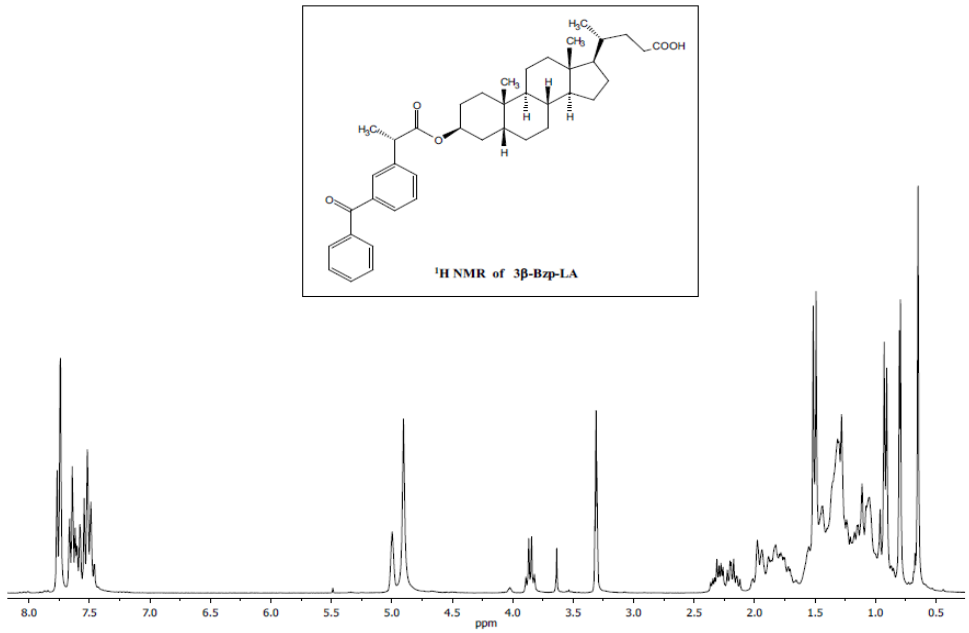
COOH
^{1}H NMR of 3β-Bzp-LA
8.0 7.5 7.0 6.5 6.0 5.5 5.0 4.5 4.0 3.5 3.0 2.5 2.0 1.5 1.0 0.5
ppm

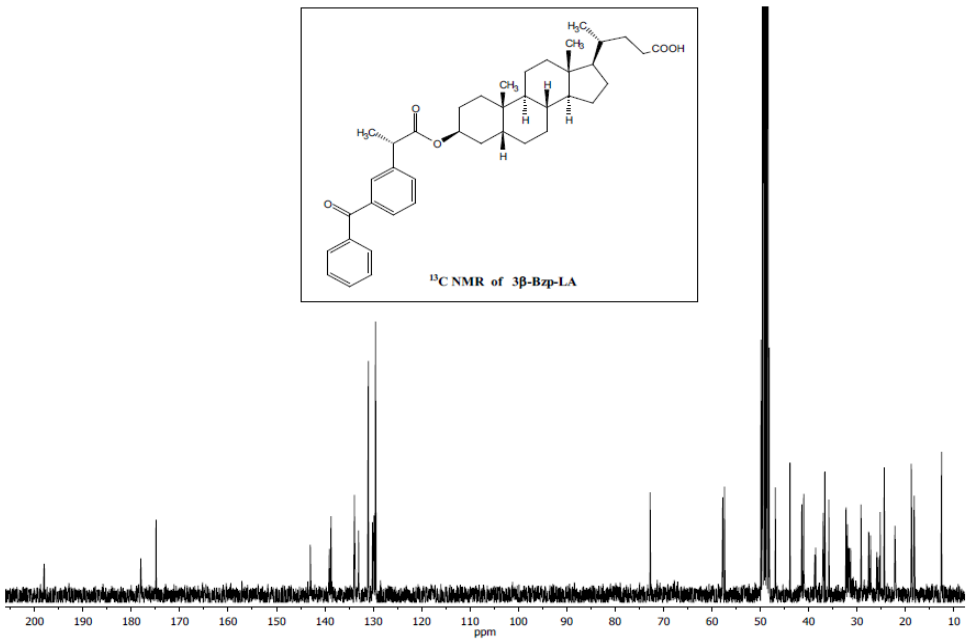
COOH
^{13}C NMR of 3β-Bzp-LA
200 190 180 170 160 150 140 130 120 110 100 90 80 70 60 50 40 30 20 10
ppm

4.6.2.7. Synthesis of 3β-Bzp-LA-Npt

To a stirred solution of **3β-Bzp-LA** (0.057 g, 0.093 mmol) and TBTU (0.060 g, 0.186 mmol) in DMF (5 mL), NEA (0.03 mL, 0.186 mmol) and DIEA (0.065 mL, 3.72 mmol) were added dropwise and then the reaction mixture was allowed to react overnight at rt. Afterwards, it was poured into brine and extracted with CH_2Cl_2; the combined organic layers were washed with brine, dried over $MgSO_4$ and concentrated under reduced pressure. Purification by column chromatography (Li Chroprep RP-18, CH_3CN:H_2O:EtOAc, 70:10:20) gave **3β-Bzp-LA-Npt** as a colorless oil (0.063 g, 88%). ^{1}H NMR (300 MHz, $CDCl_3$): δ (ppm) 0.58 (s, 3H, CH_3); 0.65-2.30 (complex signal, 28H); 0.84 (m, 6H, CH_3+21-CH_3); 1.54 (d, *J* = 7.2 Hz, 3H, KP-CH_3); 1.65 (d, *J* = 6.6 Hz, 3H, NEA-CH_3); 3.78 (q, *J* = 7.2 Hz, 1H, KP-CH); 5.03 (*br* s, 1H, 3α-H); 5.74 (d, *J* = 8.1 Hz, 1H, NEA-NH); 5.92 (m, 1H, NEA-CH); 7.36-7.91 (m, 15H, arom); 8.08 (d, *J* = 8.4 Hz, 1H, arom). ^{13}C NMR (75 MHz, $CDCl_3$): δ (ppm) 196.6 (C), 173.4 (C), 172.5 (C), 141.4 (C), 138.5 (C), 137.9 (C), 137.7 (C), 134.0 (C), 132.6 (CH), 131.7 (CH), 131.3 (C), 130.1 (2xCH), 129.3 (CH), 129.0 (CH), 128.8 (CH), 128.5 (CH), 128.4 (CH), 128.3 (2xCH), 126.6 (CH), 126.0 (CH), 125.2 (CH), 123.7 (CH), 122.6 (CH), 71.5 (CH), 56.6 (CH), 56.2 (CH), 46.0 (CH), 44.6 (CH), 42.8 (C), 40.3 (CH_2), 39.9 (CH), 37.4 (CH), 35.7 (CH), 35.5 (CH), 34.8 (C), 33.8 (CH_2), 31.9 (CH_2), 30.7 (CH_2), 30.5 (CH_2), 28.3 (CH_2), 26.6 (CH_2), 26.2 (CH_2), 25.0 (CH_2), 24.3 (CH_2), 23.9 (CH_3), 21.2 (CH_2), 20.7 (CH_3), 18.4 (CH_3), 18.1 (CH_3), 12.1 (CH_3); m/z found 766.4835, calculated for $C_{52}H_{64}NO_4$ (MH^+) 766.4860.

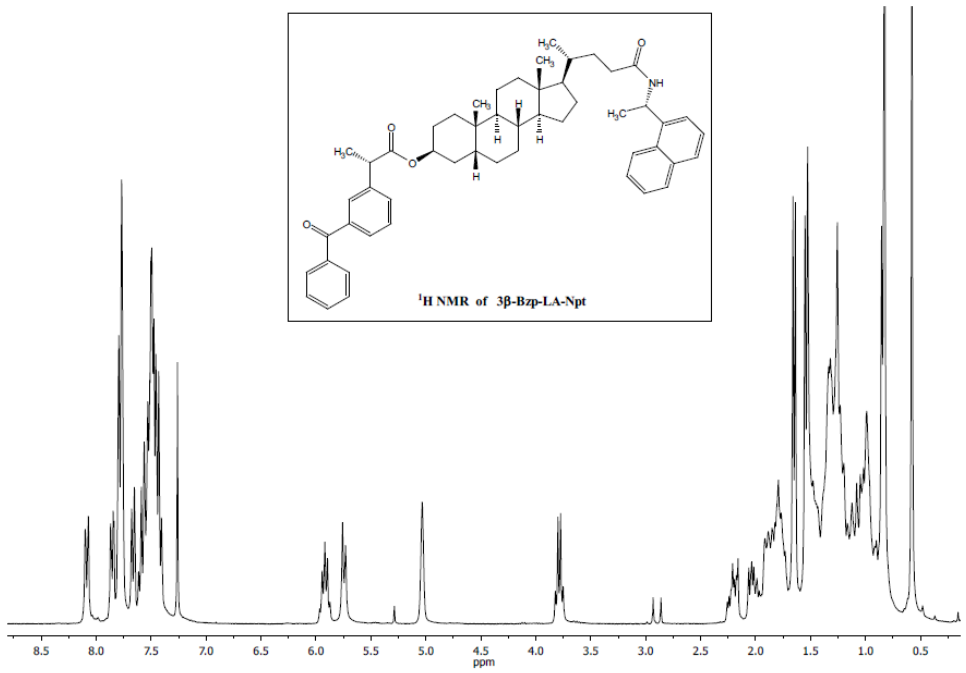
^{1}H NMR of 3β-Bzp-LA-Npt
8.5 8.0 7.5 7.0 6.5 6.0 5.5 5.0 4.5 4.0 3.5 3.0 2.5 2.0 1.5 1.0 0.5
ppm

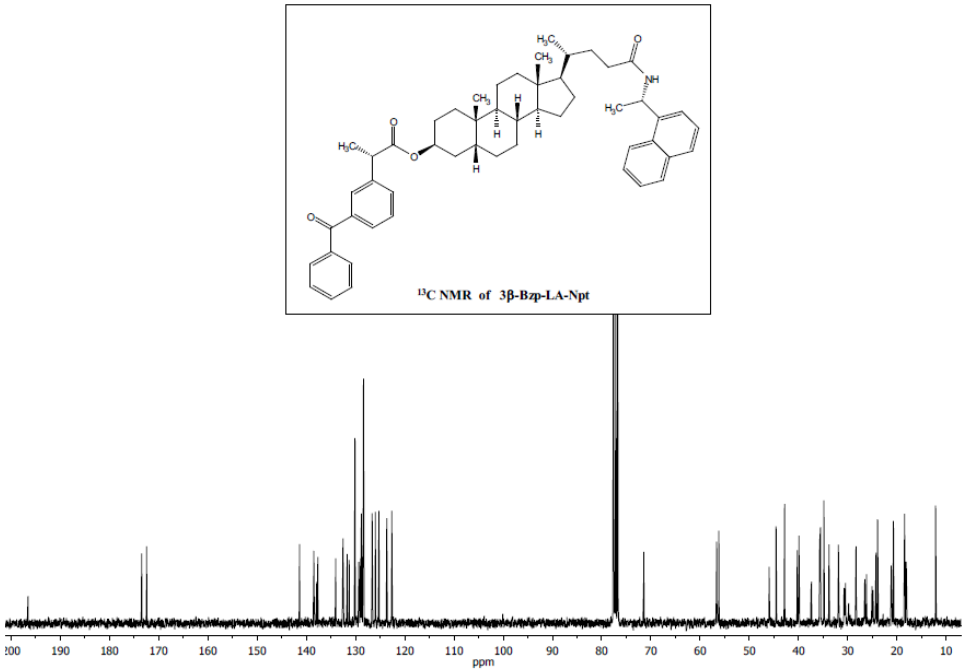
^{13}C NMR of 3β-Bzp-LA-Npt
190 180 170 160 150 140 130 120 110 100 90 80 70 60 50 40 30 20 10
ppm

4.6.2.8. Synthesis of 3β-Bzp-LA-Bip

To a stirred solution of **3β-Bzp-LA** (0.148 g, 0.25 mmol), TBTU (0.094 g, 0.29 mmol) and PBA (0.053 g, 0.29 mmol) in DMF (3 mL), DIEA (0.105 mL, 0.6 mmol) was added dropwise, and then the reaction mixture was allowed to react overnight at rt. Afterwards, it was poured into brine and extracted with CH_2Cl_2; the combined organic layers were washed with brine, dried over $MgSO_4$ and concentrated under reduced pressure. Purification by column chromatography (SiO_2,EtOAc:Hexane, 10:90) gave **3β-Bzp-LA-Bip** as a colorless oil (0.107 g, 57%). ^{1}H NMR (300 MHz, $CDCl_3$): δ (ppm) 0.61 (s, 3H, CH_3); 0.75-2.47 (complex signal, 26H); 0.84 (s, 3H, CH_3); 0.90 (d, *J* = 6.0 Hz, 3H, 21-CH_3); 1.55 (d, *J* = 7.2 Hz, 3H, KP-CH_3); 3.37 (m, 2H, CH_2); 3.80 (q, *J* = 6.9 Hz, 1H, KP-CH); 5.06 (*br* s, 1H, 3α-H); 5.16 (m, 2H, CH_2); 7.30-7.88 (m, 18H, arom). ^{13}C NMR (75 MHz, $CDCl_3$): δ (ppm) 196.5 (C), 174.2 (C), 173.4 (C), 141.4 (C), 141.2 (C), 140.8 (C), 137.9 (C), 137.7 (C), 135.2 (C), 132.5 (CH), 131.7 (CH), 130.1 (2xCH), 129.3 (CH), 129.0 (CH), 128.9 (2xCH), 128.8 (2xCH), 128.5 (CH), 128.4 (2xCH), 127.5 (CH), 127.4 (2xCH), 127.2 (2xCH), 71.4 (CH), 65.9 (CH_2), 56.6 (CH), 56.1 (CH), 46.0 (CH), 42.8 (C), 40.2 (CH_2), 39.9 (CH), 37.5 (CH), 35.7 (CH), 35.4 (CH), 34.8 (C), 31.4 (CH_2), 31.1 (CH_2), 30.7 (CH_2), 30.5 (CH_2), 28.3 (CH_2), 26.6 (CH_2), 26.2 (CH_2), 25.1(CH_2), 24.3 (CH_2), 23.9 (CH_3), 21.2 (CH_2), 18.4 (CH_3), 18.1 (CH_3), 12.1 (CH_3); m/z found 801.4520, calculated for $C_{53}H_{62}O_5Na$ (MNa^+) 801.4495.

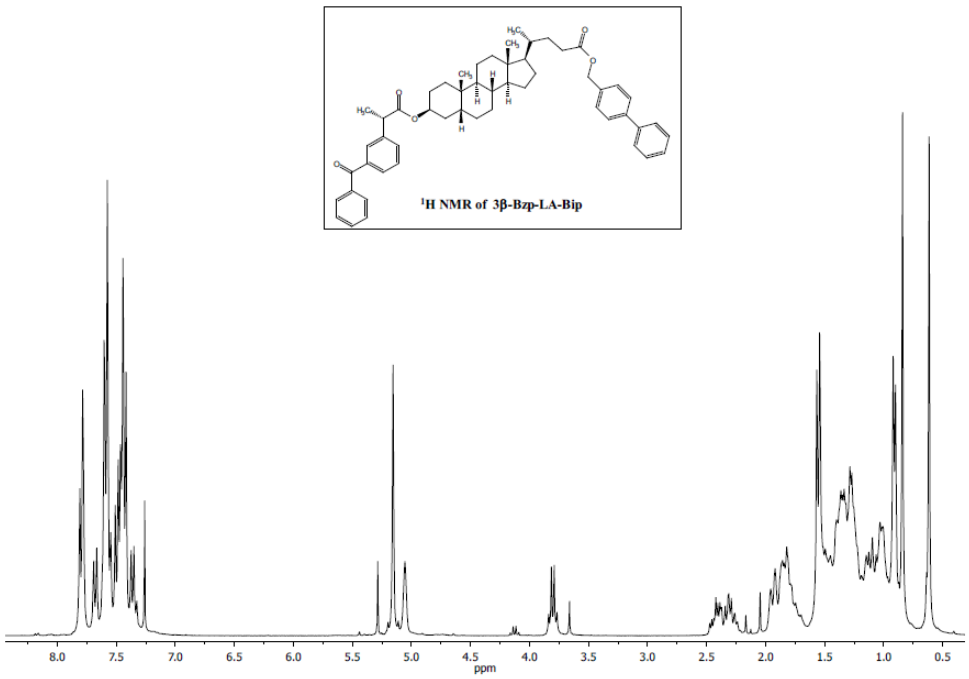
^{1}H NMR of 3β-Bzp-LA-Bip
8.0
7.5
7.0
6.5
6.0
5.5
5.0
4.5
4.0
3.5
3.0
2.5
2.0
1.5
1.0
0.5
ppm

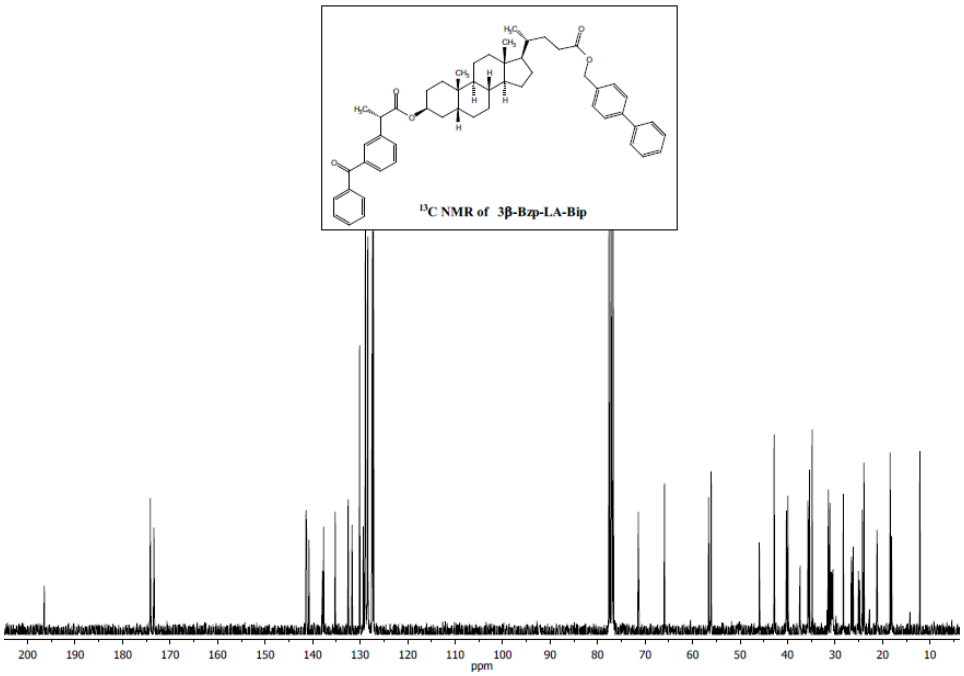
^{13}C NMR of 3β-Bzp-LA-Bip
200
190
180
170
160
150
140
130
120
110
100
90
80
70
60
50
40
30
20
10
ppm

4.6.2.9. Synthesis of LA-Bip

To a stirred solution of **LA** (0.200 g, 0.55 mmol) and TBTU (0.212 g, 0.66 mmol) in anhydrous DMF (1 mL), PBA (0.121 g, 0.66 mmol) in DMF (4 mL) followed by DIEA (0.285 mL, 1.65 mmol) were added dropwise, and then the reaction mixture was allowed to react overnight at rt. Afterwards, it was poured into brine and extracted with CH_2Cl_2; the combined organic layers were washed with brine, dried over $MgSO_4$ and concentrated under reduced pressure. Purification by column chromatography (SiO_2, EtOAc:Hexane, 10:90) gave **LA-Bip** as a colorless oil (0.218 g, 76%). ^{1}H NMR (300 MHz, $CDCl_3$): δ (ppm) 0.62 (s, 3H, CH_3); 0.86-1.97 (complex signal, 26H); 0.91 (m, 6H, 2xCH_3); 2.35 (m, 2H, CH_2); 3.63 (m, 1H, 3β-H); 5.15 (m, 2H, CH_2); 7.30-7.65 (m, 9H, arom). ^{13}C NMR (75 MHz, $CDCl_3$): δ (ppm) 174.3 (C), 141.3 (C), 140.8 (C), 135.3 (C), 128.9 (2xCH), 128.8 (2xCH), 127.6 (CH), 127.5 (2xCH), 127.3 (2xCH), 72.0 (CH), 66.0 (CH_2), 56.6 (CH), 56.1 (CH), 42.9 (C), 42.2 (CH), 40.6 (CH), 40.3 (CH_2), 36.6 (CH_2), 36.0 (CH), 35.5 (CH_2+CH), 34.7 (C), 31.5 (CH_2), 31.1 (CH_2), 30.7 (CH_2), 28.3 (CH_2), 27.3 (CH_2), 26.6 (CH_2), 24.4 (CH_2), 23.5 (CH_3), 21.0 (CH_2), 18.4 (CH_3), 12.2 (CH_3); m/z found 565.3668, calculated for $C_{37}H_{50}O_3Na$ (MNa^+) 565.3658.

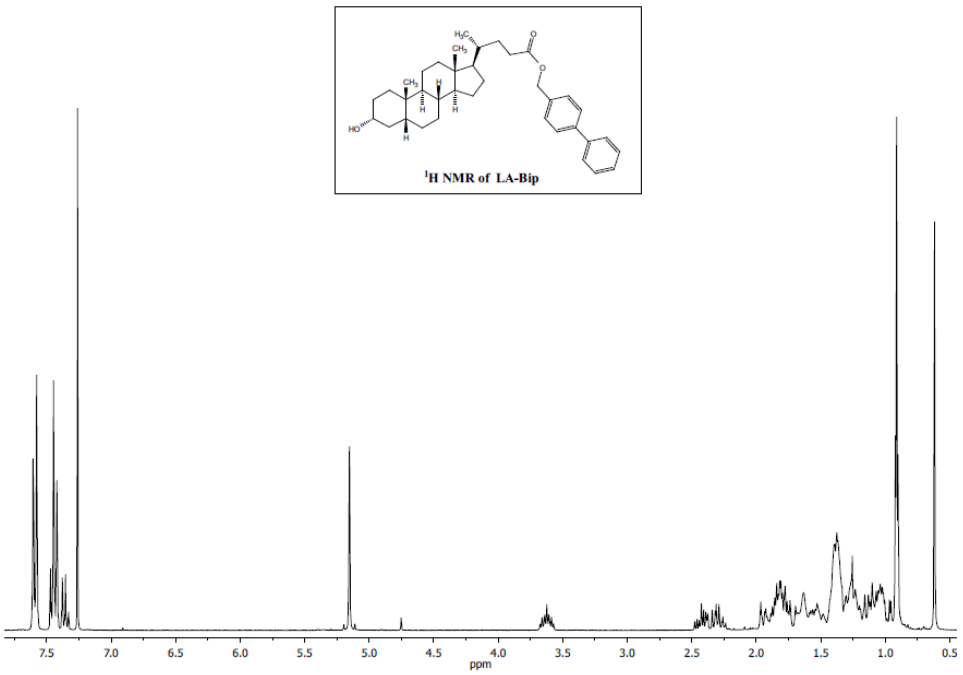
^{1}H NMR of LA-Bip
7.5
7.0
6.5
6.0
5.5
5.0
4.5
4.0
3.5
3.0
2.5
2.0
1.5
1.0
0.5
ppm

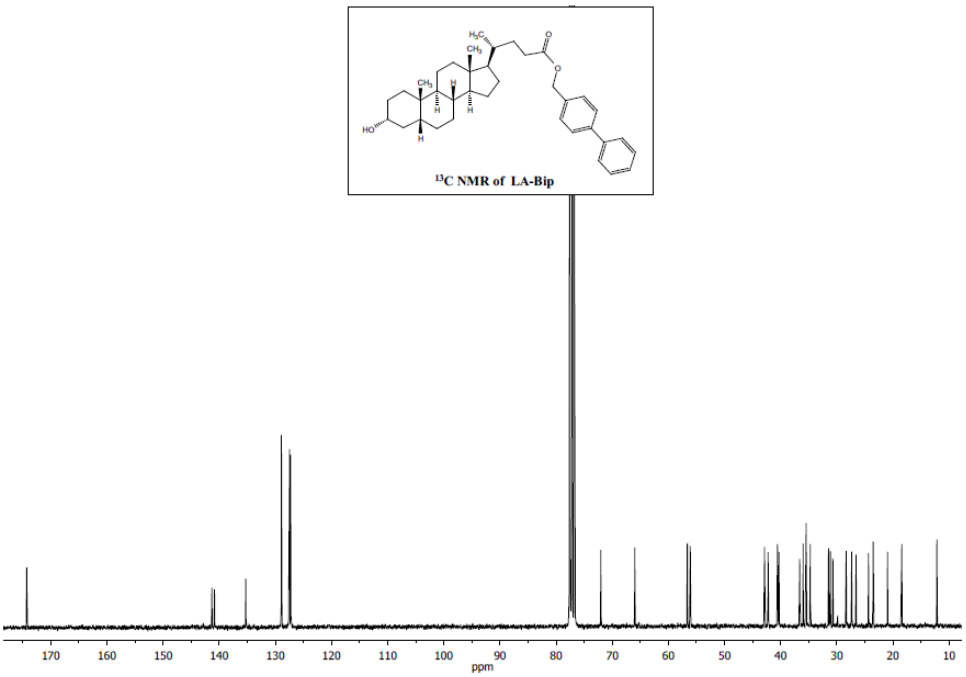
^{13}C NMR of LA-Bip
170
160
150
140
130
120
110
100
90
80
70
60
50
40
30
20
10
ppm

4.6.2.10. Synthesis of 3α-Bzp-LA-Bip

To a stirred solution of **LA-Bip** (0.100 g, 0.16 mmol) and TBTU (0.063 g, 0.20 mmol) in anhydrous DMF (1 mL), NEA (0.037 g, 0.20 mmol) in DMF (4 mL) followed by DIEA (0.084 mL, 0.48 mmol) were added dropwise, and then the reaction mixture was allowed to react overnight at rt. Afterwards, it was poured into brine and extracted with CH_2Cl_2; the combined organic layers were washed with brine, dried over $MgSO_4$ and concentrated under reduced pressure. Purification by column chromatography (SiO_2, EtOAc:Hexane, 10:90) gave **3α-Bzp-LA-Bip** as a colorless oil (0.088 g, 69%). ^{1}H NMR (300 MHz, $CDCl_3$): δ (ppm) 0.62 (s, 3H, CH_3); 0.77-2.05 (complex signal, 26H); 0.91 (m, 6H, 2xCH_3); 1.52 (d, *J* = 7.2 Hz, 3H, KP-CH_3); 2.35 (m, 2H, CH_2); 3.75 (q, *J* = 7.2 Hz, 1H, KP-CH); 4.73 (m, 1H, 3β-H); 5.16 (m, 2H, CH_2); 7.32-7.84 (m, 18H, arom). ^{13}C NMR (75 MHz, $CDCl_3$): δ (ppm) 196.6 (C), 174.2 (C), 173.7 (C), 141.3 (2xC), 140.8 (C), 138.0 (C), 137.7 (C), 135.2 (C), 132.6 (CH), 131.5 (CH), 130.2 (2xCH), 129.3 (CH), 128.9 (5xCH), 128.6 (CH), 128.4 (2xCH), 127.5 (CH), 127.4 (2xCH), 127.2 (2xCH), 75.0 (CH), 66.0 (CH_2), 56.5 (CH), 56.1 (CH), 45.8 (CH), 42.8 (C), 42.1 (CH), 40.5 (CH), 40.2 (CH_2), 35.9 (CH), 35.4 (CH), 35.1 (CH_2), 34.7 (C), 32.3 (CH_2), 31.4 (CH_2), 31.1 (CH_2), 28.3 (CH_2), 27.1 (CH_2), 26.6 (CH_2), 26.4 (CH_2), 24.3 (CH_2), 23.4 (CH_3), 21.0 (CH_2), 18.7 (CH_3), 18.4 (CH_3), 12.2 (CH_3); m/z found 779.4693, calculated for $C_{53}H_{63}O_5$ (MH^+) 779.4676.

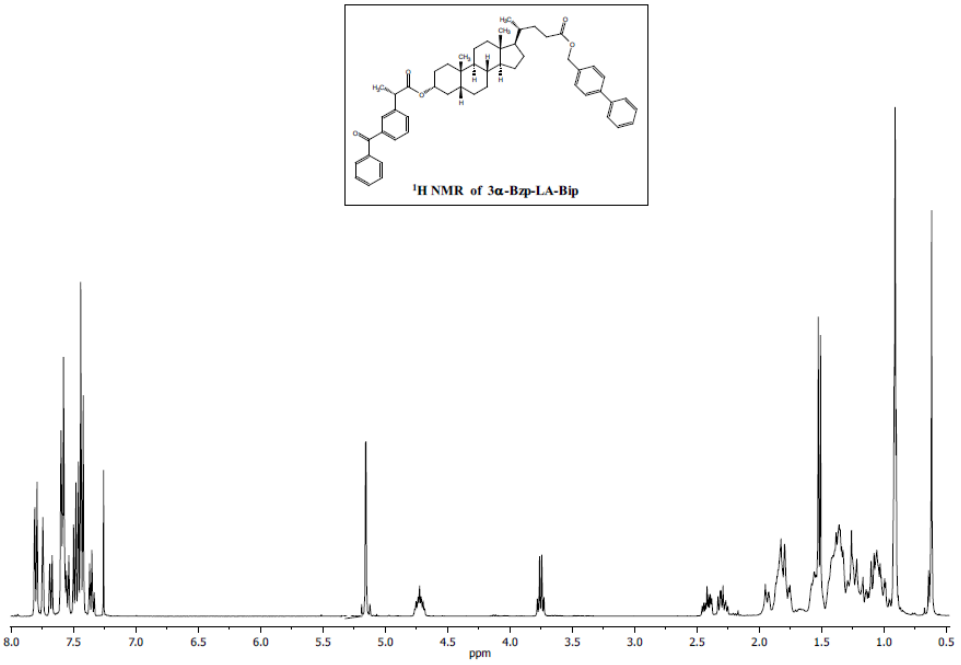
^{1}H NMR of 3α-Bzp-LA-Bip
8.0
7.5
7.0
6.5
6.0
5.5
5.0
4.5
4.0
3.5
3.0
2.5
2.0
1.5
1.0
0.5
ppm

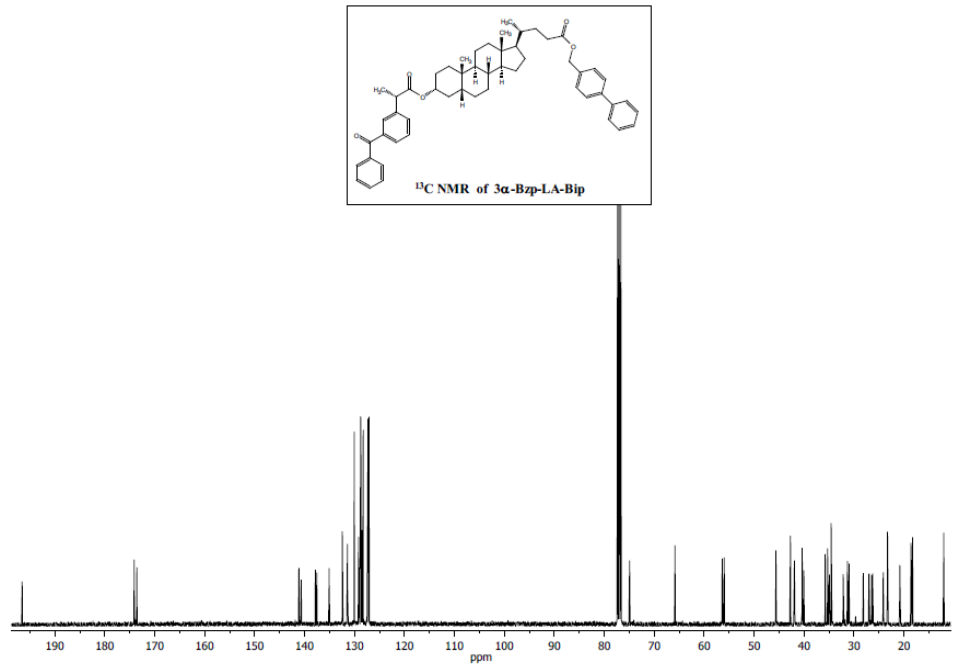
^{13}C NMR of 3α-Bzp-LA-Bip
190
180
170
160
150
140
130
120
110
100
90
80
70
60
50
40
30
20
ppm

4.6.2.11. Synthesis of Bzp-Npt

To a solution of KP (0.203 g, 0.8 mmol) in CH_2Cl_2 (10 mL), EDC (0.163 g, 0.85 mmol) was added as solid. The mixture was stirred at rt and then a solution of NEA (0.137 g, 0.8 mmol) in CH_2Cl_2 was added dropwise. After one day, the crude product was washed with diluted $NaHCO_3$, HCl 1 M and brine. Purification by preparative layer chromatography (SiO_2 Merck 60 PF254, EtOAc:Hexane, 50:50) followed by recrystallization gave **Bzp-Npt** (0.280 g, 82%). ^{1}H NMR (400 MHz, $CDCl_3$): δ (ppm) 1.54 (d, *J* = 7.2 Hz, 3H, CH_3); 1.63 (d, *J* = 6.8 Hz, 3H, CH_3); 3.57 (q, *J* = 7.2 Hz, 1H, KP-CH); 5.66 (*br* d, *J* = 7.6 Hz, 1H, NEA-NH); 5.85 (m, 1H, NEA-CH); 7.27-7.86 (m, 16H, arom). ^{13}C NMR (100 MHz, $CDCl_3$): δ (ppm) 196.6 (C), 172.4 (C), 141.7 (C), 138.1 (2xC), 137.5 (C), 134.0 (C), 132.6 (CH), 131.5 (CH), 131.1 (C), 130.1 (2xCH), 129.2 (CH), 129.1 (CH), 128.8 (2xCH), 128.5 (CH), 128.4 (2xCH), 126.4 (CH), 125.9 (CH), 125.2 (CH), 123.3 (CH), 122.5 (CH), 47.2 (CH), 45.1 (CH), 20.7 (CH_3), 18.6 (CH_3); m/z found 408.1964, calculated for $C_{28}H_{25}NO_2$ (MH^+) 408.1967.

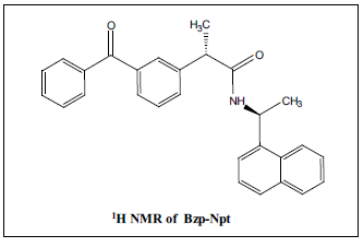

^{1}H NMR of Bzp-Npt

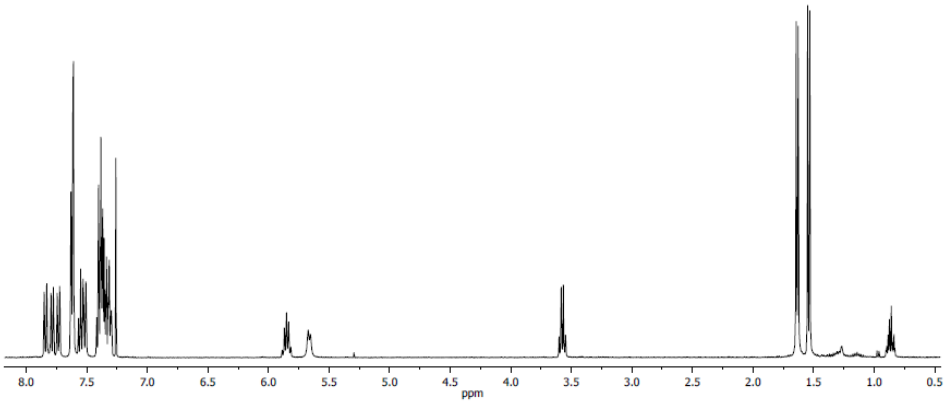

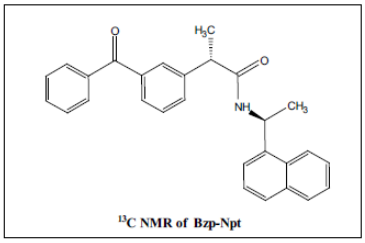

^{13}C NMR of Bzp-Npt

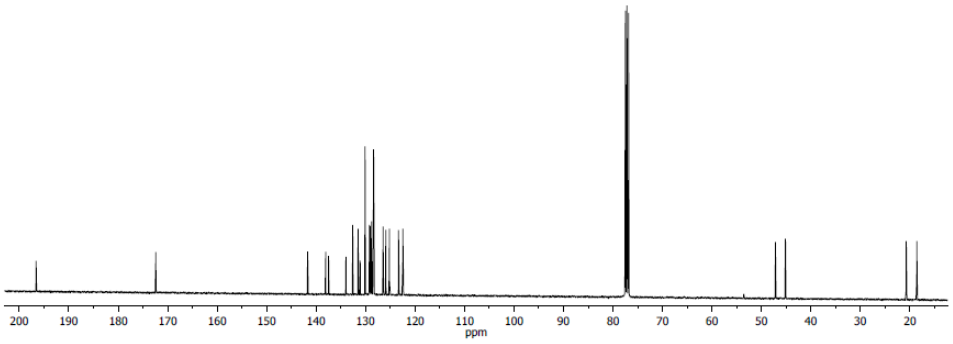

4.6.2.12. Synthesis of Bzp-Bip

To a solution of KP (0.270 g, 1.1 mmol) in CH_2Cl_2 (10 mL), DCC (0.250 g, 1.1mmol) and 4-DMAP (catalytic amount) were added as solids. The mixture was stirred at rt and then a solution of PBA (0.200 g, 1.09 mmol) in CH_2Cl_2 was added dropwise. After 2 h, the crude product was washed with diluted $NaHCO_3$, HCl 1 M and brine. Purification by preparative layer chromatography (SiO_2 Merck 60 PF254, EtOAc:Hexane, 20:80) gave **Bzp-Bip** (0.416 g, 90%). ^{1}H NMR (400 MHz, $CDCl_3$): δ (ppm) 1.61 (d, J = 8.0 Hz, 3H, KP-CH_3); 3.91 (q, J = 8.0 Hz, 1H, KP-CH); 5.19 (m, 2H, CH_2); 7.34-7.49 (m, 8H, arom); 7.55-7.59 (m, 6H, arom); 7.71-7.82 (m, 4H, arom). ^{13}C NMR (100 MHz, $CDCl_3$): δ (ppm) 196.3 (C), 173.7 (C), 141.0 (C), 140.6 (C), 140.5 (C), 137.8 (C), 137.4 (C), 134.2 (C), 132.4 (C), 131.4 (CH), 129.9 (2xCH), 129.2 (CH), 128.9 (CH), 128.7 (2xCH), 128.5 (CH), 128.3 (2xCH), 128.2 (2xCH), 127.3 (CH), 127.1 (2xCH), 127.0 (2xCH), 66.3 (CH_2), 45.3 (CH), 18.3 (CH_3); m/z found 443.1628, calculated for $C_{29}H_{24}O_3Na$ (MNa^+) 443.1623.

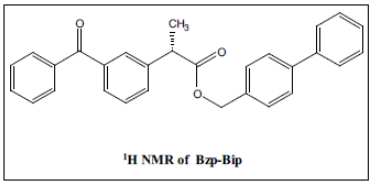

^{1}H NMR of Bzp-Bip

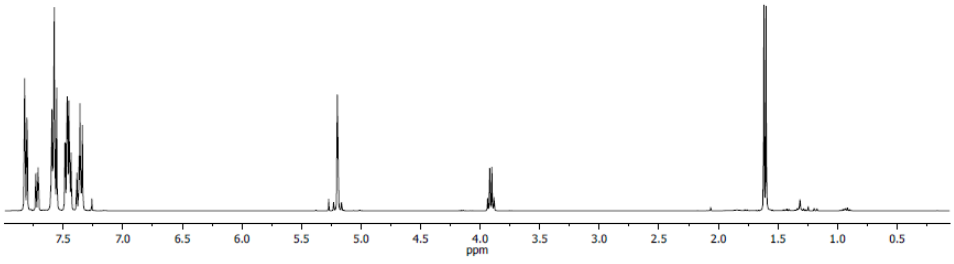

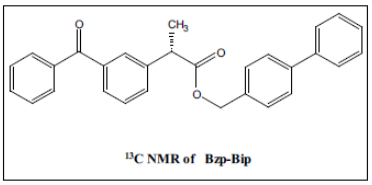

^{13}C NMR of Bzp-Bip

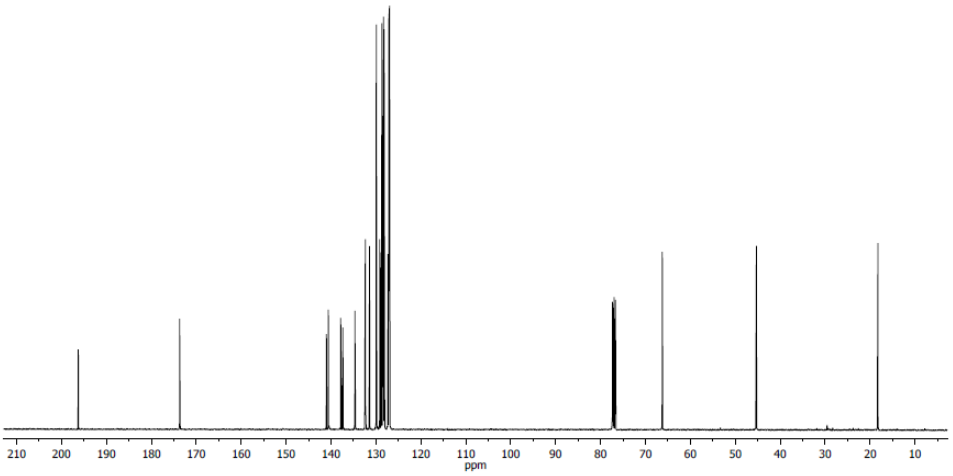

4.6.2.13. Synthesis of LA-OH

To a stirred suspension of $LiAlH_4$ (0.29 g, 7.59 mmol) in anhydrous THF (5.5 mL) at −10 °C, a solution of **LA** (1.00 g, 2.66 mmol) in anhydrous THF (100 mL) was slowly added and then the reaction mixture was refluxed overnight. Afterwards, it was quenched with saturated aqueous NH_4Cl solution, poured into aqueous HCl 1M and extracted with EtOAc. The combined organic layers were washed with brine, dried over $MgSO_4$ and concentrated. Purification by column chromatography (Li Chroprep RP-18, MeOH:H_2O, 90:10) gave **LA-OH** as a colorless solid (0.85 g, 88 %). ^{1}H NMR (300 MHz, $CDCl_3$): δ (ppm) 0.64 (s, 3H, 18-CH_3); 0.88-2.02 (complex signal, 28H); 0.92 (s, 3H, 19-CH_3); 0.93 (d, J = 6.3 Hz, 3H, 21-CH_3); 3.61 (m, 3H, 3β-H+CH_2). ^{13}C NMR (75 MHz, $CDCl_3$): δ (ppm) 72.0 (CH), 63.8 (CH_2), 56.7 (CH), 56.3 (CH), 42.9 (C), 42.3 (CH), 40.6 (CH), 40.4 (CH_2), 36.6 (CH_2), 36.0 (CH), 35.7 (CH), 35.5 (CH_2), 34.7 (C), 32.0 (CH_2), 30.7 (CH_2), 29.6 (CH_2), 28.5 (CH_2), 27.4 (CH_2), 26.6 (CH_2), 24.4 (CH_2), 23.5 (CH_3), 21.0 (CH_2), 18.8 (CH_3), 12.2 (CH_3).

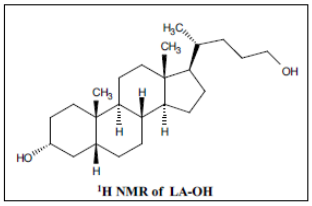

^{1}H NMR of LA-OH

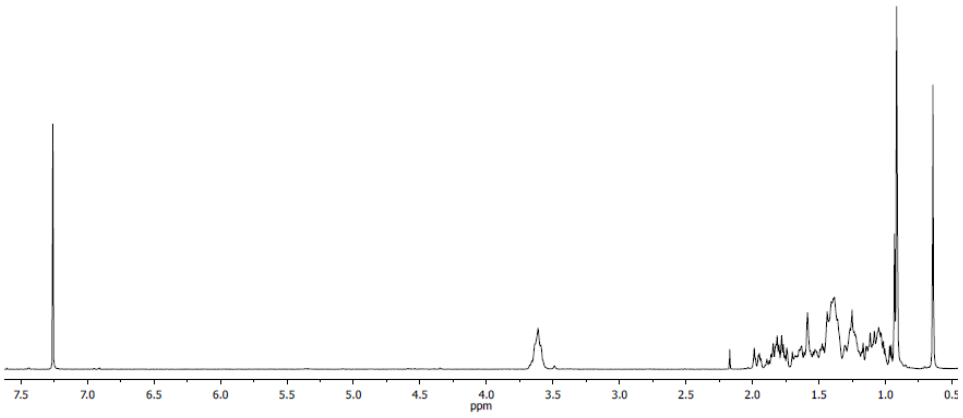

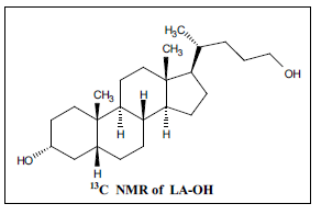

^{13}C NMR of LA-OH

4.6.2.14. Synthesis of LA-Thy

To a stirred solution of **LA-OH** (0.56 g, 1.54 mmol) and TBTU (0.59 g, 1.85 mmol) in anhydrous DMF (8 mL), Thy-CH_2CO_2H (0.30 g, 1.62 mmol) in DMF (6 mL) followed by DIEA (0.80 mL, 4.62 mmol) were added dropwise, and then the reaction mixture was allowed to react overnight at rt. Afterwards, it was poured into brine and extracted with CH_2Cl_2; the combined organic layers were washed with brine, dried over $MgSO_4$ and concentrated under reduced pressure. Purification by column chromatography (SiO_2, EtOAc:Hexane, 70:30) followed by (Li Chroprep RP-18, CH_3CN:H_2O, 90:10) gave **LA-Thy** as a colorless oil (0.29 g, 36%). ^{1}H NMR (300 MHz, $CDCl_3$): δ (ppm) 0.65 (s, 3H, CH_3); 0.91-2.03 (complex signal, 28H); 0.92 (d, *J* = 6.3 Hz, 3H, 21-CH_3); 0.93 (s, 3H, CH_3); 1.94 (d, *J* = 1.2 Hz, 3H, Thy-CH_3); 3.64 (m, 1H, 3β-H); 4.16 (m, 2H, CH_2), 4.45 (s, 2H, Thy-CH_2); 6.95 (*br* s, 1H, Thy-CH); 9.06 (s, 1H, Thy-NH). ^{13}C NMR (75 MHz, $CDCl_3$): δ (ppm) 167.7 (C), 164.2 (C), 150.9 (C), 140.3 (CH), 111.4 (C), 72.0 (CH), 66.9 (CH_2), 56.6 (CH), 56.1 (CH), 48.7 (CH_2), 42.9 (C), 42.2 (CH), 40.6 (CH), 40.3 (CH_2), 36.6 (CH_2), 36.0 (CH), 35.4(CH+CH_2), 34.7 (C), 32.0 (CH_2), 30.7 (CH_2), 28.4 (CH_2), 27.3 (CH_2), 26.6 (CH_2), 25.2 (CH_2), 24.4 (CH_2), 23.5 (CH_3), 21.0 (CH_2), 18.7 (CH_3), 12.5 (CH_3), 12.2 (CH_3); m/z found 529.3638, calculated for $C_{31}H_{49}N_2O_5$ (MH^+) 529.3641.

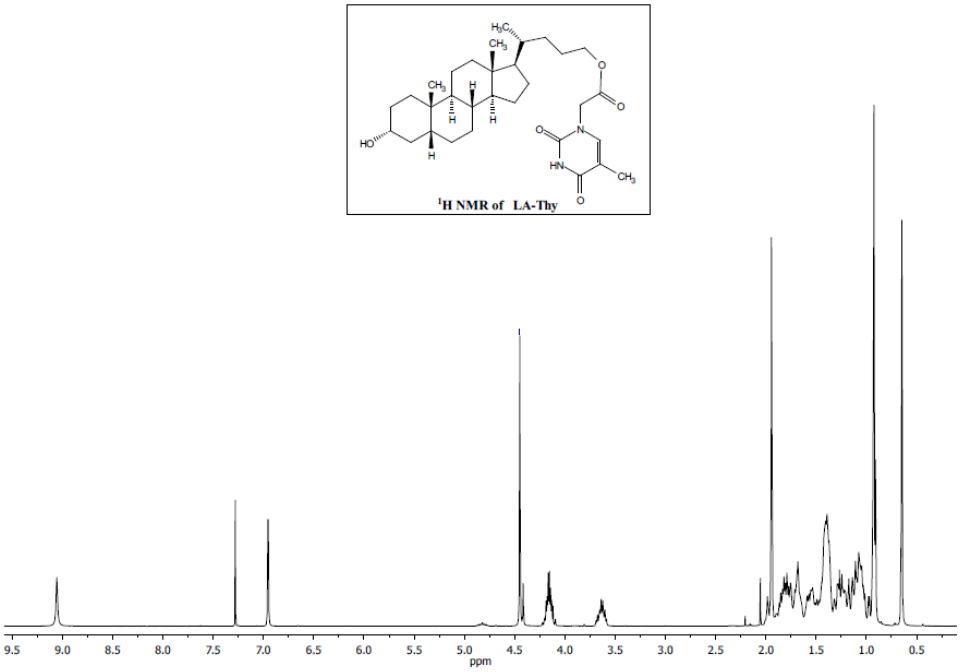
^{1}H NMR of LA-Thy
9.5 9.0 8.5 8.0 7.5 7.0 6.5 6.0 5.5 5.0 4.5 4.0 3.5 3.0 2.5 2.0 1.5 1.0 0.5
ppm

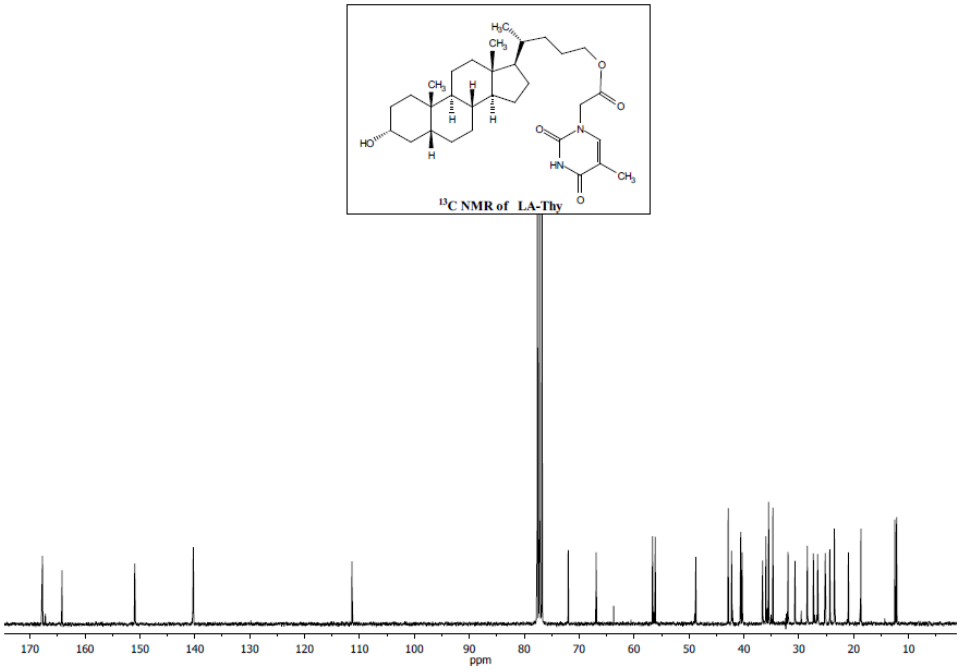
^{13}C NMR of LA-Thy
170 160 150 140 130 120 110 100 90 80 70 60 50 40 30 20 10
ppm

4.6.2.15. Synthesis of 3α-Cbz-LA-Thy

To a stirred solution of **LA-Thy** (0.09 g, 0.18 mmol) and TBTU (0.09 g, 0.26 mmol) in anhydrous DMF (1 mL), 9-carbazole acetic acid (0.06 g, 0.27 mmol) in DMF (2 mL) followed by DIEA (0.12 mL, 0.7 mmol) were added dropwise, and then the reaction mixture was allowed to react overnight at rt. Afterwards, it was poured into brine and extracted with CH_2Cl_2; the combined organic layers were washed with brine, dried over $MgSO_4$ and concentrated under reduced pressure. Purification by column chromatography (SiO_2, EtOAc:Hexane, 60:40) followed by (Li Chroprep RP-18, CH_3CN:H_2O, 95:5) gave **3α-Cbz-LA-Thy** as a colorless oil (0.11 g, 86%). ^{1}H NMR (300 MHz, $CDCl_3$): δ (ppm) 0.63 (s, 3H, CH_3); 0.79-1.97 (complex signal, 28H); 0.91 (*br* s, 6H, CH_3+21-CH_3); 1.91 (*br* d, *J* = 0.9 Hz, 3H, Thy-CH_3); 4.15 (m, 2H, CH_2), 4.39 (s, 2H, Thy-CH_2); 4.80 (m, 1H, 3β-H); 4.97 (s, 2H, Cbz-CH_2); 6.88 (s, 1H, Thy-CH); 7.22-7.37 (m, 4H, arom); 7.39-7.49 (m, 2H, arom); 8.10 (d, *J* = 7.8 Hz, 2H, arom); 9.20 (s, 1H, Thy-NH). ^{13}C NMR (75 MHz, $CDCl_3$): δ (ppm) 168.1 (C), 167.7 (C), 164.2 (C), 150.9 (C), 140.7 (2xC), 140.2 (CH), 126.0 (2xCH), 123.3 (2xC), 120.5 (2xCH), 119.7 (2xCH), 111.3 (C), 108.5 (2xCH), 76.3 (CH), 66.8 (CH_2), 56.5 (CH), 56.1 (CH), 48.7 (CH_2), 45.2 (CH_2), 42.8 (C), 42.0 (CH), 40.5 (CH), 40.2 (CH_2), 35.9 (CH), 35.4 (CH), 35.0 (CH_2), 34.6 (C), 32.2 (CH_2), 31.9 (CH_2), 28.4 (CH_2), 27.0 (CH_2), 26.7 (CH_2), 26.4 (CH_2), 25.1 (CH_2), 24.3 (CH_2), 23.4 (CH_3), 20.9 (CH_2), 18.7 (CH_3), 12.4 (CH_3), 12.1 (CH_3); m/z found 736.4345, calculated for $C_{45}H_{58}N_3O_6$ (MH^+) 736.4326.

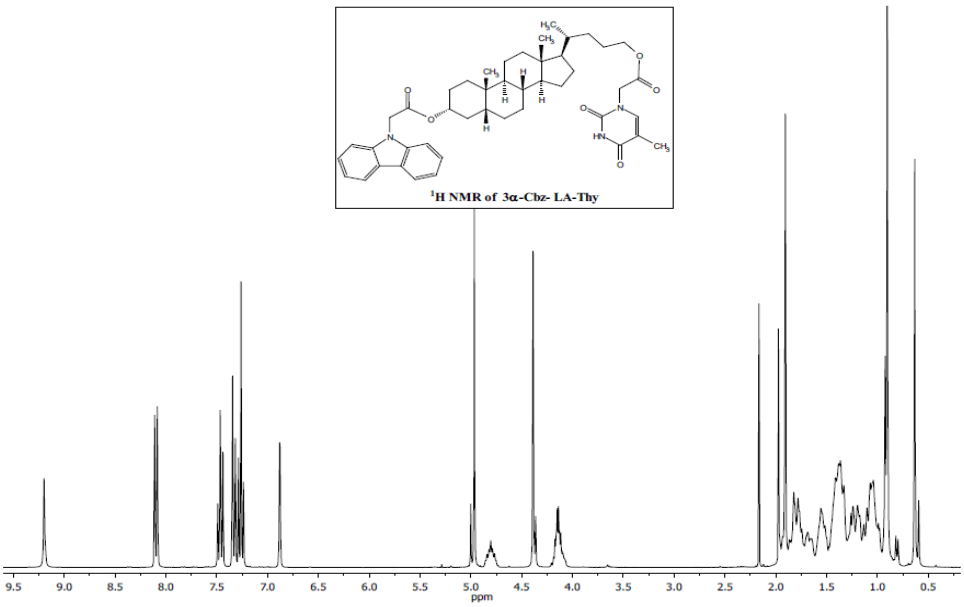
^{1}H NMR of 3α-Cbz- LA-Thy
9.5 9.0 8.5 8.0 7.5 7.0 6.5 6.0 5.5 5.0 4.5 4.0 3.5 3.0 2.5 2.0 1.5 1.0 0.5
ppm

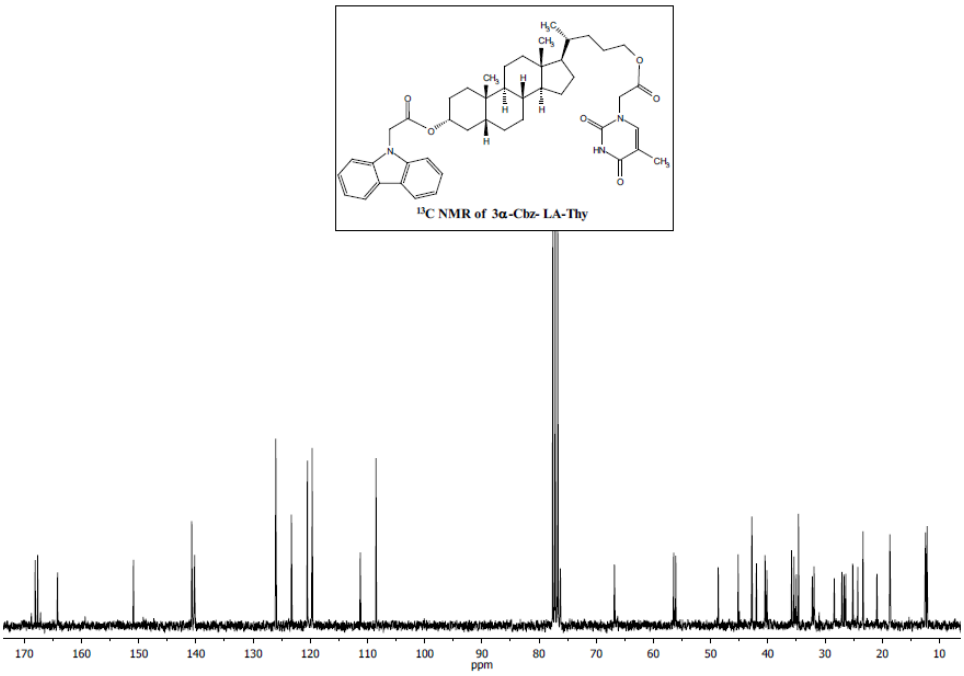
^{13}C NMR of 3α-Cbz- LA-Thy
170 160 150 140 130 120 110 100 90 80 70 60 50 40 30 20 10
ppm

4.6.2.16. Synthesis of 3α-Cbz-LA

To a stirred solution of **LA** (0.25 g, 0.66 mmol) and TBTU (0.32 g, 1.00 mmol) in anhydrous DMF (2.5 mL), 9-carbazole acetic acid (0.22 g, 1.00 mmol) in anhydrous DMF (2.5 mL) followed by DIEA (0.43 mL, 2.48 mmol) were added dropwise, and then the reaction mixture was allowed to react overnight at rt. Afterwards, it was poured into brine and extracted with CH_2Cl_2; the combined organic layers were washed with brine, dried over $MgSO_4$ and concentrated under reduced pressure. Purification by column chromatography (SiO_2, EtOAc:Hexane, 30:70) followed by (Li Chroprep RP-18, CH_3CN:H_2O, 95:5) gave **3α-Cbz-LA** as a white solid (0.18 g, 46%). ^{1}H NMR (300 MHz, $CDCl_3$): δ (ppm) 0.64 (s, 3H, CH_3); 0.85-2.46 (complex signal, 28H); 0.91 (s, 3H, CH_3); 0.92 (d, J = 6.6 Hz, 3H, 21-CH_3); 4.81 (m, 1H, 3β-H) 4.97 (s, 2H, CH_2); 7.23-7.38 (m, 4H, arom); 7.42-7.52 (m, 2H, arom); 8.10 (d, J = 7.8 Hz, 2H, arom). ^{13}C NMR (75 MHz, $CDCl_3$): δ (ppm) 180.0 (C), 168.2 (C), 140.8 (2xC), 126.1 (2xCH), 123.4 (2xC), 120.6 (2xCH), 119.7 (2xCH), 108.6 (2xCH), 76.3 (CH), 56.5 (CH), 56.1 (CH), 45.3 (CH_2), 42.9 (C), 42.0 (CH), 40.5 (CH), 40.2 (CH_2), 35.9 (CH), 35.4 (CH), 35.1 (CH_2), 34.7 (C), 32.3 (CH_2), 31.1 (CH_2), 30.9 (CH_2), 28.3 (CH_2), 27.1 (CH_2), 26.7 (CH_2), 26.4 (CH_2), 24.3 (CH_2), 23.4 (CH_3), 21.0 (CH_2), 18.4 (CH_3), 12.2 (CH_3); m/z found 584.3743, calculated for $C_{38}H_{50}NO_4$ (MH^+) 584.3740.

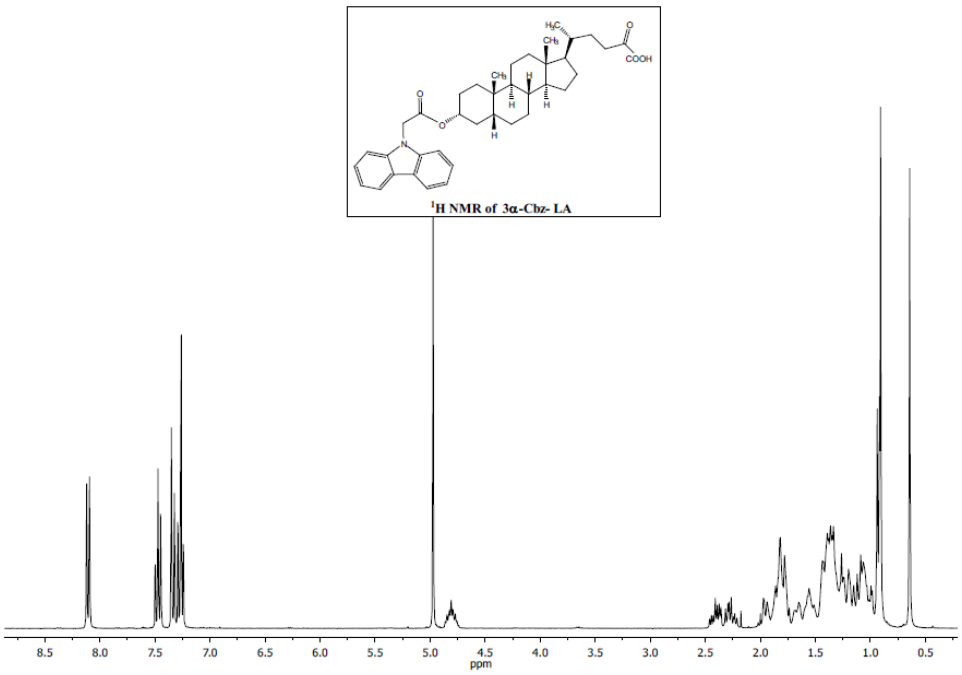
^{1}H NMR of 3α-Cbz- LA
8.5 8.0 7.5 7.0 6.5 6.0 5.5 5.0 4.5 4.0 3.5 3.0 2.5 2.0 1.5 1.0 0.5
ppm

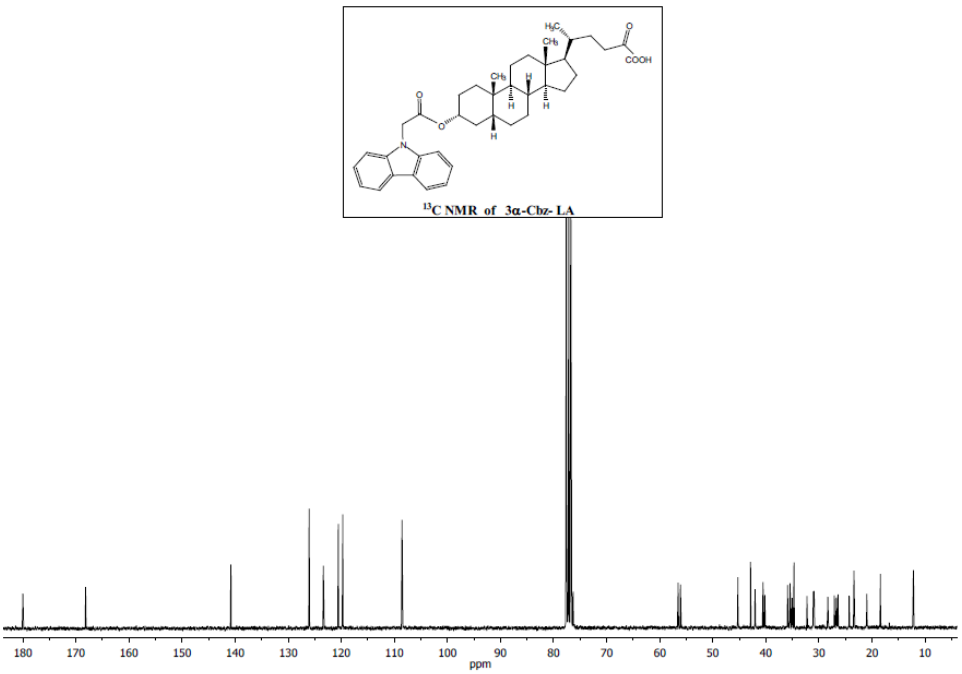
^{13}C NMR of 3α-Cbz- LA
180 170 160 150 140 130 120 110 100 90 80 70 60 50 40 30 20 10
ppm

4.6.2.17. Synthesis of 3α-Cbz-LA-Npt

To a stirred solution of **3α-Cbz-LA** (0.047 mg, 0.08 mmol) in CH_2Cl_2 (5 mL) containing EDC (0.019 mg, 0.085 mmol), a solution of NEA (0.013 mg, 0.08 mmol) in CH_2Cl_2 (2 mL) was added dropwise and the mixture was stirred overnight at rt. The crude product was washed consecutively with diluted $NaHCO_3$, HCl 1M and brine. Final purification by preparative layer chromatography (SiO_2 Merck 60 PF254,EtOAc:CH_2Cl_2, 20:80) gave **3α-Cbz-LA-Npt** (0.024 mg, 43%). ^{1}H NMR (300 MHz, $CDCl_3$): δ (ppm) 0.59 (s, 3H, CH_3); 0.86 (d, *J* = 6.4 Hz, 3H, 21-CH_3); 0.87-2.25 (complex signal, 28H); 0.90 (s, 3H, CH_3); 1.67 (d, *J* = 6.8 Hz, 3H, NEA-CH_3); 4.80 (m, 1H, 3β-H); 4.97 (s, 2H, CH_2); 5.62 (d, *J* = 8.4 Hz, 1H, NEA-NH); 5.94 (m, 1H, NEA-CH); 7.22-7.29 (m, 2H, arom); 7.29-7.38 (m, 2H, arom); 7.43-7.59 (m, 6H, arom), 7.78-7.89 (m, 2H, arom); 8.10 (d, *J* = 7.6 Hz, 3H, arom). ^{13}C NMR (100 MHz, $CDCl_3$): δ (ppm) 172.5 (C), 168.2 (C), 140.8 (2xC), 138.4 (C), 134.1 (C), 131.3 (C), 128.9 (CH), 128.5 (CH), 126.7 (CH), 126.1 (3xCH), 125.3 (CH), 123.7 (CH), 123.4 (2xC), 122.7 (CH), 120.6 (2xCH), 119.7 (2xCH), 108.5 (2xCH), 76.3 (CH), 56.5 (CH), 56.2 (CH), 45.2 (CH_2), 44.6 (CH), 42.8 (C), 42.0 (CH), 40.5 (CH), 40.2 (CH_2), 35.9 (CH), 35.6 (CH), 35.0 (CH_2), 34.7 (C), 33.9 (CH_2), 32.2 (CH_2), 31.9 (CH_2), 28.4 (CH_2), 27.1 (CH_2), 26.7 (CH_2), 26.4 (CH_2), 24.3 (CH_2), 23.4 (CH_3), 21.0 (CH_2), 20.7 (CH_3), 18.5 (CH_3), 12.2 (CH_3); m/z found , 736.4654, calculated for $C_{50}H_{61}N_2O_3$ (MH^+), 736.4602.

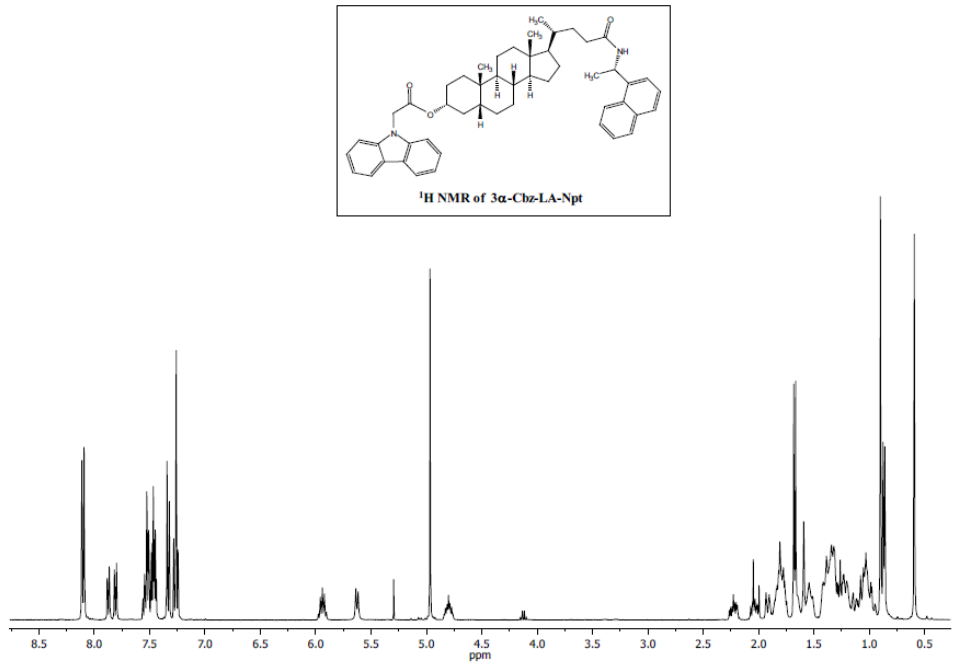
^{1}H NMR of 3α-Cbz-LA-Npt
8.5
8.0
7.5
7.0
6.5
6.0
5.5
5.0
4.5
4.0
3.5
3.0
2.5
2.0
1.5
1.0
0.5
ppm

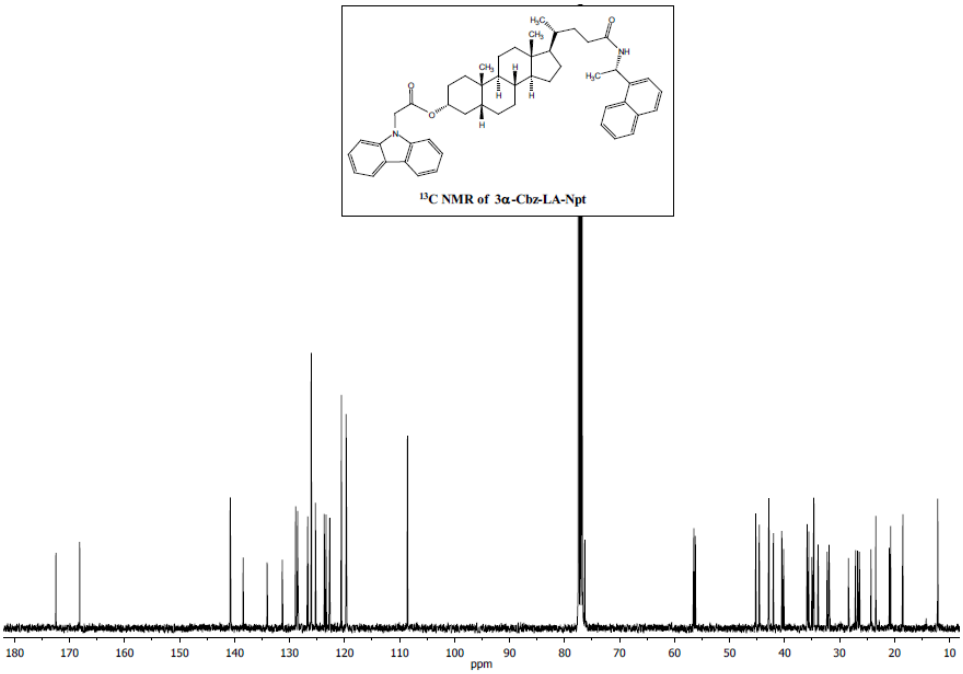
^{13}C NMR of 3α-Cbz-LA-Npt
180
170
160
150
140
130
120
110
100
90
80
70
60
50
40
30
20
10
ppm

4.7. Supplementary material

4.7.1. UV-Vis characterization

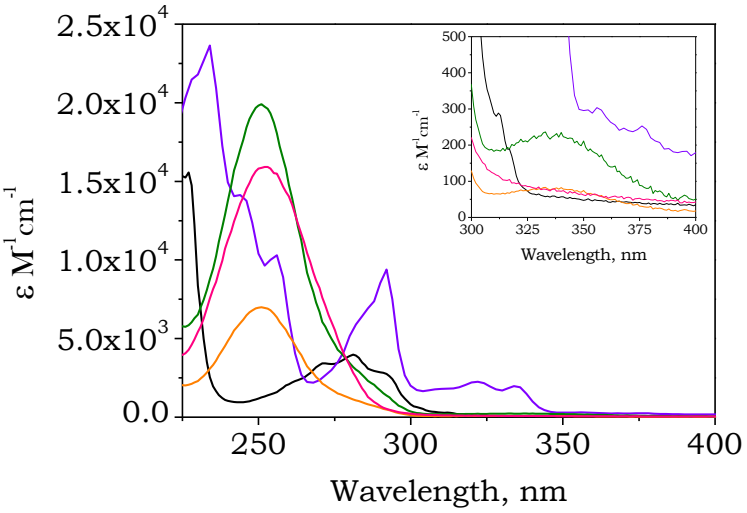

Figure 4.19. UV-Vis absorption spectra of **3α-Bzp-LA** (green), **3α-Cbz-LA** (purple), **LA-Npt** (black), **LA-Bip** (red) and **LA-Thy** (orange). Inset: zoom of the 300 – 400 nm region.

4.7.2. Instrumentation

Laser flash photolysis at 355 nm. Transient spectra were recorded at room temperature using N_2-purged solutions of the corresponding compound at 5 x 10^{-5} M in CH_2Cl_2.

Laser flash photolysis at 308 nm. Transient spectra were recorded at room temperature using N_2-purged solutions of 2.5 x 10^{-5} M in CH_2Cl_2.

Phosphorescence. Samples were dissolved in ethanol, cooled at 77 K and excited at 355 nm except of **LA-Npt** (λ_{exc}= 266 nm) and **LA-Bip** (λ_{exc}= 285 nm) for the measurements.

4.7.3. Additional NMR spectra

4.7.3.1. 3α-Bzp-LA

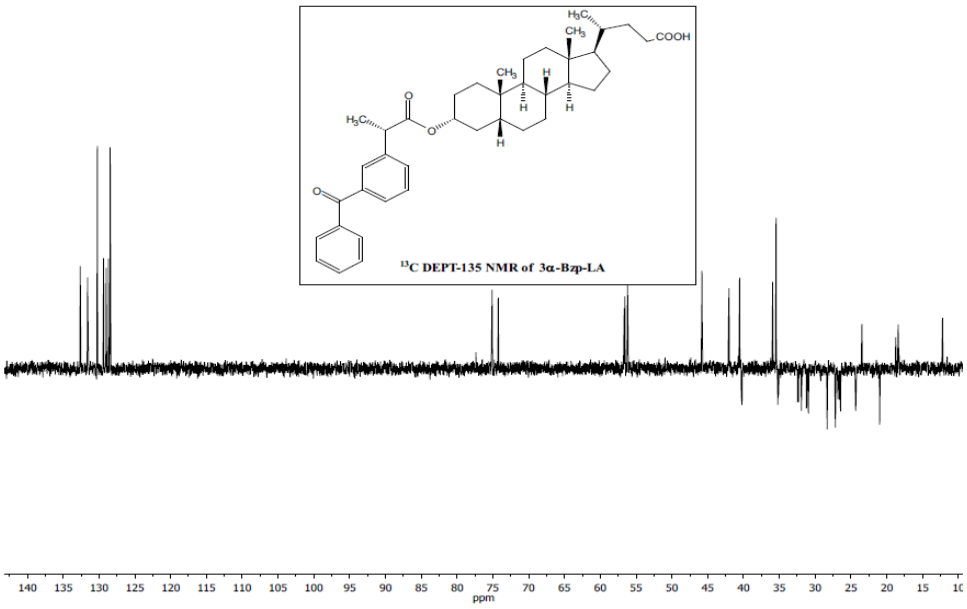

4.7.3.2. 3α-Bzp-LA-Npt

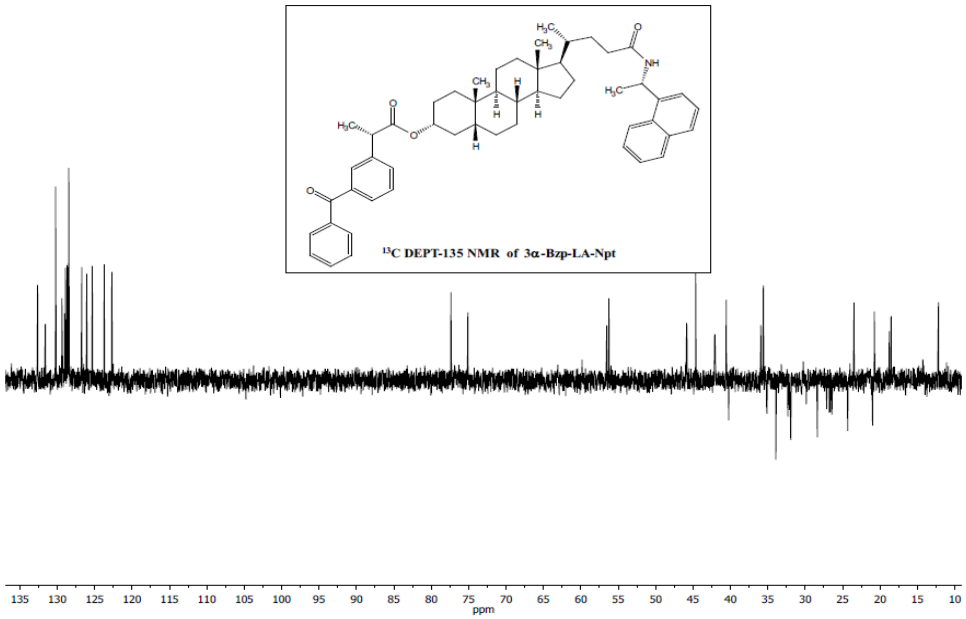

4.7.3.3. LA-Npt

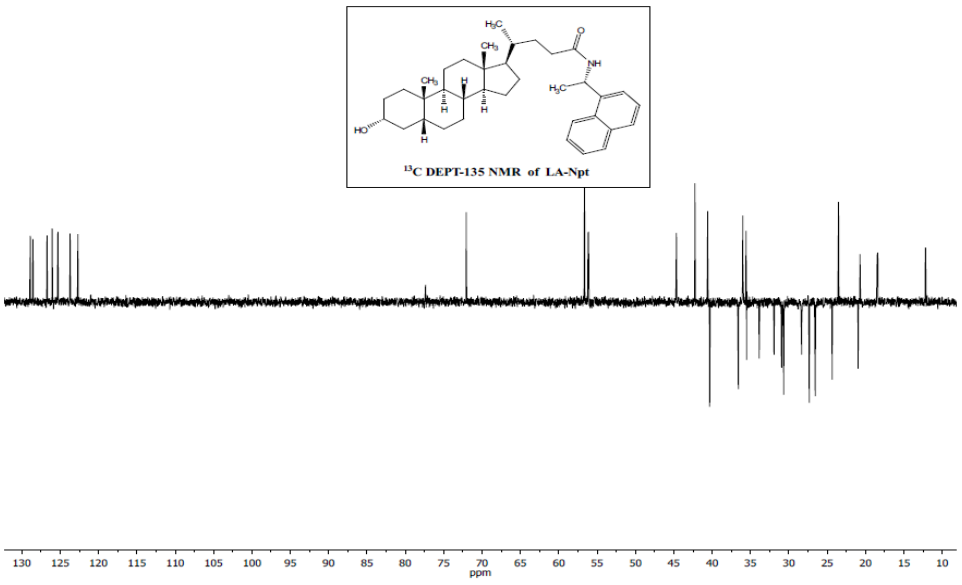

4.7.3.4. 3 β -NBz-LA

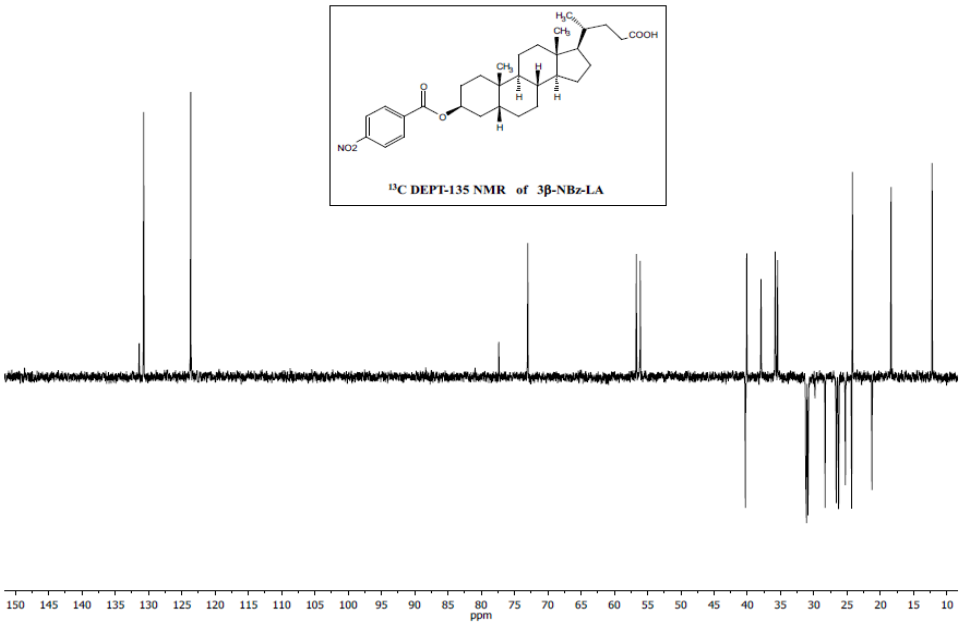

4.7.3.5. 3 β -OH-LA

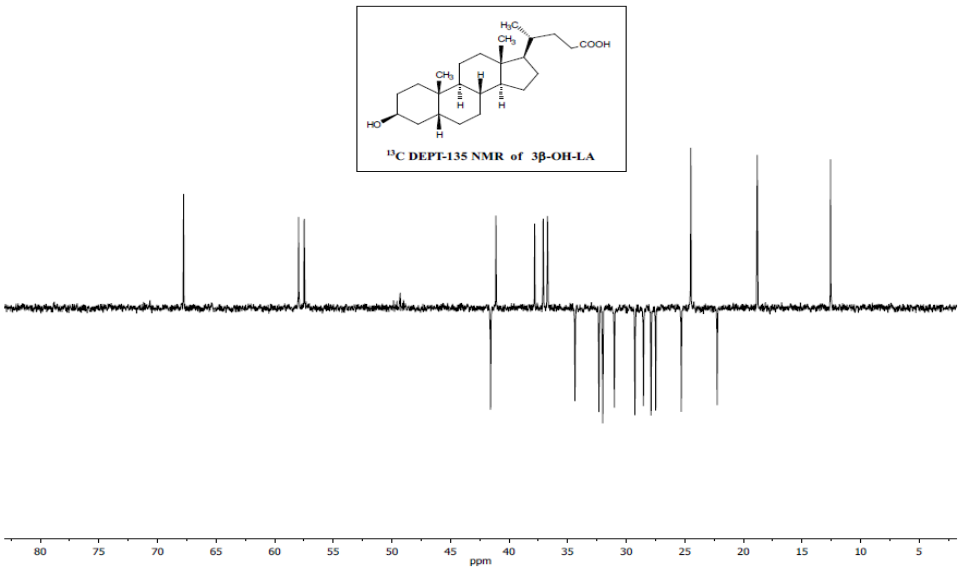

4.7.3.6. 3 β -Bzp-LA

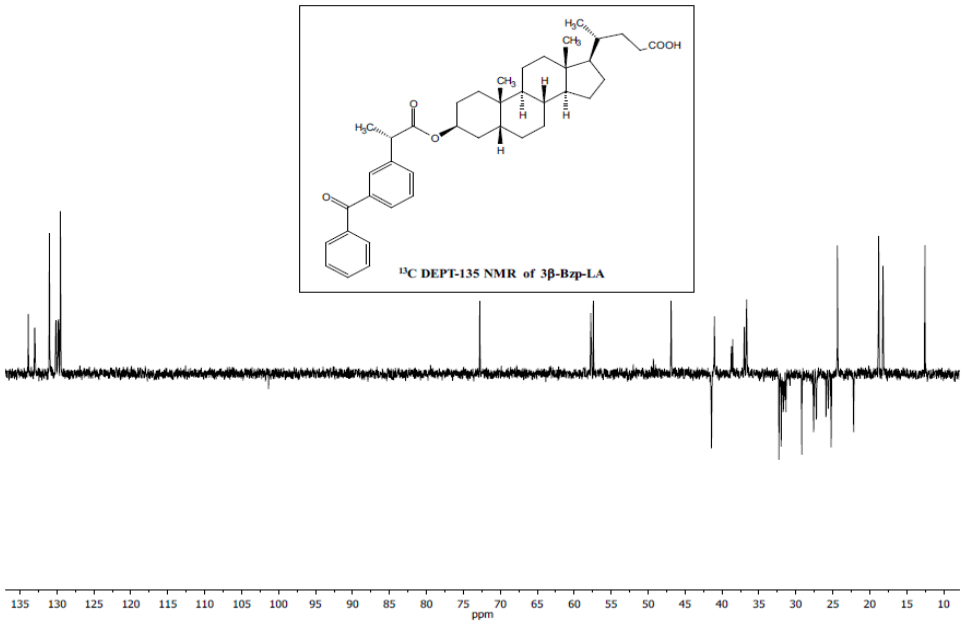

4.7.3.7. 3 β -Bzp-LA-Npt

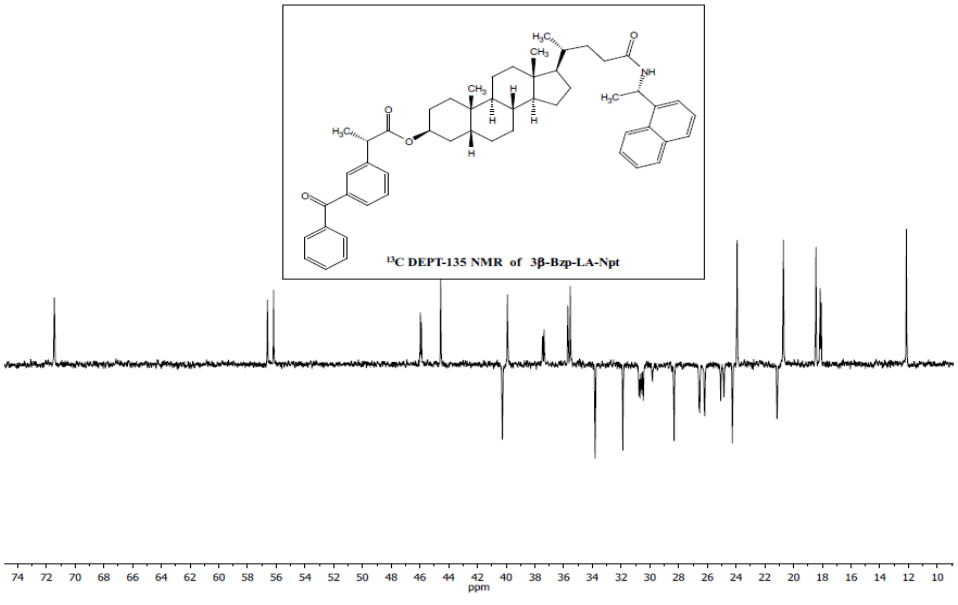

4.7.3.8. 3 β -Bzp-LA-Bip

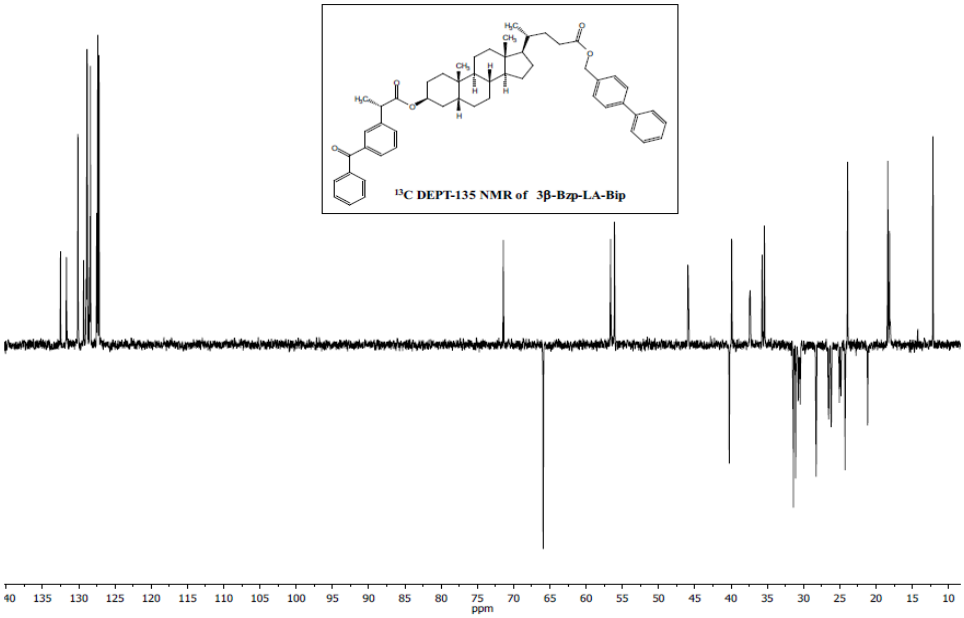

4.7.3.9. LA-Bip

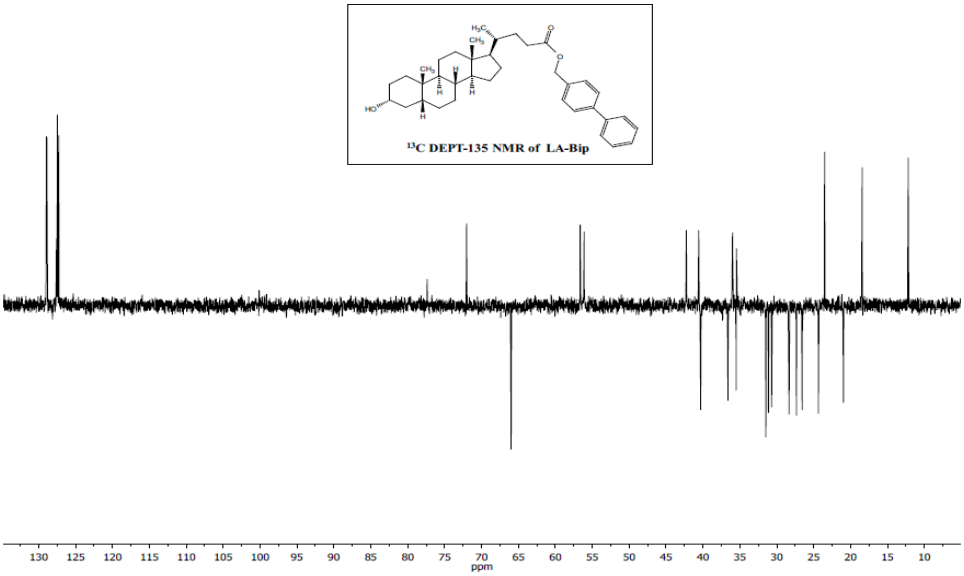

4.7.3.10. 3α-Bzp-LA-Bip

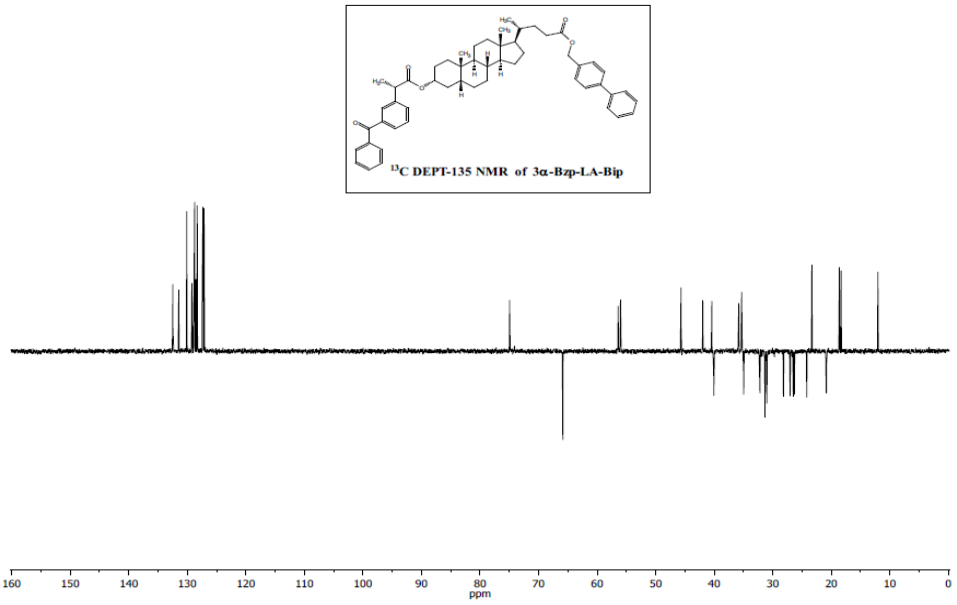

4.7.3.11. Bzp-Npt

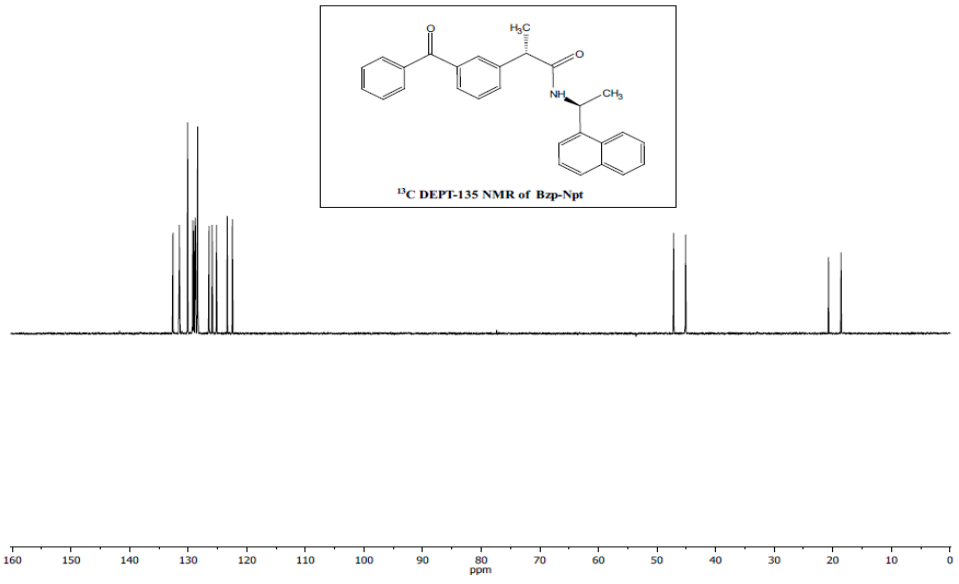

4.7.3.12. Bzp-Bip

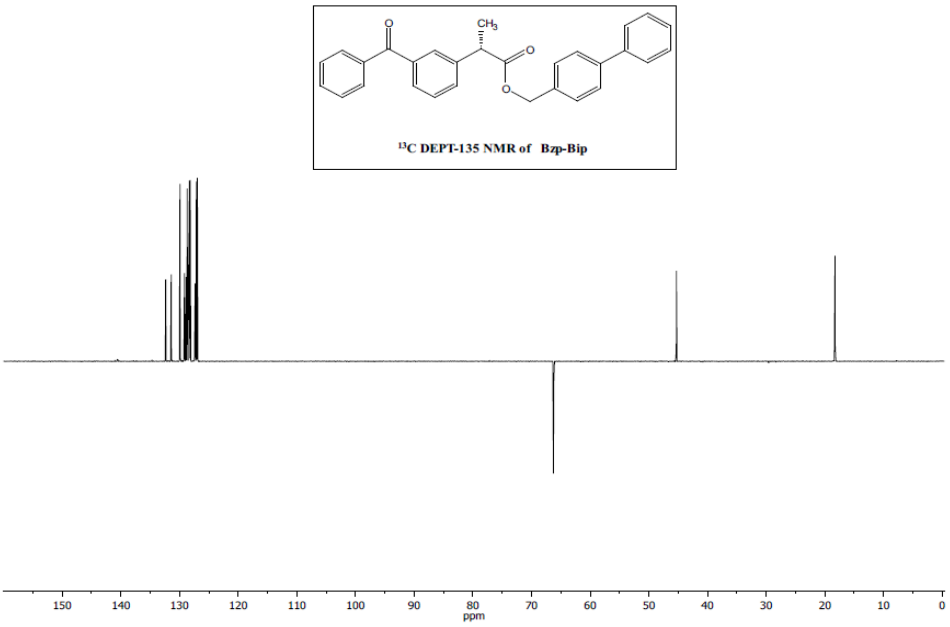

4.7.3.13. LA-OH

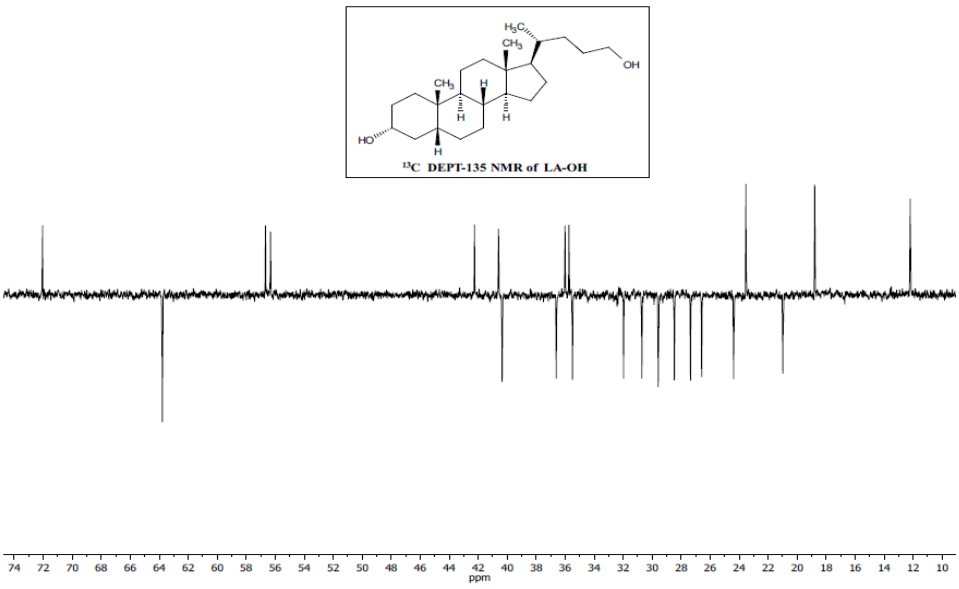

4.7.3.14. LA-Thy

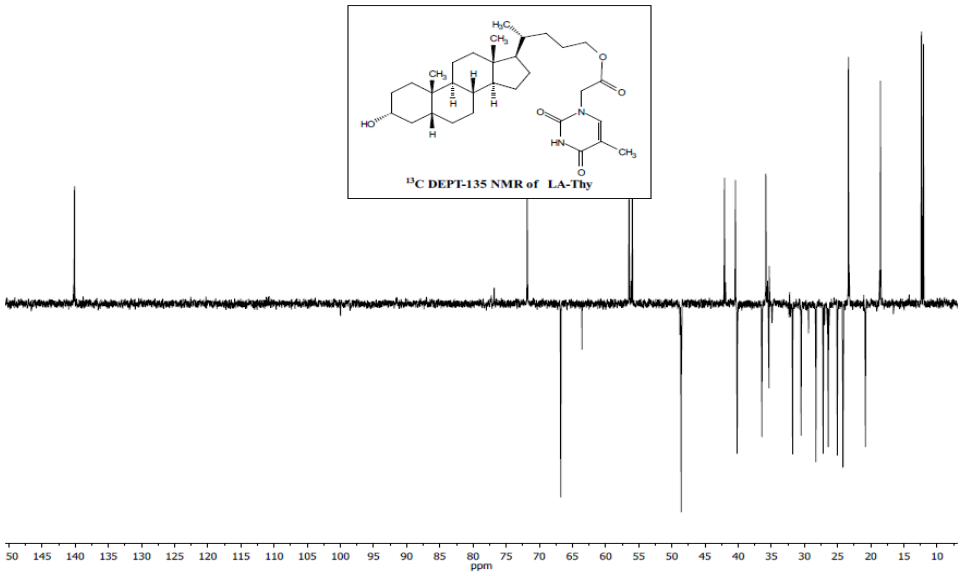

4.7.3.15. 3α-Cbz-LA-Thy

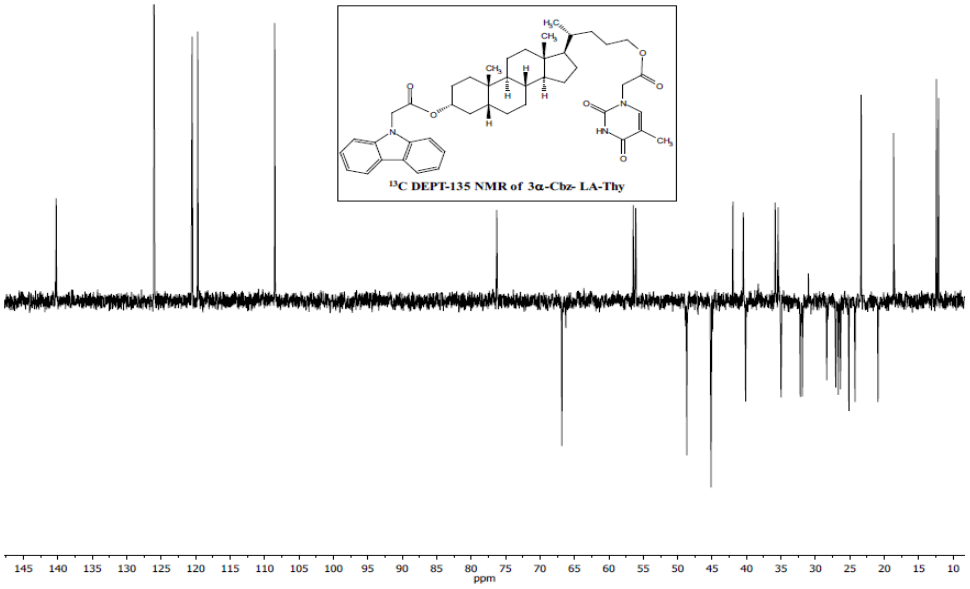

4.7.3.16. 3α-Cbz-LA

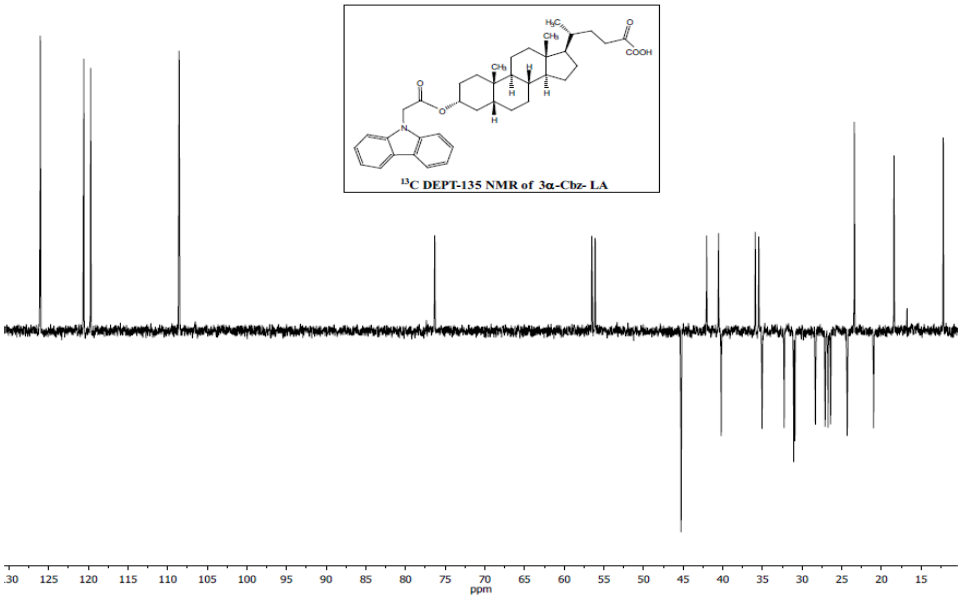

4.7.3.17. 3α-Cbz-LA-Npt

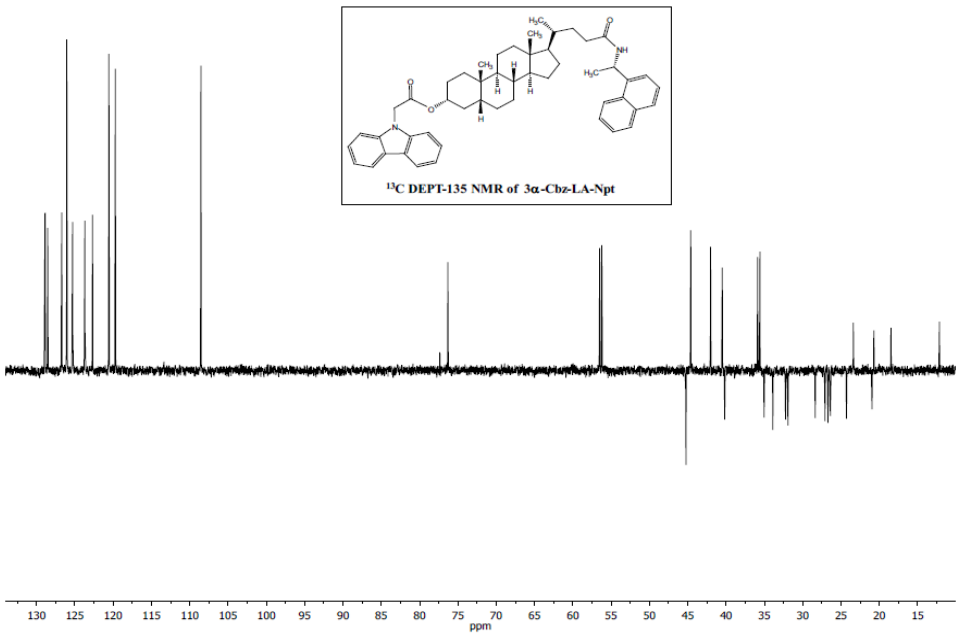

4.7.4. Molecular dynamics

Molecular dynamics were performed using the widely used Universal force field[132] (UFF) as well as a modified version, which we will call modified-UFF. Universal Force Field (UFF) has been used in previous studies with reasonable results for the two- three- and four-body interactions and here a modification has been introduced in the van der Waals interactions. Due to the presence of two chromophores containing aromatic rings at either end of the molecules **3α-Bzp-LA-Bip** and **3β-Bzp-LA-Bip**, the dispersion interactions will play an important role, and hence we have employed a force field (modified-UFF) containing dispersion coefficients taken from recent quantum chemistry results.

In the modified-UFF, the usual 12-6 Lennard-Jones term has been maintained with a slight modification. The repulsive term and the corresponding parameters have been kept, whilst the dispersive-attractive terms have been replaced by that of Grimme-D2,[133] recently introduced in DFT in order to account for dispersive interactions. In this term, a damping function has been introduced, which removes the artifact at short distances without noticeable changes in the region of the minimum.

After making several comparisons with the DFT results it was observed that UFF energetically overfavoured the folded conformations with respect to the unfolded due to the very large dispersive coefficients in the van der Waals term. Therefore, the modified-UFF, which corrected this misbehavior by using smaller dispersive coefficients, was used throughout.

The GULP software[134,135] (version 4.3.2) has been used, able to run in parallel for the evaluation of the energy and first derivatives using MPI, based on a replicated data algorithm. This version allows for the introduction in the force field of the Grimme-D2 functional to describe the dispersion interactions. The use of an atomistic (rather than quantum) approach allowed us two advantages in the calculations: a) the simulations could be extended to a much longer simulation time, which means that a statistically significant number of configurations were sampled, and b) the solvent molecules could be included in the simulations. Solvent molecules were included in a continuum model

according to the COSMIC algorithm introduced in GULP since version 4.0. The solvent included was dichloromethane. Molecular dynamics were carried out in the Npt ensemble using a time step of 1 fs, and with relaxation times for thermostat and bar stat set to 1 ps. The simulations comprised one molecule of **3α-Bzp-LA-Bip** or **3β-Bzp-LA-Bip** and run for 2 ns.

Chapter 5: Photosensitized Thymine Dimerization *via* Triplet Exciplexes*

5.1. Introduction

Ultraviolet solar radiation reaching the Earth surface has been widely reported as a potential mutagenic agent.[136] Fortunately, the ozone layer is able to block UVC below *ca.* 290 nm, which would be directly absorbed by biomolecules;[137] however, UVB (290–320 nm) and UVA (320–400 nm) are less efficiently filtered by the atmosphere and may cause photochemical alterations of the DNA structure, eventually leading to skin cancer.[138]

Nucleobases are able to absorb UVB light, causing direct photoreactions such as formation of cyclobutane thymine dimers (Thy<>Thy) or (6–4) photoproducts that have been reported among the most mutagenic alterations.[139–141]

*Reproduced in part from: P. Miro, V. Lhiaubet-Vallet, M. L. Marin and M. A. Miranda, *Chem. Eur. J.*, 2015, **21**, 17051 - 17056, with permission from ChemPubSoc Europe

Although the UVA fraction of solar light is less efficiently absorbed by the nucleobases, the presence of endogenous or exogenous photosensitizers that can be excited in that region, may greatly enhance UVA-mediated photochemical disorders. In this context, benzophenone (Bzp) and drugs containing the Bzp chromophore have been widely reported as DNA photosensitizers,[40,48,142] due to the following Bzp properties: i) it extends the active fraction of solar light up to 360 nm; ii) it exhibits a high intersystem crossing quantum yield;[22] iii) its triplet energy is close to that of Thy, the nucleobase with the lowest triplet state (in the order of 74 kcal mol^{-1})[22,48,131] and iv) it has a moderate triplet lifetime.[22]

It is assumed that Bzp-photosensitized DNA damage includes triplet-triplet energy transfer (TTET) from ^{3}Bzp* to Thy (whose triplet energy in DNA is 270 kJ mol^{-1})[143], followed by 2+2 cycloaddition yielding Thy<>Thy.[40,48,142] This occurs along with the Paternò-Büchi reaction between ^{3}Bzp* and Thy resulting in the formation of oxetanes, which have been claimed as models to mimic the highly unstable intermediates involved in the repair of (6-4) photoproducts.[48-52]

The rate constant for TTET should be related to the energy gap between ^{3}Bzp* and ^{3}Thy*.[144] Although it seems a slightly disfavored process in solution (70 and 74 kcal mol^{-1} for Bzp and Thy, respectively), it is still feasible at room temperature through population of the upper vibrational states. Thus, it can compete with the formation of oxetanes, which is possible because of the $n\pi^*$ configuration of the lowest triplet of ^{3}Bzp* and the absence of back reaction due to the lack of absorbance of the formed oxetanes in the UVA region.

In fact, previous studies have demonstrated that in solution ^{3}Bzp* is efficiently quenched by Thy derivatives (k_q in the range of 10^8-10^9 $M^{-1}s^{-1}$).[49,145,146] Sandros equation[144] states that for endergonic triplet energy transfer reactions, the bimolecular rate constant decreases exponentially with the increasing energy gap between the donor and the acceptor (Eq. 5.1).

$$k_{ET} = k_D \frac{1}{(e^{-\frac{\Delta E}{RT}}+1)} \qquad \text{Eq. 5.1}$$

Where k_{ET} is the energy transfer rate constant, k_D is the diffusion rate constant in liquid solution and ΔE is the energy gap between the triplets of the donor and the acceptor.

According to Sandros equation, the expected rate constant for TTET in solution is at least one order of magnitude lower than formation of oxetanes due to the almost isoenergetic ^{3}Bzp* and ^{3}Thy* involved; hence, the quenching rate constant essentially accounts for the formation of oxetanes.

The intramolecular version of this reaction has also been investigated, attaching directly one molecule of the chromophore to the sugar moiety of thymidine (Thd). Irradiation of the dyad leads to a mixture of photoproducts, in which the oxetanes are the major ones.[147]

A simplified mechanistic explanation of the reaction between ^{3}Bzp* and Thy is summarized in equations 5.2–5.4:[148]

^{3}Bzp* + Thy ⟶ oxetanes Eq. 5.2

^{3}Bzp* + Thy ⟶ Bzp + ^{3}Thy* Eq. 5.3

^{3}Thy* + Thy ⟶ Thy<>Thy Eq. 5.4

Interestingly, irradiation of Bzp in the presence of Thy derivatives (2:1 ratio) gives mainly oxetanes, while dimers predominate in the presence of large excess of Thy.[49,146] Although formation of dimers is dependent on Thy concentration according to Eq. 5.3, also the formation of oxetanes may be according to Eq. 5.2, so the observed changes in the oxetane to dimer ratio are clearly more marked than expected from kinetic analysis. Moreover, the unambiguous detection of cytosine (Cyt) dimers (Cyt<>Cyt) in photosensitized DNA (in spite of the triplet energy of Cyt, *ca.* 77 kcal mol^{-1})[131] suggests

that formation of locally excited pyrimidine triplet states may not be the only mechanism of dimerization and that cooperative excited states may play a significant role.[149]

In this context, excited termolecular complexes (triplet triplexes) have previously been proposed to explain the results obtained upon photosensitization of a variety of 4+2 and 2+2 cycloadditions.[127,150-152] However, the involvement of triplet triplexes has never been described in the case of DNA, but it could account for most of the experimental observations on the Bzp-photosensitized pyrimidine dimerization. This hypothesis is illustrated in equations 5.5 to 5.8:

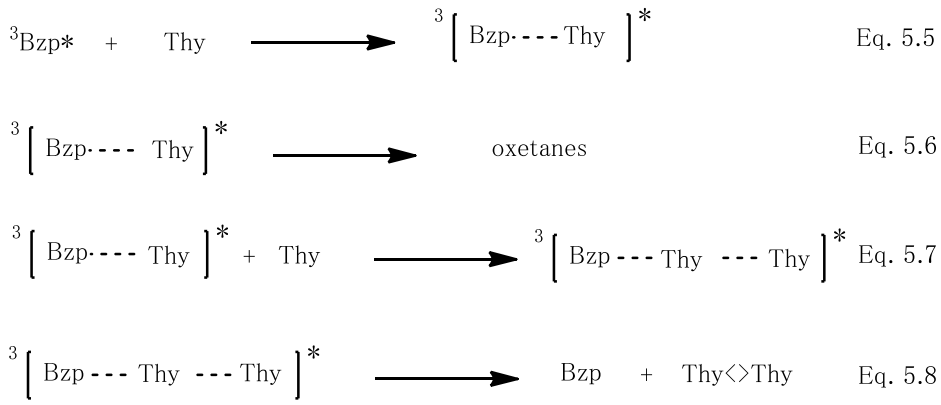

Thus, quenching of $^3Bzp^*$ by Thy would lead to oxetanes *via* triplet exciplexes, while interaction of the latter with a second Thy unit would afford triplet triplexes, the immediate precursor of Thy<>Thy. This mechanistic pathway, indeed agrees with the observed experimental tendency, which implies the higher formation of Thy<>Thy over oxetanes when the concentration of Thy increases.

In order to provide experimental evidence supporting the proposed triplex mechanism, two Thy units have been now tethered to an appropriate bile acid (BA) scaffold. For this purpose, deoxycholic acid (**DCA**) has been selected as an appropriate skeleton, since it offers a rigid structure with two hydroxyl groups on the same face of the molecule allowing covalent attachment of the Thy bases. Linking the carboxylic acid

of the lateral chain with a Bzp moiety would lead to a fully intramolecular system where binary Bzp/Thy and Thy/Thy interactions (required in the currently accepted mechanism) are possible; by contrast, ternary Bzp/Thy/Thy interactions (involved in the novel proposal) would be prevented due to geometrical strain. Conversely, increasing the degrees of freedom by replacement of the intramolecular with an intermolecular Bzp chromophore should allow assembling a reactive triplet triplex, providing an experimental proof of the concept.

5.2. Synthesis

Two analogs have been synthesized using the skeleton of **DCA** (see Scheme 5.1). In the first one, the two Thy units were covalently attached at positions 3α- and 12α- and the Bzp chromophore was esterified at the lateral chain; while in the second analog, Bzp was replaced with a benzyl group, which does not absorb in the UVA.

The developed synthetic strategy outlined in Scheme 5.1 started with the esterification of the carboxylic acid moiety of **DCA** with the (*S*)-enantiomer of reduced ketoprofen (KP-OH) to give **DCA-Bzp**. Then, in the presence of an excess of Thy-CH_2CO_2H, the two hydroxyl groups at 3α- plus 12α- were simultaneously esterified providing **3α,12α-2Thy-DCA-Bzp**. To prepare the derivative without the Bzp unit, the carboxylic group at the lateral chain of **DCA** was reacted with benzyl bromide, giving **DCA-Bn**. Subsequent treatment with Thy-CH_2CO_2H yielded **3α,12α-2Thy-DCA-Bn**.

Synthetic procedures, NMR spectroscopic data and exact mass for the new compounds are detailed in the experimental section of this chapter. Further NMR experiments and experimental procedures can be found in the supplementary material of this chapter.

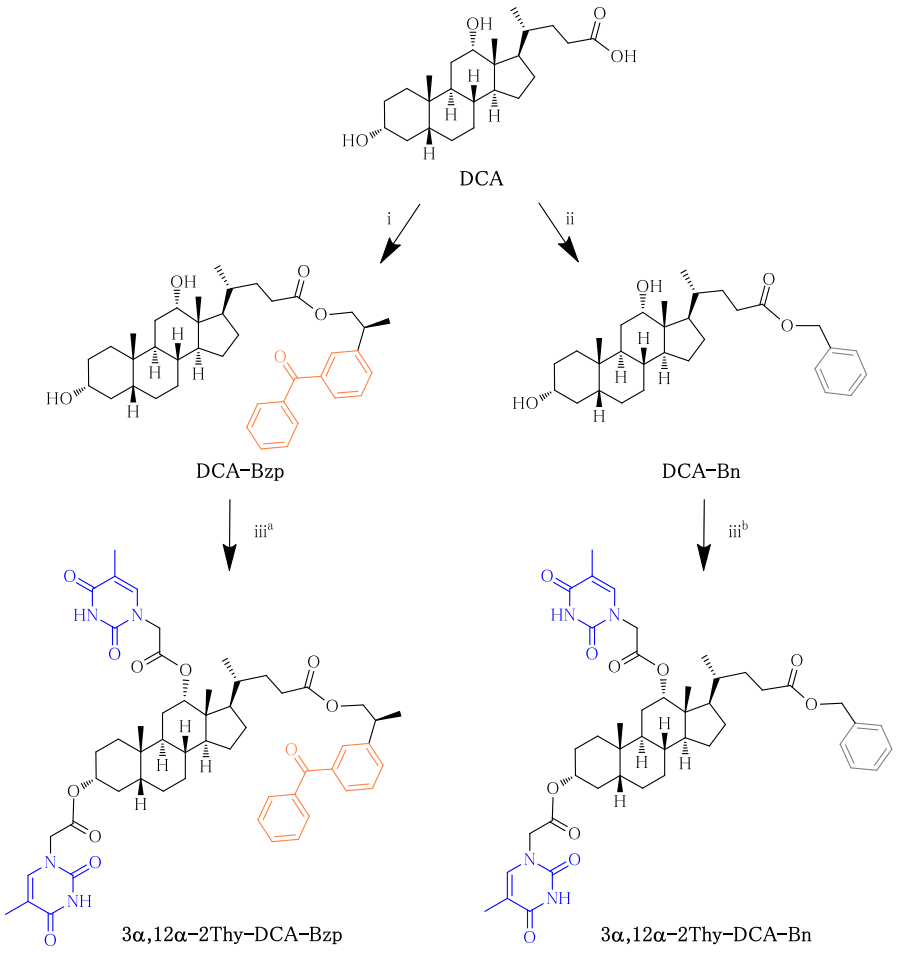

Scheme 5.1. Developed synthetic strategy to prepare **DCA** derivatives incorporating Bzp or Bn at the lateral chain plus two Thy units. Reagents and conditions: (i) KP-OH, 4-DMAP, EDC, C_5H_5N, (55%); (ii) benzyl bromide, DBU, DMF, (57%); (iii) Thy-CH_2CO_2H, Et_3N, 2,4,6-trichlorobenzoyl chloride, 4-DMAP, THF, [a](94%), [b](95%).

5.3. Results and discussion

5.3.1. Photophysics

Laser flash photolysis (LFP) was employed to monitor the triplet state obtained upon 355 nm excitation of the Bzp chromophore in the presence of two Thy units in the following systems: i) the fully intramolecular **3α,12α-2Thy-DCA-Bzp** and ii) the intermolecular mixture of the parent Bzp and the non-absorbing **3α,12α-2Thy-DCA-Bn**. Although at this stage determination of the Bzp triplet lifetimes should provide useful information on excited state interactions, this was not expected to discriminate between the Thy dimerization mechanism actually involving triplet energy transfer and that occurring *via* formation of triplet triplexes.

Thus, the triplet of **3α,12α-2Thy-DCA-Bzp** was monitored at 530 nm (Figure 5.1, left) and compared to that of **DCA-Bzp**, as a reference compound with the Bzp bound to the BA, but lacking the two Thy units. Decays were fitted to a first order exponential equation and their lifetimes (τ) resulted to be 0.08 and 1.01 μs, respectively. More accurate determination was achieved by means of energy transfer to naphthalene (Npt)[51] (Figure 5.1, right), which led to a value of 0.097 μs. This indicates a fast intramolecular deactivation of the triplet, with a rate constant of 9.3 x 10^6 s^{-1} (k = $1/\tau_{\text{3α,12α-2Thy-DCA-Bzp}} - 1/\tau_{\text{DCA-Bzp}}$).

Then, the lifetime of ^{3}Bzp* was monitored upon addition of increasing concentrations of **3α,12α-2Thy-DCA-Bn** (Figure 5.2, left). Stern-Volmer plots of the reciprocal lifetimes obtained in each case allowed determining the quenching rate constant, which was found to be 3.7 x 10^8 M^{-1} s^{-1} (Figure 5.2, right). For comparison, quenching of ^{3}Bzp* by Thy occurred with k = 1.4 x 10^8 M^{-1} s^{-1}, which is reasonably in agreement with the quenching of ^{3}Bzp* by **3α,12α-2Thy-DCA-Bn**, which contains two units of Thy per molecule.

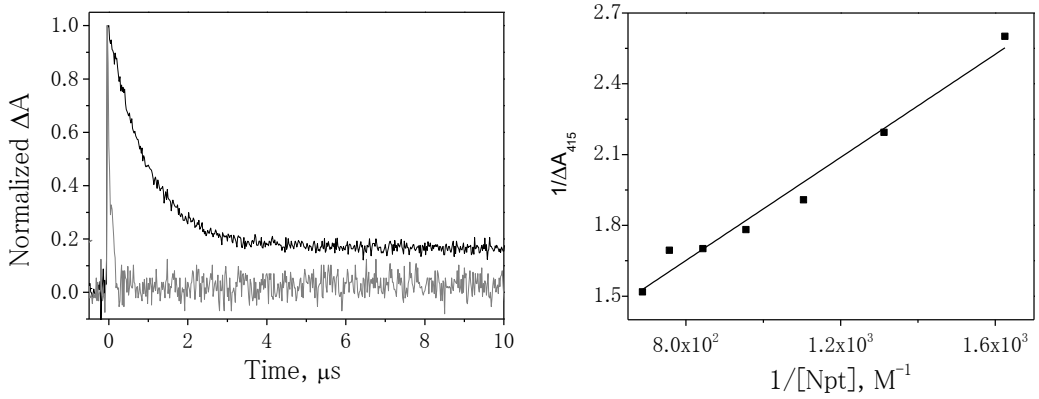

Figure 5.1. Left: LFP decays monitored at 530 nm of **DCA-Bzp** (black) and **3α,12α-2Thy-DCA-Bzp** (grey) in 4 CH_3CN:1H_2O obtained upon excitation at 355 nm. Right: double reciprocal plot for energy transfer from **3α,12α-2Thy-DCA-Bzp** to Npt, revealed through the absorbance of the ^{3}Npt* at 415 nm, immediately after the laser pulse.

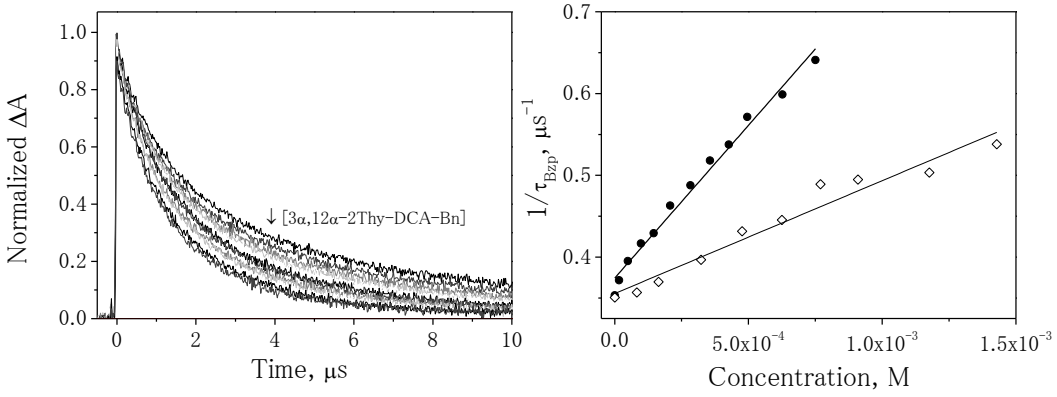

Figure 5.2. Left: LFP decays of ^{3}Bzp* monitored at 530 nm with increasing concentrations of **3α,12α-2Thy-DCA-Bn** in 4 CH_3CN:1H_2O obtained upon excitation at 355 nm. Right: Stern-Volmer plot for the quenching of ^{3}Bzp* by **3α,12α-2Thy-DCA-Bn** (●) or by Thy (◊).

5.3.2. Photochemistry

After completing the photophysical studies, the same systems were submitted to steady-state photolysis, in order to investigate their photoreactivity and the nature of the obtained photoproducts. Thus, selective irradiation of the Bzp chromophore at λ_{max} = 350 nm was monitored through the changes in the UV-visible spectra (Figures 5.3 and 5.4, left). The results for **3α,12α-2Thy-DCA-Bzp** are shown in Figure 5.3, and those corresponding to the intermolecular mixture **Bzp:3α,12α-2Thy-DCA-Bn** can be found in Figure 5.4.

A progressive decrease of the absorbance was observed in both systems, whereas the control mixture of Bzp:Thy (1:2 ratio) was almost unreactive (Figures 5.3, right and 5.4, right). Furthermore, when the residual UV spectra of **3α,12α-2Thy-DCA-Bzp** and **Bzp:3α,12α-2Thy-DCA-Bn** after reaction completion were compared to the hypothetical absorption due to unreacted Bzp or Thy (orange or blue traces, respectively, in Figures 5.3, left and 5.4, left), a different reaction pattern was envisioned. In fact, the UV spectrum of **3α,12α-2Thy-DCA-Bzp** at the end of the reaction was comparable to the one of Thy, pointing to the formation of an oxetane; conversely, the UV spectrum of the **Bzp:3α,12α-2Thy-DCA-Bn** system after irradiation resembled the one of Bzp, thus indicating formation of Thy<>Thy. Indeed, this was confirmed by analysis of the resulting photoproduct mixtures.

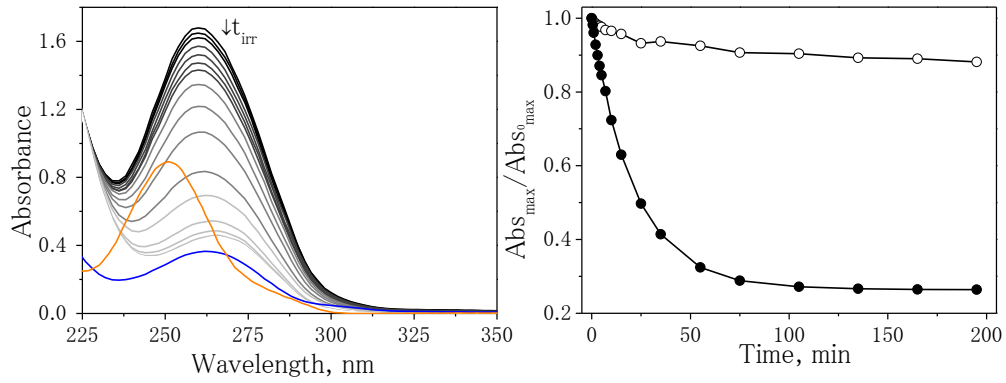

Figure 5.3. Left: UV-Vis spectra of **3α,12α-2Thy-DCA-Bzp** monitored at different irradiation (λ_{max} = 350 nm) times (C_i = 4.4 x 10^{-5}M in 4 CH_3CN:1H_2O); UV spectra of **Bzp** (orange) and **Thy** (blue) recorded at 4.4 x 10^{-5} M. Right: photoreaction kinetics of **3α,12α-2Thy-DCA-Bzp** (●) compared to **1Bzp:2Thy** (○).

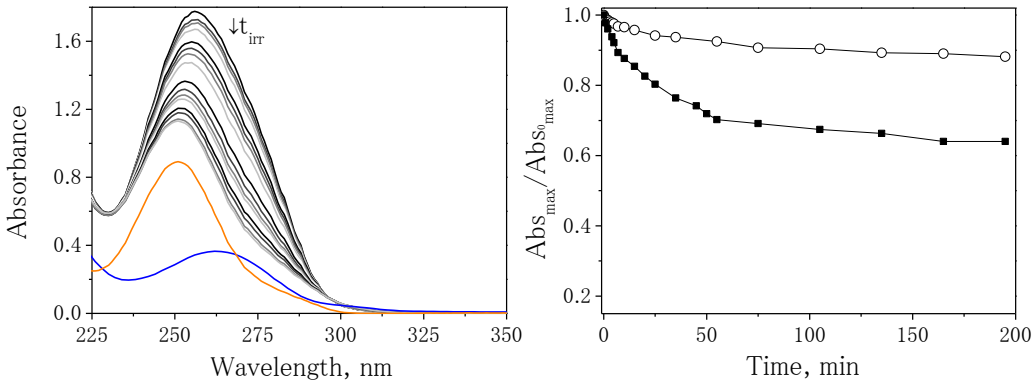

Figure 5.4. Left: UV-Vis spectra of **Bzp:3α,12α-2Thy-DCA-Bn** monitored at different irradiation (λ_{max} = 350 nm) times (C_i = 4.4 x 10^{-5}M in 4 CH_3CN:1H_2O); UV spectra of **Bzp** (orange) and **Thy** (blue) recorded at 4.4 x 10^{-5} M. Right: photoreaction kinetics of **Bzp:3α,12α-2Thy-DCA-Bn** (■) compared to **1Bzp:2Thy** (○).

Thus, **3α,12α-2Thy-DCA-Bzp** was independently irradiated in acetonitrile under inert atmosphere, and the resulting crude was purified by reverse-phase column chromatography (Scheme 5.2). Only one photoproduct was obtained, whose structural characterization was achieved on the basis of ^{1}H and ^{13}C NMR spectroscopy, including ^{13}C DEPT-135, ^{1}H-^{1}H COSY and ^{1}H-^{13}C HSQC experiments, and also on exact mass determination. The photoproduct resulted to be one single oxetane derived from the Paternò-Büchi reaction between the Bzp moiety and the Thy unit at 12α-(**3α-Thy-DCA-12α-Thy <O>Bzp**). This was assessed by the appearance of a new singlet in the ^{1}H NMR at 4.72 ppm, concomitantly with the disappearance of one of the olefinic protons and with the upfield displacement of the aromatic signals. Furthermore, upon formation of the new ring, the ^{13}C-NMR signal corresponding to the original carbonyl group at 196.9 ppm shifted to 91.7 ppm, in accordance with the values reported for analogous oxetanes.[147,153] The regiochemistry assignment depicted in Scheme 5.2 was based on the comparison of the chemical shifts of the two carbons formerly belonging to the Thy moiety with those found for related oxetanes.[147,153] In fact, the obtained values of δ_C = 76.3 ppm and δ_{CH} = 68.4 ppm are in complete agreement with the expected values (δ_C = 76.5-78.0 and δ_{CH} = 60.8-66.5 ppm) and far from those reported for the alternative regioisomers (δ_C = 52.7-57.8 and δ_{CH} = 80.0-90.0 ppm).

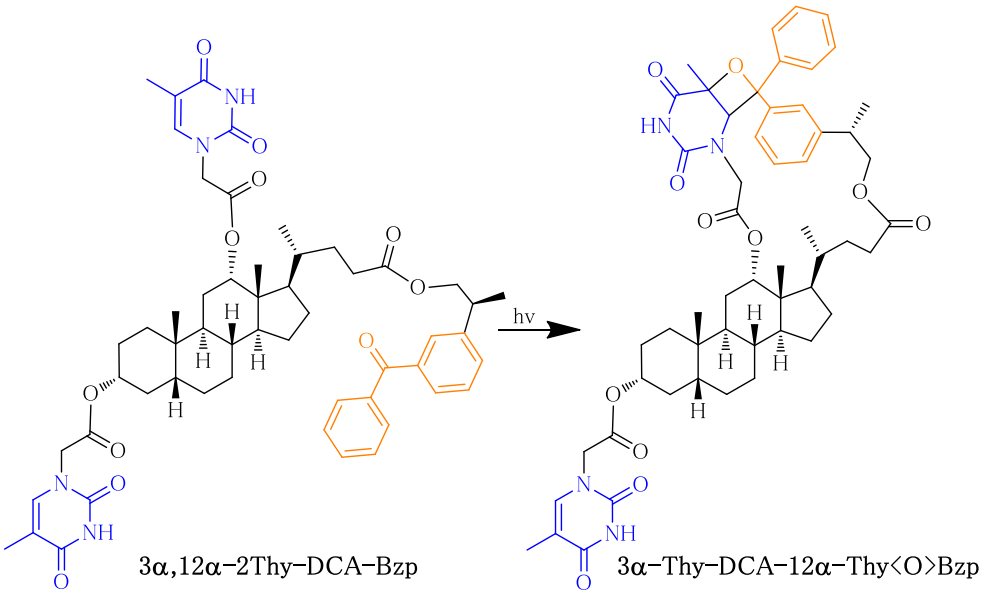

Scheme 5. 2. Irradiation (λ_{max} = 350 nm) of **3α,12α-2Thy-DCA-Bzp** in CH_3CN under N_2 to give **3α-Thy-DCA-12α-Thy-DCA<O>Bzp**, (64%).

Next, the intermolecular system **Bzp:3α,12α-2Thy-DCA-Bn** was irradiated in CH_3CN under nitrogen (Scheme 5.3). The main photoproduct (82%) was isolated by column chromatography and was found to be *trans-syn* Thy<>Thy (**3α,12α-Thy<>Thy-DCA-Bn**), whose structure was unambiguously established by crystal data (Figure 5.5).

It should be noted that when the crude resulting from irradiation of **Bzp:3α,12α-2Thy-DCA-Bn** was analyzed by UPLC-MS-MS, minor peaks corresponding to adducts compatible with formation of oxetanes were found, although to a much lesser extent (m/z 997.5033, calculated for $C_{58}H_{69}N_4O_{11}$ (MH^+) 997.4963); by contrast, in the case of **3α,12α-2Thy-DCA-Bzp**, the major reaction pathway was the Paternò-Büchi cycloaddition, and Thy<>Thy dimers were not even detected.

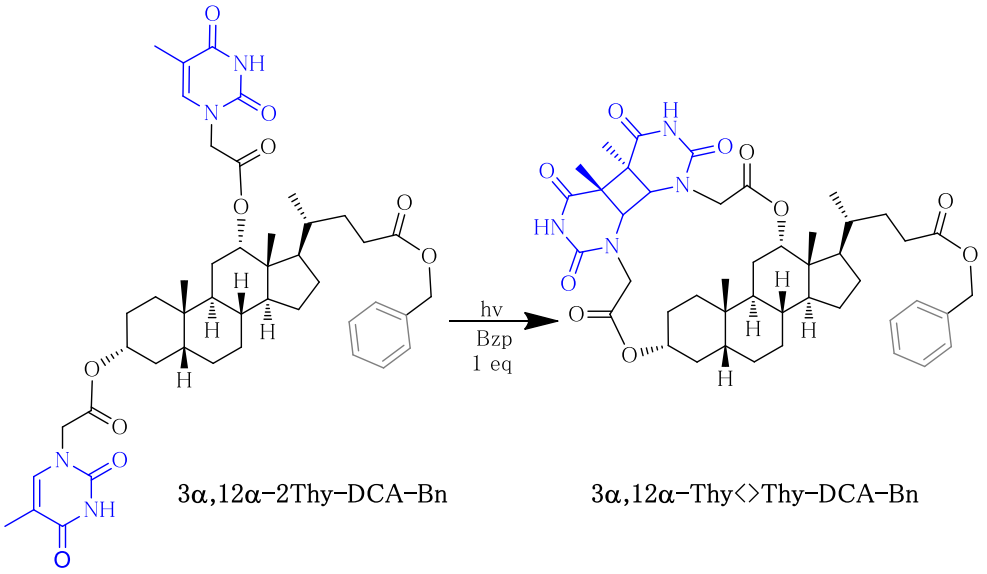

Scheme 5.3. Irradiation (λ_{max} = 350 nm) of **Bzp:3α,12α-2Thy-DCA-Bn** in CH_3CN under N_2 to give **3α,12α-Thy<>Thy-DCA-Bn**, (82%).

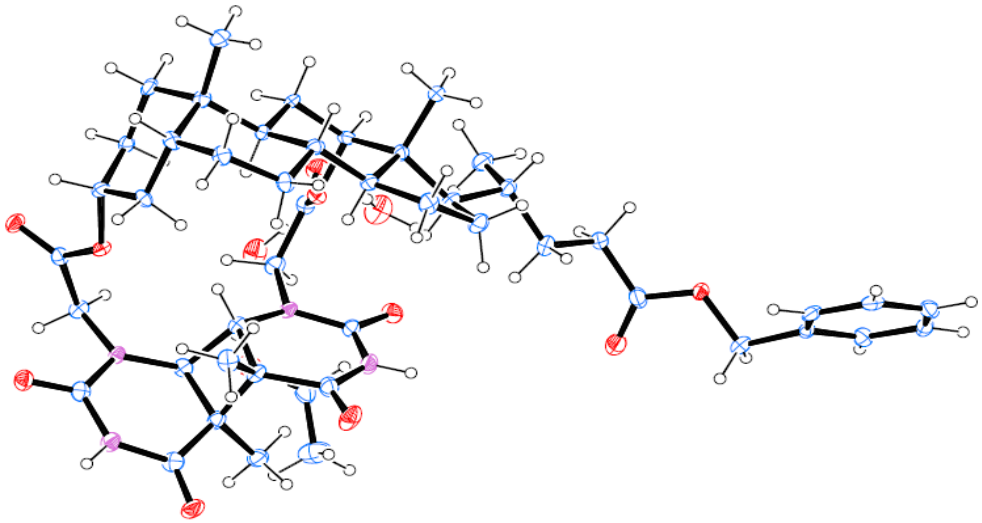

Figure 5.5. X-ray crystal structure of **3α,12α-Thy<>Thy-DCA-Bn** coming from the irradiation (λ_{max} = 350 nm) of **Bzp:3α,12α-2Thy-DCA-Bn** in CH_3CN under N_2. CCDC: 1031373.

The obtained results revealed that the photochemical behavior of the inter- and intramolecular systems is dramatically diverging. In principle, the arrangement of the two Thy bases and a Bzp unit covalently attached to the same scaffold was expected to favor formation of Thy<>Thy; however, the predominating process was by far production of an oxetane. This could be related to the known orientation dependence in the formation and evolution of exciplexes, as the degrees of freedom in **3α,12α-2Thy-DCA-Bzp** are markedly limited, and the geometry of the purported ^{3}[Bzp···Thy]* exciplex might be appropriate for production of the oxetane but not for triplex formation. In the intermolecular mixture, the free arrangement of the ketone relative to the nucleobases allows assembling of the partners in the triplet triplex ^{3}[Bzp···Thy···Thy]* with the appropriate geometry to afford Thy dimers as the final products.

5.4. Related systems with different Bzp/Thy/Thy or Thy/Thy combinations

5.4.1. Introduction

The synthesis of DCA derivatives containing two Thy units at 3α- and 12α- and a Bzp or Bn at the lateral chain has led to the formation of **3α,12α-2Thy-DCA-Bzp** and **3α,12α-2Thy-DCA-Bn**. Next, irradiation at 350 nm of **3α,12α-2Thy-DCA-Bzp** gives rise to the formation of an oxetane between the Thy at 12α- and the Bzp at the lateral chain, while the formation of Thy<>Thy is prevented in this system, due to the impossible simultaneous interaction between the two Thy and the Bzp needed for the formation of the purported triplet triplex to form the Thy<>Thy. However, that simultaneous interaction can happen in the intermolecular system upon irradiation for **3α,12α-2Thy-DCA-Bn:Bzp**, where the degrees of freedom are not restricted, allowing the formation of the triplet triplex needed for the generation of Thy<>Thy.

With this background, further investigation of the influence of the relative positions of the Thy and Bzp units on the formation of photoproducts, either coming from the intramolecular or the intermolecular sensitization from $^3Bzp^*$, appeared interesting.

For this purpose, different systems have been prepared using **DCA** as the skeleton but attaching the Bzp at C-3. Moreover, selecting **CDCA** as scaffold with the hydroxyl groups at C-3 and C-7, a variety of systems with different relative positions has been studied.

5.4.2. Synthesis

Three new families of compounds have been synthesized using the skeletons of **CDCA** and **DCA**. In the first prepared family, two Thy units were attached at 3α- and 7α- of **CDCA**, and the chromophore Bzp or the Bn group at the lateral chain (Scheme 5.4). In the second and third families, the chromophore Bzp was esterified at the 3α- position and the two Thy units were attached to the reduced lateral chain and to the 12α- in the case of **DCA** or to the reduced lateral chain and 7α- positions of **CDCA** (Schemes 5.5 and 5.6).

More in detail, the developed synthetic strategy outlined in Scheme 5.4 started with the esterification of the carboxylic acid moiety of **CDCA** with the (*S*)-enantiomer of reduced ketoprofen (KP-OH) to give **CDCA-Bzp**. Then, in the presence of an excess of Thy-CH_2CO_2H, the two hydroxyl groups at 3α- and 7α- were simultaneously esterified providing **3α,7α-2Thy-CDCA-Bzp**. To prepare the analogous derivative without the Bzp unit, the carboxylic group at the lateral chain of **CDCA** was reacted with benzyl bromide, giving **CDCA-Bn**. Subsequent treatment with Thy-CH_2CO_2H yielded **3α,7α -2Thy-CDCA-Bn**.

Moreover, the designed synthetic strategy to prepare the analogs with the Bzp chromophore at the 3α- position (Schemes 5.5 and 5.6), started with the reduction of

DCA or **CDCA** to the corresponding alcohols **DCAOH** or **CDCAOH**. Then, the first Thy unit was covalently attached at the lateral chain using Thy-CH_2CO_2H to give **DCA-Thy** or **CDCA-Thy**, respectively. Following step was the regioselective introduction of the chromophore at the 3α- position to yield **3α-Bzp-DCA-Thy** or **3α-Bzp-CDCA-Thy**. Alternatively, the 3α- position was blocked using $PhCH_2CO_2H$ or $PhCO_2H$, leading to **3α-Pa-DCA-Thy** or **3α-Bz-CDCA-Thy**, respectively. Introduction of the second Thy unit, at 12α- or 7α-, was finally achieved by treatment with Thy-CH_2CO_2H in Et_3N using 4-DMAP as catalyst, leading to **3α-Bzp,12α-Thy-DCA-Thy**, **3α-Bzp,7α-Thy-CDCA-Thy**, **3α-Pa,12α-Thy-DCA-Thy** or **3α-Bz, 7α-Thy-CDCA-Thy**.

Overall, the first family of compounds exhibit the Bzp or Bn at the lateral chain and two Thy units at 3α- and 7α- (**3α,7α-2Thy-CDCA-Bzp** and **3α,7α-2Thy-CDCA-Bn**) parallel to the previously described **DCA** analogues (Scheme 5.1). Conversely, the second and third families exhibit the Bzp at 3α- and two Thy moieties at the lateral chain and 12α-, or at the lateral chain and 7α-, that are **3α-Bzp,12α-Thy-DCA-Thy** and **3α-Bzp,7α-Thy-CDCA-Thy**. Finally, the derivatives lacking the Bzp chromophore maintaining the two Thy at the same relative positions, namely **3α-Pa,12α-Thy-DCA-Thy** and **3α-Bz,7α-Thy-CDCA-Thy** were also prepared.

Synthetic procedures, NMR spectroscopic data and exact mass for the new compounds are detailed in the experimental section of this chapter. Further NMR experiments and experimental procedures can be found in the supplementary material of this chapter.

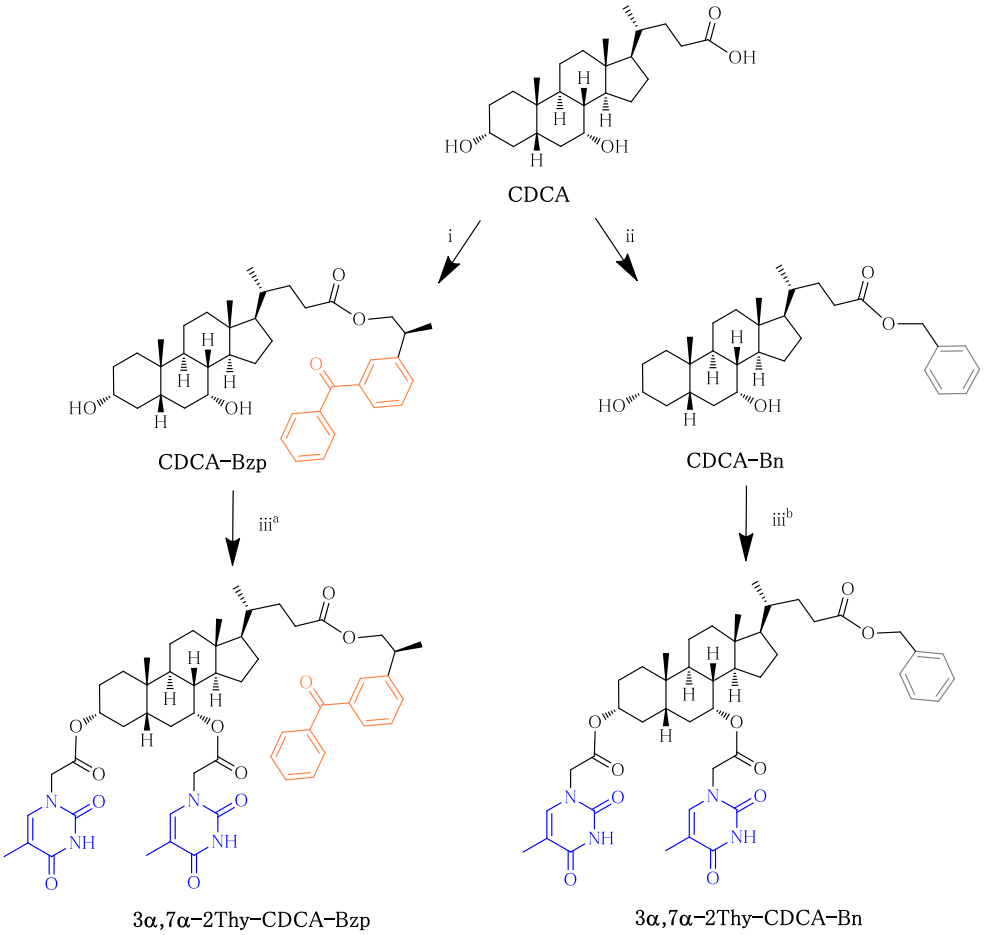

Scheme 5.4. Developed synthetic strategy to prepare **CDCA** derivatives incorporating Bzp or Bn at the lateral chain and two Thy units at 3 α − and 7 α −. Reagents and conditions: (i) KP−OH, 4−DMAP, EDC, C_5H_5N, (76%); (ii) benzyl bromide, DBU, DMF, (97%); (iii) Thy−CH_2CO_2H, Et_3N, 2,4,6−trichlorobenzoyl chloride, 4−DMAP, THF, [a](72%), [b](75%).

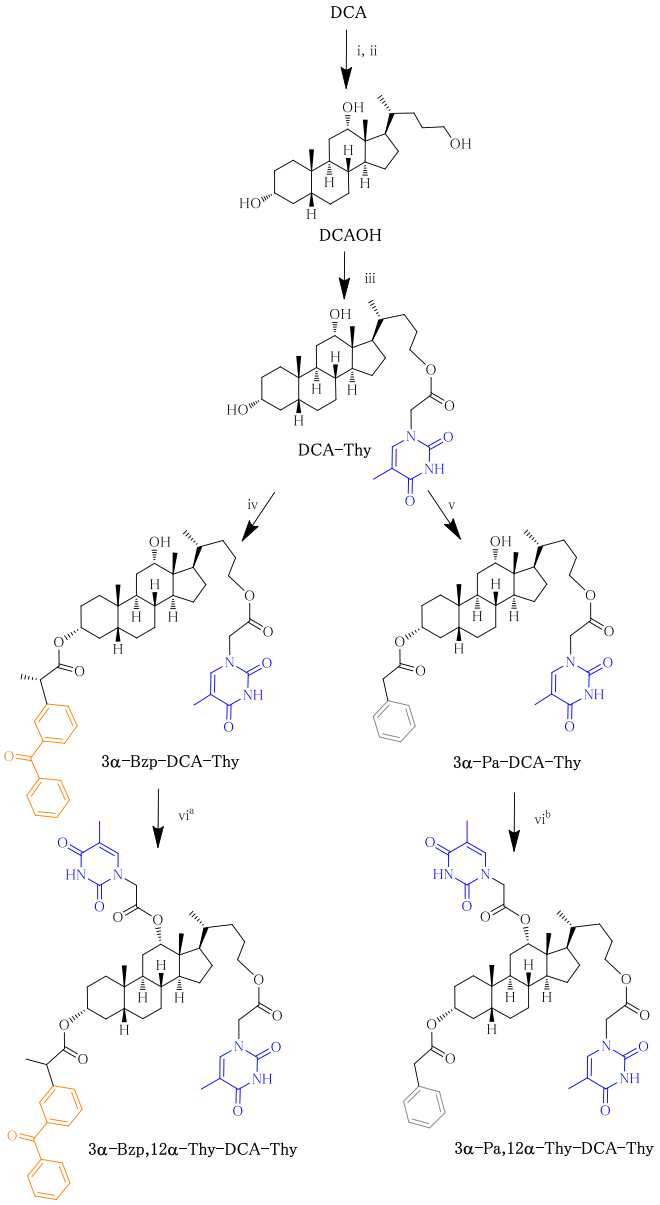

Scheme 5.5. Developed synthetic strategy to prepare **DCA** derivatives incorporating or lacking Bzp at 3α–, and two Thy units. Reagents and conditions: (i) benzyl bromide, DBU, DMF, (57%); (ii) $LiAlH_4$, refluxing THF, (87%); (iii) Thy–CH_2COOH, TBTU, DIEA, DMF, (56%); (iv) KP, TBTU, DIEA, DMF, (63%); (v) Ph–CH_2CO_2H, TBTU, DIEA, DMF, (49%); (vi) Thy–CH_2CO_2H, Et_3N, 2,4,6–trichlorobenzoyl chloride, 4–DMAP, THF, [a](58%), [b](61%).

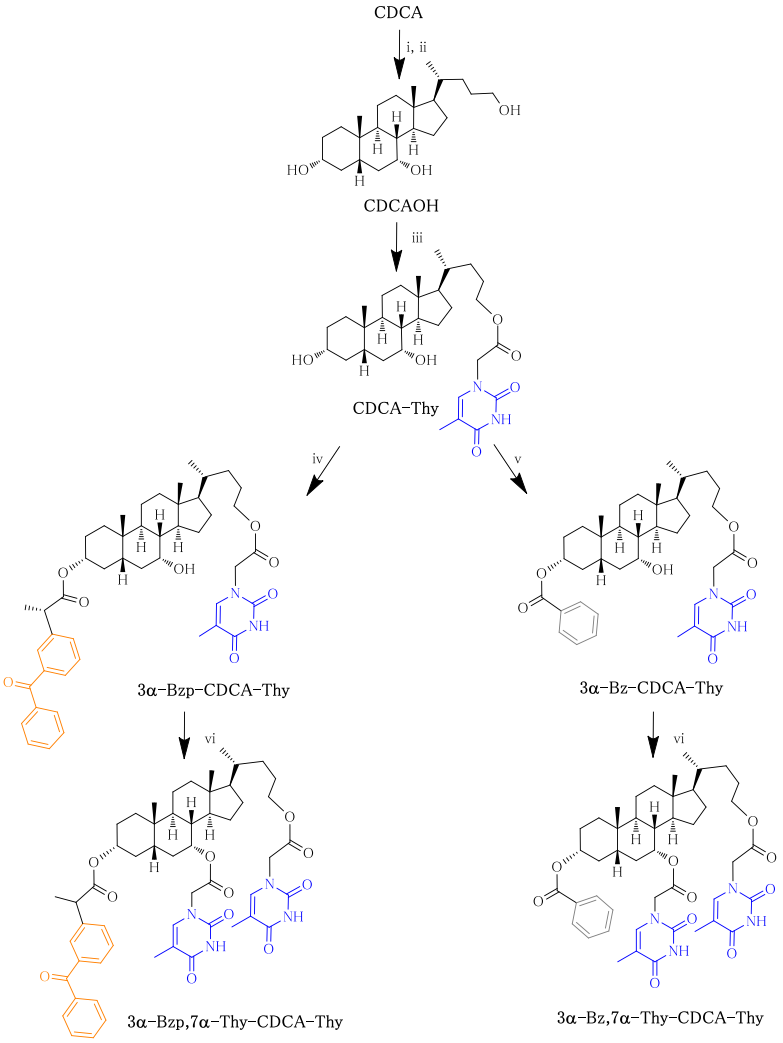

Scheme 5.6. Developed synthetic strategy to prepare **CDCA** derivatives incorporating or lacking Bzp at 3α–, and two Thy units. Reagents and conditions: (i) benzyl bromide, DBU, DMF, (97%); (ii) $LiAlH_4$, refluxing THF, (61%); (iii) Thy–CH_2COOH, TBTU, DIEA, DMF, (72%); (iv) KP, TBTU, DIEA, DMF, (22%); (v) Ph–CO_2H, TBTU, DIEA, DMF, (78%); (vi) Thy–CH_2CO_2H, Et_3N, 2,4,6–trichlorobenzoyl chloride, 4–DMAP, THF [a](20%), [b](88%).

5.4.3. Results and discussion

5.4.3.1. Photophysics

Initially the influence of the number and relative positions of the Thy units on the lifetime of the ^{3}Bzp* in the fully intramolecular systems was investigated. Thus, the derivatives with the Bzp at the lateral chain: **3α,7α-2Thy-CDCA-Bzp** and the ones exhibiting the Bzp at 3α-: **3α-Bzp,12α-Thy-DCA-Thy** and **3α-Bzp,7α-Thy-CDCA-Thy** together with the references **CDCA-Bzp, 3α-Bzp-DCA-Thy and 3α-Bzp-CDCA-Thy** were monitored by LFP upon selective excitation of Bzp at 355 nm (Figure 5.6). Decays were fitted to a first order exponential equation and their lifetimes are shown in Table 5.1. Then, the rate constants for the intramolecular deactivation of the triplet were evaluated in each case by comparison with the corresponding reference.

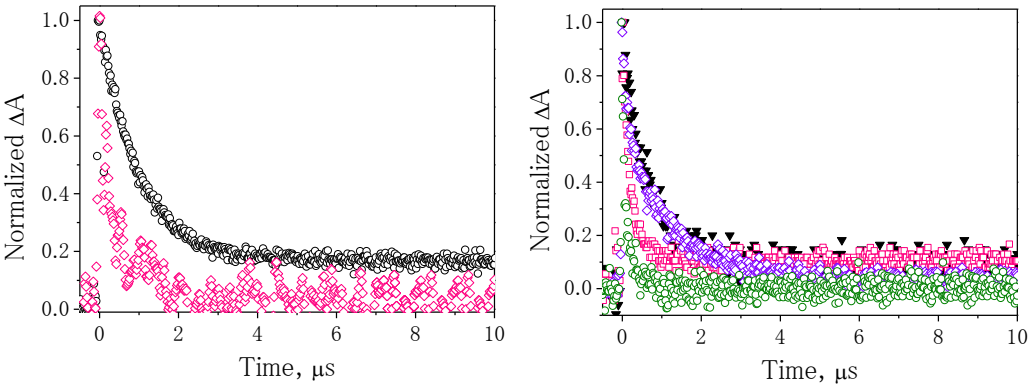

Figure 5.6. LFP decays monitored at 530 nm in 4 CH_3CN:1H_2O (λ_{exc}=355 nm). Left: **CDCA-Bzp** (○) and **3α,7α-2Thy-CDCA-Bzp** (◊). Right: **3α-Bzp-DCA-Thy** (▼), **3α-Bzp,12α-Thy-DCA-Thy** (□), **3α-Bzp-CDCA-Thy** (◊), **3α-Bzp,7α-Thy-CDCA-Thy** (○).

Table 5.1. Triplet lifetimes of Bzp in different systems.

Compound	τ_{Bzp} (μs)	k (s^{-1})
CDCA-Bzp	1.01	-
3α,7α-2Thy-CDCA-Bzp	0.08	1.2 x 10^{7a}
3α-Bzp -DCA-Thy	0.65	-
3α-Bzp,12α-Thy-DCA-Thy	0.19	3.7 x 10^{6b}
3α-Bzp -CDCA-Thy	0.94	-
3α-Bzp,7α-Thy-CDCA-Thy	0.09	1.0 x 10^{7c}

[a] $k=(1/\tau_{3\alpha,7\alpha\text{-2Thy-CDCA-Bzp}}-1/\tau_{CDCA\text{-Bzp}})$; [b] $k=(1/\tau_{3\alpha\text{-Bzp,12}\alpha\text{-Thy-DCA-Thy}}-1/\tau_{3\alpha\text{-Bzp -DCA-Thy}})$; [c] $k=(1/\tau_{3\alpha\text{-Bzp,7}\alpha\text{-Thy-CDCA-Thy}}-1/\tau_{3\alpha\text{-Bzp -CDCA-Thy}})$.

These results were compared with the intermolecular quenching of ^{3}Bzp* upon increasing concentrations of the scaffold containing two Thy units attached at the different positions of DCA or CDCA. Therefore, the lifetime of ^{3}Bzp* was monitored upon addition of increasing concentrations of **3α,7α-2Thy-CDCA-Bn**, **3α-Pa,12α-Thy-DCA-Thy** and **3α-Bz,7α-Thy-CDCA-Thy**. Stern-Volmer plots of the reciprocal lifetimes obtained in each case allowed determining the quenching rate constants, which were found to be 2.9 x 10^8 M^{-1} s^{-1}, 1.3 x 10^9 M^{-1} s^{-1} and 9.4 x 10^8 M^{-1} s^{-1} for **3α,7α-2Thy-CDCA-Bn**, **3α-Pa,12α-Thy-DCA-Thy** and **3α-Bz,7α-Thy-CDCA-Thy**, respectively (Figure 5.7). For comparison, quenching of ^{3}Bzp* by Thy resulted in a k = 1.4 x 10^8 M^{-1} s^{-1}.

An overall analysis of the intra- and intermolecular quenching evidenced a more efficient intermolecular one, which in principle could lead to different photoproducts as demonstrated in the previous section (see Section 5.3. Results and discussion).

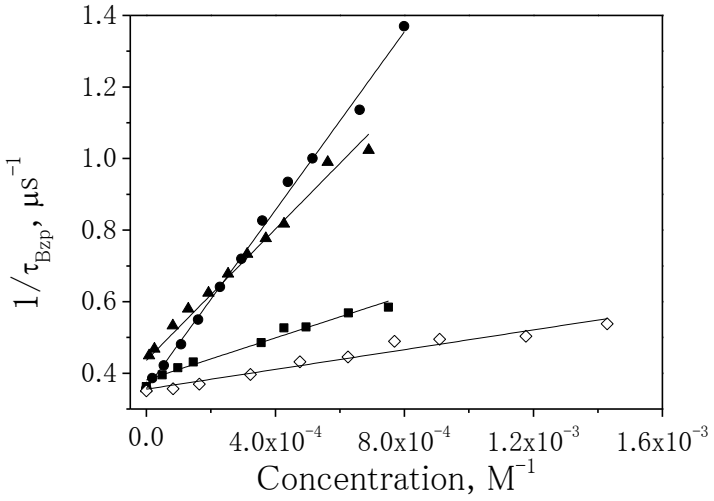

Figure 5.7. Stern-Volmer plots for LFP decays of Bzp monitored at 530 nm in 4 CH_3CN:1H_2O (λ_{exc}= 355 nm) upon increasing concentrations of **3α,7α-2Thy-CDCA-Bn** (■), **3α-Pa,12α-Thy-DCA-Thy** (●), **3α-Bz,7α-Thy-CDCA-Thy** (▲) and **Thy** (◊).

5.4.3.2. Photochemistry

Inter- and intramolecular photobehavior of 1Bzp:2Thy systems with increasing degree of organization were initially evaluated in parallel upon selective irradiation of the Bzp chromophore at λ_{max} = 350 nm, by monitoring changes in the UV-visible spectra. Firstly, the intermolecular mixture **1Bzp:2Thy**; secondly, the fully intramolecular derivatives: **3α,7α-2Thy-CDCA-Bzp**, **3α-Bzp,12α-Thy-DCA-Thy** and **3α-Bzp,7α-Thy-CDCA-Thy**; and finally the intermolecular 1:1 systems in which only the two Thy are covalently attached to a BA skeleton, namely: **Bzp:3α,7α-2Thy-CDCA-Bn**; **Bzp:3α-Pa,12α-Thy-DCA-Thy** and **Bzp:3α-Bz,7α-Thy-CDCA-Thy**.

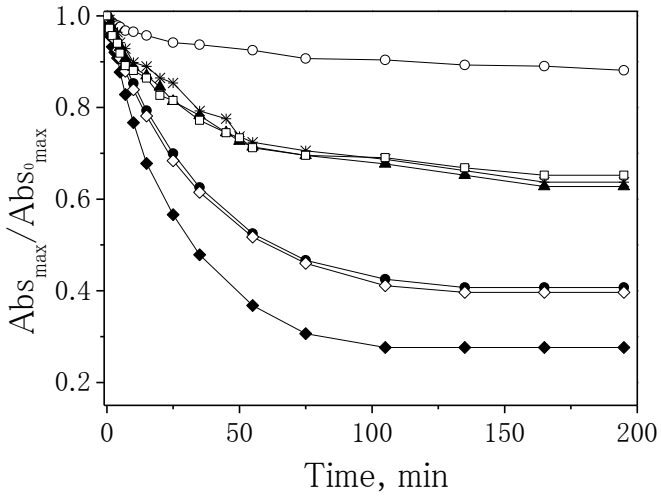

Figure 5.8. Photoreaction kinetics of the intermolecular **1Bzp:2Thy** (○), the intramolecular derivatives: **3α,7α-2Thy-CDCA-Bzp** (♦); **3α-Bzp,12α-Thy-DCA-Thy** (●) and **3α-Bzp,7α-Thy-CDCA-Thy** (◊) and the intermolecular 1:1 systems **Bzp:3α,7α-2Thy-CDCA-Bn** (▲); **Bzp:3α-Pa,12α-Thy-DCA-Thy** (*) and **Bzp:3α-Bz,7α-Thy-CDCA-Thy** (□) (C_i = 4.4 x 10^{-5}M in $4CH_3CN:1H_2O$, λ_{max} = 350 nm).

As expected, the intermolecular mixture **1Bzp:2Thy** was almost unreactive, while a significant decrease in the absorbance was observed for the intermolecular systems with the two Thys linked to the BA (see Figure 5.8). More interestingly, the most remarkable absorbance changes were found for the fully intramolecular derivatives, being the regioisomer having the chromophore at the lateral chain more reactive than those with the Bzp at 3α- .

The different behavior between the intramolecular and intermolecular systems was in agreement with that observed for **3α,12α-2Thy-DCA-Bzp** (Figure 5.3) and **Bzp:3α,12α-2Thy-DCA-Bn** (Figure 5.4) systems, discussed in Section 5.3. Briefly, in the case of **3α,12α-2Thy-DCA-Bzp,** the maximum absorbance decreased almost three fourths until reaching a plateau, while for **Bzp:3α,12α-2Thy-DCA-Bn**, the maximum absorbance decreased only one forth. The residual absorbance was correlated to the

chromophores remaining unreactive, so in the case of **3α,12α-2Thy-DCA-Bzp** irradiation, as the isolated photoproduct was exclusively an oxetane, the residual absorbance at 250-260 nm region was due to one Thy unit, while in the case of **Bzp:3α,12α-2Thy-DCA-Bn** irradiation, as the isolated photoproduct was a dimer, the residual absorbance at 250-260 nm region corresponded to the Bzp unit. This explanation is supported by the molar absorptivity at 262 nm, which is *ca.* 2-fold for Bzp than for Thy.

An analogous rationale could be applied to the results obtained upon irradiation of these three families, so the observed absorbance variations are associated with different product distributions (see Figure 5.8). Hence, for a proper evaluation of the observed photoreactivity, it seemed appropriate to perform independent irradiations and analyze the resulting photoproduct mixtures.

Thus, **3α,7α-2Thy-CDCA-Bzp** was independently irradiated in acetonitrile under inert atmosphere, and the corresponding crude was purified by reverse-phase column chromatography (Scheme 5.7). Only one photoproduct was obtained, whose structural characterization was achieved on the basis of ^{1}H and ^{13}C NMR spectroscopy, including ^{13}C DEPT-135, ^{1}H-^{1}H COSY and ^{1}H-^{13}C HSQC experiments, and also on exact mass determination. The photoproduct resulted to be an oxetane derived from the Paternò-Büchi reaction between the Bzp moiety and the Thy unit at 7α-. This was assessed by the appearance of a new singlet in the ^{1}H NMR at 4.54 ppm, concomitant with the disappearance of one of the olefinic protons and the upfield displacement of the aromatic signals. Furthermore, upon formation of the oxetane ring, the ^{13}C-NMR signal corresponding to the original carbonyl group at 196.7 ppm shifted to 91.1 ppm, in complete agreement with the values reported for analogous oxetanes.[147,153] The assignment of the regiochemistry depicted in Scheme 5.7 was based on the comparison of the chemical shifts of the other two carbons of the oxetane ring (formerly belonging to the Thy moiety, δ_C = 75.6 ppm and δ_{CH} = 68.4 ppm) with the ones reported for related oxetanes.[147,153] In fact, they are in complete agreement with the values reported for

similar oxetanes and far from the values that would be expected for the alternative regioisomers (δ_C = 52.7–57.8 or δ_{CH} = 80.0–90.0 ppm).

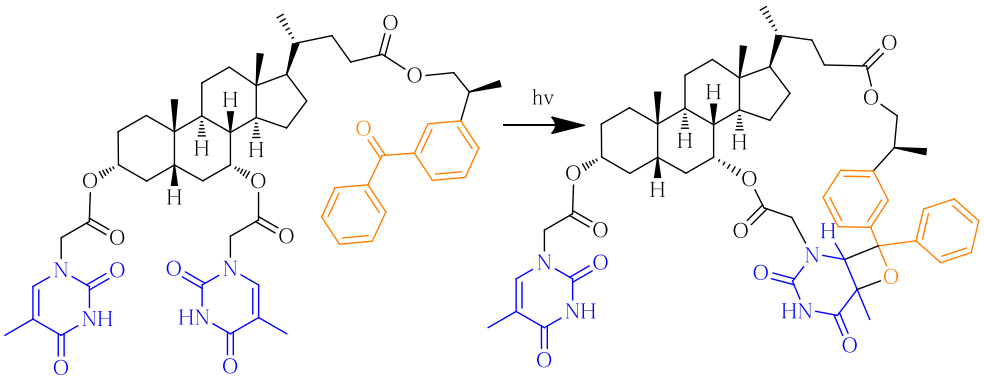

3α,7α-2Thy-CDCA-Bzp　　3α-Thy-CDCA-7α-Thy<O>Bzp

Scheme 5.7. Irradiation (λ_{max} = 350 nm) of **3α,7α-2Thy-CDCA-Bzp** in CH_3CN under N_2 to give **3α-Thy-CDCA-7α-Thy<O>Bzp** (23%).

Then, independent irradiations of **3α-Bzp,12α-Thy-DCA-Thy** or **3α-Bzp,7α-Thy-CDCA-Thy** at 350 nm were performed under inert atmosphere, and the crudes were purified by column chromatography (Scheme 5.8.). Again formation of oxetanes occurred between the chromophore at 3α- and the Thy at 7α- or 12α-, with the same regiochemistry as above. The structures of those oxetanes were assigned on the basis of the ^1H and ^{13}C NMR spectral data and exact mass.

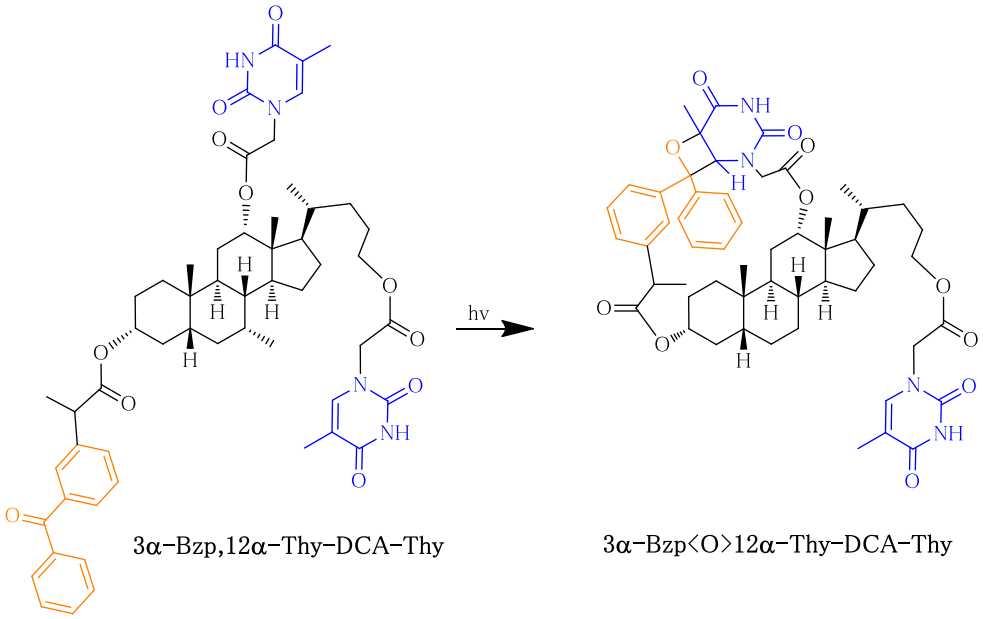

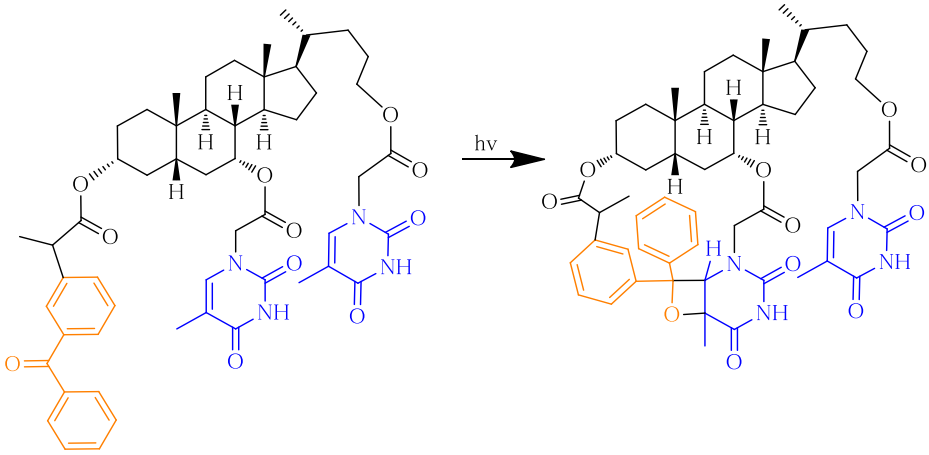

Scheme 5.8. Photoirradiation (λ_{max} = 350 nm) of **3α-Bzp,12α-Thy-DCA-Thy** to give **3α-Bzp<O>12α-Thy-DCA-Thy** (63%) or **3α-Bzp,7α-Thy-CDCA-Thy** to give **3α-Bzp<O>7α-Thy-CDCA-Thy** (30%) in CH_3CN under N_2.

Then, the intermolecular systems **Bzp:3α,7α-2Thy-CDCA-Bn**, **Bzp:3α-Pa,12α-Thy-DCA-Thy** or **Bzp:3α-Bz,7α-Thy-CDCA-Thy** were independently irradiated in CH_3CN under nitrogen and the crude mixtures were submitted to column chromatography to isolate the corresponding photoproducts. In the three cases, the corresponding Thy<>Thy were obtained as one single *trans-syn* regioisomer with yields higher than 40% (Schemes 5.9 and 5.10).

Their structural characterization was achieved on the basis of ^{1}H, ^{13}C and ^{1}H-^{13}C-HSQC NMR experiments. In the three systems, the dimerization produced an upfield shift of the olefinic protons of both Thys when becoming aliphatic (from the 6.56-7.55 ppm region to the 3.08-4.09 ppm region in the ^{1}H NMR experiments). Also an upfield shift of the aromatic carbons was observed upon dimerization (from the 140 ppm region to the 61.2-66.4 ppm region in the ^{13}C NMR spectra).

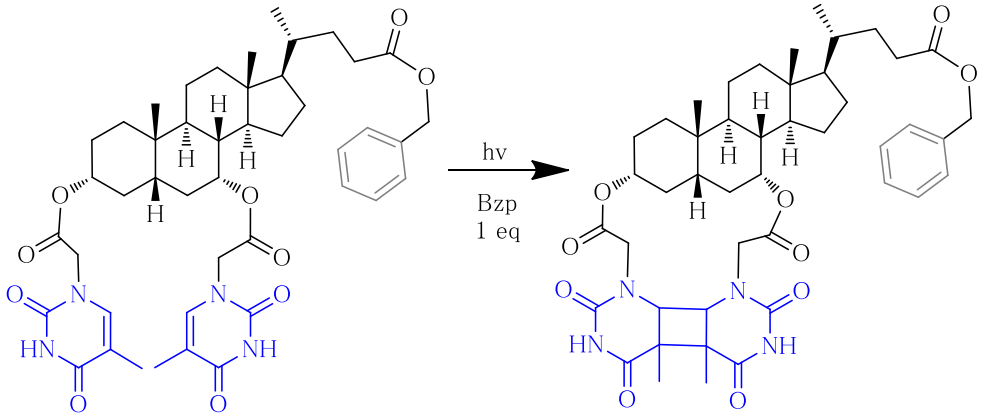

Scheme 5.9. Photoirradiation (λ_{max} = 350 nm) of **Bzp:3α,7α-2Thy-CDCA-Bn** to give **3α,7α-Thy<>Thy-CDCA-Bn** (40%) in CH_3CN under N_2.

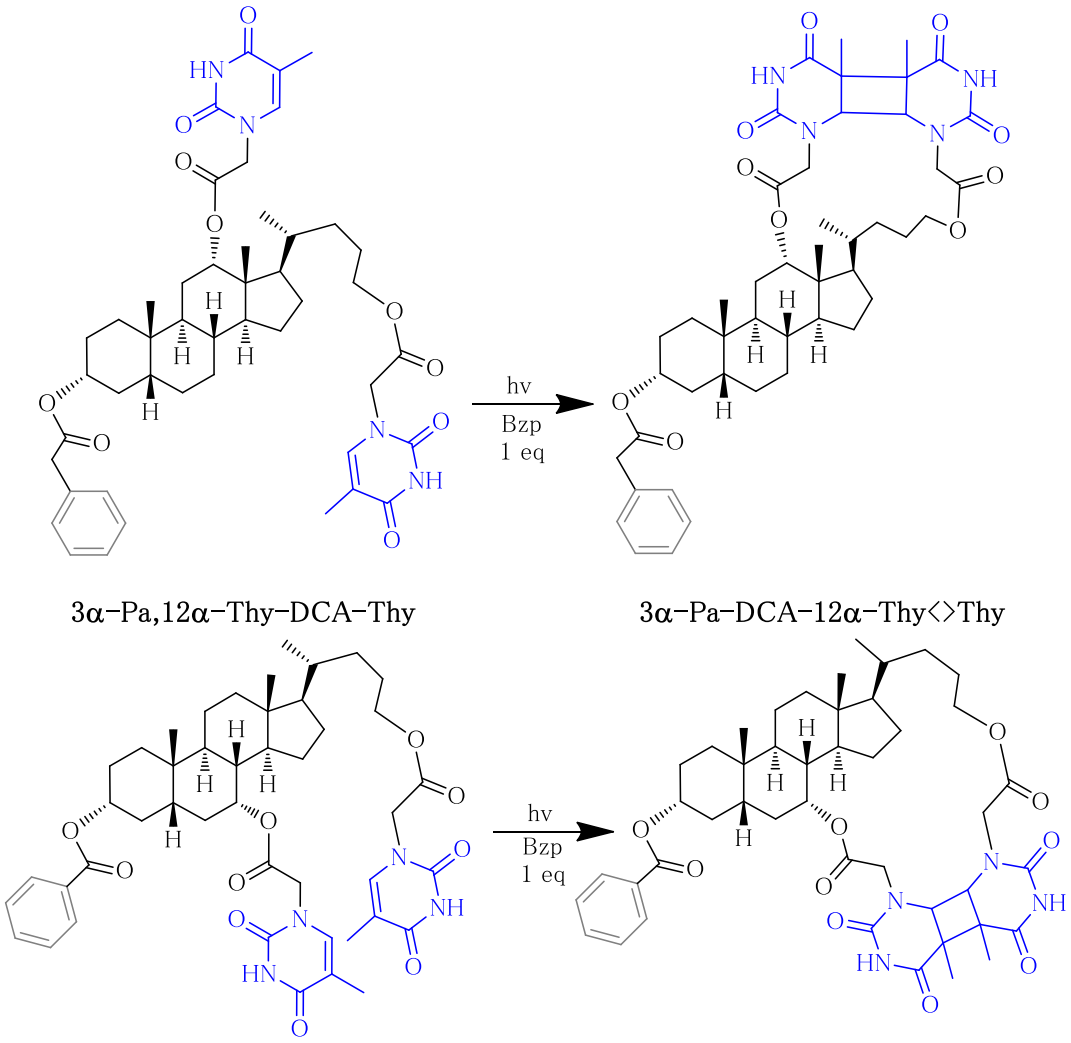

Scheme 5.10. Photoirradiation (λ_{max} = 350 nm) of **Bzp:3α-Pa,12α-Thy-DCA-Thy** to give **3α-Pa-DCA-12α-Thy <>Thy** (41%) or **Bzp:3α-Bz,7α-Thy-CDCA-Thy** to give **3α-Bz-CDCA-7α-Thy <>Thy** (48%) in CH_3CN under N_2.

5.5. Conclusions

A new mechanistic pathway leading to photosensitized formation of cyclobutane pyrimidine dimers is proposed, in which the key step involves generation of a triplet triplex. The concept has been illustrated with different systems combining one benzophenone (Bzp) and two thymine (Thy) units with different degrees of freedom. The photoreactivity of all the synthesized systems can be switched from a clean Paternò–Büchi when the Bzp and the two Thy are all linked to the skeleton to a fully chemo–, regio– and stereoselective [2+2] dimerization when the Bzp intermolecular and the two Thy units are attached to the BA skeleton. This finding underlines the importance of cooperative triplet excited states in DNA photodamage. Such delocalized chemical entities may predominate over locally excited triplet states when the thermodynamic requirement for energy transfer is not fulfilled.

5.6. Experimental

5.6.1. Synthesis and characterization

5.6.1.1. Synthesis of *(S)*–KP–OH

To a stirred solution of KP (1.400 g, 5.50 mmol) in anhydrous THF (14 mL) at –20 °C, borane–tetrahydrofuran complex (6.600 mL of a 1M solution, 6.60 mmol) was added dropwise, and the reaction mixture was allowed to warm overnight until room temperature. Then, the solution was cooled down again to 5 °C and treated with a MeOH:H_2O mixture (15:85, 17 mL). Afterwards, the solvents were concentrated in vacuum, the crude was redissolved in CH_2Cl_2 and poured into brine, extracted with CH_2Cl_2, washed with $NaHCO_3$ (5%), dried over $MgSO_4$ and evaporated under reduced pressure. Purification of the crude by column chromatography (SiO_2, CH_2Cl_2:MeOH, 95:5) gave the *(S)*–enantiomer (**KP–OH**) as an oil (0.728 g, 55%). ^1H NMR (300 MHz,

$CDCl_3$): δ (ppm) 1.31 (d, *J* = 7.2 Hz, 3H, CH_3); 1.49 (*br* s, 1H, OH); 3.04 (m, 1H, CH); 3.75 (m, 2H, CH_2); 7.40–7.84 (m, 9H, arom). ^{13}C NMR (75 MHz, $CDCl_3$): δ (ppm) 197.0 (C), 144.5 (C), 137.7 (C), 137.6 (C), 132.5 (CH), 131.8 (CH), 130.1 (2xCH), 128.9 (CH), 128.5 (CH), 128.4 (CH), 128.3 (2xCH), 68.3 (CH_2), 42.3 (CH), 17.6 (CH_3); m/z found 241.1219, calculated for $C_{16}H_{17}O_2$ (MH^+) 241.1229.

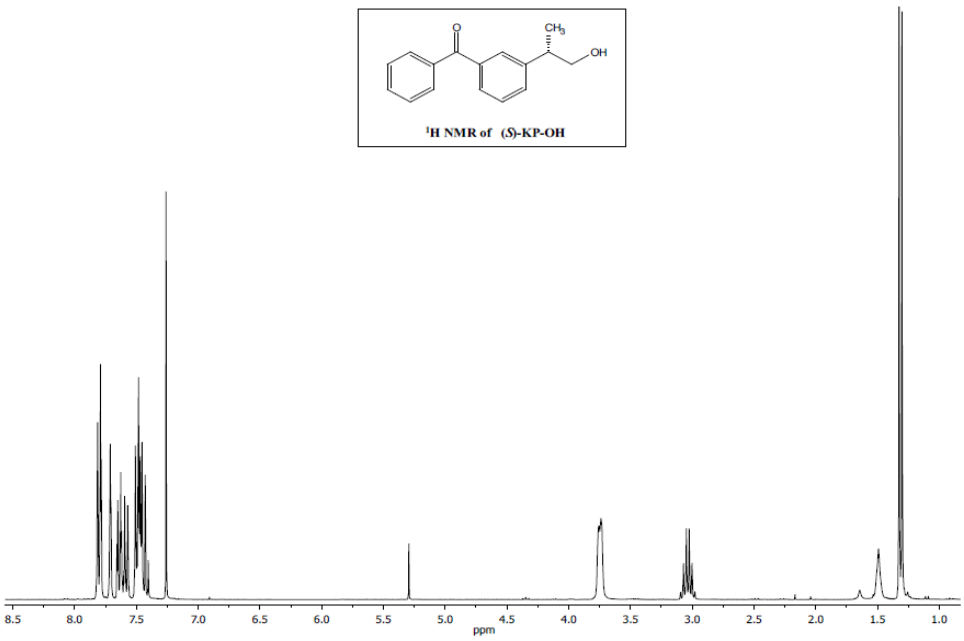

^{1}H NMR of (*S*)-KP-OH

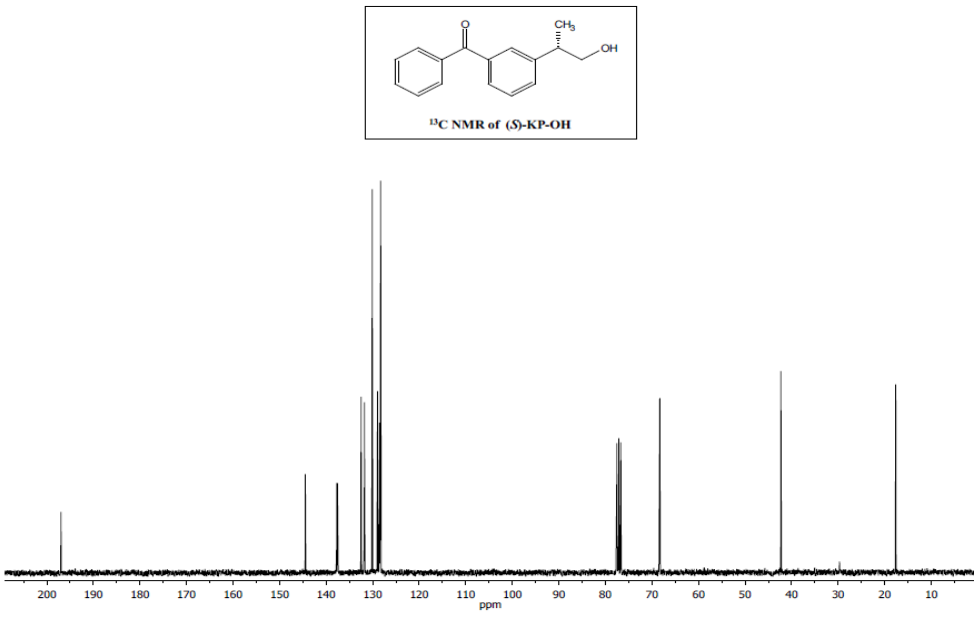

^{13}C NMR of (*S*)-KP-OH

5.6.1.2. Synthesis of DCA-Bzp

To a stirred mixture of **DCA** (0.772 g, 1.97 mmol), KP-OH (0.394 g, 1.64 mmol) and 4-DMAP (0.200 g, 1.64 mmol) in anhydrous C_5H_5N (8 mL) at 0 °C, EDC (0.348 mL, 1.97 mmol) was added dropwise and the reaction mixture was allowed to react for one hour at 0 ºC and then overnight at room temperature. Afterwards, the suspension was poured into HCl 1M and extracted with CH_2Cl_2; the combined organic layers were washed with brine, dried over $MgSO_4$ and concentrated under reduced pressure. Purification by column chromatography (SiO_2, EtOAc:Hexane, 60:40) gave **DCA-Bzp** as a colorless solid (0.666 g, 55%). ^{1}H NMR (300 MHz, $CDCl_3$): δ (ppm) 0.64 (s, 3H, CH_3); 0.78-1.89 (complex signal, 24H); 0.90 (s, 3H, CH_3); 0.92 (d, J = 6.3 Hz, 3H, 21-CH_3); 1.33 (d, J = 7.2 Hz, 3H, KP-CH_3); 2.20 (m, 2H, CH_2); 3.17 (m, 1H, KP-CH); 3.61 (m, 1H, 3β-H); 3.95 (*br* s, 1H, 12β-H); 4.16 (dd, J = 10.8 and 6.6 Hz, 1H, KP-CH_2); 4.21 (dd, J = 10.8 and 7.2 Hz, 1H, KP-CH_2); 7.39-7.82 (m, 9H, arom). ^{13}C NMR (75 MHz, $CDCl_3$): δ (ppm) 196.9 (C), 174.2 (C), 143.8 (C), 137.9 (C), 137.7 (C), 132.6 (CH), 131.5 (CH), 130.2 (2xCH), 129.1 (CH), 128.8 (CH), 128.5 (CH), 128.4 (2xCH), 73.2 (CH), 72.0 (CH), 69.0 (CH_2), 48.4 (CH), 47.4 (CH), 46.6 (C), 42.2 (CH), 39.0 (CH), 36.6 (CH_2), 36.2 (CH), 35.3 (CH_2), 35.2 (CH), 34.2 (C), 33.8 (CH), 31.4 (CH_2), 31.0 (CH_2), 30.7 (CH_2), 28.8 (CH_2), 27.5 (CH_2), 27.3 (CH_2), 26.3 (CH_2), 23.8 (CH_2), 23.3 (CH_3), 18.1 (CH_3), 17.4 (CH_3), 12.9 (CH_3); m/z found 615.4038, calculated for $C_{40}H_{55}O_5$ (MH^+) 615.4050.

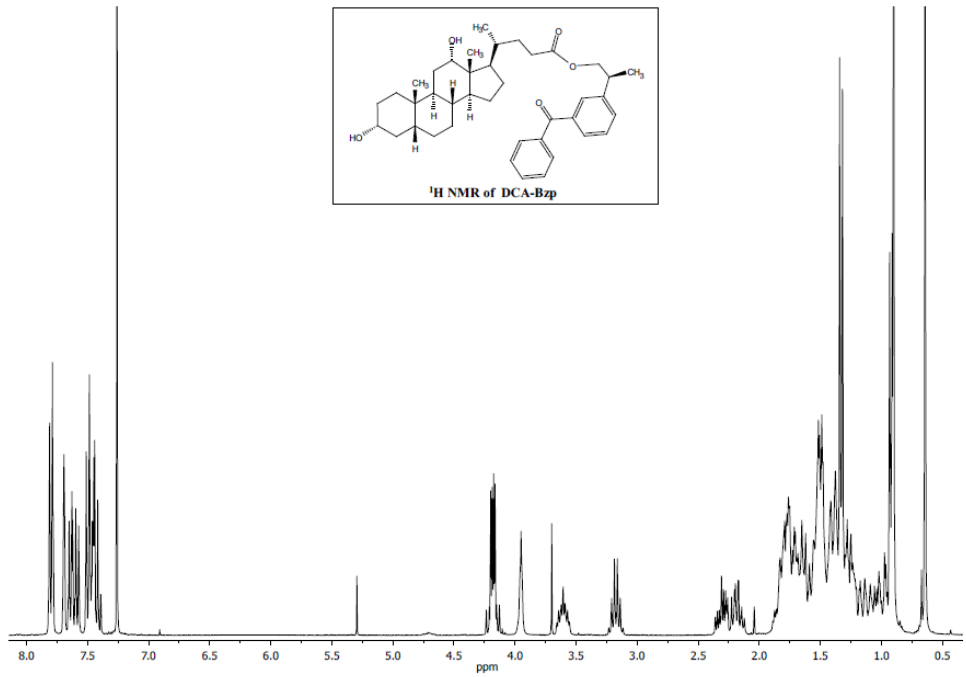
^{1}H NMR of DCA-Bzp
8.0 7.5 7.0 6.5 6.0 5.5 5.0 4.5 4.0 3.5 3.0 2.5 2.0 1.5 1.0 0.5
ppm

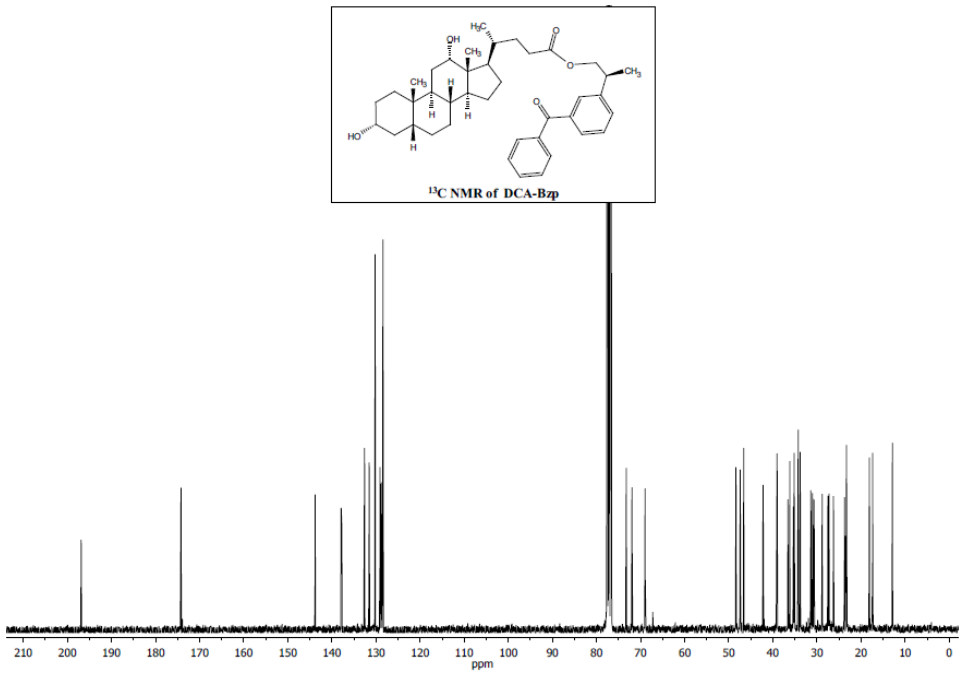
^{13}C NMR of DCA-Bzp
210 200 190 180 170 160 150 140 130 120 110 100 90 80 70 60 50 40 30 20 10 0
ppm

5.6.1.3. Synthesis of 3α,12α-2Thy-DCA-Bzp

A stirred suspension of Thy-CH_2CO_2H (1.192 g, 6.47 mmol) in anhydrous THF (40 mL) was treated with Et_3N (1.810 mL, 12.99 mmol) and 2,4,6-trichlorobenzoyl chloride (1.230 mL, 7.85 mmol) and the resulting mixture was allowed to react for 1.5 h. Then, a solution of 4-DMAP (0.527 g, 1.32 mmol) and **DCA-Bzp** (0.663 g, 1.08 mmol) in anhydrous THF (25 mL) was added and the resulting reaction mixture was stirred overnight. Afterwards, it was poured into $NaHCO_3$ (5%), extracted with CH_2Cl_2 and the combined extracts were washed with brine, dried over $MgSO_4$ and concentrated under vacuum. Purification by column chromatography (SiO_2, CH_2Cl_2:MeOH, 97:3, followed by (Li Chroprep RP-18, CH_3CN:H_2O, 80:20) gave **3α,12α-2Thy-DCA-Bzp** as a yellow solid (0.959 g, 94%). ^{1}H NMR (300 MHz, $CDCl_3$): δ (ppm) 0.68 (s, 3H, CH_3); 0.74 (d, *J* = 6.3 Hz, 3H, 21-CH_3); 0.78-2.34 (complex signal, 26H); 0.88 (s, 3H, CH_3); 1.33 (d, *J* = 6.9 Hz, 3H, KP-CH_3); 1.89 (*br* s, 3H, Thy-CH_3); 1.90 (*br* s, 3H, Thy-CH_3); 3.17 (m, 1H, KP-CH); 4.17 (d, *J* = 6.9 Hz, 2H, KP-CH_2); 4.41 (d, *J* = 17.1 Hz, 1H, Thy-CH_2); 4.45 (*br* s, 2H, Thy-CH_2); 4.58 (d, *J* = 17.1 Hz, 1H, Thy-CH_2); 4.71 (*br* s, 1H, 3β-H); 5.12 (*br* s, 1H ,12β-H); 6.97 (*br* s, 1H, Thy-CH); 7.11 (*br* s, 1H, Thy-CH); 7.39-7.85 (m, 9H, arom). ^{13}C NMR (100 MHz, $CDCl_3$): δ (ppm) 196.9 (C), 174.1 (C), 167.2 (C), 166.8 (C), 164.7 (C), 164.3 (C), 151.6 (C), 150.9 (C), 143.8 (C), 140.9 (CH), 140.3 (CH), 137.8 (C), 137.7 (C), 132.7 (CH), 131.5 (CH), 130.2 (2xCH), 129.2 (CH), 128.9 (CH), 128.5 (CH), 128.4 (2xCH), 111.5 (C), 110.8 (C), 78.1 (CH), 76.9 (CH), 69.1 (CH_2), 49.7 (CH_2), 49.5 (CH), 49.4 (CH_2), 47.6 (CH), 45.3 (C), 41.9 (CH), 39.1 (CH), 35.7 (CH), 34.8 (CH), 34.7 (CH_2), 34.5 (CH), 34.2 (C), 32.1 (CH_2), 31.4 (CH_2), 31.0 (CH_2), 27.5 (CH_2), 27.0 (CH_2), 26.1 (CH_2), 25.9 (CH_2), 25.6 (CH_2), 23.6 (CH_2), 23.1 (CH_3), 18.1 (CH_3), 17.8 (CH_3), 12.5 (2xCH_3), 12.4 (CH_3); m/z found 947.4810, calculated for $C_{54}H_{67}N_4O_{11}$ (MH^+) 947.4807.

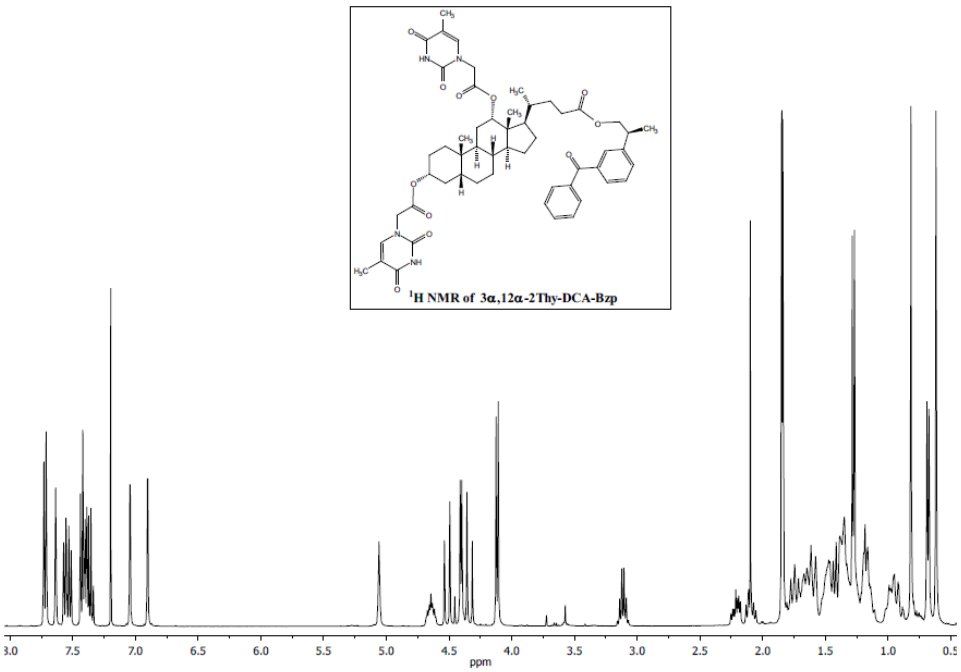
^{1}H NMR of 3α,12α-2Thy-DCA-Bzp
ppm

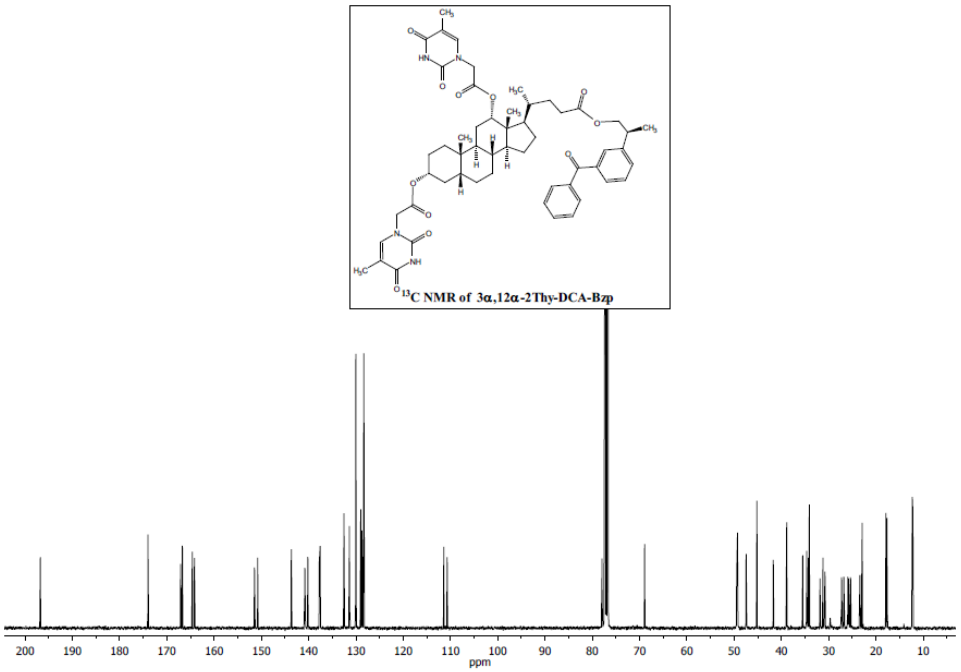
^{13}C NMR of 3α,12α-2Thy-DCA-Bzp
ppm

5.6.1.4. Synthesis of DCA-Bn

A stirred solution of **DCA** (2.510 g, 6.39 mmol) in anhydrous DMF (8 mL) was treated with DBU (1.060 mL, 7.19 mmol). Ten minutes later, benzyl bromide (0.850 mL, 7.18 mmol) was added dropwise and the solution was allowed to react overnight at room temperature. Then, the solvent was evaporated and the crude was redissolved with EtOAc, washed with $NaHCO_3$ (5%), HCl 1 M and brine, dried over $MgSO_4$ and concentrated under reduced pressure. Purification by column chromatography (SiO_2, EtOAc:Hexane, 90:10) gave **DCA-Bn** as a colorless solid (1.770 g, 57%). ^{1}H NMR (300 MHz, $CDCl_3$): δ (ppm) 0.64 (s, 3H, CH_3); 0.83-1.91 (complex signal, 24H); 0.90 (s, 3H, CH_3); 0.95 (d, *J* = 6.0 Hz, 3H, 21-CH_3); 2.38 (m, 2H, CH_2); 3.60 (m, 1H, 3β-H); 3.95 (*br* s, 1H, 12β-H)); 5.08 (d, *J* = 12.3 Hz, 1H, CH_2); 5.13 (d, *J* = 12.3 Hz, 1H, CH_2); 7.38-7.28 (m, 5H, arom). ^{13}C NMR (75 MHz, $CDCl_3$): δ (ppm) 174.1 (C), 136.2 (C), 128.7 (2xCH), 128.4 (2xCH), 128.3 (CH), 73.2 (CH), 71.9 (CH), 66.2 (CH_2), 48.4 (CH), 47.4 (CH), 46.6 (C), 42.2 (CH), 36.6 (CH_2), 36.1 (CH), 35.3 (CH_2), 35.2 (CH), 34.2 (C), 33.8 (CH), 31.5 (CH_2), 31.0 (CH_2), 30.6 (CH_2), 28.8 (CH_2), 27.6 (CH_2), 27.3 (CH_2), 26.2 (CH_2), 23.8 (CH_2), 23.3 (CH_3), 17.4 (CH_3), 12.8 (CH_3); m/z found 483.3480, calculated for $C_{31}H_{47}O_4$ (MH^+) 483.3474.

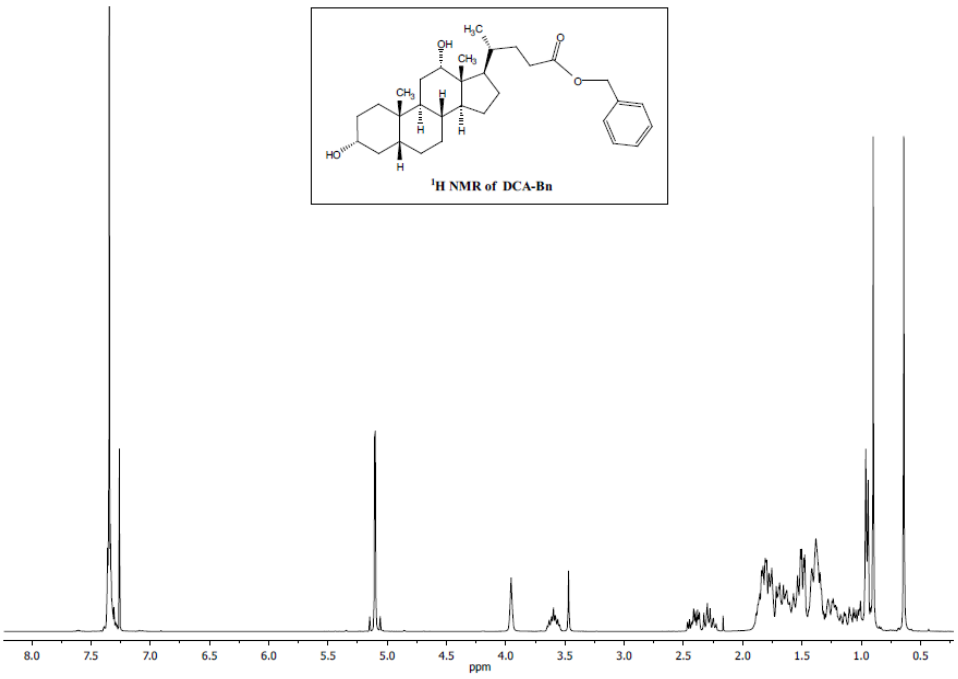
^{1}H NMR of DCA-Bn
8.0
7.5
7.0
6.5
6.0
5.5
5.0
4.5
4.0
3.5
3.0
2.5
2.0
1.5
1.0
0.5
ppm

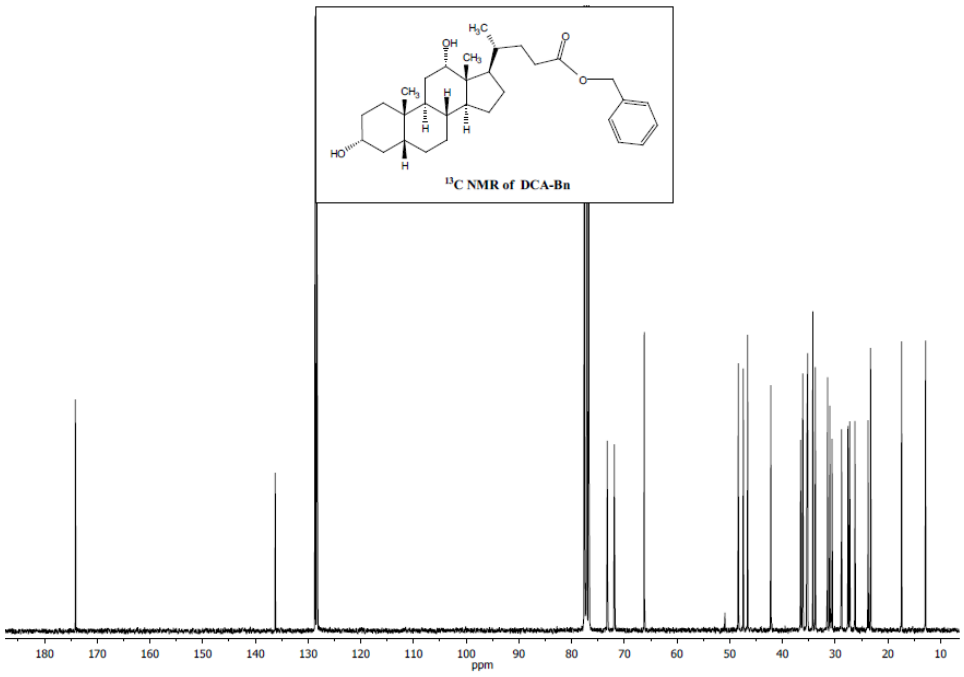
^{13}C NMR of DCA-Bn
180
170
160
150
140
130
120
110
100
90
80
70
60
50
40
30
20
10
ppm

5.6.1.5. Synthesis of 3α,12α-2Thy-DCA-Bn

A stirred suspension of Thy-CH_2CO_2H (1.720 g, 9.36 mmol) in anhydrous THF (60 mL) was treated with Et_3N (2.620 mL, 18.80 mmol) and 2,4,6-trichlorobenzoyl chloride (1.750 mL, 11.23 mmol) and the resulting mixture was allowed to react for 1.5 h. Then a solution of 4-DMAP (0.232 g, 1.91 mmol) and **DCA-Bn** (0.752 g, 1.56 mmol) in anhydrous THF (25 mL) was added and stirred overnight. Afterwards, the reaction mixture was poured into $NaHCO_3$ (5%), extracted with CH_2Cl_2 and the combined extracts were washed with brine, dried over $MgSO_4$ and concentrated under vacuum. Purification by column chromatography (SiO_2, CH_2Cl_2:MeOH, 98:2) followed by (Li Chroprep RP-18, CH_3CN:H_2O, 80:20), gave **3α,12α-2Thy-DCA-Bn** as a white solid (1.210 g, 95%). ^{1}H NMR (300 MHz, $CDCl_3$): δ (ppm) 0.65 (s, 3H, CH_3); 0.77 (d, *J* = 5.7 Hz, 3H, 21-CH_3); 0.78-2.42 (complex signal, 26H); 0.86 (s, 3H, CH_3); 1.87 (*br* s, 3H, Thy-CH_3); 1.89 (*br* s, 3H, Thy-CH_3); 4.38 (d, *J* = 17.4 Hz, 1H, Thy-CH_2); 4.40 (d, *J* = 17.4 Hz, 1H, Thy-CH_2); 4.49 (d, *J* = 17.4 Hz, 1H, Thy-CH_2); 4.57 (d, *J* = 17.4 Hz, 1H, Thy-CH_2); 4.70 (m, 1H, 3β-H); 5.08 (*br* s, 2H, CH_2); 5.11 (*br* s, 1H, 12β-H); 6.98 (*br* s, 1H, Thy-CH); 7.05 (*br* s, 1H, Thy-CH); 7.26-7.37 (m, 5H, arom); 10.12 (s, 1H, Thy-NH); 10.21 (s, 1H, Thy-NH). ^{13}C NMR (75 MHz, $CDCl_3$): δ (ppm) 174.0 (C), 167.3 (C), 166.7 (C), 164.7 (C), 164.6 (C), 151.5 (C), 150.9 (C), 140.8 (CH), 140.5 (CH), 136.0 (C), 128.6 (2xCH), 128.3 (3xCH), 111.2 (C), 110.7 (C), 77.9 (CH), 76.5 (CH), 66.2 (CH_2), 49.3 (CH+2xCH_2), 47.5 (CH), 45.2 (C), 41.7 (CH), 35.5 (CH), 34.7 (CH+CH_2), 34.2 (CH), 34.1 (C), 31.9 (CH_2), 31.3 (CH_2), 30.8 (CH_2), 27.3 (CH_2), 26.8 (CH_2), 26.0 (CH_2), 25.9 (CH_2), 25.3 (CH_2), 23.4 (CH_2), 22.9 (CH_3), 17.7 (CH_3), 12.4 (2xCH_3), 12.2 (CH_3); m/z found 815.4200, calculated for $C_{45}H_{59}N_4O_{10}$ (MH^+) 815.4231.

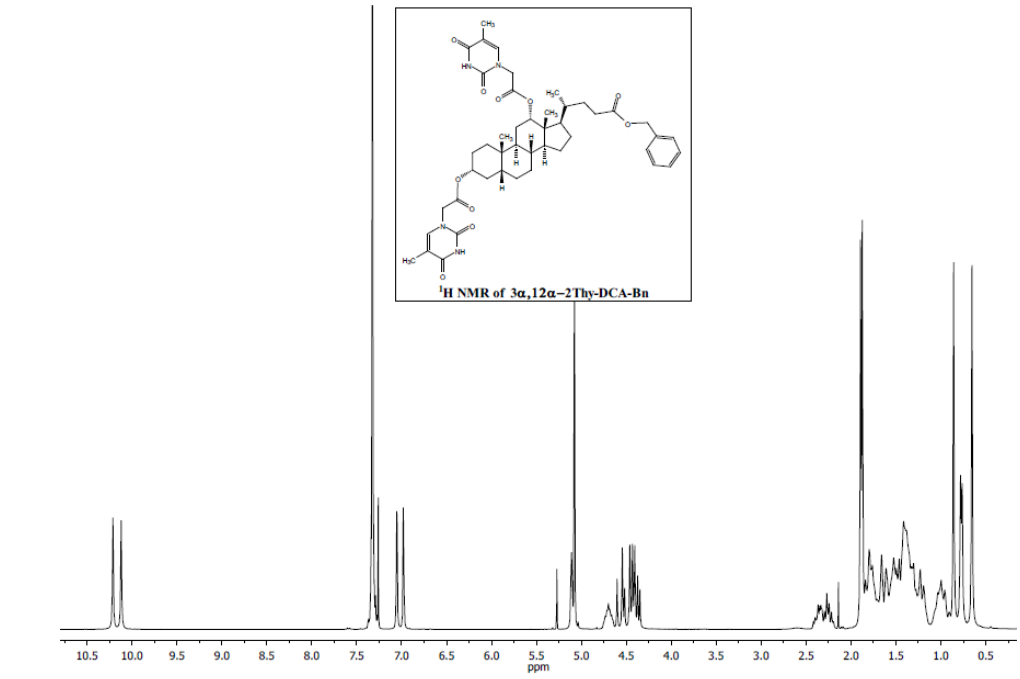
^{1}H NMR of 3α,12α−2Thy-DCA-Bn
10.5 10.0 9.5 9.0 8.5 8.0 7.5 7.0 6.5 6.0 5.5 5.0 4.5 4.0 3.5 3.0 2.5 2.0 1.5 1.0 0.5
ppm

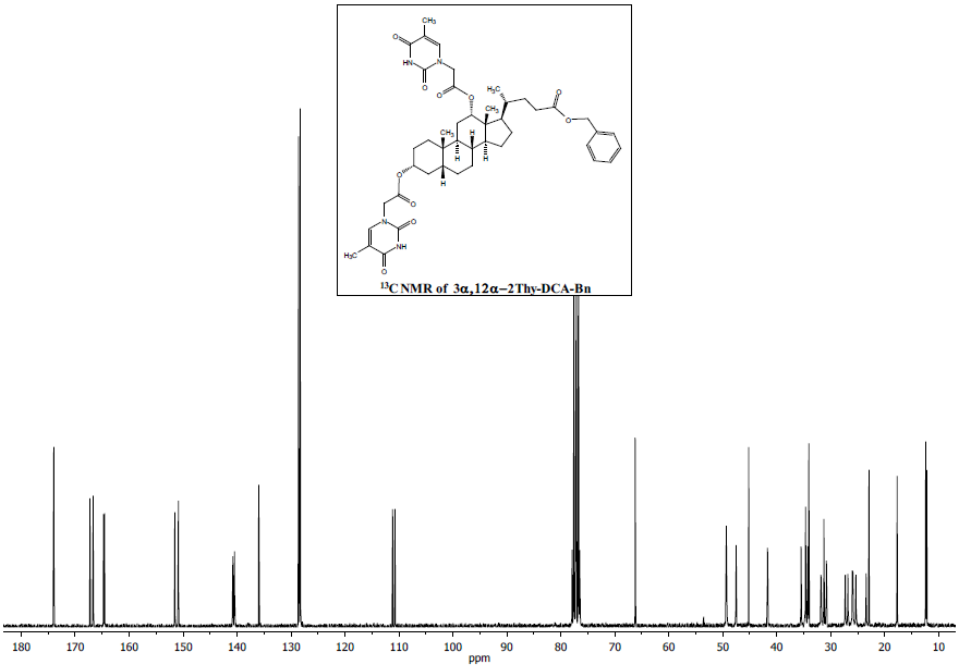
^{13}C NMR of 3α,12α−2Thy-DCA-Bn
180 170 160 150 140 130 120 110 100 90 80 70 60 50 40 30 20 10
ppm

5.6.1.6. Synthesis of CDCA-Bzp

To a stirred mixture of **CDCA** (0.915 g, 2.33 mmol), KP-OH (0.588 g, 2.45 mmol) and TBTU (0.898 g, 2.79 mmol) in anhydrous DMF (7 mL), DIEA (1.22 mL, 6.99 mmol) was added dropwise and the reaction mixture was allowed to react overnight. Afterwards, it was poured into brine and extracted with CH_2Cl_2; the combined organic layers were washed with brine, dried over $MgSO_4$ and concentrated under reduced pressure. Purification by column chromatography (SiO_2, EtOAc:Hexane, 60:40) gave **CDCA-Bzp** as a colorless solid (1.09 g, 76%); ^{1}H NMR (300 MHz, $CDCl_3$): δ (ppm) 0.57 (s, 3H, CH_3); 0.81-2.31 (complex signal, 26H); 0.82 (m, 6H, CH_3 + 21-CH_3); 1.27 (d, J = 7.2 Hz, 3H, KP-CH_3); 2.68 (*br* s, 2H, 2xOH); 3.11 (m, 1H, KP-CH); 3.37 (m, 1H, 3β-H); 3.76 (*br* s, 1H, 7β-H); 4.12 (m, 2H, KP-CH_2); 7.32-7.80 (m, 9H, arom). ^{13}C NMR (75 MHz, $CDCl_3$): δ (ppm) 196.5 (C), 174.0 (C), 143.6 (C), 137.6 (C), 137.5 (C), 132.4 (CH), 131.4 (CH), 130.0 (2xCH), 128.8 (CH), 128.6 (CH), 128.3 (CH), 128.2 (2xCH), 71.7 (CH), 68.8 (CH_2), 68.2 (CH), 55.8 (CH), 50.3 (CH), 42.5 (C), 41.5 (CH), 39.6 (2xCH_2), 39.4 (CH), 38.8 (2xCH), 35.4 (CH_2), 35.2 (CH), 35.0 (C), 34.7 (CH_2), 32.8 (CH), 31.1 (CH_2), 30.9 (CH_2), 30.6 (CH_2), 28.1 (CH_2), 23.5 (CH_2), 22.9 (CH_3), 20.6 (CH_2), 18.2 (CH_3), 17.9 (CH_3), 11.7 (CH_3); m/z found 615.4077, calculated for $C_{40}H_{55}O_5$ (MH^+) 615.4050.

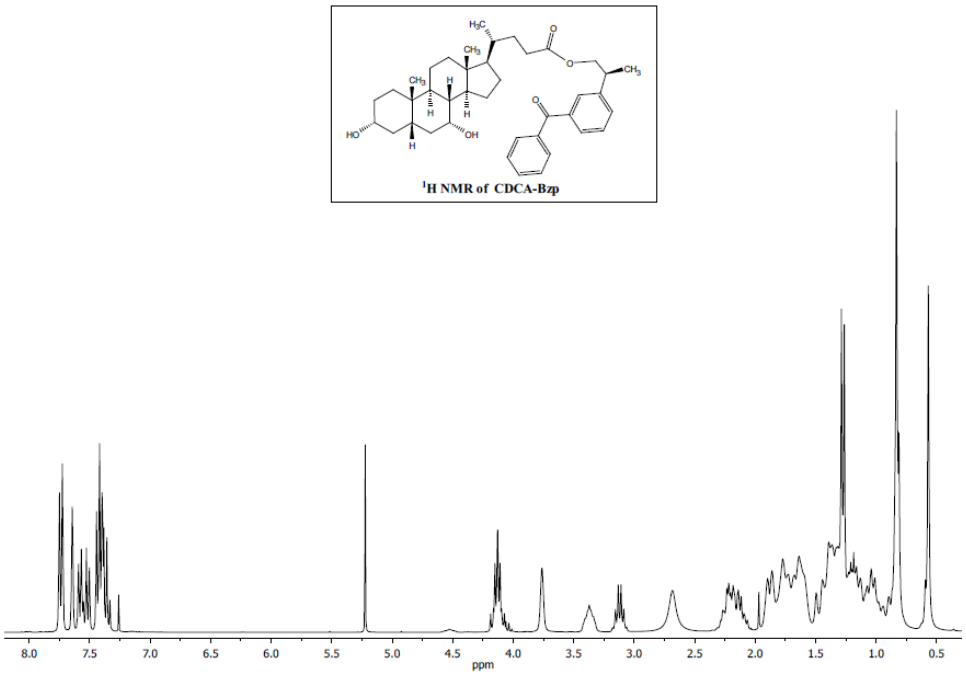
^{1}H NMR of CDCA-Bzp
8.0 7.5 7.0 6.5 6.0 5.5 5.0 4.5 4.0 3.5 3.0 2.5 2.0 1.5 1.0 0.5
ppm

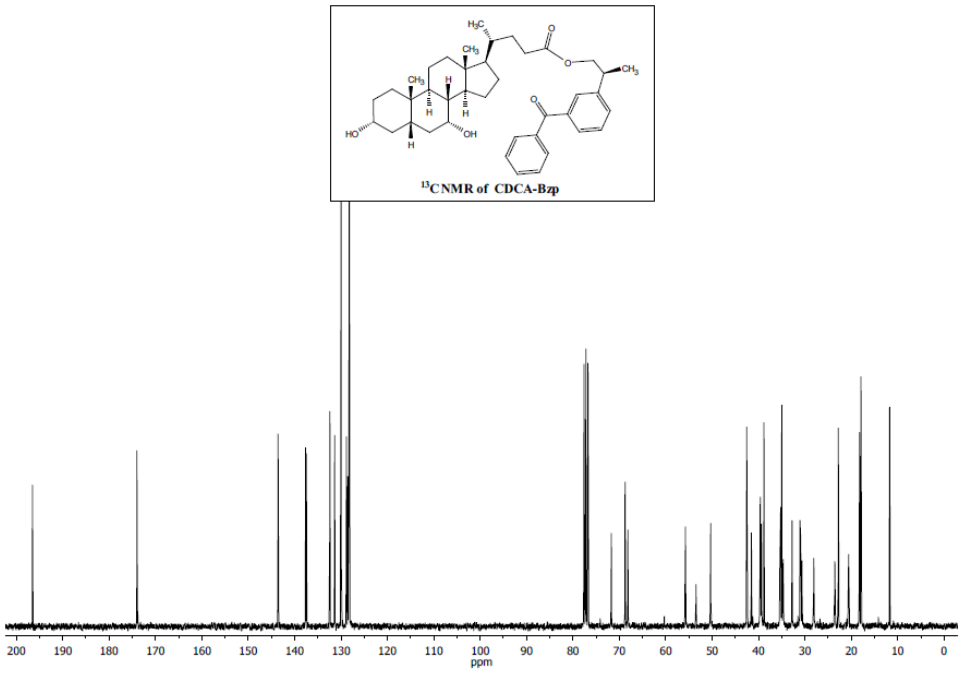
^{13}CNMR of CDCA-Bzp
200 190 180 170 160 150 140 130 120 110 100 90 80 70 60 50 40 30 20 10 0
ppm

5.6.1.7. Synthesis of 3α,7α-2Thy-CDCA-Bzp

A stirred suspension of Thy-CH_2CO_2H (2.96 g, 16.05 mmol) in anhydrous THF (50 mL) was treated with Et_3N (6.10 mL) and 2,4,6-trichlorobenzoyl chloride (3.03 mL, 19.4 mmol) and the resulting mixture was allowed to react for 1.5 h. Then, a solution of 4-DMAP (0.265 g, 2.17 mmol) and **CDCA-Bzp** (1.10 g, 1.78 mmol) in anhydrous THF (20 mL) was added and the resulting reaction mixture was stirred overnight. Afterwards, it was poured into brine, extracted with CH_2Cl_2 and the combined extracts were washed again with brine, dried over $MgSO_4$ and concentrated under vacuum. Purification by column chromatography (Li Chroprep RP-18, CH_3CN:H_2O, 85:15), gave **3α,7α-2Thy-CDCA-Bzp** as a colorless solid (1.22 g, 72%); ^{1}H NMR (300 MHz, $CDCl_3$): δ (ppm) 0.55 (s, 3H, CH_3); 0.67-2.31 (complex signal, 26H); 0.81 (d, J = 6.3 Hz, 3H, 21-CH_3); 0.86 (s, 3H, CH_3); 1.29 (d, J = 6.9 Hz, 3H, KP-CH_3); 1.85 (*br* s, 3H, Thy-CH_3); 1.87 (*br* s, 3H, Thy-CH_3); 3.12 (m, 1H, KP-CH); 4.14 (m, 2H, KP-CH_2); 4.36 (AB_q, 2H, J_{AB}= 17.7 Hz, Thy-CH_2); 4.47-4.64 (m, 3H, Thy-CH_2 + 3β-H); 4.86 (*br* s, 1H, 7β-H); 7.05 (*br* s, 1H, Thy-CH); 7.12 (*br* s, 1H, Thy-CH); 7.34-7.80 (m, 9H, arom); 10.25 (m, 2H, 2xThy-NH). ^{13}C NMR (100 MHz, $CDCl_3$): δ (ppm) 196.7 (C), 174.0 (C), 167.5 (C), 166.9 (C), 164.7 (2xC), 151.6 (C), 151.0 (C), 143.6 (C), 141.0 (2xCH), 137.6 (C), 137.5 (C), 132.5 (CH), 131.4 (CH), 130.0 (2xCH), 128.9 (CH), 128.6 (CH), 128.4 (CH), 128.3 (2xCH), 111.0 (C), 110.5 (C), 76.1 (CH), 73.7 (CH), 68.8 (CH_2), 55.7 (CH), 50.4 (CH), 49.4 (CH_2), 49.0 (CH_2), 42.6 (C), 40.5 (CH), 39.5 (CH_2), 38.9 (CH), 37.9 (CH), 35.3 (CH), 34.6 (C+CH_2), 34.4 (CH_2), 34.2 (CH), 31.3 (CH_2), 30.8 (2xCH_2), 27.9 (CH_2), 26.5 (CH_2), 23.4 (CH_2), 22.6 (CH_3), 20.5 (CH_2), 18.1 (CH_3), 17.9 (CH_3), 12.4 (CH_3), 12.3 (CH_3), 11.6 (CH_3); m/z found 947.4783, calculated for $C_{54}H_{67}N_4O_{11}$ (MH^+) 947.4807.

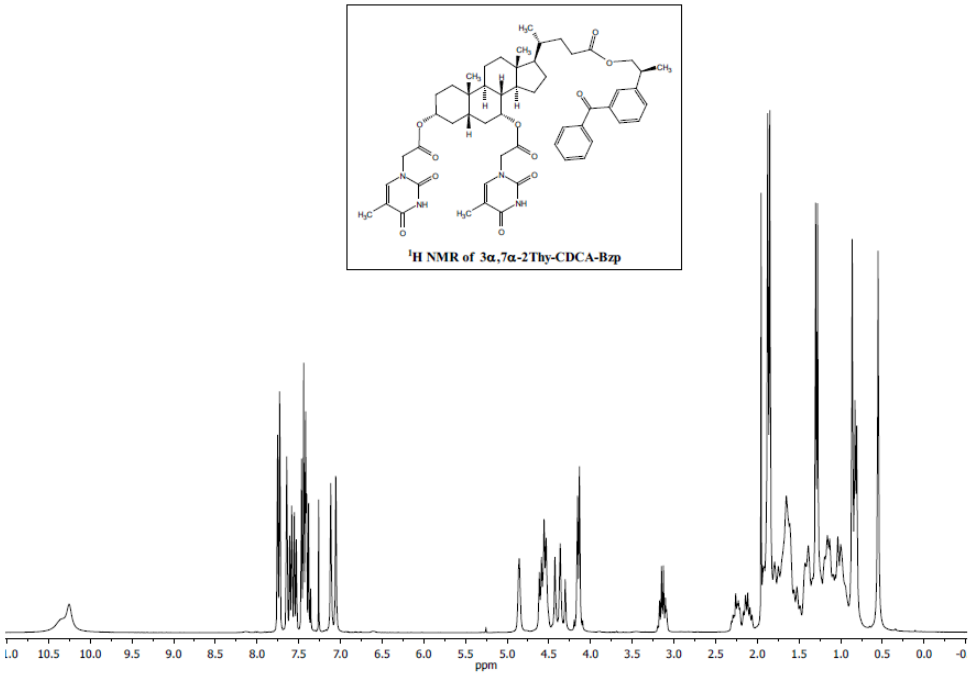
^{1}H NMR of 3α,7α-2Thy-CDCA-Bzp
ppm

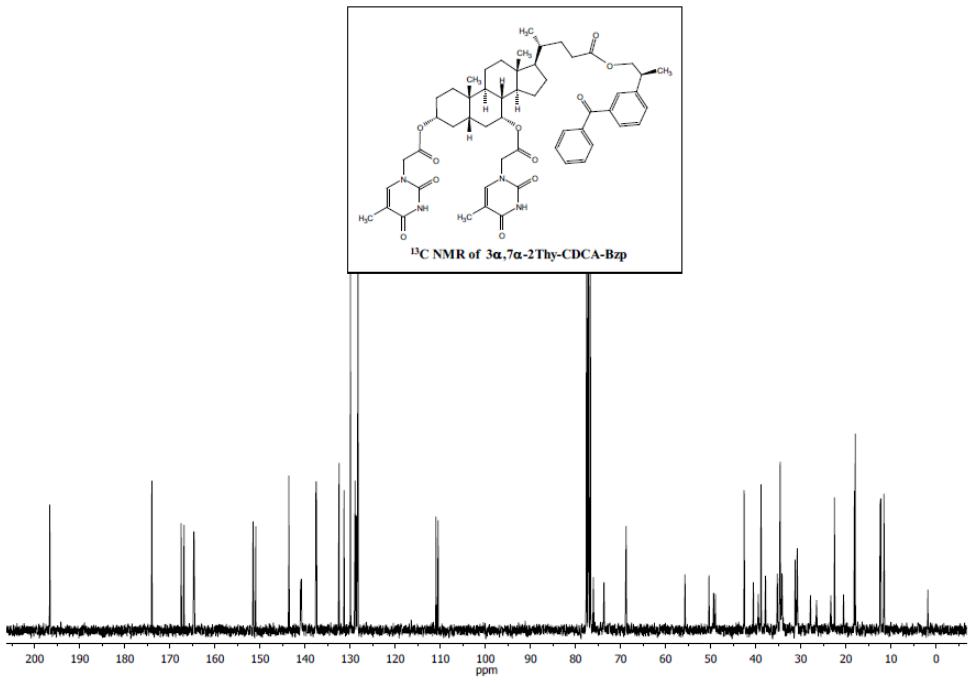
^{13}C NMR of 3α,7α-2Thy-CDCA-Bzp
ppm

5.6.1.8. Synthesis of CDCA-Bn

A stirred solution of **CDCA** (1.00 g, 2.55 mmol) in anhydrous DMF (10 mL) was treated with DBU (0.429 mL, 2.87 mmol). Ten minutes later, benzyl bromide (0.32 mL, 2.71 mmol) was added dropwise and the reaction mixture was allowed to react overnight at rt. Then, the solvent was evaporated and the crude was extracted with CH_2Cl_2; the combined organic layers were washed with brine, dried over $MgSO_4$ and concentrated under reduced pressure. Purification by column chromatography (SiO_2, EtOAc:Hexane, 70:30) gave **CDCA-Bn** as a colorless solid (1.19 g, 97%); ^{1}H NMR (300 MHz, $CDCl_3$): δ (ppm) 0.62 (s, 3H, CH_3); 0.87-2.44 (complex signal, 26H); 0.88 (s, 3H, CH_3); 0.90 (d, *J* = 6.3 Hz, 3H, 21-CH_3); 3.43 (m, 1H, 3β-H); 3.82 (*br* s, 1H, 7β-H)); 5.08 (d, *J* = 12.6 Hz, 1H, CH_2); 5.12 (d, *J* = 12.6 Hz, 1H, CH_2); 7.26-7.38 (m, 5H, arom). ^{13}C NMR (75 MHz, $CDCl_3$): δ (ppm) 173.9 (C), 136.0 (C), 128.4 (2xCH), 128.0 (3xCH), 71.6 (CH), 68.0 (CH), 65.9 (CH_2), 55.8 (CH), 50.3 (CH), 42.4 (C), 41.5 (CH), 39.6 (CH_2), 39.5 (CH_2), 39.3 (CH), 35.4 (CH_2), 35.1 (CH), 34.9 (C), 34.7 (CH_2), 32.8 (CH), 31.0 (CH_2), 30.8 (CH_2), 30.5 (CH_2), 28.1 (CH_2), 23.5 (CH_2), 22.8 (CH_3), 20.5 (CH_2), 18.2 (CH_3), 11.7 (CH_3); m/z found 505.3280, calculated for $C_{31}H_{46}O_4Na$ (MNa^+) 505.3294.

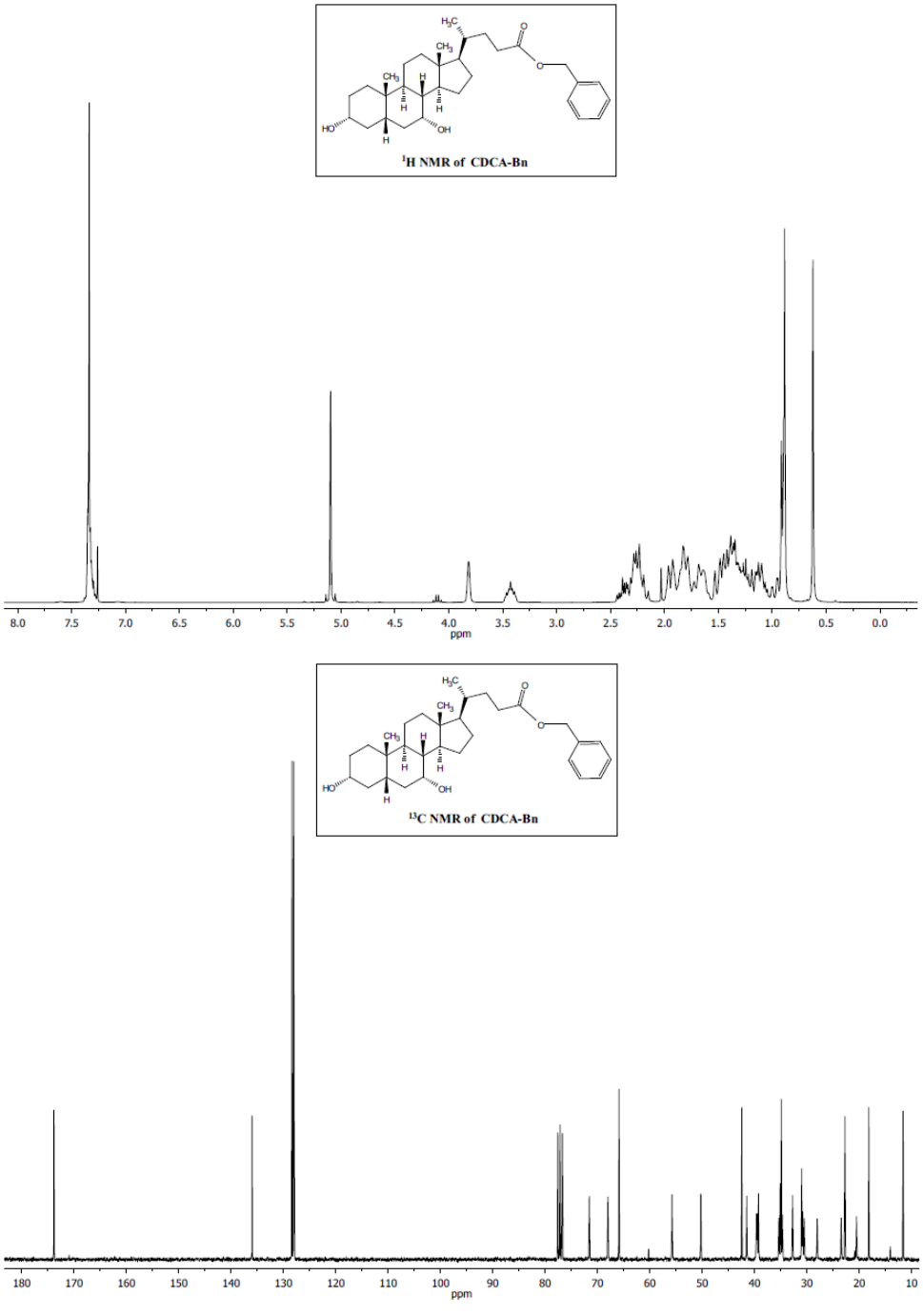
^{1}H NMR of CDCA-Bn
8.0 7.5 7.0 6.5 6.0 5.5 5.0 4.5 4.0 3.5 3.0 2.5 2.0 1.5 1.0 0.5 0.0
ppm
^{13}C NMR of CDCA-Bn
180 170 160 150 140 130 120 110 100 90 80 70 60 50 40 30 20 10
ppm

5.6.1.9. Synthesis of 3α,7α-2Thy-CDCA-Bn

A stirred suspension of Thy-CH_2CO_2H (4.08 g, 22.18 mmol) in anhydrous THF (60 mL) was treated with Et_3N (0.610 mL) and 2,4,6-trichlorobenzoyl chloride (4.21 mL, 26.9 mmol) and the resulting mixture was allowed to react for 1.5 h. Then a solution of 4-DMAP (0.368 g, 3.02 mmol) and **CDCA-Bn** (1.19 g, 2.47 mmol) in anhydrous THF (40 mL) was added and stirred overnight. Afterwards, the reaction mixture was poured into brine, extracted with CH_2Cl_2 and the combined extracts were washed with brine, dried over $MgSO_4$ and concentrated under vacuum. Purification by column chromatography (SiO_2, EtOAc:Hexane, 80:20) followed by (Li Chroprep RP-18, CH_3CN:H_2O, 80:20), gave **3α,7α-2Thy-CDCA-Bn** as a white solid (1.51 g, 75%). **3α,7α-2Thy-CDCA-Bn** was christalized from C_5H_5N; ^{1}H NMR (300 MHz, C_5D_5N): δ (ppm) 0.55 (s, 3H, CH_3); 0.75-2.49 (complex signal, 26H); 0.82 (s, 3H, CH_3); 0.86 (d, *J* = 6.3 Hz, 3H, 21-CH_3); 1.93 (*br* s, 3H, Thy-CH_3); 2.14 (*br* s, 3H, Thy-CH_3); 4.71-4.97 (m, 5H, 2xThy-CH_2+3β-H); 5.02 (*br* s, 1H, 7β-H); 5.28 (m, 2H, CH_2); 7.31-7.47 (m, 5H, arom); 7.47-7.55 (m, 2H, 2xThy-CH); 13.47 (*br* s, 1H, Thy-NH); 13.54 (*br* s, 1H, Thy-NH). ^{13}C NMR (75 MHz, C_5D_5N): δ (ppm) 174.1 (C), 168.9 (C), 168.2 (C), 165.8 (2xC), 153.1 (C), 152.7 (C), 142.0 (CH), 141.9 (CH), 137.6 (C), 129.4 (2xCH), 129.1 (2xCH), 128.9 (CH), 110.9 (C), 110.7 (C), 76.6 (CH); 73.9 (CH), 66.5 (CH_2), 56.6 (CH), 51.0 (CH), 50.7 (2xCH_2), 43.3 (C), 41.3 (CH), 40.3 (CH_2), 38.5 (CH), 36.1 (CH), 35.3 (CH_2), 35.2 (CH_2+C), 35.0 (CH), 32.2 (CH_2), 31.5 (CH_2), 31.4 (CH_2), 28.6 (CH_2), 27.3 (CH_2), 24.0 (CH_2), 23.0 (CH_3), 21.3 (CH_2), 18.7 (CH_3), 13.3 (CH_3), 12.9 (CH_3), 12.2 (CH_3); m/z found 815.4216, calculated for $C_{45}H_{59}N_4O_{10}$ (MH^+) 815.4231.

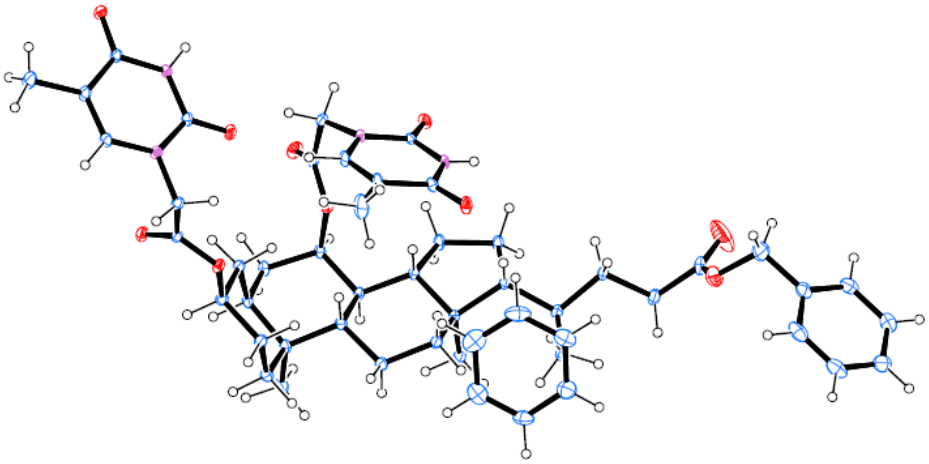

Figure 5.9 X-ray crystal structure of **3α,7α-2Thy-CDCA-Bn.**

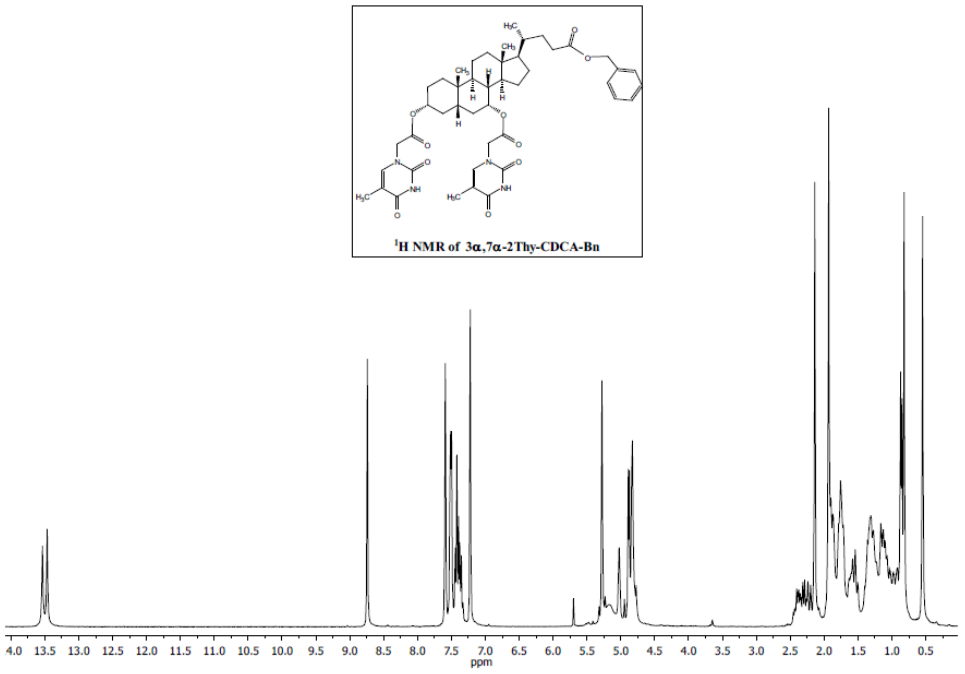
^{1}H NMR of 3α,7α-2Thy-CDCA-Bn
4.0 13.5 13.0 12.5 12.0 11.5 11.0 10.5 10.0 9.5 9.0 8.5 8.0 7.5 7.0 6.5 6.0 5.5 5.0 4.5 4.0 3.5 3.0 2.5 2.0 1.5 1.0 0.5
ppm

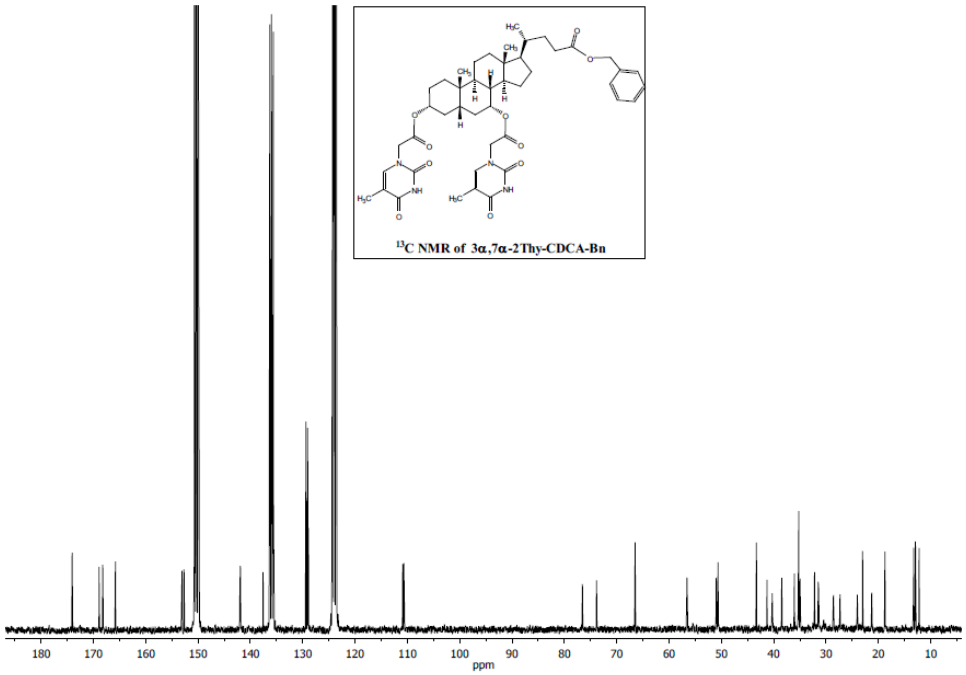
^{13}C NMR of 3α,7α-2Thy-CDCA-Bn
180 170 160 150 140 130 120 110 100 90 80 70 60 50 40 30 20 10
ppm

5.6.1.10. Synthesis of DCAOH

A stirred suspension of $LiAlH_4$ (0.33 g, 9.13 mmol) in anhydrous THF (8.5 mL) was cooled to −10 ° C, treated with a solution of **DCA-Bn** (1.54 g, 3.19 mmol) in anhydrous THF (6 mL), and then the reaction mixture was refluxed overnight (70 ° C). Afterwards, the reaction was quenched with saturated aqueous NH_4Cl solution (5 mL), redissolved with EtOAc, poured into aqueous HCl 1M and extracted with EtOAc. The combined organic layers were washed with brine, dried over $MgSO_4$ and concentrated. Purification by column chromatography (Li Chroprep RP-18, MeOH: EtOAc: H_2O, 8:1:1) gave **DCAOH** as a colorless solid (1.05 g, 87%); ^{1}H NMR (300 MHz, $CDCl_3$): δ (ppm) 0.68 (s, 3H, CH_3); 0.91 (s, 3H, CH_3); 0.93-1.89 (complex signal, 26H); 0.98 (d, *J* = 6.3 Hz, 3H, 21-CH_3); 3.61 (m, 3H, 3β-H + CH_2); 3.99 (*br* s, 1H, 12β-H). ^{13}C NMR (75 MHz, $CDCl_3$): δ (ppm) 72.4 (CH), 71.0 (CH), 62.7 (CH_2), 47.5 (CH), 46.8 (CH), 45.7 (C), 41.3 (CH), 35.6 (CH_2), 35.2 (CH), 34.5 (CH), 34.4 (CH_2), 33.3 (C), 32.9 (CH), 30.9 (CH_2), 29.7 (CH_2), 28.7 (CH_2), 27.8 (CH_2), 26.7 (CH_2), 26.3 (CH_2), 25.3 (CH_2), 22.8 (CH_2), 22.3 (CH_3), 16.9 (CH_3), 11.9 (CH_3); m/z found 379.3214, calculated for calculated for $C_{24}H_{43}O_3$ (MH^+) 379.3212.

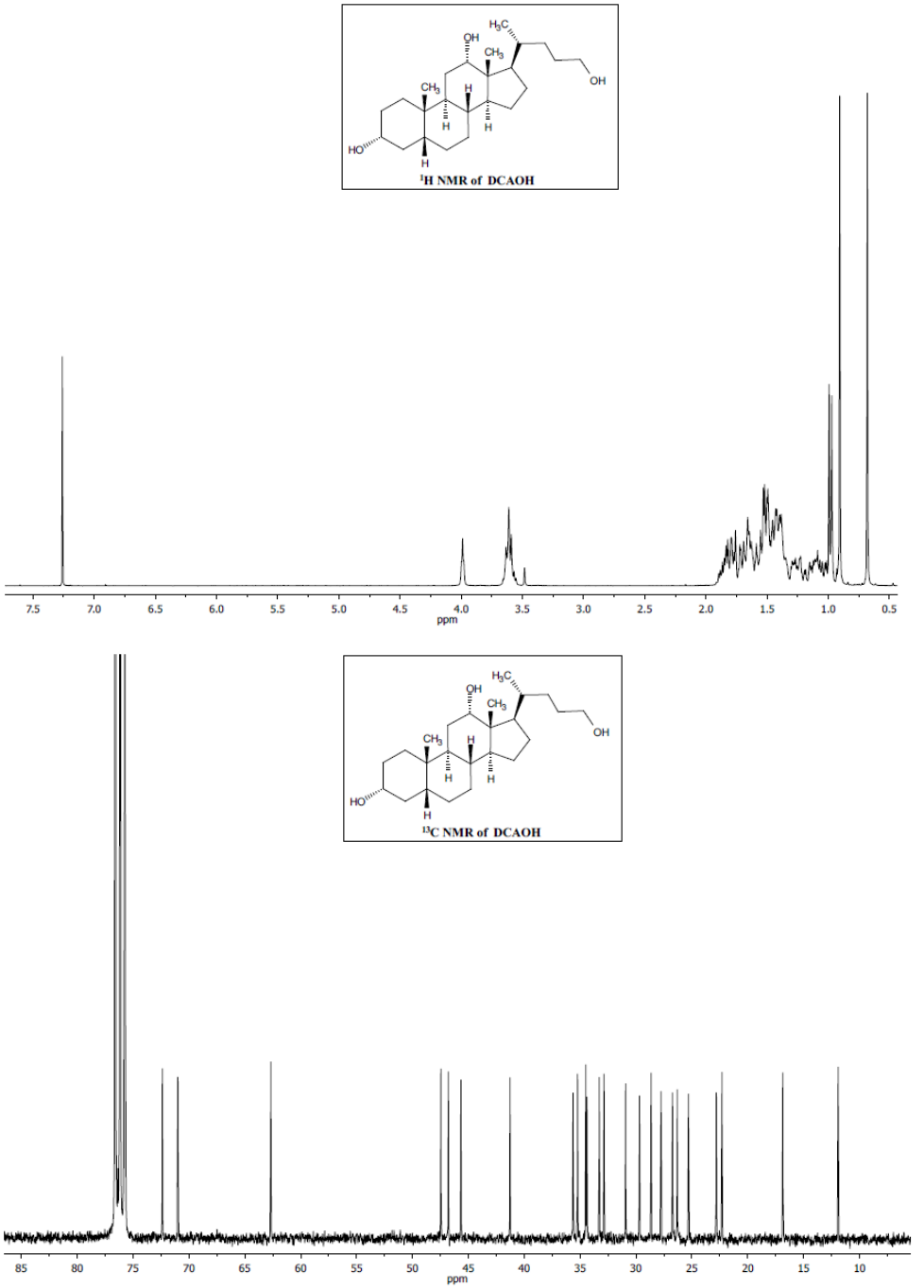
^{1}H NMR of DCAOH
7.5 7.0 6.5 6.0 5.5 5.0 4.5 4.0 3.5 3.0 2.5 2.0 1.5 1.0 0.5
ppm
^{13}C NMR of DCAOH
85 80 75 70 65 60 55 50 45 40 35 30 25 20 15 10
ppm

5.6.1.11. Synthesis of DCA-Thy

DCAOH (0.44 g, 1.17 mmol) and TBTU (0.45 g, 1.41 mmol) were dissolved in anhydrous DMF (3 mL). Then a solution of Thy-CH_2CO_2H (0.226 g, 1.23 mmol) in anhydrous DMF (2 mL) was added, followed by DIEA (0.61 mL, 3.51 mmol) and the resulting reaction mixture was allowed to react at rt for 7 h. Then it was poured into brine and extracted with CH_2Cl_2. The combined organic extracts were washed with brine, dried over $MgSO_4$ and concentrated under reduced pressure. Purification by column chromatography (SiO_2, CH_2Cl_2:MeOH, 97:3, followed by Li Chroprep RP-18, CH_3CN:H_2O, 80:20) gave **DCA-Thy** as a yellowish solid (0.353 g, 56%); ^{1}H NMR (300 MHz, $CDCl_3$): δ (ppm) 0.63 (s, 3H, CH_3); 0.82-1.90 (complex signal, 26H);0.86 (s, 3H, CH_3); 0.93 (d, J = 6.6 Hz, 3H, 21-CH_3); 1.88 (d, J = 1.2 Hz, 3H, Thy-CH_3); 2.52 (*br* s, 1H, OH); 2.76 (*br* s, 1H, OH); 3.58 (m, 1H, 3β-H); 3.94 (*br* s, 1H, 12β-H); 4.10 (m, 2H, CH_2); 4.42 (s, 2H, Thy-CH_2); 6.96 (s, 1H, Thy-CH); 10.01 (*br* s, 1H, Thy-NH). ^{13}C NMR (75 MHz, $CDCl_3$): δ (ppm) 167.8 (C), 164.6 (C), 151.2 (C), 140.4 (CH), 111.2 (C), 73.2 (CH), 71.7 (CH), 66.7 (CH_2), 48.8 (CH_2), 48.3 (CH), 47.3 (CH), 46.5 (C), 42.1 (CH), 36.3 (CH_2), 36.0 (CH), 35.4 (CH_2), 35.3 (CH), 34.2 (C), 33.5 (CH), 31.8 (CH_2), 30.3 (CH_2), 28.6 (CH_2), 27.7 (CH_2), 27.2 (CH_2), 26.2 (CH_2), 25.2 (CH_2), 23.8 (CH_2), 23.1 (CH_3), 17.5 (CH_3), 12.8 (CH_3), 12.4 (CH_3); m/z found 545.3599, calculated for $C_{31}H_{49}N_2O_6$ (MH^+) 545.3591.

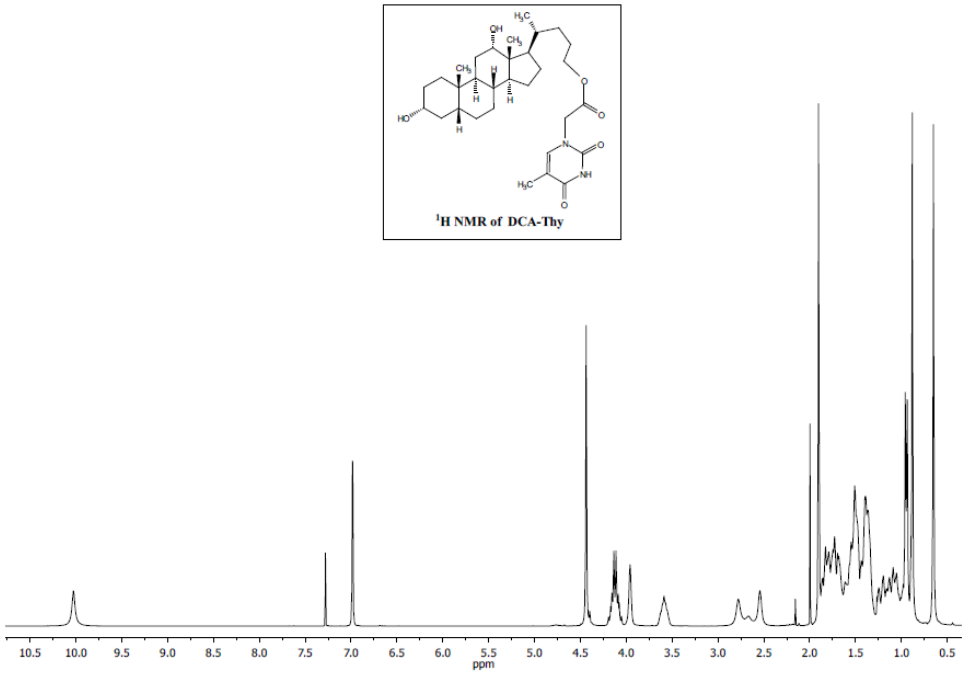
^{1}H NMR of DCA-Thy
10.5 10.0 9.5 9.0 8.5 8.0 7.5 7.0 6.5 6.0 5.5 5.0 4.5 4.0 3.5 3.0 2.5 2.0 1.5 1.0 0.5
ppm

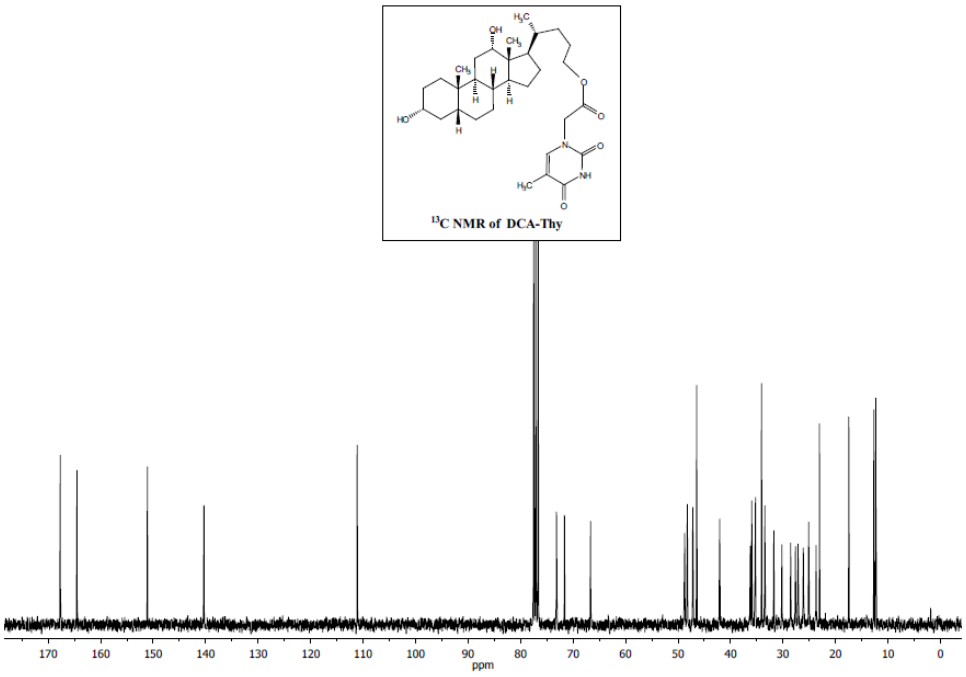
^{13}C NMR of DCA-Thy
170 160 150 140 130 120 110 100 90 80 70 60 50 40 30 20 10 0
ppm

5.6.1.12. Synthesis of 3α-Bzp-DCA-Thy

To a stirred solution of **DCA-Thy** (0.40 g, 0.73 mmol), TBTU (0.28 g, 0.87 mmol) and (*S*)-KP (0.20 g, 0.80 mmol) in anhydrous DMF (5 mL), DIEA (0.38 mL, 2.18 mmol) was added dropwise and then the reaction mixture was allowed to react at rt for 7 h. Afterwards, it was poured into brine and extracted with CH_2Cl_2; the combined organic layers were washed with brine, dried over $MgSO_4$ and concentrated under vacuum. Purification by column chromatography (SiO_2, CH_2Cl_2: MeOH, 98:2, followed by Li Chroprep RP-18, CH_3CN:H_2O, 90:10) gave **3α-Bzp-DCA-Thy** as a yellow solid (0.360 g, 63%); ^{1}H NMR (300 MHz, $CDCl_3$): δ (ppm) 0.65 (s, 3H, CH_3); 0.89 (s, 3H, CH_3); 0.84-2.00 (complex signal, 26H); 0.94 (d, *J* = 6.0 Hz, 3H, 21-CH_3); 1.48 (d, 3H, *J* = 7.2 Hz, KP-CH_3); 1.89 (d, *J* = 1.2 Hz, 3H, Thy-CH_3); 3.73 (q, *J* = 6.9 Hz, 1H, KP-CH); 3.97 (*br* s, 1H, 12β-H); 4.12 (m, 2H, CH_2); 4.42 (s, 2H, Thy-CH_2); 4.70 (m, 1H, 3β-H); 6.94 (s, 1H, Thy-CH); 7.36-7.82 (m, 9H, arom); 9.38 (s, 1H, Thy-NH). ^{13}C NMR (75 MHz, $CDCl_3$): δ (ppm) 196.7 (C), 173.7 (C), 167.7 (C), 164.3 (C), 151.0 (C), 141.2 (C), 140.3 (CH), 137.9 (C), 137.6 (C), 132.6 (CH), 131.6 (CH), 130.2 (2xCH), 129.3 (CH), 129.0 (CH), 128.6 (CH), 128.4 (2xCH), 111.3 (C), 75.0 (CH), 73.2 (CH), 66.7 (CH_2), 48.8 (CH_2), 48.3 (CH), 47.5 (CH), 46.5 (C), 45.8 (CH), 42.0 (CH), 36.1 (CH), 35.2 (CH), 34.9 (CH_2), 34.2 (C), 33.7 (CH), 32.0 (CH_2), 31.8 (CH_2), 28.8 (CH_2), 27.7 (CH_2), 27.1 (CH_2), 26.5 (CH_2), 26.1 (CH_2), 25.2 (CH_2), 23.7 (CH_2), 23.2 (CH_3), 18.7 (CH_3), 17.6 (CH_3), 12.8 (CH_3), 12.5 (CH_3); m/z found 781.4429, calculated for $C_{47}H_{61}N_2O_8$ (MH^+) 781.4428.

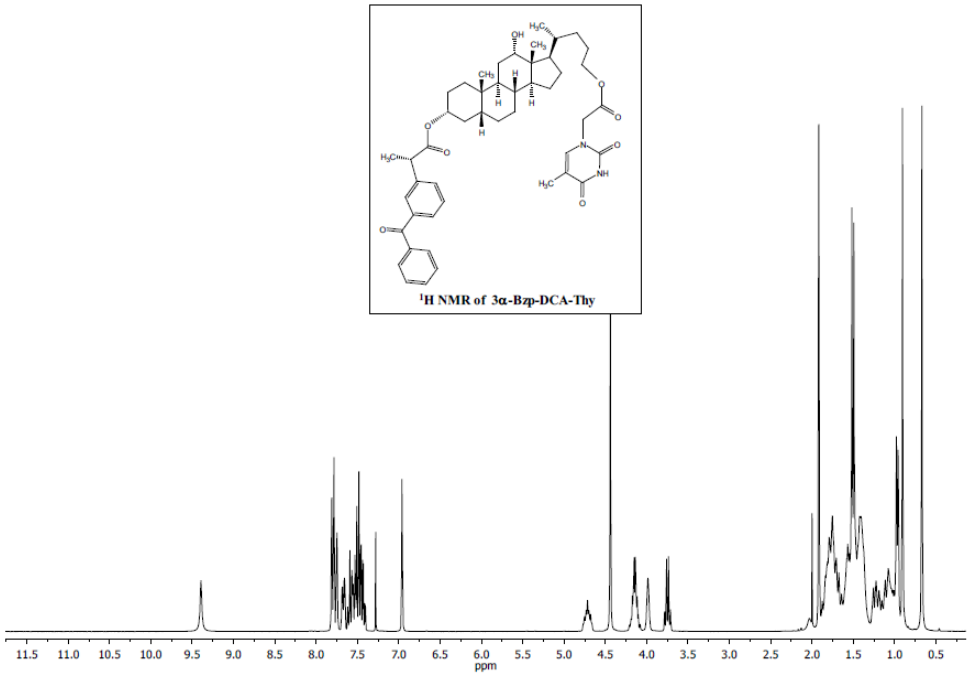
^{1}H NMR of 3α-Bzp-DCA-Thy
11.5 11.0 10.5 10.0 9.5 9.0 8.5 8.0 7.5 7.0 6.5 6.0 5.5 5.0 4.5 4.0 3.5 3.0 2.5 2.0 1.5 1.0 0.5
ppm

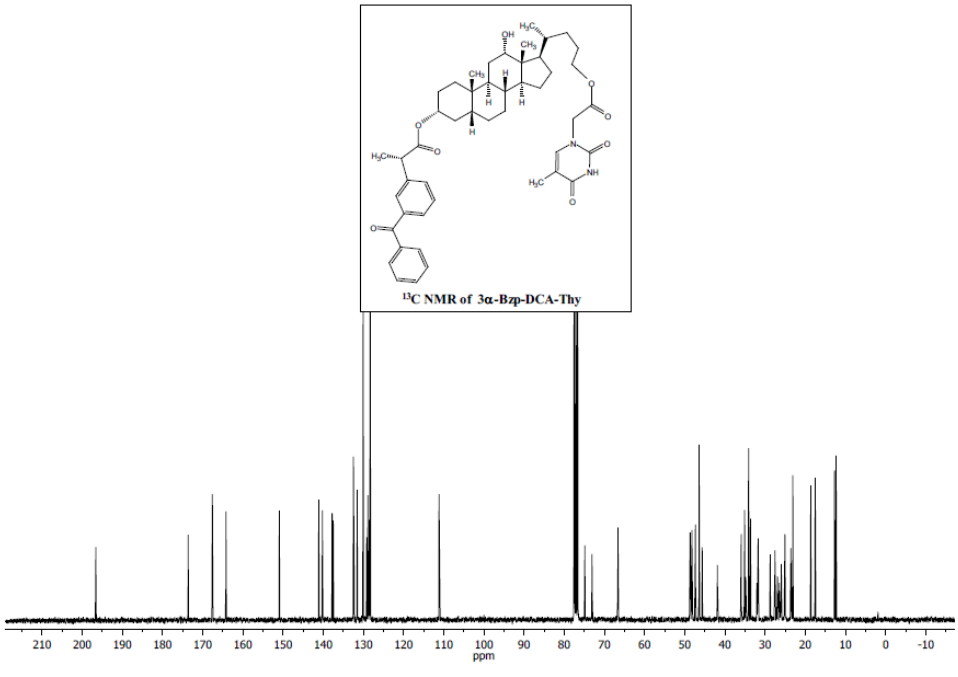
^{13}C NMR of 3α-Bzp-DCA-Thy
210 200 190 180 170 160 150 140 130 120 110 100 90 80 70 60 50 40 30 20 10 0 -10
ppm

5.6.1.13. Synthesis of 3α-(*R* or *S*) Bzp,12α-Thy-DCA-Thy

A stirred suspension of Thy-CH_2CO_2H (0.25 g, 1.37 mmol) and Et_3N (0.38 mL) in anhydrous THF (9 mL) was treated with 2,4,6-trichlorobenzoyl chloride (0.26 mL, 1.64 mmol) and the resulting suspension was allowed to react for 1.5 h. After that, a solution of 4-DMAP (0.068 g, 0.56 mmol) and **3α-Bzp-DCA-Thy** (0.36 g, 0.46 mmol) in anhydrous THF (11 mL) was added and the reaction mixture was allowed to stir overnight. Then, it was poured into brine and extracted with CH_2Cl_2. The combined organic extracts were washed with brine, dried over $MgSO_4$ and concentrated under vacuum. Purification by column chromatography (SiO_2, CH_2Cl_2: CH_3CN, 83:17, followed by Li Chroprep RP-18, CH_3CN:H_2O, 90:10) gave **3α-(*R* or *S*) Bzp,12α-Thy-DCA-Thy** as a pale yellow solid (0.175 g, 58%). ^{1}H NMR (300 MHz, $CDCl_3$): δ (ppm) 0.67 (s, 3H, CH_3); 0.69-1.80 (complex signal, 26H); 0.77 (d, *J* = 6.0 Hz, 3H, 21-CH_3); 0.88 (s, 3H, CH_3); 1.54 (d, *J* = 6.9 Hz, 3H, KP-CH_3); 1.79 (d, *J* = 0.9 Hz, 3H, Thy-CH_3); 1.93 (d, *J* = 1.2 Hz, 3H, Thy-CH_3); 3.79 (q, *J* = 7.2 Hz, 1H, KP-CH); 4.18 (m, 2H); 4.20 (d, *J* = 17.4 Hz, 1H, Thy-CH_2); 4.26 (d, *J* = 17.1 Hz, 1H, Thy-CH_2); 4.50 (d, *J* = 17.1 Hz, 1H, Thy-CH_2); 4.69 (d, *J* = 17.4 Hz, 1H, Thy-CH_2); 4.72 (m, 1H, 3β-H); 5.14 (*br* s, 1H, 12β-H); 6.90 (s, 1H, Thy-CH) ; 6.96 (s, 1H, Thy-CH); 7.36-7.88 (m, 9H, arom); 10.66 (s, 1H, Thy-NH); 10.80 (s, 1H, Thy-NH). ^{13}C NMR (75 MHz, $CDCl_3$): δ (ppm) 196.5 (C), 173.5 (C), 167.5 (C), 166.4 (C), 165.0 (C), 164.5 (C), 152.1 (C), 151.5 (C), 141.2 (C), 140.6 (CH), 140.2 (CH), 138.0 (C), 137.4 (C), 132.8 (CH), 131.5 (CH), 130.0 (2xCH), 129.3 (CH), 128.9 (CH), 128.6 (CH), 128.5 (2xCH), 111.6 (C), 111.1 (C), 78.1 (CH), 75.1 (CH), 66.8 (CH_2), 50.3 (CH_2), 50.0 (CH_2), 49.8 (CH), 47.9 (CH), 46.0 (CH), 45.1 (C), 41.8 (CH), 35.8 (CH), 35.6 (CH), 34.8 (CH_2), 34.3 (CH), 34.0 (C), 32.1 (CH_2), 31.9 (CH_2), 27.4 (CH_2), 26.9 (CH_2), 26.7 (CH_2), 26.3 (CH_2), 26.2 (CH_2), 25.3 (CH_2), 23.4 (CH_2), 23.0 (CH_3), 18.6 (CH_3), 17.6 (CH_3), 12.6 (CH_3), 12.5 (CH_3), 12.4 (CH_3); m/z found 947.4754, calculated for $C_{54}H_{67}N_4O_{11}$ (MH^+) 947.4807. Under the reaction conditions, partial racemization of the methyl group of the Bzp was observed.

Therefore, the stereochemistry of the methyl group in the Bzp chromophore was not unequivocally assigned.

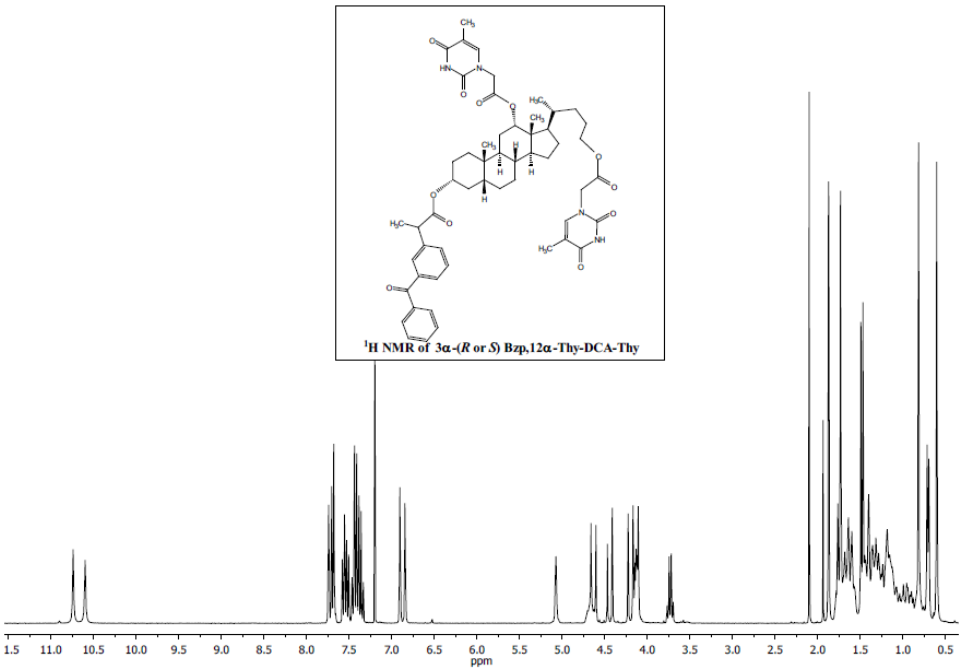
^{1}H NMR of 3α-(*R* or *S*) Bzp,12α-Thy-DCA-Thy
1.5 11.0 10.5 10.0 9.5 9.0 8.5 8.0 7.5 7.0 6.5 6.0 5.5 5.0 4.5 4.0 3.5 3.0 2.5 2.0 1.5 1.0 0.5
ppm

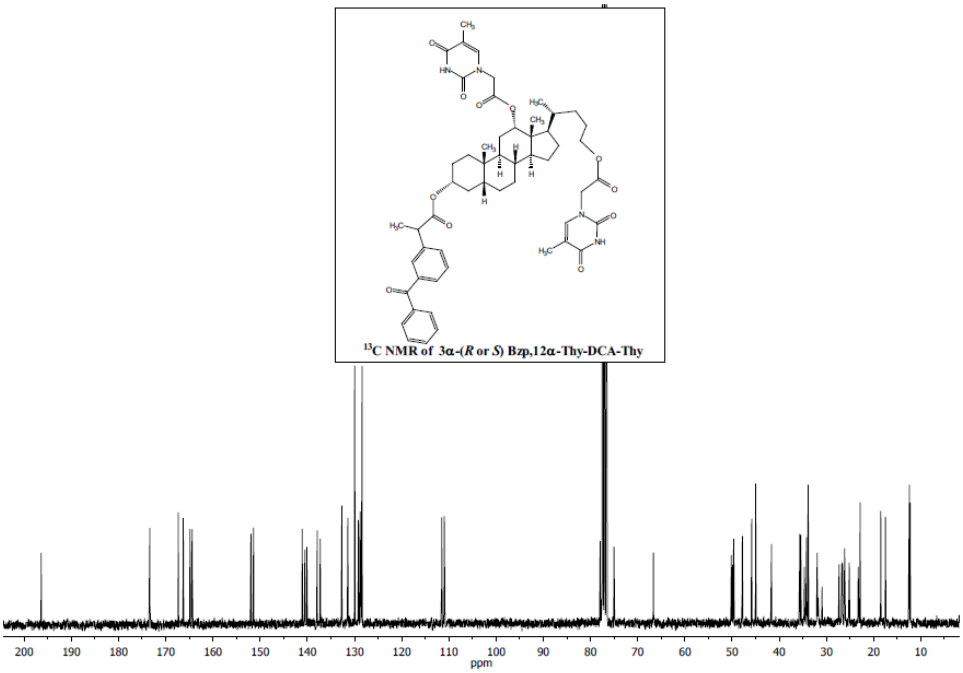
^{13}C NMR of 3α-(*R* or *S*) Bzp,12α-Thy-DCA-Thy
200 190 180 170 160 150 140 130 120 110 100 90 80 70 60 50 40 30 20 10
ppm

5.6.1.14. Synthesis of 3α-Pa-DCA-Thy

To a stirred solution of **DCA-Thy** (0.40 g, 0.73 mmol) and TBTU (0.35 g, 1.10 mmol) in anhydrous DMF (3 mL), phenylacetic acid (0.13 g, 0.96 mmol) in anhydrous DMF (2 mL) followed by DIEA (0.47 mL, 2.72 mmol) were added dropwise and then the reaction mixture was allowed to react at rt for 7 h. Afterwards, it was poured into brine and extracted with CH_2Cl_2; the combined organic layers were washed with brine, dried over $MgSO_4$ and concentrated under vacuum. Purification by column chromatography (SiO_2, EtOAc:Hexane, 50:50) followed by (Li Chroprep RP-18, CH_3CN:H_2O, 80:20) gave **3α-Pa-DCA-Thy** as a yellow solid (0.24 g, 49%); ^{1}H NMR (300 MHz, $CDCl_3$): δ (ppm) 0.65 (s, 3H, CH_3); 0.79-1.95 (complex signal, 26H); 0.88 (s, 3H, CH_3); 0.95 (d, *J* = 6.6 Hz, 3H, 21-CH_3); 1.91 (d, *J* = 1.2 Hz, 3H, Thy-CH_3); 3.55 (s, 2H, Ph-CH_2); 3.97 (*br* s, 1H, 12β-H); 4.13 (m, 2H, CH_2); 4.40 (s, 2H, Thy-CH_2); 4.70 (m, 1H, 3β-H); 6.91 (*br* s, 1H, Thy-CH); 7.19-7.33 (m, 5H, arom); 8.51 (s, 1H, Thy-NH). ^{13}C NMR (75 MHz, $CDCl_3$): δ (ppm) 171.3 (C), 167.6 (C), 163.9 (C), 150.7 (C), 140.3 (CH), 134.5 (C), 129.3 (2xCH), 128.7 (2xCH), 127.1 (CH), 111.4 (C), 74.9 (CH), 73.3 (CH), 66.8 (CH_2), 48.8 (CH_2), 48.4 (CH), 47.6 (CH), 46.6 (C), 42.0 (CH), 41.9 (CH_2), 36.1 (CH), 35.2 (CH), 35.0 (CH_2), 34.3 (C), 33.8 (CH), 32.3 (CH_2), 31.9 (CH_2), 28.9 (CH_2), 27.7 (CH_2), 27.1 (CH_2), 26.7 (CH_2), 26.2 (CH_2), 25.2 (CH_2), 23.8 (CH_2), 23.3 (CH_3), 17.7 (CH_3), 12.9 (CH_3), 12.5 (CH_3); m/z found 663.4017, calculated for $C_{39}H_{55}N_2O_7$ (MH^+) 663.4009.

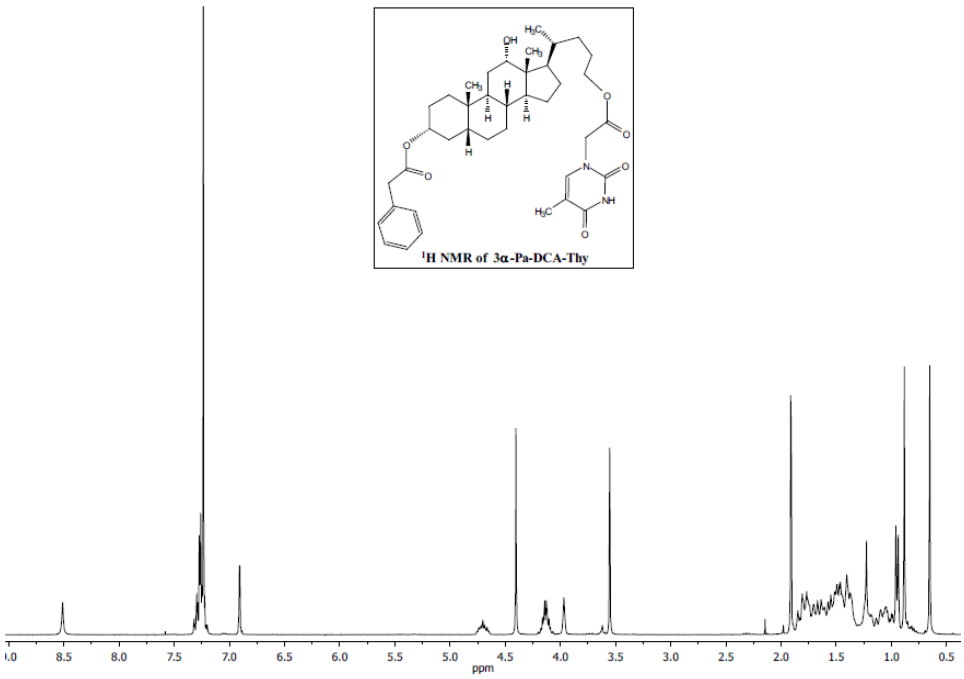
^{1}H NMR of 3α-Pa-DCA-Thy
ppm

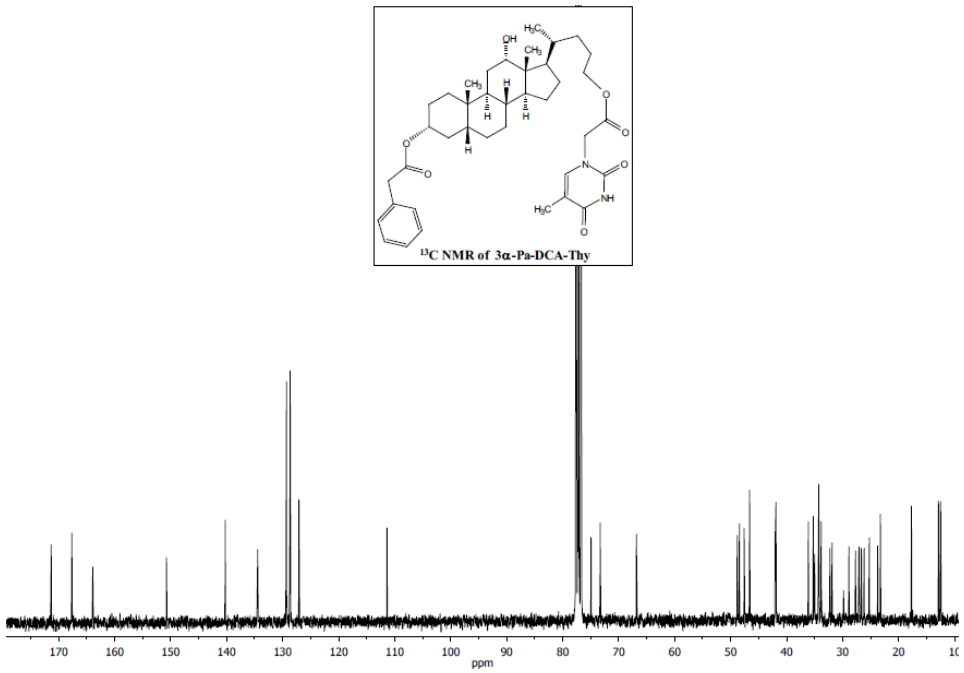
^{13}C NMR of 3α-Pa-DCA-Thy
ppm

5.6.1.15. Synthesis of 3α-Pa,12α-Thy-DCA-Thy

A stirred suspension of Thy-CH_2CO_2H (0.18 g, 0.95 mmol) and Et_3N (0.27 mL) in anhydrous THF (5 mL) was treated with 2,4,6-trichlorobenzoyl chloride (0.18 mL, 1.14 mmol). The resulting suspension was allowed to react for 1.5 h; after that, a solution of 4-DMAP (0.047 g, 0.39 mmol) and **3α-Pa-DCA-Thy** (0.21 g, 0.32 mmol) in anhydrous THF (6.5 mL) was added and the reaction mixture was allowed to stir overnight. Then, it was poured into brine and extracted with CH_2Cl_2. The combined organic extracts were washed with brine, dried over $MgSO_4$ and concentrated under vacuum. Purification by column chromatography (SiO_2, EtOAc:Hexane, 60:40) followed by (Li Chroprep RP-18, CH_3CN:H_2O, 80:20) gave **3α-Pa,12α-Thy-DCA-Thy** as a pale yellow solid, 0.16 g, 61%); ^{1}H NMR (300 MHz, $CDCl_3$): δ (ppm) 0.67 (s, 3H, CH_3); 0.78 (d, *J* = 6.0 Hz, 3H, 21-CH_3); 0.78-2.05 (complex signal, 26H); 0.89 (s, 3H, CH_3; 1.91 (d, *J* = 0.9 Hz, 3H, Thy-CH_3); 1.96 (d, *J* = 0.9 Hz, 3H, Thy-CH_3); 3.61 (d, *J* = 15.0 Hz, 1H, Ph-CH_2); 3.68 (d, *J* = 15.0 Hz, 1H, Ph-CH_2); 3.80 (d, *J* = 17.4 Hz, 1H, Thy-CH_2); 4.22 (m, 2H, CH_2); 4.23 (d, *J* = 17.1 Hz, 1H, Thy-CH_2); 4.55 (d, *J* = 17.1 Hz, 1H, Thy-CH_2); 4.69 (d, *J* = 17.4 Hz, 1H, Thy-CH_2); 4.78 (m, 1H, 3β-H); 5.12 (*br* s, 1H, 12β-H); 6.56 (*br* s, 1H, Thy-CH); 6.99 (*br* s, 1H, Thy-CH); 7.17-7.34 (m, 5H, arom); 10.85 (s, 1H, Thy-NH); 11.05 (s, 1H, Thy-NH). ^{13}C NMR (75 MHz, $CDCl_3$) δ (ppm) 170.9 (C), 167.4 (C), 166.1 (C), 165.1 (C), 164.5 (C), 152.2 (C), 151.5 (C), 140.5 (CH), 140.2 (CH), 134.6 (C), 129.2 (2xCH), 128.8 (2xCH), 127.2 (CH), 111.7 (C), 111.0 (C), 78.2 (CH), 74.7 (CH), 66.7 (CH_2), 50.4 (CH_2), 50.2 (CH_2), 50.1 (CH), 48.0 (CH), 45.1 (C), 42.2 (CH_2), 41.6 (CH), 35.8 (CH), 35.4 (CH), 34.7 (CH_2), 34.1 (CH), 33.8 (C), 32.1 (CH_2), 31.7 (CH_2), 27.4 (CH_2), 26.7 (CH_2), 26.5 (CH_2), 26.3 (CH_2), 26.2 (CH_2), 25.0 (CH_2), 23.3 (CH_2), 22.8 (CH_3), 17.6 (CH_3), 12.6 (CH_3), 12.5 (CH_3), 12.4 (CH_3); m/z found 829.4363, calculated for $C_{46}H_{61}N_4O_{10}N_4$ (MH^+) 829.4388.

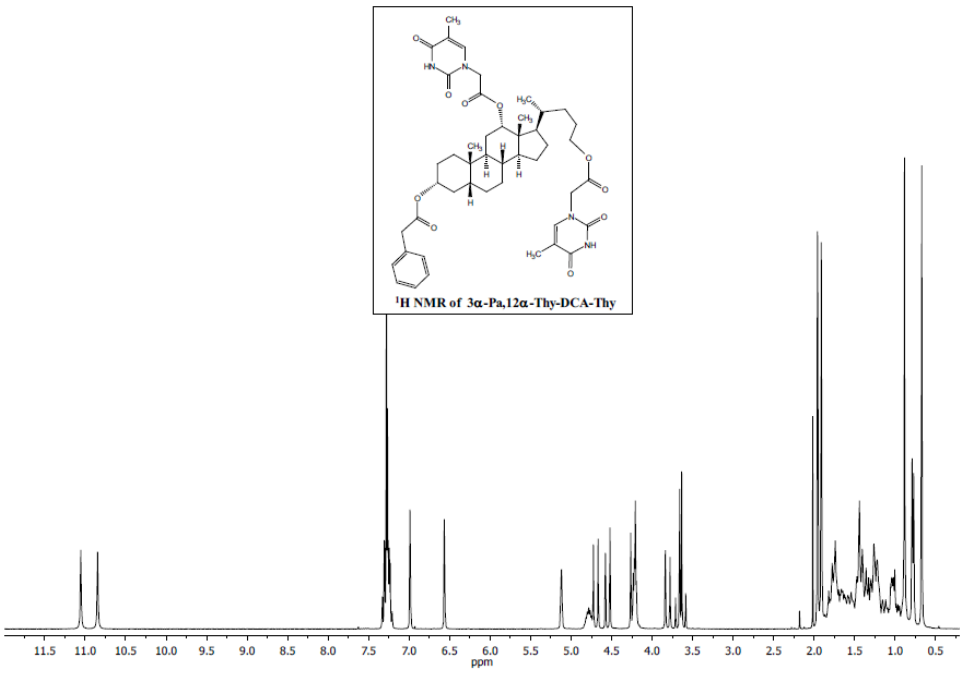
^{1}H NMR of 3α-Pa,12α-Thy-DCA-Thy
11.5 11.0 10.5 10.0 9.5 9.0 8.5 8.0 7.5 7.0 6.5 6.0 5.5 5.0 4.5 4.0 3.5 3.0 2.5 2.0 1.5 1.0 0.5
ppm

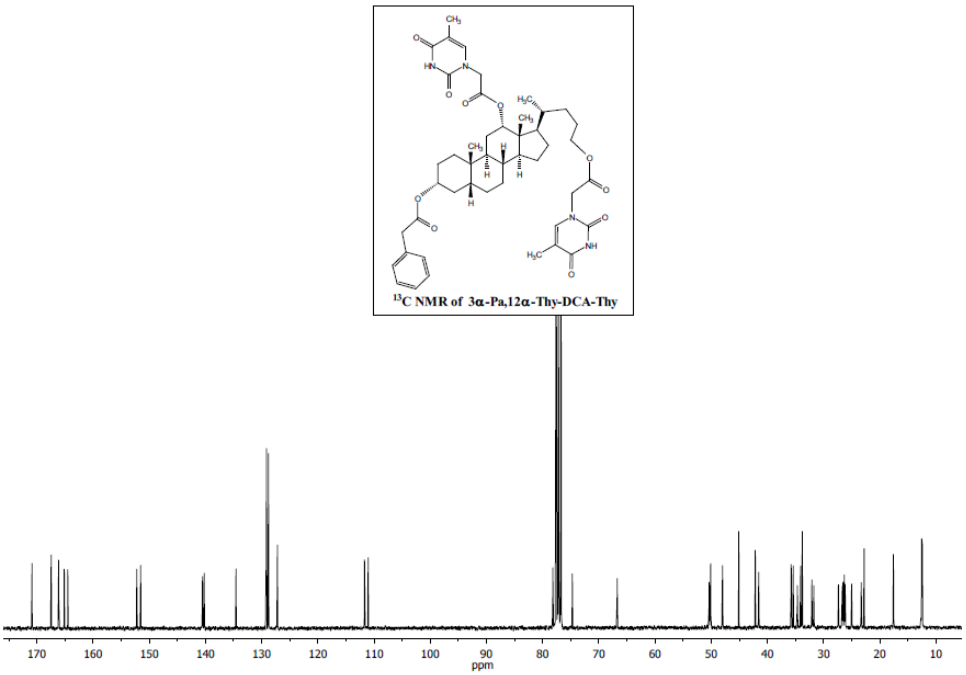
^{13}C NMR of 3α-Pa,12α-Thy-DCA-Thy
170 160 150 140 130 120 110 100 90 80 70 60 50 40 30 20 10
ppm

5.6.1.16. Synthesis of CDCAOH

A stirred suspension of $LiAlH_4$ (1.68 g, 46.9 mmol) in anhydrous THF (60 mL) was cooled to −10 ° C, treated with a solution of **CDCA-Bn** (6.82 g, 15.6 mmol) in anhydrous THF (37 mL) and refluxed overnight (70 °C). Afterwards, it was quenched with saturated aqueous NH_4Cl solution (20 mL), redissolved with EtOAc, poured into aqueous HCl 1M and extracted with EtOAc. The combined organic layers were washed with brine, dried over $MgSO_4$ and concentrated. Purification by column chromatography (Li Chroprep RP-18, CH_3CN: H_2O, 90:10) gave **CDCAOH** as a colorless solid (5.28 g, 61%); ^1H NMR (300 MHz, CD_3OD): δ (ppm) 0.69 (s, 3H, CH_3); 0.91-2.05 (complex signal, 25H); 0.93 (s, 3H, CH_3); 0.96 (d, J = 6.6 Hz, 3H, 21-CH_3); 2.27 (q, J = 13.2 Hz, 1H, CH_2); 3.37 (m, 1H, 3 β -H); 3.50 (m, 2H, CH_2); 3.79 (*br* s, 1H,7- β H). ^{13}C NMR (75 MHz, CD_3OD): δ (ppm) 71.8 (CH), 68.0 (CH), 62.6 (CH_2), 56.5 (CH), 50.5 (CH), 42.6 (C), 42.2 (CH), 40.1 (CH_2), 39.8 (CH), 39.5 (CH_2), 36.1 (CH), 35.6 (CH_2), 35.2 (C), 34.9 (CH_2), 33.0 (CH), 32.2 (CH_2), 30.4 (CH_2), 29.3 (CH_2), 28.4 (CH_2), 23.6 (CH_2), 22.4 (CH_3), 20.8 (CH_2), 18.3 (CH_3), 11.2 (CH_3); m/z found 379.3225, calculated for $C_{24}H_{43}O_3$ (MH^+) 379.3212.

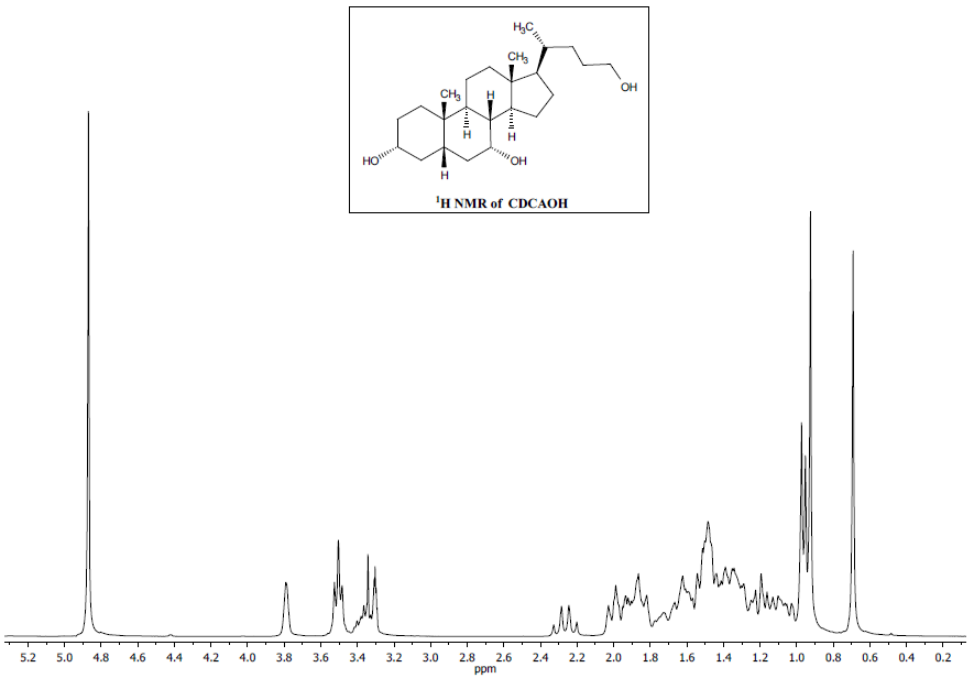
^{1}H NMR of CDCAOH
5.2 5.0 4.8 4.6 4.4 4.2 4.0 3.8 3.6 3.4 3.2 3.0 2.8 2.6 2.4 2.2 2.0 1.8 1.6 1.4 1.2 1.0 0.8 0.6 0.4 0.2
ppm

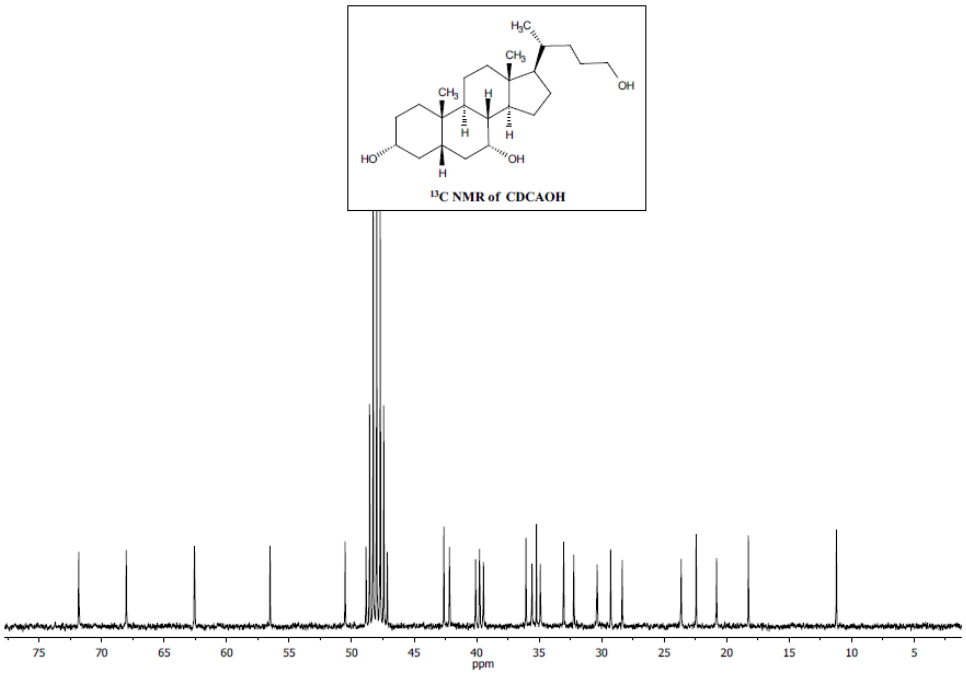
^{13}C NMR of CDCAOH
75 70 65 60 55 50 45 40 35 30 25 20 15 10 5
ppm

5.6.1.17. Synthesis of CDCA-Thy

CDCAOH (2.72 g, 7.19 mmol), TBTU (2.77 g, 8.63 mmol) and Thy-CH_2CO_2H (1.33 g, 7.55 mmol) were dissolved in anhydrous DMF (18 mL). Then, DIEA (0.376 mL, 21.57 mmol) was added and the resulting reaction mixture was allowed to react at rt overnight. Afterwards, it was poured into brine and extracted with CH_2Cl_2. The combined organic extracts were washed with brine, dried over $MgSO_4$ and concentrated under reduced pressure. Purification by column chromatography (SiO_2, CH_2Cl_2:CH_3COCH_3, 60:40, followed by Li Chroprep RP-18, CH_3CN:H_2O, 80:20) gave **CDCA-Thy** as a white solid (2.82 g, 72%); ^{1}H NMR (300 MHz, $CDCl_3$): δ (ppm) 0.59 (s, 3H, CH_3); 0.75-2.02 (complex signal, 26H); 0.83 (s, 3H, CH_3); 0.86 (d, *J* = 6.6 Hz, 3H, 21-CH_3); 1.86 (s, 3H, Thy-CH_3); 2.56 (*br* s, 2H, 2xOH); 3.38 (m, 1H, 3β-H); 3.78 (*br* s, 1H, 7β-H); 4.06 (m, 2H, CH_2); 4.40 (s, 2H, Thy-CH_2) ; 9.99 (s, 1H, Thy-CH); 10.0 (s, 1H, Thy-NH). ^{13}C NMR (75 MHz, $CDCl_3$): δ (ppm) 167.7 (C), 164.5 (C), 151.1 (C), 140.3 (CH), 111.1 (C), 71.8 (CH), 68.3 (CH), 66.6 (CH_2), 55.7 (CH), 50.4 (CH), 48.7 (CH_2), 42.6 (C), 41.5 (CH), 39.7 (2xCH_2), 39.4 (CH), 35.4 (CH_2), 35.3 (CH), 35.0 (C), 34.6 (CH_2), 32.8 (CH), 31.8 (CH_2), 30.6 (CH_2), 28.3 (CH_2), 24.9 (CH_2), 23.6 (CH_2), 22.8 (CH_3), 20.6 (CH_2), 18.6 (CH_3), 12.3 (CH_3), 11.8 (CH_3); m/z found 545.3577, calculated for $C_{31}H_{49}N_2O_6$ (MH^+) 545.3591.

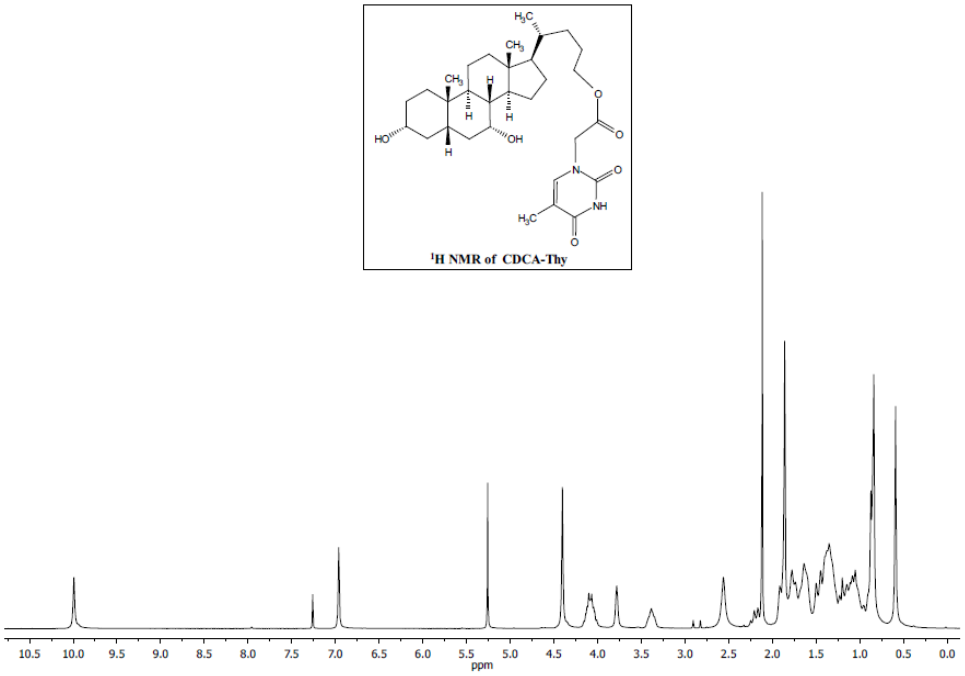
^{1}H NMR of CDCA-Thy
10.5 10.0 9.5 9.0 8.5 8.0 7.5 7.0 6.5 6.0 5.5 5.0 4.5 4.0 3.5 3.0 2.5 2.0 1.5 1.0 0.5 0.0
ppm

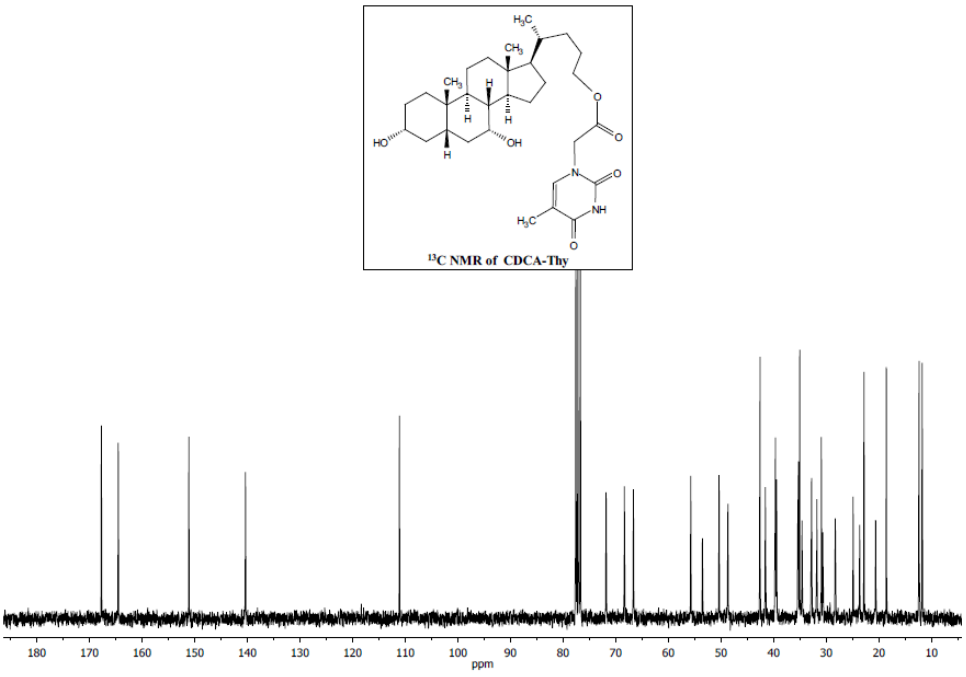
^{13}C NMR of CDCA-Thy
180 170 160 150 140 130 120 110 100 90 80 70 60 50 40 30 20 10
ppm

5.6.1.18. Synthesis of 3α-Bzp-CDCA-Thy

To a stirred solution of **CDCA-Thy** (2.04 g, 3.75 mmol), TBTU (1.44 g, 4.5 mmol) and (*S*)-KP (1.14 g, 4.5 mmol) in anhydrous DMF (14 mL), DIEA (2.0 mL, 11.25 mmol) was added dropwise and then the reaction mixture was allowed to react overnight. Afterwards, it was poured into brine and extracted with CH_2Cl_2; the combined organic layers were washed with brine, dried over $MgSO_4$ and concentrated under vacuum. Purification by column chromatography (SiO_2, EtOAc:Hexane:CH_3COOH, 70:30:1, followed by Li Chroprep RP-18, CH_3CN:H_2O, 90:10) gave **3α-Bzp-CDCA-Thy** as a colorless oil (0.636 g, 22%); ^{1}H NMR (300 MHz, $CDCl_3$): δ (ppm) 0.58 (s, 3H, CH_3); 0.75-2.30 (complex signal, 25H); 0.85 (m, 6H, CH_3 + 21-CH_3); 1.43 (d, *J* = 7.2 Hz, 3H, KP-CH_3); 1.83 (s, 3H, Thy-CH_3); 2.28 (m, 1H, CH_2); 3.68 (m, 1H, KP-CH); 3.77 (*br* s, 1H, 7β-H); 4.06 (m, 2H, CH_2); 4.40 (s, 2H, Thy-CH_2); 4.53 (m, 1H, 3β-H); 6.96 (s, 1H, Thy-CH); 7.30-7.80 (m, 9H, arom); 10.00 (s, 1H, Thy-NH). ^{13}C NMR (75 MHz, $CDCl_3$): δ (ppm) 196.4 (C), 173.6 (C), 167.6 (C), 164.5 (C), 151.0 (C), 141.1 (C), 140.0 (CH), 137.6 (C), 137.4 (C), 132.4 (CH), 131.5 (CH), 129.9 (2xCH), 129.0 (CH), 128.7 (CH), 128.4 (CH), 128.2 (2xCH), 110.9 (C), 75.0 (CH), 68.0 (CH), 66.5 (CH_2), 55.6 (CH), 50.2 (CH), 48.5 (CH_2), 45.5 (CH), 42.5 (C), 41.2 (CH), 39.4 (CH_2), 39.3 (CH), 35.2 (CH), 35.0 (CH_2+C+CH_2), 34.3 (CH_2), 32.7 (CH), 31.7 (CH_2), 28.1 (CH_2), 26.6 (CH_2), 24.9 (CH_2), 23.5 (CH_2), 22.6 (CH_3), 20.5 (CH_2), 18.6 (2xCH_3), 12.2 (CH_3), 11.7 (CH_3); m/z found 781.4438, calculated for $C_{47}H_{61}N_2O_8$ (MH^+) 781.4428.

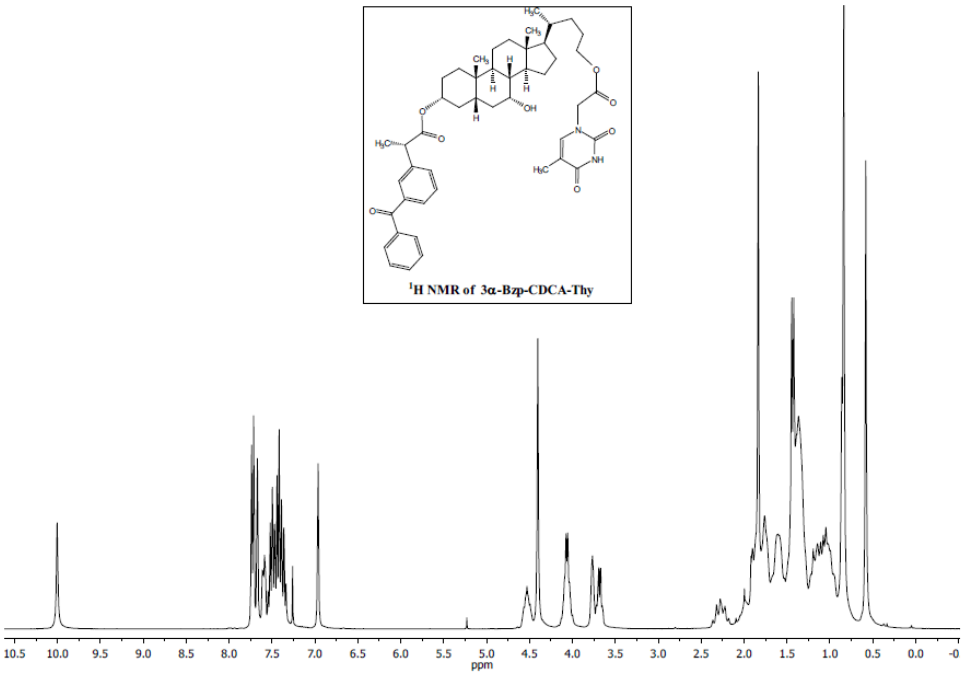
^{1}H NMR of 3α-Bzp-CDCA-Thy
10.5 10.0 9.5 9.0 8.5 8.0 7.5 7.0 6.5 6.0 5.5 5.0 4.5 4.0 3.5 3.0 2.5 2.0 1.5 1.0 0.5 0.0 -0
ppm

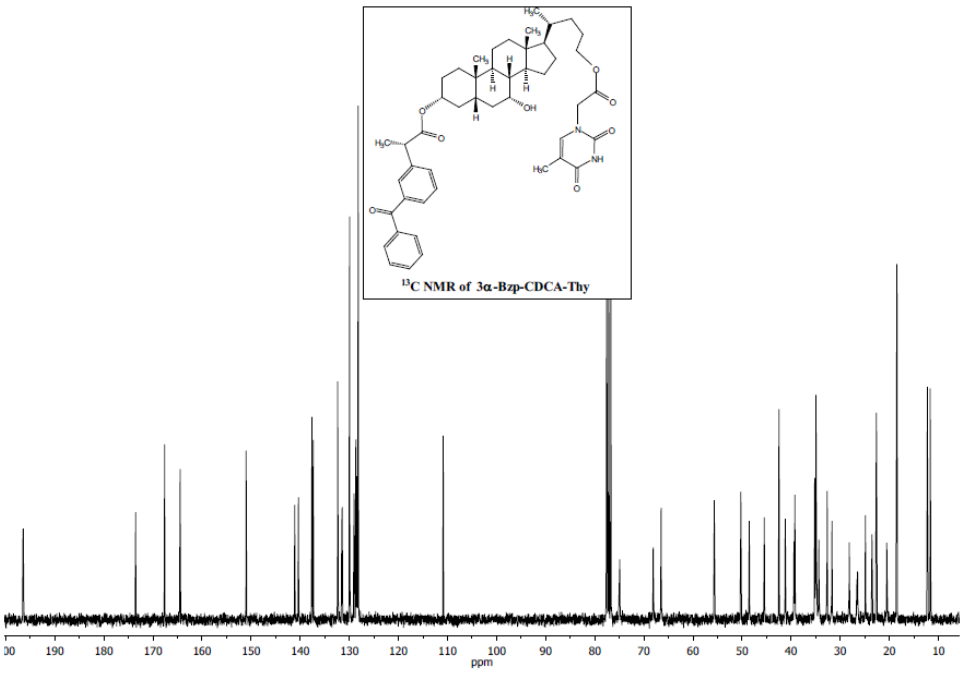
^{13}C NMR of 3α-Bzp-CDCA-Thy
190 180 170 160 150 140 130 120 110 100 90 80 70 60 50 40 30 20 10
ppm

5.6.1.19. Synthesis of 3α-(*R* or *S*) Bzp,7α-Thy-CDCA-Thy

A stirred suspension of Thy-CH_2CO_2H (4.0 g, 21.69 mmol) and Et_3N (6.10 mL) in anhydrous THF (60 mL) was treated with 2,4,6-trichlorobenzoyl chloride (4.10 mL, 26.29 mmol). The resulting suspension was allowed to react for 1.5 h, and a solution of 4-DMAP (0.358 g, 2.94 mmol) and **3α-Bzp-CDCA-Thy** (1.88 g, 2.41 mmol) in anhydrous THF (20 mL) was added and the reaction mixture was allowed to stir overnight. Then, it was poured into brine and extracted with CH_2Cl_2. The combined organic extracts were washed with brine, dried over $MgSO_4$ and concentrated under vacuum. Purification by column chromatography (Li Chroprep RP-18, CH_3CN:H_2O, 80:20) gave **3α-(*R* or *S*) Bzp,7α-Thy-CDCA-Thy** (less polar 0.277g, 12%) and **3α-(*R* or *S*) Bzp,7α-Thy-CDCA-Thy** (more polar 0.178g, 8%). Under the reaction conditions, partial racemization of the methyl group of the Bzp was observed. However, the stereochemistry of the methyl group in the Bzp chromophore was not unequivocally assigned. Therefore, after their isolation, the two resulting products were named as more or less polar. **3α-(*R* or *S*) Bzp,7α-Thy-CDCA-Thy** (less polar) ^{1}H NMR (300 MHz, $CDCl_3$): δ (ppm) 0.54 (s, 3H, CH_3); 0.75-2.02 (complex signal, 26H); 0.81 (d, *J* = 6.0 Hz, 3H, 21-CH_3); 0.85 (s, 3H, CH_3); 1.49 (d, *J* = 6.9 Hz, 3H, KP-CH_3); 1.78 (s, 3H, Thy-CH_3); 1.88 (s, 3H, Thy-CH_3); 3.76 (m, 1H, KP-CH); 3.87 (d, *J* = 17.1 Hz, 1H, Thy-CH_2); 4.12 (m, 1H, CH_2); 4.24 (m, 1H, CH_2); 4.32-4.49 (m, 3H, 3xThy-CH_2); 4.61 (m, 1H, 3β-H); 4.78 (*br* s, 1H, 7β-H); 6.47 (s, 1H, Thy-CH); 6.99 (s, 1H, Thy-CH); 7.16-7.85 (m, 9H, arom); 10.60 (s, 1H, Thy-NH); 10.74 (s, 1H, Thy-NH). ^{13}C NMR (75 MHz, $CDCl_3$): δ (ppm) 196.2 (C), 173.2 (C), 167.6 (C), 166.3 (C), 164.6 (C), 164.4 (C), 152.0 (C), 151.4 (C), 141.8 (C), 140.9 (CH), 140.4 (CH), 138.2 (C), 136.9 (C), 132.9 (CH), 131.3 (CH), 129.9 (2xCH), 128.9 (CH), 128.7 (CH), 128.5 (3xCH), 111.3 (C), 110.5 (C), 74.3 (CH), 73.6 (CH), 66.3 (CH_2), 56.6 (CH), 50.5 (CH), 49.7 (2xCH_2), 45.6 (CH), 42.4 (C), 40.6 (CH), 39.8 (CH_2), 37.7 (CH), 35.6 (CH), 34.7 (2xCH_2), 34.5 (C), 32.0 (CH_2), 30.9 (CH), 30.8 (CH_2), 28.0 (CH_2), 26.7 (CH_2), 25.5 (CH_2), 23.1 (CH_2), 22.6 (CH_3), 20.6 (CH_2), 18.6 (CH_3), 18.3 (CH_3), 12.4 (2xCH_3), 11.6 (CH_3); m/z found

947.4814, calculated for $C_{54}H_{67}N_4O_{11}$ (MH^+) 947.4807. **3α-(*R* or *S*) Bzp,7α-Thy-CDCA-Thy** (more polar) ^{1}H NMR (300 MHz, $CDCl_3$): δ (ppm) 0.56 (s, 3H, CH_3); 0.75-1.98 (complex signal, 26H); 0.83 (d, *J* = 6.0 Hz, 3H, 21-CH_3); 0.87 (s, 3H, CH_3); 1.53 (d, *J* = 7.2 Hz, 3H, KP-CH_3); 1.77 (s, 3H, Thy-CH_3); 1.89 (s, 3H, Thy-CH_3); 3.78 (m, 1H, KP-CH); 4.08-4.60 (complex signal, 7H, 2xThy-CH_2 + CH_2 + 3β-H); 4.86 (*br* s, 1H, 7β-H); 6.90 (s, 1H, Thy-CH); 6.97 (s, 1H, Thy-CH); 7.34-7.88 (m, 9H, arom); 10.53 (s, 1H, Thy-NH); 10.62 (s, 1H, Thy-NH). ^{13}C NMR (75 MHz, $CDCl_3$): δ (ppm) 196.4 (C), 173.4 (C), 167.6 (C), 166.6 (C), 164.5 (2xC), 151.8 (C), 151.5 (C), 141.2 (C), 140.9 (CH), 140.4 (CH), 137.9 (C), 137.3 (C), 132.7 (CH), 131.6 (CH), 130.0 (2xCH), 129.2 (CH), 128.8 (CH), 128.5 (CH), 128.4 (2xCH), 111.3 (C), 110.8 (C), 74.7 (CH), 73.8 (CH), 66.4 (CH_2), 56.5 (CH), 50.5 (CH), 49.7 (2xCH_2), 45.9 (CH), 42.5 (C), 40.9 (CH), 39.7 (CH_2), 37.9 (CH), 35.6 (CH), 34.7 (2xCH_2), 34.6 (C), 32.1 (CH_2), 31.8 (CH), 31.1 (CH_2), 29.3 (CH_3), 28.1 (CH_2), 26.7 (CH_2), 25.5 (CH_2), 23.3 (CH_2), 22.6 (CH_3), 20.6 (CH_2), 18.5 (CH_3), 12.4 (2xCH_3), 11.6 (CH_3); m/z found 947.4814, calculated for $C_{54}H_{67}N_4O_{11}$ (MH^+) 947.4807.

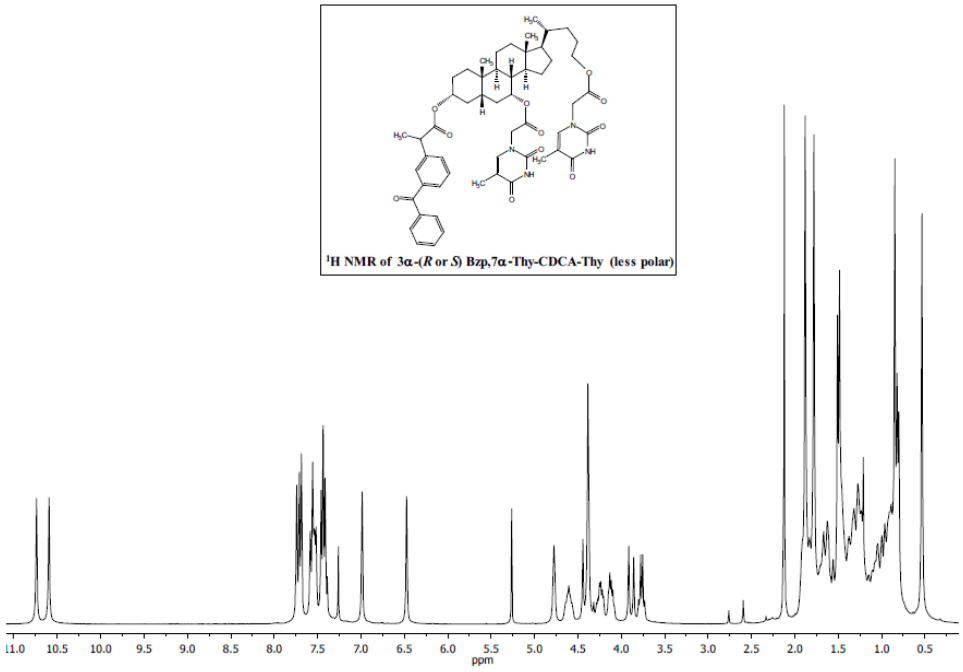
^{1}H NMR of 3α-(*R* or *S*) Bzp,7α-Thy-CDCA-Thy (less polar)
11.0 10.5 10.0 9.5 9.0 8.5 8.0 7.5 7.0 6.5 6.0 5.5 5.0 4.5 4.0 3.5 3.0 2.5 2.0 1.5 1.0 0.5
ppm

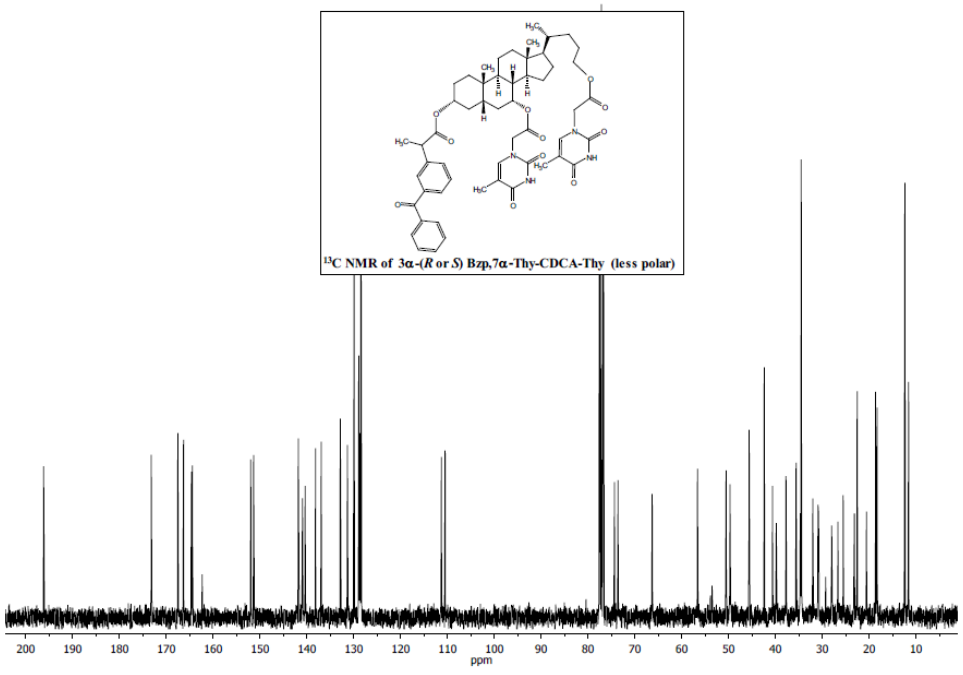
^{13}C NMR of 3α-(*R* or *S*) Bzp,7α-Thy-CDCA-Thy (less polar)
200 190 180 170 160 150 140 130 120 110 100 90 80 70 60 50 40 30 20 10
ppm

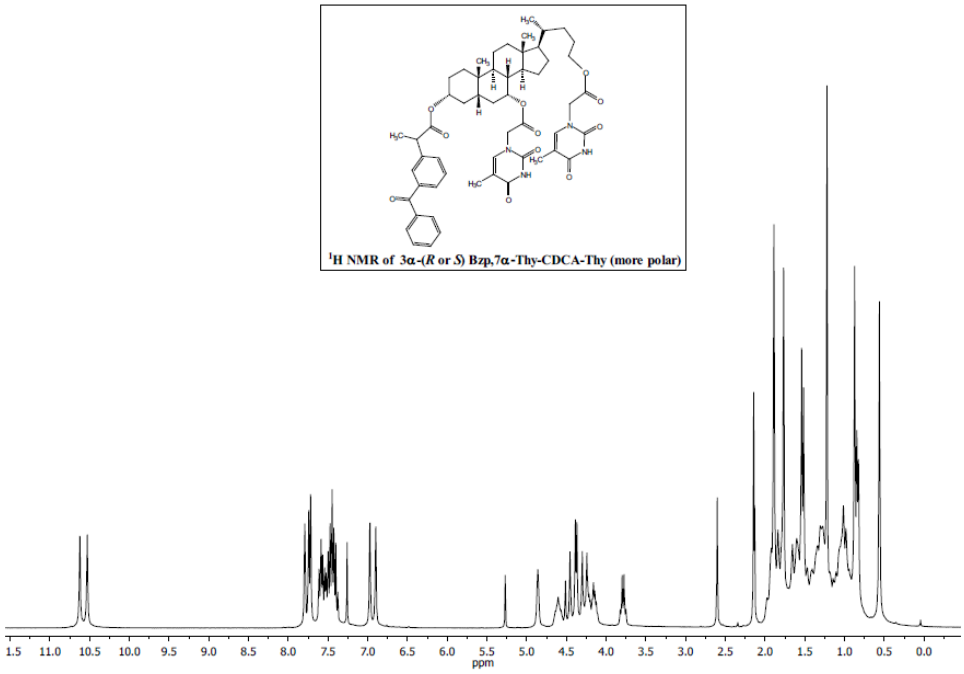
^{1}H NMR of 3α-(*R* or *S*) Bzp,7α-Thy-CDCA-Thy (more polar)
1.5 11.0 10.5 10.0 9.5 9.0 8.5 8.0 7.5 7.0 6.5 6.0 5.5 5.0 4.5 4.0 3.5 3.0 2.5 2.0 1.5 1.0 0.5 0.0
ppm

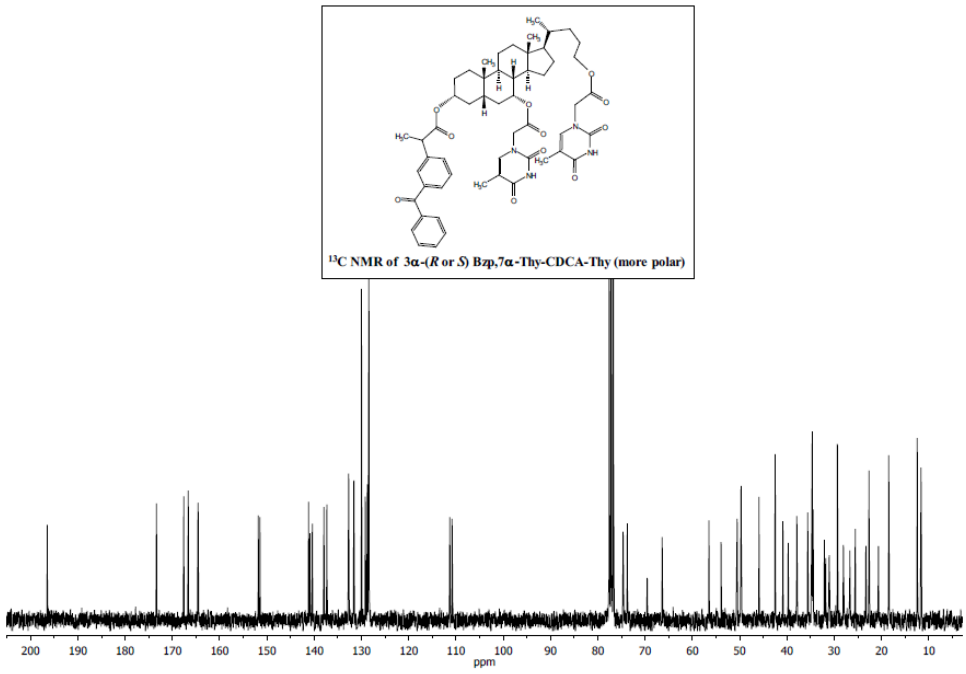
^{13}C NMR of 3α-(*R* or *S*) Bzp,7α-Thy-CDCA-Thy (more polar)
200 190 180 170 160 150 140 130 120 110 100 90 80 70 60 50 40 30 20 10
ppm

5.6.1.20. Synthesis of 3α-Bz-CDCA-Thy

To a stirred solution of **CDCA-Thy** (2.34 g, 4.30 mmol), TBTU (1.65 g, 5.16 mmol) and benzoic acid (0.63 g, 5.16 mmol) in anhydrous DMF (14 mL), DIEA (2.24 mL, 12.9 mmol) was added dropwise and then the reaction mixture was allowed to react overnight. Afterwards, it was poured into brine and extracted with CH_2Cl_2; the combined organic layers were washed with brine, dried over $MgSO_4$ and concentrated under vacuum. Purification by column chromatography (SiO_2, CH_2Cl_2:MeOH, 95:5) followed by (Li Chroprep RP-18, CH_3CN:H_2O, 85:15) gave **3α-Bz-CDCA-Thy** as a yellow solid (0.251 g, 78%); ^{1}H NMR (300 MHz, $CDCl_3$): δ (ppm) 0.65 (s, 3H, CH_3); 0.84-2.03 (complex signal, 25H); 0.92 (m, 6H, CH_3+21-CH_3); 1.91 (s, 3H, Thy-CH_3); 2.45 (m, 1H, CH_2); 3.85 (*br* s, 1H, 7β-H); 4.12 (m, 2H, CH_2); 4.42 (s, 2H, Thy-CH_2); 4.82 (m, 1H, 3β-H); 6.93 (*br* s, 1H, Thy-CH); 7.34-7.60 (m, 3H, arom); 8.02 (d, *J* = 8.4 Hz, 2H, arom); 9.36 (s, 1H, Thy-NH). ^{13}C NMR (75 MHz, $CDCl_3$): δ (ppm) 167.7 (C), 166.3 (C), 164.3 (C), 151.0 (C), 140.3 (CH), 132.7 (CH), 131.0 (C), 129.6 (2xCH), 128.3 (2xCH), 111.3 (C), 75.1 (CH), 68.5 (CH), 66.8 (CH_2), 55.9 (CH), 50.6 (CH), 48.7 (CH_2), 42.8 (C), 41.4 (CH), 39.7 (CH_2), 39.5 (CH), 35.5 (CH_2), 35.4 (CH), 35.2 (C+CH_2), 34.6 (CH_2), 33.0 (CH), 31.9 (CH_2), 28.4 (CH_2), 26.9 (CH_2), 25.1 (CH_2), 23.8 (CH_2), 22.9 (CH_3), 20.7 (CH_2), 18.6 (CH_3), 12.5 (CH_3), 11.9 (CH_3); m/z found 649.3865, calculated for $C_{38}H_{53}N_2O_7$ (MH^+) 649.3853.

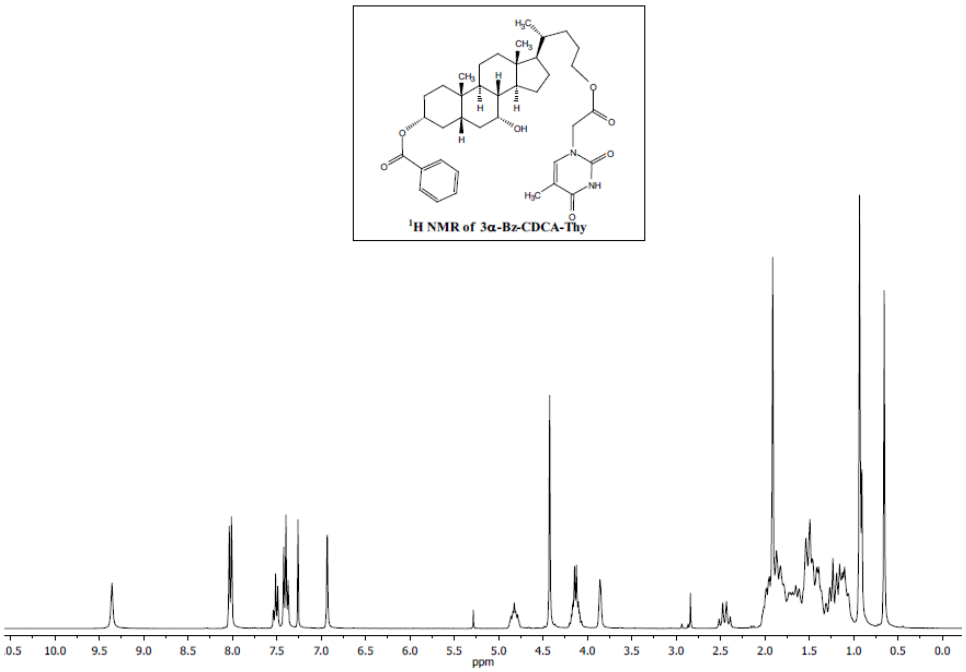
^{1}H NMR of 3α-Bz-CDCA-Thy
0.5 10.0 9.5 9.0 8.5 8.0 7.5 7.0 6.5 6.0 5.5 5.0 4.5 4.0 3.5 3.0 2.5 2.0 1.5 1.0 0.5 0.0
ppm

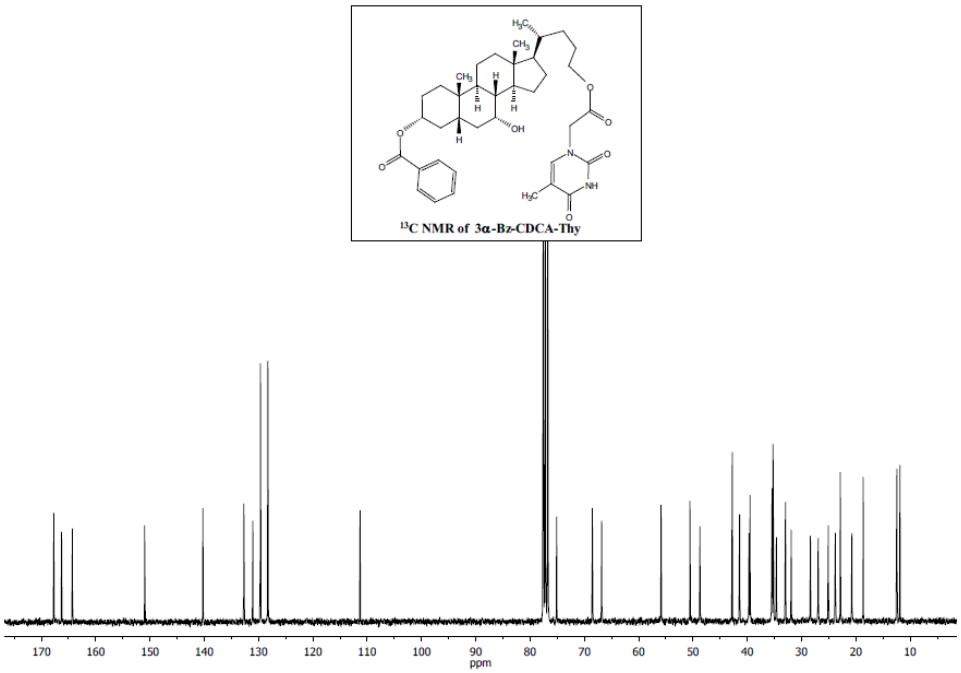
^{13}C NMR of 3α-Bz-CDCA-Thy
170 160 150 140 130 120 110 100 90 80 70 60 50 40 30 20 10
ppm

5.6.1.21. Synthesis of 3α-Bz,7α-Thy-CDCA-Thy

A stirred suspension of Thy-CH_2CO_2H (1 g, 5.96 mmol) and Et_3N (1.5 mL) in anhydrous THF (20 mL) was treated with 2,4,6-trichlorobenzoyl chloride (1.13 mL, 7.2 mmol). The resulting suspension was allowed to react for 1.30 h; after that, a solution of 4-DMAP (0.098 g, 0.81 mmol) and **3α-Bz-CDCA-Thy** (0.430 g, 0.66 mmol) in anhydrous THF (10 mL) was added, and the reaction mixture was allowed to stir overnight. Then, it was poured into brine and extracted with CH_2Cl_2. The combined organic extracts were washed with brine, dried over $MgSO_4$ and concentrated under vacuum. Purification by column chromatography (Li Chroprep RP-18, CH_3CN:H_2O, 80:20) gave **3α-Bz,7α-Thy-CDCA-Thy** as a pale yellow solid (0.476 g, 88%); ^{1}H NMR (300 MHz, $CDCl_3$): δ (ppm) 0.59 (s, 3H, CH_3); 0.75-2.03 (complex signal, 26H); 0.85 (d, *J* = 6.3 Hz, 3H, 21-CH_3); 0.93 (s, 3H, CH_3); 1.89 (s, 3H, Thy-CH_3); 1.93 (s, 3H, Thy-CH_3); 4.08-4.47 (complex signal, 6H, CH_2+Thy-CH_2+Thy-CH_2); 4.82 (m, 1H, 3β-H); 4.91 (*br* s, 1H, 7β-H); 6.98 (s, 1H, Thy-CH); 7.01 (s, 1H, Thy-CH); 7.32-7.59 (m, 3H, arom); 8.01 (d, *J* = 7.2 Hz, 2H, arom); 10.57 (s, 1H, Thy-NH); 10.65 (s, 1H, Thy-NH). ^{13}C NMR (75 MHz, $CDCl_3$) δ (ppm) 167.6 (C), 166.6 (C), 166.1 (C), 164.7 (2xC), 151.8 (C), 151.4 (C), 140.7 (CH), 140.5 (CH), 133.0 (CH), 130.7 (C), 129.5 (2xCH), 128.5 (2xCH), 111.3 (C), 111.0 (C), 74.9 (CH), 73.9 (CH), 66.4 (CH_2), 56.5 (CH), 50.6 (CH), 49.7 (2xCH_2), 42.5 (C), 40.8 (CH), 39.8 (CH_2), 37.9 (CH), 35.6 (CH), 35.0 (CH_2), 34.8 (CH_2), 34.7 (C), 34.5 (CH), 32.1 (CH_2), 31.2 (CH_2), 28.1 (CH_2), 26.9 (CH_2), 25.5 (CH_2), 23.3 (CH_2), 22.7 (CH_3), 20.7 (CH_2), 18.4 (CH_3), 12.5 (CH_3), 12.4 (CH_3), 11.7 (CH_3); m/z found 815.4238, calculated for $C_{45}H_{59}N_4O_{10}$ (MH^+) 815.4231.

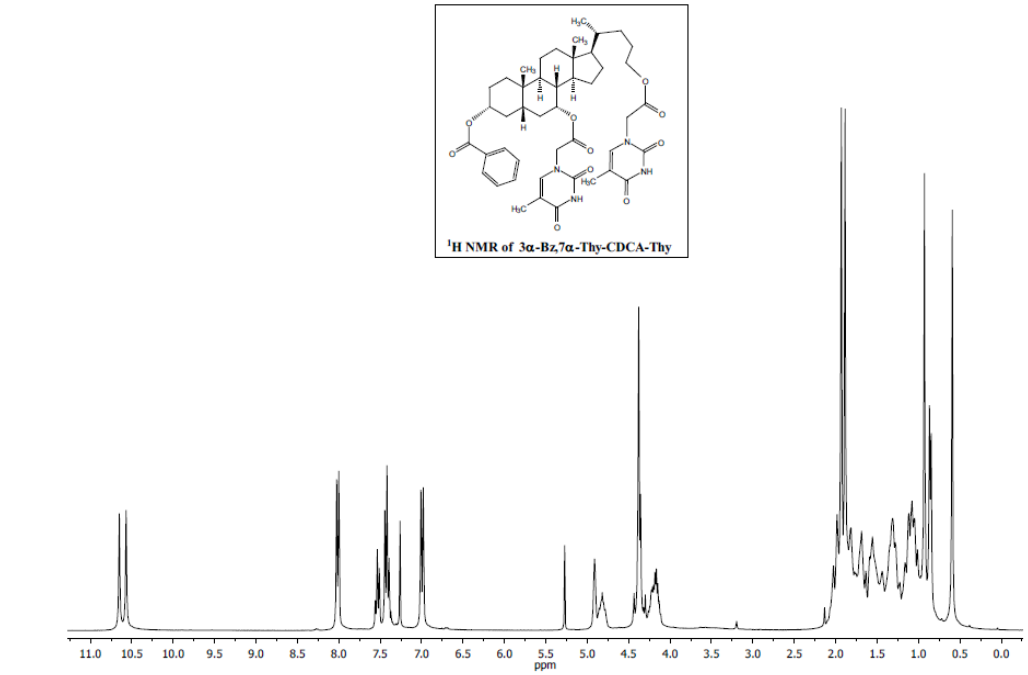
^{1}H NMR of 3α-Bz,7α-Thy-CDCA-Thy
11.0 10.5 10.0 9.5 9.0 8.5 8.0 7.5 7.0 6.5 6.0 5.5 5.0 4.5 4.0 3.5 3.0 2.5 2.0 1.5 1.0 0.5 0.0
ppm

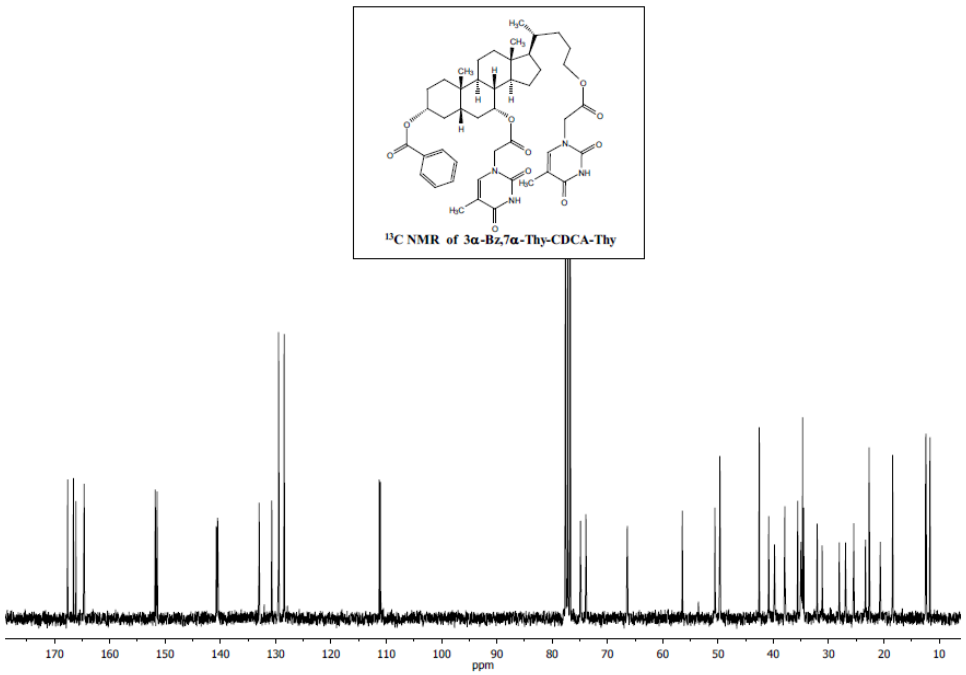
^{13}C NMR of 3α-Bz,7α-Thy-CDCA-Thy
170 160 150 140 130 120 110 100 90 80 70 60 50 40 30 20 10
ppm

5.6.2. Preparative irradiations

5.6.2.1. Photochemical synthesis of 3α-Thy-DCA-12α-Thy<O>Bzp

A solution of **3α,12α-2Thy-DCA-Bzp** (0.148 g, 0.16 mmol) in CH_3CN (250 mL), placed in a Pyrex® round-bottom flask was purged with N_2 and irradiated in a photoreactor using 8 lamps (λ_{max}= 350 nm) for two hours. Then, the solvent was concentrated under vacuum and the crude was purified by column chromatography (SiO_2, CH_2Cl_2:MeOH, 99:1) followed by (Li Chroprep RP-18, CH_3CN:H_2O, 80:20) to give **3α-Thy-DCA-12α-Thy<O>Bzp** (0.095 g, 64%). ^{1}H NMR (300 MHz, $CDCl_3$): δ (ppm) 0.75 (s, 3H, CH_3); 0.76-2.02 (complex signal, 24H); 0.86 (m, 6H, CH_3+21-CH_3); 1.35 (d, *J* = 7.2 Hz, 3H, KP-CH_3); 1.82 (*br* s, 3H, Thy-CH_3); 1.92 (*br* s, 3H, Thy-CH_3); 2.23 (m, 2H, CH_2); 3.10 (m, 1H, KP-CH); 3.57 (d, *J* = 17.7 Hz, 1H, Thy-CH_2); 4.02 (t, *J* = 10.5 Hz, 1H, KP-CH_2); 4.21 (d, *J* = 17.1 Hz, 1H, Thy-CH_2); 4.51 (d, *J* = 17.1 Hz, 1H, Thy-CH_2); 4.53 (dd, *J* = 3.9 and 10.5 Hz, 1H, KP-CH_2); 4.61 (m, 1H, 3β-H); 4.62 (d, *J* = 17.7 Hz, 1H, Thy-CH_2); 4.72 (*br* s, 1H, oxetane-CH); 5.27 (s, 1H, 12β-H); 6.91 (s, 1H, Thy-CH); 7.10-7.46 (m, 9H, arom); 8.96 (s, 1H, Thy-NH); 9.38 (s, 1H, Thy-NH). ^{13}C NMR (75 MHz, $CDCl_3$) δ (ppm) 173.5 (C), 170.5 (C), 167.0 (C), 166.7 (C), 164.0 (C), 151.6 (C), 150.7 (C), 144.3 (C), 143.3 (C), 140.0 (CH), 138.2 (C), 129.6 (CH), 128.9 (2xCH), 128.8 (CH), 126.2 (CH), 126.1 (2xCH), 124.9 (CH), 124.6 (CH), 111.8 (C), 91.7 (C), 77.6 (CH), 77.2 (CH), 76.3 (C), 69.1 (CH_2), 68.4 (CH), 50.1 (CH), 50.0 (CH_2), 49.2 (CH_2), 47.7 (CH), 45.2 (C), 41.9 (CH), 39.8 (CH), 36.4 (CH), 35.7 (CH), 35.1 (CH), 34.7 (CH_2), 34.5 (C), 32.2 (CH_2), 31.7 (CH_2), 30.0 (CH_2), 28.0 (CH_2), 27.0 (CH_2), 26.2 (CH_2), 25.9 (CH_2), 25.7 (CH_2), 24.5 (CH_3), 23.5 (CH_2), 23.3 (CH_3), 17.9 (CH_3), 17.8 (CH_3), 12.5 (CH_3), 12.4 (CH_3); m/z found 947.4805, calculated for $C_{54}H_{67}N_4O_{11}$ (MH^+) 947.4807.

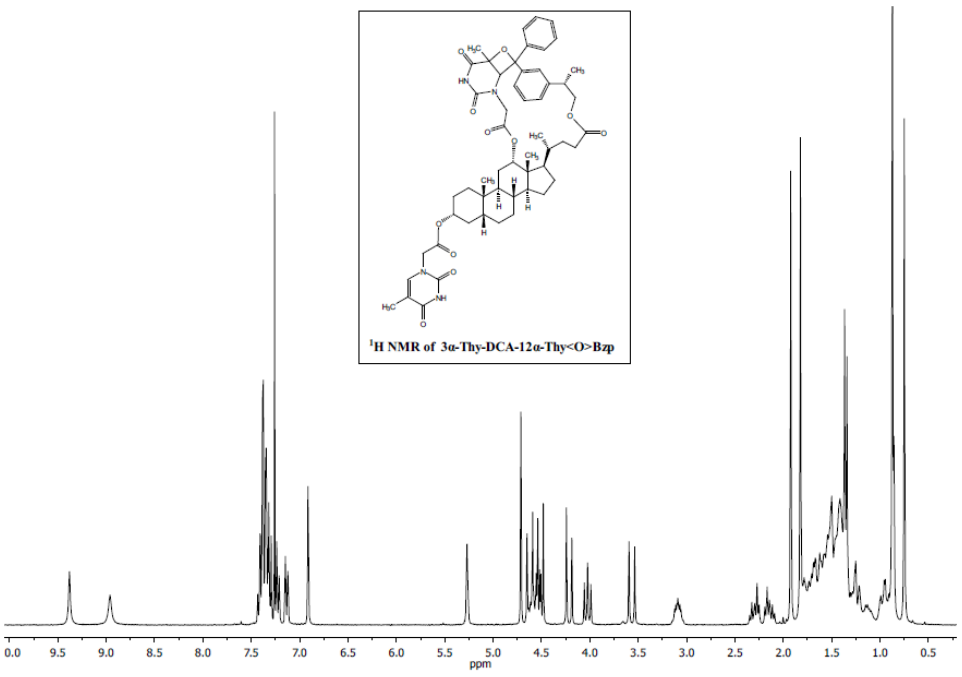
^{1}H NMR of 3α-Thy-DCA-12α-Thy<O>Bzp
0.0 9.5 9.0 8.5 8.0 7.5 7.0 6.5 6.0 5.5 5.0 4.5 4.0 3.5 3.0 2.5 2.0 1.5 1.0 0.5
ppm

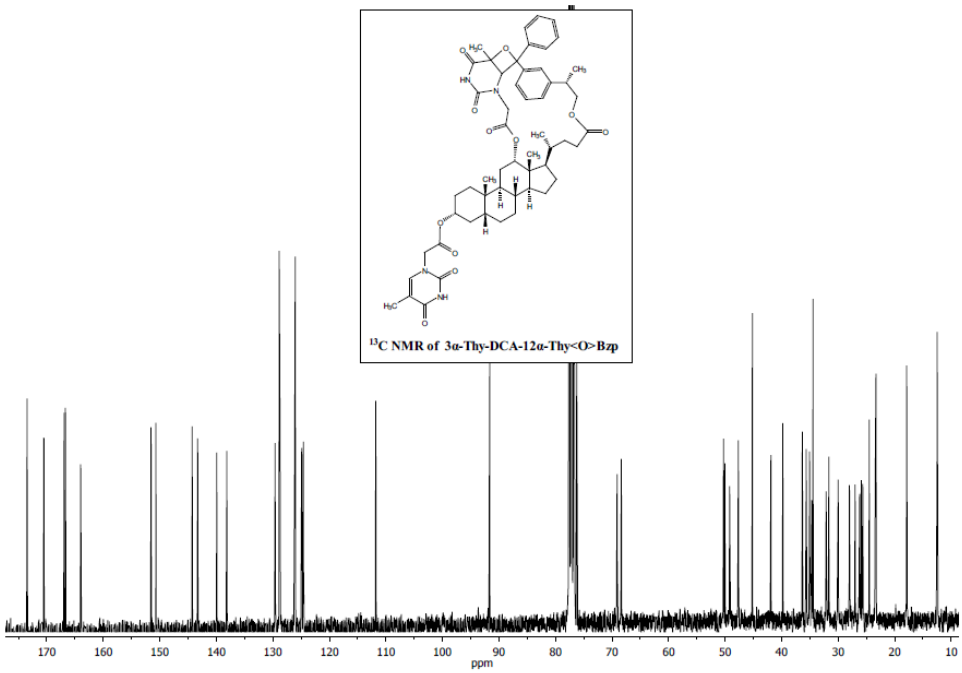
^{13}C NMR of 3α-Thy-DCA-12α-Thy<O>Bzp
170 160 150 140 130 120 110 100 90 80 70 60 50 40 30 20 10
ppm

5.6.2.2. Photochemical synthesis of 3α,12α-Thy<>Thy-DCA-Bn

A solution of **3α,12α-2Thy-DCA-Bn** (0.102 g, 0.12 mmol) and **Bzp** (0.022 g, 0.12 mmol) in CH_3CN (150 mL), placed in a Pyrex® round-bottom flask was purged with N_2 and irradiated in a photoreactor using 8 lamps (λ_{max}= 350 nm) for six hours. Then, the solvent was concentrated under vacuum and the crude was purified by column chromatography (SiO_2, CH_2Cl_2: Acetone, 90:10) to give **3α,12α-Thy<>Thy-DCA-Bn** (0.084 g, 82%). **3α,12α-Thy<>Thy-DCA-Bn** was christalized from a CH_3CN:H_2O mixture; ^{1}H NMR (300 MHz, $CDCl_3$): δ (ppm) 0.70 (s, 3H, CH_3); 0.75-2.00 (complex signal, 26H); 0.83 (d, *J* = 4.5 Hz, 3H, 21-CH_3); 0.88 (s, 3H, CH_3); 1.59 (s, 3H, Thy-CH_3); 1.68 (s, 3H, Thy-CH_3); 3.40-3.56 (m, 2H, Thy-CH_2); 3.60 (*br* s, 1H, Thy<>Thy-CH); 4.16 (*br* s, 1H, Thy<>Thy-CH); 4.35-4.56 (m, 2H, Thy-CH_2); 4.92 (m, 1H, 3β-H); 5.12 (*br* s, 3H, CH_2+12β-H); 7.24-7.38 (m, 5H, arom); 8.40 (s, 1H, Thy-NH); 8.58 (s, 1H, Thy-NH). ^{13}C NMR (75 MHz, $CDCl_3$): δ (ppm) 174.3 (C), 168.4 (C), 168.2 (C), 166.6 (2xC), 150.5 (C), 150.4 (C), 136.0 (C), 128.7 (2xCH), 128.5 (2xCH), 128.3 (CH), 79.0 (CH), 74.1 (CH), 66.5 (CH_2), 63.6 (CH), 52.5 (CH), 51.3 (CH_2), 49.4 (CH_2), 46.7 (CH), 45.3 (2xC), 45.0 (C), 39.9 (CH), 34.9 (CH), 34.5 (CH), 34.0 (CH_2), 33.2 (CH), 32.4 (C), 31.0 (CH), 30.6 (CH_2), 30.2 (CH_2), 29.6 (CH_2), 27.4 (CH_2), 25.7 (CH_2), 25.6 (CH_2), 25.1 (CH_2), 23.4 (CH_2), 23.1 (CH_2), 22.8 (CH_3), 22.4 (CH_3), 21.5 (CH_3), 17.1 (CH_3), 12.5 (CH_3); m/z found 815.4266, calculated for $C_{45}H_{59}N_4O_{10}$ (MH^+) 815.4231.

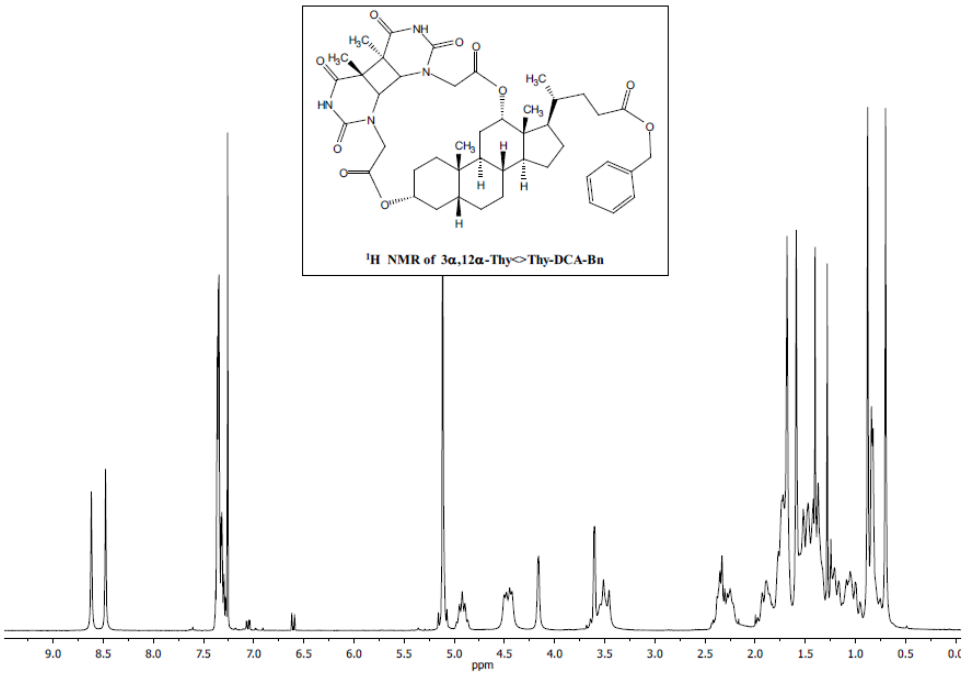
^{1}H NMR of 3α,12α-Thy<>Thy-DCA-Bn
9.0 8.5 8.0 7.5 7.0 6.5 6.0 5.5 5.0 4.5 4.0 3.5 3.0 2.5 2.0 1.5 1.0 0.5
ppm

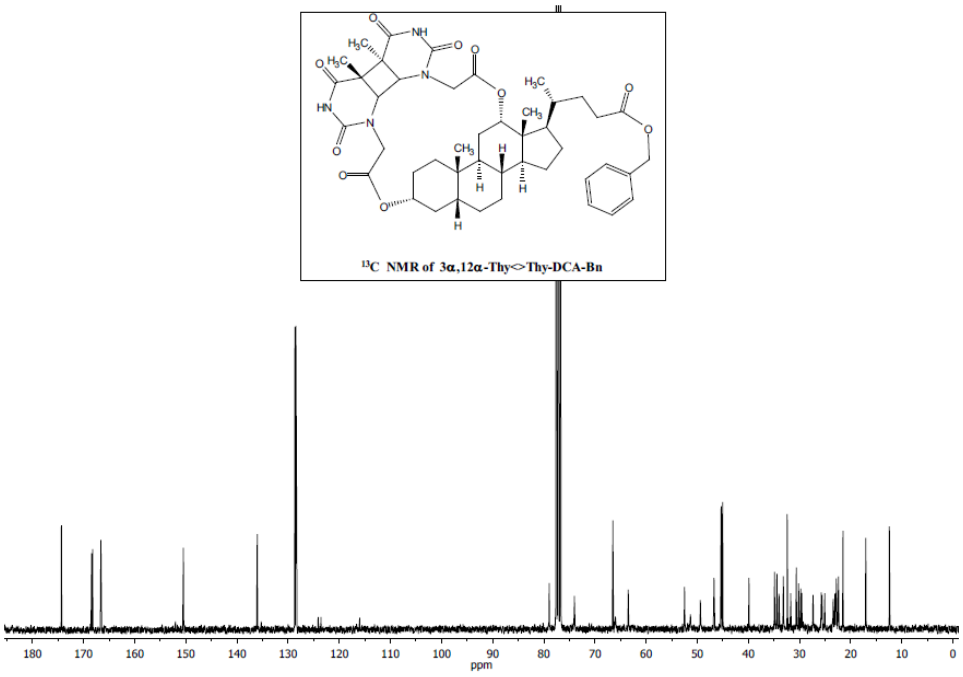
^{13}C NMR of 3α,12α-Thy<>Thy-DCA-Bn
180 170 160 150 140 130 120 110 100 90 80 70 60 50 40 30 20 10 0
ppm

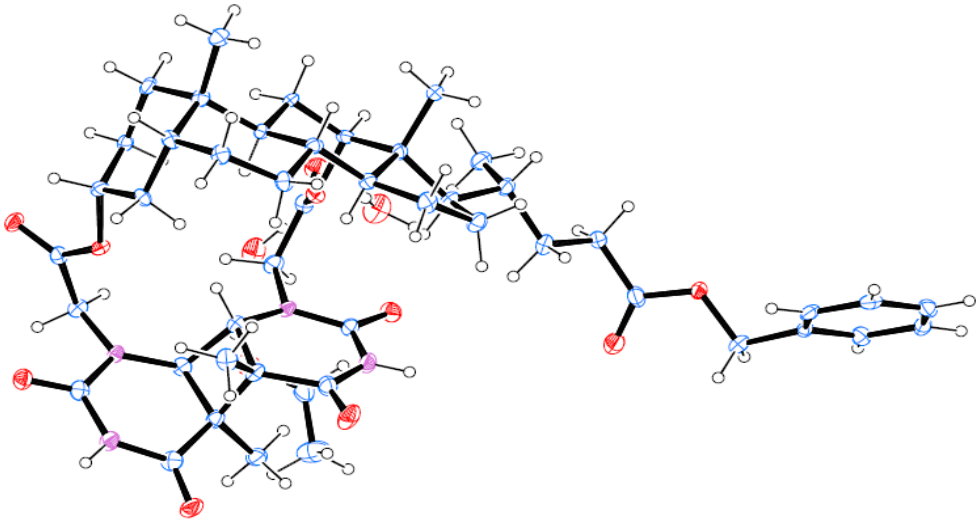

Figure 5.10. X-ray crystal structure of **3α,12α-Thy<>Thy-DCA-Bn** obtained from the irradiation (λ_{max} = 350 nm) of **Bzp:3α,12α-2Thy-DCA-Bn** in CH_3CN under N_2. CCDC: 1031373.

5.6.2.3. Photochemical synthesis of 3α-Thy-CDCA-7α-Thy<O>Bzp

A solution of **3α,7α-2Thy-CDCA-Bzp** (0.150 g, 0.1 mmol) in CH_3CN (100 mL) placed in a Pyrex® round-bottom flask was purged with N_2 and irradiated in a photoreactor using 8 lamps (λ_{max}= 350 nm) for 4 h. Then, the solvent was concentrated under vacuum and the crude was purified by column chromatography (SiO_2, CH_2Cl:Acetone 90:10) to give **3α-Thy-CDCA-7α-Thy<O>Bzp** (0.035 g, 23%); ^1H NMR (400 MHz, $CDCl_3$): δ (ppm) 0.62 (s, 3H, CH_3); 0.75-2.12 (complex signal, 26H); 0.80 (d, *J* = 6.8 Hz, 3H, 21-CH_3); 0.89 (s, 3H, CH_3); 1.14 (d, 3H, *J* = 7.2 Hz, KP-CH_3); 1.87 (*br* s, 3H, Thy-CH_3); 1.90 (*br* s, 3H, Thy-CH_3); 3.12 (m, 1H, KP-CH); 3.41 (d, *J* = 18.4 Hz, 1H, Thy-CH_2); 4.02 (dd, *J* = 5.6 and 11.2 Hz, 1H, KP-CH_2); 4.46-4.57 (m, 3H, Thy-CH_2+3β-H+oxetane-CH); 4.61 (dd, *J* = 11.2 and 12.0 Hz, 1H, KP-CH_2); 4.68 (d, *J* = 17.2 Hz, 1H, Thy-CH_2); 4.73 (d, *J* = 18.4 Hz, 1H, Thy-CH_2); 5.11 (*br* s, 1H, 7β-H); 6.98 (s, 1H, Thy-CH); 7.05 (d, *J* = 8.4 Hz, 1H, arom); 7.16 (*br* d, *J* = 7.6 Hz, 1H, arom); 7.25-7.47 (m, 7H, arom); 9.22 (s, 1H, Thy-NH); 9.60 (s, 1H, Thy-NH). ^{13}C NMR (100 MHz, $CDCl_3$): δ (ppm) 174.1 (C), 169.7 (C), 167.7 (C), 167.6 (C), 163.7 (C), 151.7 (C), 150.4 (C), 145.0 (C), 143.9 (C), 140.1 (CH), 137.7 (C), 128.9 (2xCH), 128.8 (CH), 128.6 (CH), 127.0 (CH), 126.1 (2xCH), 124.7 (CH), 121.8 (CH), 112.0 (C), 91.1 (C), 76.2 (CH), 75.6 (C), 73.5 (CH), 67.5 (CH), 67.3 (CH_2), 53.4 (CH), 51.8 (CH), 49.0 (CH_2), 46.9 (CH_2), 42.8 (C), 40.5 (CH), 40.2 (CH), 39.5 (CH_2), 37.6 (CH), 35.5 (CH), 34.6 (CH_2), 34.5 (C), 34.3 (CH_2), 33.2 (CH), 31.3 (CH_2), 29.9 (CH_2), 27.3 (2xCH_2), 27.0 (CH_2), 25.9 (CH_3), 23.5 (CH_2), 22.7 (CH_3), 20.8 (CH_2), 18.5 (CH_3), 18.2 (CH_3), 12.5 (CH_3), 11.9 (CH_3); m/z found 947.4815, calculated for $C_{54}H_{67}N_4O_{11}$ (MH^+) 947.4807.

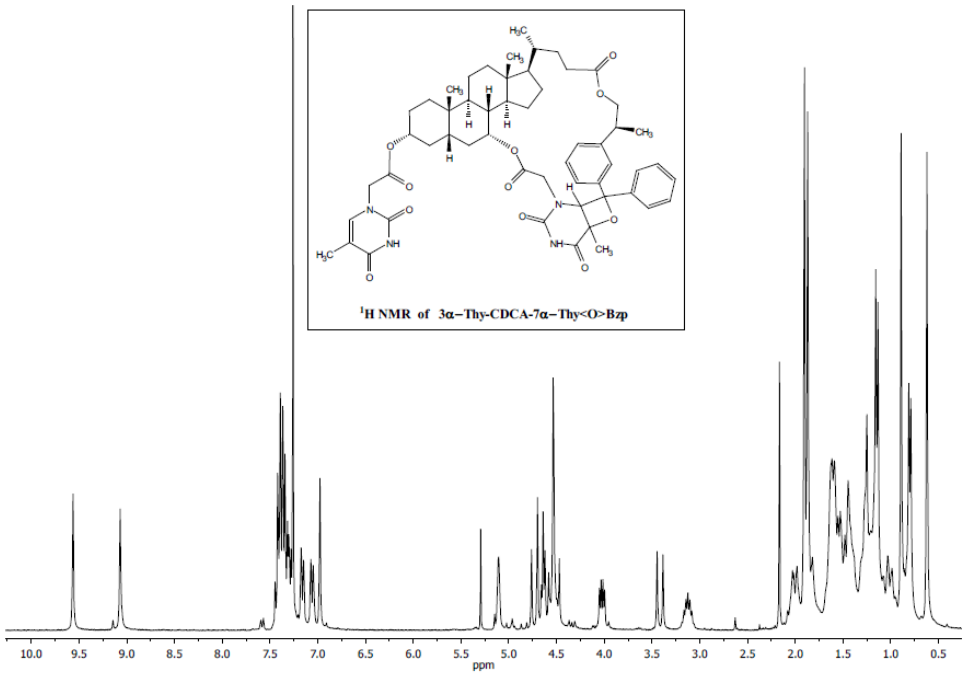
^{1}H NMR of 3α−Thy-CDCA-7α−Thy<O>Bzp
10.0 9.5 9.0 8.5 8.0 7.5 7.0 6.5 6.0 5.5 5.0 4.5 4.0 3.5 3.0 2.5 2.0 1.5 1.0 0.5
ppm

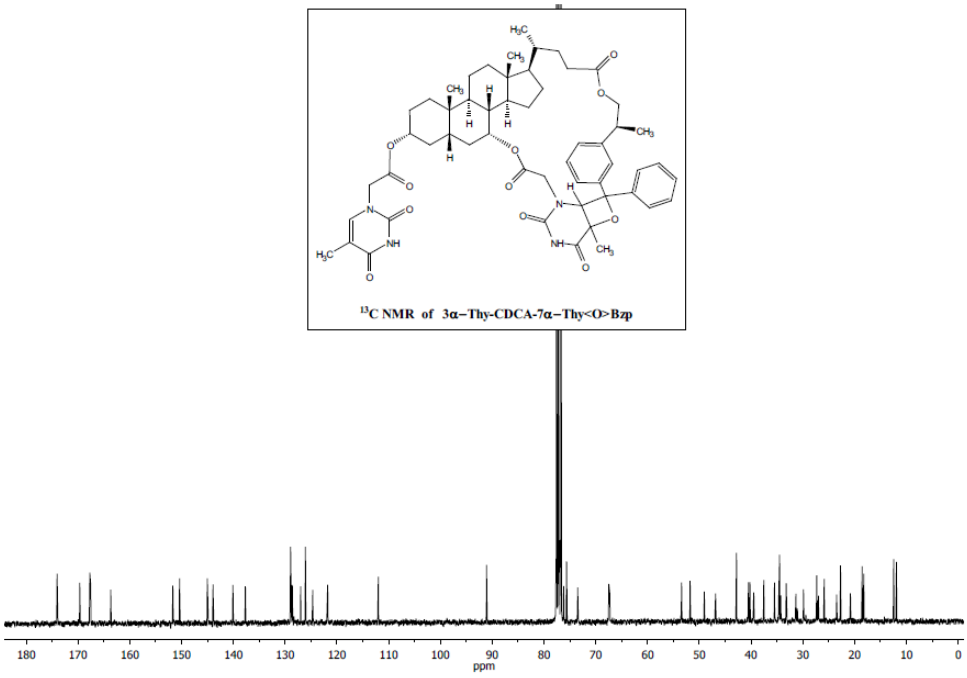
^{13}C NMR of 3α−Thy-CDCA-7α−Thy<O>Bzp
180 170 160 150 140 130 120 110 100 90 80 70 60 50 40 30 20 10 0
ppm

5.6.2.4. Photochemical synthesis of 3α,7α-Thy<>Thy-CDCA-Bn

A solution of **3α,7α-2Thy-CDCA-Bn** (0.031 g, 0.038 mmol) and **Bzp** (0.007 g, 0.038 mmol) in CH_3CN (70 mL) placed in a Pyrex® round-bottom flask was purged with N_2 and irradiated in a photoreactor using 8 lamps (λ_{max}= 350 nm) for six hours. Then, the solvent was concentrated under vacuum and the crude was purified by column chromatography (SiO_2, CH_2Cl_2: Acetone, 85:15) to give **3α,7α-Thy<>Thy-CDCA-Bn** (0.012 g, 40%); ^{1}H NMR (400 MHz, $CDCl_3$): δ (ppm) 0.64 (s, 3H, CH_3); 0.92 (d, *J* = 6.4 Hz, 3H, 21-CH_3); 0.94 (s, 3H, CH_3); 1.02-2.07 (complex signal, 26H); 1.66 (s, 3H, Thy-CH_3); 1.72 (s, 3H, Thy-CH_3); 2.99-3.20 (m, 1H, Thy-CH_2); 3.31-3.53 (m, 2H, Thy-CH_2+Thy<>Thy-CH); 3.58 (d, *J* = 2.0 Hz, 1H, Thy<>Thy-CH); 4.49-4.72 (m, 3H, 3β-H+7β-H+1xThy-CH_2); 4.81-5.00 (*m*, 1H, Thy-CH_2); 5.09 (d, *J*=12.4 Hz, 1H, Bn-CH_2); 5.14 (d, *J* = 12.4 Hz, 1H, Bn-CH_2); 7.28-7.44 (m, 5H, arom); 7.76-7.88 (m, 2H, 2xThy-NH). ^{13}C NMR (100 MHz, $CDCl_3$): δ (ppm) 174.2 (C), 168.7 (C), 168.0 (C), 167.9 (C), 166.3 (C), 150.8 (C), 150.2 (C), 136.2 (C), 128.7 (2xCH), 128.4 (2xCH), 128.3 (CH), 76.6 (CH), 76.5 (CH), 66.3 (CH+CH_2), 61.2 (CH), 56.1 (CH), 50.1 (CH), 49.1 (CH_2), 48.4 (CH_2), 45.3 (C), 45.2 (C) 42.9 (C), 40.2 (CH), 39.5 (CH_2), 38.9 (CH), 35.4 (CH), 34.7 (C), 34.3 (CH), 34.2 (CH_2), 33.9 (CH_2), 31.4 (CH_2), 31.1 (CH_2), 28.6 (CH_2), 28.1 (CH_2), 26.0 (CH_2), 23.6 (CH_2), 22.7 (CH_3), 22.5 (CH_3), 21.2 (CH_3), 20.9 (CH_2), 18.4 (CH_3), 11.8 (CH_3); m/z found 815.4218, calculated for $C_{45}H_{59}N_4O_{10}$ (MH^+) 815.4231.

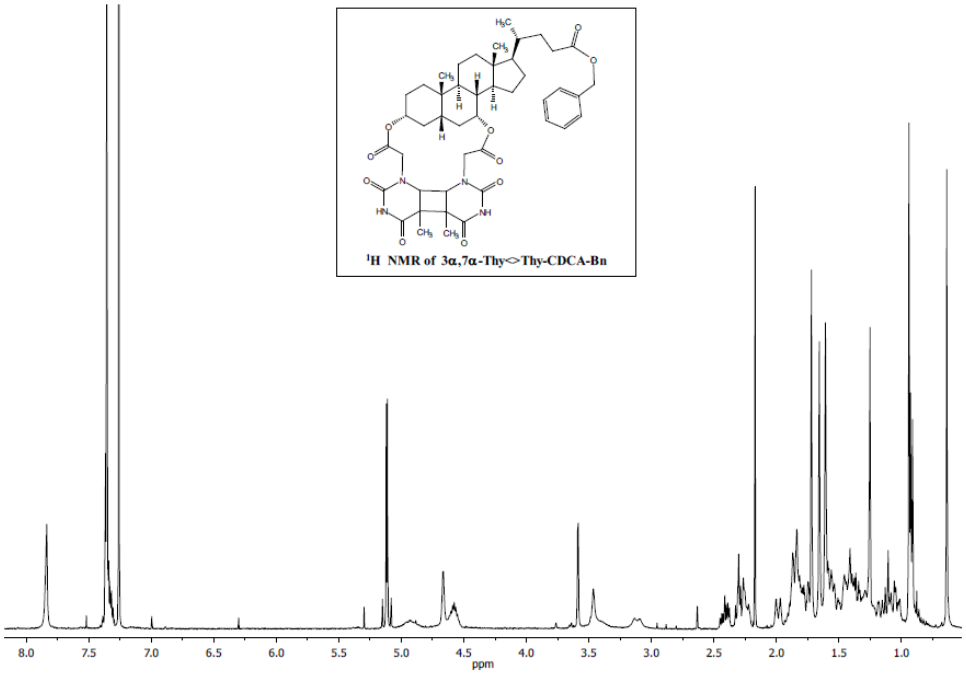
^{1}H NMR of 3α,7α-Thy<>Thy-CDCA-Bn
8.0
7.5
7.0
6.5
6.0
5.5
5.0
4.5
4.0
3.5
3.0
2.5
2.0
1.5
1.0
ppm

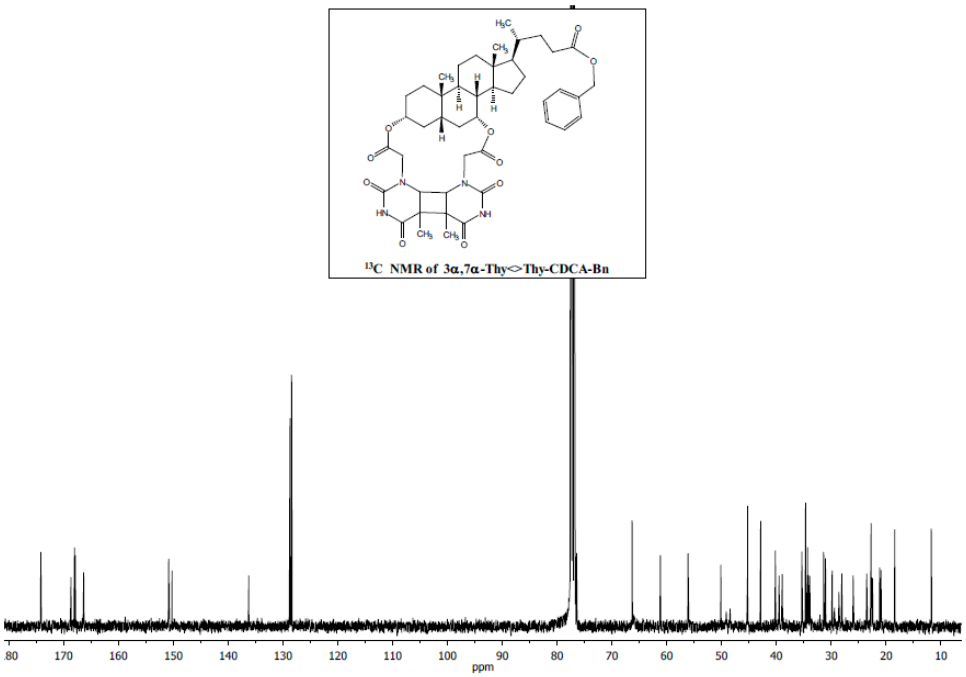
^{13}C NMR of 3α,7α-Thy<>Thy-CDCA-Bn
180
170
160
150
140
130
120
110
100
90
80
70
60
50
40
30
20
10
ppm

5.6.2.5. Photochemical synthesis of 3α-Bzp<O>12α-Thy-DCA-Thy

A solution of **3α-(*R* or *S*)Bzp,12α-Thy-DCA-Thy** more polar (0.030 g, 0.03 mmol) in CH_3CN (50 mL), placed in a Pyrex® round-bottom flask, was purged with N_2 and irradiated in a photoreactor using 8 lamps (λ_{max}= 350 nm) for 4.5 h. Then, the solvent was concentrated under vacuum and the crude was purified by column chromatography (SiO_2, CH_2Cl:MeOH 97:3) followed by (Li Chroprep RP-18, CH_3CN:H_2O, 80:20) to give **3α-Bzp<O>12α-Thy-DCA-Thy** (0.019 g, 63%); ^{1}H NMR (300MHz, $CDCl_3$): δ (ppm) 0.69 (s, 3H, CH_3); 0.74 (d, *J* = 6.3 Hz, 3H, 21-CH_3); 0.82-1.95 (complex signal, 26H); 0.91 (s, 3H, CH_3); 1.61 (d, *J* = 7.2 Hz, 3H, KP-CH_3); 1.92 (d, *J* = 0.9 Hz, 3H, Thy-CH_3); 2.03 (*br* s, 3H, Thy-CH_3); 3.41 (d, *J* = 17.4 Hz, 1H, Thy-CH_2); 3.78 (q, *J* = 7.2 Hz, 1H, KP-CH); 4.16 (m, 2H); 4.20 (d, *J* = 17.1 Hz, 1H, Thy-CH_2); 4.41 (d, *J* = 17.1 Hz, 1H, Thy-CH_2); 4.49 (s, 1H, oxetane-CH); 4.60 (d, *J* = 17.1 Hz, 1H, Thy-CH_2); 4.80 (m, 1H, 3β-H); 5.12 (*br* s, 1H, 12β-H); 6.90 (s, 1H, Thy-CH); 6.94-7.49 (m, 8H, arom); 8.05 (s, 1H, arom); 10.27 (s, 1H, Thy-NH); 10.31 (s, 1H, Thy-NH). ^{13}C NMR (75 MHz, $CDCl_3$): δ (ppm) 173.0 (C), 171.2 (C), 167.3 (C), 166.6 (C), 164.2 (C), 152.2 (C), 151.4 (C), 142.9 (C), 140.8 (C), 140.0 (CH), 136.5 (C), 128.7 (3xCH), 128.5 (2xCH), 126.5 (2xCH), 125.8 (CH), 125.2 (CH), 111.8 (C), 91.7 (C), 78.3 (CH), 76.1 (C), 74.1 (CH), 71.5 (CH), 66.7 (CH_2), 50.8 (CH), 50.4 (CH_2), 50.2 (CH_2), 48.0 (CH), 47.0 (CH), 45.3 (C), 41.4 (CH), 36.4 (CH), 35.5 (CH), 34.5 (CH_2), 34.3 (CH), 33.8 (C), 32.1 (CH_2), 31.9 (CH_2), 27.5 (CH_2), 26.9 (CH_2), 26.8 (CH_2), 26.4 (CH_2), 26.1 (CH_2), 24.9 (CH_2), 24.2 (CH_3), 23.2 (CH_2), 22.8 (CH_3), 18.4 (CH_3), 17.0 (CH_3), 12.6 (2xCH_3); m/z found 947.4802, calculated for $C_{54}H_{67}N_4O_{11}$ (MH^+) 947.4807.

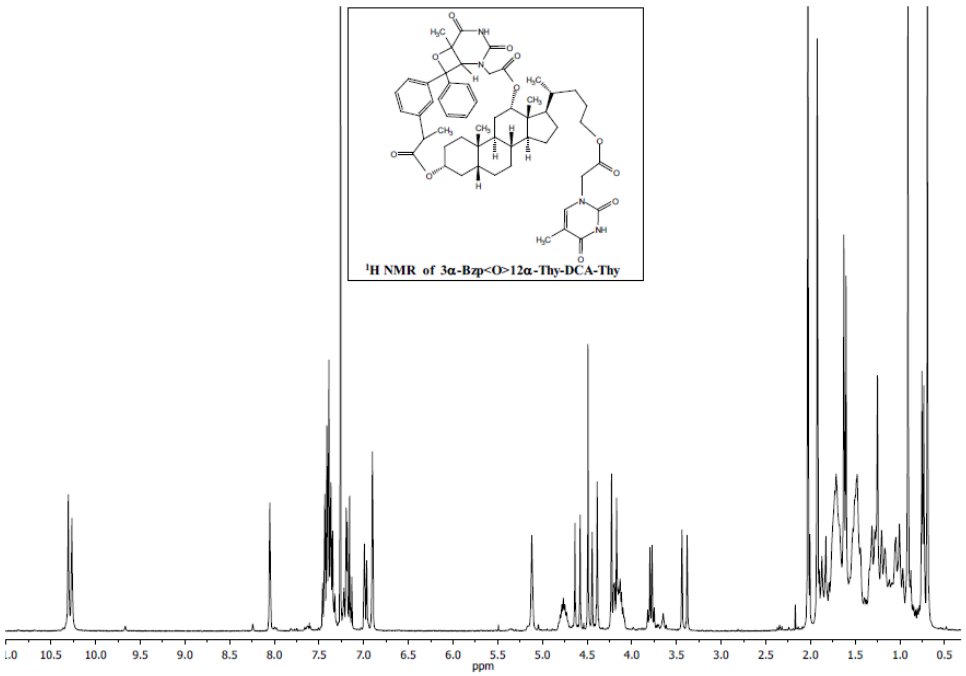
^{1}H NMR of 3α-Bzp<O>12α-Thy-DCA-Thy
ppm

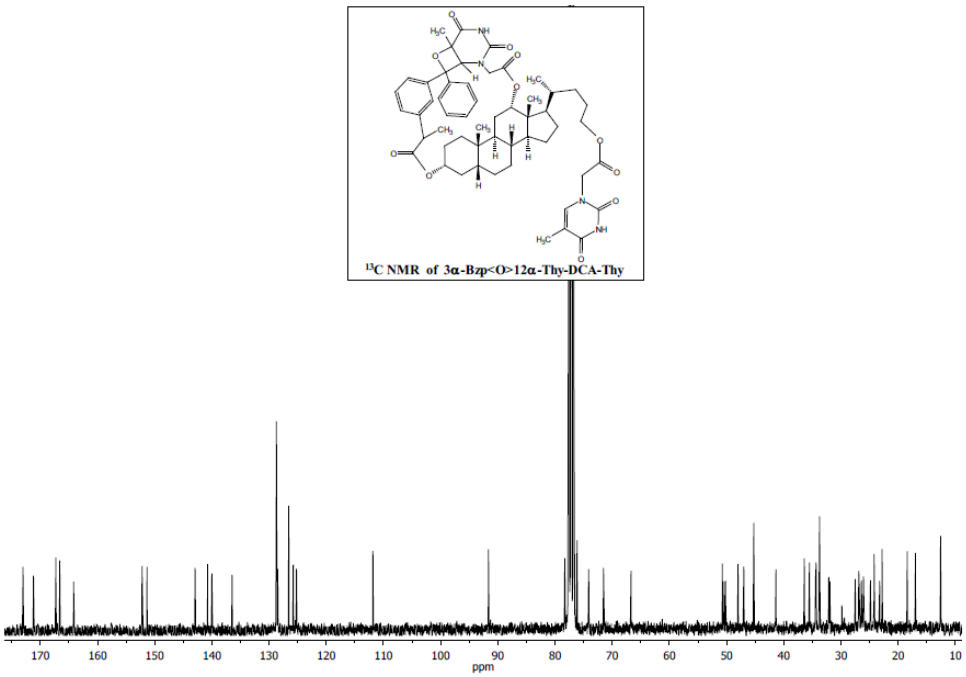
^{13}C NMR of 3α-Bzp<O>12α-Thy-DCA-Thy
ppm

5.6.2.6. Photochemical synthesis of 3α-Pa-DCA- 12α-Thy <>Thy

A solution of **3α-Pa,12α-Thy-DCA-Thy** (0.151 g, 0.18 mmol) and **Bzp** (0.033 g, 0.18 mmol) in CH_3CN (100 mL), placed in a Pyrex® round-bottom flask, was purged with N_2 and irradiated in a photoreactor using 8 lamps (λ_{max}= 350 nm) for 6 h. Then, the solvent was concentrated under vacuum and the crude was purified by column chromatography (SiO_2, CH_2Cl:MeOH 99:1) to give **3α-Pa-DCA-12α-Thy<>Thy** (0.072 g, 21%); ^{1}H NMR (300 MHz, $CDCl_3$): δ (ppm) 0.79 (s, 3H, CH_3); 0.88 (d, *J* = 7.2 Hz, 3H, 21-CH_3); 0.91 (s, 3H, CH_3); 0.99-1.82 (complex signal, 26H); 1.50 (s, 3H, Thy-CH_3); 1.52 (s, 3H, Thy-CH_3); 3.60 (s, 2H, Ph-CH_2); 3.79-3.86 (m, 1H, CH_2); 3.91 (d, *J* = 15.9 Hz, 1H, Thy-CH_2); 4.03 (d, *J* = 6.6 Hz, 1H, Thy<>Thy-CH); 4.09 (d, *J* = 16.8 Hz, 1H, Thy-CH_2); 4.12 (d, *J* = 6.6 Hz, 1H, Thy<>Thy-CH); 4.28 (d, *J* = 15.9 Hz, 1H, Thy-CH_2); 4.34 (d, *J* = 16.8 Hz, 1H, Thy-CH_2); 4.72 (m, 1H, 3β-H); 4.86-4.98 (m, 1H, CH_2); 5.09 (*br* s, 1H, 12β-H); 7.21-7.32 (m, 5H, arom); 7.33 (s, 1H, Thy-NH); 7.77 (s, 1H, Thy-NH). ^{13}C NMR (75 MHz, $CDCl_3$): δ (ppm) 171.4 (C), 171.2 (C), 170.8 (C), 169.2 (2xC), 151.1 (C), 150.3 (C), 134.6 (C), 129.3 (2xCH), 128.6 (2xCH), 127.1 (CH), 78.3 (CH), 75.4 (CH), 66.6 (CH_2), 66.4 (CH), 65.9 (CH), 51.0 (CH_2), 50.3 (CH_2), 49.2 (CH), 46.9 (C+CH), 46.3 (C), 45.6 (C), 42.3 (CH), 41.9 (CH_2), 36.6 (CH), 35.7 (CH), 35.1 (CH_2), 34.9 (CH), 34.8 (C), 33.7 (CH_2), 32.8 (CH_2), 27.5 (CH_2), 27.2 (CH_2), 26.6 (CH_2), 26.5 (CH_2), 26.1 (CH_2), 25.5 (CH_2), 23.5 (CH_2+CH_3), 22.4 (CH_3), 22.2 (CH_3), 16.3 (CH_3), 14.5 (CH_3);); m/z found 829.4398, calculated for $C_{46}H_{61}N_4O_{10}N_4$ (MH^+) 829.4388.

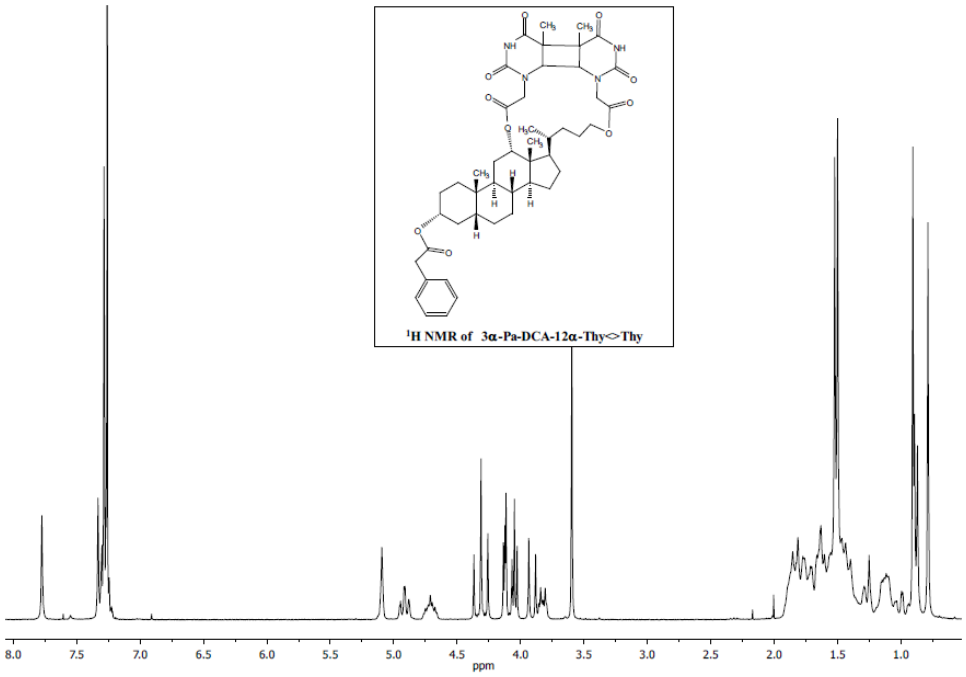
^{1}H NMR of 3α-Pa-DCA-12α-Thy<>Thy
8.0
7.5
7.0
6.5
6.0
5.5
5.0
4.5
4.0
3.5
3.0
2.5
2.0
1.5
1.0
ppm

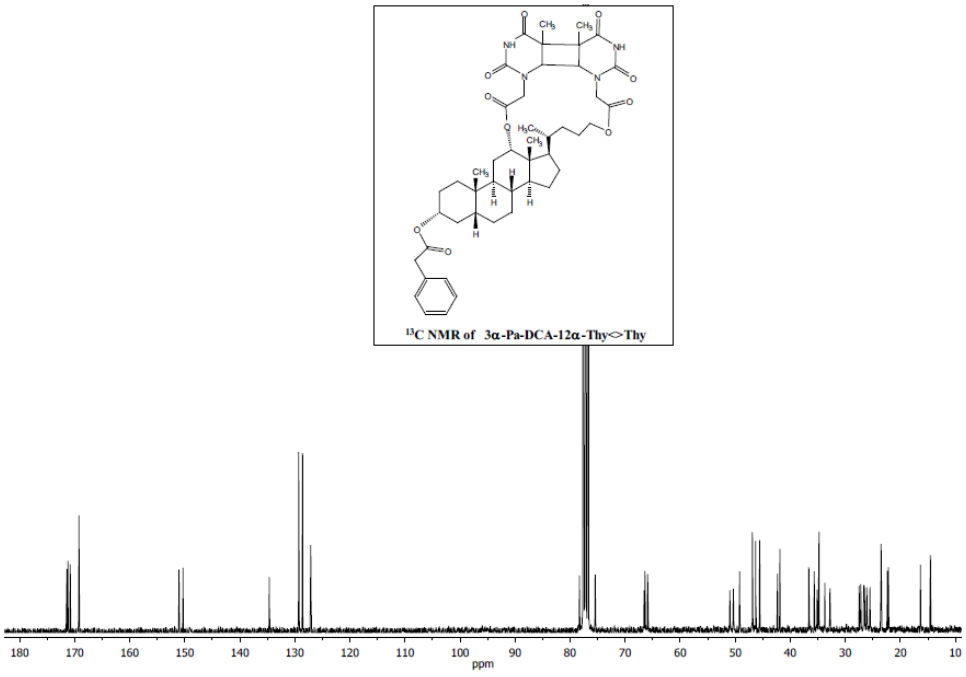
^{13}C NMR of 3α-Pa-DCA-12α-Thy<>Thy
180
170
160
150
140
130
120
110
100
90
80
70
60
50
40
30
20
10
ppm

5.6.2.7. Photochemical synthesis of 3α-Bzp<O>7α-Thy-CDCA-Thy

A solution of **3α-(*R* or *S*) Bzp,7α-Thy-CDCA-Thy** (0.105 g, 0.11 mmol) in CH_3CN (75 mL), placed in a Pyrex® round-bottom flask, was purged with N_2 and irradiated in a photoreactor using 8 lamps (λ_{max} = 350 nm) for 5 h. Then, the solvent was concentrated under vacuum and the crude was purified by column chromatography (SiO_2, CH_2Cl:Acetone, 95:5) followed by (SiO_2, EtOAc:Hexane, 65:35) to give **3α-Bzp<O>7α-Thy-CDCA-Thy** (0.031 g, 30%); ^{1}H NMR (400 MHz, $CDCl_3$): δ (ppm) 0.61 (s, 3H, CH_3); 0.75-2.10 (complex signal, 24H); 0.86 (d, *J* = 6.8 Hz, 3H, 21-CH_3); 0.94 (s, 3H, CH_3); 1.62 (m, 3H, KP-CH_3); 1.91 (s, 3H, Thy-CH_3); 2.13 (s, 3H, Thy-CH_3); 2.89 (s, 1H, CH); 2.96 (s, 1H, CH); 3.19 (d, *J* = 16.8 Hz, 1H, Thy-CH_2); 3.80 (q, *J* = 7.2 Hz, 1H, KP-CH); 4.09-4.21 (m, 2H, Thy-CH_2+CH_2); 4.24 (m, 1H, CH_2); 4.43 (d, *J* = 17.1 Hz, 1H, Thy-CH_2); 4.57 (d, *J* = 17.2 Hz, 1H, Thy-CH_2); 4.73 (m, 1H, 3β-H); 4.81 (*br* s, 1H, 7β-H); 4.84 (s, 1H, oxetane-CH); 6.82 (*br* d, *J* = 8.4 Hz, 1H, arom); 6.91 (*br* s, 1H, Thy-CH); 7.13-7.48 (m, 7H, arom); 8.17 (s, 1H, arom); 9.86 (s, 1H, Thy-NH); 10.24 (s, 1H, Thy-NH). ^{13}C NMR (100 MHz, $CDCl_3$): δ (ppm) 173.0 (C), 170.4 (C), 167.5 (C), 167.2 (C), 163.9 (C), 152.3 (C), 151.6 (C), 142.6 (C), 140.9 (C), 139.9 (CH), 135.6 (C), 129.1 (CH), 128.9 (CH), 128.7 (2xCH), 128.6 (CH), 127.0 (2xCH), 126.4 (CH), 125.9 (CH), 111.9 (C), 91.2 (C), 75.6 (C), 74.5 (CH), 74.0 (CH), 70.6 (CH), 66.6 (CH_2), 56.9 (CH), 51.8 (CH), 49.8 (CH_2), 49.3 (CH_2), 47.5 (CH), 42.7 (C), 40.8 (CH), 40.1 (CH_2), 37.8 (CH), 35.8 (CH), 35.2 (CH), 35.3 (CH_2), 34.8 (CH_2), 34.7 (C), 32.2 (CH_2), 30.7 (CH_2), 28.4 (CH_2), 27.1 (CH_2), 25.2 (CH_2), 24.1 (CH_3), 23.2 (CH_2), 22.8 (CH_3), 20.9 (CH_2), 19.9 (CH_3), 18.8 (CH_3), 12.5 (CH_3), 11.8 (CH_3); m/z found 947.4821, calculated for $C_{54}H_{67}N_4O_{11}$ (MH^+) 947.4807.

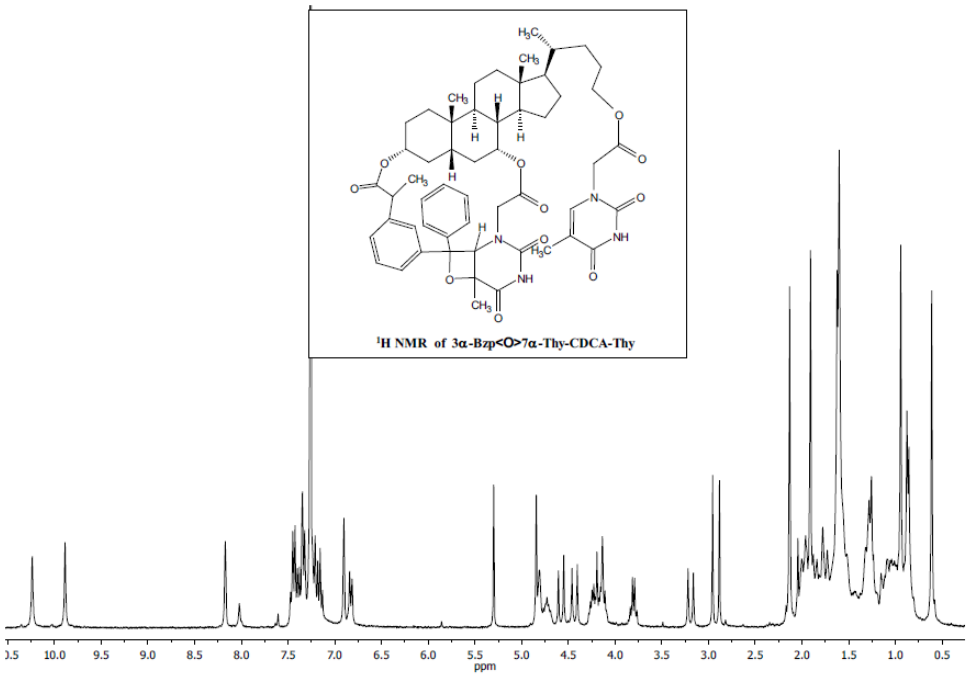
^{1}H NMR of 3α-Bzp<O>7α-Thy-CDCA-Thy
ppm

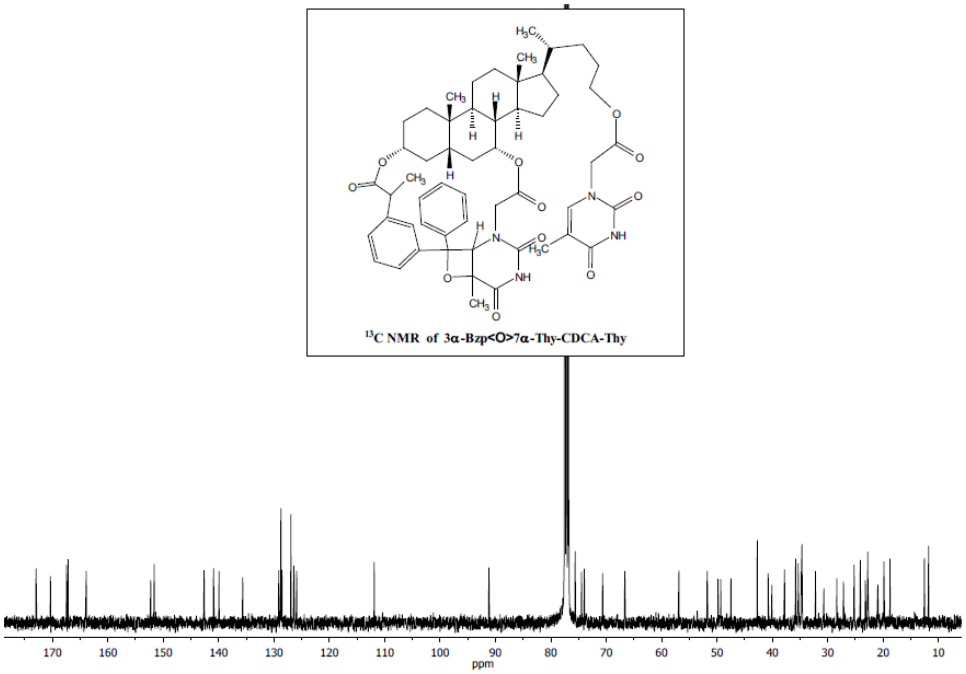
^{13}C NMR of 3α-Bzp<O>7α-Thy-CDCA-Thy
ppm

5.6.2.8. Photochemical synthesis of 3α-Bz-CDCA- 7α-Thy <>Thy

A solution of **3α-Bz,7α-Thy-CDCA-Thy** (0.040 g, 0.049 mmol) and **Bzp** (0.009 g, 0.049 mmol) in CH_3CN (70 mL), placed in a Pyrex® round-bottom flask was purged with N_2 and irradiated in a photoreactor using 8 lamps (λ_{max}= 350 nm) for six hours. Then, the solvent was concentrated under vacuum and the crude was purified by column chromatography (SiO_2, CH_2Cl_2: Acetone, 85:15) to give **3α-Bz-CDCA-7α-Thy<>Thy** (0.019 g, 48%). ^{1}H NMR (300 MHz, $CDCl_3$): δ (ppm) 0.69 (s, 3H, CH_3); 0.75-2.25 (complex signal, 26H); 0.95 (m, 6H, 21-CH_3+CH_3); 1.58 (s, 3H, Thy-CH_3); 1.59 (s, 3H, Thy-CH_3); 3.41 (d, *J* = 15.6 Hz, 1H, Thy-CH_2); 3.63 (d, *J* = 18.3 Hz, 1H, Thy-CH_2); 3.71 (d, *J* = 4.2 Hz, 1H, Thy<>Thy-CH); 3.80 (d, *J* = 4.5 Hz, 1H, Thy<>Thy-CH); 3.96 (m, 1H, CH_2); 4.15 (d, *J* = 15.6 Hz, 1H, Thy-CH_2); 4.48 (m, 1H, CH_2); 4.87 (m, 1H, 3β-H); 4.97 (d, *J* = 18.3 Hz, 1H, Thy-CH_2); 5.01 (*br* s, 1H, 7β-H); 7.33-7.86 (m, 5H, arom); 8.03 (s, 1H, Thy-NH); 8.05 (s, 1H, Thy-NH). ^{13}C NMR (75 MHz, $CDCl_3$): δ (ppm) 168.7 (C),168.5 (C), 168.0 (C), 167.5 (C), 166.3 (C), 151.0 (C), 150.9 (C), 132.8 (C), 130.9 (C), 129.7 (2xCH), 128.4 (2xCH), 74.5 (CH), 73.9 (CH), 66.8 (CH_2), 63.9 (CH), 61.6 (CH), 53.4 (CH), 51.4 (CH), 48.8 (CH_2), 46.3 (C), 46.1 (C), 45.0 (CH_2), 42.3 (C), 40.8 (CH), 39.4 (CH_2), 38.2 (CH), 35.1 (CH_2), 35.0 (CH), 34.8 (CH_2), 34.6 (CH), 31.7 (C+CH_2), 29.6 (CH_2), 28.6 (CH_2), 27.0 (CH_2), 23.9 (CH_2), 22.6 (CH_3), 21.7 (CH_2), 21.5 (2xCH_3), 20.5 (CH_2), 17.7 (CH_3), 11.3 (CH_3); m/z found 815.4238, calculated for $C_{45}H_{59}N_4O_{10}$ (MH^+) 815.4231.

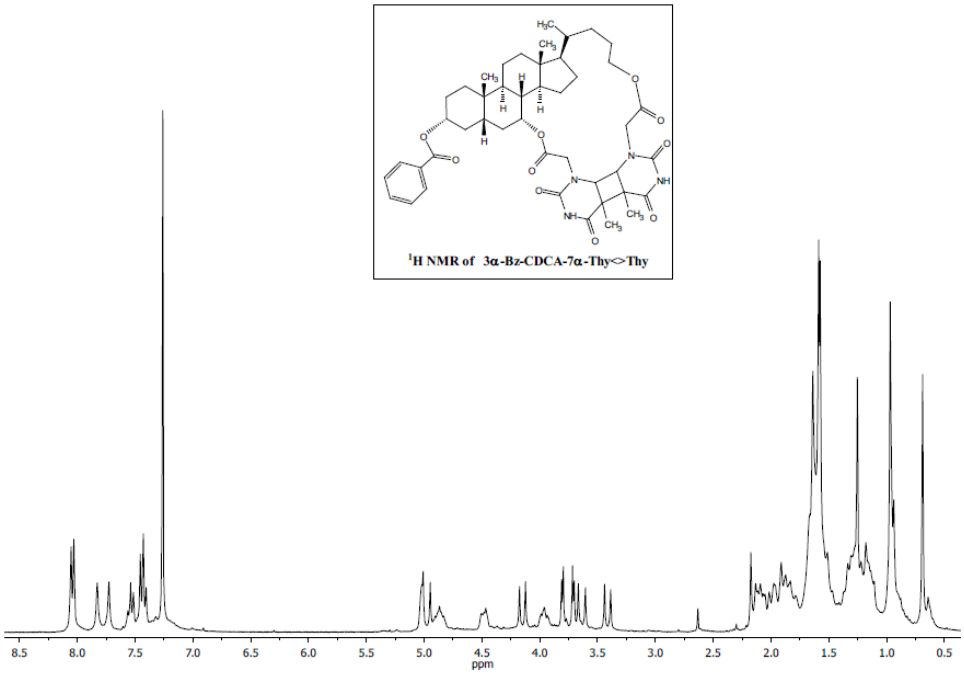
^{1}H NMR of 3α-Bz-CDCA-7α-Thy<>Thy
8.5 8.0 7.5 7.0 6.5 6.0 5.5 5.0 4.5 4.0 3.5 3.0 2.5 2.0 1.5 1.0 0.5
ppm

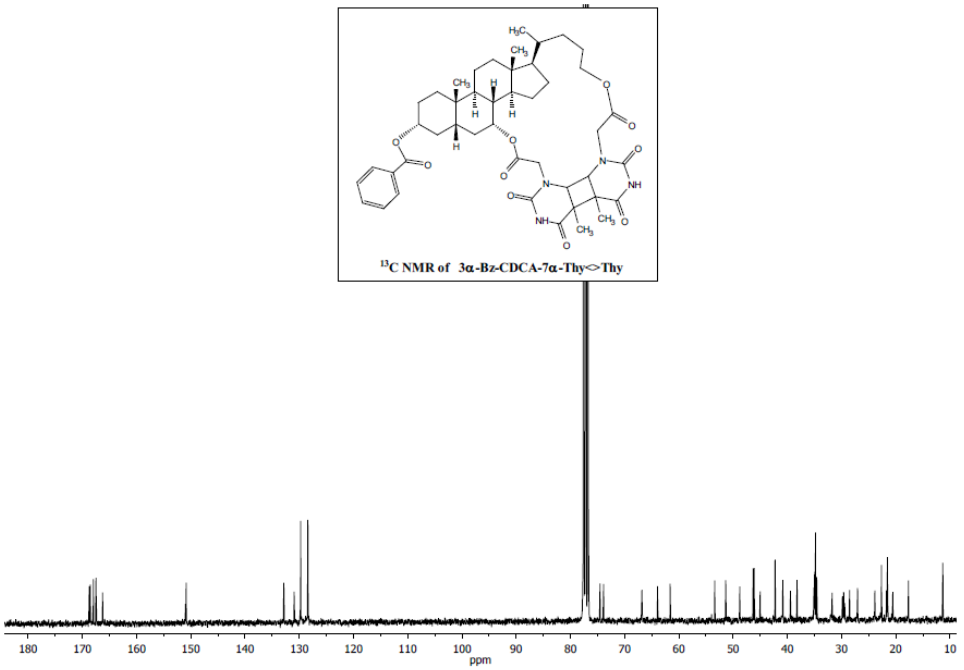
^{13}C NMR of 3α-Bz-CDCA-7α-Thy<>Thy
180 170 160 150 140 130 120 110 100 90 80 70 60 50 40 30 20 10
ppm

5.7. Supplementary material

5.7.1. Determination of τ_T of Bzp by energy transfer to Npt

When the triplet lifetime (τ_T) of a chromophore is in the order of the laser pulse, it is difficult to obtain a direct reliable value. Thus, triplet lifetime determination by energy transfer to a lower energetic triplet is a useful tool.[154–156] In this case, the short-lived τ_T of Bzp in **3α, 12α-2Thy-DCA-Bzp** was determined by energy transfer to Npt (triplet energies of Bzp and Npt 68.9 kcal mol^{-1} and 60.9 kcal mol^{-1}, respectively).[22] Laser flash photolysis of **3α,12α-2Thy-DCA-Bzp** was performed upon selective excitation of Bzp at 355 nm in the presence of increasing amounts of Npt, and the triplet-triplet absorption of Npt was monitored at 415 nm (Figure 5.10, left). As the plot of the absorbance at 415 nm against the concentration of Npt was not fitted to a straight line (Figure 5.10, right), the reverse of that Stern-Volmer plot was calculated and the corresponding double reciprocal equation[51,154–157] was obtained:

$$\frac{1}{A_{415}} = \alpha + \alpha/(k_q \tau_T\,[\mathrm{Npt}]) \qquad \text{Eq. 5.9}$$

Where A_{415} is the absorbance of the triplet Npt at 415 nm, k_q is the bimolecular rate constant for the quenching of DCA-Bzp triplet by Npt (8 x 10^9 M^{-1} s^{-1}), τ_T is the unknown triplet lifetime of the chromophore in **3α, 12α-2Thy-DCA-Bzp** and α is a constant. The fitting of the previous data to this equation is shown in Figure 5.1, right (see page 134).

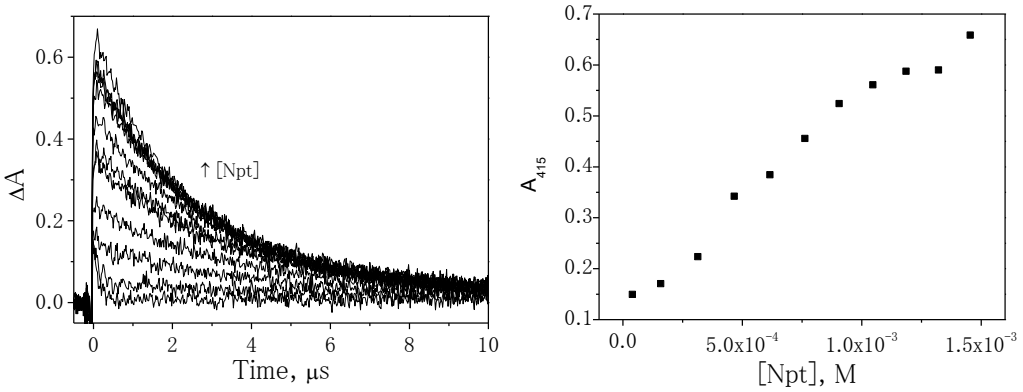

Figure 5.10. Left: LFP decays obtained upon excitation at 355 nm and monitored at 415 nm of **3α,12α-2Thy-DCA-Bzp** with increasing concentrations of Npt in 4 CH_3CN:1H_2O. **Right:** Stern-Volmer plot of the absorbance at 415 nm *versus* Npt concentration immediately after the laser pulse.

5.7.2. UPLC analysis of the irradiated samples

The crude of the irradiation of **3α,12α-2Thy-DCA-Bzp** or **Bzp:3α,12α-2Thy-DCA-Bn** was analyzed by UPLC-MS-MS and compared to the corresponding standards, **3α,12α-2Thy-DCA-Bzp** and **3α-Thy-DCA-12α-Thy<O>Bzp** or **3α,12α-2Thy-DCA-Bn** and **3α,12α-Thy<>Thy-DCA-Bn**, respectively. The chromatograms confirmed that the main photoproduct from each irradiation corresponds to the isolated one.

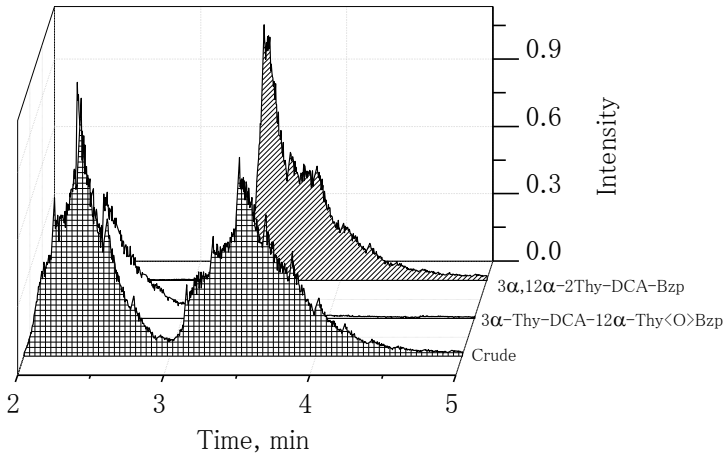

Figure 5.11. UPLC analysis of the crude of the irradiation (λ_{max} = 350 nm) of **3α,12α-2Thy-DCA-Bzp** in $4CH_3CN$:$1H_2O$.

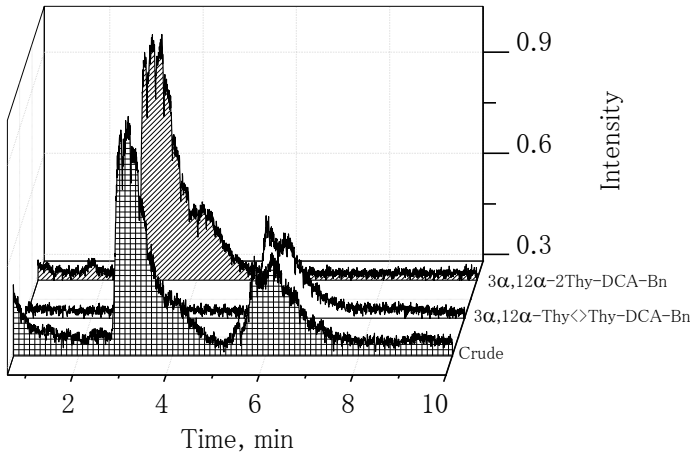

Figure 5.12. UPLC analysis of the crude of the irradiation (λ_{max} = 350 nm) of **Bzp:3α,12α-2Thy-DCA-Bn** in $4CH_3CN$:$1H_2O$.

5.7.3. Instrumentation

Laser flash photolysis at 355 nm. Transient spectra were recorded at room temperature using N_2-purged $4CH_3CN$:$1H_2O$ solutions of 5 x 10^{-4} M of the compound of interest. Intermolecular quenchings of Bzp (5 x 10^{-4} M) were determined upon addition of increasing concentrations of quencher and recorded at 530 nm. Energy transfer experiment was performed with 5 x 10^{-4} M of 3α,12α-2Thy-DCA-Bzp and increasing concentrations of Npt up to 1.4 x 10^{-3} M (monitored at 415 nm).

Irradiations for the UV-Vis analysis. Irradiation of solutions at the concentration of 4.4 x 10^{-5} M in $4CH_3CN$:$1H_2O$ and N_2 atmosphere were performed in the Luzchem photoreactor with lamps centred at 350 nm.

UPLC-MS-MS. The analysis of the photoproducts from the intramolecular irradiation of **3α,12α-2Thy-DCA-Bzp** was achieved with and isocratic elution using 77% MeOH and 23% H_2O (containing 0.01% formic acid) as the mobile phase during the first 10 minutes followed by a gradient to reach 100% of MeOH. The injection volume was 2μL. The analysis of the intermolecular irradiation of **Bzp:3α,12α-2Thy-DCA-Bn** was achieved with isocratic elution using 70% MeOH and 30% H_2O (containing 0.01% formic acid) as the mobile phase during the first 12 minutes followed by a gradient to reach 100% of MeOH. The injection volume was 1μL.

5.7.4. Additional NMR spectra

5.7.4.1. *(S)*-KP-OH

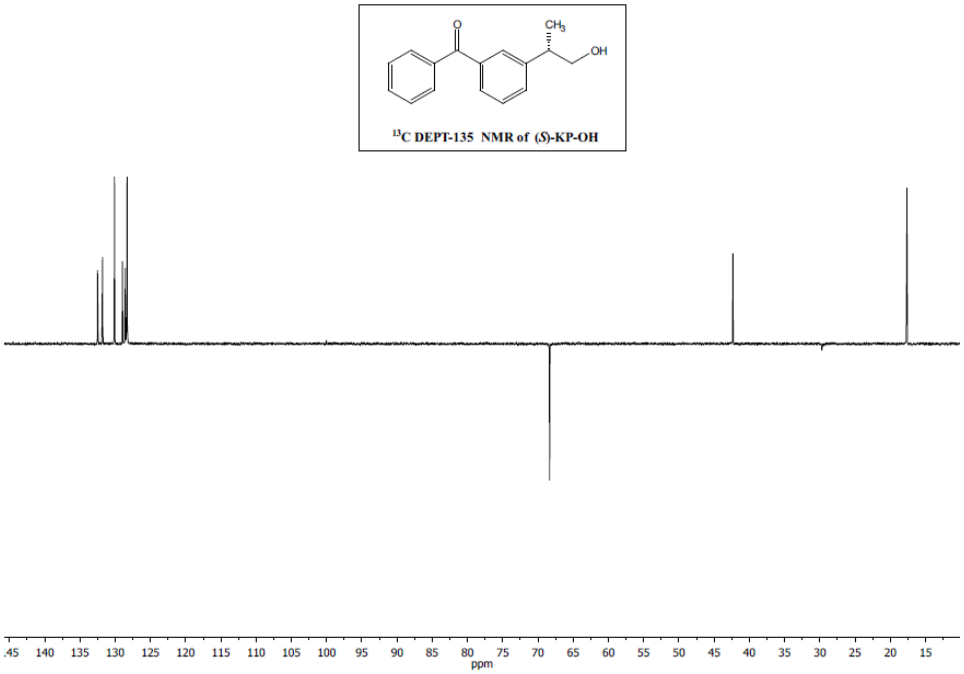

5.7.4.2. DCA–Bzp

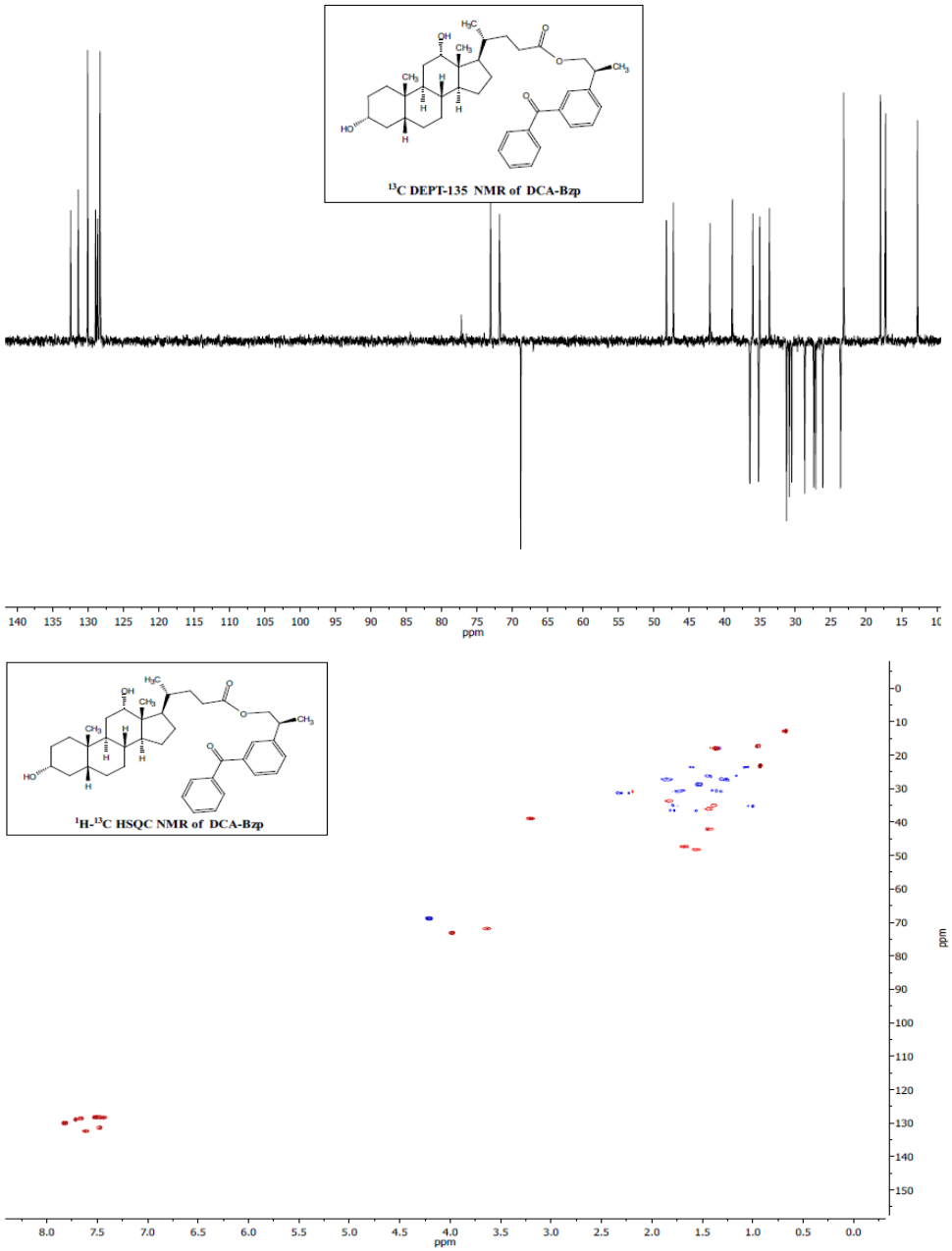
^{13}C DEPT-135 NMR of DCA-Bzp
ppm
^{1}H-^{13}C HSQC NMR of DCA-Bzp
ppm
ppm

5.7.4.3. 3α,12α-2Thy-DCA-Bzp

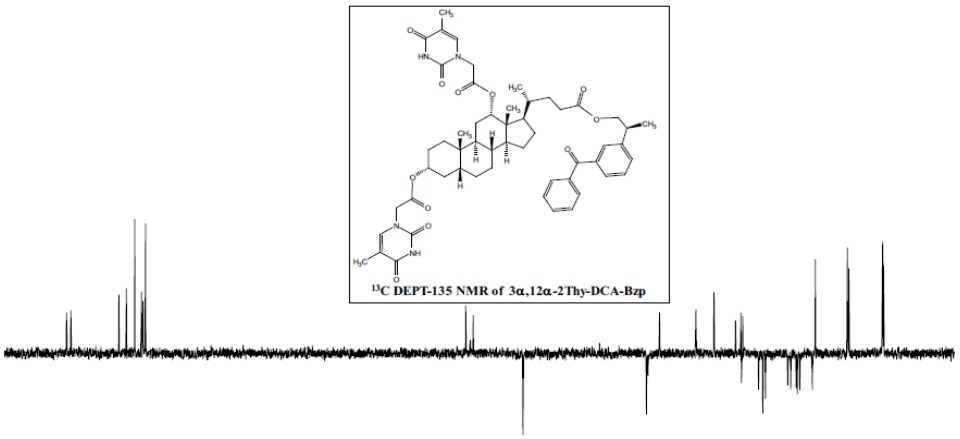

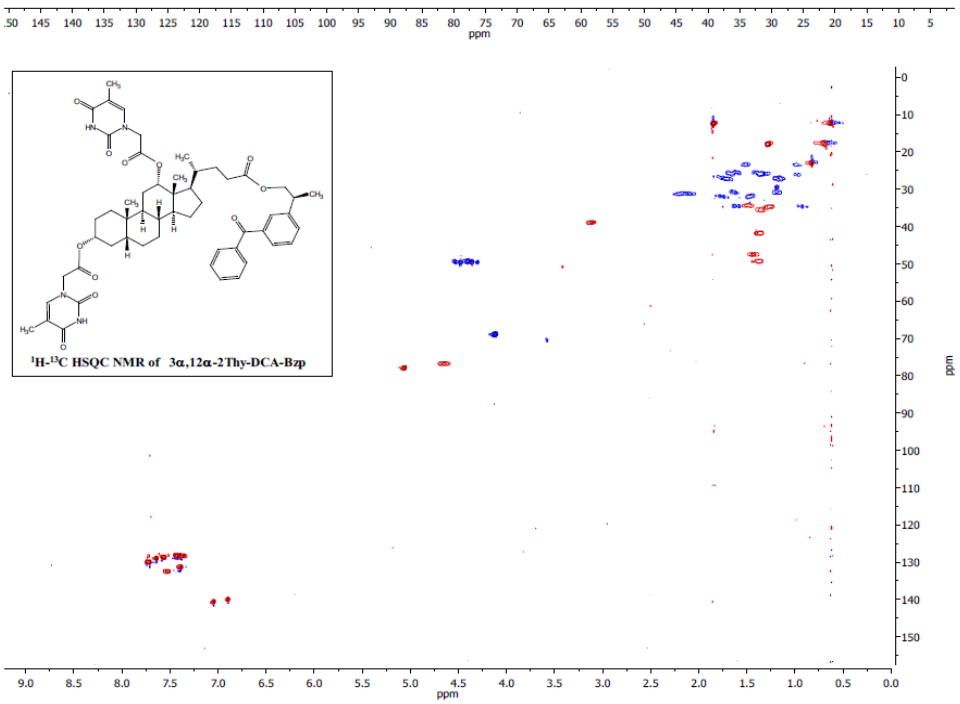

5.7.4.4. DCA-Bn

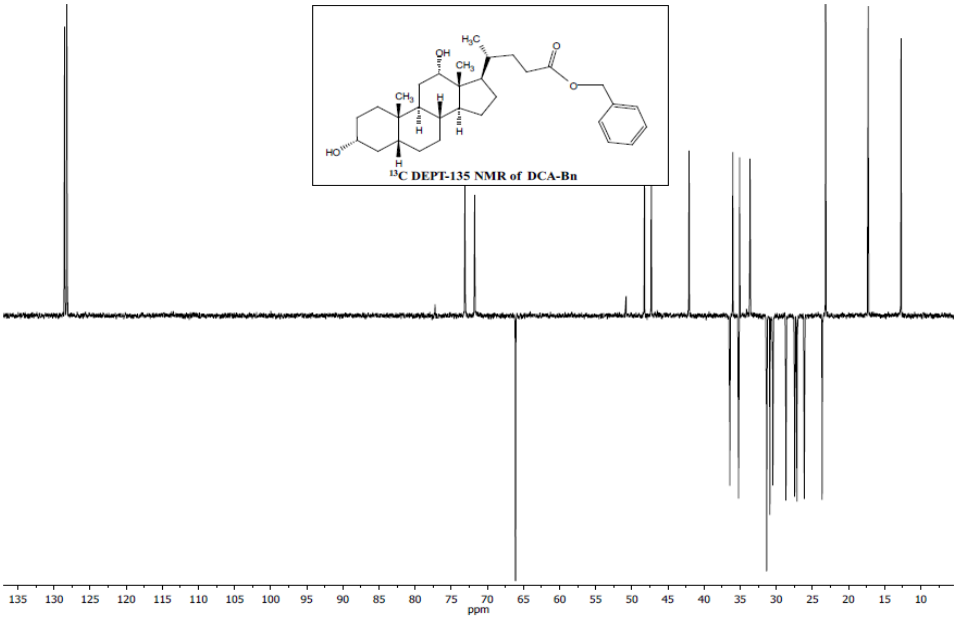
^{13}C DEPT-135 NMR of DCA-Bn
135 130 125 120 115 110 105 100 95 90 85 80 75 70 65 60 55 50 45 40 35 30 25 20 15 10
ppm

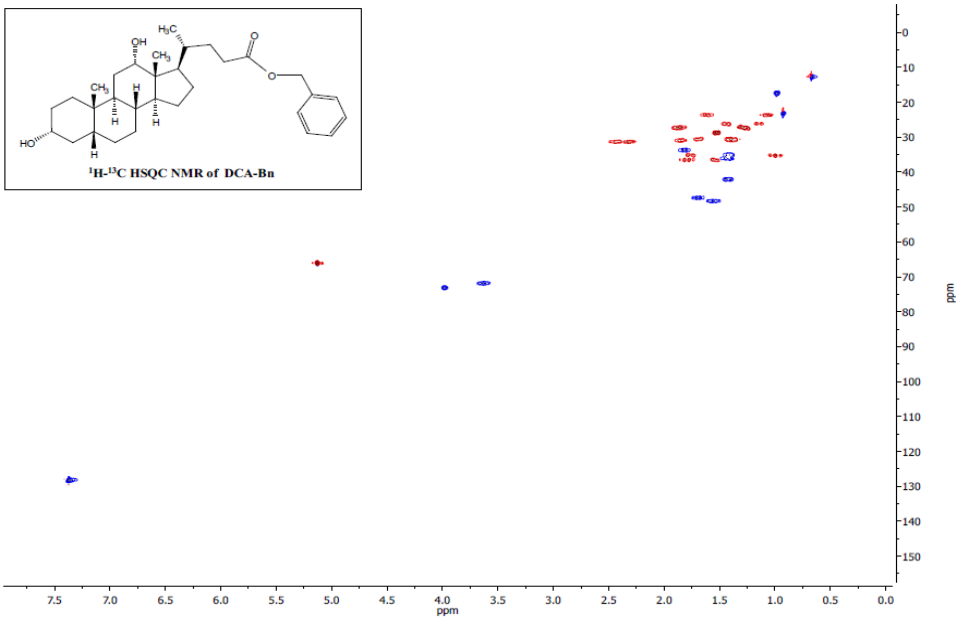
^{1}H-^{13}C HSQC NMR of DCA-Bn
0 10 20 30 40 50 60 70 80 90 100 110 120 130 140 150
ppm
7.5 7.0 6.5 6.0 5.5 5.0 4.5 4.0 3.5 3.0 2.5 2.0 1.5 1.0 0.5 0.0
ppm

5.7.4.5. 3α,12α-2Thy-DCA-Bn

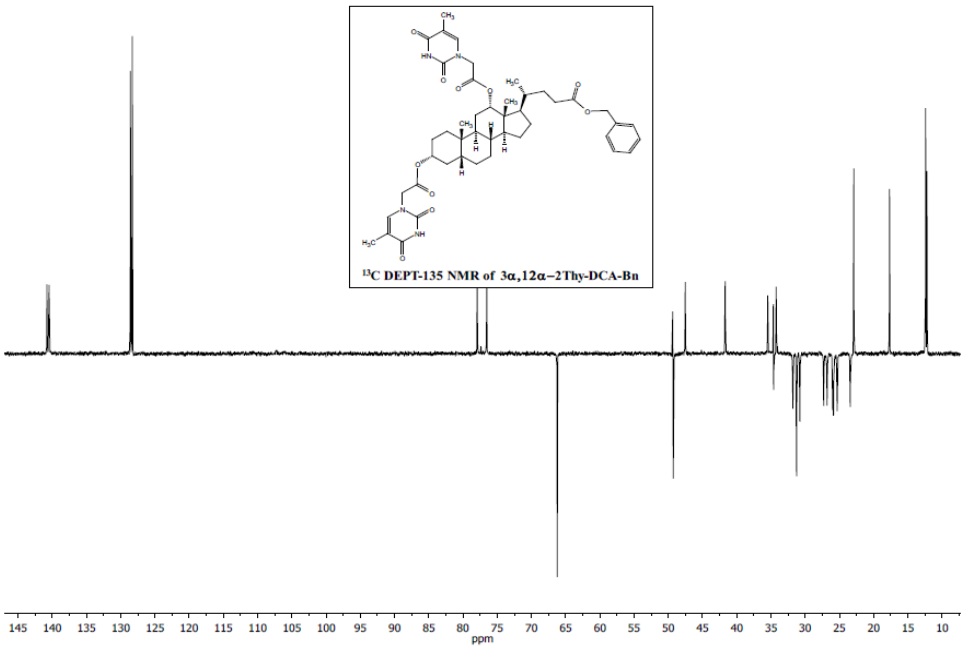

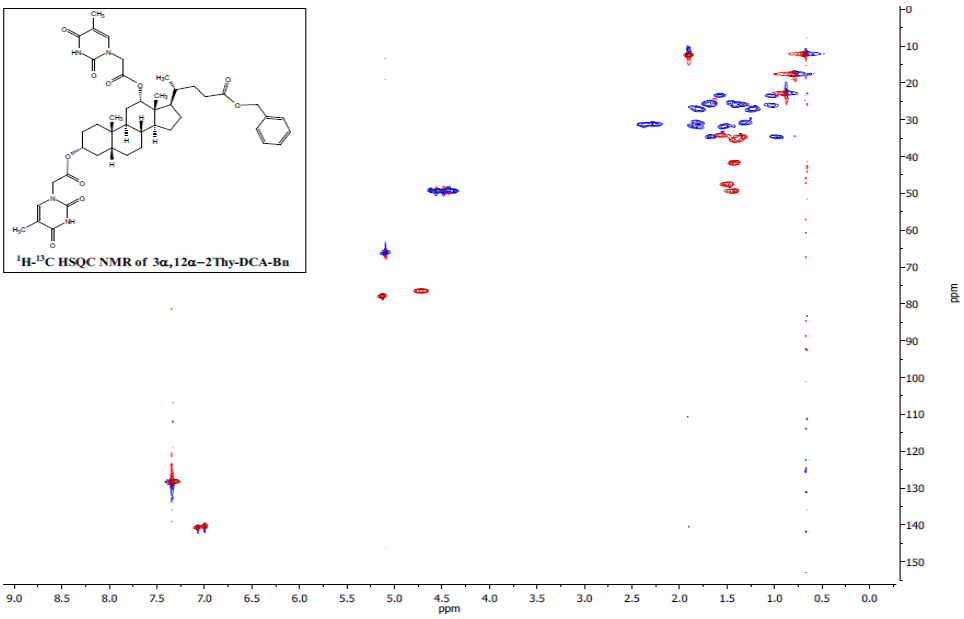

5.7.4.6. CDCA-Bzp

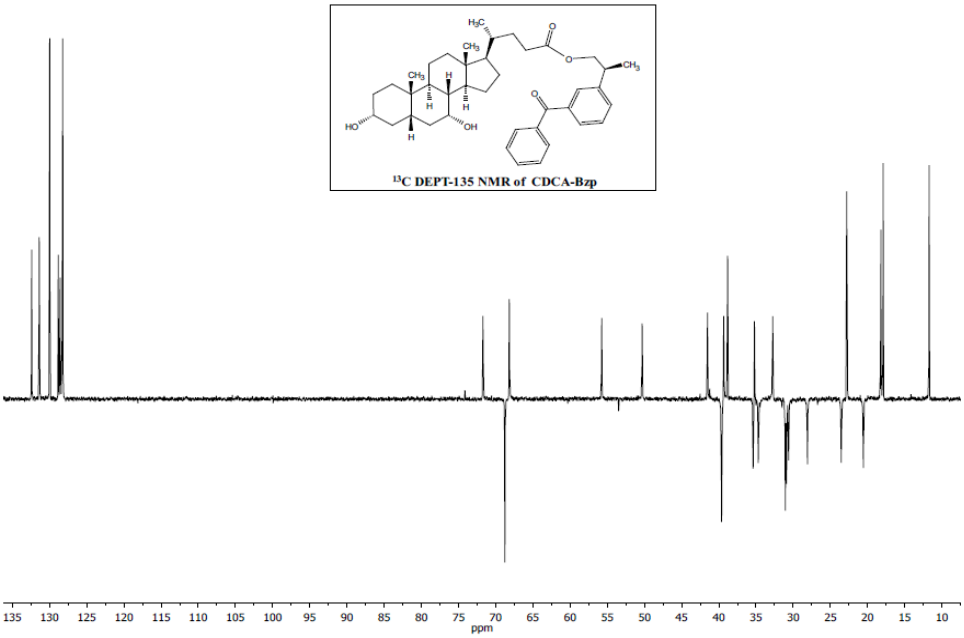

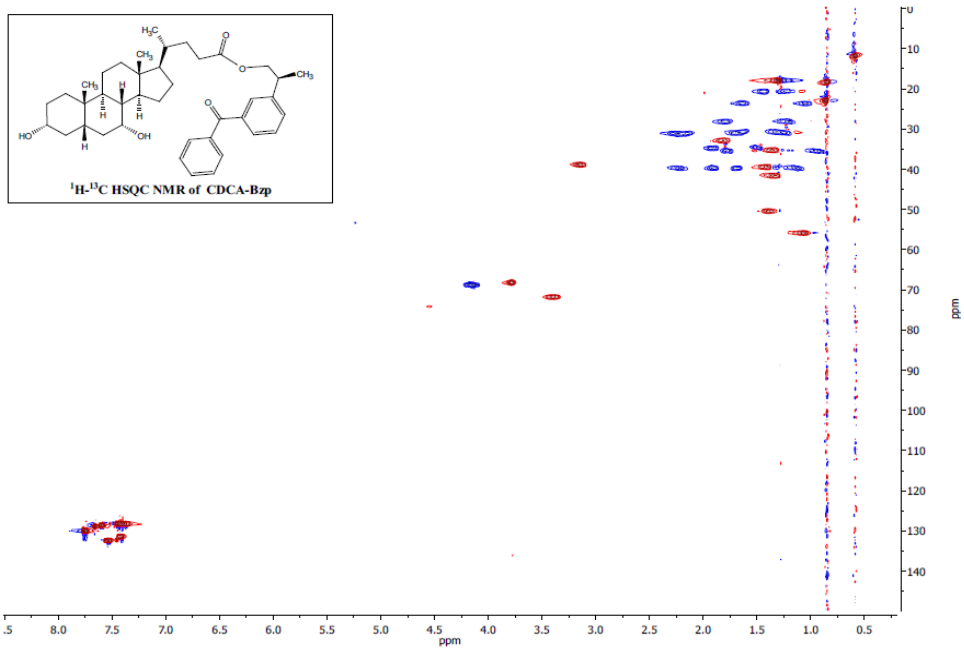

5.7.4.7. 3α,7α-2Thy-CDCA-Bzp

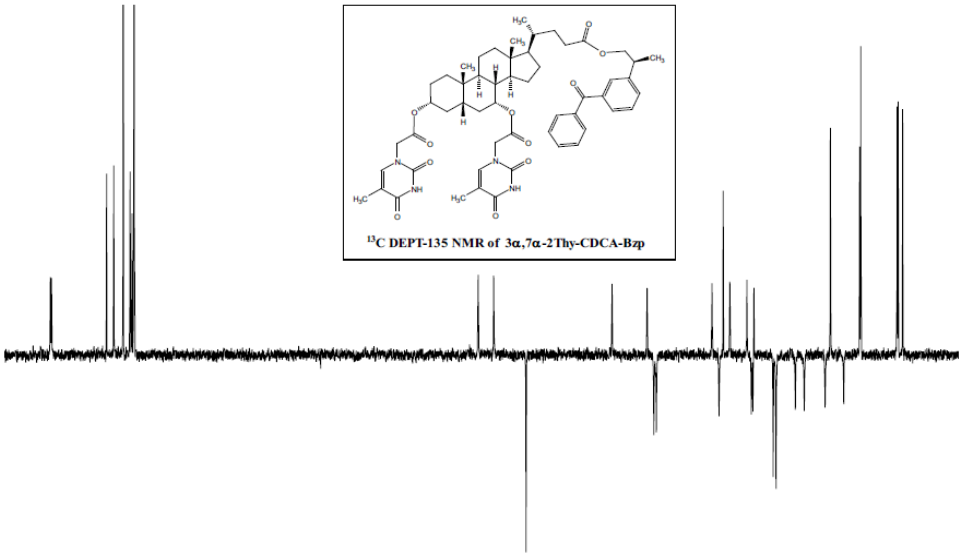

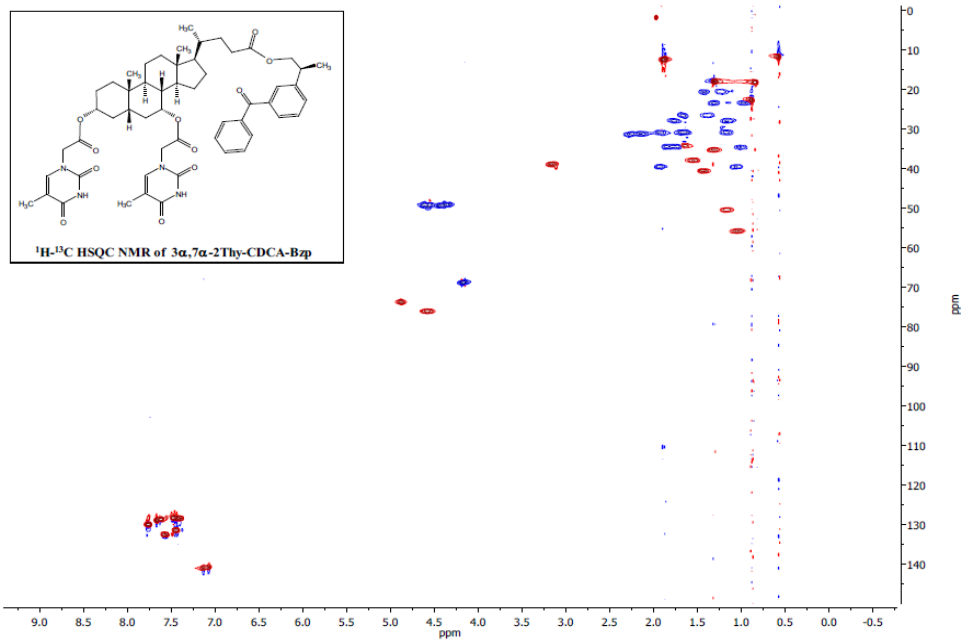

5.7.4.8. CDCA-Bn

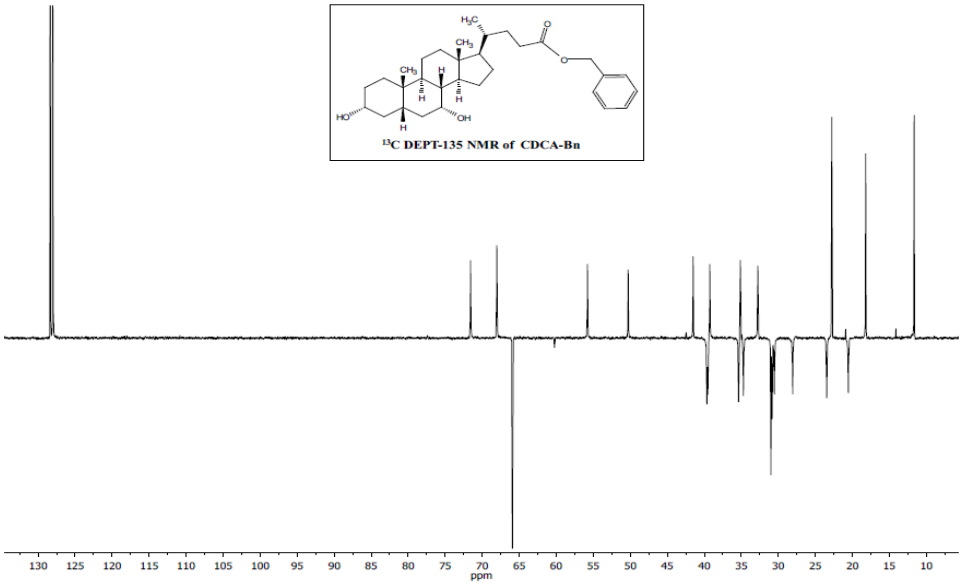
^{13}C DEPT-135 NMR of CDCA-Bn
130 125 120 115 110 105 100 95 90 85 80 75 70 65 60 55 50 45 40 35 30 25 20 15 10
ppm

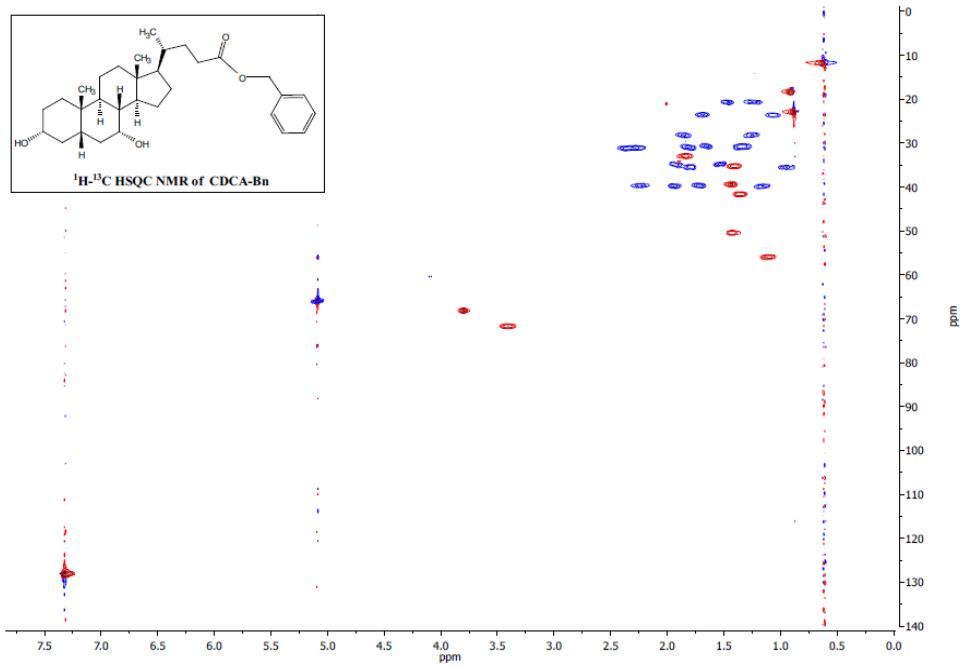
^{1}H-^{13}C HSQC NMR of CDCA-Bn
7.5 7.0 6.5 6.0 5.5 5.0 4.5 4.0 3.5 3.0 2.5 2.0 1.5 1.0 0.5 0.0
ppm
0 10 20 30 40 50 60 70 80 90 100 110 120 130 140
ppm

5.7.4.9. 3α,7α-2Thy-CDCA-Bn

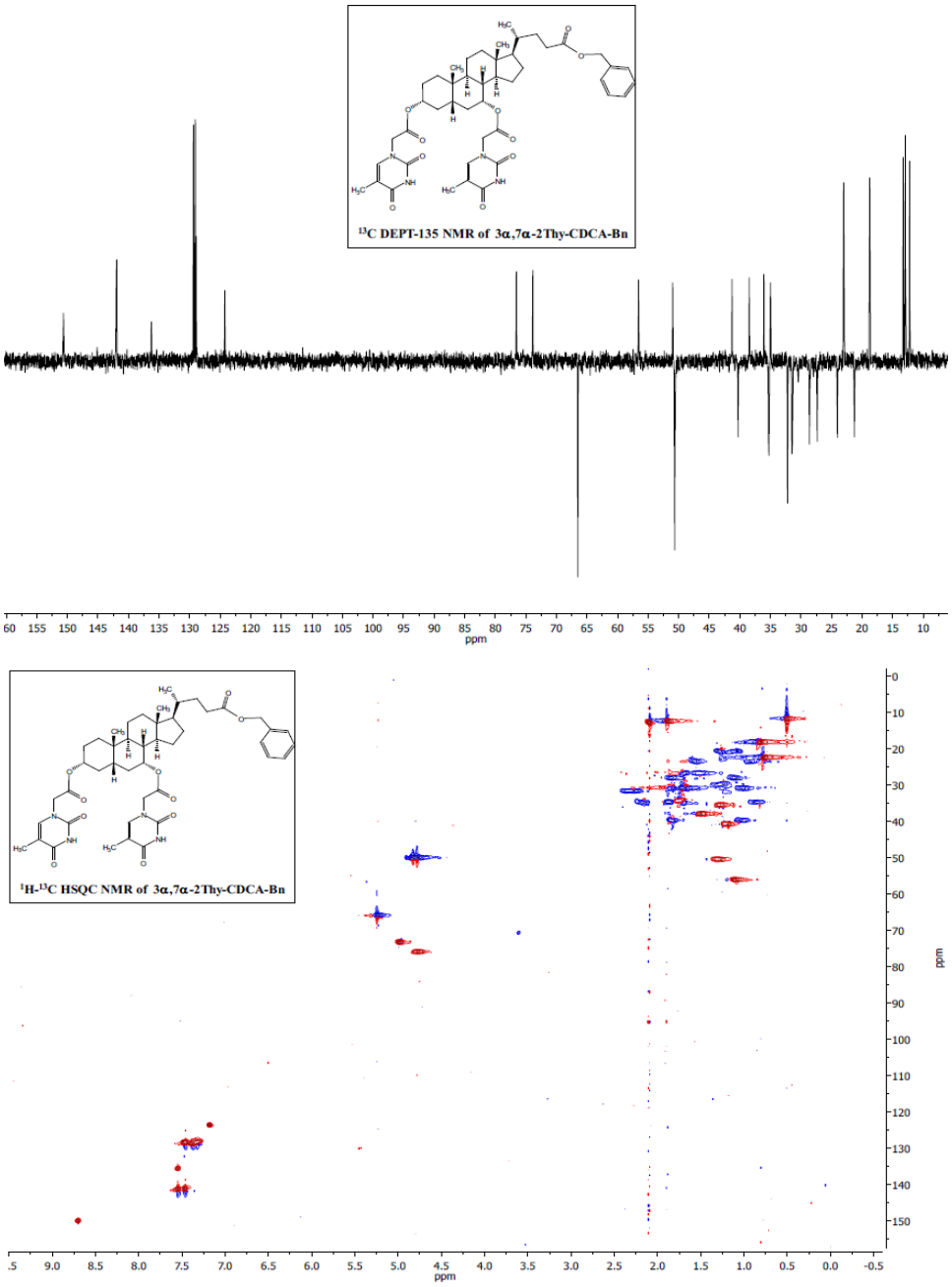

5.7.4.10. DCAOH

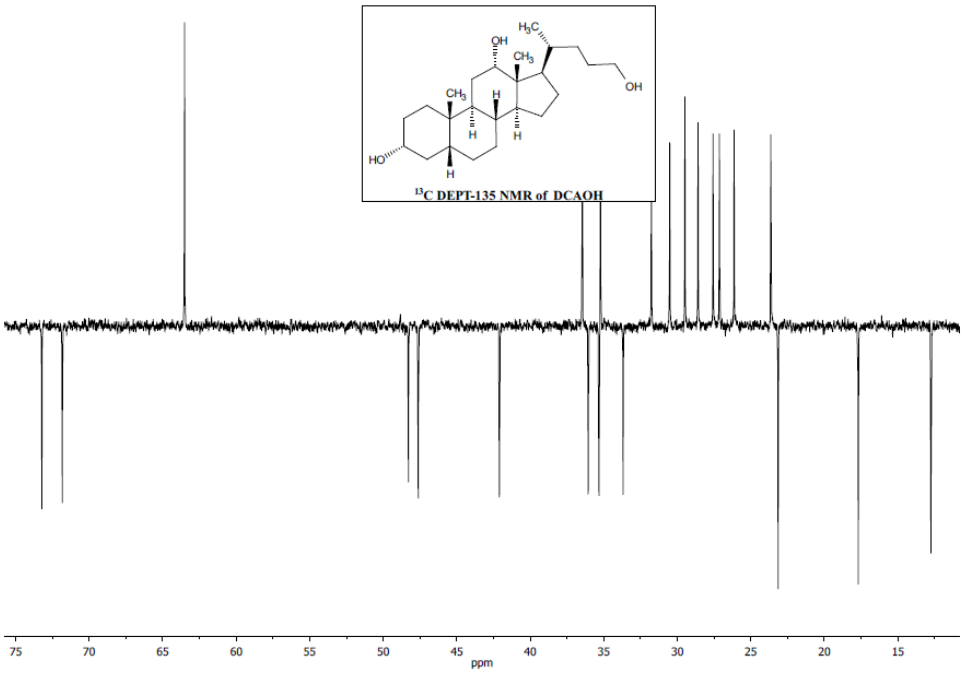
OH
H_3C
CH_3
OH
CH_3
H
H
H
H
HO
H
^{13}C DEPT-135 NMR of DCAOH
75
70
65
60
55
50
45
40
35
30
25
20
15
ppm

5.7.4.11. DCA-Thy

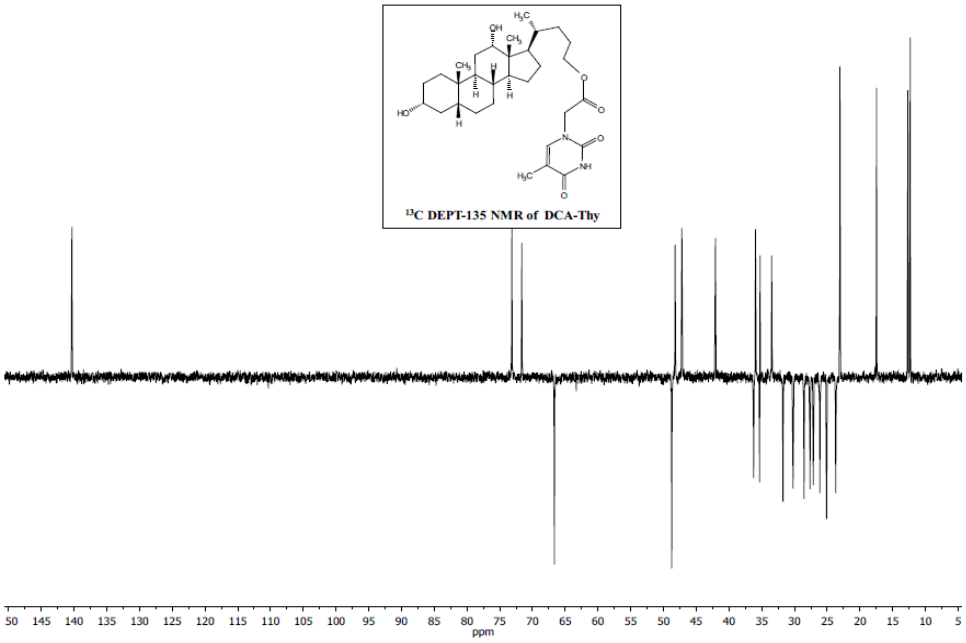

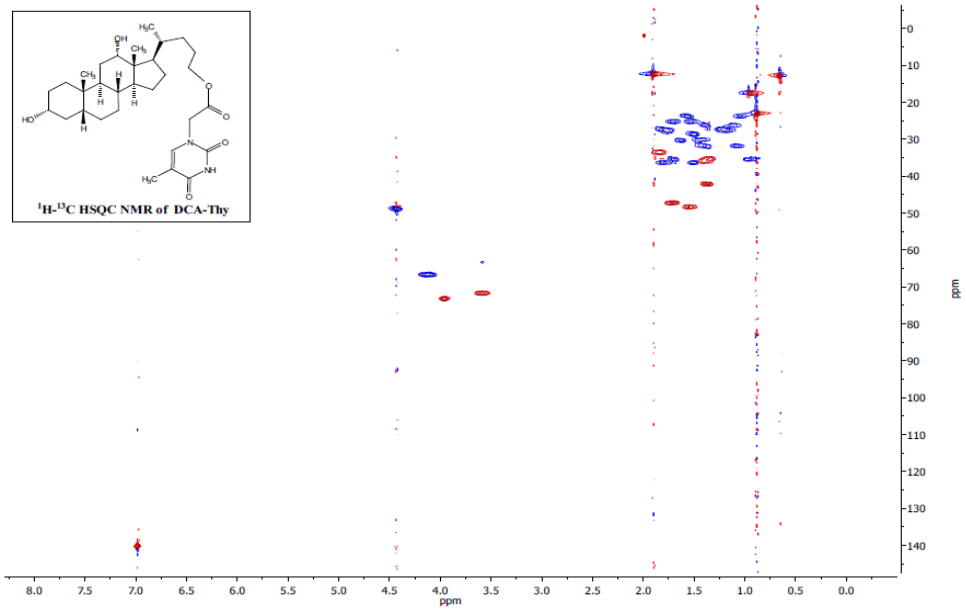

5.7.4.12. 3α-Bzp-DCA-Thy

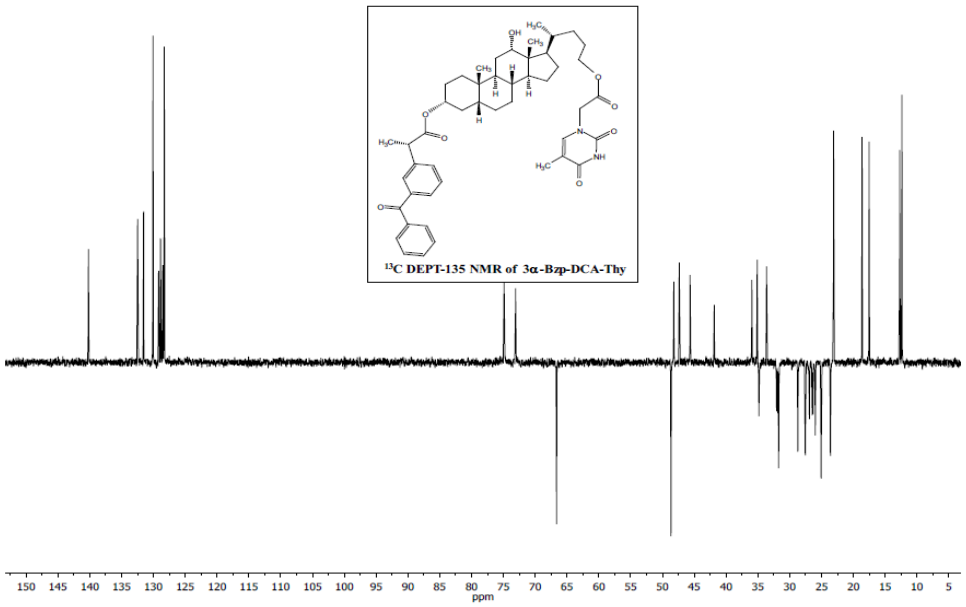

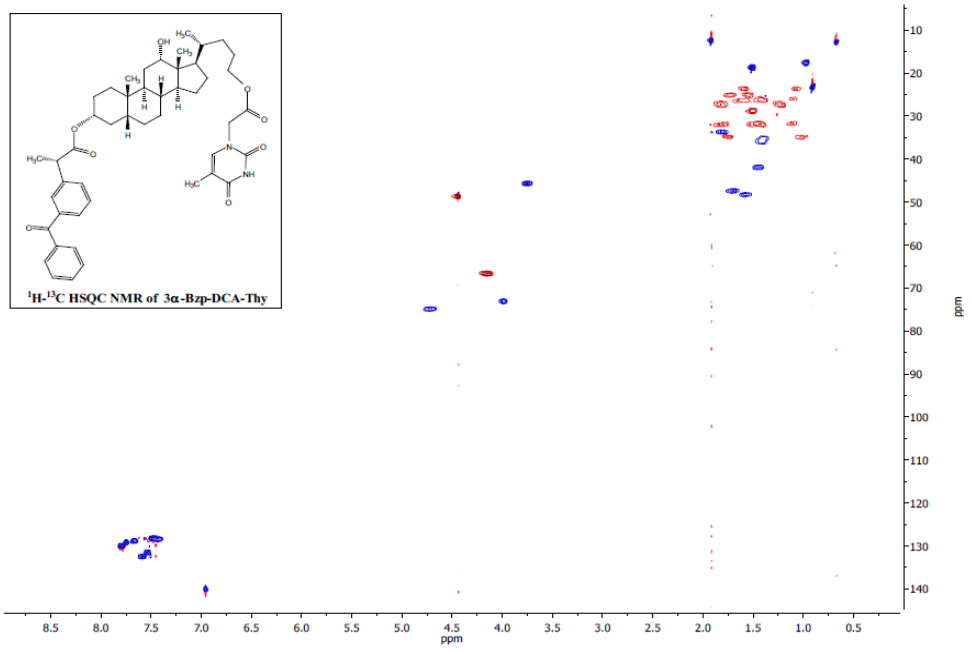

5.7.4.13. 3α-(*R* or *S*) Bzp, 12α-Thy -DCA-Thy

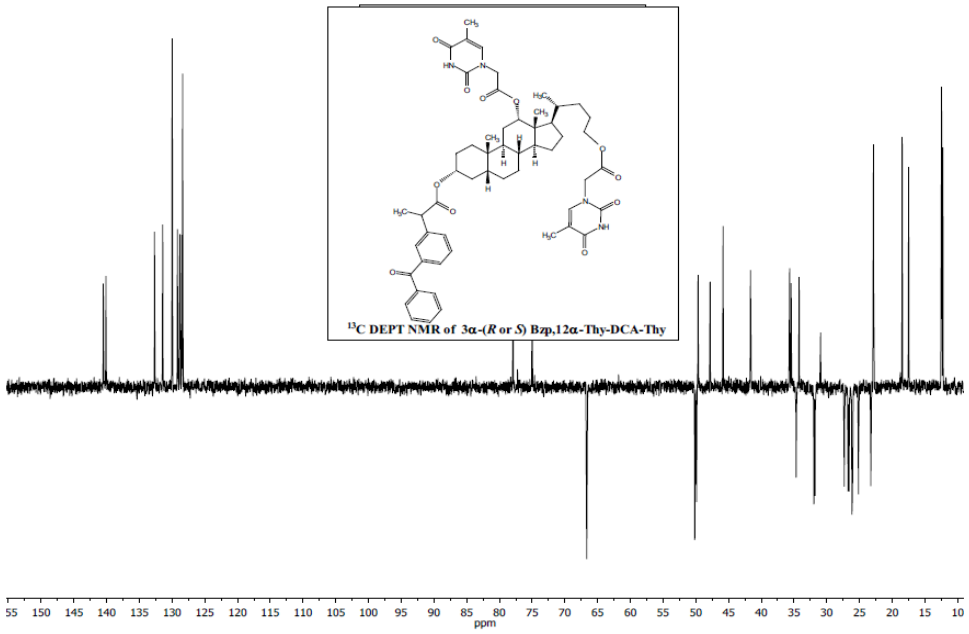

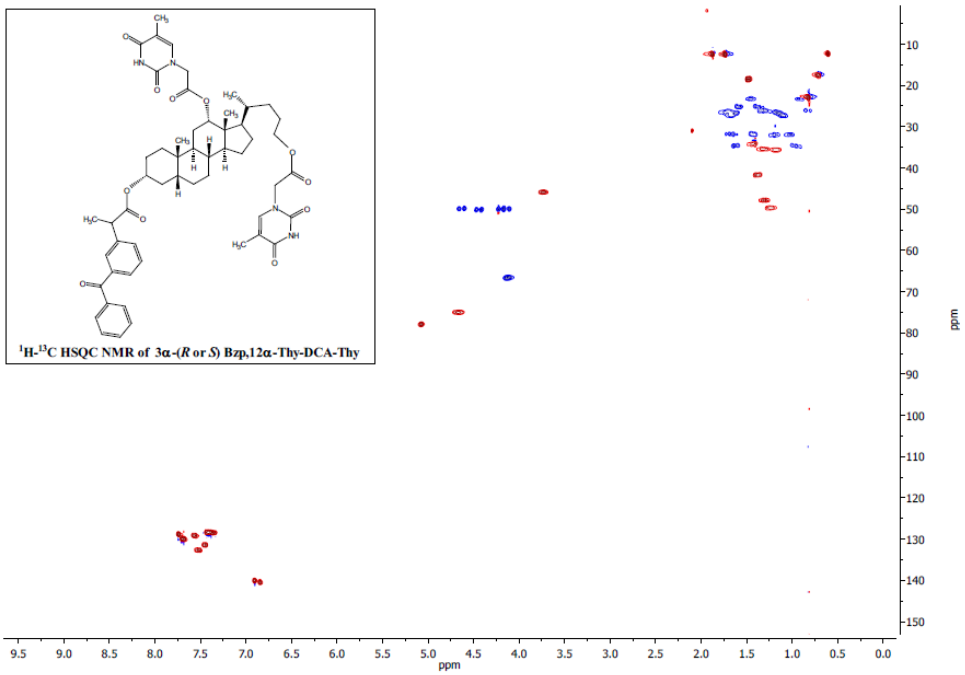

5.7.4.14. 3α-Pa-DCA-Thy

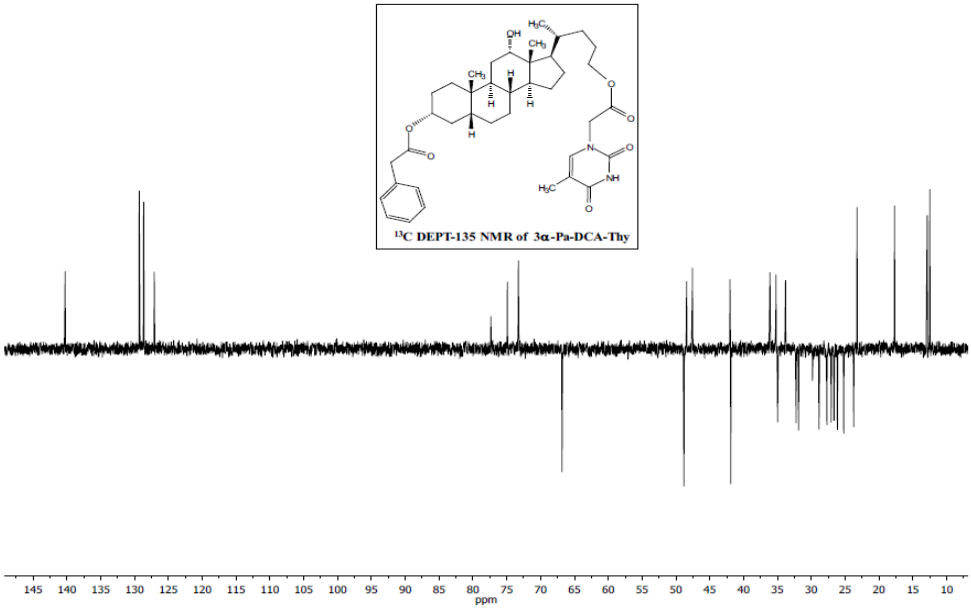

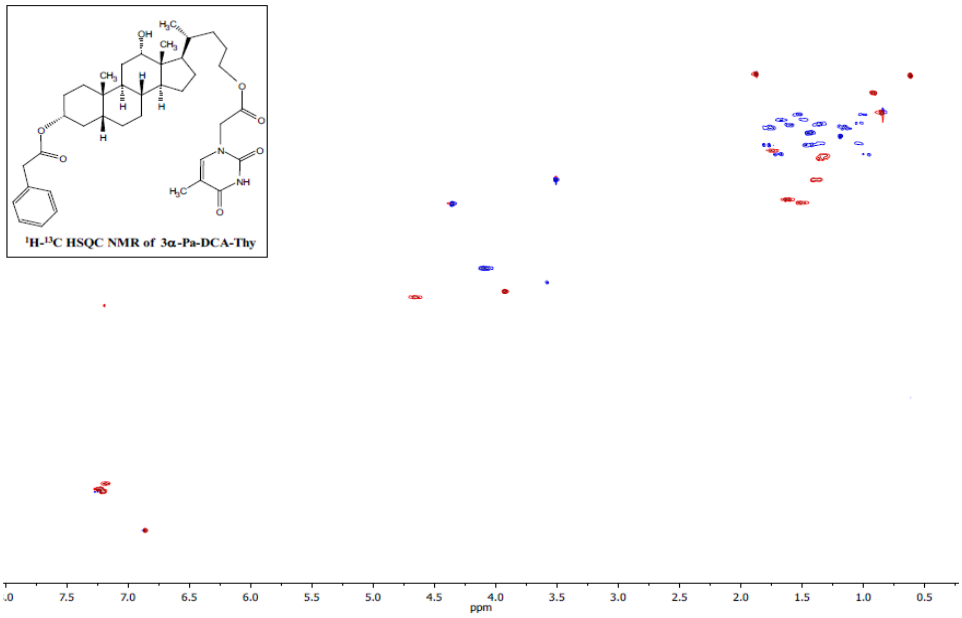

5.7.4.15. 3α-Pa,12α-Thy-DCA-Thy

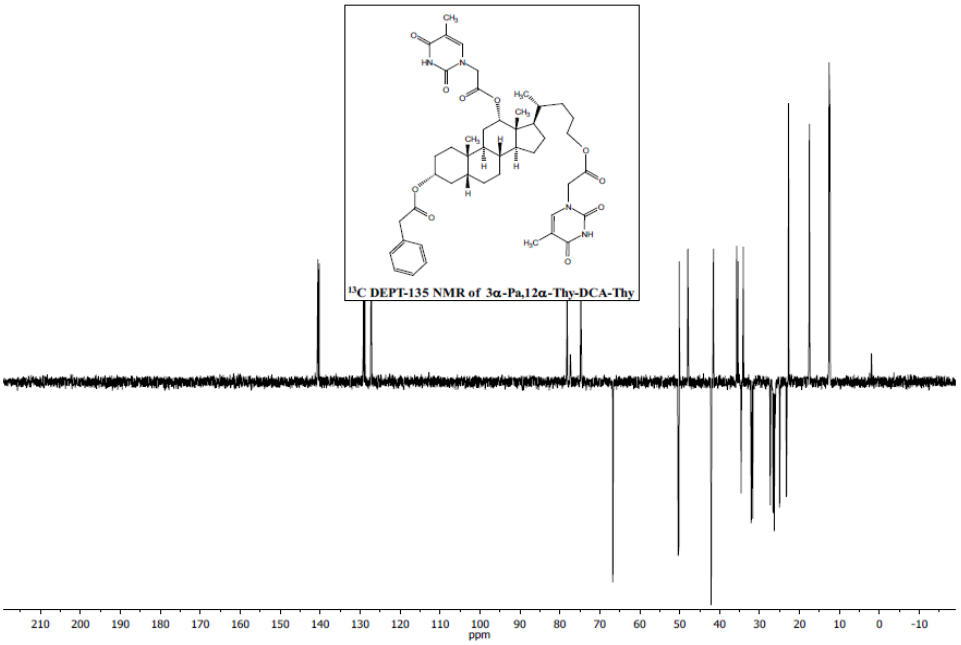

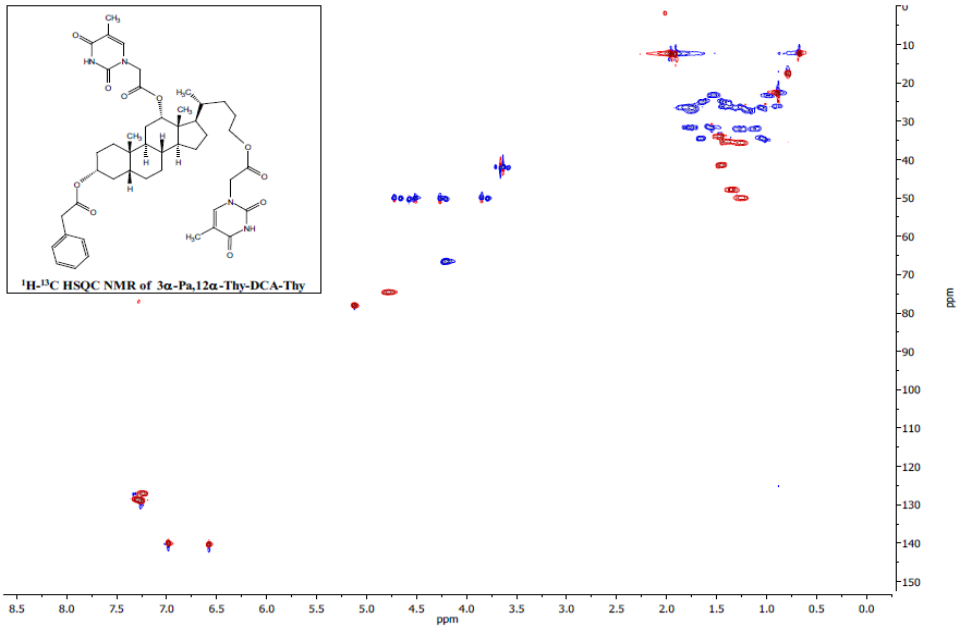

5.7.4.16. CDCAOH

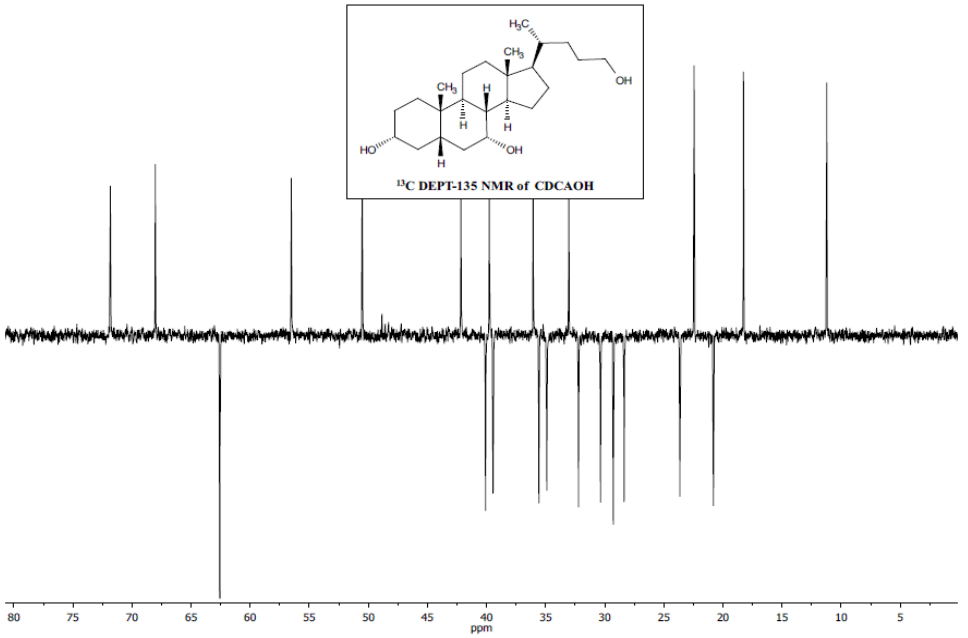

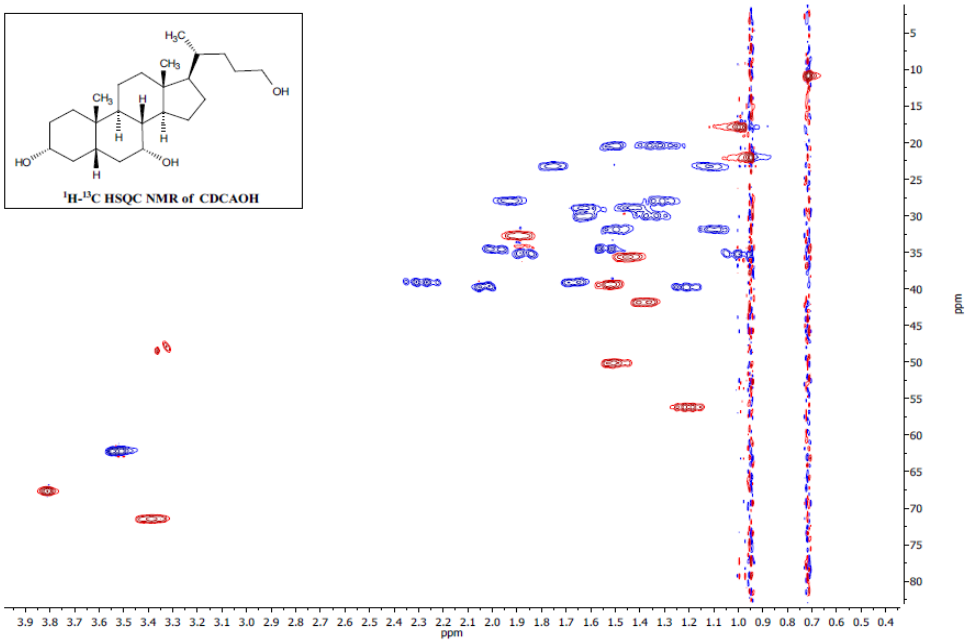

5.7.4.17. CDCA-Thy

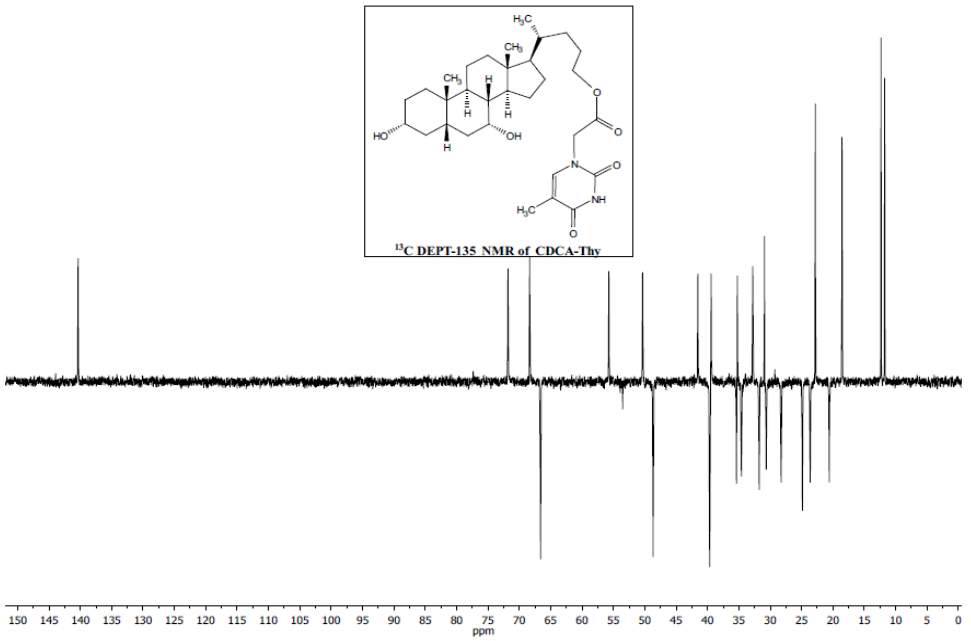

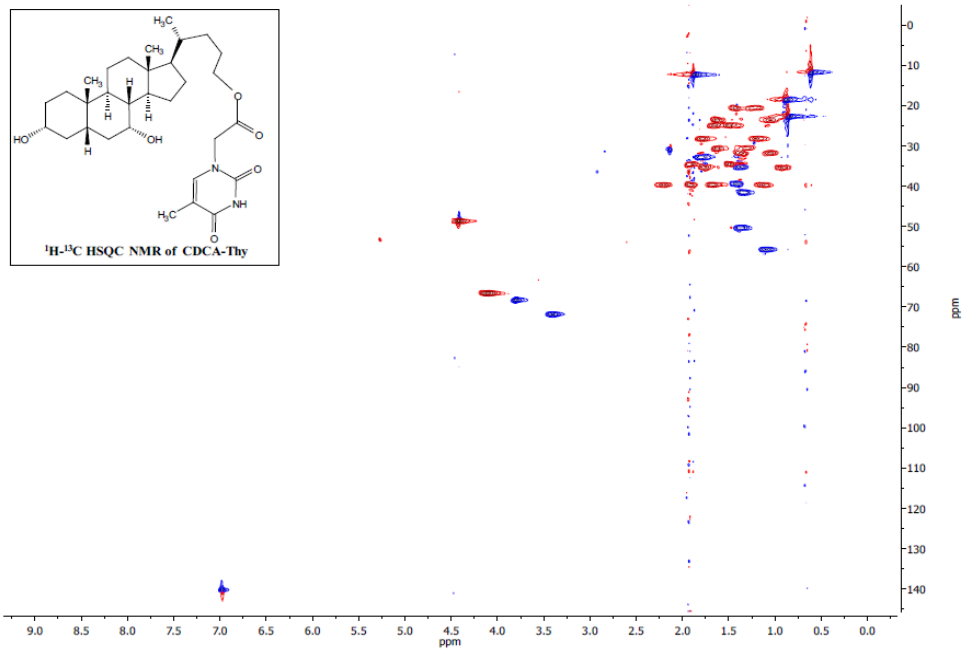

5.7.4.18. 3α-Bzp-CDCA-Thy

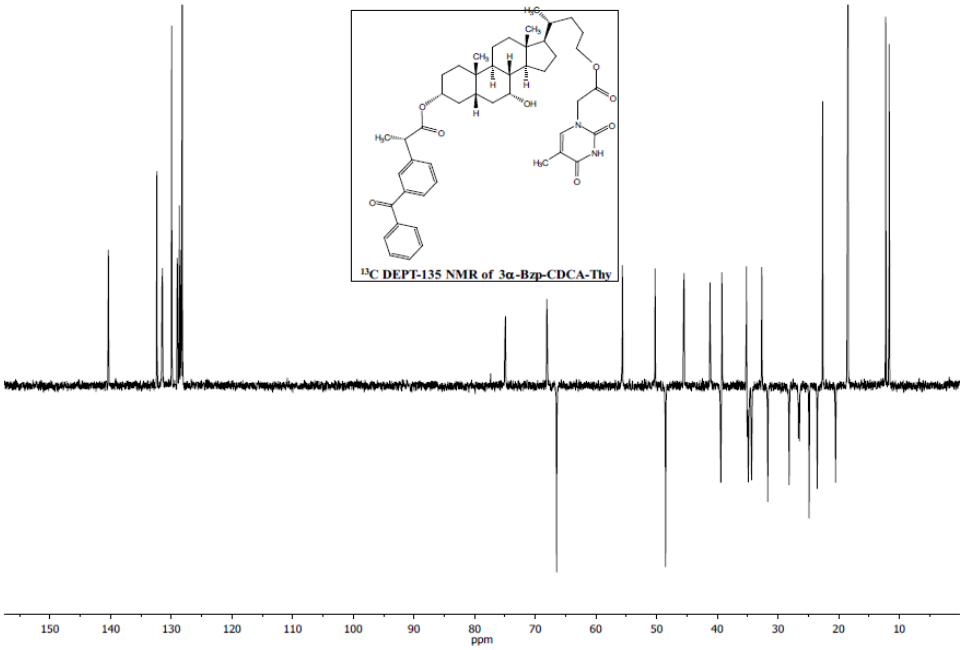

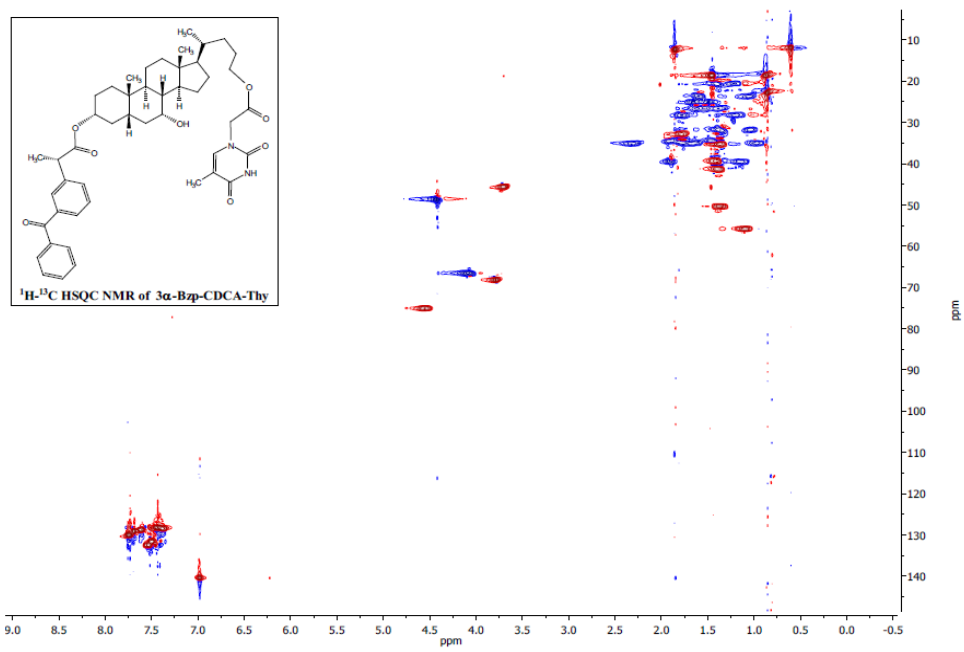

5.7.4.19. 3α-(*R* or *S*) Bzp,7α-Thy-CDCA-Thy

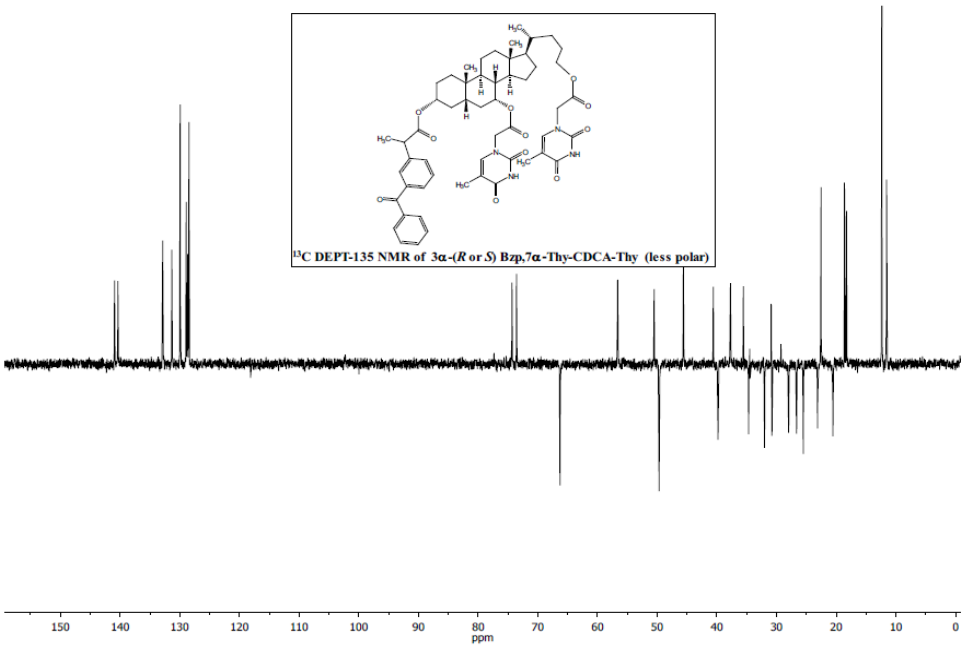

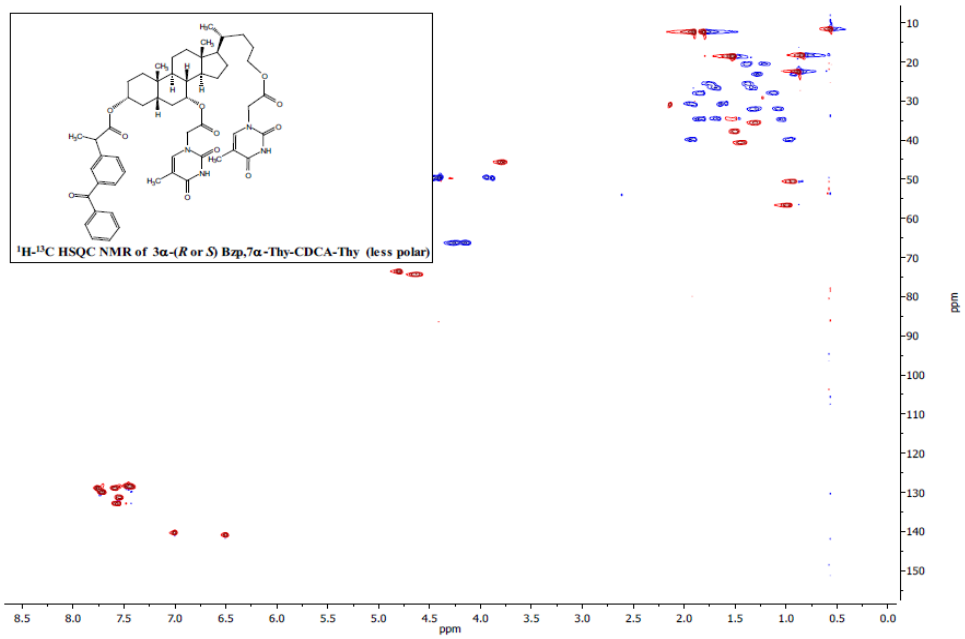

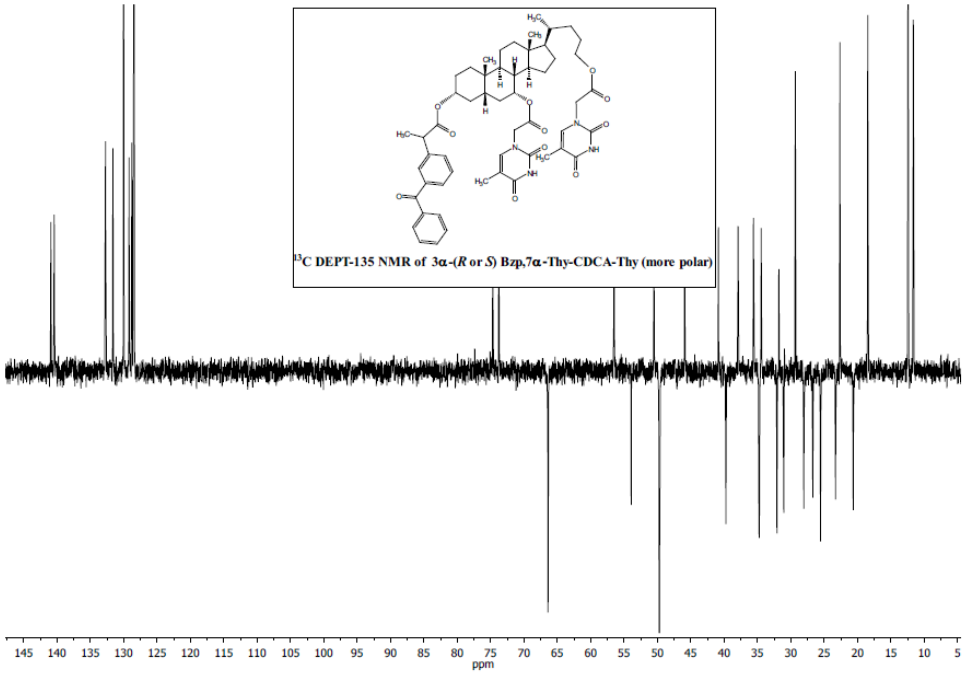
^{13}C DEPT-135 NMR of 3α-(*R* or *S*) Bzp,7α-Thy-CDCA-Thy (more polar)
ppm

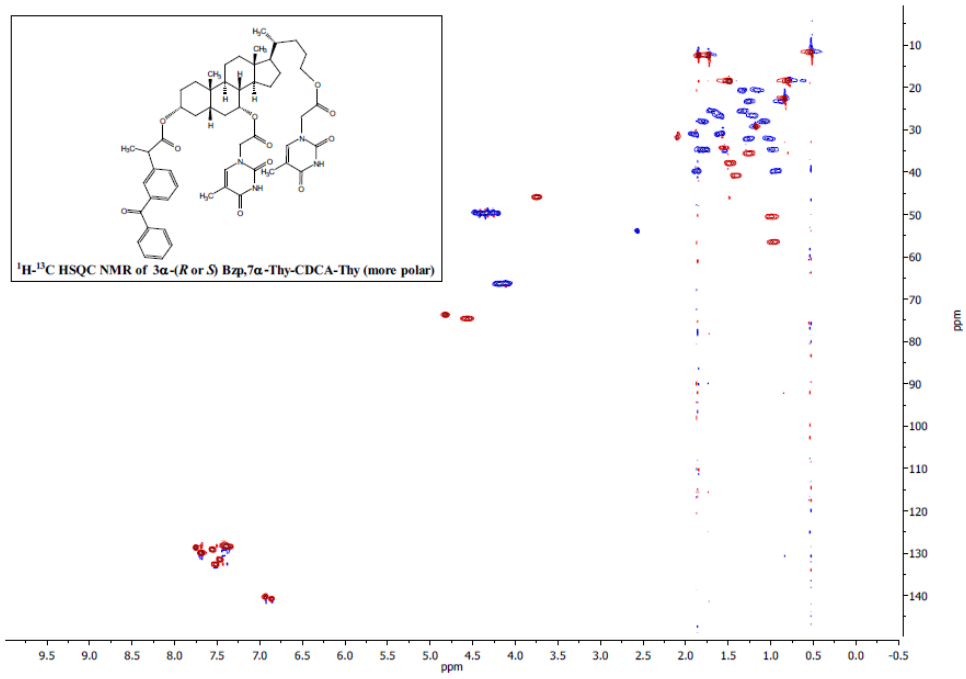
^{1}H-^{13}C HSQC NMR of 3α-(*R* or *S*) Bzp,7α-Thy-CDCA-Thy (more polar)
ppm
ppm

5.7.4.20. 3α-Bz-CDCA-Thy

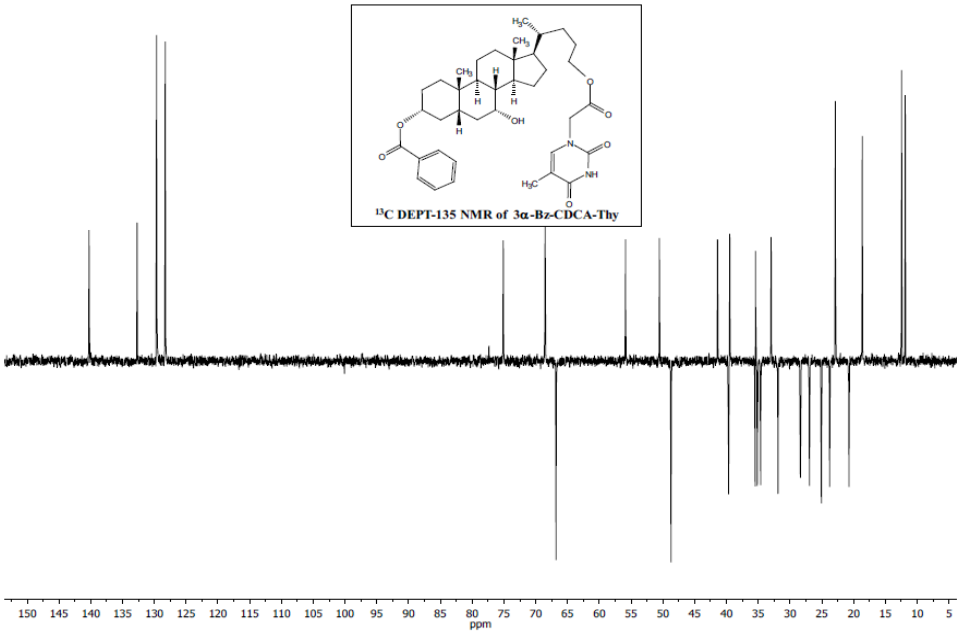

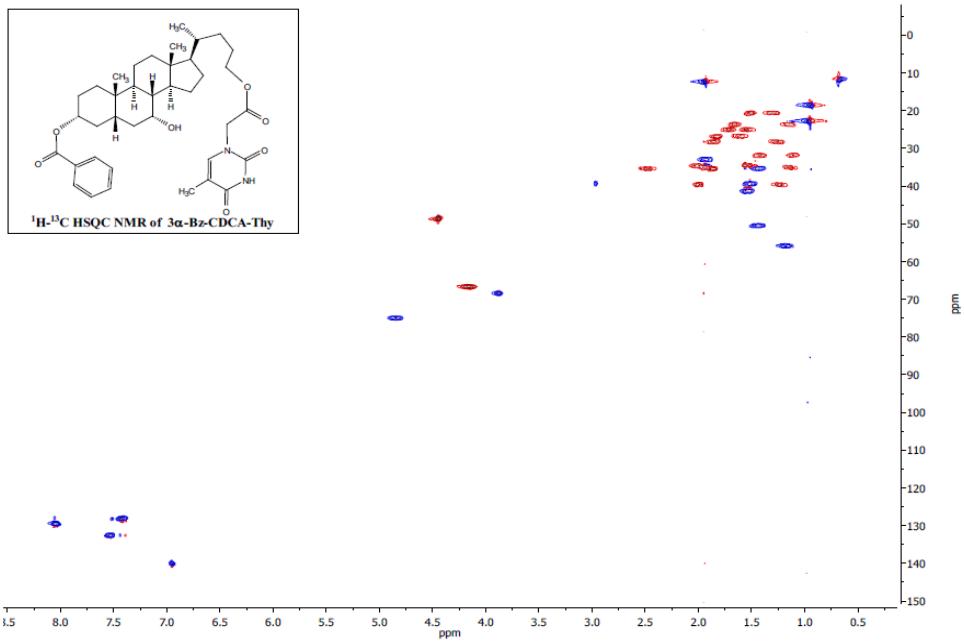

5.7.4.21. 3α-Bz,7α-Thy-CDCA-Thy

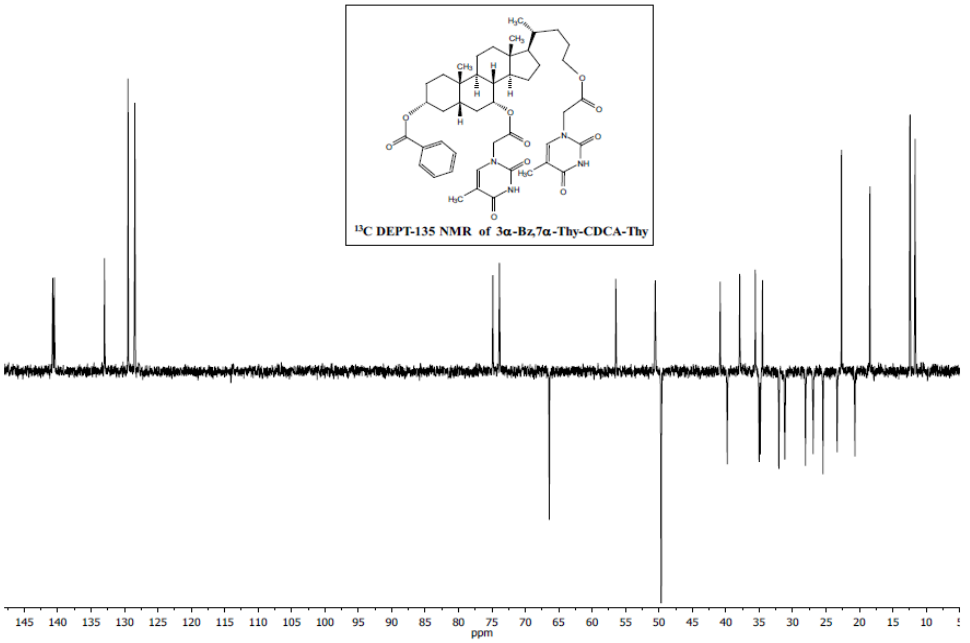

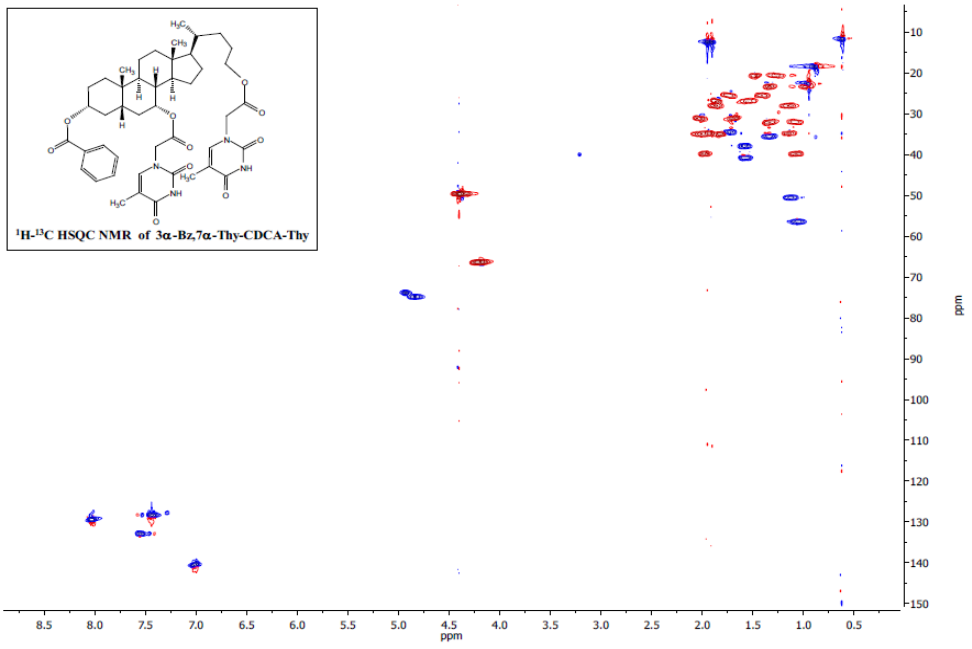

5.7.4.22. 3α-Thy-DCA-12α-Thy<O>Bzp

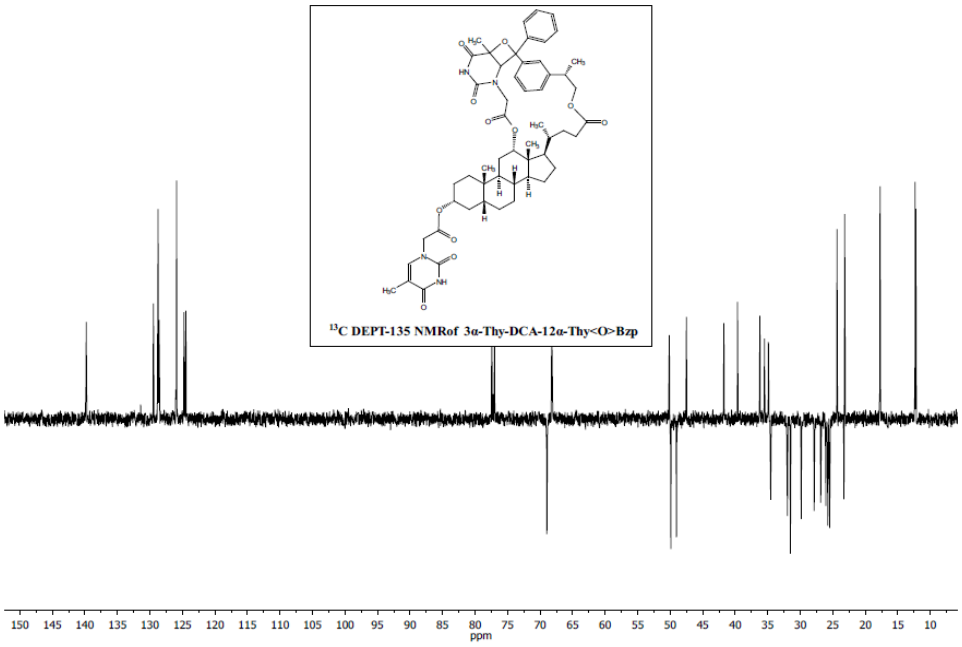

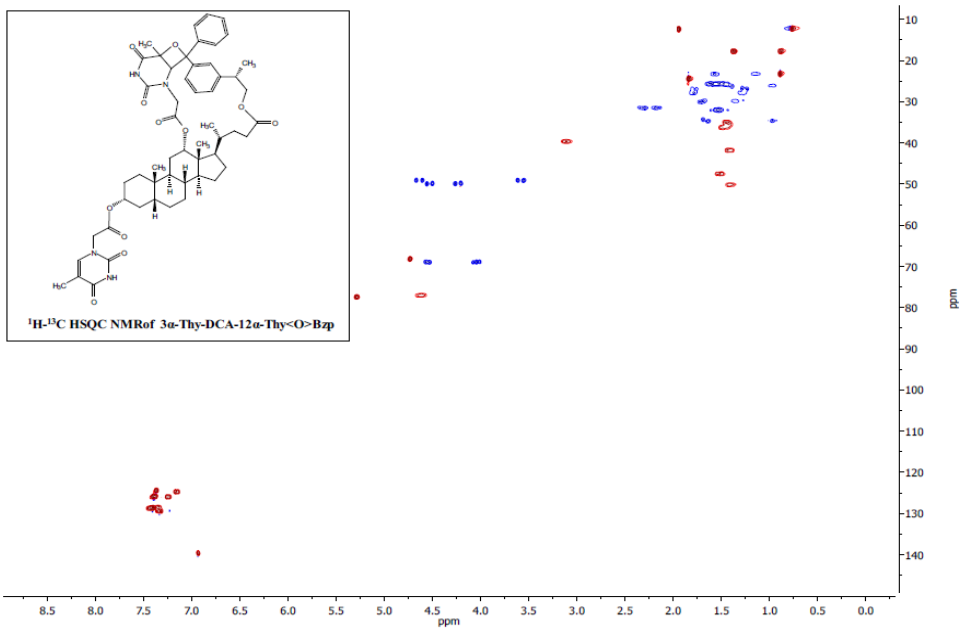

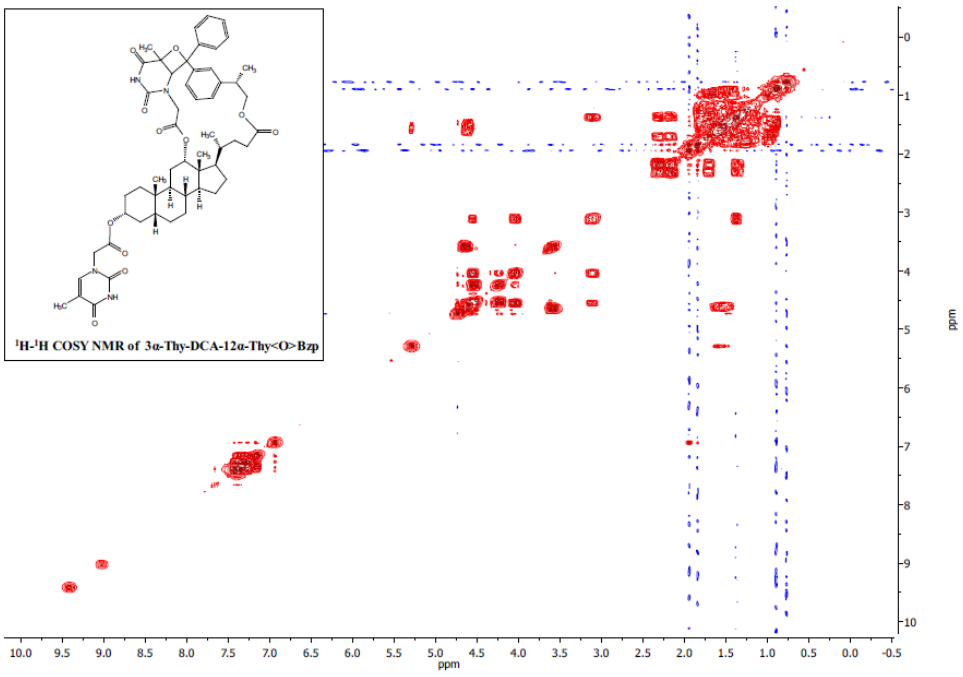
^{1}H-^{1}H COSY NMR of 3α-Thy-DCA-12α-Thy<O>Bzp
ppm

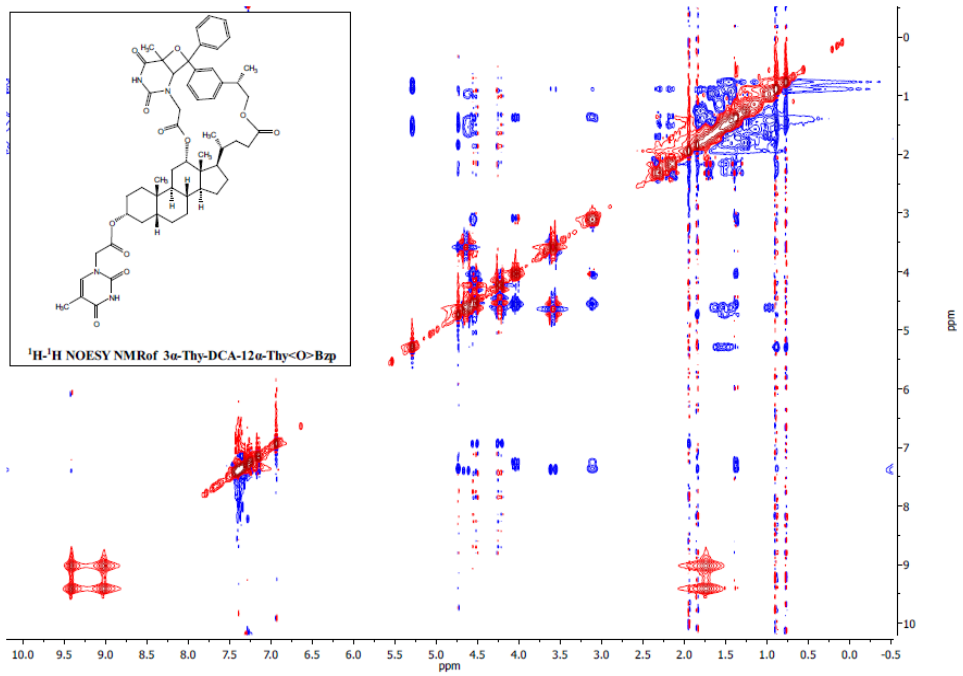
^{1}H-^{1}H NOESY NMRof 3α-Thy-DCA-12α-Thy<O>Bzp
ppm

5.7.4.23. 3α,12α-Thy<>Thy-DCA-Bn

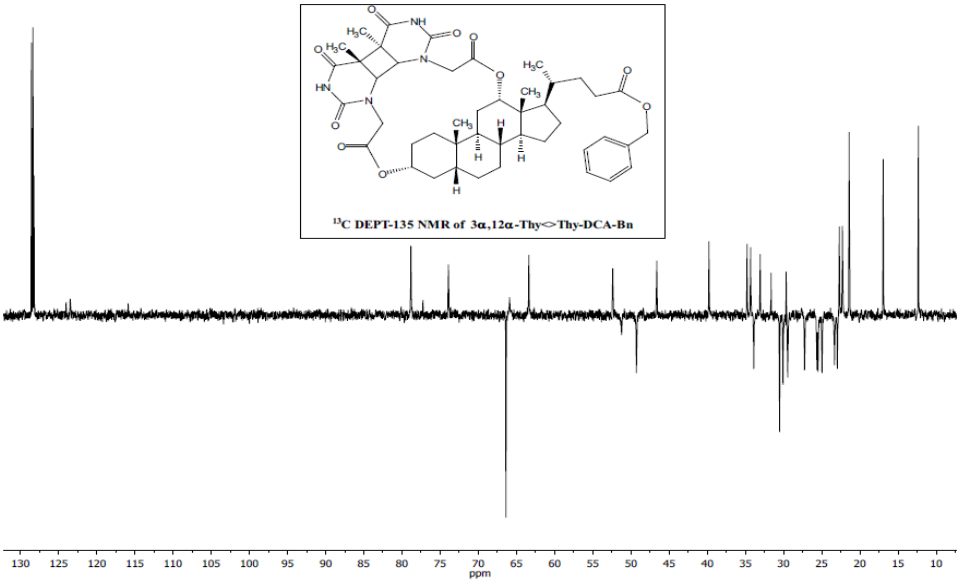

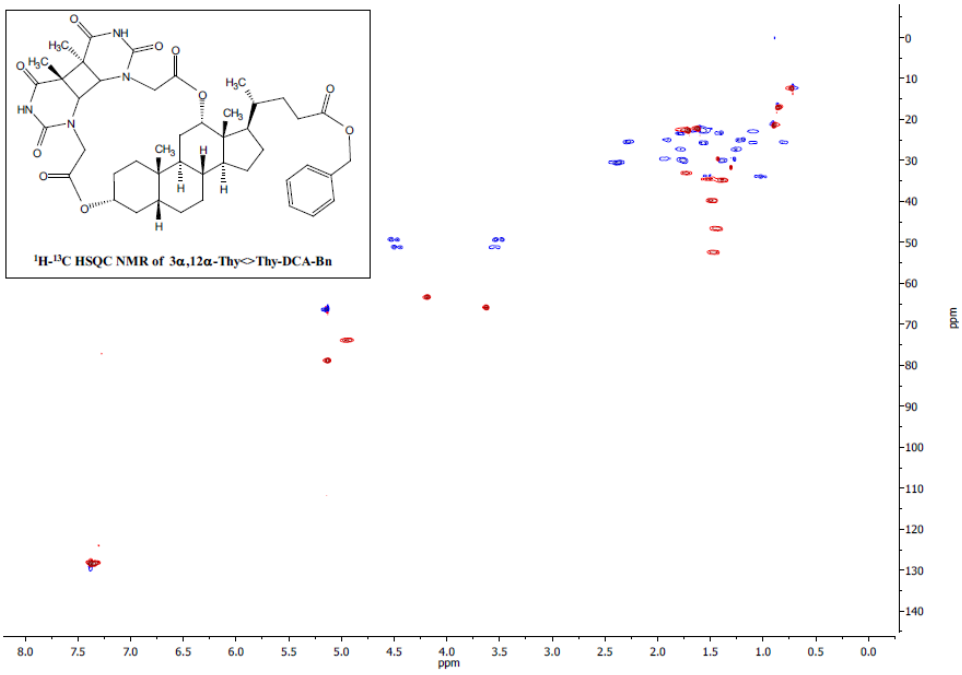

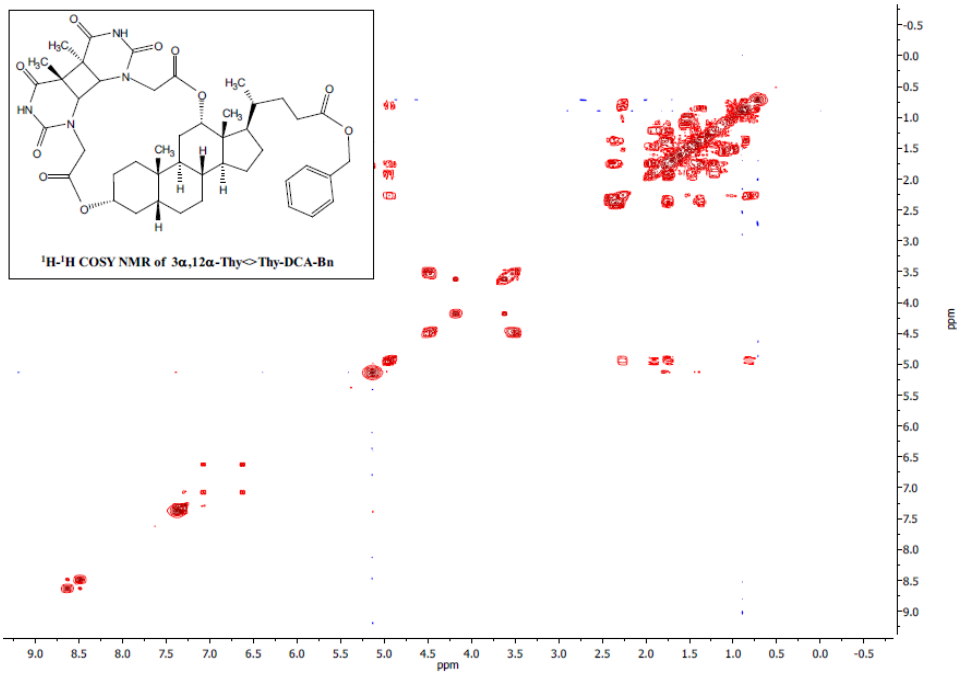
^{1}H-^{1}H COSY NMR of 3α,12α-Thy<>Thy-DCA-Bn
ppm
ppm

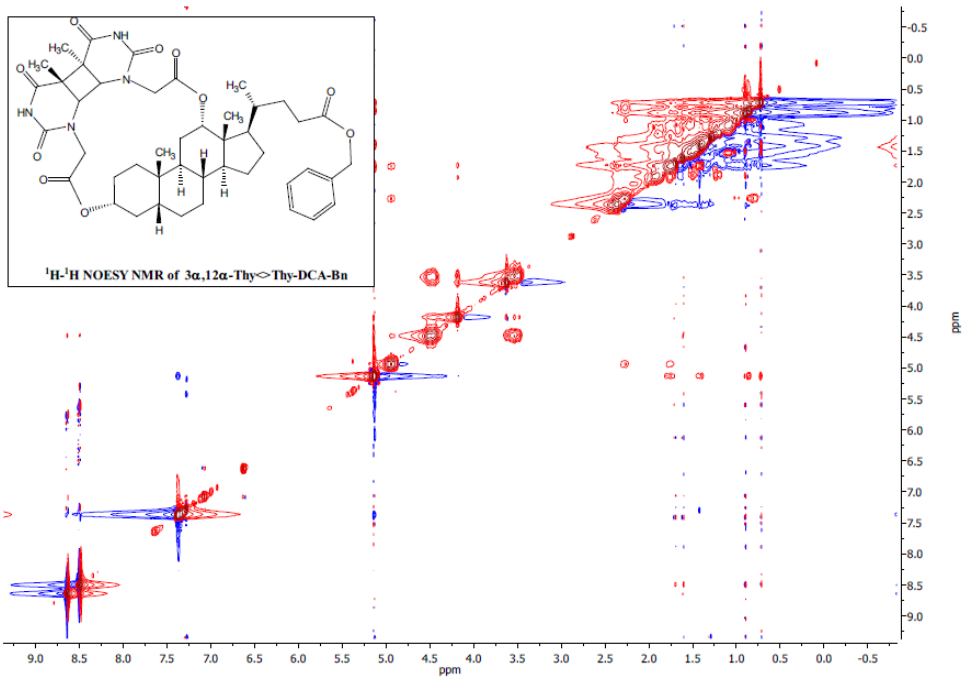
^{1}H-^{1}H NOESY NMR of 3α,12α-Thy<>Thy-DCA-Bn
ppm
ppm

5.7.4.24. 3α-Thy-CDCA-7α-Thy<O>Bzp

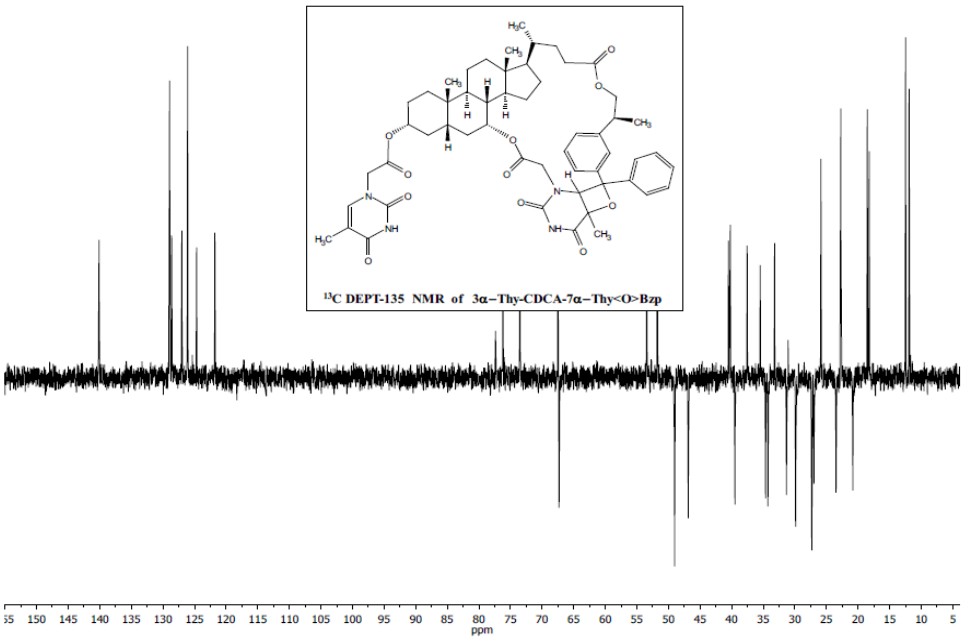

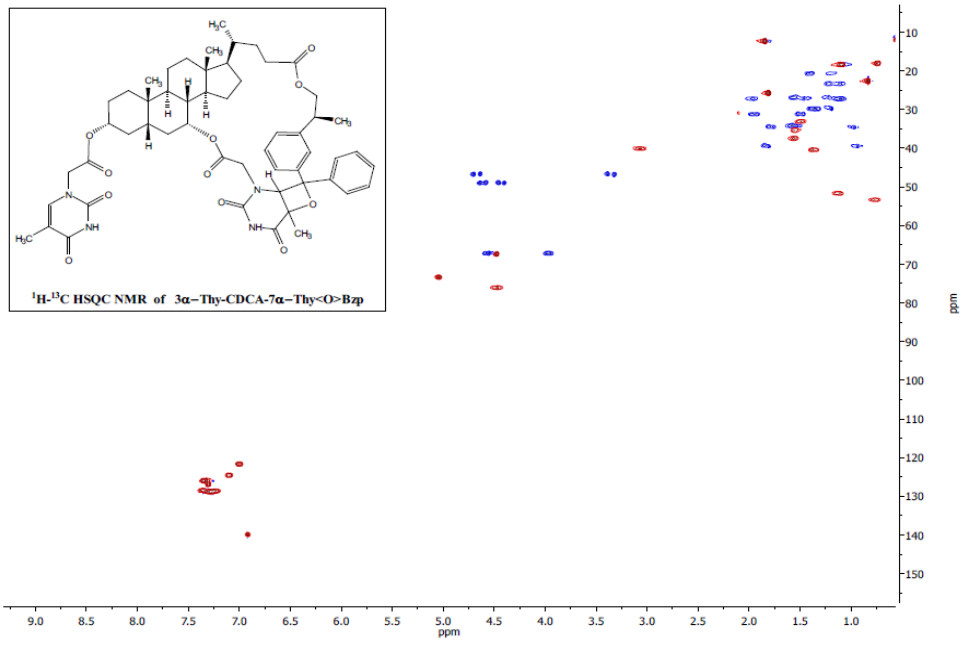

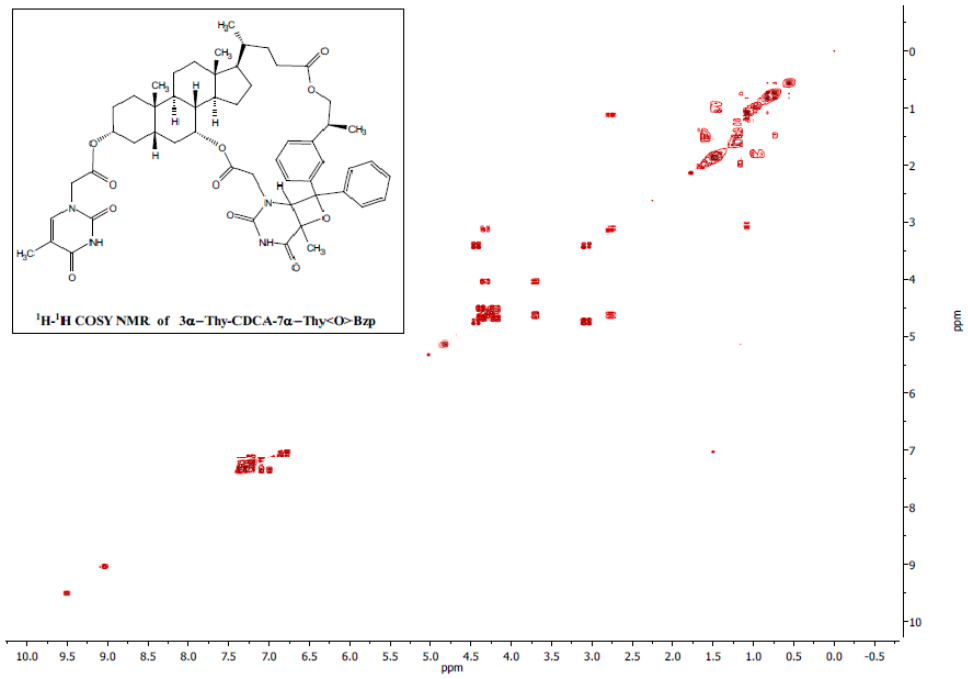
^{1}H-^{1}H COSY NMR of 3α−Thy-CDCA-7α−Thy<O>Bzp
ppm
ppm

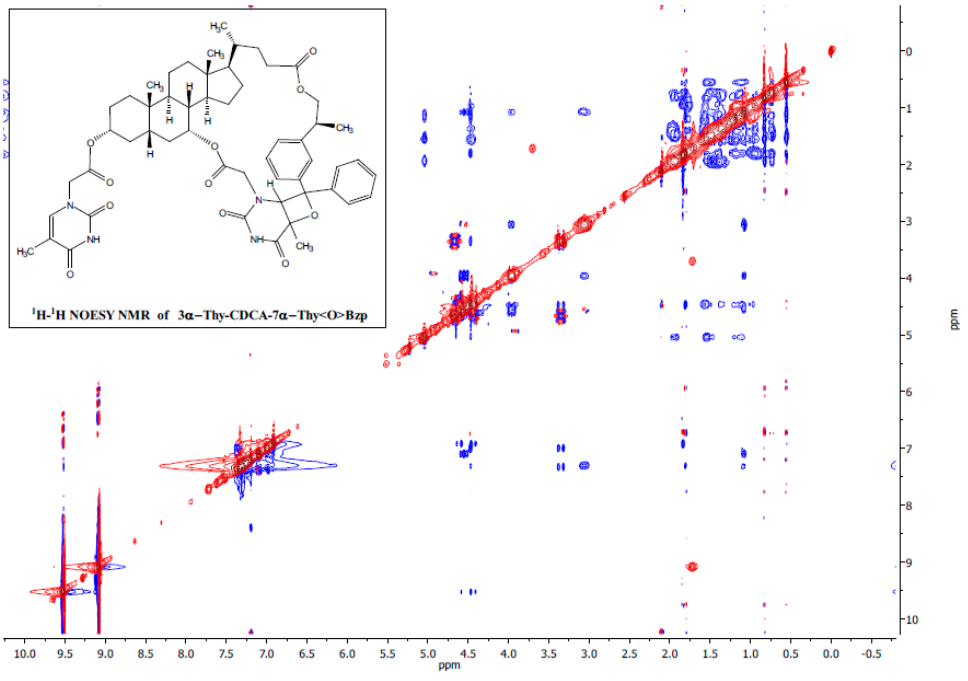
^{1}H-^{1}H NOESY NMR of 3α−Thy-CDCA-7α−Thy<O>Bzp
ppm
ppm

5.7.4.25. 3α,7α-Thy<>Thy-CDCA-Bn

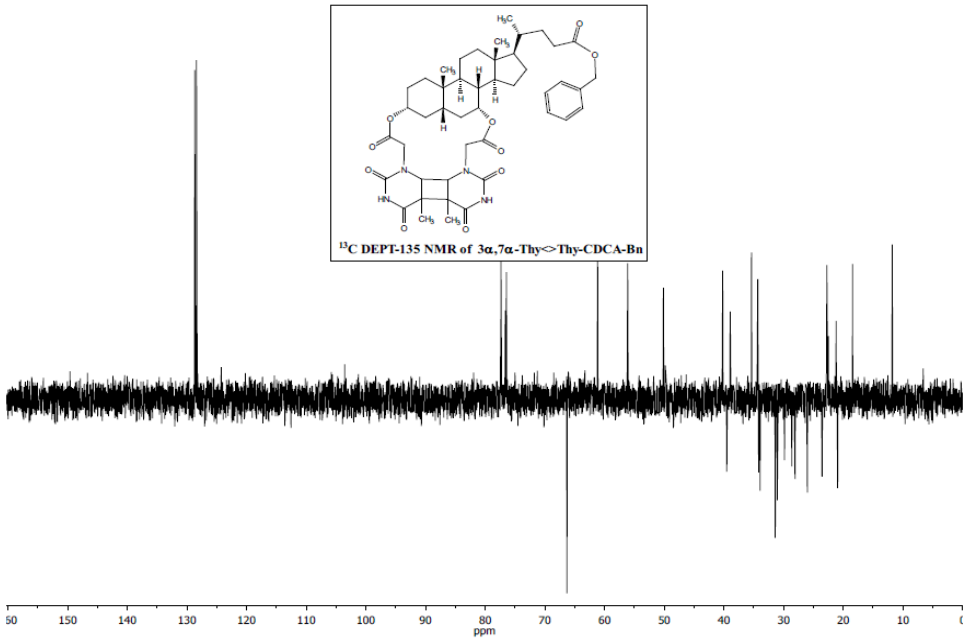

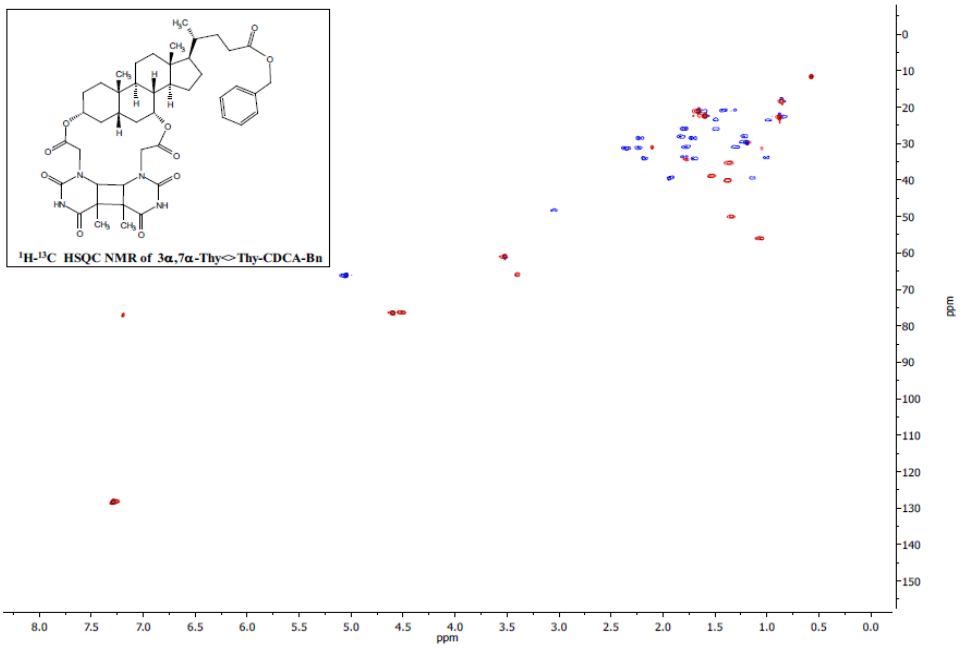

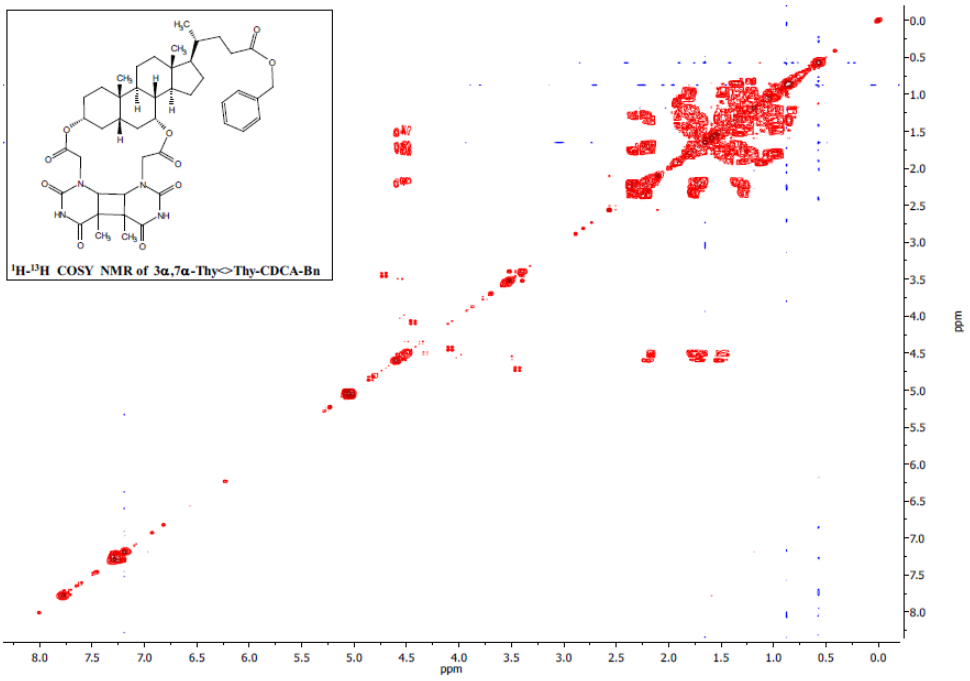
^{1}H-^{13}H COSY NMR of 3α,7α-Thy<>Thy-CDCA-Bn
ppm
ppm

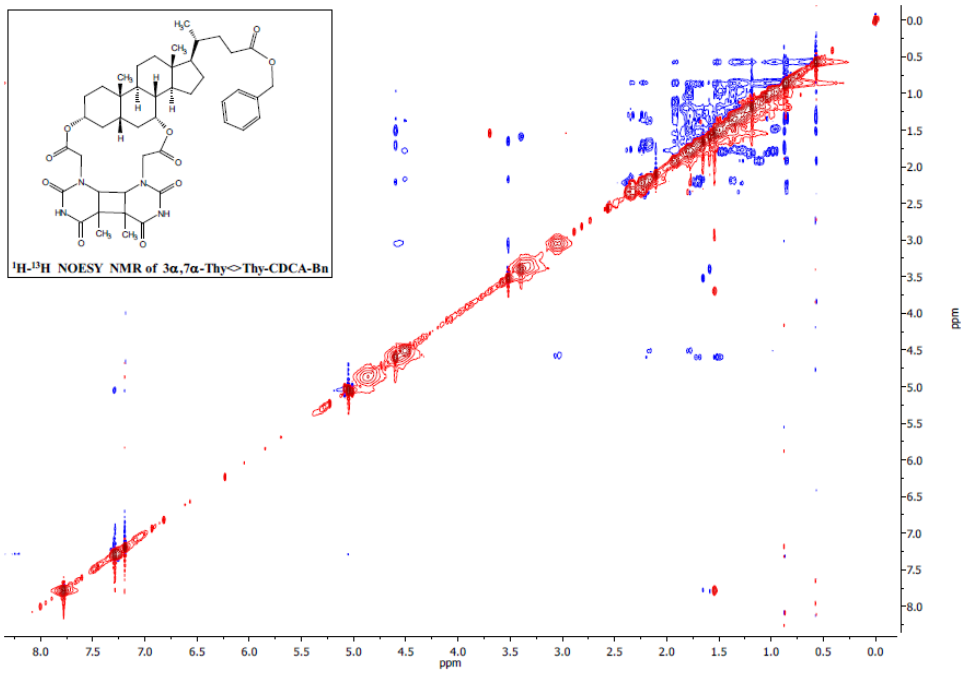
^{1}H-^{13}H NOESY NMR of 3α,7α-Thy<>Thy-CDCA-Bn
ppm
ppm

5.7.4.26. 3α-Bzp<O>12α-Thy -DCA-Thy

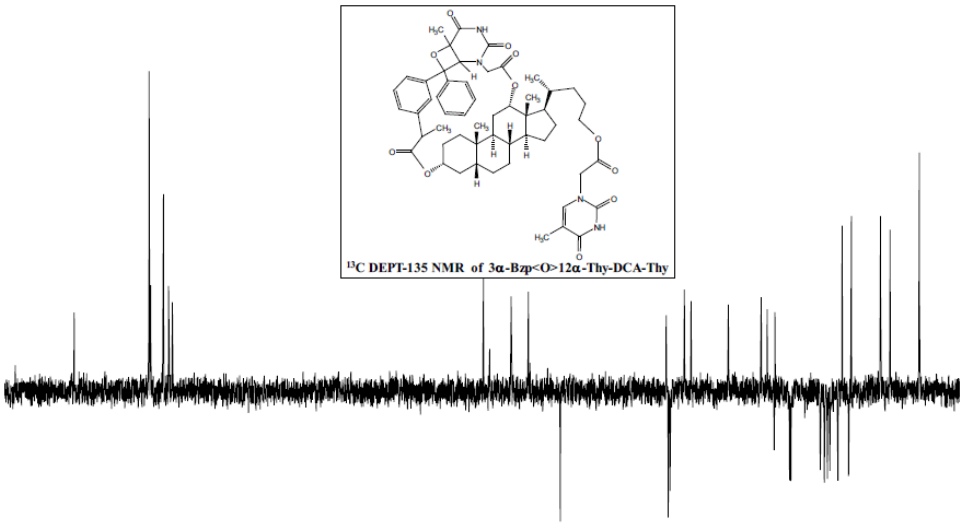

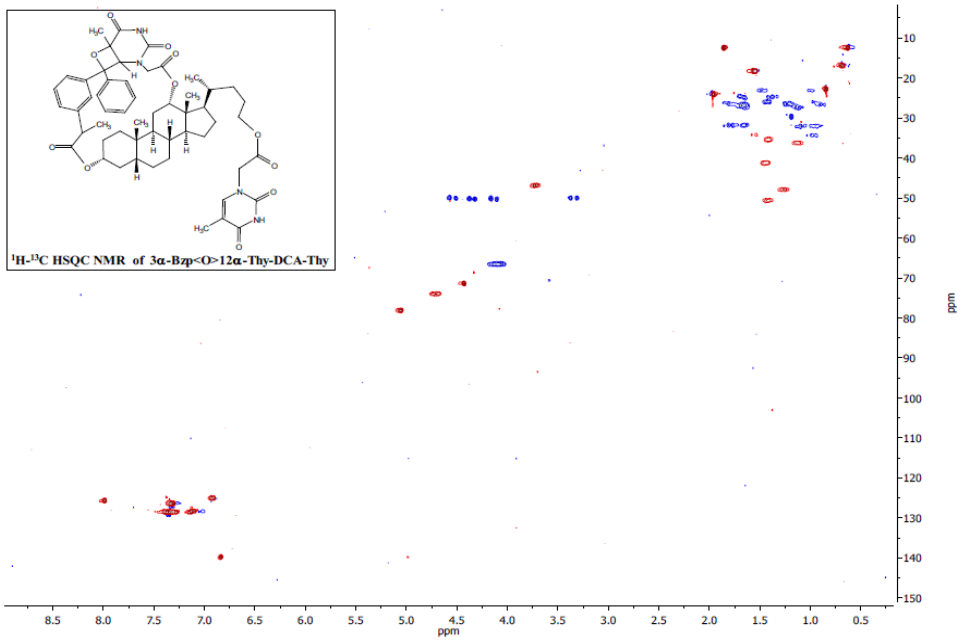

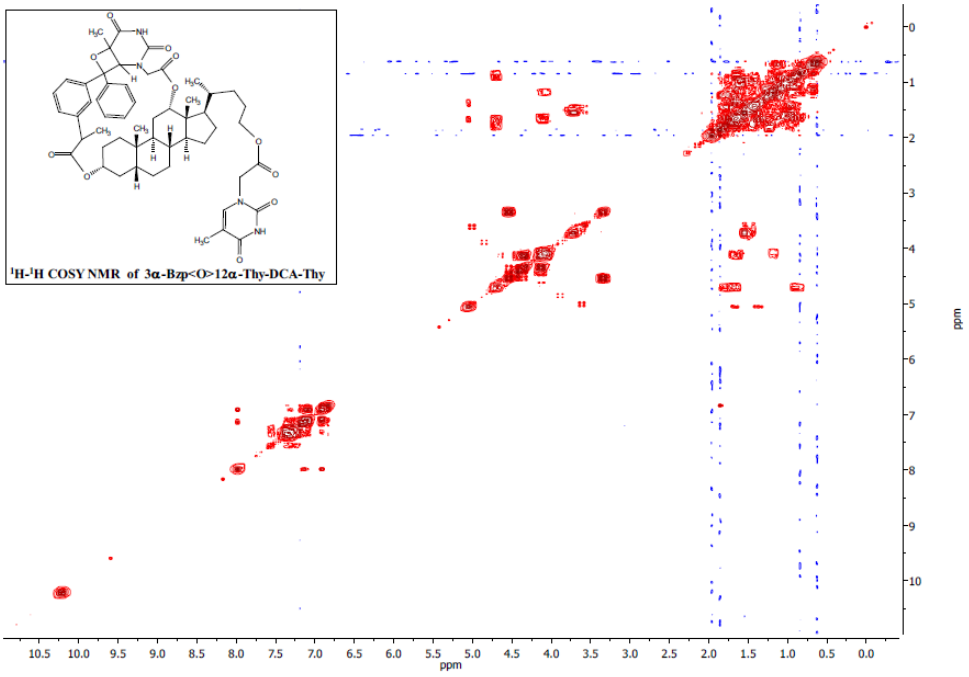
^{1}H-^{1}H COSY NMR of 3α-Bzp<O>12α-Thy-DCA-Thy
ppm
ppm

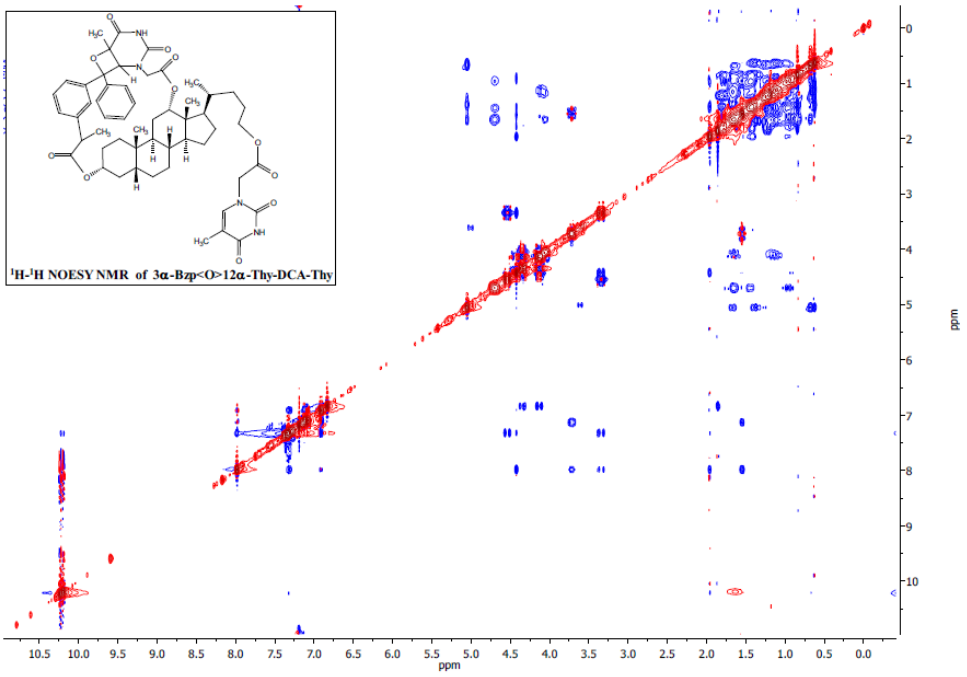
^{1}H-^{1}H NOESY NMR of 3α-Bzp<O>12α-Thy-DCA-Thy
ppm
ppm

5.7.4.27. 3α-Pa-DCA- 12α-Thy <>Thy

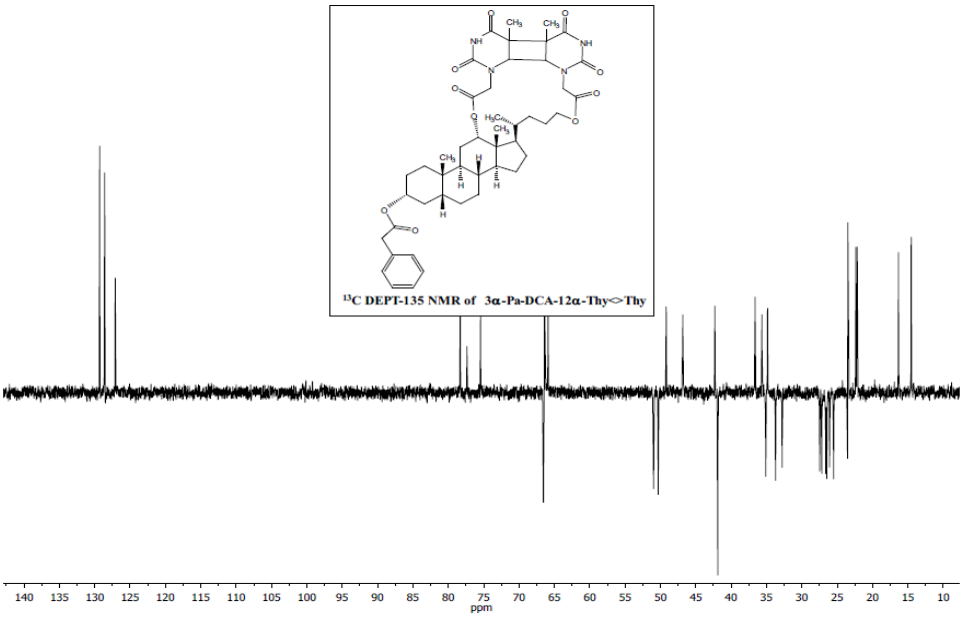

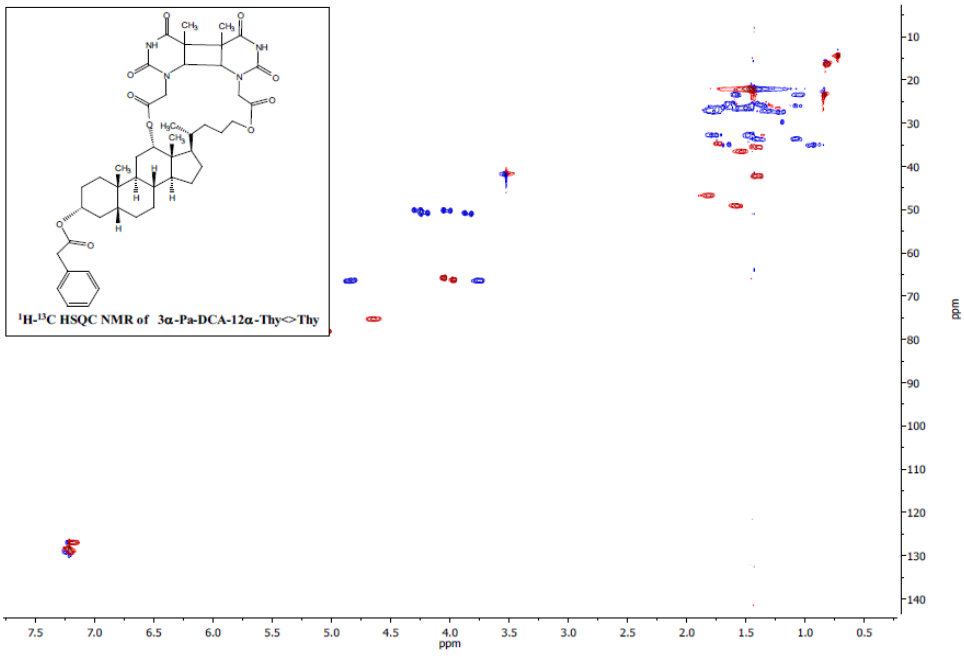

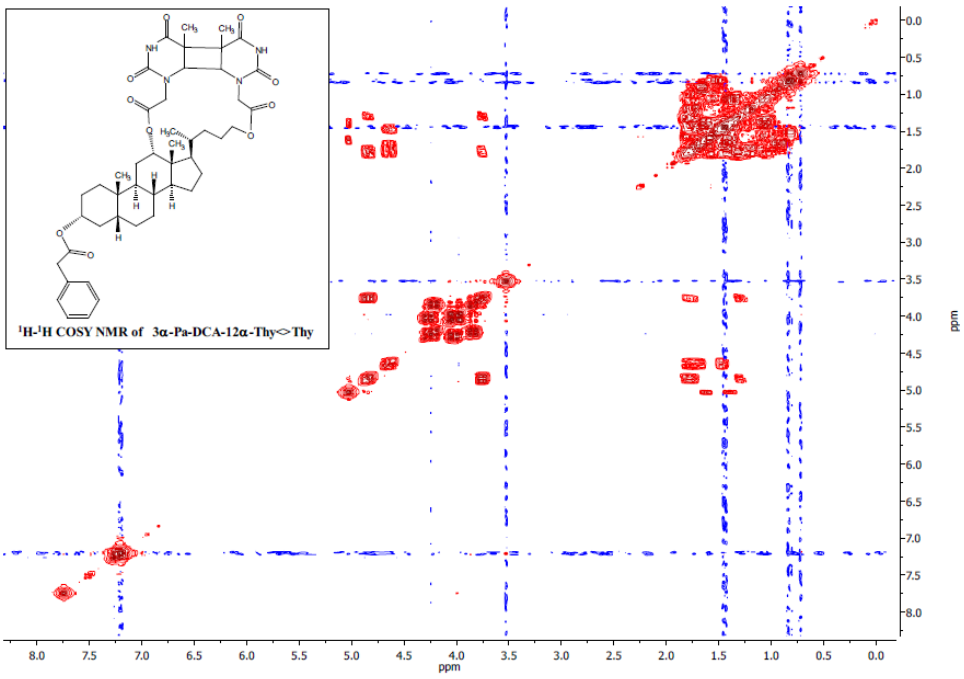
^{1}H-^{1}H COSY NMR of 3α-Pa-DCA-12α-Thy<>Thy
ppm
ppm

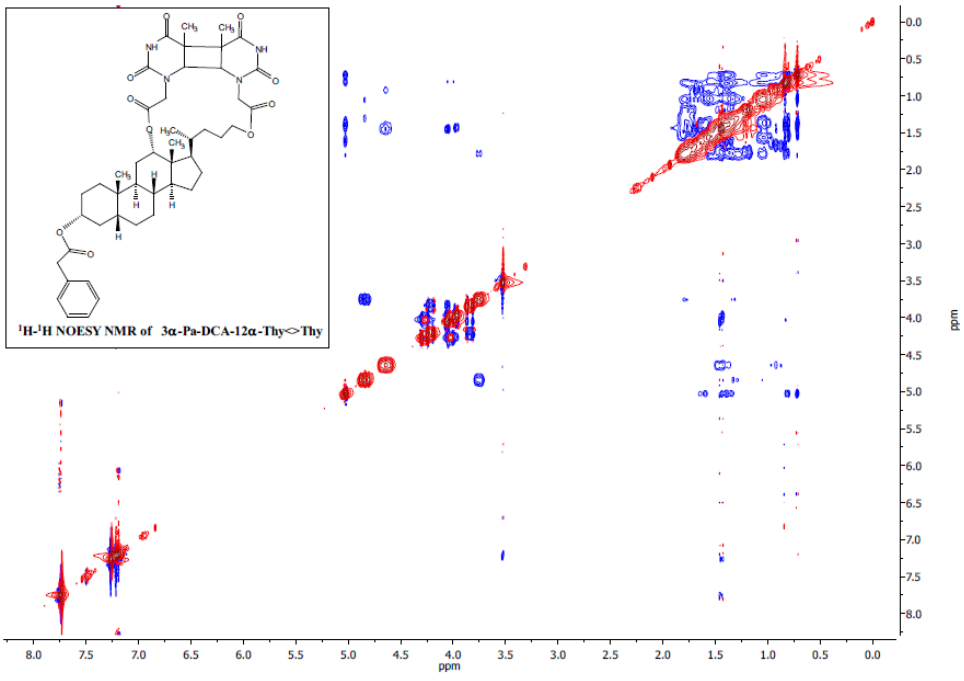
^{1}H-^{1}H NOESY NMR of 3α-Pa-DCA-12α-Thy<>Thy
ppm
ppm

5.7.4.28. 3α-Bzp<O>7α-Thy-CDCA-Thy

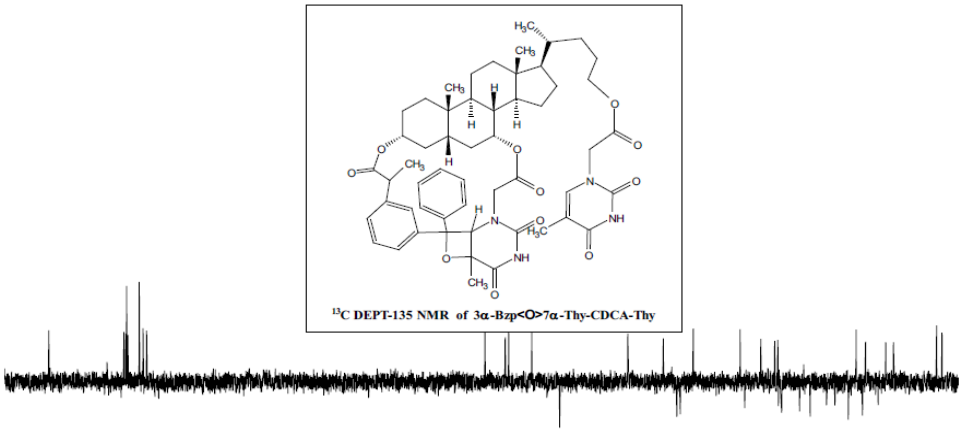

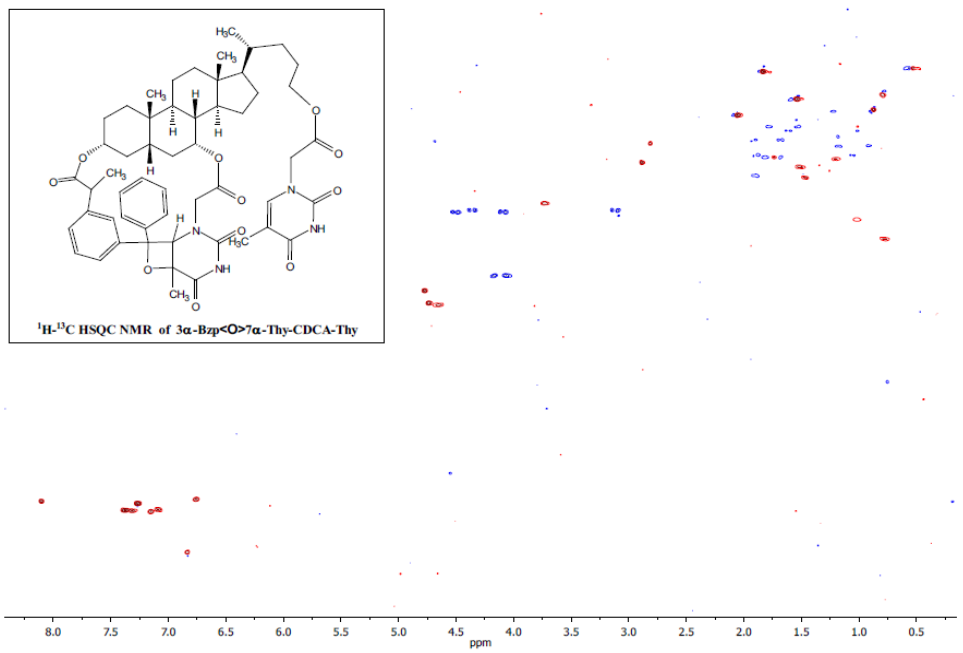

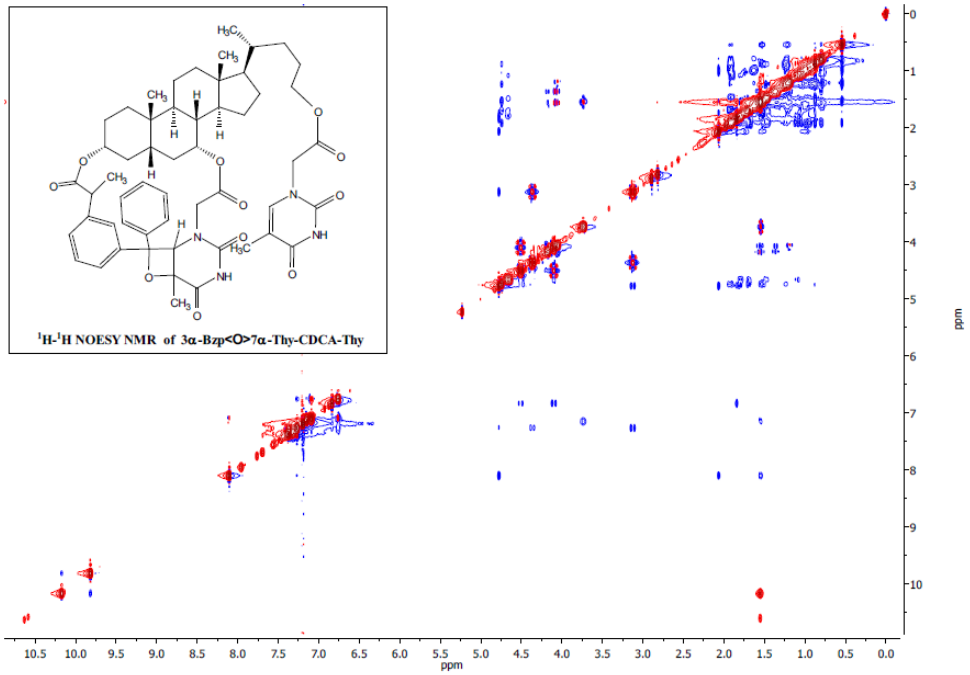
^{1}H-^{1}H NOESY NMR of 3α-Bzp<O>7α-Thy-CDCA-Thy
ppm
ppm

5.7.4.29. 3α-Bz-CDCA- 7α-Thy <>Thy

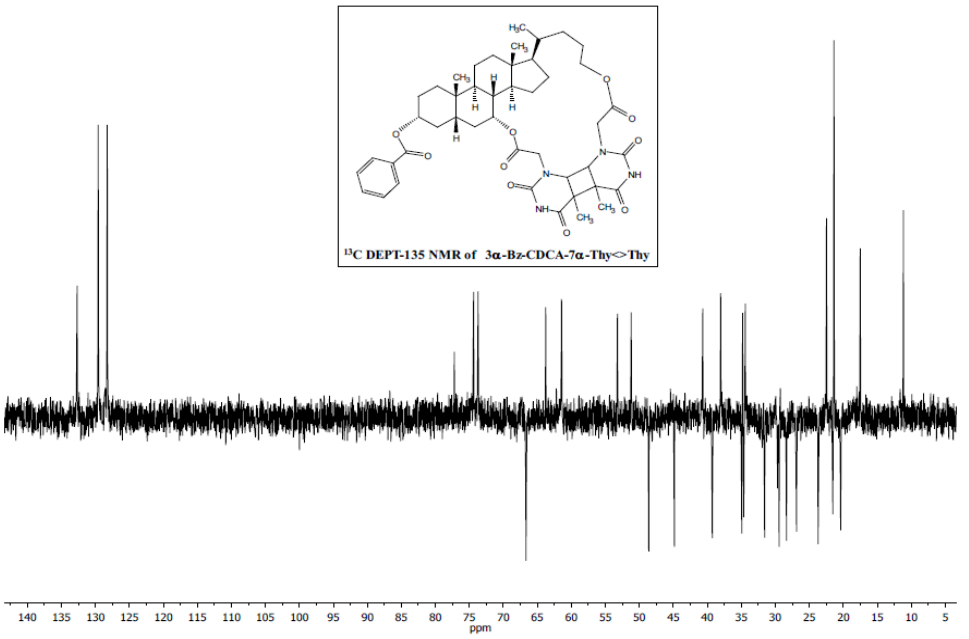

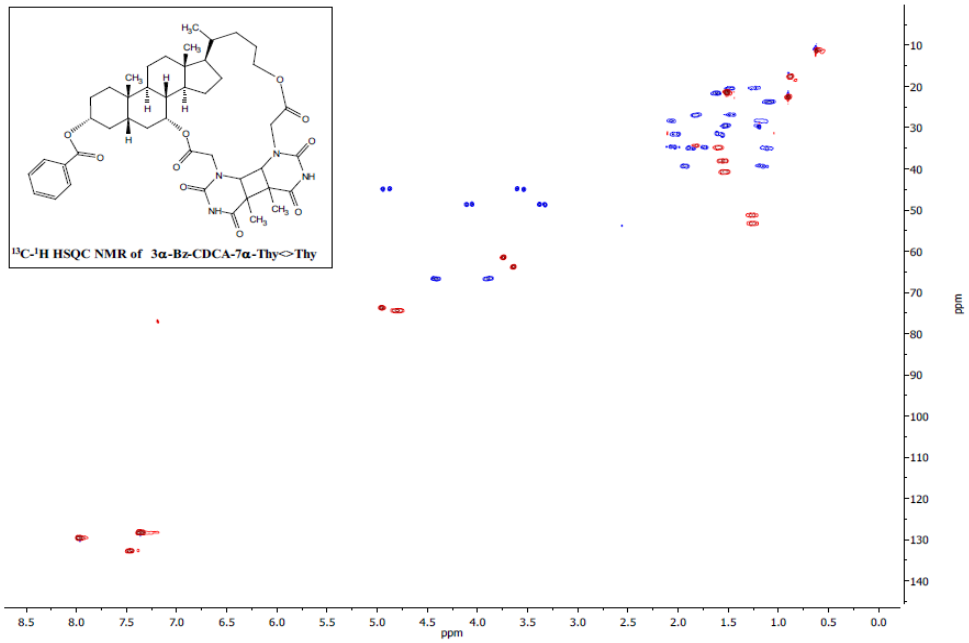

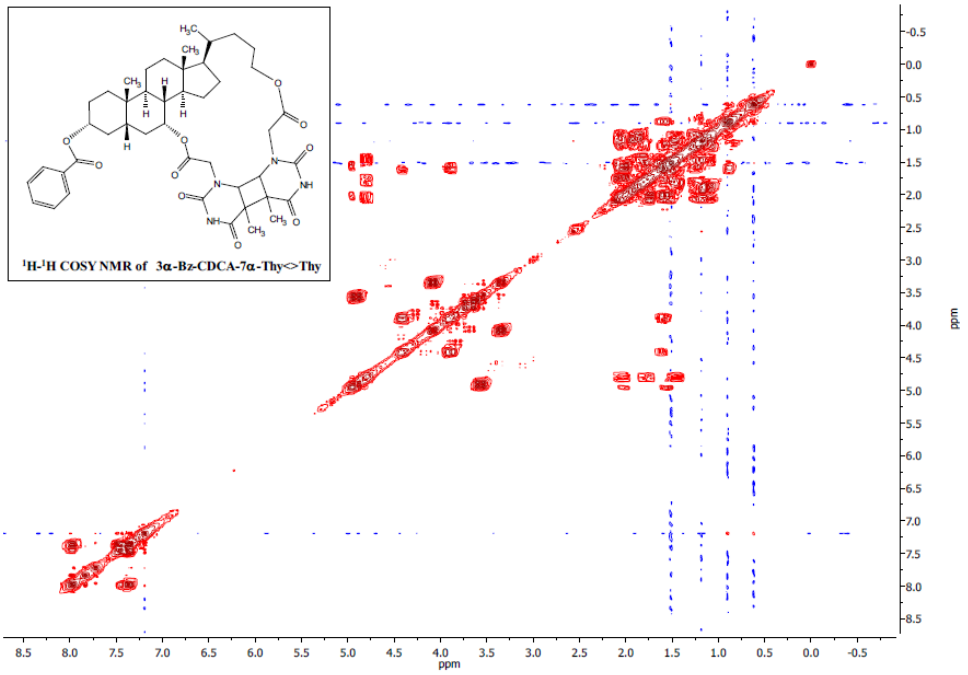
^{1}H-^{1}H COSY NMR of 3α-Bz-CDCA-7α-Thy<>Thy
ppm
ppm

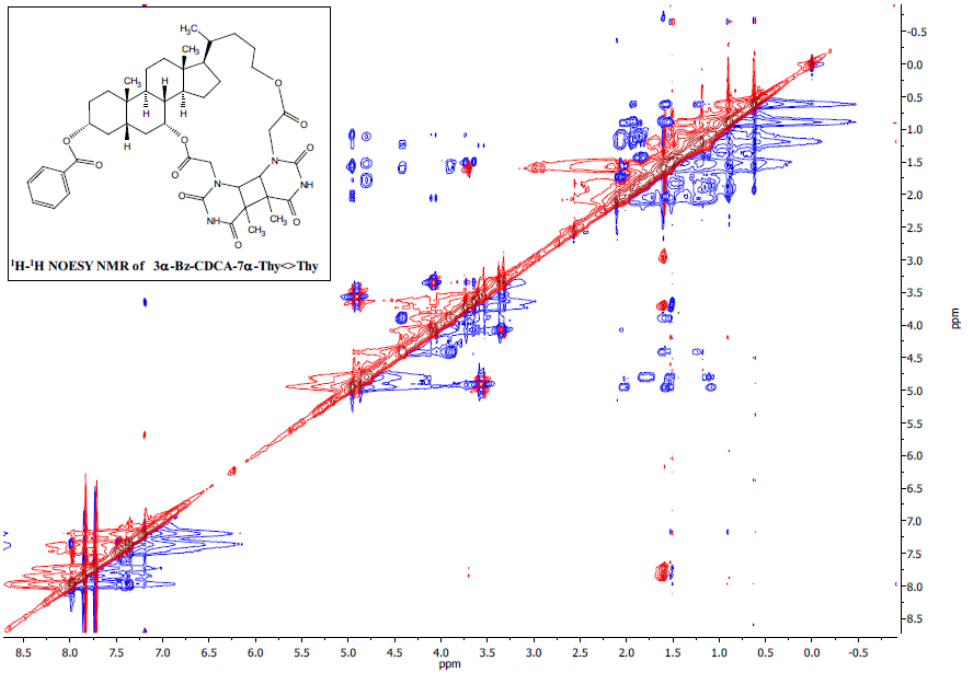
^{1}H-^{1}H NOESY NMR of 3α-Bz-CDCA-7α-Thy<>Thy
ppm
ppm

Chapter 6: Generation of Thymine Triplet by Through-Bond Sensitization from Benzophenone*

6.1. Introduction

The ultraviolet (UV) fraction of solar radiation incident on the Earth surface has been demonstrated to be harmful for living organisms, since it can cause photochemical alterations in the DNA structure.[138,158,159] Specifically, UVB is absorbed by the nucleobases themselves, causing direct photoreactions between adjacent Thy and/or Cyt units. This gives mainly rise to CPDs, which have been reported among the most mutagenic lesions.[139,140] Specifically, formation of CPDs (Thy<>Thy, Thy<>Cyt or Cyt<>Cyt) starts with the absorption of UVB light by one pyrimidine followed by a [2+2] photochemical cycloaddition between the C5-C6 double bonds of the excited Thy or Cyt with another pyrimidine in its ground state, leading to the final photolesion.

*Reproduced in part from: P. Miro, M. L. Marin and M. A. Miranda, *Chem. Eur. J.*, 2016, under revision, with permission from ChemPubSoc Europe

Fortunately, years of evolution are responsible for the intrinsic photostability properties of the nucleobases, since they exhibit an extremely short-lived singlet excited state and a very low ISC quantum yield.[160,161]

Although the UVA fraction of solar light is not efficiently absorbed by the nucleobases, UVA-absorbing endogenous or exogenous photosensitizers can mediate additional photochemical disorders. Among them, Bzp and drugs containing the Bzp chromophore,[48] such as the non-steroidal antiinflammatory drug (*S*)-ketoprofen (KP), have been widely reported as DNA photosensitizers.[131,142,162]

The KP-photosensitized generation of CPDs between two Thy nucleobases is assumed to occur by triplet-triplet energy transfer (TTET) from KP (E_T *ca.* 69 kcal/mol)[22] to Thy (E_T *ca.* 74 kcal/mol),[48] followed by [2+2] cycloaddition. Although TTET is a slightly disfavored process in solution (*ca.* 5 kcal/mol uphill), it is still feasible at room temperature due to the reasonable population of the upper vibrational states.[144] Furthermore, the unambiguous detection of Cyt<>Cyt in Bzp-photosensitized DNA has recently been reported, despite the high triplet state energy of Cyt (E_T *ca.* 77 kcal/mol).[163]

A mechanistic explanation for the interaction between ^{3}Bzp* and Thy is outlined in Scheme 1. Thus, reaction between ^{3}Bzp* and Thy could give rise directly to ^{3}Thy* by TTET or to the exciplex ^{3}[BP····Thy]* (discussed in detail in Chapter 5 of this Thesis), which subsequently would evolve to ^{3}Thy* or to the oxetane BP<^{O}>Thy.[164,165]

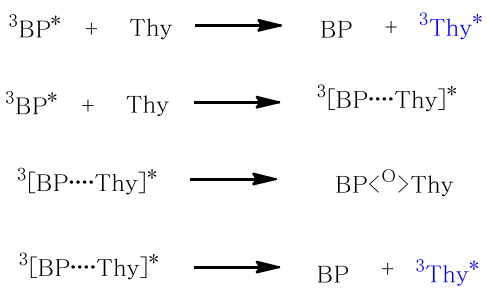

Scheme 6.1. Postulated mechanisms to explain interaction between triplet benzophenone and thymine.

Surprisingly, a direct evidence supporting formation of the key species ^{3}Thy* upon Bzp photosensitization has never been provided. The main reasons to explain this fact are: i) the TTET process has to compete with the more efficient Paternò-Büchi reaction between the carbonyl moiety of ^{3}Bzp* ($n\pi^*$ nature) and the C5-C6 olefinic region of Thy;[49,50,52,148] ii) the very low absorption coefficient of the Thy T-T absorption band, centred at 370 nm[164,166] and iii) the spectral overlap between ^{3}Bzp* (with two bands peaking at 320 and 530 nm) and ^{3}Thy* (a broad band centered at 370 nm). Therefore, until now, only with more energetic triplet ketones such as acetone, acetophenone, propiophenone and 1-indanone, it has been possible to generate ^{3}Thy* by TTET.[164]

In order to provide a direct evidence for the Bzp-photosensitized formation of ^{3}Thy* it would be necessary to block formation of oxetanes, which constitutes the main deactivation pathway of ^{3}Bzp*. In Chapter 4 of this Thesis, it has been demonstrated that thermodynamically favored TTET from ^{3}Bzp* to naphthalene (Npt) or biphenyl (Bip) can efficiently happen through-bond (TB) in intramolecular systems in which the two chromophores are separated by a rigid hydrocarbon bridge. In fact, formation of ^{3}Npt* or ^{3}Bip* upon selective excitation of Bzp has been demonstrated by laser flash photolysis (LFP) in dyads in which Bzp/Npt or Bzp/Bip are covalently attached to the 3α-position (donor) and lateral chain (acceptor) of lithocholic acid (LA).[167] However, no examples of TB-TTET in systems where the process is uphill have been reported to date.

With this background, the aim of the present work is to obtain a direct spectroscopic evidence for the formation of ^{3}Thy* (by TB-TTET) from ^{3}Bzp*. To achieve this goal two new systems have been designed and synthesized, in which one Bzp and one Thy are covalently linked to both ends of the rigid skeleton of the natural bile acids cholic acid (CA) or LA (see design of the experimental hypothesis in Figure 6.1). This way, the formation of oxetanes is prevented due to the long (non-bonding) distance between the chromophores imposed by the bile acid scaffold. Thus, the predominance of TB-TTET over other secondary processes is secured. In addition, the use of LA would minimize interactions between ^{3}Bzp* and the secondary alcohol moieties which may also

be involved in alternative reactions such as H-abstraction, as it is shown in Chapter 3 of this Thesis.

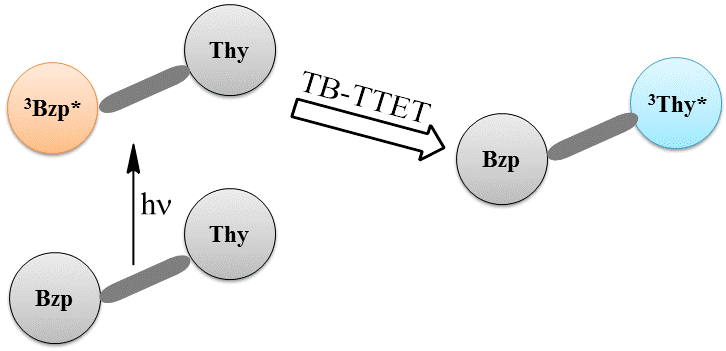

Figure 6.1. TB-TTET in a Bzp/Thy pair linked through a rigid bridge at non-bonding distance.

6.2. Synthesis

Target compounds **3α-Thy-CA-Bzp** and **3α-Bzp-LA-Thy** in addition to the controls **CA-Bzp** and **3α-Bzp-LA** were obtained as shown in Scheme 6.1. First, CA was esterified using reduced KP to give compound **CA-Bzp**, which was used as a control. Subsequent esterification of the most reactive C-3 position of **CA-Bzp**, using thymine-1-acetic acid ($ThyCH_2CO_2H$), gave dyad **3α-Thy-CA-Bzp**. Analogously, **LA** was reduced with $LiAlH_4$, to give the corresponding alcohol (**LA-OH**). Subsequent derivatization with thymine 1-acetic acid ($Thy-CH_2CO_2H$) yielded **LA-Thy**. Then, **LA-Thy** was reacted with *(S)*-ketoprofen (KP) under esterification conditions to give **3α-Bzp-LA-Thy**. In parallel, **3α-Bzp-LA** was obtained upon esterification of the 3α-position of LA with KP.

Synthetic procedures, NMR spectroscopic data and exact mass for the new compounds are detailed in the experimental section of this chapter. Synthesis and characterization of **LA-OH**, **LA-Thy** and **3α-Bzp-LA** has already been described in

Chapter 4. Further NMR experiments and experimental procedures can be found in the supplementary material of this chapter.

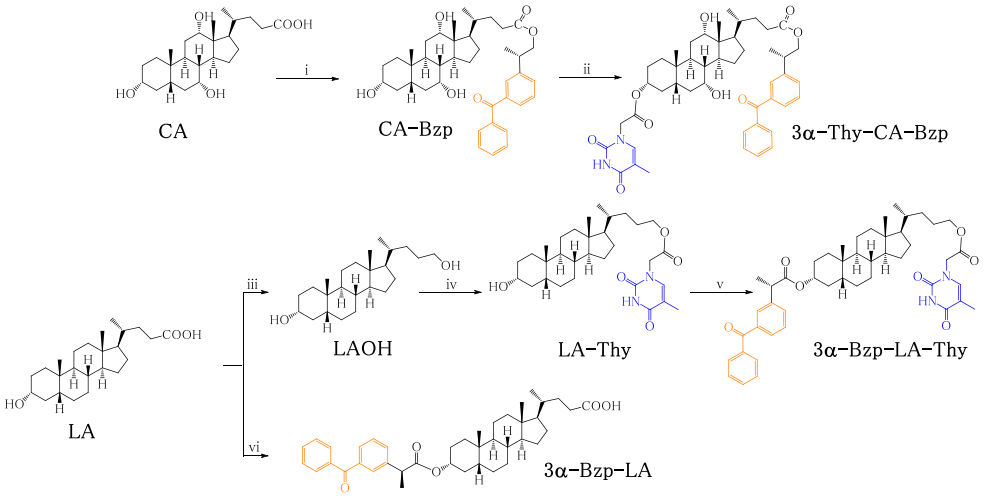

Scheme 6.1. Synthetic strategy to prepare **CA** and **LA** derivatives incorporating **Thy** and/or **Bzp**. Reagents and conditions: (i) KP-OH, 4-DMAP, EDC, C_5H_5N (50%); (ii) $ThyCH_2CO_2H$, 4-DMAP, EDC, DMF (63%); (iii) $LiAlH_4$, THF, (88%); (iv) $ThyCH_2CO_2H$, TBTU, DIEA, DMF, (36%); (v) KP, TBTU, DIEA, DMF, (73%); (vi) KP, DCC, 4-DMAP, CH_2Cl_2 (70%).hb

6.3. Results and discussion

Next, the transient absorption spectra were recorded upon LFP excitation at 355 nm from **3α-Thy-CA-Bzp** and the typical bands of ^{3}Bzp* (λ_{max} *ca.* 320 and 530 nm) were observed at first sight (Figure 6.2, left). Likewise, **CA-Bzp** was subjected to LFP excitation at 355 nm, and the characteristic bands of ^{3}Bzp* were observed (Figure 6.2, right). When the two spectra were compared, clear differences were noticed in the region between 350 and 400 nm, which are consistent with the presence of ^{3}Thy* that would result from TB-TTET.[164] Parallel experiments were performed with **3α-Bzp-LA-Thy** and the control **3α-Bzp-LA**, with identical results (Figure 6.3, left and right).

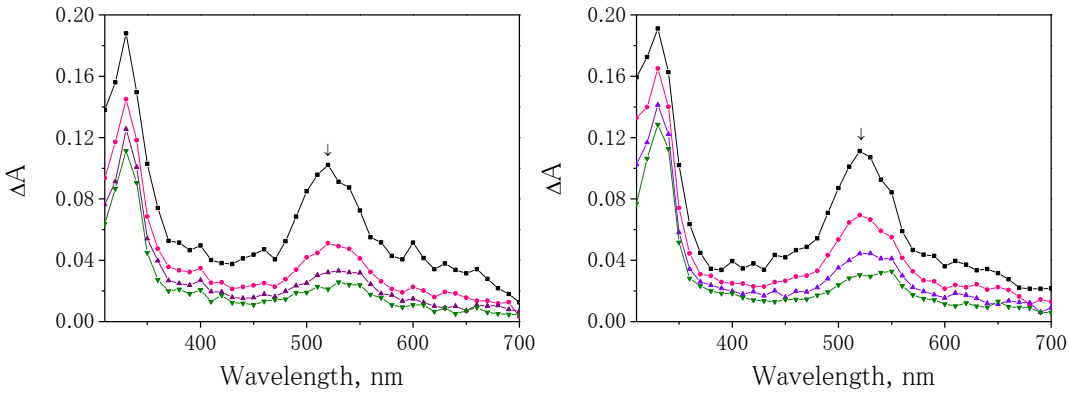

Figure 6.2. LFP (λ_{exc} = 355 nm, CH_2Cl_2, N_2, 5 × 10^{-4} M) of **3α-Thy-CA-Bzp** (left) and **CA-Bzp** (right). Transient absorption spectra obtained at 0.5 μs (black), 0.7 μs (red), 1.1 μs (purple) and 1.5 μs (green) after the laser pulse.

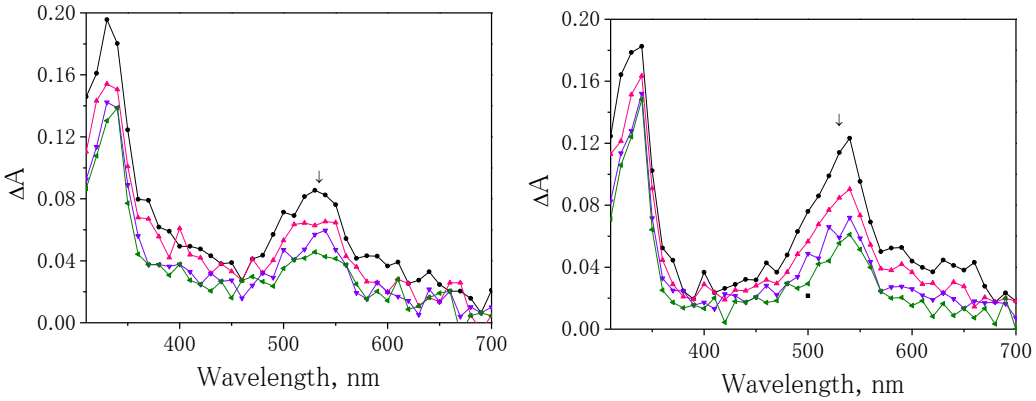

Figure 6.3. LFP (λ_{exc} = 355 nm, CH_2Cl_2, N_2, 5 × 10^{-4} M) of **3α-Bzp-LA-Thy** (left) and **3α-Bzp-LA** (right). Transient absorption spectra obtained at 0.5 μs (black), 1.0 μs (red), 1.5 μs (purple) and 2.0 μs (green), after the laser pulse.

Due to the spectral overlap and to the low molar absorption coefficient of $^3Thy^*$, in order to get an unambiguous piece of evidence for its formation, algorithmic subtractions of the spectra (**3α-Thy-CA-Bzp** minus **CA-Bzp** and **3α-Bzp-LA-Thy** minus **3α-Bzp-LA**) were performed. Thus, subtraction of the spectrum obtained for **CA-Bzp** (Figure 6.2, right) from the one of **3α-Thy-CA-Bzp** (Figure 6.2, left), both taken 0.5

μs after the laser pulse, resulted in a spectrum, which was essentially coincident with the one already reported for ^{3}Thy*, and obtained by TTET from the more energetic triplet of acetone (Figure 6.4, black trace).[164] Analogously, subtraction of the spectrum obtained for **3α-Bzp-LA** (Figure 6.3, right) from the one of **3α-Bzp-LA-Thy** (Figure 6.3, left), both taken 0.5 μs after the laser pulse, gave the trace corresponding to ^{3}Thy*, as shown in Figure 6.4, red trace.

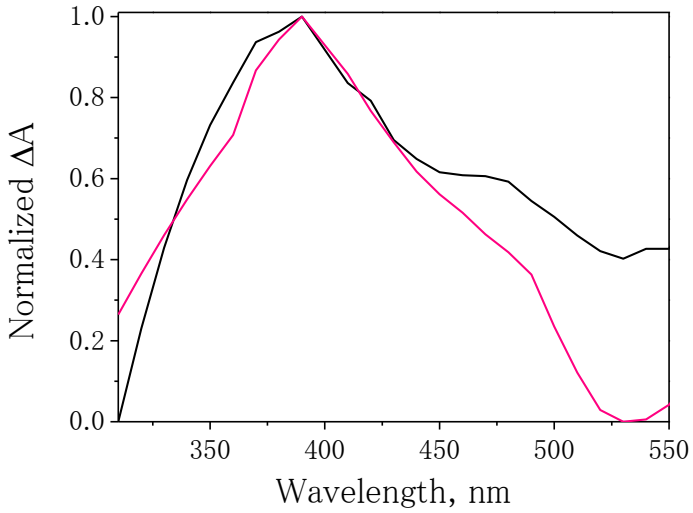

Figure 6.4. Transient absorption spectra obtained from the algorithmic subtraction of the LFP traces corresponding to **3α-Thy-CA-Bzp** minus **CA-Bzp** (black trace) and **3α-Bzp-LA-Thy** minus **3α-Bzp-LA** (red trace) at 0.5 μs.

A further control experiment was performed to rule out a possible interference due to intermolecular TTET. Hence, a 1:1 mixture of **3α-Bzp-LA** and $ThyCH_2COOH$ was submitted to LFP, and the transient absorption spectrum was recorded at the same times after the laser pulse (See Figure 6.5). As expected, a clean spectrum was obtained exhibiting only the typical bands of $^3Bzp^*$, indicating that intermolecular TTET is negligible at the employed concentrations.

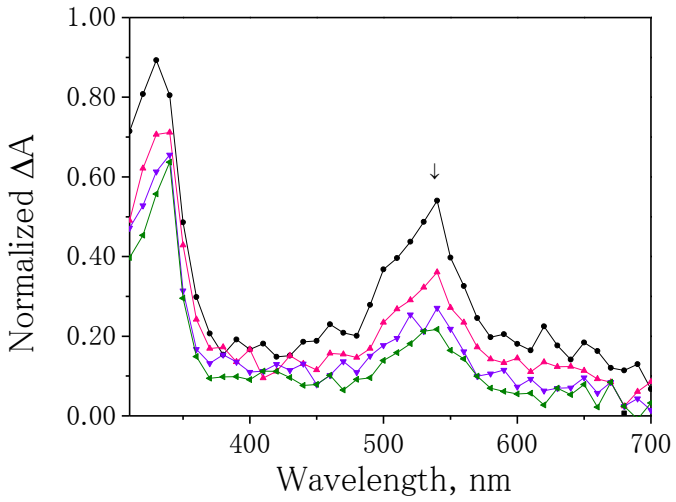

Figure 6.5. LFP (λ_{exc} = 355 nm, CH_2Cl_2, N_2, 5 × 10^{-4} M) of **3α-Bzp-LA:** $ThyCH_2COOH$, 1:1. Transient absorption spectra obtained at 0.5 μs (black), 1.0 μs (red), 1.5 μs (purple) and 2.0 μs (green) after the laser pulse.

Then, the lifetime behavior of $^3Bzp^*$ in the different systems was recorded providing a kinetic evidence for the occurrence of TB-TTET from $^3Bzp^*$ to Thy. In the compounds derived from CA, the decay of $^3Bzp^*$ in dyad **3α-Thy-CA-Bzp** was monitored at 520 nm, and a clear decrease in the lifetime was observed if compared to the reference **CA-Bzp** (Figure 6.6, left). A similar behavior was observed in the LA-based systems when comparing the dyad **3α-Bzp-LA-Thy** and the reference **3α-Bzp-LA** (Figure 6.6, right), in which $^3Bzp^*$ lives longer due to the lower contribution of hydrogen abstraction

from the CH of the secondary alcohols. All the decays were fitted to a first order exponential equation, and the lifetimes are summarized in Table 6.1. The rate constants of TB-TTET were determined for **3α-Thy-CA-Bzp** and **3α-Bzp-LA-Thy**, and found to be 8.3 x 10^5 s^{-1} and x 9.7 x 10^5 s^{-1}, respectively.

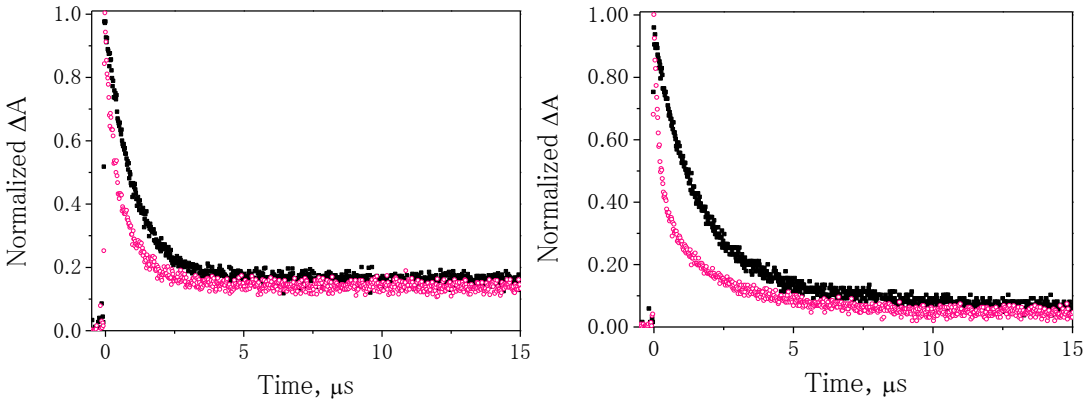

Figure 6.6. LFP (λ_{exc} = 355 nm, CH_2Cl_2, N_2, 5 × 10^{-4} M) of left: **3α-Thy-CA-Bzp** (○) and **CA-Bzp** (■) and right: **3α-Bzp-LA-Thy** (○) and **3α-Bzp-LA** (■). Decays monitored at 520 nm.

Table 6.1. Triplet lifetimes and rate constants for TB-TTET in Bzp/Thy systems

System[a]	τ (^{3}BP*)[b]	k[c]
CA-Bzp	1.01	N.A.
3α-Thy-CA-Bzp	0.55	8.3 × $10^{5,d}$
3α-Bzp-LA	1.77	N.A.
3α-Bzp-LA-Thy	0.65	9.7 × $10^{5,e}$

[a]In all cases, the concentration was 5 × 10^{-4} M; [b]Units: μs; [c]Units: s^{-1}; [d]Determined as ($1/\tau_{\text{3α-Thy-CA-Bzp}} - 1/\tau_{\text{CA-Bzp}}$);[e]Determined as ($1/\tau_{\text{3α-Bzp-LA-Thy}} - 1/\tau_{\text{3α-Bzp-LA}}$)

.

6.4. Conclusions

Unambiguous spectroscopic evidence for the formation of ^{3}Thy* from ^{3}Bzp* has been provided in two different systems. Although in principle it is a thermodynamically disfavored process that has to compete with the Paternò-Büchi reaction, a careful experimental design has been applied to circumvent these problems. Thus, one Bzp and one Thy have been covalently linked to the two ends of rigid skeletons of the natural CA and LA. This way, population of ^{3}Thy* by triplet-triplet energy transfer from ^{3}Bzp* has to occur through-bond, and competitive formation of oxetanes is avoided by placing the two chromophores at non-bonding distances.

6.5. Experimental

6.5.1. Synthesis and characterization

6.5.1.1. Synthesis of CA-Bzp

To a stirred mixture of **CA** (0.671 g, 1.64 mmol), (*S*)-KP-OH (0.328 g, 1.37 mmol) and 4-DMAP (0.2 g, 1.64 mmol) in 8 mL of anhydrous pyridine at 0° C, EDC (0.290 mL, 1.64 mmol) was added dropwise and the reaction mixture was allowed to react for one hour and then overnight at rt. The suspension was poured into HCl 1M and extracted with CH_2Cl_2. Then, the combined organic layers were washed with brine, dried over $MgSO_4$ and concentrated under reduced pressure. Purification by column chromatography (SiO_2, CH_2Cl_2: MeOH, 95:5) gave **CA-Bzp** as a colorless solid (0.516 g, 50%). ^{1}H NMR (300 MHz, $CDCl_3$): δ (ppm) 0.66 (s, 3H, 18-CH_3); 0.89 (s, 3H, 19-CH_3); 0.92-2.01 (complex signal, 24H); 0.94 (d, *J* = 6.3 Hz, 3H, 21-CH_3); 1.34 (d, 3H, *J* = 7.2 Hz, KP-CH_3); 3.18 (m, 1H, KP-CH); 3.46 (m, 1H, 3β-H); 3.84 (br s, 1H, 7β-H); 3.96 (br s, 1H, 12β-H); 4.16 (dd, *J* = 10.8, 6.9 Hz, 1H, KP-CH_2); 4.21 (dd, *J* = 10.8, 7.2 Hz, 1H, KP-CH_2); 7.38-7.83 (m, 9H, arom). ^{13}C NMR (75 MHz, $CDCl_3$): δ (ppm) 196.8 (C), 174.3 (C), 143.8 (C), 137.8 (C), 137.7 (C), 132.6 (CH), 131.5 (CH), 130.1 (2xCH), 129.0 (CH), 128.7 (CH), 128.5 (CH), 128.4 (2xCH), 73.1 (CH), 72.0 (CH), 68.9 (CH_2), 68.5 (CH), 47.1 (CH), 46.5 (C), 41.7 (CH), 41.6 (CH), 39.6 (CH), 39.0 (CH), 35.4 (CH_2), 35.3 (CH), 34.9 (C), 34.8 (CH_2), 31.4 (CH_2), 31.0 (CH_2), 30.5 (CH_2), 29.8 (CH_2), 28.3 (CH_2), 27.6 (CH_2), 26.4 (CH), 23.3 (CH_2), 22.6 (CH_3), 18.1 (CH_3), 17.4 (CH_3), 12.6 (CH_3).; m/z found 631.3989, calculated for $C_{40}H_{55}O_6$ (MH^+) 631.3999.

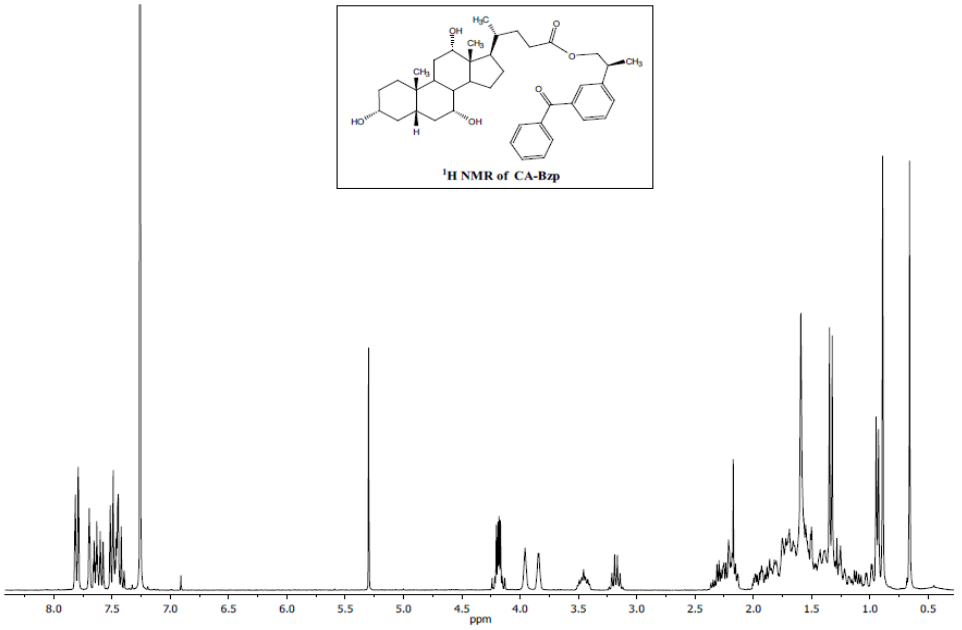
^{1}H NMR of CA-Bzp
8.0
7.5
7.0
6.5
6.0
5.5
5.0
4.5
4.0
3.5
3.0
2.5
2.0
1.5
1.0
0.5
ppm

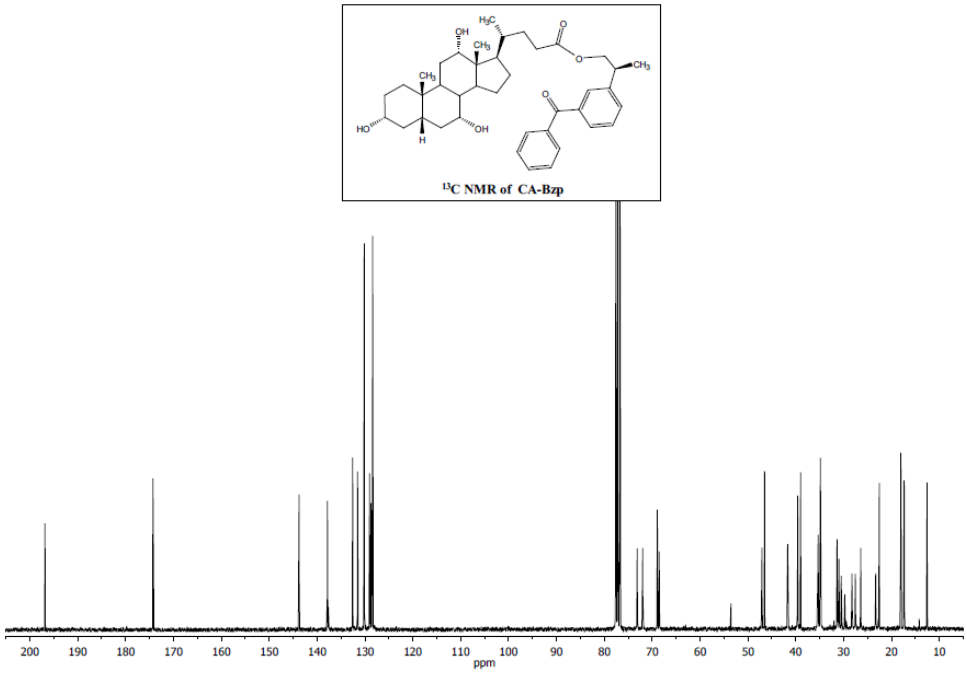
^{13}C NMR of CA-Bzp
200
190
180
170
160
150
140
130
120
110
100
90
80
70
60
50
40
30
20
10
ppm

6.5.1.2. Synthesis of 3α-Thy-CA-Bzp

To a stirred solution of Thy-CH_2COOH (0.360 g, 1.96 mmol) in anhydrous DMF (2.5 mL), a solution of 4-DMAP (0.093 g, 0.77 mmol) and **CA-Bzp** (0.374 g, 0.59 mmol) in DMF (2 mL) was added dropwise. Then the resulting suspension was cooled at 0 ° C, EDC (0.35 mL, 1.96 mmol) was added and after one hour at 0 ° C, the reaction mixture was allowed to stir overnight at rt. Then, the suspension was poured into HCl 1M, extracted with CH_2Cl_2 and the combined organic extracts were washed with brine, dried over $MgSO_4$ and concentrated. After purification by column chromatography (SiO_2, AcOEt:hexane, 90:10) followed by (Li Chroprep RP-18, CH_3CN:H_2O, 80:20), **3α-Thy-CA-Bzp** was obtained as a colorless solid (0.298 g, 63%). ^{1}H NMR (300 MHz, $CDCl_3$): δ (ppm) 0.64 (s, 3H, 18-CH_3); 0.82-1.93 (complex signal, 24H); 0.88 (s, 3H, 19-CH_3); 0.94 (d, J = 6.0 Hz, 3H, 21-CH_3); 1.32 (d, 3H, J = 6.9 Hz, KP-CH_3); 1.86 (br s, 3H, Thy-CH_3); 3.16 (m, 1H, KP-CH); 3.82 (br s, 1H, 7β-H); 3.96 (br s, 1H, 12β-H); 4.17 (m, 2H, KP-CH_2); 4.34 (d, 1H, J = 16.8 Hz, Thy-CH_2); 4.47 (d, 1H, J = 16.8 Hz, Thy-CH_2); 4.59 (m, 1H, 3β-H); 7.10 (s, 1H, Thy-CH); 7.38-7.80 (m, 9H, arom); 9.20 (br s, 1H, Thy-NH). ^{13}C NMR (75 MHz, $CDCl_3$): δ (ppm) 196.8 (C), 174.2 (C), 167.7 (C), 164.6 (C), 151.4 (C), 143.8 (CH), 141.3 (C), 137.8 (C), 137.7 (C), 132.6 (CH), 131.5 (CH), 130.1 (2xCH), 129.0 (CH), 128.7 (CH), 128.4 (CH), 128.3 (2xCH), 110.6 (C), 76.9 (CH), 72.8 (CH), 68.9 (CH_2), 68.2 (CH), 49.5 (CH_2), 47.1 (CH), 46.4 (C), 42.0 (CH), 41.3 (CH), 39.7 (CH), 39.0 (CH), 35.1 (CH), 35.0 (CH_2), 34.9 (CH_2), 34.8 (C), 34.4 (CH_2), 31.3 (CH_2), 31.0 (CH_2), 28.5 (CH_2), 27.5 (CH_2), 26.7 (CH), 26.3 (CH_2), 23.2 (CH_2), 22.6 (CH_3), 18.1 (CH_3), 17.3 (CH_3), 12.6 (CH_3), 12.3 (CH_3); m/z found 797.4388, calculated for $C_{47}H_{61}N_2O_9$ (MH^+) 797.4377.

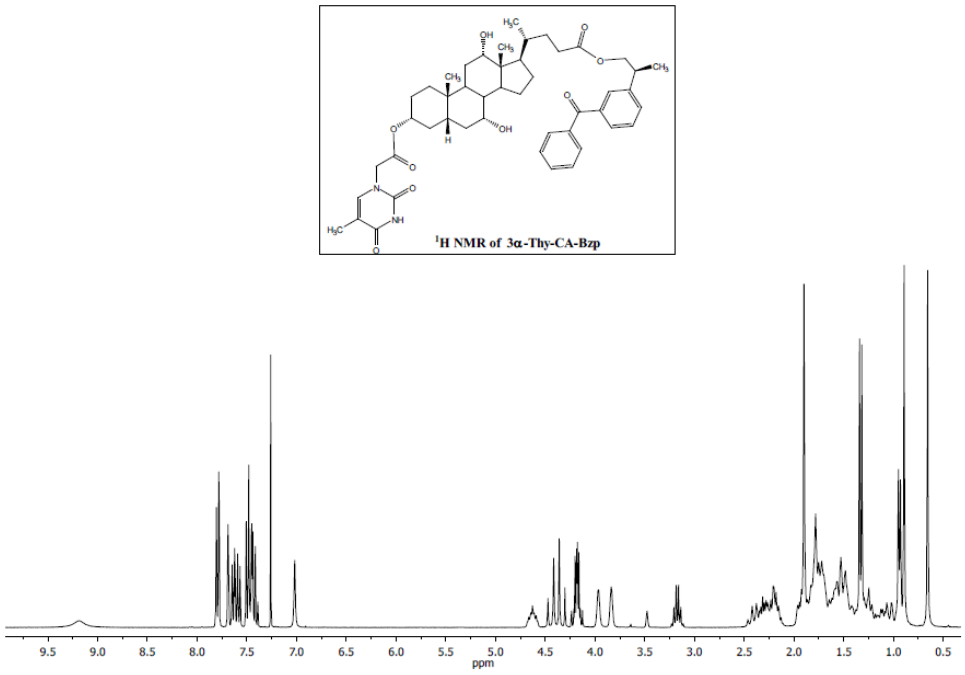
^{1}H NMR of 3α-Thy-CA-Bzp
9.5 9.0 8.5 8.0 7.5 7.0 6.5 6.0 5.5 5.0 4.5 4.0 3.5 3.0 2.5 2.0 1.5 1.0 0.5
ppm

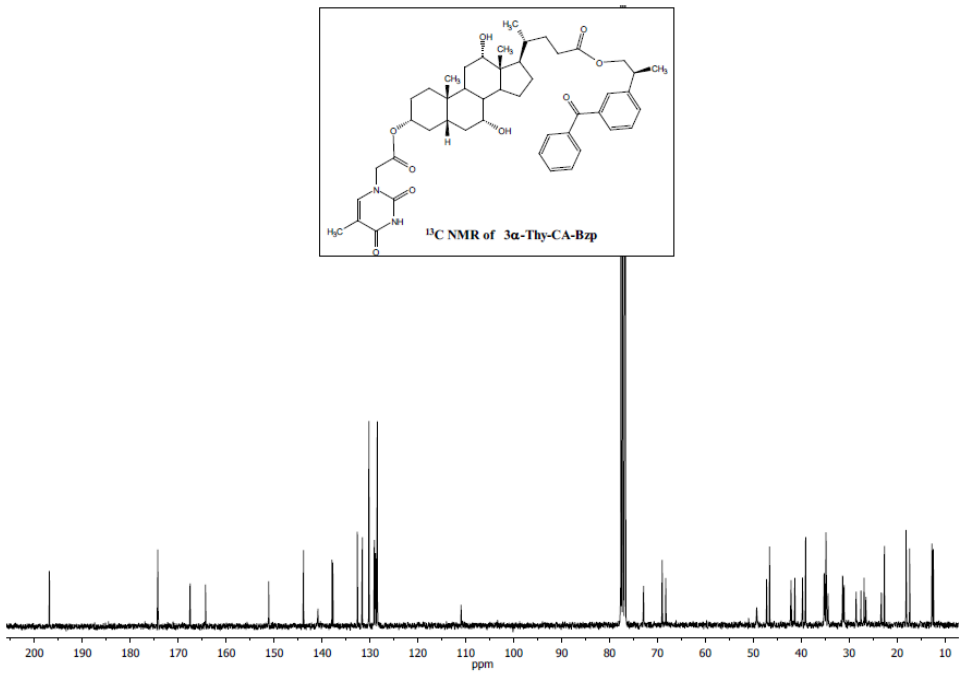
^{13}C NMR of 3α-Thy-CA-Bzp
200 190 180 170 160 150 140 130 120 110 100 90 80 70 60 50 40 30 20 10
ppm

6.5.1.3. Synthesis of 3α-Bzp-LA-Thy

To a stirred solution of **LA-Thy** (0.129 g, 0.24 mmol) and TBTU (0.12 g, 0.36 mmol) in anhydrous DMF (1 mL), KP (0.09 g, 0.36 mmol) in DMF (2.5 mL) followed by DIEA (0.16 mL, 0.9 mmol) were added dropwise and then the reaction mixture was allowed to react overnight at rt. Afterwards, it was poured into brine and extracted with CH_2Cl_2; the combined organic layers were washed with brine, dried over $MgSO_4$ and concentrated under reduced pressure. Purification by column chromatography (SiO_2, EtOAc:Hexane, 50:50) followed by (Li Chroprep RP-18, CH_3CN:H_2O, 90:10) gave **3α-Bzp-LA-Thy** as a colorless oil (0.14 g, 73%). ^{1}H NMR (300 MHz, $CDCl_3$): δ (ppm) 0.62 (s, 3H, CH_3); 0.79-2.01 (complex signal, 28H); 0.89 (*br* s, 6H, CH_3+CH_3); 1.49 (d, *J* = 6.9 Hz, 3H, KP-CH_3); 1.91 (d, *J* = 1.2 Hz, 3H, Thy-CH_3); 3.74 (m, 1H, KP-CH); 4.12 (m, 2H, CH_2), 4.43 (s, 2H, Thy-CH_2); 4.72 (m, 1H, 3β-H); 6.94 (*br* s, 1H, Thy-CH); 7.37-7.81 (m, 9H, arom); 9.35 (s, 1H, Thy-NH). ^{13}C NMR (75 MHz, $CDCl_3$) : δ (ppm) 196.7 (C), 173.7 (C), 167.7 (C), 164.3 (C), 151.0 (C), 141.2 (C), 140.3 (CH), 137.9 (C), 137.6 (C), 132.6 (CH), 131.6 (CH), 130.2 (2xCH), 129.3 (CH), 128.9 (CH), 128.6 (CH), 128.4 (2xCH), 111.3 (C), 75.0 (CH), 66.8 (CH_2), 56.5 (CH), 56.1 (CH), 48.7 (CH_2), 45.8 (CH), 42.8 (C), 42.0 (CH), 40.5 (CH), 40.2 (CH_2), 35.9 (CH), 35.4 (CH), 35.0 (CH_2), 34.7 (C), 32.1 (CH_2), 31.9 (CH_2), 28.4 (CH_2), 27.1 (CH_2), 26.7 (CH_2), 26.4 (CH_2), 25.1 (CH_2), 24.3 (CH_2), 23.4 (CH_3), 20.9 (CH_2), 18.7 (CH_3), 18.6 (CH_3), 12.5 (CH_3), 12.1 (CH_3); m/z found 765.4500, calculated for $C_{47}H_{61}N_2O_7$ (MH^+) 765.4479.

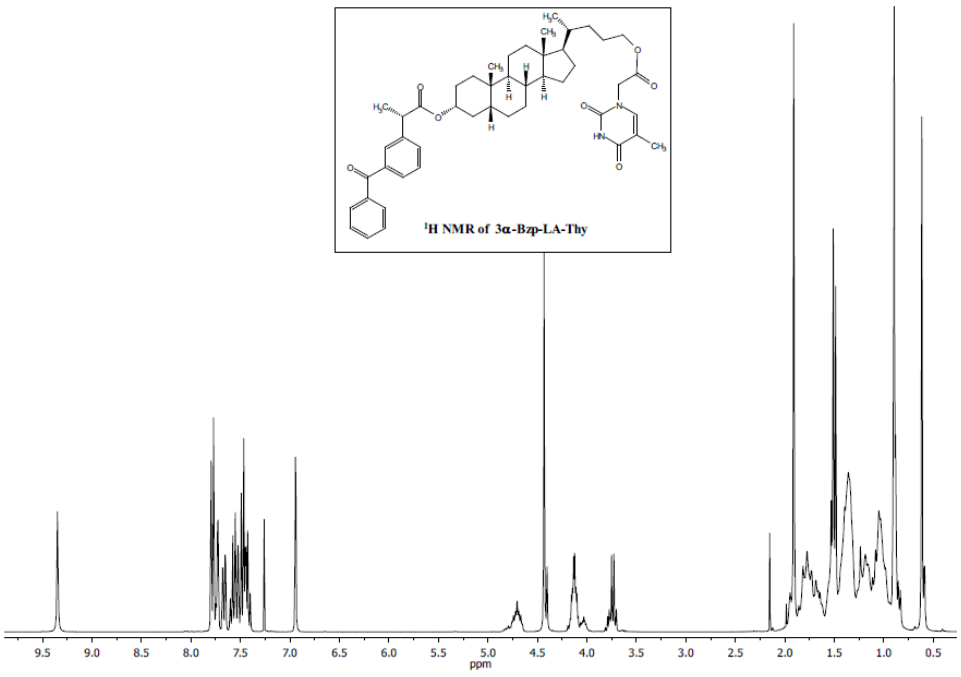
^{1}H NMR of 3α-Bzp-LA-Thy
9.5 9.0 8.5 8.0 7.5 7.0 6.5 6.0 5.5 5.0 4.5 4.0 3.5 3.0 2.5 2.0 1.5 1.0 0.5
ppm

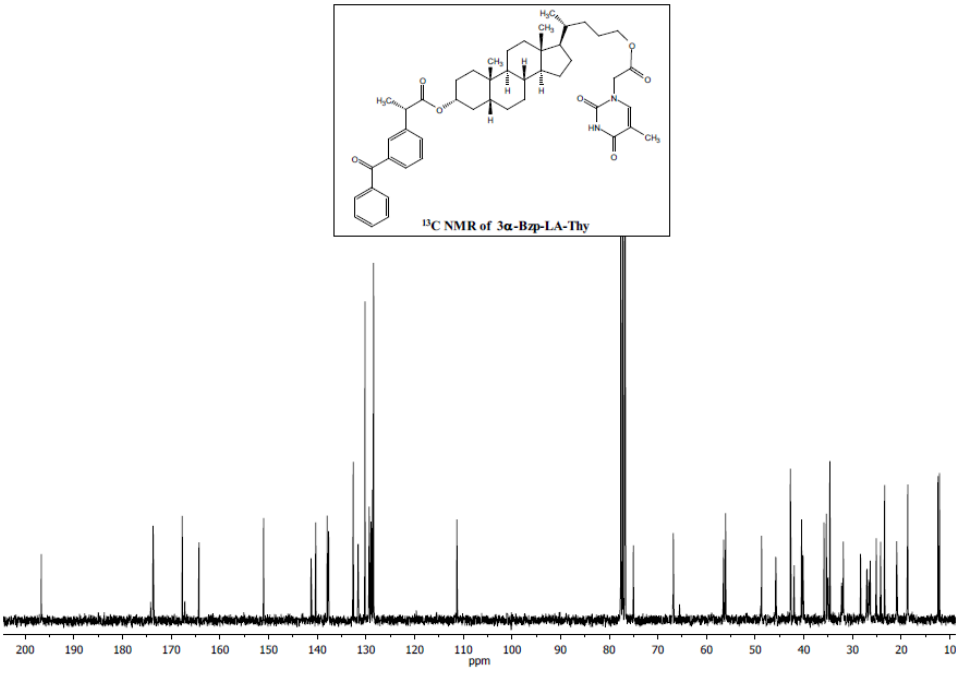
^{13}C NMR of 3α-Bzp-LA-Thy
200 190 180 170 160 150 140 130 120 110 100 90 80 70 60 50 40 30 20 10
ppm

6.6. Supplementary material

6.6.1. Instrumentation

Laser flash photolysis at 355 nm. Transient spectra were recorded at room temperature using N_2-purged solutions of 5 x 10^{-4} M of specified sample in CH_2Cl_2.

6.6.2. Additional NMR spectra

6.6.2.1. CA-Bzp

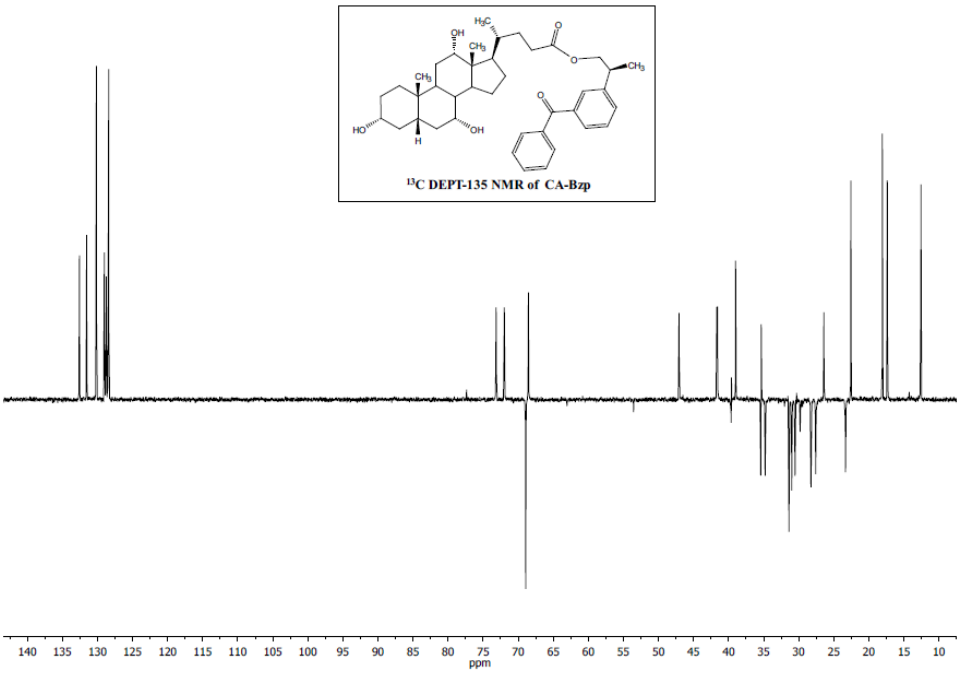

6.6.2.1. 3α-Thy-CA-Bzp

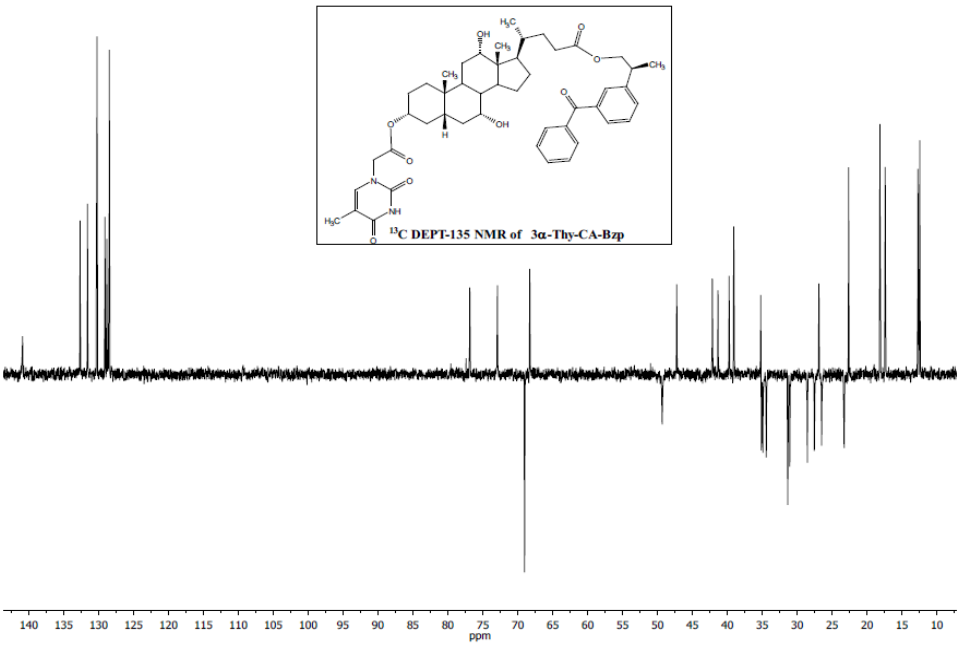

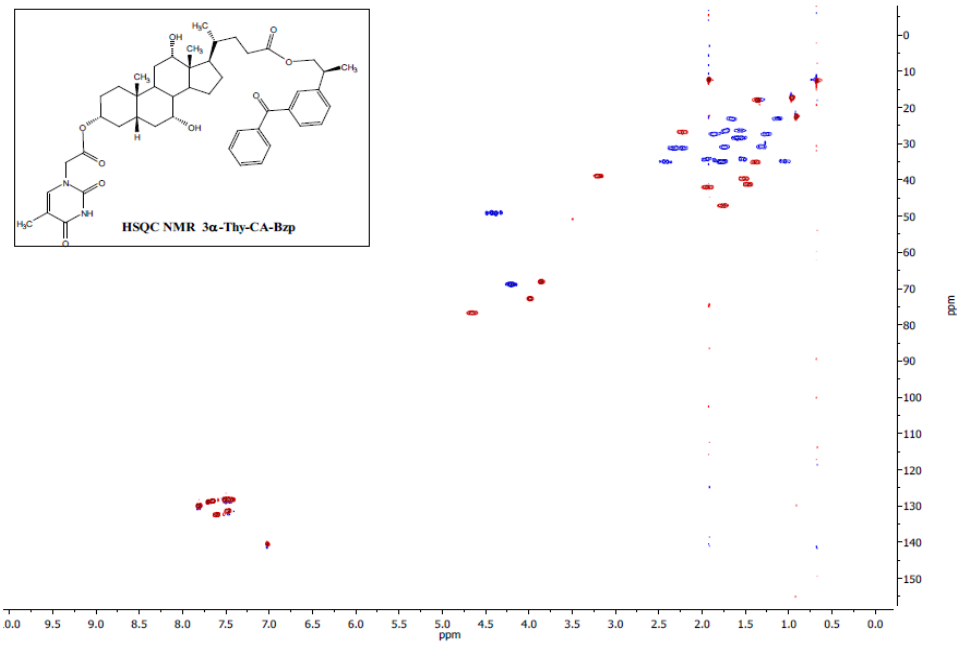

6.6.2.3. 3α-Bzp-LA-Thy

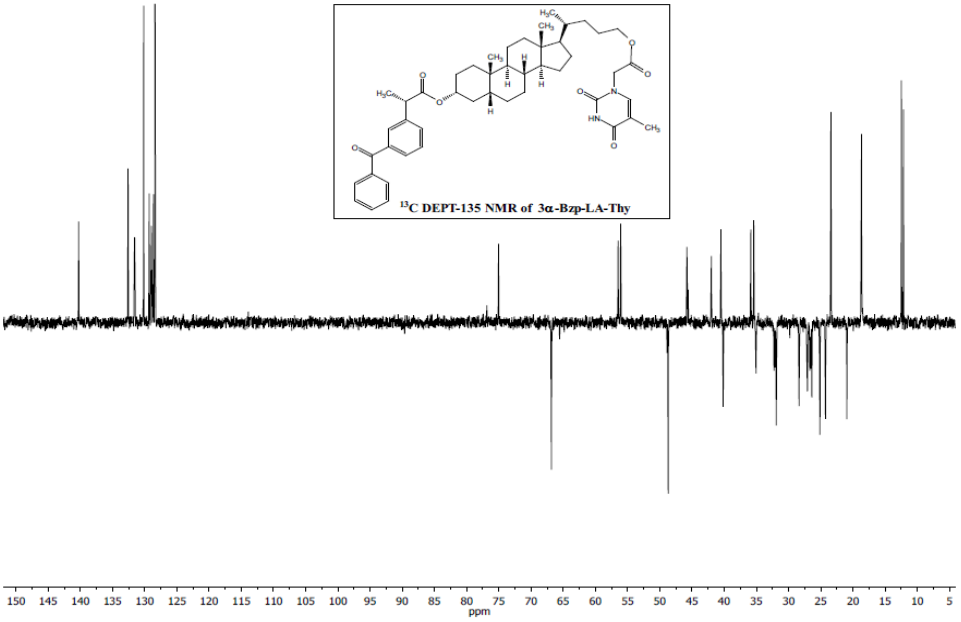

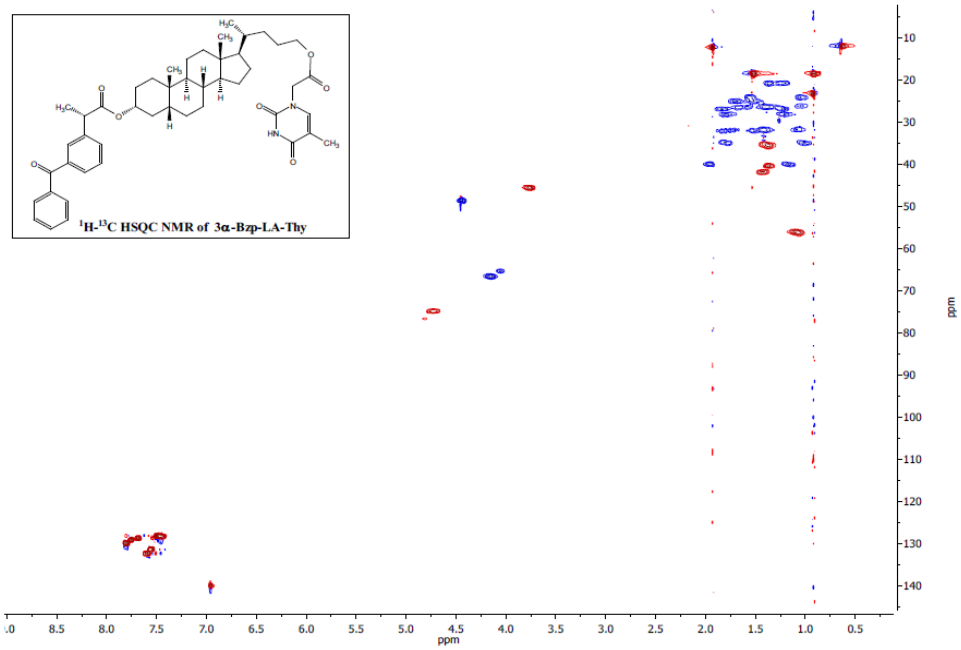

Chapter 7: Thymine–Thymine Dimers: Direct *vs* Photosensitized Formation

7.1. Introduction

Solar light arriving at the Earth is essential for humans, but at the same time it can cause deleterious effects. Its minor UVB radiation component is responsible for most of the melanoma skin cancer cases caused by solar light since it can be absorbed by the thymine (Thy) or cytosine (Cyt) nucleobases giving rise to the formation of cyclopyrimidine dimers (CPDs) such as Thy<>Thy, Cyt<>Thy or Cyt<>Cyt and also pyrimidine–(6–4)–pyrimidone adducts and their related Dewar isomers.[168–170] However, the effects of UVA (from 320 to 400 nm) should not be disregarded, in particular when they can be mediated by photosensitizers absorbing in this region. In such a way, formation of dimers is thought to procced through an initial triplet–triplet energy transfer step (TTET).[148,171] To be efficient, TTET requires selective excitation of a donor chromophore with a high intersystem crossing quantum yield, a triplet energy above that of Thy and long triplet lifetime. The reported quantum yields for photodimerization range

from 10^{-5} to 10^{-2}.[40] However, alternative mechanisms involving the participation of triplet triplexes have been demonstrated to play a role in the sensitized formation of Thy<>Thy using Bzp (see Chapter 5).[172]

Although DNA irradiation produces Cyt<>Cyt and Thy<>Cyt,[169,173] Thy<>Thy are the photoproducts with higher yields and therefore the most biologically significant.[174,175] With respect to the regio- and stereoselectivity of the dimers, up to four diastereoisomers can be obtained for Thy in solution[149] that are *cis–syn*, *cis–anti*, *trans–anti* and *trans–syn*. Distribution of diastereoisomers can be influenced by, for instance, solvent polarity being the *cis–syn* dimer the major one in polar solvents when Bzp is used as the photosensitizer.[40]

In many organisms, CPDs are repaired by photolyases. They act through a light-dependent single-electron transfer mechanism (Figure 7.1.)[176,177] with quantum yields for the repair of Thy<>Thy as high as 0.7–0.98.[178] The redox-active flavin adenine dinucleotide (FAD) cofactor plays a pivotal role in the photorepair activity of photolyases since its fully reduced and protonated form ($FADH^-$) can be excited to reach its singlet excited state ($^1FADH^{-*}$) *via* energy transfer from an antenna chromophore present in the medium, absorbing at long wavelengths. Although this chromophore is not essential for the reaction to happen, it helps to populate $^1FADH^{-*}$, since direct absorption by $FADH^-$ is very slow. Then, the excited $^1FADH^{-*}$ transfers one electron to the CPD and leads to the dimer radical anion, inducing the spontaneous cleavage of the cyclobutane, eventually followed by back electron transfer to $FADH^*$ which then relaxes to $FADH^-$, finally giving rise to the restored pyrimidine. [176,177]

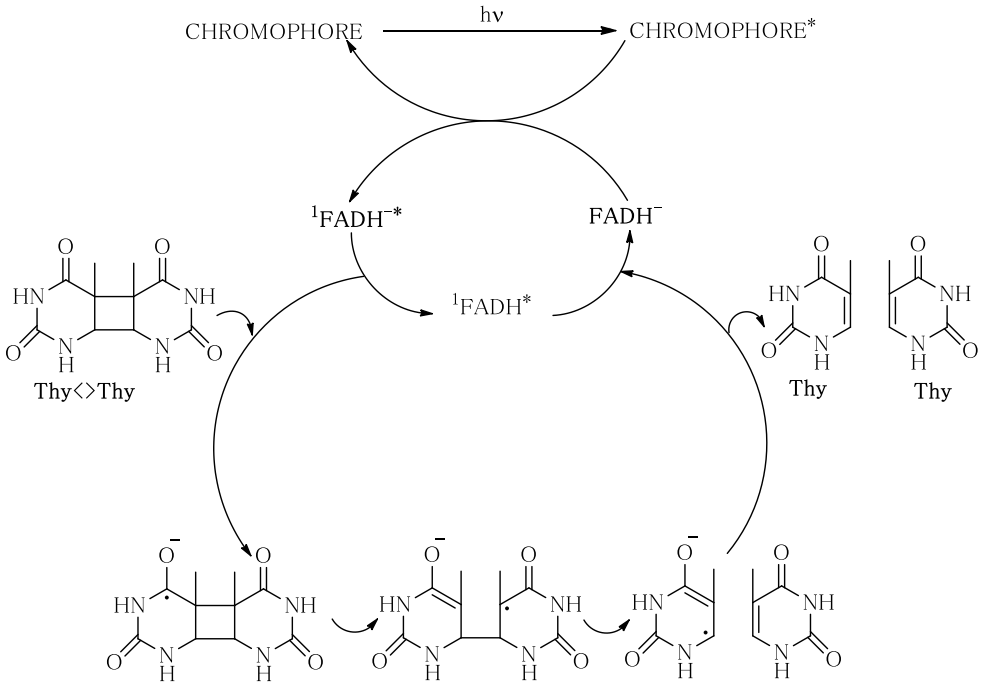

Figure 7.1. Schematic mechanism for Thy<>Thy repair induced by CPDs photolyase in the presence of $FADH^-$.

Model compounds, which mimic the performance of the CPD-photolyase have reported to achieve the CPDs photorepair.[179-183] Among them, the activity of the Cbz chromophore, known to act as an electron donor[184] has been tested in intermolecular[52,185] and intramolecular[186] systems giving strong evidence for the photocatalytic Thy<>Thy cleavage. Moreover, a dual performance for Cbz has been claimed[52] since its suitability to photosensitize Thy<>Thy formation could compromise its photorepair activity. In fact, Cbz is a chromophore with a moderate intersystem crossing quantum yield (0.36),[22] a relatively high triplet energy (70.2 kcal mol^{-1}),[22] a long triplet lifetime and also a $\pi\,\pi^*$ triplet configuration (free from the problems associated with the competitive hydrogen-abstraction, as described in the systems including intramolecular benzophenone, see

Chapter 5).[187] Therefore, it is able to act as a TTET photosensitizer when irradiated at wavelengths near 300 nm.

With this background, the aim of this chapter is to evaluate the direct *versus* Cbz–intramolecular photosensitized formation of Thy<>Thy, as well as the intermolecular *versus* intramolecular photorepair dynamics mediated by Cbz.

The use of different systems including two or three Thy units anchored to the rigid skeleton of BAs (CA, DCA and CDCA) is planned for studying regioselectivity in direct Thy<>Thy formation (Figure 7.2). Even more, with Cbz covalently attached to different positions of the scaffold in an additional family of derivatives (Figure 7.3) it appears feasible to investigate intramolecular Cbz–photosensitized Thy<>Thy formation.

In the second part, using the directly obtained dimers toghether with the photosensitized ones (keeping intact the intramolecular Cbz unit), it is intended to investigate the inter– *versus* intramolecular Cbz photosensitized repair of Thy<>Thy.

Scaffold	Lateral chain protected	3 α – position protected
CA	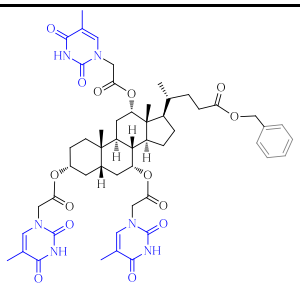 3α,7α,12α-3Thy-CA-Bn	---
DCA	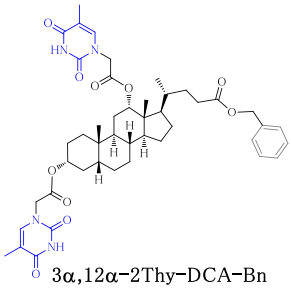 3α,12α-2Thy-DCA-Bn	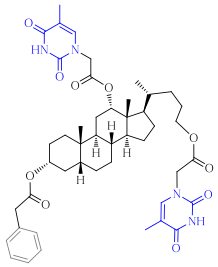 3α-Pa,12α-Thy-DCA-Thy
CDCA	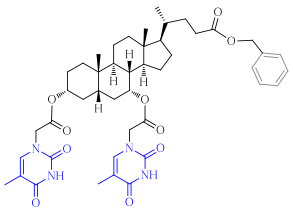 3α,7α-2Thy-CDCA-Bn	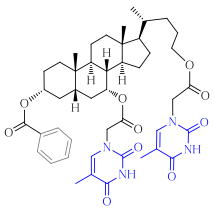 3α-Bz,7α-Thy-CDCA-Thy

Figure 7.2. Structure of BA derivatives incorporating two or three Thy units.

Scaffold	Cbz at the lateral chain	Cbz at 3α–
CA	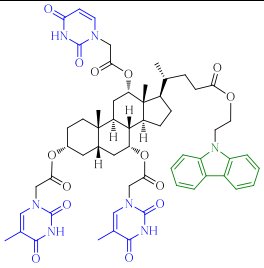 3α,7α,12α-3Thy-CA-Cbz	---
DCA	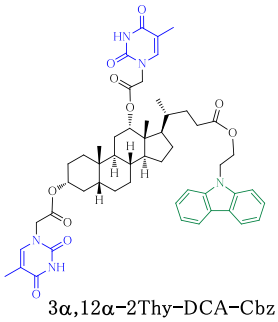 3α,12α-2Thy-DCA-Cbz	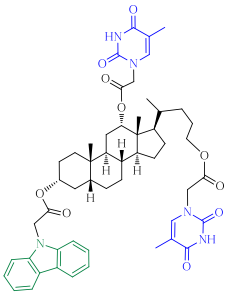 3α-Cbz, 12α-Thy-DCA-Thy
CDCA	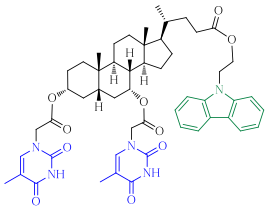 3α,7α-2Thy-CDCA-Cbz	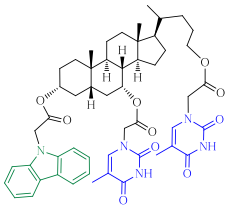 3α-Cbz,7α-Thy-CDCA-Thy

Figure 7.3. Structure of BA derivatives incorporating Cbz and two or three Thy units.

7.2. Synthesis

To prepare the systems shown in Figures 7.2 and 7.3, CA, DCA and CDCA have been used as scaffolds. For the sake of clarity in the following detailed synthesis, the compounds have been grouped on the basis os the BA used, therefore their synthesis will follow a different order from the one shown in Figures 7.2 and 7.3.

The developed synthetic strategy to prepare the derivatives coming from CA (Scheme 7.1), started with their protection as benzyloxy (**CA-Bn**) using benzyl bromide, followed by treatment with an excess of Thy-CH_2CO_2H to give **3α,7α,12α-3Thy-CA-Bn**. Moreover, under controlled conditions one single unit of Thy was introduced at 3α- giving rise to **3α-Thy-CA-Bn**, which was used in the photophysical experiments as a control. The derivatives containing Cbz at the lateral chain were synthesized beginning with the esterification of CA with Cbz-$(CH_2)_2$-OH to yield **CA-Cbz**. Then under Yamaguchi conditions, the three positions 3α-, 7α- and 12α- were esterified providing **3α,7α,12α-3Thy-CA-Cbz** whereas introduction of one Thy unit was regioselectively accomplished at 3α- position under mild esterification conditions giving rise to **3α-Thy-CA-Cbz**, a compound designed as a control.

The synthesis of the derivatives containing two Thy units and the protecting group shown in Figure 7.2 (**3α,12α-2Thy-DCA-Bn**, **3α,7α-2Thy-CDCA-Bn**, **3α-Pa,12α-Thy-DCA-Thy** and **3α-Bz,7α-Thy-CDCA-Thy**) has already been detailed in Chapter 5 of this Thesis (Schemes 5.1, 5.4 , 5.5 and 5.6, respectively in pages 132, 143, 144 and 145).

Next, to prepare the dyads with two Thy units and the Cbz (Figure 7.3), the developed strategy started with esterification of the carboxyl group of DCA or CDCA with Cbz-$(CH_2)_2$-OH giving **DCA-Cbz** or **CDCA-Cbz** (see Schemes 7.2 and 7.3, respectively). Subsequent treatment with an excess of Thy-CH_2CO_2H resulted in the esterification of the two hydroxyl groups giving rise to **3α,12α-2Thy-DCA-Cbz** or **3α,7α-2Thy-CDCA-Cbz**, respectively.

Moreover, to prepare the derivatives with two Thy moieties and the Cbz at 3α– (Schemes 7.2 and 7.3), the carboxyl group of **DCA** or **CDCA** was initially reduced to the corresponding alcohol (**DCAOH** or **CDCAOH**, respectively), which were esterified using Thy–CH_2CO_2H to give **DCA–Thy** or **CDCA–Thy** (already described in Chapter 5 of this Thesis). The following step was the introduction of the chromophore, as Cbz–CH_2–COOH at 3α–, to yield **3α–Cbz–DCA–Thy** or **3α–Cbz–CDCA–Thy**. Subsequent treatment with Thy–CH_2CO_2H led to **3α–Cbz,12α–Thy–DCA–Thy** or **3α–Cbz,7α–Thy–CDCA–Thy**, respectively.

In summary, a first set of new compounds containing two or three Thy units at different relative positions of a BA skeleton has been prepared (Figure 7.2). A second set of compounds has been synthesized, in which in addition to the two or three Thys, a Cbz moiety has also been covalently attached (Figure 7.3).

All the compounds are fully characterized and will be employed to compare direct *versus* photosensitized formation of Thy<>Thy dimers and intermolecular *versus* intramolecular Cbz–mediated photorepair.

Synthetic procedures, NMR spectroscopic data and exact mass for the new compounds are detailed in the experimental section of this chapter. Further NMR experiments and experimental procedures can be found in the supplementary material of this chapter.

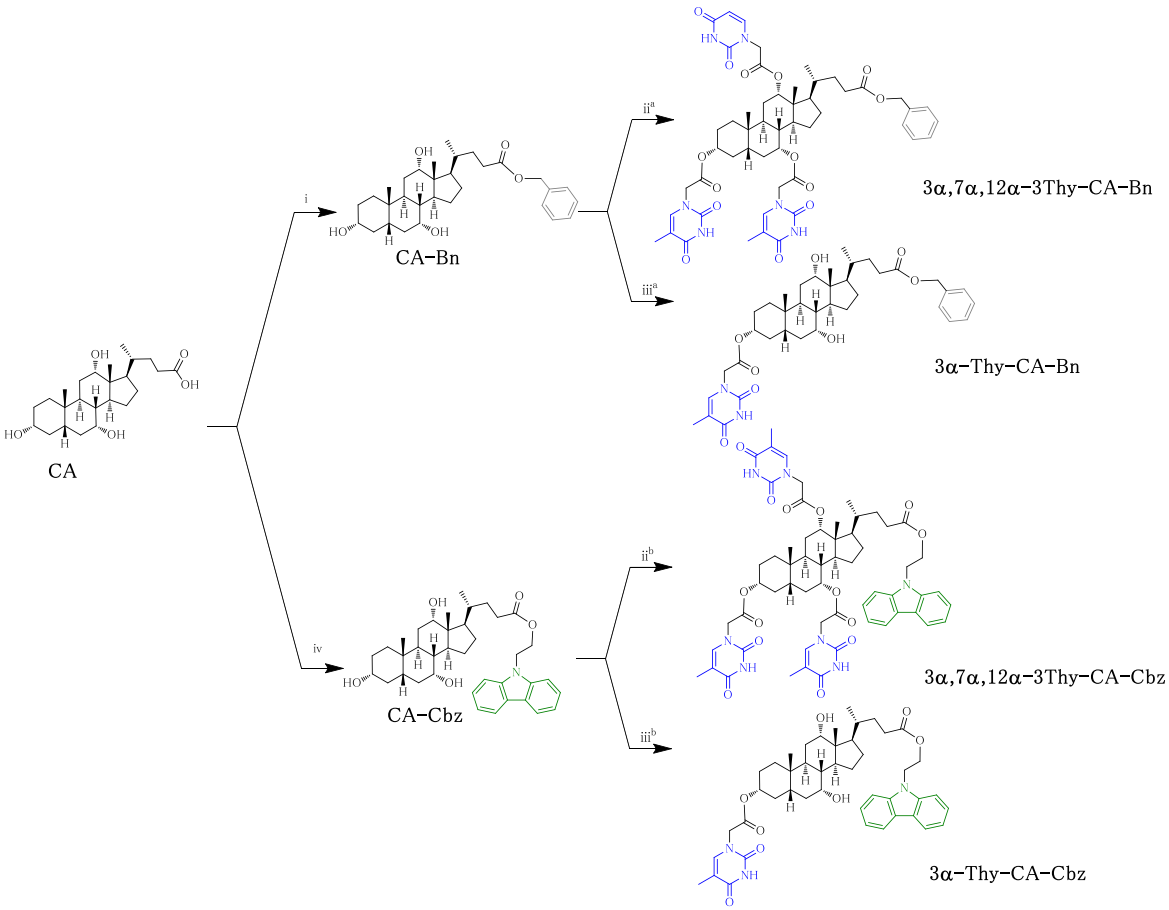

Scheme 7.1. Developed synthetic strategy to prepare the derivatives from CA with different number of Thy units and incorporating or lacking Cbz. Reagents and conditions: (i) benzyl bromide, DBU, DMF, (98%); (ii) Thy–CH_2COOH, Et_3N, 2,4,6-trichlorobenzoyl chloride, 4-DMAP, THF [a](98%), [b](64%); (iii) Thy–CH_2–COOH, 4-DMAP, EDC, DMF, [a](56%), [b](68%); iv) Cbz–$(CH_2)_2$–OH, TBTU, DIEA, DMF, (70%).

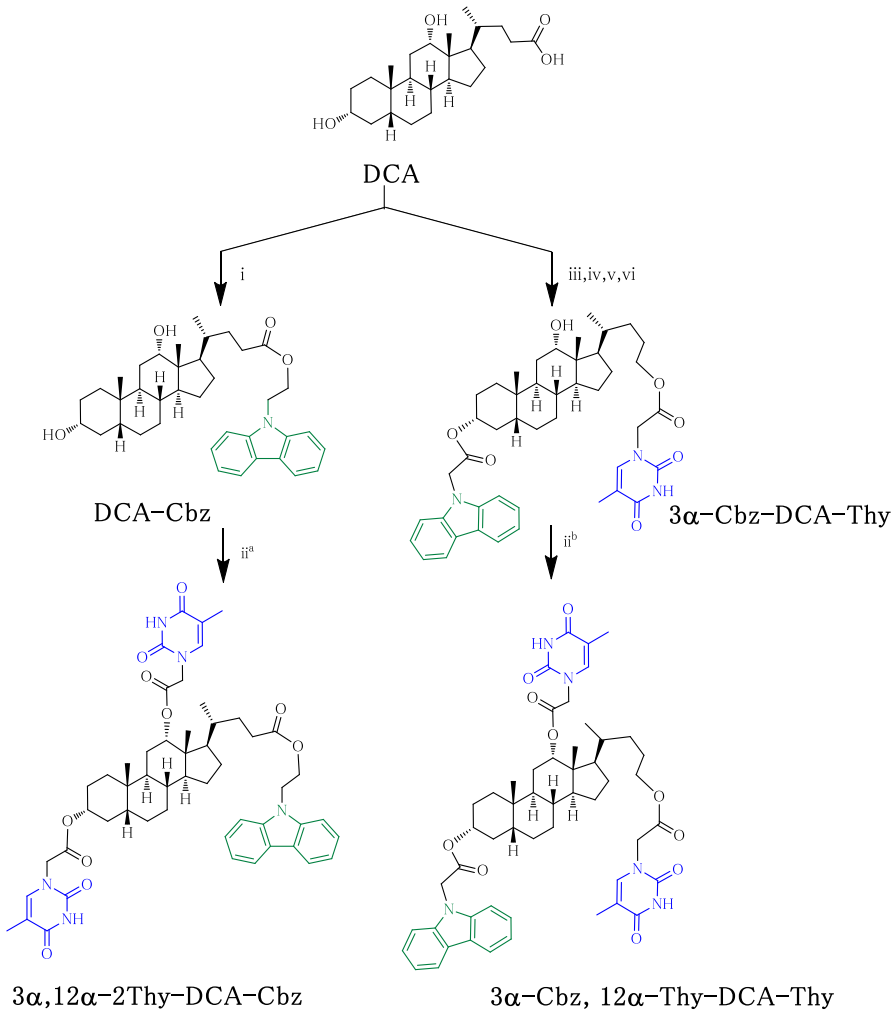

Scheme 7.2. Developed synthetic strategy to prepare the derivatives from DCA incorporating Cbz and one or two Thy units at different relative positions. Reagents and conditions: (i) Cbz–CH_2CH_2OH, TBTU, DIEA, DMF (67%); (ii) Thy–CH_2COOH, Et_3N, 2,4,6–trichlorobenzoyl chloride, 4–DMAP, THF [a](77%), [b](60%); (iii) benzyl bromide, DBU, DMF (57%); (iv) $LiAlH_4$, refluxing THF (87%); (v) Thy–CH_2COOH, TBTU, DIEA, DMF (56%); (vi) Cbz–CH_2–COOH, TBTU, DIEA, DMF (43%).

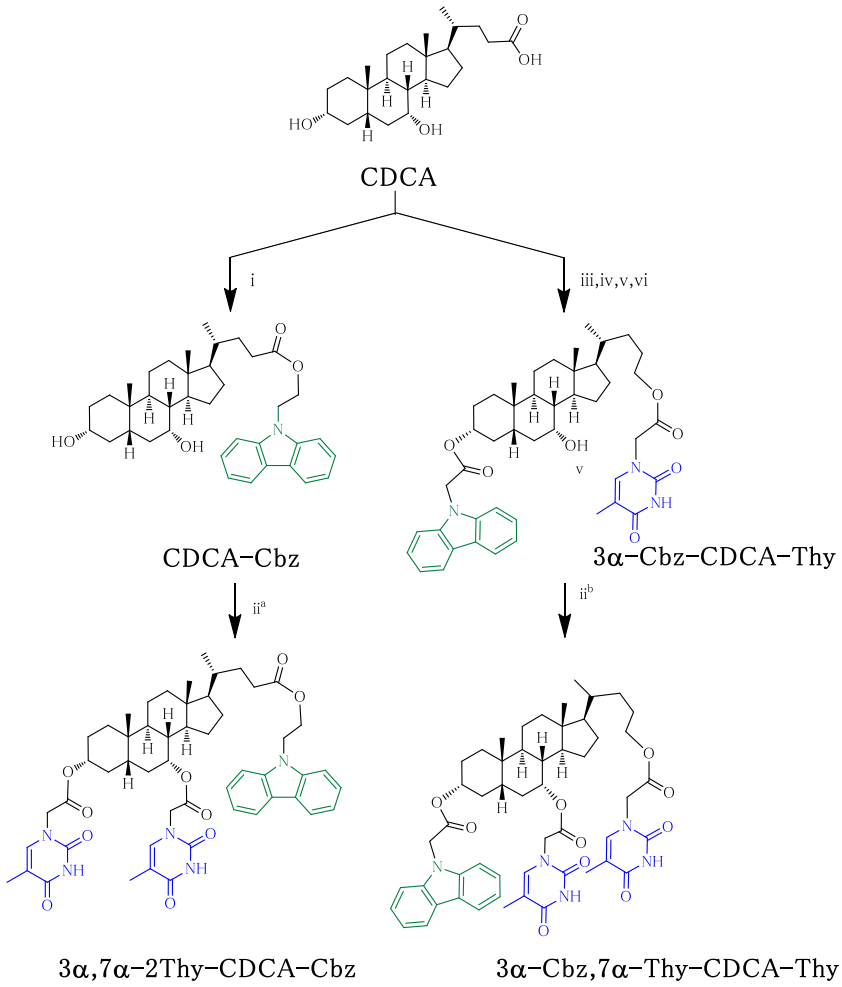

Scheme 7.3 Developed synthetic strategy to prepare the derivatives from CDCA incorporating Cbz and one or two Thy units at different relative positions. Reagents and conditions: (i) Cbz–CH_2CH_2OH, TBTU, DIEA, DMF (94%); (ii) Thy–CH_2COOH, Et_3N, 2,4,6-trichlorobenzoyl chloride, 4-DMAP, THF [a](38%), [b](21%); (iii) benzyl bromide, DBU, DMF (97%); (iv) $LiAlH_4$, refluxing THF (61%); (v) Thy–CH_2COOH, TBTU, DIEA, DMF (72%); (vi) Cbz–CH_2–COOH, TBTU, DIEA, DMF (45%).

7.3. Results and discussion

7.3.1. Photophysics

In order to check the reactivity of Cbz as a Thy<>Thy photosensitizer, laser flash photolysis (LFP) was employed, and the triplet lifetime of Cbz was monitored upon excitation at 308 nm. The potential differences in the triplet lifetime of ^{3}Cbz* depending on the number and relative position of Thy units in the BA skeleton could give useful information about the excited state interactions in the initial step of the generation of Thy<>Thy *via* TTET. Intermolecular Cbz quenching by Thy was firstly studied, followed by the intramolecular quenching in the BA derivatives incorporating Cbz and different number of Thy units in their structure (Figure 7.3) together with their corresponding controls.

In the intermolecular experiment, the decay of the signal attributed to ^{3}Cbz* was recorded at its maximum (420 nm) upon addition of one, two and three equivalents of thymidine (Thd) (Figure 7.4, left), and these data were fitted to a first order exponential equation. The corresponding lifetimes were fitted to a Stern–Volmer equation (Figure 7.4, right), and the value for the intermolecular quenching constant was obtained from the slope of the linear fitting (k_q= 4.9 x 10^8 $M^{-1}s^{-1}$).

Second, the influence of the number (one, two or three) of Thy units and also their relative positions was investigated in the systems that incorporate the Cbz moiety. Hence, the decay of the derivatives incorporating Cbz in the lateral chain of the BA skeleton (**3α,12α-2Thy-DCA-Cbz**, **3α,7α-2Thy-CDCA-Cbz** and **3α,7α,12α-3Thy-CA-Cbz**) together with their controls **CA-Cbz** and **3α-Thy-CA-Cbz** was recorded at 420 nm (Figure 7.5). A decrease in the triplet lifetime of ^{3}Cbz* when a Thy is present at 3α- (**3α-Thy-CA-Cbz**) was observed, indicating an efficient TTET through-bond as described in more detail in Chapter 4. Nevertheless, a dramatic decrease in the lifetime (down to few ns, basically below the duration of the laser pulse) was found when two or three Thy units were attached to the skeleton (**3α,12α-2Thy-**

DCA–Cbz, **3α,7α-2Thy–CDCA–Cbz** and **3α,7α,12α-3Thy–CA–Cbz**), with apparently small differences between the three systems.

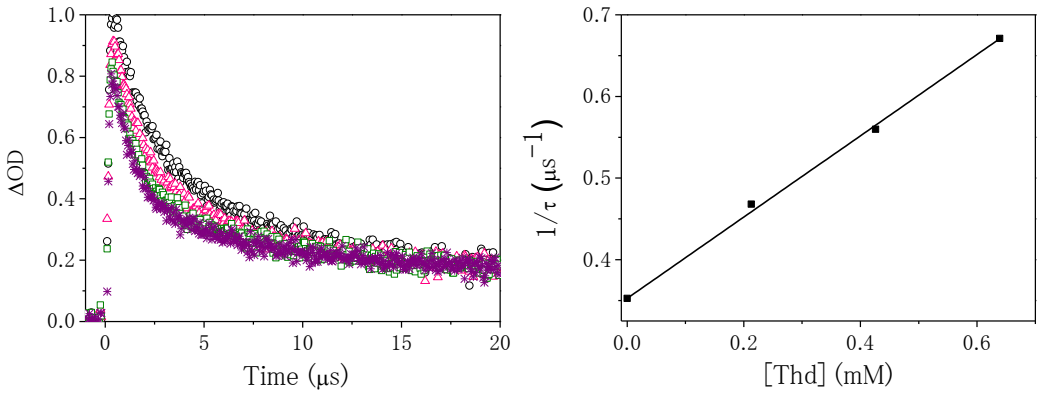

Figure 7.4. Left: LFP decays obtained upon selective excitation of Cbz at 308 nm and monitored at 420 nm for Cbz (○) and the intermolecular mixtures, 1Thd:1Cbz (△), 2Thd:1Cbz (□) and 3Thd:1Cbz (*) in deaerated $4CH_3CN:1H_2O$. **Right:** Stern–Volmer plot for the quenching of $^3Cbz^*$ by Thd.

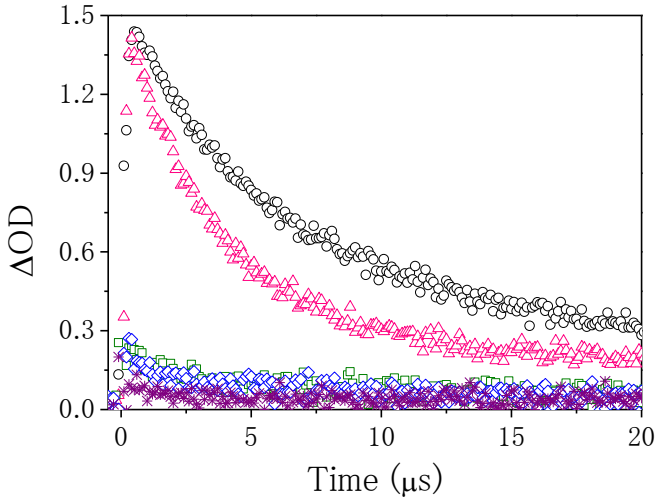

Figure 7.5. LFP decays monitored at 420 nm upon selective excitation of Cbz at 308 nm in **CA–Cbz** (○), **3α-Thy–CA–Cbz** (△), **3α,12α-2Thy–DCA–Cbz** (□), **3α,7α-2Thy–CDCA–Cbz** (*) and **3α,7α,12α-3Thy–CA–Cbz** (◇) in $4CH_3CN:1H_2O$.

The intramolecular TTET process was further investigated in the two systems in which the Cbz unit is attached at 3α- (**3α-Cbz,12α-Thy-DCA-Thy** and **3α-Cbz,7α-Thy-CDCA-Thy**) and compared to their corresponding controls (**3α-Cbz-DCA-Thy** and **3α-Cbz -CDCA-Thy**, respectively). For this purpose, they were also submitted to selective LFP excitation at 308 nm and their decays at 420 nm were plotted in Figure 7.6. Again, the introduction of a Thy in the BA structure results in a marked decrease in the ^{3}Cbz* lifetime due to TB-TTET, that is slightly less efficient than the one observed in the previous **3α-Thy-DCA-Cbz**; whereas the introduction of the second Thy produced a dramatic diminishing in the lifetime of ^{3}Cbz*, as observed when Cbz was introduced in the lateral chain. No other transient species were envisaged in the studied compounds since the introduction of the *N*-substituted Cbz prevents formation of the carbazolyl radical. Moreover, in the cases in which only one Thy is present and the TTET can only happen TB, the corresponding ^{3}Thy* was not unequivocally inferred due to the overlap between ^{3}Cbz* and ^{3}Thy* as well as the low extinction coefficient of ^{3}Thy*.

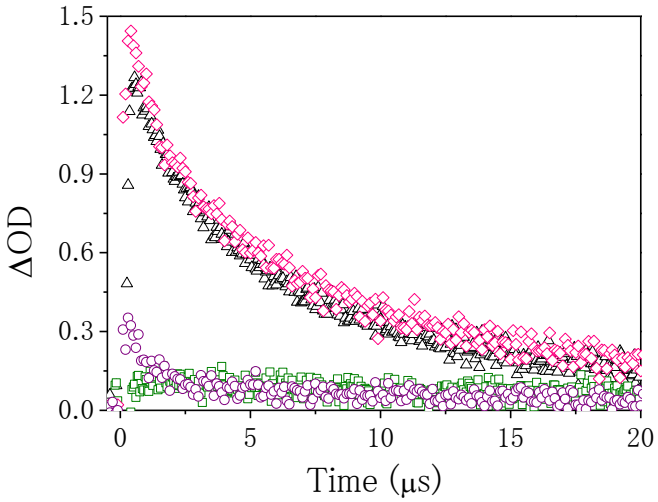

Figure 7.6. LFP decays monitored at 420 nm of the intramolecular samples **3α-Cbz-DCA-Thy** (Δ), **3α-Cbz,12α-Thy-DCA-Thy** (□), **3α-Cbz-CDCA-Thy** (◊) and **3α-Cbz,7α-Thy-CDCA-Thy** (○) in deaerated 4CH_3CN:1H_2O.

There is not any other competitive process in these systems, such as hydrogen-abstraction, so although TTET from Cbz to Thy is slightly disfavored (triplet energies of 70.2[22] and 74[131] kcal mol^{-1} for Cbz and Thy, respectively), formation of Thy<>Thy is still expected.

In fact, the above results show that in the systems containing only one Thy, the TTET from Cbz to Thy is efficient despite it only can occur through-bond, since the distance between them prevents though-space TTET, as it has been deeper studied in Chapter 4 of this Thesis. Nevertheless, when including more Thy units, through space TTET plays a major role due to the proximity between Cbz and the Thys.

7.3.2. Photochemistry

First, direct formation of the different Thy<>Thy was investigated to have in hand the dimers that were subsequently submitted to intermolecular photosensitized repair. Hence, the direct reactivity of the derivatives **3α,12α-2Thy-DCA-Bn**, **3α-Pa, 12α-Thy-DCA-Thy**, **3α,7α-2Thy-CDCA-Bn** and **3α-Bz, 7α-Thy-CDCA-Thy** was evaluated by independent irradiation of these compounds with lamps centered at 260 nm, followed by column chromatography purification to isolate the corresponding photoproducts. In all cases, only one Thy<>Thy was isolated, namely **3α,12α-Thy<>Thy-DCA-Bn**, **3α-Pa-DCA-12α-Thy<>Thy**, **3α,7α-Thy<>Thy-CDCA-Bn** and **3α-Bz-CDCA-7α-Thy <>Thy** (Figure 7.7). These compounds have already been obtained and characterized in this Thesis using intermolecular Bzp photosensitization as described in Chapter 5 (page 153 and 154).

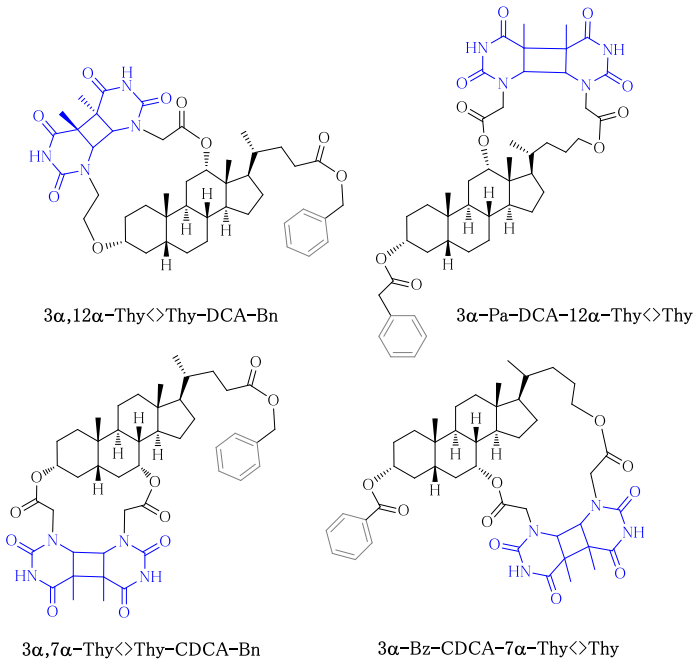

Figure 7.7. Chemical structure of the dimers obtained from the direct irradiation (λ_{max} = 260 nm) of **3α,12α-2Thy-DCA-Bn** (top, left), **3α-Pa, 12α-Thy-DCA-Thy** (top, right), **3α,7α-2Thy-CDCA-Bn** (bottom, left) and **3α-Bz, 7α-Thy-CDCA-Thy** (bottom, right) in CH_3CN under N_2.

Second, the systems exhibiting two Thys and the Cbz (see Figure 7.3), were submitted to steady-state photolysis in order to investigate the nature of the obtained photoproducts.

Initially, selective irradiation of the Cbz at λ_{max}= 300 nm through a Pyrex filter, was monitored at different irradiation times attending at the changes in the spectra at 260 nm, where the Thy chromophore has a maximum. The controls Thy, Cbz and the intermolecular 1Cbz:2Thy mixture, showed a slight decrease in the absorbance at 260 nm (Figure 7.8); however, the derivatives **3α,7α-2Thy-CDCA-Cbz** and **3α-Cbz,7α-Thy-CDCA-Thy** showed a progressive decrease in the absorbance due to Thy. Nevertheless, the derivatives coming from DCA, **3α,12α-2Thy-DCA-Cbz** and **3α-Cbz,12α-Thy-DCA-Thy** were the most reactive ones. Therefore, these results showed

a different reaction pattern between the derivatives of CDCA and DCA that can be associated with the different relative position of the Cbz and the two Thys.

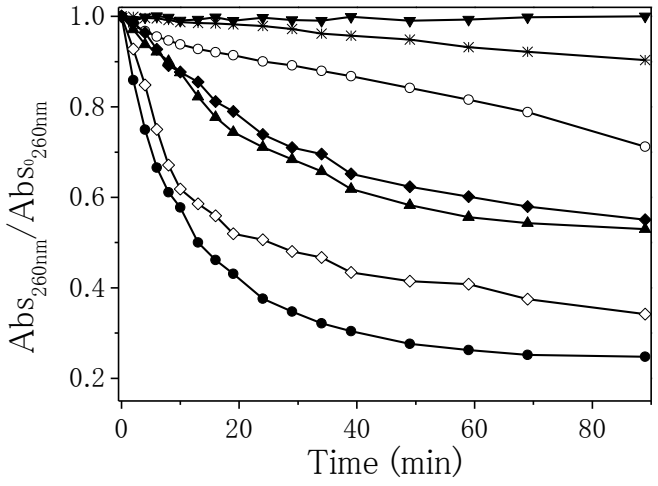

Figure 7.8. Photoreaction kinetics of Thy (▼), Cbz (*), the intermolecular 2Thy:1Cbz mixture (○) and the intramolecular systems **3α,12α-2Thy-DCA-Cbz** (●), **3α-Cbz,12α-Thy-DCA-Thy** (◊), **3α,7α-2Thy-CDCA-Cbz** (▲) and **3α-Cbz,7α-Thy-CDCA-Thy** (⧫), upon irradiation at 300 nm in deareated 4ACN:1H_2O.

Then, the four compounds (**3α,12α-2Thy-DCA-Cbz**; **3α-Cbz,12α-Thy-DCA-Thy**; **3α,7α-2Thy-CDCA-Cbz** and **3α-Cbz,7α-Thy-CDCA-Thy**) were independently irradiated (λ_{max}= 350 nm) in acetonitrile, under inert atmosphere, and the resulting photoproducts were isolated and characterized.

For the case of derivatives **3α,12α-2Thy-DCA-Cbz** and **3α-Cbz,12α-Thy-DCA-Thy**, only one Thy<>Thy dimer was isolated in each case in 54% and 35%, respectively (Scheme 7.4). These photoproducts were characterized by ^{1}H and ^{13}C spectroscopy, together with exact mass; however, the difficulties in the NOEDIFF experiments, due to the NOE zero zone fulfilled by these molecules as a result of their high molecular mass (917.46 g mol^{-1}), did not enable for the unequivocal establishment of

the stereochemistry of the cyclization achieved in each case. Attempts to obtain a crystal to submit to X-Rays analysis were also unsuccessful in both cases.

Unexpectedly, irradiation of **3α,7α-2Thy-CDCA-Cbz** or **3α-Cbz,7α-Thy-CDCA-Thy**, did not produce any photoproduct. Long irradiation times only gave polymerization.

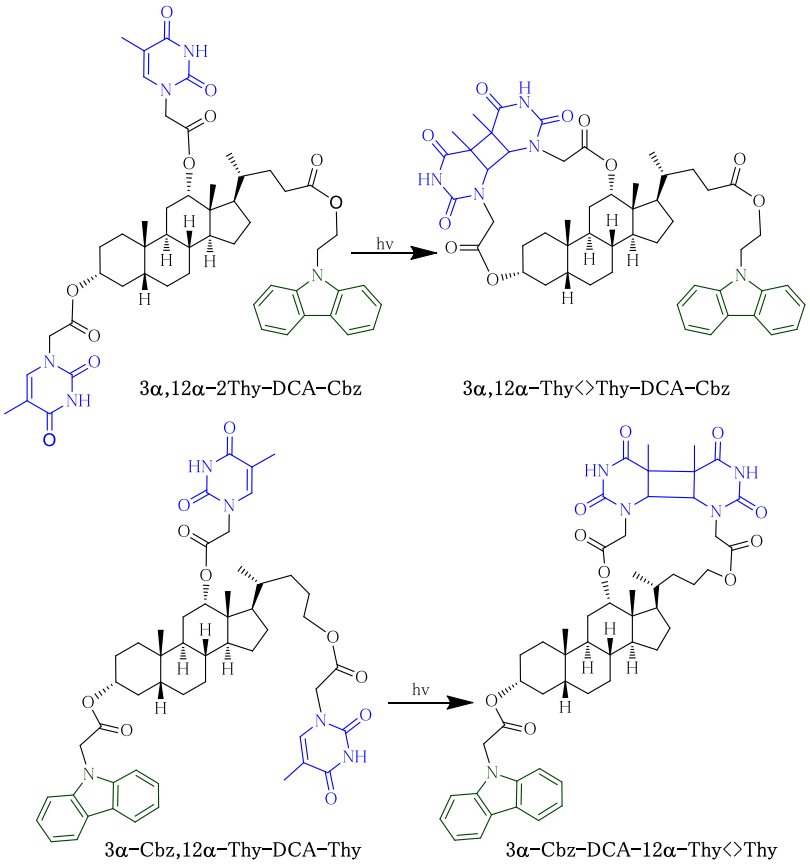

Scheme 7.4. Irradiation (λ_{max} = 350 nm) of **3α,12α-2Thy-DCA-Cbz** (top) and **3α-Cbz,12α-Thy-DCA-Thy** (bottom) in CH_3CN under N_2 to give **3α,12α-Thy<>Thy-DCA-Cbz** (54%) and **3α-Cbz, -DCA-12α-Thy <>Thy** (35%).

7.4. Conclusions and further experiments

Direct formation of Thy<>Thy from **3α,12α-2Thy-DCA-Bn**, **3α-Pa, 12α-Thy-DCA-Thy**, **3α,7α-2Thy-CDCA-Bn** and **3α-Bz,7α-Thy-CDCA-Thy** was accomplished. Moreover, the intramolecular Cbz photosensitized formation of Thy<>Thy was achieved in the case of the DCA derivatives (**3α,12α-2Thy-DCA-Cbz** and **3α-Cbz, 12α-Thy-DCA-Thy**), being the isolated photoproducts in agreement with the LFP experiments. However, although a significant quenching of ^{3}Cbz* was observed in the LFP experiments for the CDCA derivatives (**3α,7α-2Thy-CDCA-Cbz** and **3α-Cbz, 7α-Thy-CDCA-Thy**) no photoproducts were isolated in the steady-state irradiation of the samples.

In future experiments, repair of the dimers **3α,12α-Thy<>Thy-DCA-Bn**, **3α-Pa-DCA-12α-Thy<>Thy**, **3α,7α-Thy<>Thy-CDCA-Bn** and **3α-Bz-CDCA-7α-Thy<>Thy** upon intermolecular Cbz-photosensitization will be compared to the intramolecular photosensitized repair of dimers **3α,12α-Thy<>Thy-DCA-Cbz** and **3α-Cbz-DCA-12α-Thy<>Thy**. For this purpose, the Cbz-mediated photoreversion will be first followed by UV, monitoring the rise of the absorption band of the Thy, and also by HPLC. Moreover, additional emission studies will provide kinetic valuable data to understand the overall process.

7.5. Experimental

7.5.1. Synthesis and characterization

7.5.1.1. Synthesis of CA-Bn

To a stirred solution of **CA** (0.5 g, 1.2 mmol) in anhydrous DMF (0.2 mL), DBU was added (0.2 mL, 1.35 mmol). Ten minutes later, benzyl bromide (0.16 mL, 1.35 mmol) was added dropwise, and the solution was allowed to react overnight at rt. Then, the solvent was evaporated and the crude was redissolved with EtOAc, washed with $NaHCO_3$ (5%), HCl 1M and brine, dried over $MgSO_4$ and concentrated under reduced pressure. Purification by column chromatography (SiO_2, EtOAc:Hexane, 90:10) gave **CA-Bn** as a colorless solid (0.60 g, 98%); ^{1}H NMR (300 MHz, $CDCl_3$): δ (ppm) 0.64 (s, 3H, CH_3); 0.82–3.11 (complex signal, 24H); 0.87 (s, 3H, CH_3); 0.96 (d, J = 6.0 Hz, 3H, 21–CH_3); 3.43 (m, 1H, 3β–H); 3.82 (br s, 1H, 7β–H); 3.94 (br s, 1H, 12β–H); 5.08 (d, J = 12.3 Hz, 1H, CH_2); 5.13 (d, J = 12.3 Hz, 1H, CH_2); 7.37–7.28 (m, 5H, arom); ^{13}C NMR (75 MHz, $CDCl_3$): δ (ppm) 174.2 (C), 136.2 (C), 128.6 (2xCH), 128.4 (2xCH), 128.3 (CH), 73.2 (CH), 72.0 (CH), 68.6 (CH), 66.2 (CH_2), 47.2 (CH), 46.6 (C), 41.8 (CH), 41.6 (CH), 39.7 (CH_2), 39.6 (CH), 35.4 (CH_2), 35.3 (CH), 34.9 (C), 34.8 (CH_2), 31.4 (CH_2), 31.0 (CH_2), 30.6 (CH_2), 28.3 (CH_2), 27.6 (CH_2), 26.5 (CH), 23.3 (CH_2), 22.6 (CH_3), 17.4 (CH_3), 12.6 (CH_3); m/z found 499.3427, calculated for $C_{31}H_{47}O_5$ (MH^+) 499.3424.

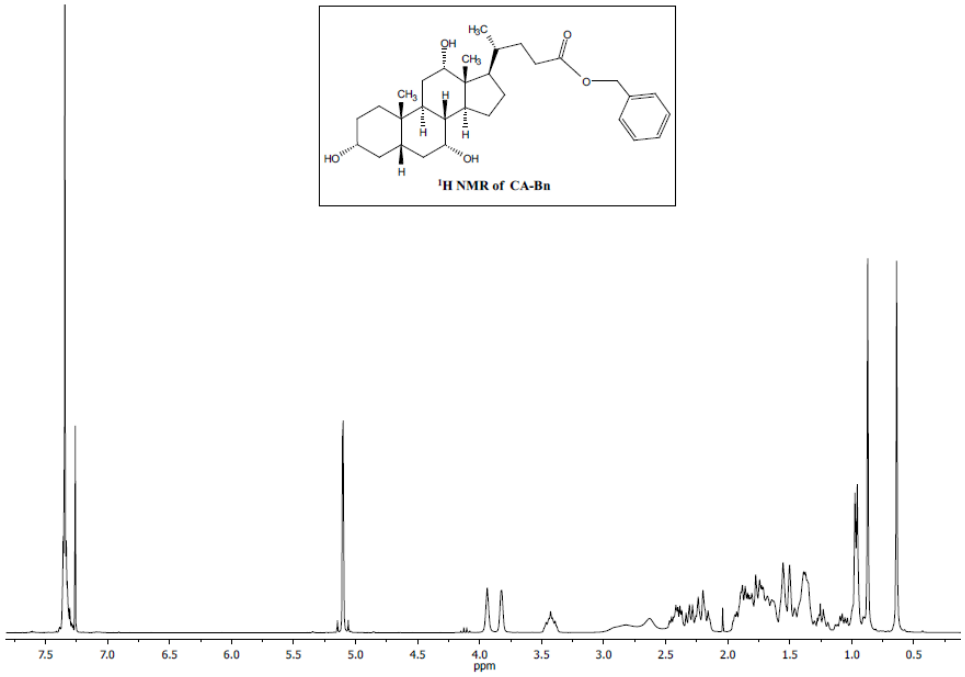
^{1}H NMR of CA-Bn
7.5
7.0
6.5
6.0
5.5
5.0
4.5
4.0
3.5
3.0
2.5
2.0
1.5
1.0
0.5
ppm

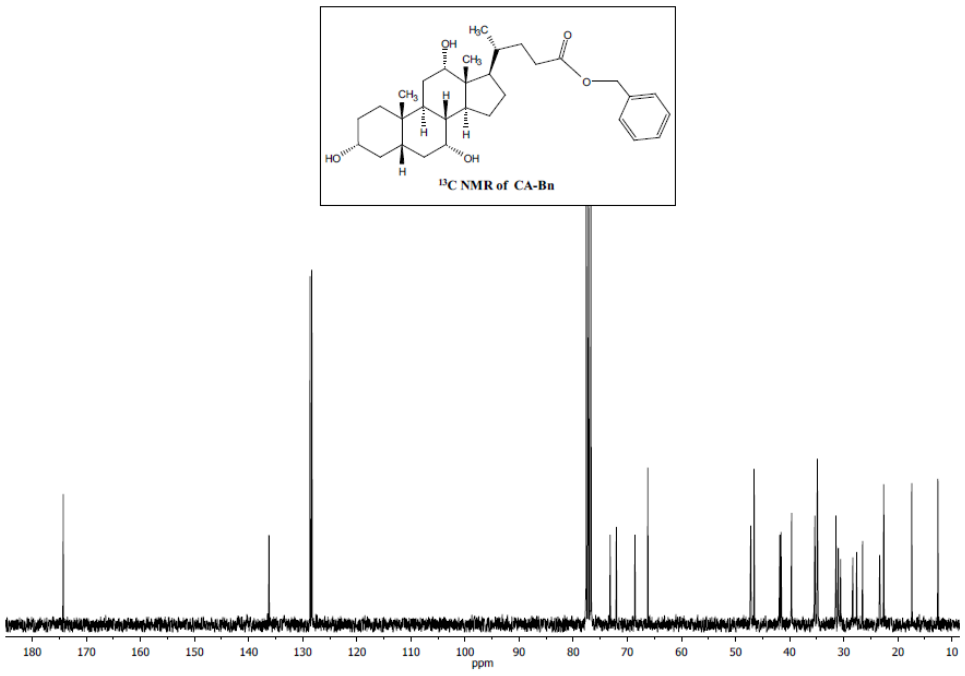
^{13}C NMR of CA-Bn
180
170
160
150
140
130
120
110
100
90
80
70
60
50
40
30
20
10
ppm

7.5.1.2. Synthesis of 3α-Thy-CA-Bn

To a stirred solution of Thy-CH_2-COOH (2.2 g, 12.03 mmol) in anhydrous DMF (15 mL), a solution of 4-DMAP (0.49 g, 4.01 mmol) and **CA-Bn** (2.00 g, 4.01 mmol) in DMF (5 mL) was added dropwise. Then the resulting suspension was cooled at 0°C, EDC (2.13 mL, 12.03 mmol) was added and after one hour at 0°C, the reaction mixture was allowed to stir overnight at rt. Then, the suspension was poured into HCl 1M, extracted with CH_2Cl_2 and the combined organic extracts were washed with brine, dried over $MgSO_4$ and concentrated. After purification by column chromatography (SiO_2, EtOAc :Hexane, 70:30) followed by (Li Chroprep RP-18, CH_3CN:H_2O, 60:40), **3α-Thy-CA-Bn** was obtained as a colorless solid (1.49 g, 56%); ^{1}H NMR (300 MHz, $CDCl_3$): δ (ppm) 0.65 (s, 3H, CH_3); 0.82-2.10 (complex signal, 22H); 0.89 (s, 3H, CH_3); 0.96 (d, *J* = 6.0 Hz, 3H, 21-CH_3); 1.85 (*br* s, 3H, Thy-CH_3); 2.32 (m, 2H, CH_2); 3.84 (*br* s, 1H, 7β-H); 3.97 (*br* s, 1H, 12β-H); 4.33 (d, *J* = 16.5 Hz, 1H, Thy-CH_2); 4.49 (d, *J* = 16.5 Hz, 1H, Thy-CH_2); 4.57 (m, 1H, 3β-H); 5.07 (d, *J* = 12.3 Hz, 1H, CH_2); 5.12 (d, *J* = 12.3 Hz, 1H, CH_2); 7.14 (s, 1H, Thy-CH) 7.27-7.37 (m, 5H, arom); 10.10 (*br* s, 1H, Thy-NH); ^{13}C NMR (75 MHz, $CDCl_3$): δ (ppm) 174.2 (C), 167.8 (C), 164.7 (C), 151.5 (C), 141.5 (CH), 136.2 (C), 128.6 (2xCH), 128.3 (2xCH), 128.2 (CH), 110.4 (C), 76.7 (CH), 72.6 (CH), 68.2 (CH), 66.2 (CH_2), 49.9 (CH_2), 47.2 (CH), 46.4 (C), 42.1 (CH), 41.2 (CH), 39.7 (CH), 35.1 (CH), 35.0 (CH_2), 34.9 (CH_2), 34.8 (C), 34.5 (CH_2), 31.3 (CH_2), 31.1 (CH_2), 28.5 (CH_2), 27.5 (CH_2), 26.7 (CH), 26.2 (CH_2), 23.3 (CH_2), 22.6 (CH_3), 17.3 (CH_3), 12.6 (CH_3), 12.3 (CH_3); m/z found 665.3812, calculated for $C_{38}H_{53}N_2O_8$ (MH^+) 665.3802.

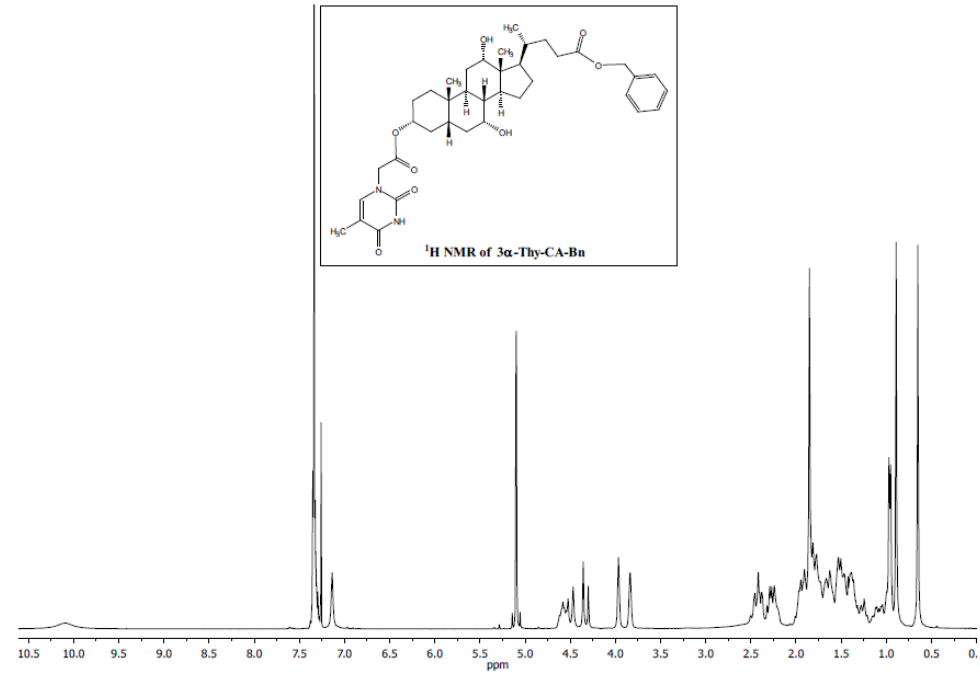
^{1}H NMR of 3α-Thy-CA-Bn
10.5 10.0 9.5 9.0 8.5 8.0 7.5 7.0 6.5 6.0 5.5 5.0 4.5 4.0 3.5 3.0 2.5 2.0 1.5 1.0 0.5
ppm

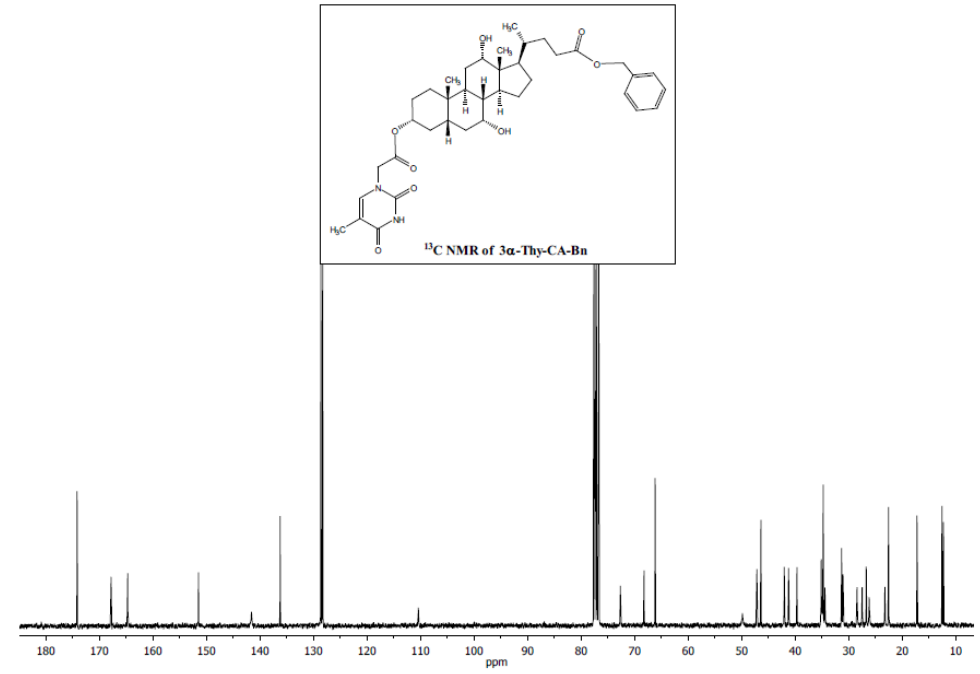
^{13}C NMR of 3α-Thy-CA-Bn
180 170 160 150 140 130 120 110 100 90 80 70 60 50 40 30 20 10
ppm

7.5.1.3. Synthesis of 3α,7α,12α-3Thy-CA-Bn

A stirred suspension of Thy-CH_2-COOH (3.33 g, 18.06 mmol) in anhydrous THF (120 mL) was treated with Et_3N (5.0 mL) and 2,4,6-trichlorobenzoyl chloride (3.45 mL, 22.08 mmol) and the resulting mixture was allowed to react for 1.5 h. Then, a solution of 4-DMAP (0.299 g, 2.45 mmol) and **CA-Bn** (1 g, 2.01 mmol) in anhydrous THF (30 mL) was added and stirred overnight. Afterwards, the reaction mixture was poured into $NaHCO_3$ (5%), extracted with CH_2Cl_2 and the combined extracts were washed with brine, dried over $MgSO_4$ and concentrated under vacuum. Purification by column chromatography (SiO_2, CH_2Cl_2:MeOH, 97:3) followed by (Li Chroprep RP-18, CH_3CN:H_2O, 70:30), gave **3α,7α,12α-3Thy-CA-Bn** as a yellow oil (1.96 g, 98%); ^{1}H NMR (300 MHz, $CDCl_3$): δ (ppm) 0.66 (s, 3H, CH_3); 0.75 (d, *J* = 6.0 Hz, 3H, 21-CH_3); 0.86 (s, 3H, CH_3); 0.92-2.00 (complex signal, 22H); 1.84 (s, 3H, Thy-CH_3); 1.87 (s, 3H, Thy-CH_3); 1.91 (s, 3H, Thy-CH_3); 2.32 (m, 2H, CH_2) 4.29-4.63 (m, 7H, 3xThy-CH_2+3β-H); 4.91 (*br* s, 1H, 7β-H); 5.08 (m, 3H, CH_2+12β-H); 7.02 (s, 1H, Thy-CH); 7.06 (s, 1H, Thy-CH); 7.11 (s, 1H, Thy-CH); 7.27-7.37 (m, 5H, arom); 10.41 (s, 1H, Thy-NH); 10.47 (s, 1H, Thy-NH); 10.60 (s, 1H, Thy-NH); ^{13}C NMR (75 MHz, $CDCl_3$): δ (ppm) 173.8 (C), 167.6 (C), 167.4 (2xC), 165.2 (C), 165.0 (C), 164.7 (C), 151.9 (C), 150.8 (2xC), 141.0 (CH), 140.8 (2xCH), 136.0 (C), 128.6 (2xCH), 128.4 (2xCH), 128.3 (CH), 111.1 (C), 110.6 (2xC), 77.3 (CH), 75.9 (CH), 72.9 (CH), 66.3 (CH_2), 49.7 (CH_2), 49.3 (CH_2), 49.2 (CH_2), 47.6 (CH), 45.3 (C), 43.5 (CH), 40.5 (CH), 37.7 (CH), 34.7 (CH), 34.4 (CH_2), 34.2 (CH_2+C), 31.5 (CH_2), 30.9 (CH_2), 30.7 (CH_2), 28.9 (CH), 27.1 (CH_2), 26.1 (CH_2), 25.4 (CH_2), 22.7 (CH_2), 22.5 (CH_3), 17.6 (CH_3), 12.4 (2xCH_3), 12.3 (CH_3), 12.2 (CH_3); m/z found 997.4525, calculated for $C_{52}H_{65}N_6O_{14}$ (MH^+) 997.4559.

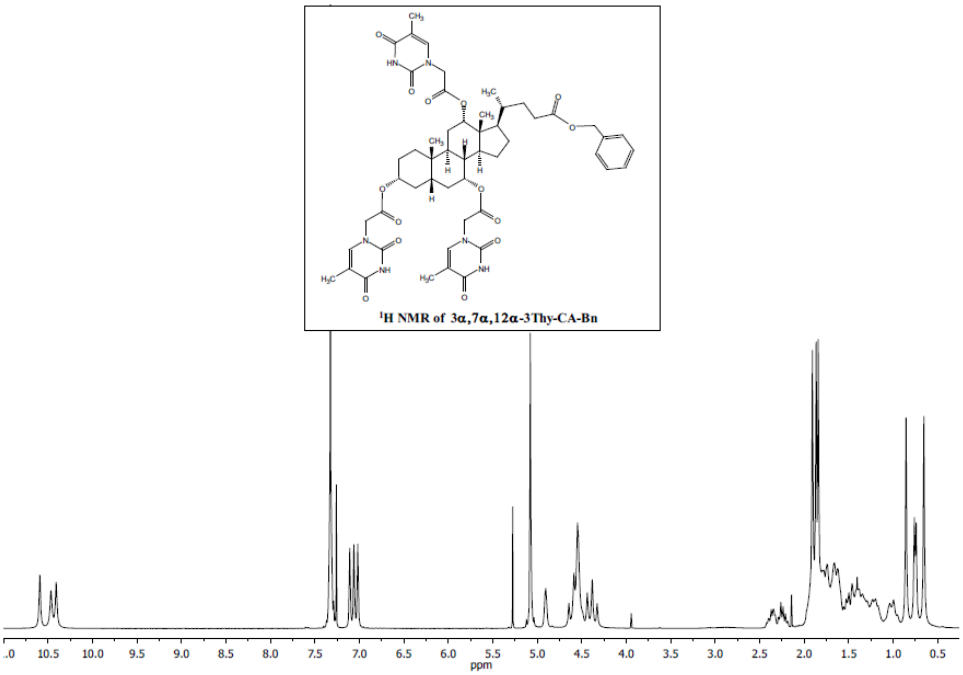
^{1}H NMR of 3α,7α,12α-3Thy-CA-Bn
ppm

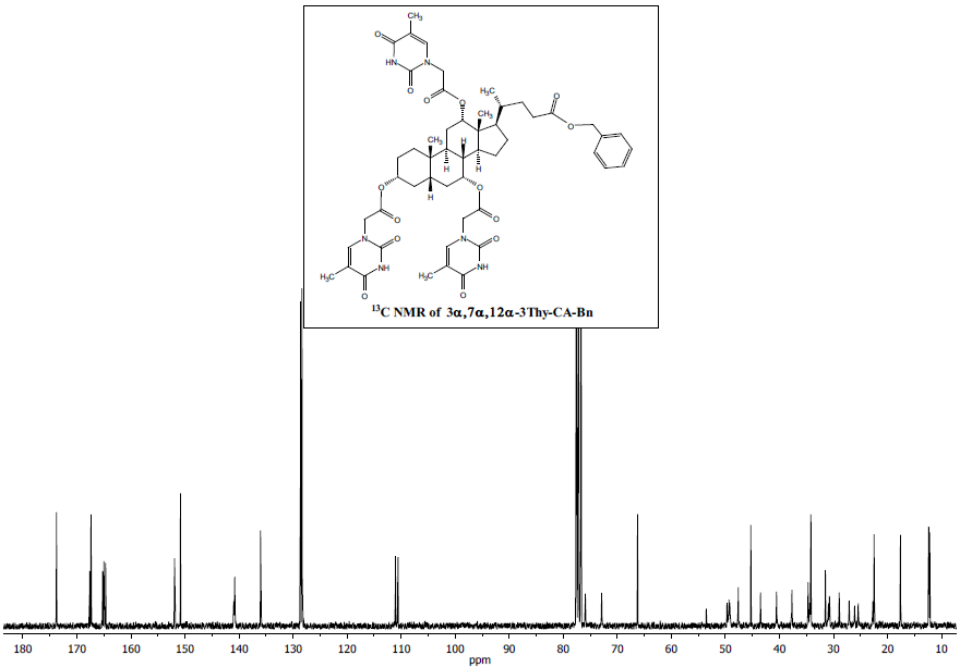
^{13}C NMR of 3α,7α,12α-3Thy-CA-Bn
ppm

7.5.1.4. Synthesis of CA–Cbz

To a stirred solution of Cbz–$(CH_2)_2$–OH (0.50 g, 2.25 mmol) and TBTU (0.87 g, 2.7 mmol) in anhydrous DMF (5 mL), **CA** (0.96 g, 2.36 mmol) in anhydrous DMF (4 mL) followed by DIEA (1.17 mL, 6.75 mmol) were added dropwise and then the reaction mixture was allowed to react overnight at rt. Afterwards, it was poured into brine and extracted with CH_2Cl_2; the combined organic layers were washed with brine, dried over $MgSO_4$ and concentrated under reduced pressure. Purification by column chromatography (SiO_2, EtOAc:Hexane, 95:5) followed by (Li Chroprep RP–18, CH_3CN:H_2O, 92:8) gave **CA–Cbz** as a white solid (0.99 g, 70%); ^{1}H NMR (300 MHz, $CDCl_3$): δ (ppm) 0.63 (s, 3H, CH_3); 0.76–2.49 (complex signal, 24H); 0.88 (s, 3H, CH_3); 0.90 (d, *J* = 6.0 Hz, 3H, 21–CH_3); 3.45 (m, 1H, 3β–H); 3.83 (*br* s, 1H, 7β–H); 3.91 (*br* s, 1H, 12β–H); 4.45 (m, 2H, CH_2); 4.54 (m, 2H, CH_2); 7.20–7.32 (m, 2H, arom); 7.37–7.55 (m, 4H, arom); 8.10 (d, *J* = 7.8 Hz, 2H, arom); ^{13}C NMR (75 MHz, $CDCl_3$) δ 174.2 (C), 140.4 (2xC), 125.8 (2xCH), 123.0 (2xC), 120.4 (2xCH), 119.3 (2xCH), 108.6 (2xCH), 73.1 (CH), 71.9 (CH), 68.5 (CH), 62.0 (CH_2), 47.0 (CH), 46.4 (C), 41.7 (CH_2), 41.5 (2xCH), 39.5 (CH+CH_2), 35.3 (CH_2), 35.2 (CH), 34.8 (C), 34.7 (CH_2), 31.2 (CH_2), 30.7 (CH_2), 30.4 (CH_2), 28.2 (CH_2), 27.5 (CH_2), 26.3 (CH), 23.2 (CH_2), 22.5 (CH_3), 17.3 (CH_3), 12.5 (CH_3); m/z found 602.3873, calculated for $C_{38}H_{52}NO_5$ (MH^+) 602.3845.

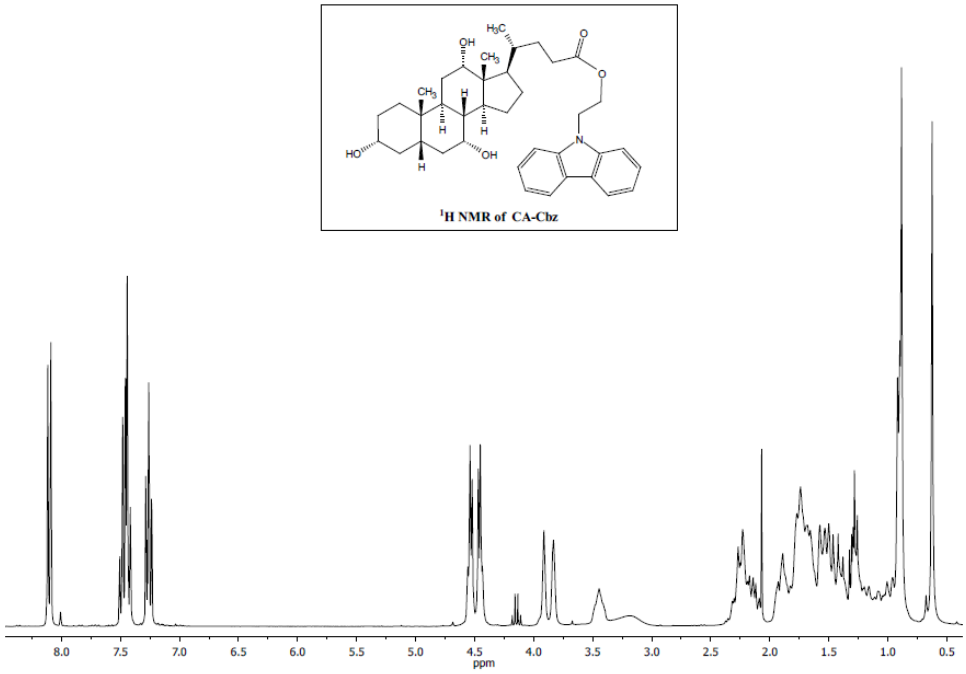
^{1}H NMR of CA-Cbz
8.0
7.5
7.0
6.5
6.0
5.5
5.0
4.5
4.0
3.5
3.0
2.5
2.0
1.5
1.0
0.5
ppm

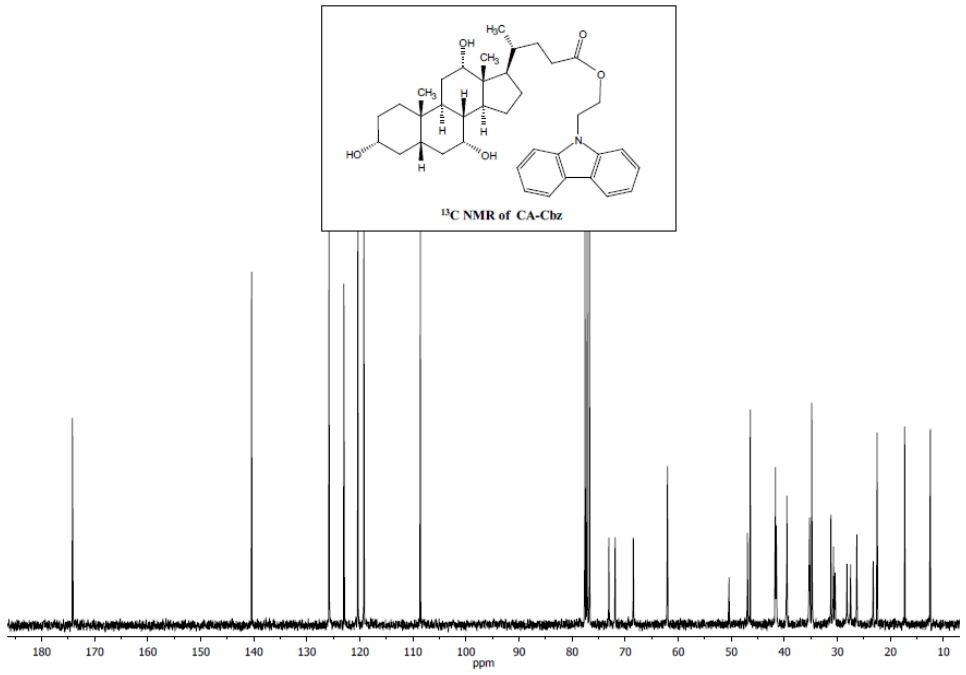
^{13}C NMR of CA-Cbz
180
170
160
150
140
130
120
110
100
90
80
70
60
50
40
30
20
10
ppm

7.5.1.5. Synthesis of 3α-Thy-CA-Cbz

To a stirred solution of Thy-CH_2-COOH (0.38 g, 2.05 mmol) in anhydrous DMF (2 mL), a solution of 4-DMAP (0.09 g, 0.75 mmol) and **CA-Cbz** (0.41 g, 0.68 mmol) in DMF (3 mL) was added dropwise. The resulting suspension was cooled at 0 °C, EDC (0.36 mL, 2.03 mmol) was added and after one hour at 0°C, the reaction mixture was allowed to stir overnight at rt. Then, the suspension was poured into brine, extracted with CH_2Cl_2 and the combined organic extracts were washed with brine, dried over $MgSO_4$ followed by (Li Chroprep RP-18, CH_3CN:H_2O, 92:8), **3α-Thy-CA-Cbz** was obtained as a colorless solid (0.36 g, 68%); ^{1}H NMR (300 MHz, $CDCl_3$): δ (ppm) 0.64 (s, 3H, CH_3); 0.78-2.51 (complex signal, 24H); 0.91 (*br* s, 6H, CH_3+21-CH_3); 1.87 (s, 3H, Thy-CH_3); 3.85 (*br* s, 1H, 7β-H); 4.00 (*br* s, 1H, 12β-H); 4.34 (d, *J* = 16.8 Hz, 1H, Thy-CH_2); 4.38-4.50 (m, 3H, Thy-CH_2+CH_2); 4.50-4.60 (m, 2H, CH_2); 4.61 (*br* s, 1H, 3β-H); 7.09 (s, 1H, Thy-CH); 7.20-7.32 (m, 2H, arom); 7.38-7.51 (m, 4H, arom); 8.10 (d, *J* = 7.5 Hz, 2H, arom); 10.16 (s, 1H, Thy-NH); ^{13}C NMR (75 MHz, $CDCl_3$) δ 174.2 (C), 167.7 (C), 164.7 (C), 151.4 (C), 141.3 (CH), 140.4 (2xC), 125.9 (2xCH), 123.0 (2xC), 120.4 (2xCH), 119.3 (2xCH), 110.5 (C), 108.6 (2xCH), 76.7 (CH), 72.7 (CH), 68.1 (CH), 62.0 (CH_2), 49.6 (CH_2), 47.0 (CH), 46.3 (C), 41.9 (CH), 41.7 (CH_2), 41.2 (CH), 39.6 (CH), 35.0 (CH), 34.9 (CH_2), 34.8 (CH_2), 34.7 (C), 34.4 (CH_2), 31.1 (CH_2), 30.8 (CH_2), 28.4 (CH_2), 27.4 (CH_2), 26.7 (CH), 26.2 (CH_2), 23.2 (CH_2), 22.5 (CH_3), 17.2 (CH_3), 12.5 (CH_3), 12.3 (CH_3); m/z found 768.4226, calculated for $C_{45}H_{58}N_3O_8$ (MH^+) 768.4224.

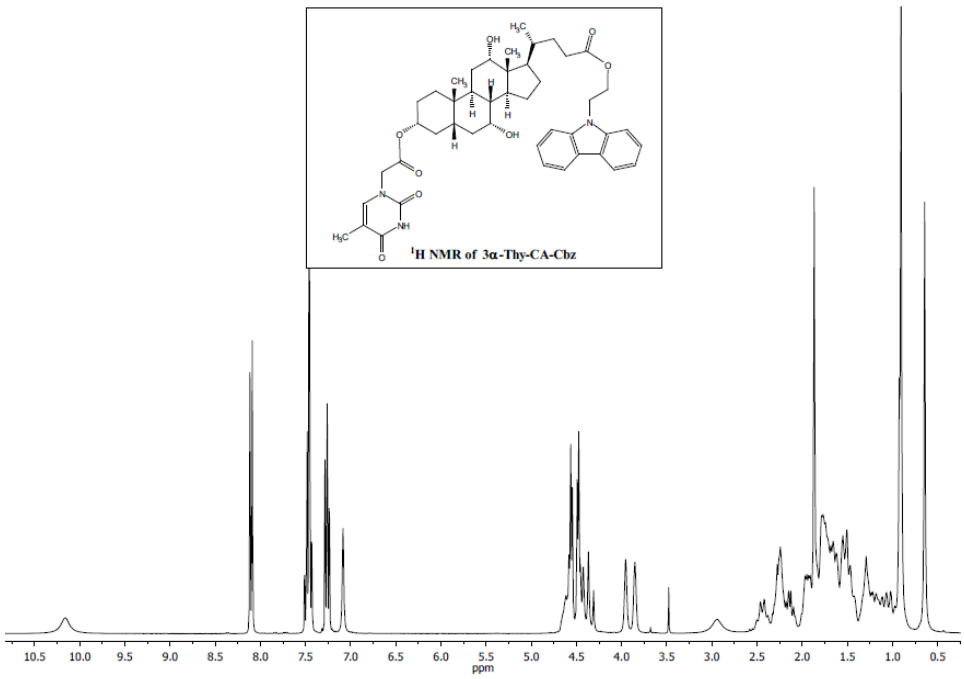
^{1}H NMR of 3α-Thy-CA-Cbz
10.5 10.0 9.5 9.0 8.5 8.0 7.5 7.0 6.5 6.0 5.5 5.0 4.5 4.0 3.5 3.0 2.5 2.0 1.5 1.0 0.5
ppm

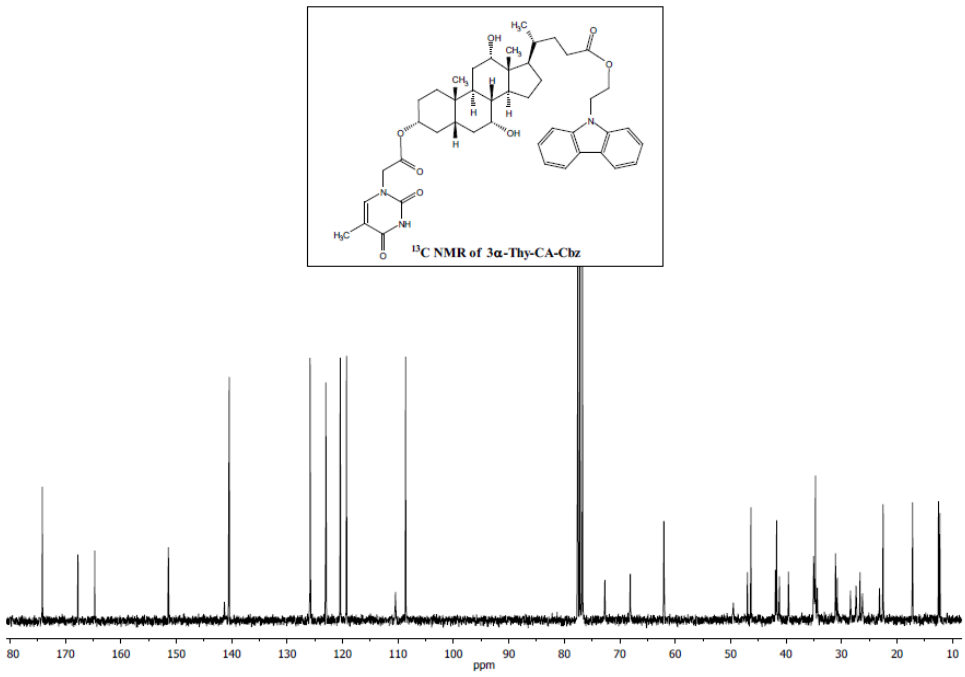
^{13}C NMR of 3α-Thy-CA-Cbz
80 170 160 150 140 130 120 110 100 90 80 70 60 50 40 30 20 10
ppm

7.5.1.6. Synthesis of 3α,7α,12α-3Thy-CA-Cbz

A stirred suspension of Thy-CH_2-COOH (0.80 g, 4.35 mmol) in anhydrous THF (19 mL) was treated with Et_3N (1.22 mL) and 2,4,6-trichlorobenzoyl chloride (0.82 mL, 5.22 mmol) and the resulting mixture was allowed to react for 1.5 h. Then, a solution of 4-DMAP (0.14 g, 1.14 mmol) and **CA-Cbz** (0.58 g, 0.97 mmol) in anhydrous THF (10 mL) was added and stirred overnight. Afterwards, the reaction mixture was poured into brine, extracted with CH_2Cl_2 and the combined extracts were washed with brine, dried over $MgSO_4$ and concentrated under vacuum. Purification by column chromatography (SiO_2, EtOAc:Hexane, 98:2) followed by (Li Chroprep RP-18, CH_3CN:H_2O, 70:30), gave **3α,7α,12α-3Thy-CA-Cbz** as a colorless oil (0.68 g, 64%); ^{1}H NMR (300 MHz, $CDCl_3$): δ (ppm) 0.64 (s, 3H, CH_3); 0.68 (d, *J* = 6.0 Hz, 3H, 21-CH_3); 0.76-2.26 (complex signal, 24H); 0.88 (s, 3H, CH_3); 1.82 (s, 3H, Thy-CH_3); 1.87 (s, 3H, Thy-CH_3); 1.92 (s, 3H, Thy-CH_3); 4.26-4.71 (m, 11H, 3xThy-CH_2+2xCH_2+3β-H); 4.93 (*br* s, 1H, 7β-H); 5.06 (*br* s, 1H, 12β-H); 6.97 (s, 1H, Thy-CH); 7.01 (s, 1H, Thy-CH); 7.11 (s, 1H, Thy-CH); 7.26 (m, 2H, arom); 7.38-7.53 (m, 4H, arom); 8.10 (d, *J* = 7.8 Hz, 2H, arom); 10.05 (*br* s, 2H, 2xThy-NH); ^{13}C NMR (75 MHz, $CDCl_3$) δ 173.8 (C), 167.6 (C), 167.4 (C), 167.3 (C), 165.3 (C), 165.0 (C), 164.7 (C), 151.9 (C), 150.8 (2xC), 141.0 (CH), 140.8 (2xCH), 140.5 (2xC), 125.9 (2xCH), 123.0 (2xC), 120.5 (2xCH), 119.4 (2xCH), 111.1 (C), 110.6 (C), 110.5 (C), 108.7 (2xCH), 77.2 (CH), 76.0 (CH), 72.9 (CH), 62.2 (CH_2), 49.8 (CH_2), 49.3 (CH_2), 49.2 (CH_2), 47.4 (CH), 45.3 (C), 43.5 (CH), 41.8 (CH_2), 40.5 (CH), 37.7 (CH), 34.6 (CH), 34.4 (CH_2), 34.2 (CH_2+C), 31.2 (CH_2), 31.0 (CH_2), 30.5 (CH_2), 28.9 (CH), 27.1 (CH_2), 26.1 (CH_2), 25.4 (CH_2), 22.7 (CH_2), 22.5 (CH_3), 17.6 (CH_3), 12.4 (2xCH_3), 12.3 (CH_3), 12.1 (CH_3); m/z found 1100.4997, calculated for $C_{59}H_{70}N_7O_{14}$ (MH^+) 1100.4975.

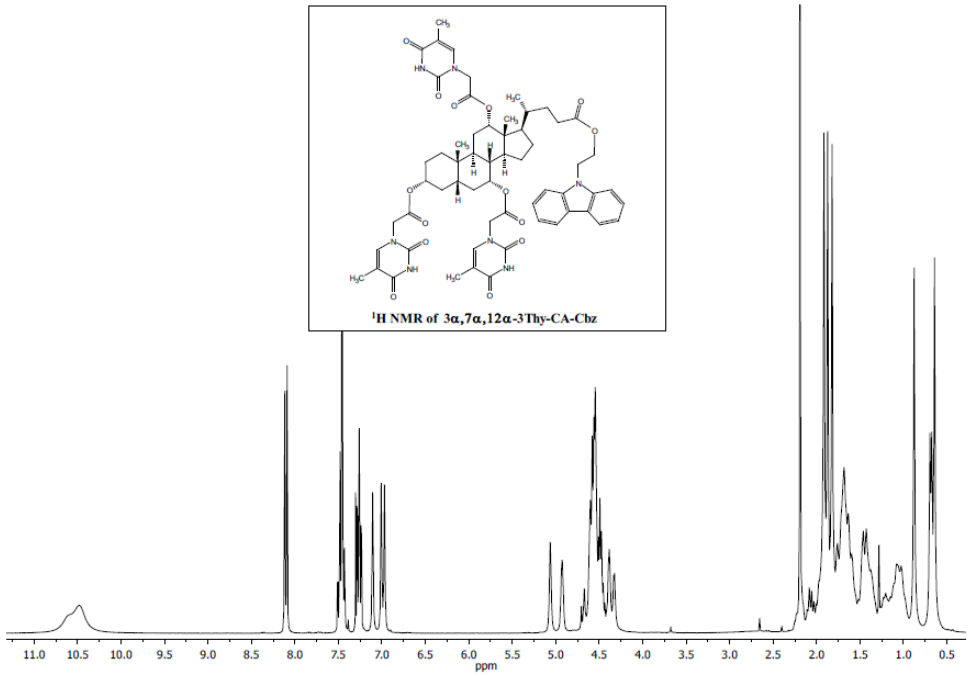
^{1}H NMR of 3α,7α,12α-3Thy-CA-Cbz
11.0 10.5 10.0 9.5 9.0 8.5 8.0 7.5 7.0 6.5 6.0 5.5 5.0 4.5 4.0 3.5 3.0 2.5 2.0 1.5 1.0 0.5
ppm

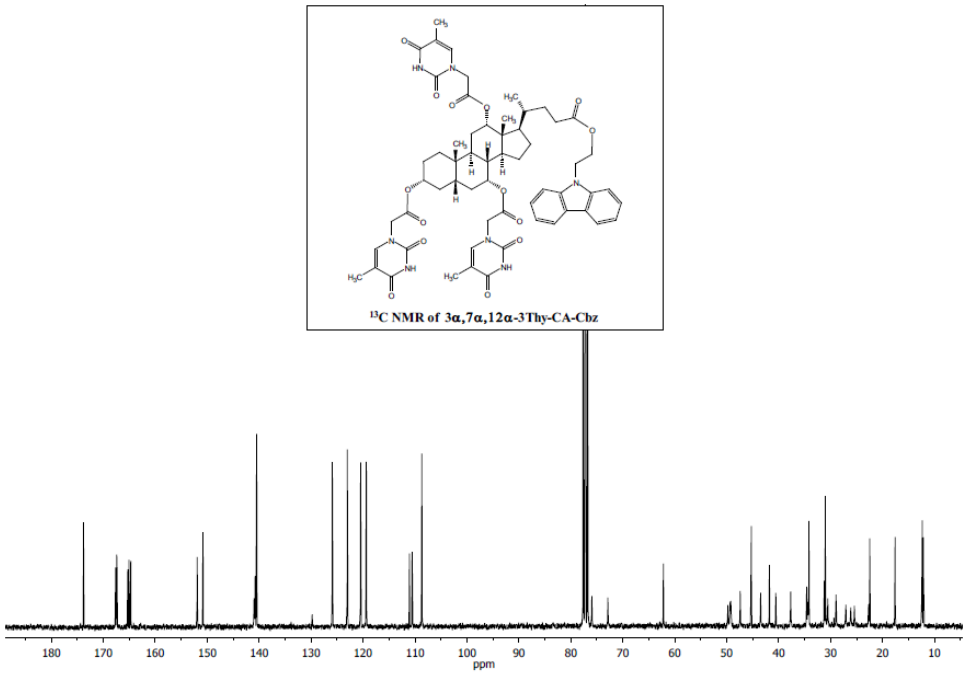
^{13}C NMR of 3α,7α,12α-3Thy-CA-Cbz
180 170 160 150 140 130 120 110 100 90 80 70 60 50 40 30 20 10
ppm

7.5.1.7. Synthesis of DCA–Cbz

To a stirred solution of Cbz-$(CH_2)_2$-OH (0.50 g, 2.25 mmol) and TBTU (0.87 g, 2.7 mmol) in anhydrous DMF (5 mL), **DCA** (0.93 g, 2.36 mmol) in anhydrous DMF (4 mL) followed by DIEA (1.17 mL, 6.75 mmol) were added dropwise and then the reaction mixture was allowed to react overnight at rt. Afterwards, it was poured into brine and extracted with CH_2Cl_2; the combined organic layers were washed with brine, dried over $MgSO_4$ and concentrated under reduced pressure. Purification by column chromatography (SiO_2, EtOAc:Hexane, 40:60) followed by (Li Chroprep RP-18, CH_3CN:H_2O, 92:8) gave **DCA–Cbz** as a white solid (0.93 g, 67%); ^{1}H NMR (300 MHz, $CDCl_3$): δ (ppm) 0.62 (s, 3H, CH_3); 0.80–2.29 (complex signal, 26H); 0.87 (d, J = 6.3 Hz, 3H, 21-CH_3); 0.91 (s, 3H, CH_3); 3.61 (m, 1H, 3β-H); 3.93 (*br* s, 1H, 12β-H); 4.47 (m, 2H, CH_2); 4.56 (m, 2H, CH_2); 7.20–7.32 (m, 2H, arom); 7.40–7.52 (m, 4H, arom); 8.10 (d, J = 7.8 Hz, 2H, arom); ^{13}C NMR (75 MHz, $CDCl_3$) δ 174.2 (C), 140.5 (2xC), 125.9 (2xCH), 123.1 (2xC), 120.4 (2xCH), 119.3 (2xCH), 108.7 (2xCH), 73.2 (CH), 71.8 (CH), 62.1 (CH_2), 48.3 (CH), 47.3 (CH), 46.5 (C), 42.2 (CH), 41.8 (CH_2), 36.5 (CH_2), 36.1 (CH), 35.3 (CH_2), 35.1 (CH), 34.2 (C), 33.7 (CH), 31.2 (CH_2), 30.7 (CH_2), 30.6 (CH_2), 28.7 (CH_2), 27.5 (CH_2), 27.2 (CH_2), 26.2 (CH_2), 23.7 (CH_2), 23.2 (CH_3), 17.3 (CH_3), 12.8 (CH_3); m/z found 586.3881, calculated for $C_{38}H_{52}NO_4$ (MH^+) 586.3896.

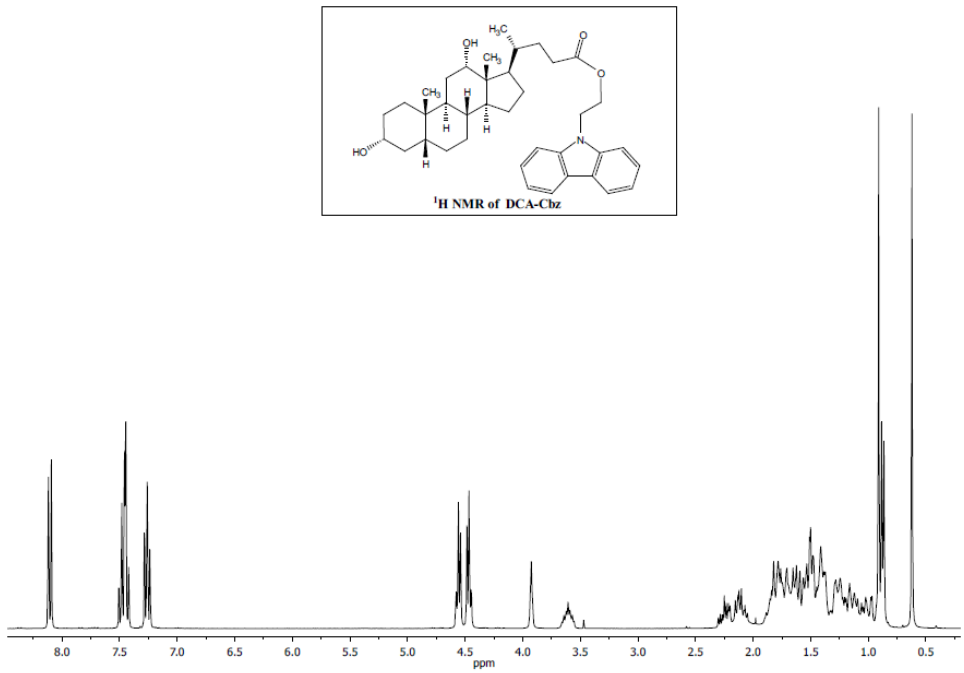
^{1}H NMR of DCA-Cbz
8.0
7.5
7.0
6.5
6.0
5.5
5.0
4.5
4.0
3.5
3.0
2.5
2.0
1.5
1.0
0.5
ppm

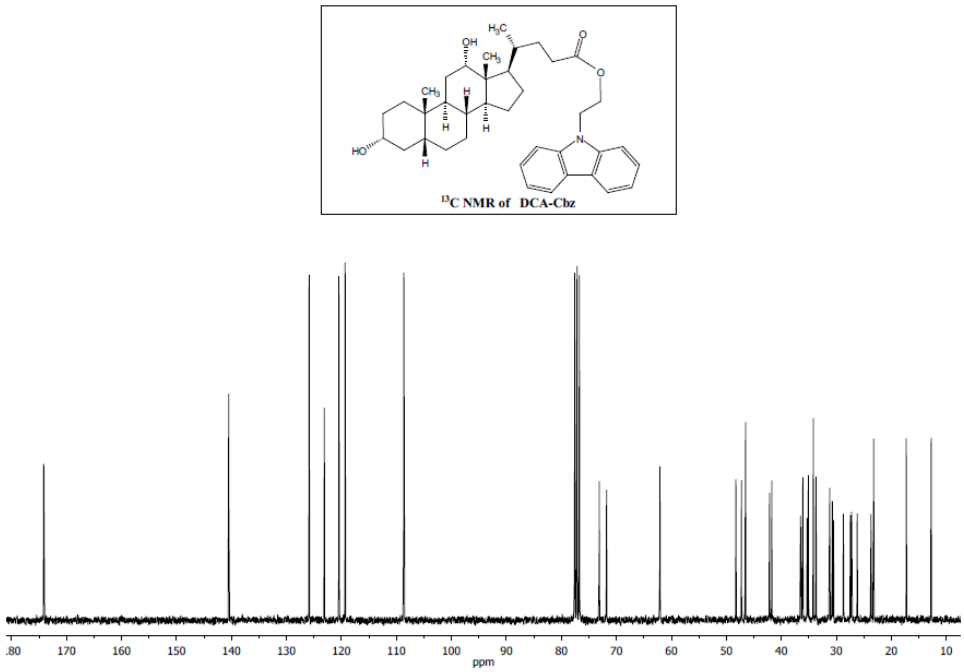
^{13}C NMR of DCA-Cbz
180
170
160
150
140
130
120
110
100
90
80
70
60
50
40
30
20
10
ppm

7.5.1.8. Synthesis of 3α, 12α-2Thy-DCA-Cbz

A stirred suspension of Thy-CH_2-COOH (0.42 g, 2.31 mmol) in anhydrous THF (10 mL) was treated with Et_3N (0.64 mL) and 2,4,6-trichlorobenzoyl chloride (0.43 mL, 2.77 mmol) and the resulting mixture was allowed to react for 1.5 h. Then, a solution of 4-DMAP (0.11 g, 0.91 mmol) and **DCA-Cbz** (0.45 g, 0.77 mmol) in anhydrous THF (10 mL) was added and stirred overnight. Afterwards, the reaction mixture was poured into brine, extracted with CH_2Cl_2 and the combined extracts were washed with brine, dried over $MgSO_4$ and concentrated under vacuum. Purification by column chromatography (SiO_2, EtOAc:Hexane, 90:10) followed by (Li Chroprep RP-18, CH_3CN:H_2O, 90:10), gave **3α,12α-2Thy-DCA-Cbz** as a yellow oil (0.54 g, 77%); ^{1}H NMR (300 MHz, $CDCl_3$): δ (ppm) 0.65 (s, 3H, CH_3); 0.71 (d, *J* = 5.7 Hz, 3H, 21-CH_3); 0.82-2.25 (complex signal, 26H); 0.88 (s, 3H, CH_3); 1.87 (*br* s, 3H, Thy-CH_3); 1.90 (*br* s, 3H, Thy-CH_3); 4.26-4.65 (m, 8H, 2xThy-CH_2+2xCH_2); 4.72 (m, 1H, 3β-H); 5.11 (*br* s, 1H, 12β-H); 6.96 (s, 1H, Thy-CH); 6.98 (s, 1H, Thy-CH); 7.18-7.32 (m, 2H, arom); 7.39-7.56 (m, 4H, arom); 8.10 (d, *J* = 7.8 Hz, 2H, arom); 10.19 (s, 1H, Thy-NH); 10.36 (s, 1H, Thy-NH); ^{13}C NMR (75 MHz, $CDCl_3$) δ 173.9 (C), 167.2 (C), 166.5 (C), 164.7 (C), 164.5 (C), 151.5 (C), 150.8 (C), 140.7 (CH), 140.5 (CH), 140.3 (2xC), 125.8 (2xCH), 122.9 (2xC), 120.3 (2xCH), 119.2 (2xCH), 111.0 (C), 110.5 (C), 108.6 (2xCH), 77.7 (CH), 76.4 (CH), 62.1 (CH_2), 49.2 (CH+2xCH_2), 47.2 (CH), 45.0 (C), 41.6 (CH_2+CH), 35.4 (CH), 34.5 (CH_2), 34.5 (CH), 34.1 (CH), 34.0 (C), 31.7 (CH_2), 30.9 (CH_2), 30.4 (CH_2), 27.1 (CH_2), 26.7 (CH_2), 25.9 (2xCH_2), 25.2 (CH_2), 23.3 (CH_2), 22.8 (CH_3), 17.5 (CH_3), 12.3 (2xCH_3), 12.0 (CH_3); m/z found 940.4497, calculated for $C_{52}H_{63}N_5O_{10}Na$ (MNa^+) 940.4473.

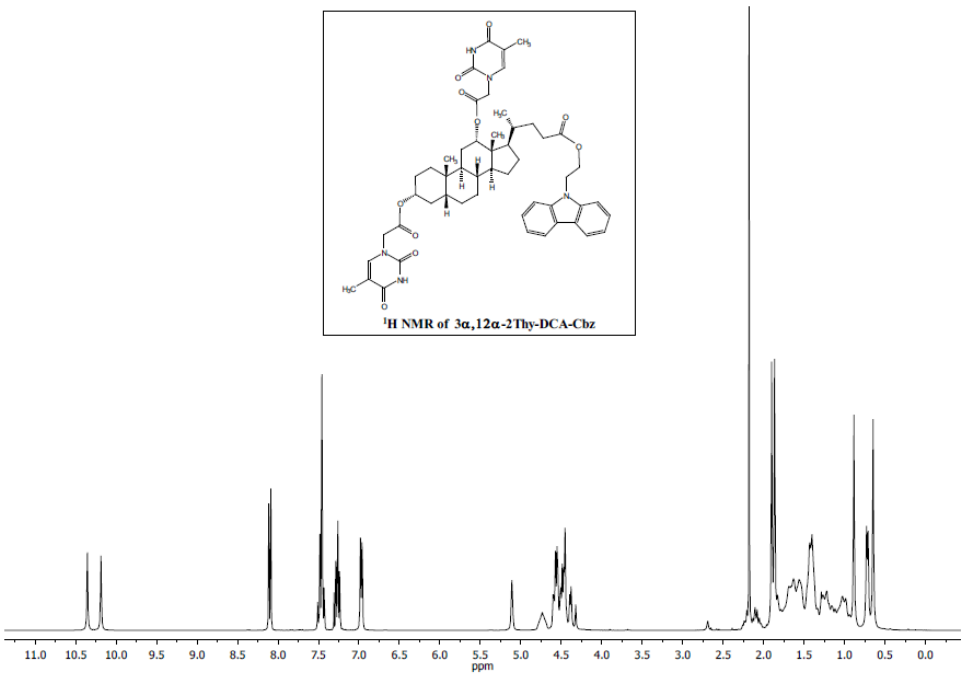
^{1}H NMR of 3α,12α-2Thy-DCA-Cbz
11.0 10.5 10.0 9.5 9.0 8.5 8.0 7.5 7.0 6.5 6.0 5.5 5.0 4.5 4.0 3.5 3.0 2.5 2.0 1.5 1.0 0.5 0.0
ppm

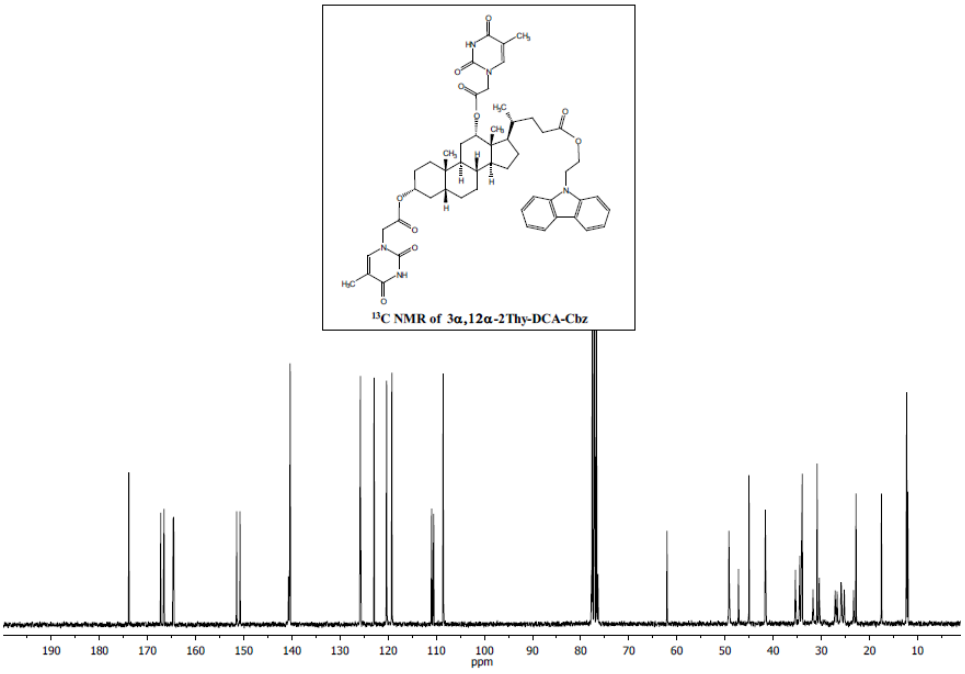
^{13}C NMR of 3α,12α-2Thy-DCA-Cbz
190 180 170 160 150 140 130 120 110 100 90 80 70 60 50 40 30 20 10
ppm

7.5.1.9. Synthesis of 3α-Cbz-DCA-Thy

To a stirred solution of **DCA-Thy** (already prepared from DCAOH, pages 175-178) (0.55 g, 1.01 mmol) and TBTU (0.40 g, 1.21 mmol) in anhydrous DMF (2 mL), a solution of Cbz-CH_2-COOH (0.25 g, 1.11 mmol) in anhydrous DMF (3 mL) followed by DIEA (0.53 mL, 3.03 mmol) were added dropwise and then the reaction mixture was allowed to react overnight at rt. Afterwards, it was poured into brine and extracted with CH_2Cl_2; the combined organic layers were washed with brine, dried over $MgSO_4$ and concentrated under reduced pressure. Purification by column chromatography (SiO_2, EtOAc:Hexane, 50:50) followed by (Li Chroprep RP-18, CH_3CN:H_2O, 90:10) gave **3α-Cbz-DCA-Thy** as a white solid (0.33 g, 43%); ^{1}H NMR (300 MHz, $CDCl_3$): δ (ppm) 0.67 (s, 3H, CH_3); 0.79-1.97 (complex signal, 26H); 0.90 (s, 3H, CH_3); 0.96 (d, *J* = 6.3 Hz, 3H, 21-CH_3); 1.91 (d, *J* = 1.2 Hz, 3H, Thy-CH_3); 3.98 (*br* s, 1H, 12β-H); 4.16 (m, 2H, CH_2); 4.39 (s, 2H, Thy-CH_2) ; 4.80 (*br* s, 1H, 3β-H); 4.96 (s, 2H, Cbz-CH_2); 6.88 (s, 1H, Thy-CH); 7.20-7.33 (m, 4H, arom); 7.43-7.52 (m, 2H, arom); 8.09 (d, *J* = 7.8 Hz, 2H, arom); 8.98 (s, 1H, Thy-NH); ^{13}C NMR (75 MHz, $CDCl_3$) δ 168.2 (C), 167.7 (C), 164.1 (C), 150.9 (C), 140.8 (2xC), 140.3 (CH), 126.1 (2xCH), 123.4 (2xC), 120.6 (2xCH), 119.7 (2xCH), 111.4 (C), 108.6 (2xCH), 76.2 (CH), 73.3 (CH), 66.8 (CH_2), 48.8 (CH_2), 48.4 (CH), 47.6 (CH), 46.6 (C), 45.2 (CH_2), 42.0 (CH), 36.1 (CH), 35.3 (CH), 34.9 (CH_2), 34.3 (C), 33.8 (CH), 32.2 (CH_2), 31.9 (CH_2), 28.8 (CH_2), 27.7 (CH_2), 27.0 (CH_2), 26.7 (CH_2), 26.1 (CH_2), 25.3 (CH_2), 23.8 (CH_2), 23.2 (CH_3), 17.7 (CH_3), 12.9 (CH_3), 12.5 (CH_3); m/z found 752.4308, calculated for $C_{45}H_{58}N_3O_7$ (MH^+) 752.4300.

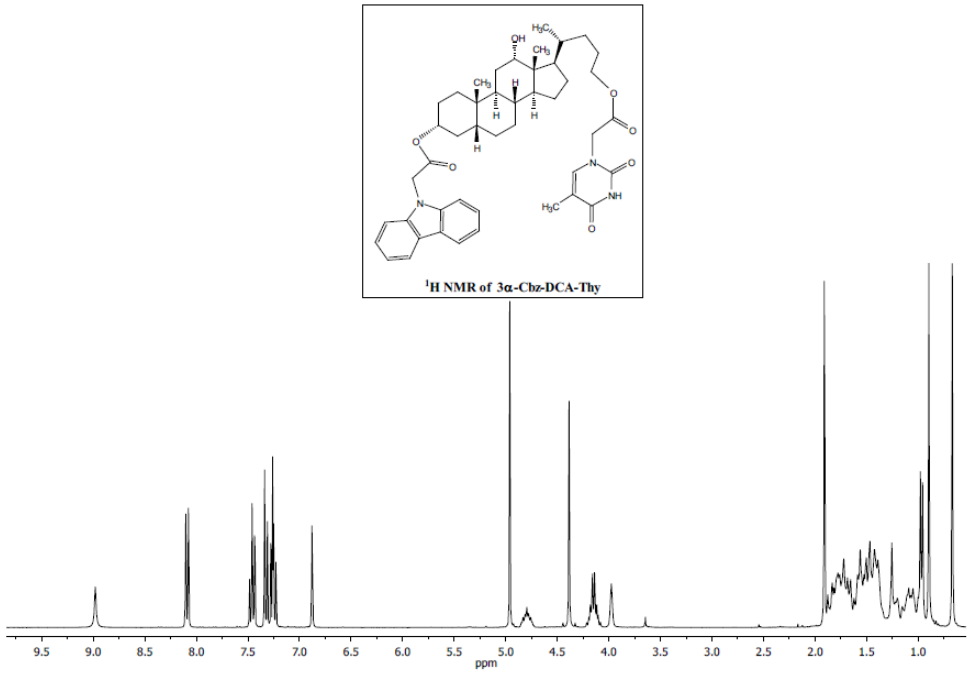
^{1}H NMR of 3α-Cbz-DCA-Thy
9.5 9.0 8.5 8.0 7.5 7.0 6.5 6.0 5.5 5.0 4.5 4.0 3.5 3.0 2.5 2.0 1.5 1.0
ppm

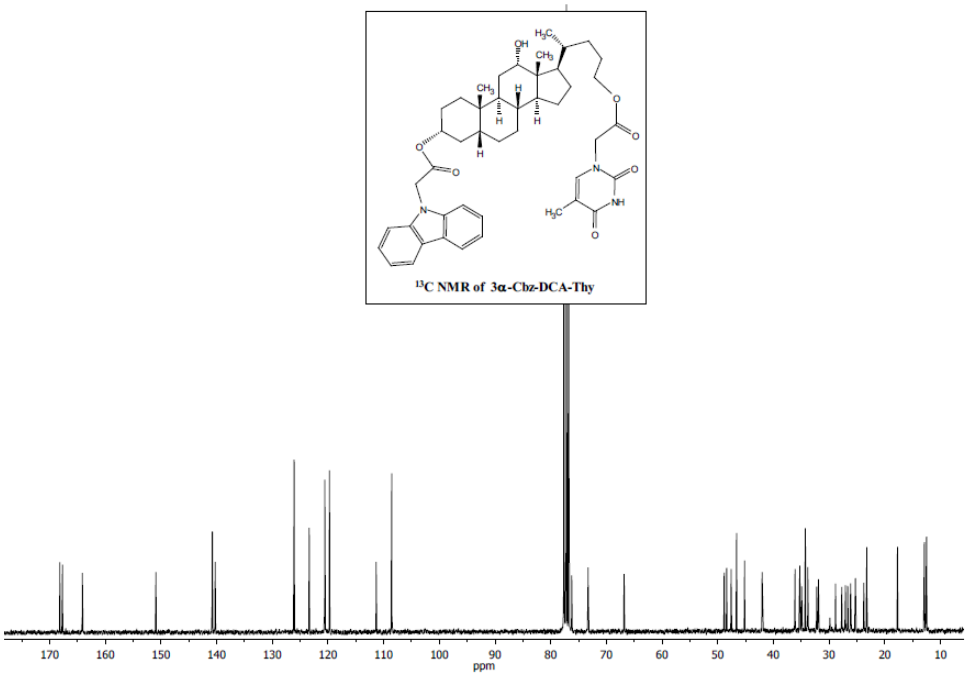
^{13}C NMR of 3α-Cbz-DCA-Thy
170 160 150 140 130 120 110 100 90 80 70 60 50 40 30 20 10
ppm

7.5.1.10. Synthesis of 3α-Cbz, 12α-Thy-DCA-Thy

A stirred suspension of Thy-CH_2-COOH (0.50 g, 2.72 mmol) in anhydrous THF (15 mL) was treated with Et_3N (0.76 mL) and 2,4,6-trichlorobenzoyl chloride (0.51 mL, 3.29 mmol) and the resulting mixture was allowed to react for 90 minutes. Then, a solution of 4-DMAP (0.064 g, 0.53 mmol) and **3α-Cbz-DCA-Thy** (0.34 g, 0.45 mmol) in anhydrous THF (11 mL) was added and stirred overnight. Afterwards, the reaction mixture was poured into brine, extracted with CH_2Cl_2 and the combined extracts were washed with brine, dried over $MgSO_4$ and concentrated under vacuum. Purification by column chromatography (SiO_2, EtOAc:Hexane, 50:50) followed by (Li Chroprep RP-18, CH_3CN:H_2O, 90:10), gave **3α-Cbz,12α-Thy-DCA-Thy** as a colorless oil (0.25 g, 60%); ^{1}H NMR (300 MHz, $CDCl_3$): δ (ppm) 0.50-1.79 (complex signal, 26H); 0.59 (s, 3H, CH_3); 0.71 (d, *J* = 4.8 Hz, 3H, 21-CH_3); 0.83 (s, 3H, CH_3); 1.12 (*br* s, 3H, Thy-CH_3); 1.95 (d, *J* = 1.2 Hz, 3H, Thy-CH_3); 2.96 (d, *J* = 17.4 Hz, 1H, Thy-CH_2); 4.19 (m, 2H, CH_2); 4.22 (d, *J* = 16.8 Hz, 1H, Thy-CH_2); 4.47 (d, *J* = 17.4 Hz, 1H, Thy-CH_2); 4.55 (d, *J* = 16.8 Hz, 1H, Thy-CH_2); 4.90 (m, 1H, 3β-H); 4.96 (*br* s, 1H, 12β-H); 4.97 (d, *J* = 17.7 Hz, 1H, Cbz-CH_2); 5.12 (d, *J* = 17.7 Hz, 1H, Cbz-CH_2); 5.53 (*br* d, *J* = 1.2 Hz, 1H, Thy-CH); 6.99 (*br* d, *J* = 1.2 Hz, 1H, Thy-CH); 7.21-7.30 (m, 2H, arom); 7.33-7.39 (d, *J* = 8.4 Hz, 2H, arom); 7.42-7.55 (m, 2H, arom); 8.00 (d, *J* = 7.8 Hz, 2H, arom); 11.02 (s, 1H, Thy-NH); 11.07 (s, 1H, Thy-NH); ^{13}C NMR (75 MHz, $CDCl_3$) δ 168.3 (C), 167.4 (C), 165.9 (C), 165.0 (C), 164.5 (C), 152.4 (C), 151.4 (C), 140.4 (2xC), 140.2 (CH), 140.0 (CH), 126.3 (2xCH), 123.0 (2xC), 120.5 (2xCH), 120.2 (2xCH), 111.7 (C), 110.6 (C), 108.3 (2xCH), 77.9 (CH), 75.8 (CH), 66.7 (CH_2), 50.3 (CH_2), 50.0 (CH_2), 49.9 (CH), 47.9 (CH), 45.5 (CH_2), 44.9 (C), 41.4 (CH), 35.8 (CH), 35.1 (CH), 34.5 (CH_2), 33.7 (CH), 33.5 (C), 32.0 (CH_2), 31.3 (CH_2), 27.2 (CH_2), 26.5 (CH_2), 26.4 (CH_2), 26.3 (CH_2), 26.0 (CH_2), 24.4 (CH_2), 23.1 (CH_2), 22.5 (CH_3), 17.4 (CH_3), 12.5 (CH_3), 12.2 (CH_3), 12.0 (CH_3); m/z found 918.4673, calculated for $C_{52}H_{64}N_5O_{10}$ (MH^+) 918.4653.

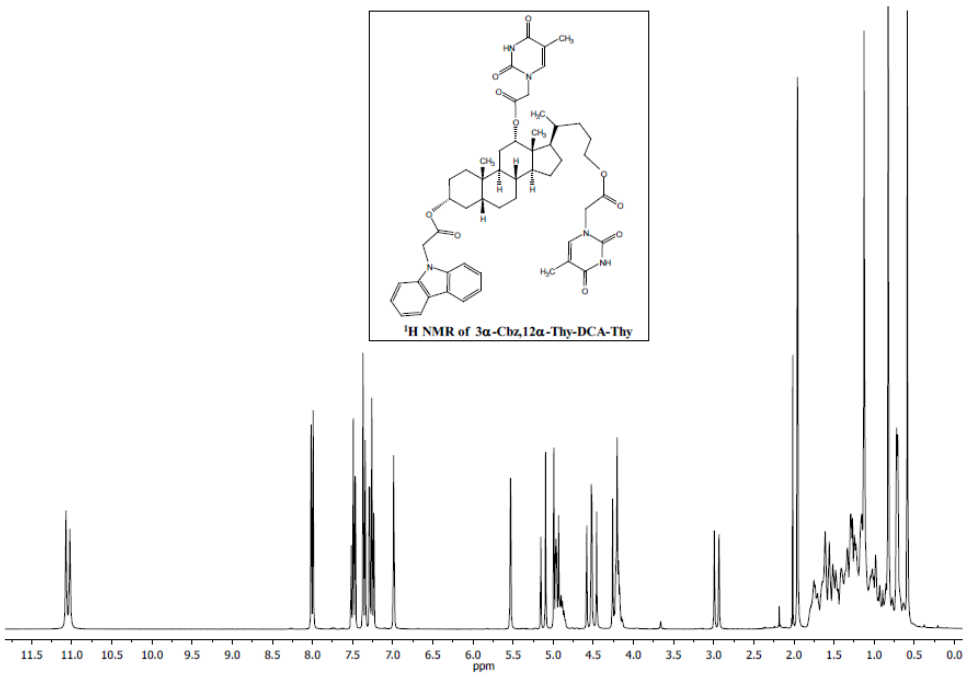
^{1}H NMR of 3α-Cbz,12α-Thy-DCA-Thy
11.5 11.0 10.5 10.0 9.5 9.0 8.5 8.0 7.5 7.0 6.5 6.0 5.5 5.0 4.5 4.0 3.5 3.0 2.5 2.0 1.5 1.0 0.5 0.0
ppm

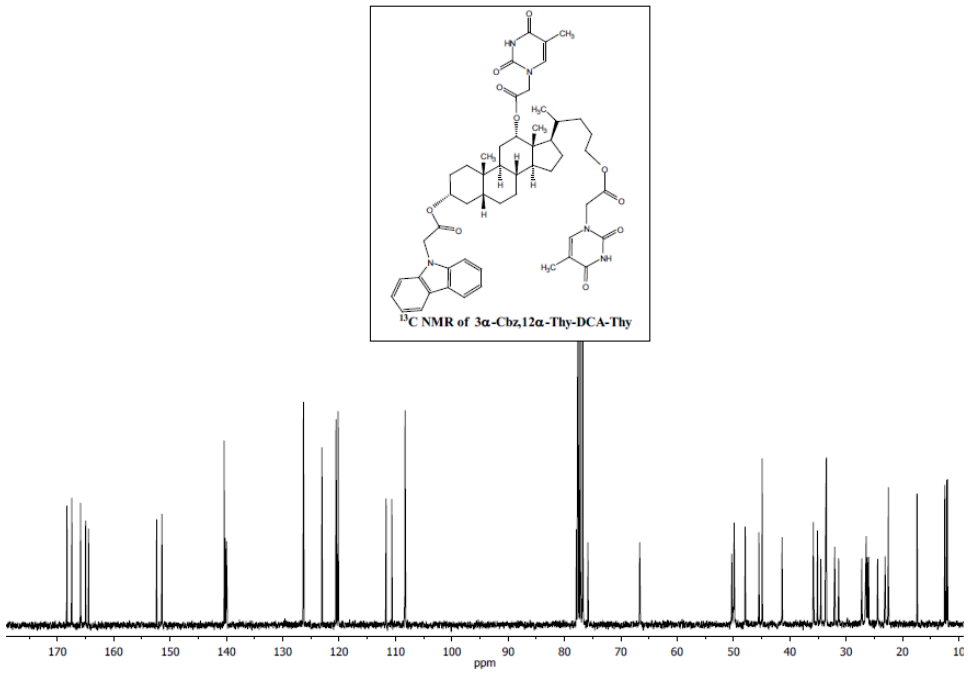
^{13}C NMR of 3α-Cbz,12α-Thy-DCA-Thy
170 160 150 140 130 120 110 100 90 80 70 60 50 40 30 20
ppm

7.5.1.11. Synthesis of CDCA–Cbz

To a stirred solution of **CDCA** (1.0 g, 2.55 mmol), Cbz–$(CH_2)_2$–OH (0.644 g, 3.05 mmol) and TBTU (0.979 g, 3.05 mmol) in anhydrous DMF (8 mL), DIEA (1.33 mL, 7.65 mmol) was added dropwise and then the reaction mixture was allowed to react overnight at rt. Afterwards, it was poured into brine and extracted with CH_2Cl_2; the combined organic layers were washed with brine, dried over $MgSO_4$ and concentrated under reduced pressure. Purification by column chromatography (SiO_2, EtOAc:Hexane, 60:40) gave **CDCA–Cbz** as a white solid (1.40 g, 94%); ^{1}H NMR (300 MHz, $CDCl_3$): δ (ppm) 0.62 (s, 3H, CH_3); 0.75–2.35 (complex signal, 26H); 0.84 (d, *J* = 6.3 Hz, 3H, 21–CH_3); 0.90 (s, 3H, CH_3); 3.45 (m, 1H, 3β–H); 3.83 (*br* s, 1H, 7β–H); 4.46 (m, 2H, CH_2); 4.54 (m, 2H, CH_2); 7.21–7.30 (m, 2H, arom); 7.39–7.52 (m, 4H, arom); 8.10 (d, *J* = 7.8 Hz, 2H, arom); ^{13}C NMR (75 MHz, $CDCl_3$) δ (ppm) 173.8 (C), 140.2 (2xC), 125.6 (2xCH), 122.8 (2xC), 120.1 (2xCH), 119.0 (2xCH), 108.4 (2xCH), 71.5 (CH), 68.0 (CH), 61.8 (CH_2), 55.6 (CH), 50.1 (CH), 42.3 (C), 41.4 (CH_2), 39.5 (2xCH_2+CH), 39.2 (CH), 35.3 (CH_2), 35.0 (CH), 34.8 (C), 34.6 (CH_2), 32.6 (CH), 30.8 (CH_2), 30.5 (2xCH_2), 27.9 (CH_2), 23.4 (CH_2), 22.7 (CH_3), 20.4 (CH_2), 18.1 (CH_3), 11.5 (CH_3); m/z found 586.3917, calculated for $C_{38}H_{52}NO_4$ (MH^+) 586.3896.

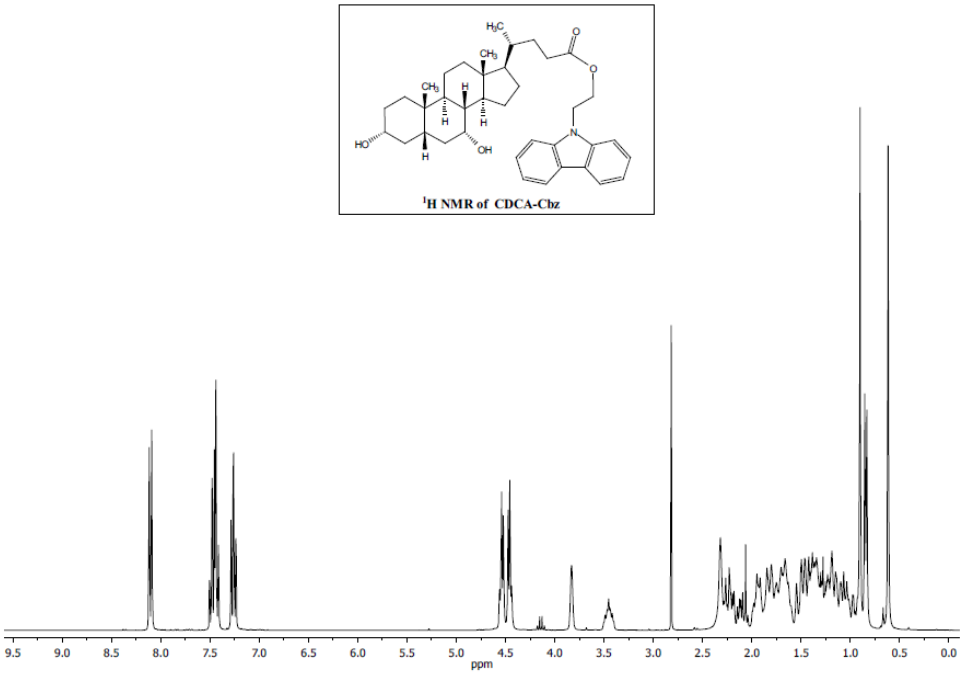
^{1}H NMR of CDCA-Cbz
9.5 9.0 8.5 8.0 7.5 7.0 6.5 6.0 5.5 5.0 4.5 4.0 3.5 3.0 2.5 2.0 1.5 1.0 0.5 0.0
ppm

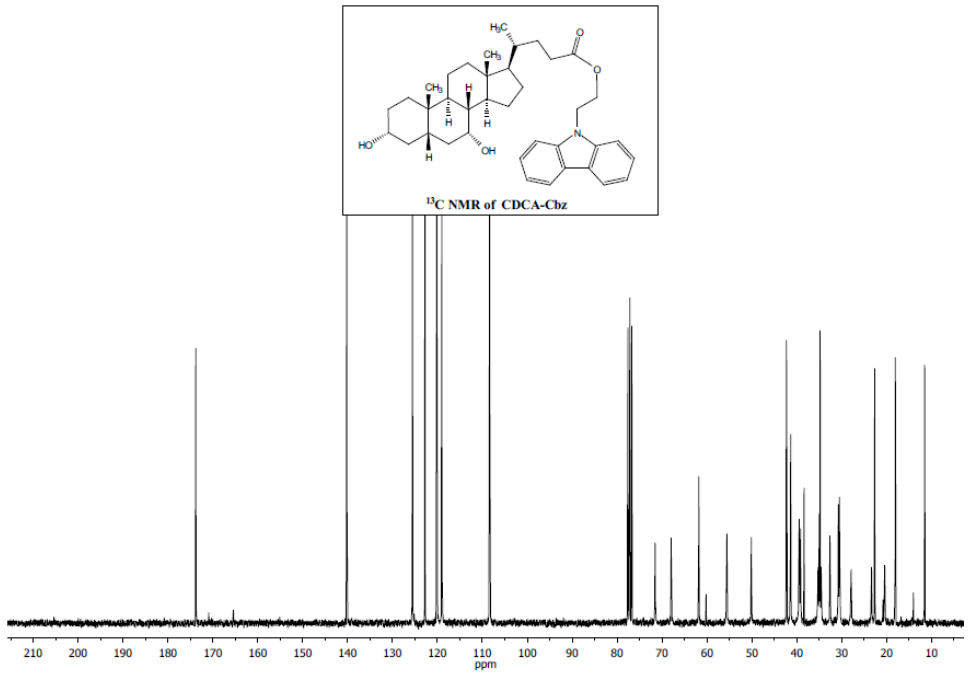
^{13}C NMR of CDCA-Cbz
210 200 190 180 170 160 150 140 130 120 110 100 90 80 70 60 50 40 30 20 10
ppm

7.5.1.12. Synthesis of 3α, 7α-2Thy-CDCA-Cbz

A stirred suspension of Thy-CH_2-COOH (5.68 g, 37.42 mmol) in anhydrous THF (100 mL) was treated with Et_3N (8.72 mL) and 2,4,6-trichlorobenzoyl chloride (5.8 mL, 37.42 mmol) and the resulting mixture was allowed to react for 1.5 h. Then, a solution of 4-DMAP (0.511 g, 4.19 mmol) and **CDCA-Cbz** (2.01 g, 3.43 mmol) in anhydrous THF (30 mL) was added and stirred overnight. Afterwards, the reaction mixture was poured into brine, extracted with CH_2Cl_2 and the combined extracts were washed with brine, dried over $MgSO_4$ and concentrated under vacuum. Purification by column chromatography (SiO_2, CH_2Cl_2:MeOH, 90:10) gave **3α,7α-2Thy-CDCA-Cbz** as a white solid (1.20 g, 38%); ^{1}H NMR (300 MHz, C_5D_5N): δ (ppm) 0.51 (s, 3H, CH_3); 0.52-2.25 (complex signal, 26H); 0.76 (d, *J* = 6.0 Hz, 3H, 21-CH_3); 0.81 (s, 3H, CH_3); 1.93 (*br* s, 3H, Thy-CH_3); 2.12 (*br* s, 3H, Thy-CH_3); 4.52-4.69 (m, 4H, 2xCH_2); 4.73-4.96 (m, 5H, 2xThy-CH_2+3β-H); 5.03 (*br* s, 1H, 7β-H); 7.30-7.73 (m, 8H, 6 arom+2xThy-CH); 8.27 (d, *J* = 7.8 Hz, 2H, arom); ^{13}C NMR (75 MHz, C_5D_5N) δ (ppm) 174.1 (C), 168.9 (C), 168.2 (C), 165.8 (2xC), 153.0 (C), 152.7 (C), 142.0 (CH), 141.9 (CH), 141.5 (2xC), 126.7 (2xCH), 123.8 (2xC), 121.1 (2xCH), 120.1 (2xCH), 110.9 (C), 110.6 (C), 109.9 (2xCH), 76.5 (CH), 73.9 (CH), 62.9 (CH_2), 56.5 (CH), 50.9 (CH), 50.6 (2xCH_2), 43.3 (C), 42.5 (CH_2), 41.3 (CH), 40.2 (CH_2), 38.5 (CH), 35.9 (CH), 35.3 (2xCH_2+C), 35.0 (CH), 32.0 (CH_2), 31.4 (CH_2), 31.2 (CH_2), 28.5 (CH_2), 27.3 (CH_2), 24.0 (CH_2), 23.0 (CH_3), 21.3 (CH_2), 18.7 (CH_3), 12.2 (CH_3), 12.9 (CH_3), 13.2 (CH_3); m/z found 918.4651, calculated for $C_{52}H_{64}N_5O_{10}$ (MH^+) 918.4653.

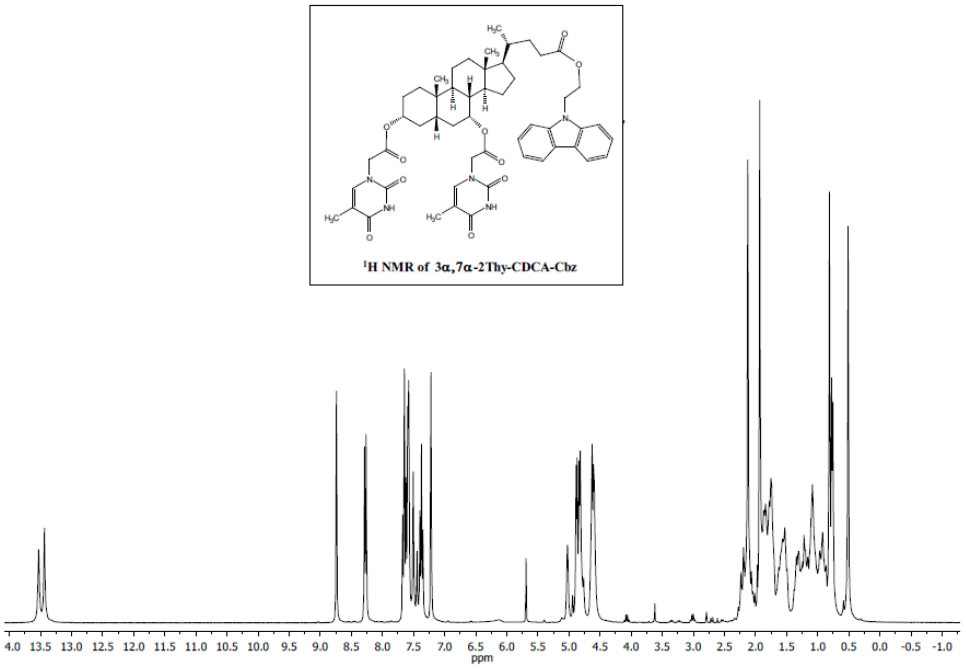
^{1}H NMR of 3α,7α-2Thy-CDCA-Cbz
4.0 13.5 13.0 12.5 12.0 11.5 11.0 10.5 10.0 9.5 9.0 8.5 8.0 7.5 7.0 6.5 6.0 5.5 5.0 4.5 4.0 3.5 3.0 2.5 2.0 1.5 1.0 0.5 0.0 -0.5 -1.0
ppm

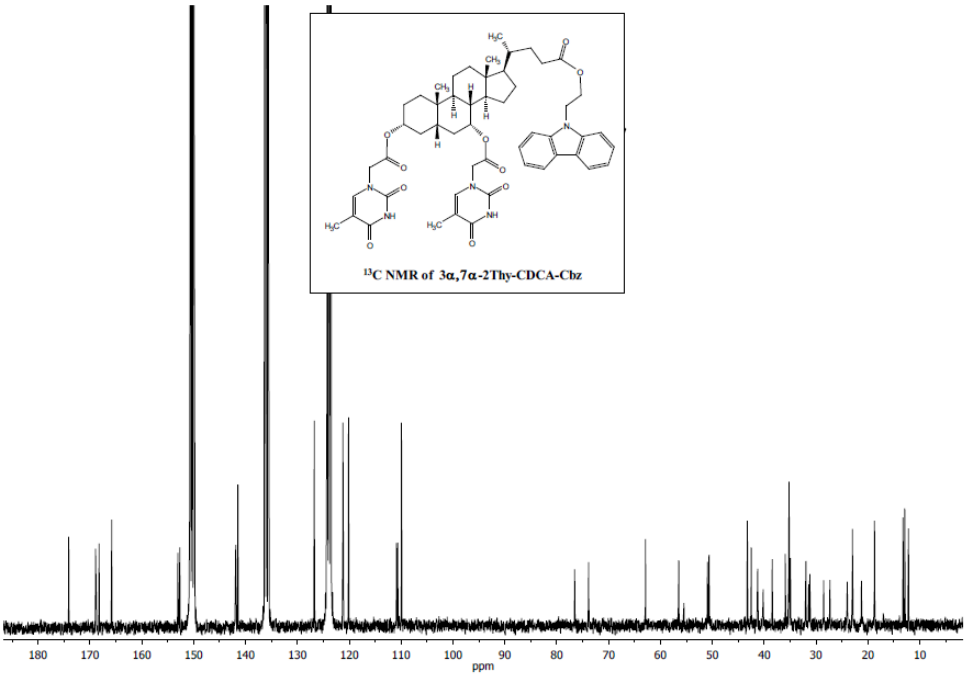
^{13}C NMR of 3α,7α-2Thy-CDCA-Cbz
180 170 160 150 140 130 120 110 100 90 80 70 60 50 40 30 20 10
ppm

7.5.1.13. Synthesis of 3α-Cbz-CDCA-Thy

To a stirred solution of **CDCA-Thy** (already prepared from CDCAOH, pages 188-191) (0.748 g, 1.38 mmol), TBTU (0.529 g, 1.65 mmol) and Cbz-CH_2-COOH (0.372 g, 1.65 mmol) in anhydrous DMF (14 mL), DIEA (0.718 mL, 3.03 mmol) was added dropwise and then the reaction mixture was allowed to react overnight at rt. Afterwards, it was poured into brine and extracted with CH_2Cl_2; the combined organic layers were washed with brine, dried over $MgSO_4$ and concentrated under reduced pressure. Purification by column chromatography (SiO_2, EtOAc:Hexane, 50:50) followed by (Li Chroprep RP-18, CH_3CN:H_2O, 90:10) gave **3α-Cbz-CDCA-Thy** as a white solid (0.468 g, 45%); ^{1}H NMR (300 MHz, $CDCl_3$): δ (ppm) 0.64-2.49 (complex signal, 26H); 0.65 (s, 3H, CH_3); 0.90 (s, 3H, CH_3); 0.93 (d, *J* = 6.3 Hz, 3H, 21-CH_3); 1.86 (s, 3H, Thy-CH_3); 3.82 (*br* s, 1H, 7β-H); 4.12 (m, 2H, CH_2); 4.31 (s, 2H, Thy-CH_2) ; 4.68 (m, 1H, 3β-H); 4.95 (s, 2H, Cbz-CH_2) ; 6.80 (s, 1H, Thy-CH); 7.17-7.52 (m, 6H, arom); 8.08 (d, *J* = 7.8 Hz, 2H, arom); 9.85 (*br* s, 1H, Thy-NH); ^{13}C NMR (75 MHz, $CDCl_3$) δ 168.1 (C), 167.7 (C), 164.4 (C), 151.0 (C), 140.6 (2xC), 140.3 (CH), 125.9 (2xCH), 123.1 (2xC), 120.3 (2xCH), 119.5 (2xCH), 111.0 (C), 108.5 (2xCH), 76.2 (CH), 68.2 (CH), 66.6 (CH_2), 55.7 (CH), 50.3 (CH), 48.6 (CH_2), 44.9 (CH_2), 42.6 (C), 41.2 (CH), 39.5 (CH_2), 39.3 (CH), 35.3 (CH), 35.1 (CH_2), 35.0 (C), 34.9 (CH_2), 34.3 (CH_2), 32.8 (CH), 31.8 (CH_2), 28.2 (CH_2), 26.7 (CH_2), 25.0 (CH_2), 23.6 (CH_2), 22.7 (CH_3), 20.6 (CH_2), 18.5 (CH_3), 12.3 (CH_3), 11.8 (CH_3); m/z found 752.4275, calculated for $C_{45}H_{58}N_3O_7$ (MH^+) 752.4300.

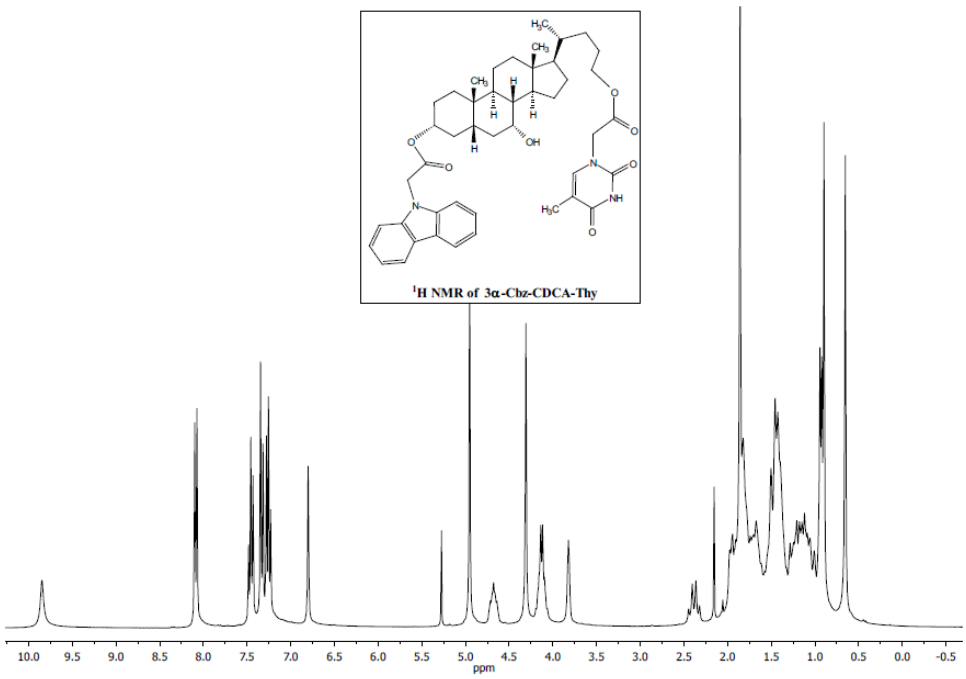
^{1}H NMR of 3α-Cbz-CDCA-Thy
10.0 9.5 9.0 8.5 8.0 7.5 7.0 6.5 6.0 5.5 5.0 4.5 4.0 3.5 3.0 2.5 2.0 1.5 1.0 0.5 0.0 -0.5
ppm

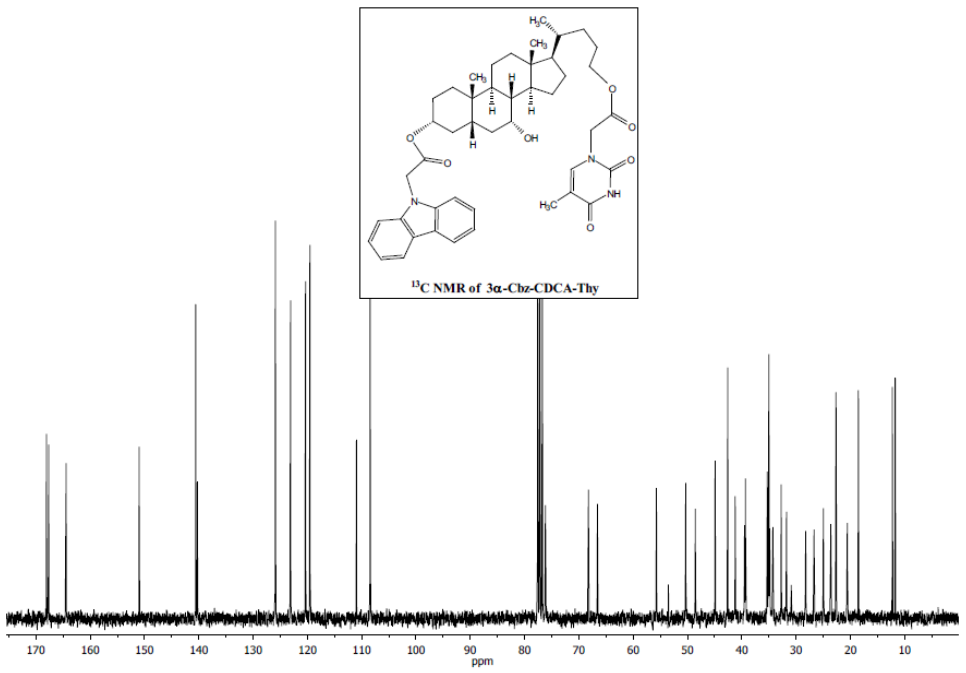
^{13}C NMR of 3α-Cbz-CDCA-Thy
170 160 150 140 130 120 110 100 90 80 70 60 50 40 30 20 10
ppm

7.5.1.14. Synthesis of 3α-Cbz, 7α-Thy -CDCA-Thy

A stirred suspension of Thy-CH_2-COOH (4.0 g, 26.29 mmol) in anhydrous THF (60 mL) was treated with Et_3N (6.10 mL) and 2,4,6-trichlorobenzoyl chloride (4.10 mL, 26.29 mmol) and the resulting mixture was allowed to react for 1.5 h. Then, a solution of 4-DMAP (0.359 g, 2.94 mmol) and **3α-Cbz-CDCA-Thy** (1.88 g, 2.41 mmol) in anhydrous THF (20 mL) was added and stirred overnight. Afterwards, the reaction mixture was poured into brine, extracted with CH_2Cl_2 and the combined extracts were washed with brine, dried over $MgSO_4$ and concentrated under vacuum. Purification by column chromatography (Li Chroprep RP-18, CH_3CN:H_2O, 80:20), gave **3α-Cbz,7α-Thy-CDCA-Thy** as a colorless oil (0.25 g, 21%); ^{1}H NMR (300 MHz, $CDCl_3$): δ (ppm) 0.31-2.10 (complex signal, 26H); 0.49 (s, 3H, CH_3); 0.78 (d, *J* = 6.3 Hz, 3H, 21-CH_3); 0.82 (s, 3H, CH_3); 1.02 (*br* s, 3H, Thy-CH_3); 1.93 (*br* s, 3H, Thy-CH_3); 3.97 (d, *J* = 17.1 Hz, 1H, Thy-CH_2); 4.11 (m, 1H, CH_2); 4.25-4.50 (m, 4H, 1xThy-CH_2+1xCH_2+Thy-CH_2); 4.60 (*br* s, 1H, 7β-H); 4.76 (m, 1H, 3β-H); 4.95 (d, *J* = 17.7 Hz, 1H, Cbz-CH_2); 5.14 (d, *J* = 17.7 Hz, 1H, Cbz-CH_2); 5.32 (s, 1H, Thy-CH); 6.96 (s, 1H, Thy-CH); 7.19-7.53 (m, 6H, arom); 8.01 (d, *J* = 7.8 Hz, 2H, arom); 10.65 (s, 1H, Thy-NH); 10.88 (s, 1H, Thy-NH); ^{13}C NMR (75 MHz, $CDCl_3$): δ 168.2 (C), 167.6 (C), 165.9 (C), 164.5 (C), 164.4 (C), 152.3 (C), 151.5 (C), 140.5 (CH), 140.4 (2xC), 140.3 (CH), 126.4 (2xCH), 123.0 (2xC), 120.7 (2xCH), 120.2 (2xCH), 111.6 (C), 110.6 (C), 108.4 (2xCH), 75.5 (CH), 73.8 (CH), 66.4 (CH_2), 56.8 (CH), 50.5 (CH), 50.0 (2xCH_2), 45.5 (CH_2), 42.2 (C), 40.7 (CH), 39.7 (CH_2), 37.7 (CH), 35.7 (CH), 34.8 (CH_2), 34.4 (CH_2+C+CH), 32.1 (CH_2), 30.3 (CH_2), 28.0 (CH_2), 26.6 (CH_2), 25.8 (CH_2), 23.0 (CH_2), 22.6 (CH_3), 20.6 (CH_2), 18.3 (CH_3), 12.5 (CH_3), 11.8 (CH_3), 11.5 (CH_3); m/z found 918.4623, calculated for $C_{52}H_{64}N_5O_{10}$ (MH^+) 918.4653.

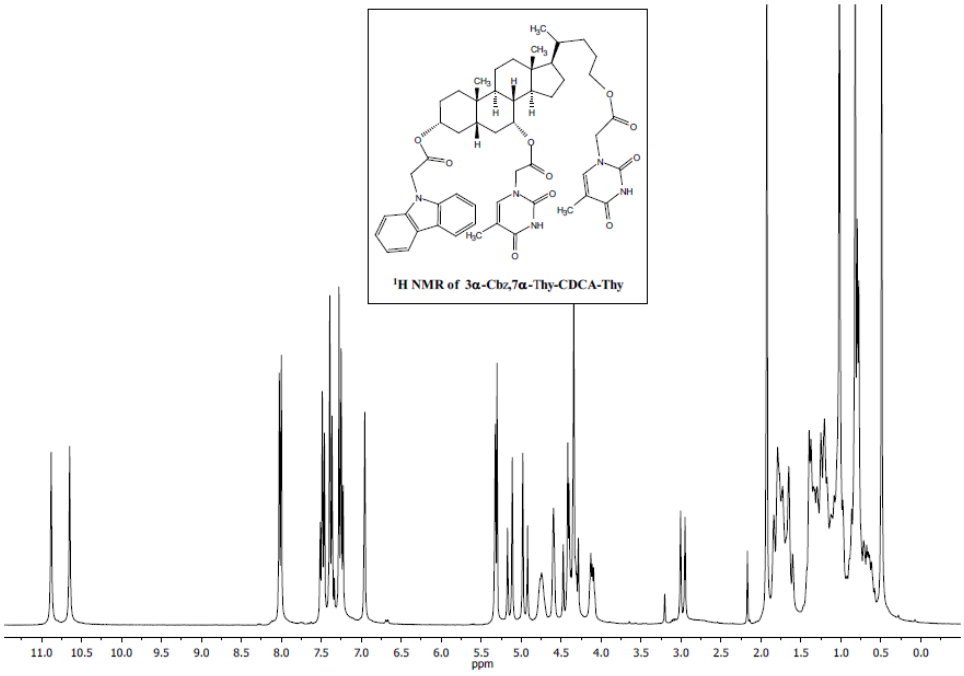
^{1}H NMR of 3α-Cbz,7α-Thy-CDCA-Thy
11.0 10.5 10.0 9.5 9.0 8.5 8.0 7.5 7.0 6.5 6.0 5.5 5.0 4.5 4.0 3.5 3.0 2.5 2.0 1.5 1.0 0.5 0.0
ppm

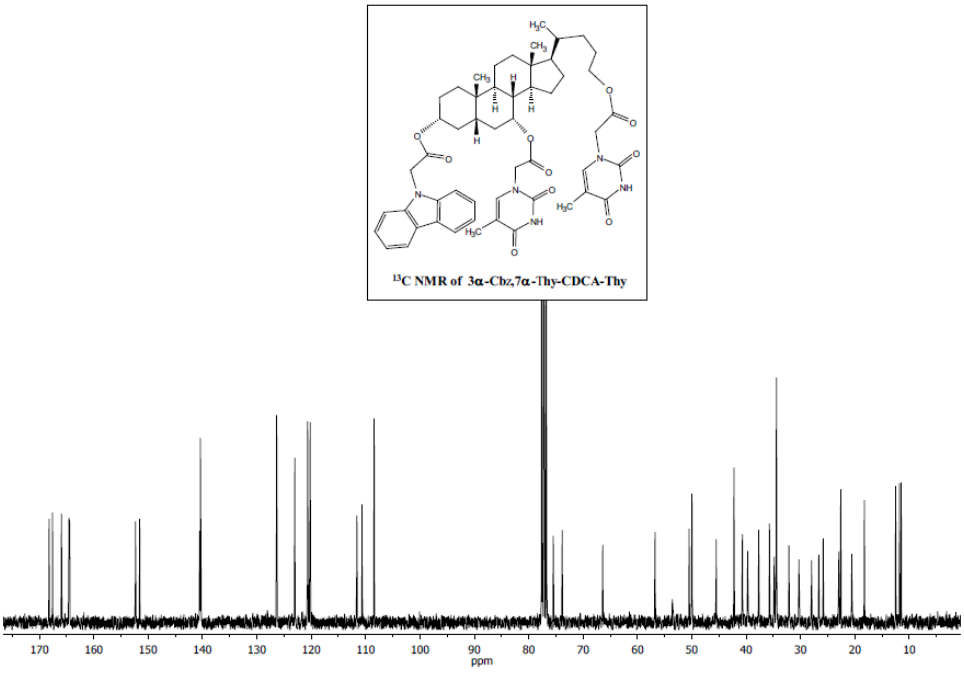
^{13}C NMR of 3α-Cbz,7α-Thy-CDCA-Thy
170 160 150 140 130 120 110 100 90 80 70 60 50 40 30 20 10
ppm

7.5.2. Preparative irradiations

7.5.2.1. Photochemical synthesis of 3α,12α-Thy<>Thy-DCA-Cbz

A solution of **3α,12α-2Thy-DCA-Cbz** (0.267 g, 0.27 mmol) in CH_3CN (350 mL), placed in a Pyrex® round-bottom flask was purged with N_2 and irradiated in a photoreactor using 8 lamps (λ_{max}= 350 nm) for four hours. Then, the solvent was concentrated under vacuum and the crude was purified by column chromatography (SiO_2, CH_2Cl_2:MeOH, 99:1) followed by (Li Chroprep RP-18, CH_3CN:H_2O, 90:10) to give **3α,12α-Thy<>Thy-DCA-Cbz** (0.144 g, 54%); ^{1}H NMR (400 MHz, C_5D_5N): δ (ppm) 0.48 (s, 3H); 0.65 (s, 3H); 0.62-2.25 (complex signal, 26H); 0.86 (d, *J* = 6.0 Hz, 3H); 1.75 (s, 3H, Thy-CH_3); 2.02 (s, 3H, Thy-CH_3); 3.94 (d, *J* = 17.2 Hz, 1H, Thy-CH_2); 4.01 (d, *J* = 2.8 Hz, 1H, ciclobutane-CH); 4.15 (*br* d, *J* = 16.8 Hz, 1H, Thy-CH_2); 4.30-4.41 (m, 2H, CH_2); 4.42-4.50 (m, 3H, CH_2+ciclobutane-CH); 4.72 (d, *J* = 17.2 Hz, 1H, Thy-CH_2); 4.83 (m, 1H, Thy-CH_2); 4.96 (m, 1H, 3β-H); 5.22 (s, 1H, 12β-H); 7.22-7.30 (m, 2H, arom); 7.43-7.56 (m, 4H, arom); 8.15 (d, *J* = 7.6 Hz, 2H, arom); 13.06 (*br* s, 1H, Thy-NH); 13.13 (*br* s, 1H, Thy-NH); ^{13}C NMR (100 MHz, C_5D_5N) δ 173.5 (C), 170.4 (C), 170.3 (C), 168.1 (C), 167.7 (C), 152.3 (C), 152.2 (C), 141.0 (2XC), 126.3 (2XCH), 123.5 (2XC), 120.8 (2XCH), 119.7 (2XCH), 109.5 (2XCH), 78.2 (CH), 73.2 (CH), 66.0 (CH), 64.2 (CH), 62.4 (CH_2), 52.4 (CH), 52.0 (CH_2), 50.1 (CH_2), 47.8 (CH), 45.6 (C), 45.5 (C), 45.2 (C), 42.0 (CH_2), 39.9 (CH), 35.4 (CH), 34.5 (CH), 34.1 (CH_2), 33.3 (CH), 32.4 (C), 31.5 (CH_2), 30.6 (CH_2), 29.8 (CH_2), 27.4 (CH_2), 25.8 (2XCH_2), 25.2 (CH_2), 23.9 (CH_2), 23.3 (CH_3), 23.2 (CH_2), 22.4 (CH_3), 21.4 (CH_3), 17.0 (CH_3), 12.5 (CH_3); m/z found 918.4664, calculated for $C_{52}H_{64}N_5O_{10}$ (MH^+) 918.4653.

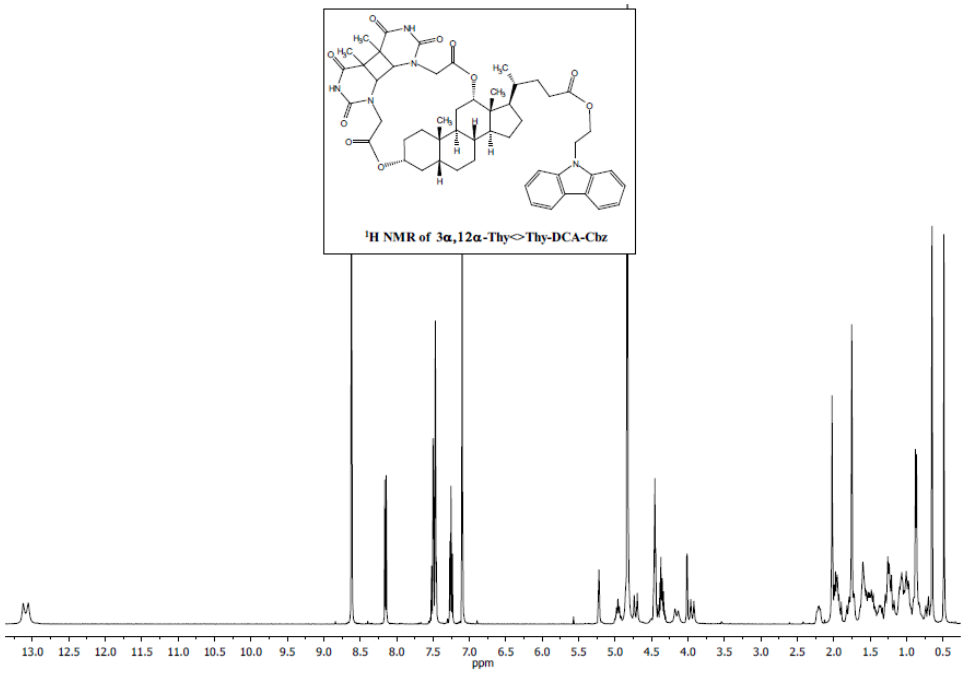
^{1}H NMR of 3α,12α-Thy<>Thy-DCA-Cbz
13.0 12.5 12.0 11.5 11.0 10.5 10.0 9.5 9.0 8.5 8.0 7.5 7.0 6.5 6.0 5.5 5.0 4.5 4.0 3.5 3.0 2.5 2.0 1.5 1.0 0.5
ppm

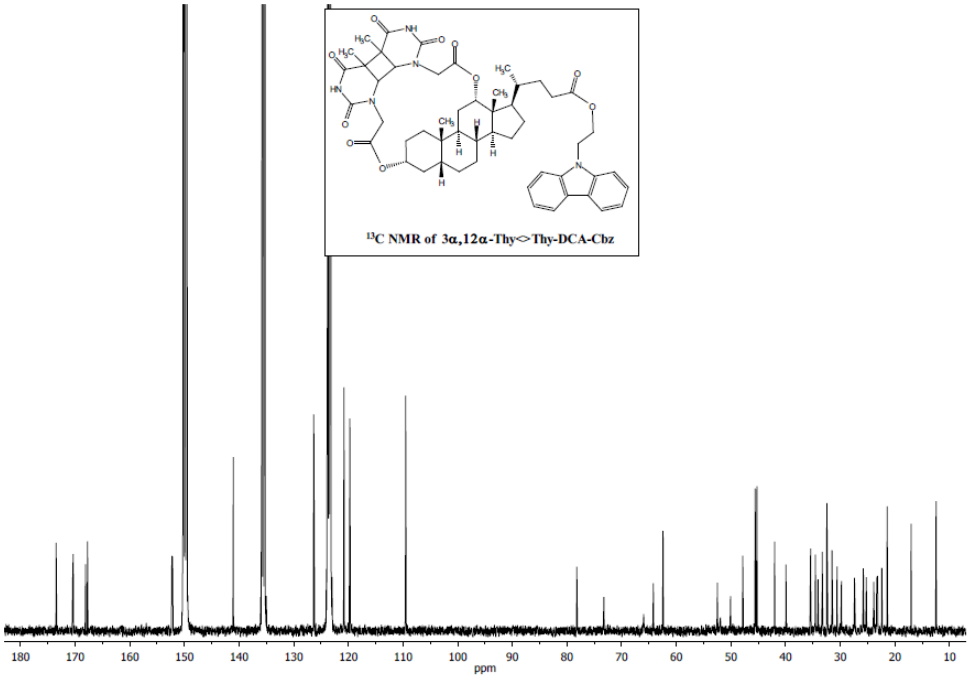
^{13}C NMR of 3α,12α-Thy<>Thy-DCA-Cbz
180 170 160 150 140 130 120 110 100 90 80 70 60 50 40 30 20 10
ppm

7.5.2.2. Photochemical synthesis of 3α-Cbz-DCA-12α-Thy<>Thy

A solution of **3α-Cbz,12α-Thy-DCA-Thy** (0.155 g, 0.17 mmol) in CH_3CN (100 mL), placed in a Pyrex® round-bottom flask, was purged with N_2 and irradiated in a photoreactor using 8 lamps (λ_{max}= 350 nm) for eight hours. Then, the solvent was concentrated under vacuum and the crude was purified by column chromatography (SiO_2, CH_2Cl_2:MeOH, 95:5) followed by (Li Chroprep RP-18, CH_3CN:H_2O, 90:10) to give **3α-Cbz-DCA-12α-Thy<> Thy** (0.054 g, 35%); ^{1}H NMR (300 MHz, $CDCl_3$): δ (ppm) 0.78 (s, 3H, CH_3); 0.82-1.81 (complex signal, 26H); 0.87 (*br* s, 6H, CH_3+21-CH_3); 1.50 (s, 3H, Thy-CH_3); 1.55 (s, 3H, Thy-CH_3); 3.82 (m, 1H); 3.88 (d, *J* = 16.2 Hz, 1H, Thy-CH_2); 4.02 (d, *J* = 6.3 Hz, 1H, Thy-CH); 4.07 (d, *J* = 16.8 Hz, 1H, Thy-CH_2); 4.11 (d, *J* = 6.3 Hz, 1H, Thy-CH); 4.20 (d, *J* = 16.2 Hz, 1H, Thy-CH_2); 4.33 (d, *J* = 16.8 Hz, 1H, Thy-CH_2); 4.76 (m, 1H, 3β-H); 4.90 (m, 1H); 4.92 (d, *J* = 17.4 Hz, 1H, Cbz-CH_2); 4.98 (d, *J* = 17.4 Hz, 1H, Cbz-CH_2); 5.09 (*br* s, 1H, 12β-H); 7.18-7.26 (m, 2H, arom), 7.32 (d, *J* = 8.1 Hz, 2H, arom); 7.39-7.46 (m, 2H, arom); 7.50 (s, 1H, Thy-NH), 8.04-8.10 (m, 3H, arom+Thy-NH); ^{13}C NMR (75 MHz, $CDCl_3$) 171.2 (C), 170.8 (C), 169.4 (2XC), 168.3 (C), 151.3 (C), 150.3 (C), 140.8 (2xC), 125.9 (2xCH), 123.3 (2xC), 120.5 (2xCH), 119.6 (2xCH), 108.6 (2xCH), 78.2 (CH), 76.7 (CH), 66.6 (CH_2), 66.3 (CH), 65.9 (CH), 50.9 (CH_2), 50.3 (CH_2), 49.2 (CH), 46.8 (C), 46.7 (CH), 46.2 (C), 45.5 (C), 45.3 (CH_2), 42.2 (CH), 36.5 (CH), 35.6 (CH), 35.0 (CH_2), 34.8 (CH), 34.6 (C), 33.7 (CH_2), 32.7 (CH_2), 27.4 (CH_2), 27.0 (CH_2), 26.6 (CH_2), 26.4 (CH_2), 25.9 (CH_2), 25.6 (CH_2), 23.5 (CH_2), 23.4 (CH_3), 22.3 (CH_3), 22.2 (CH_3), 16.4 (CH_3), 14.4 (CH_3); m/z found 918.4662, calculated for $C_{52}H_{64}N_5O_{10}$ (MH^+) 918.4653.

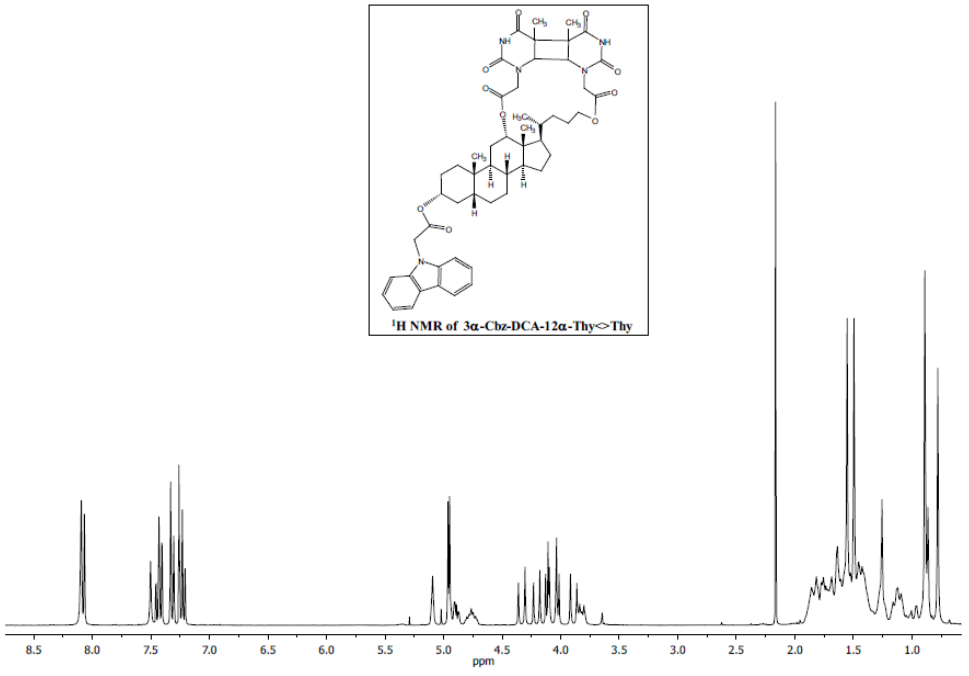
^{1}H NMR of 3α-Cbz-DCA-12α-Thy<>Thy
8.5
8.0
7.5
7.0
6.5
6.0
5.5
5.0
4.5
4.0
3.5
3.0
2.5
2.0
1.5
1.0
ppm

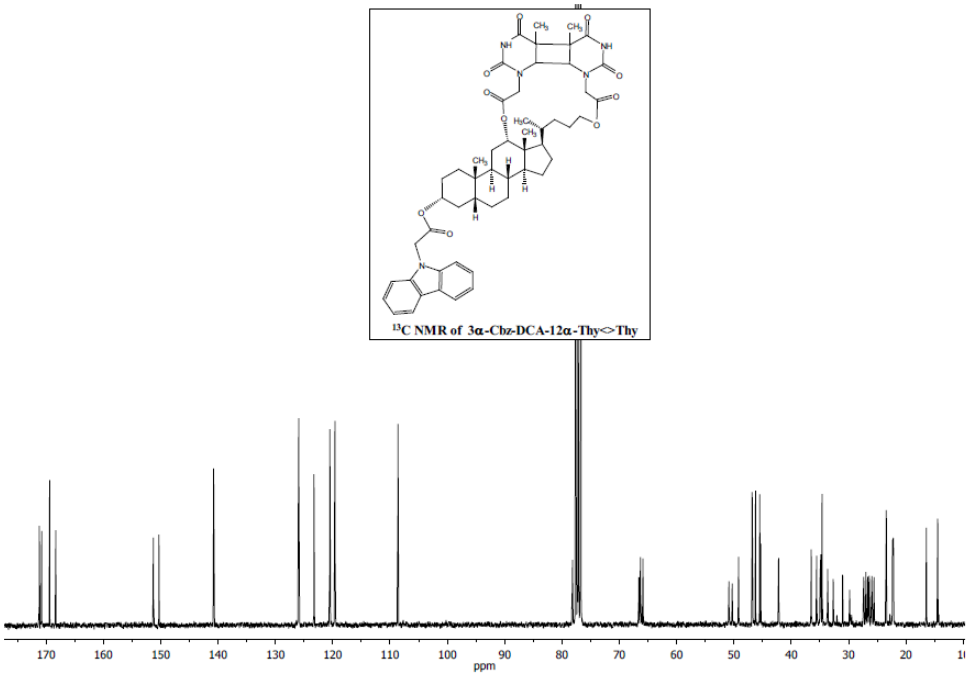
^{13}C NMR of 3α-Cbz-DCA-12α-Thy<>Thy
170
160
150
140
130
120
110
100
90
80
70
60
50
40
30
20
ppm

7.6.Supplementary material

7.6.1. Instrumentation

Laser flash photolysis at 308 nm. Transient spectra were recorded at room temperature using N_2–purged $4CH_3CN$:$1H_2O$ solutions of 9 x 10^{-5} M of the compound of interest. The decays were recorded at 420 nm.

Irradiations for the UV–Vis analysis. Irradiation of solutions of $4CH_3CN$:$1H_2O$ at the concentration of 4.4 x 10^{-5} M in N_2 atmosphere were performed in the Luzchem photoreactor with all lamps centred at 300 nm.

7.6.2 Additional NMR spectra

7.6.2.1. CA-Bn

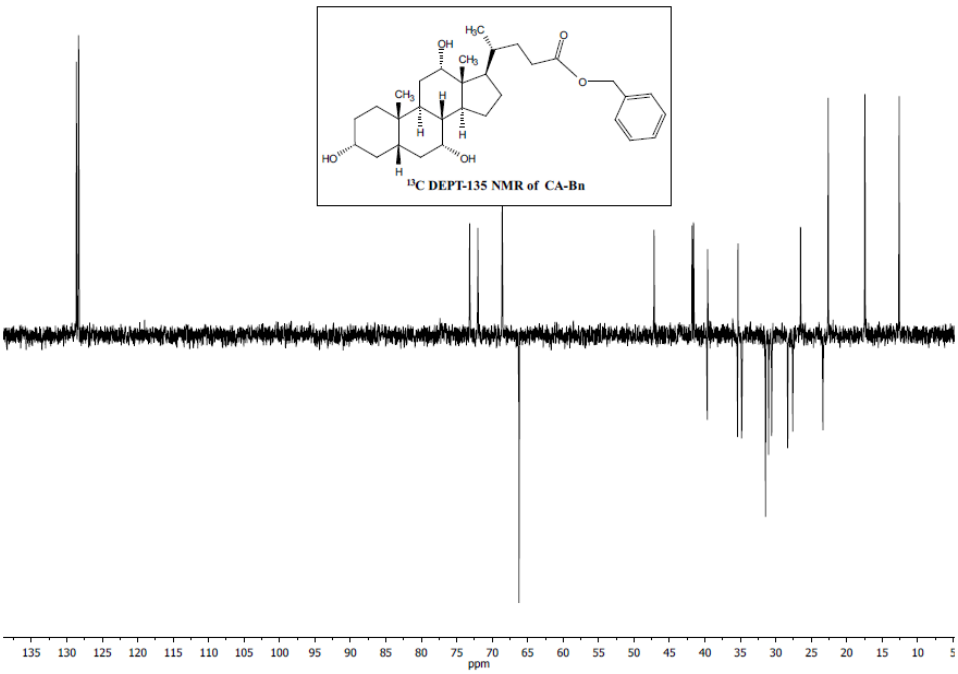

7.6.2.2. 3α-Thy-CA-Bn

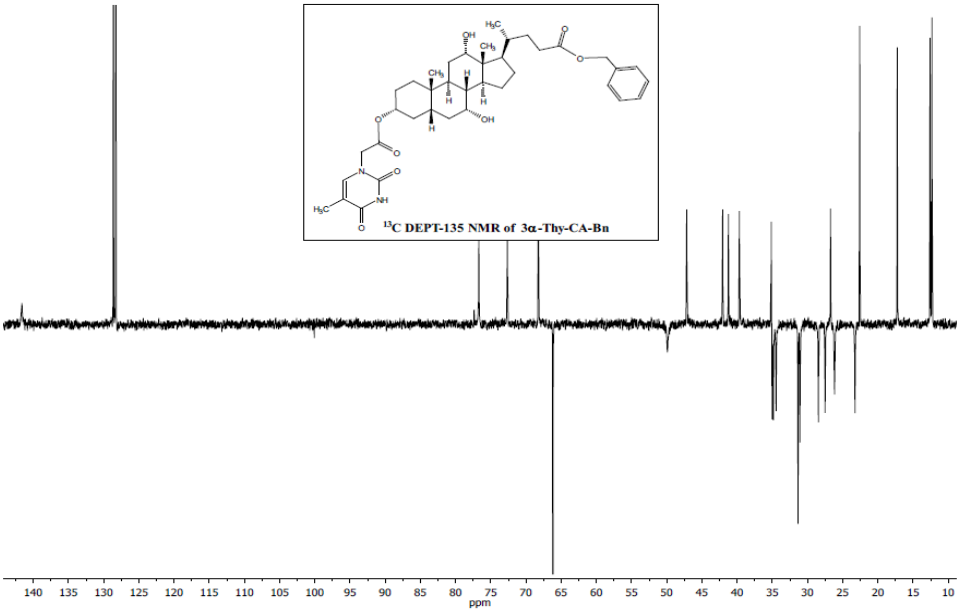

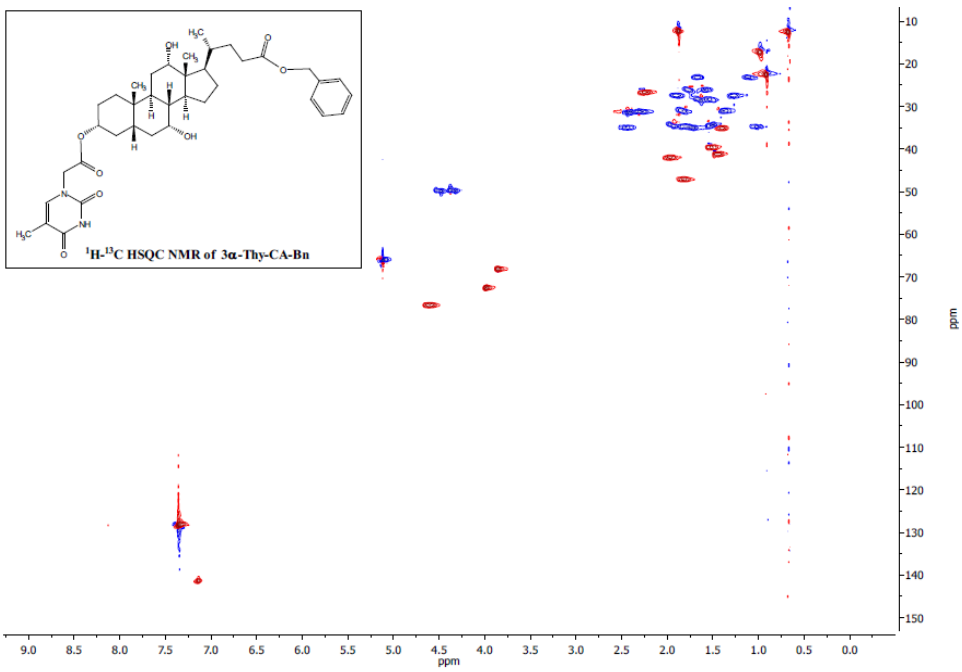

7.6.2.3. 3α,7α,12α-3Thy-CA-Bn

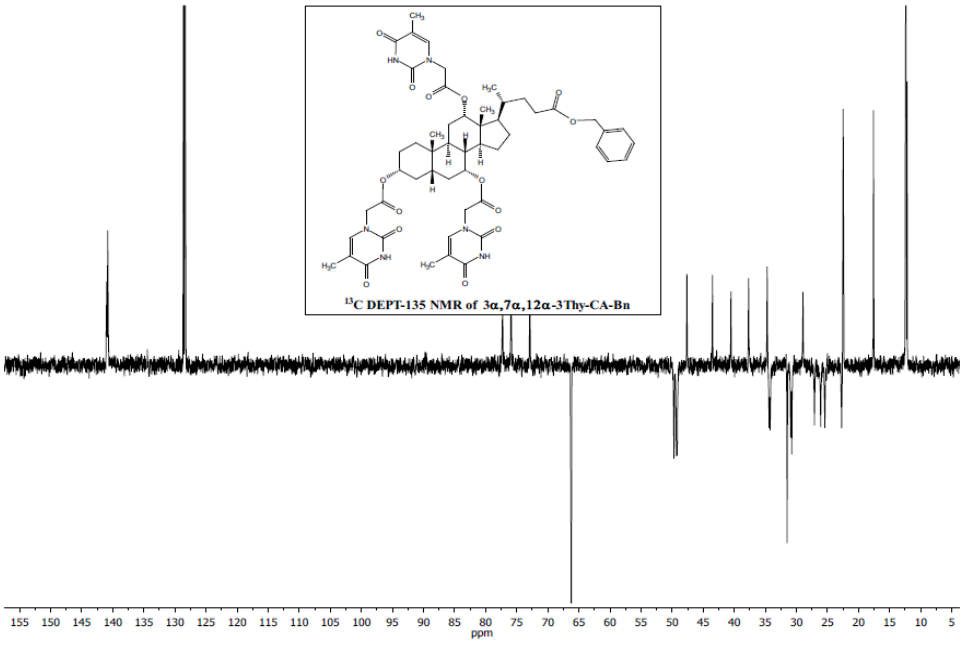

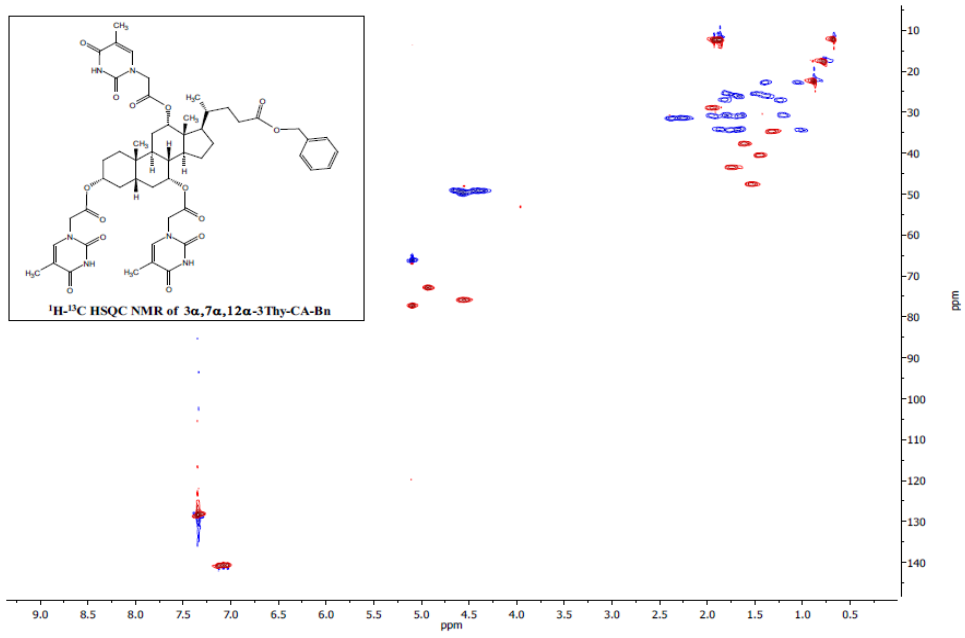

7.6.2.4. CA-Cbz

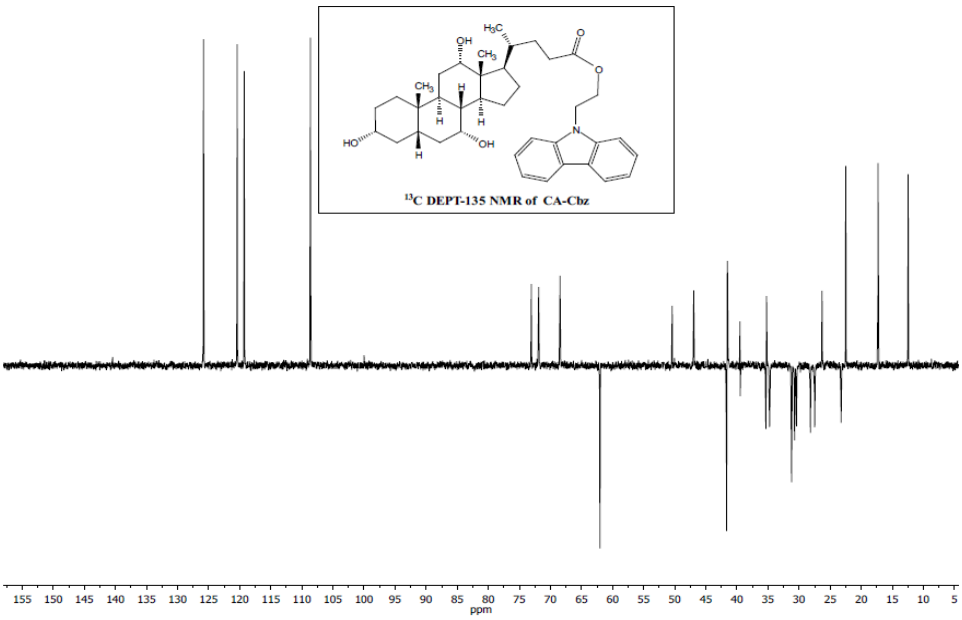
^{13}C DEPT-135 NMR of CA-Cbz
155 150 145 140 135 130 125 120 115 110 105 100 95 90 85 80 75 70 65 60 55 50 45 40 35 30 25 20 15 10 5
ppm

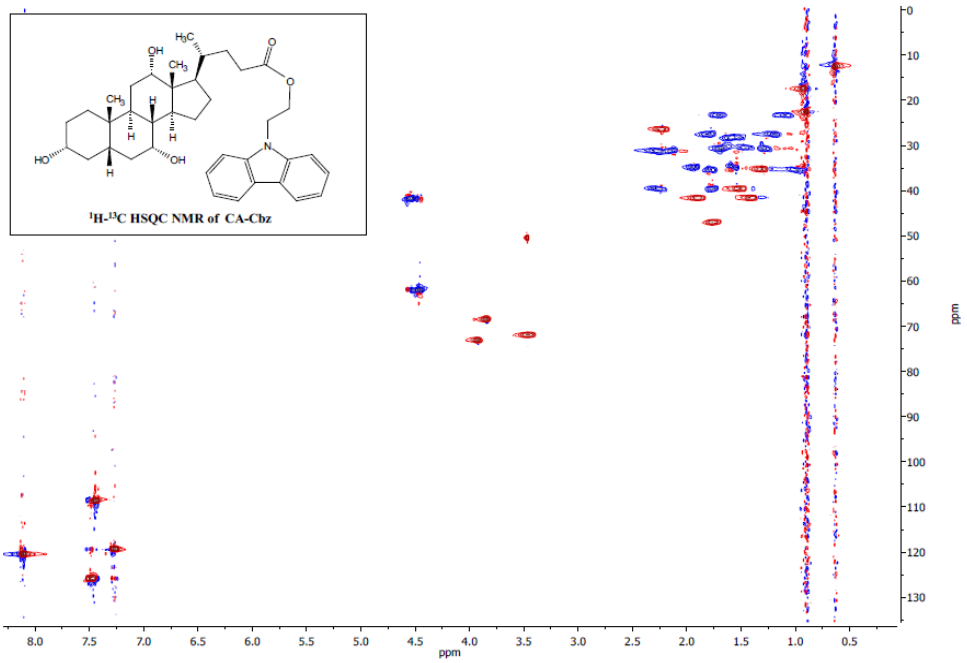
^{1}H-^{13}C HSQC NMR of CA-Cbz
8.0 7.5 7.0 6.5 6.0 5.5 5.0 4.5 4.0 3.5 3.0 2.5 2.0 1.5 1.0 0.5
ppm
0 10 20 30 40 50 60 70 80 90 100 110 120 130
ppm

7.6.2.5. 3α-Thy-CA-Cbz

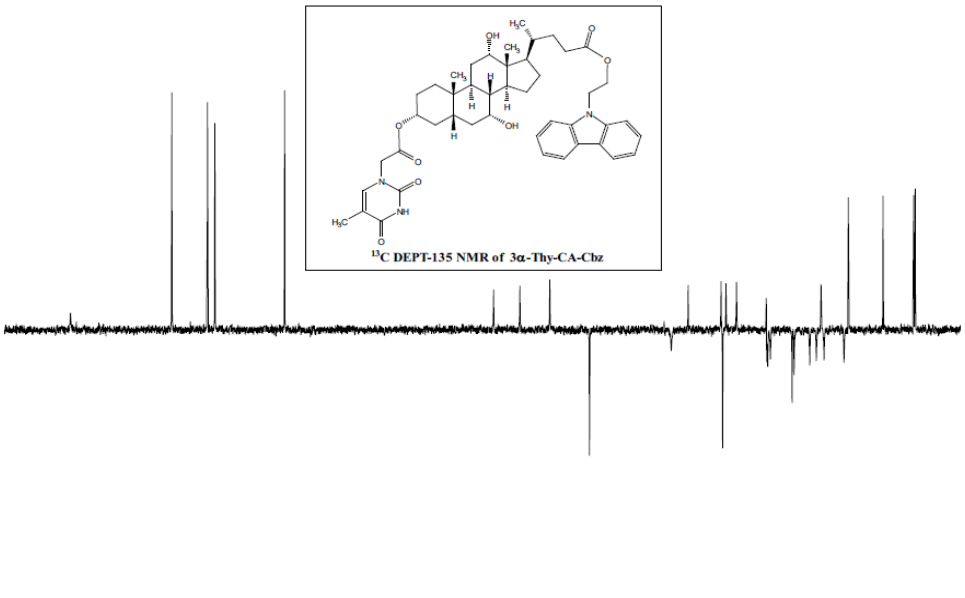

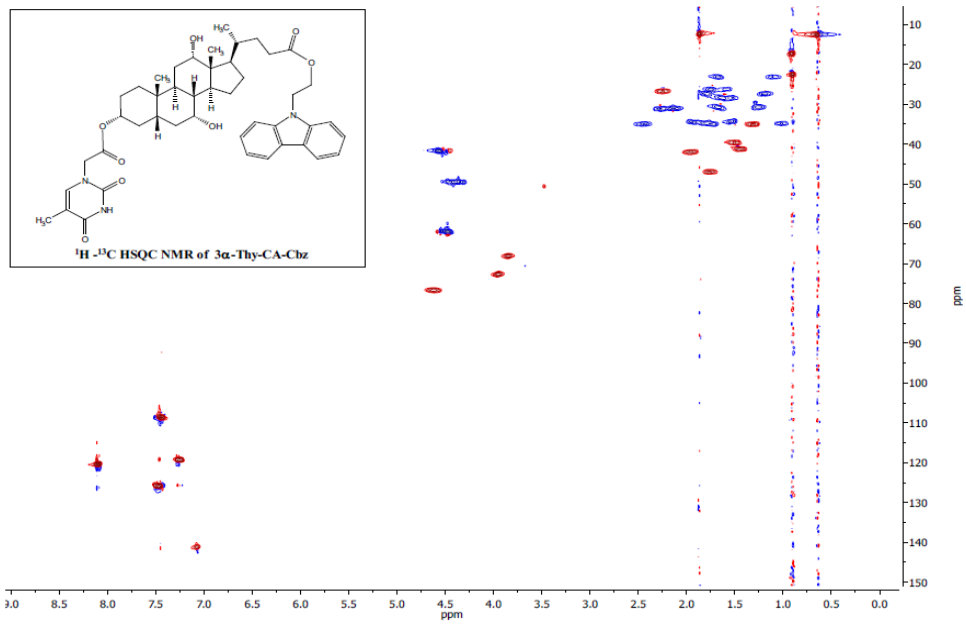

7.6.2.6. 3α,7α,12α-3Thy-CA-Cbz

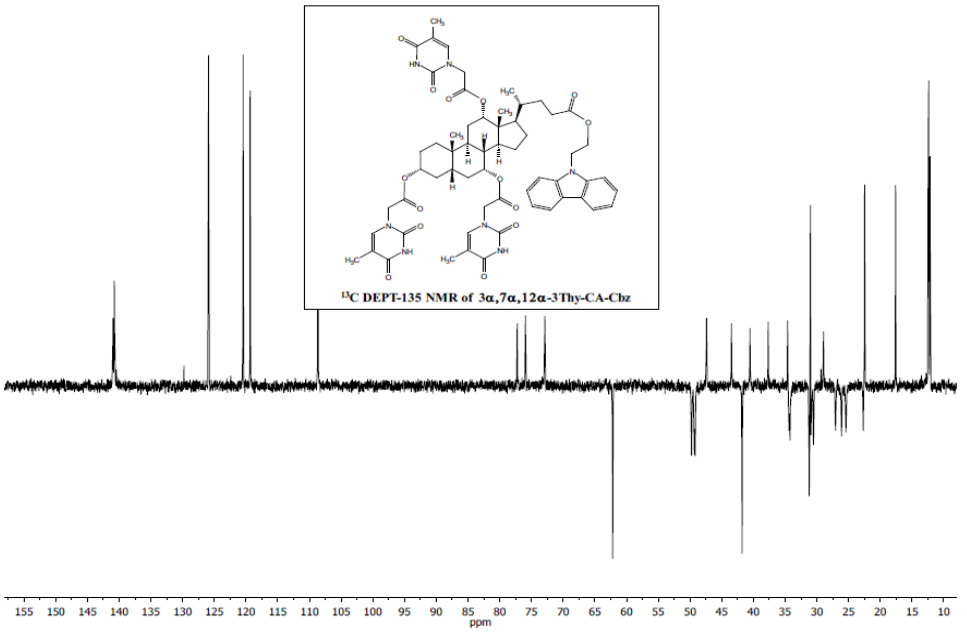

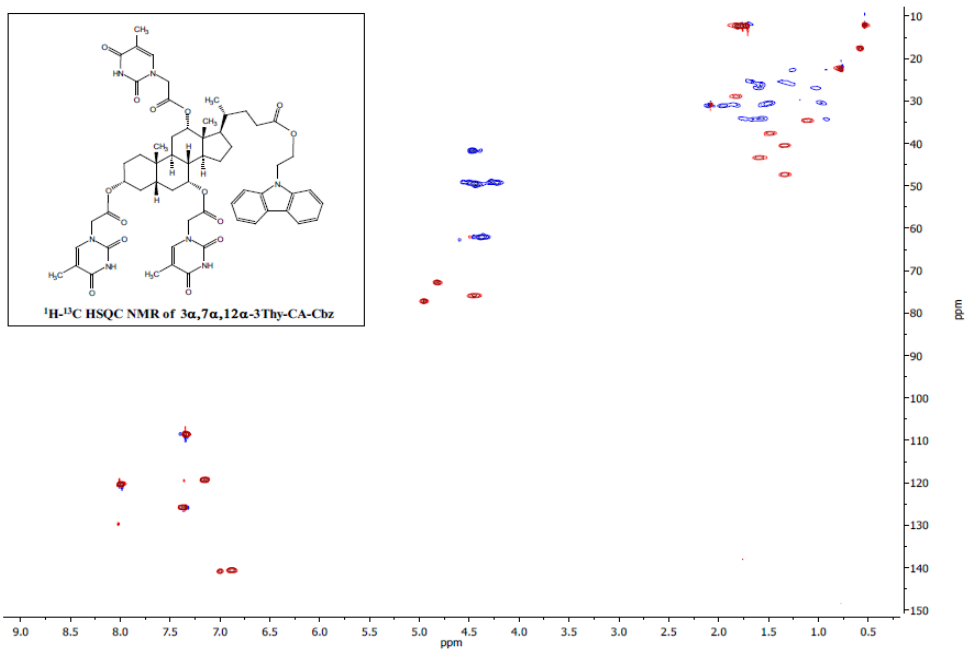

7.6.2.7. DCA–Cbz

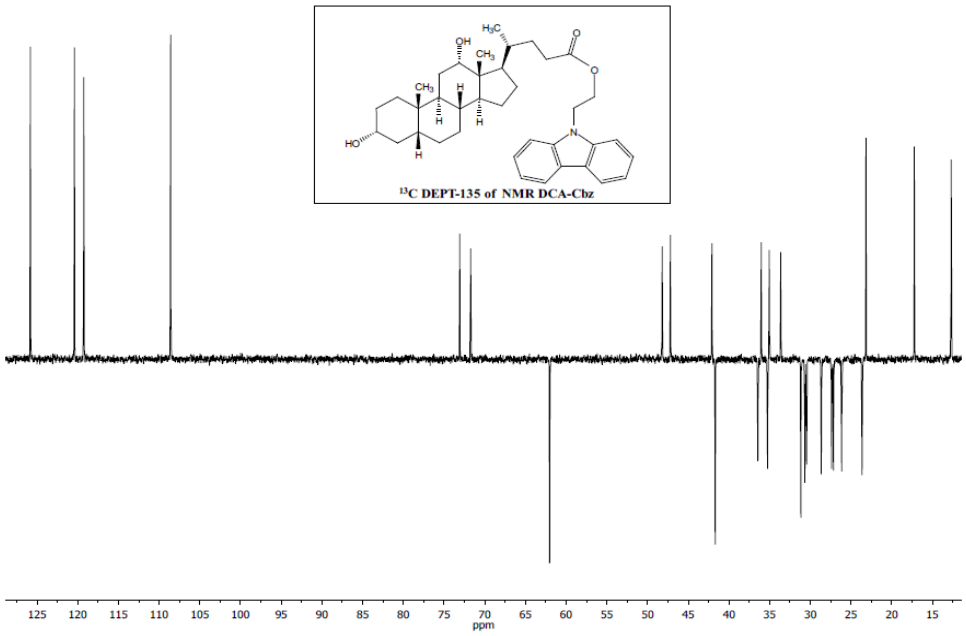
^{13}C DEPT-135 of NMR DCA-Cbz
125 120 115 110 105 100 95 90 85 80 75 70 65 60 55 50 45 40 35 30 25 20 15
ppm

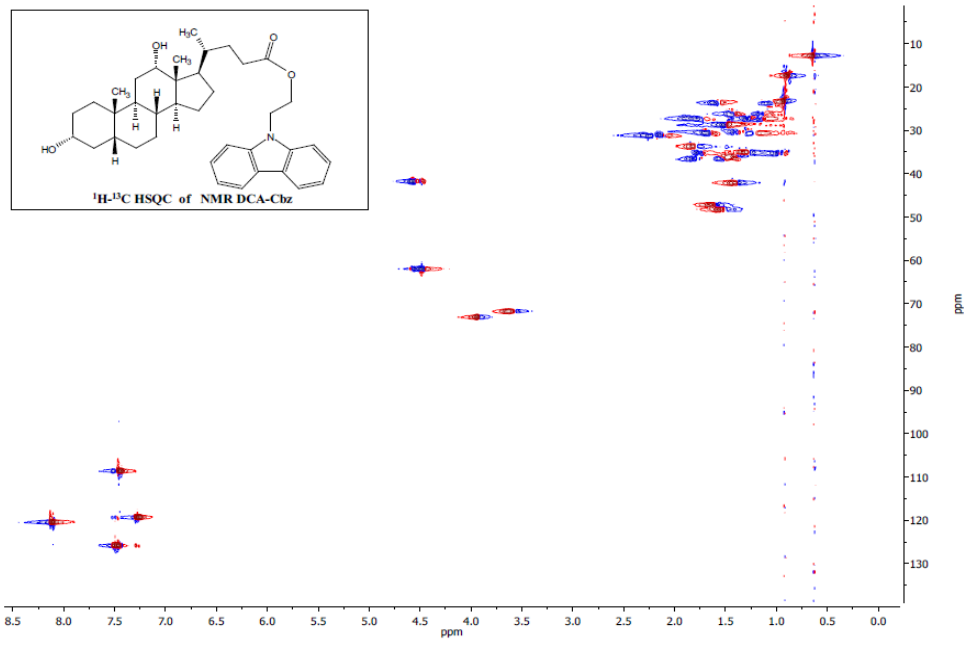
^{1}H-^{13}C HSQC of NMR DCA-Cbz
8.5 8.0 7.5 7.0 6.5 6.0 5.5 5.0 4.5 4.0 3.5 3.0 2.5 2.0 1.5 1.0 0.5 0.0
ppm
10 20 30 40 50 60 70 80 90 100 110 120 130
ppm

7.6.2.8. 3α, 12α-2Thy-DCA-Cbz

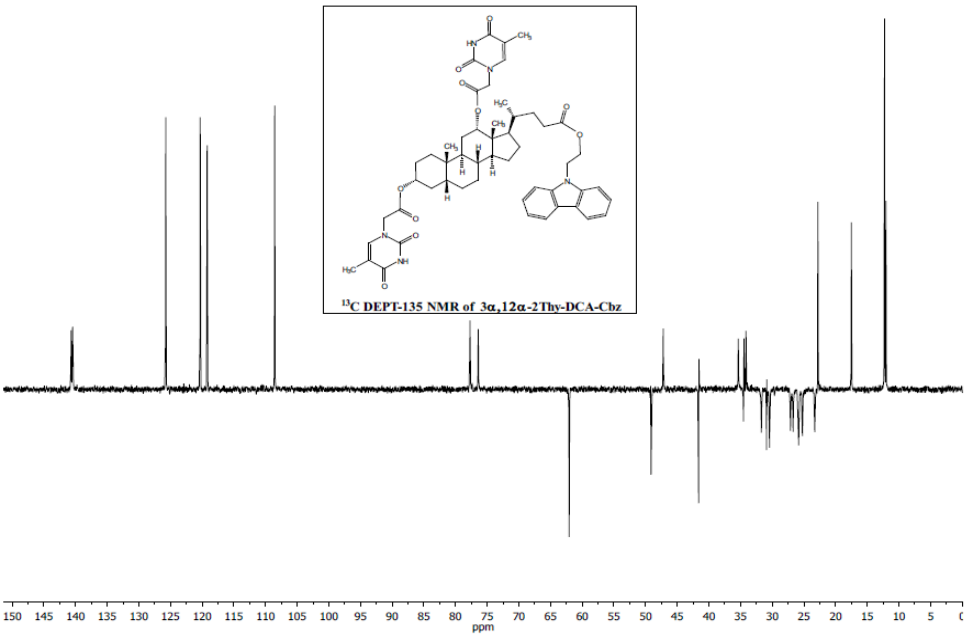

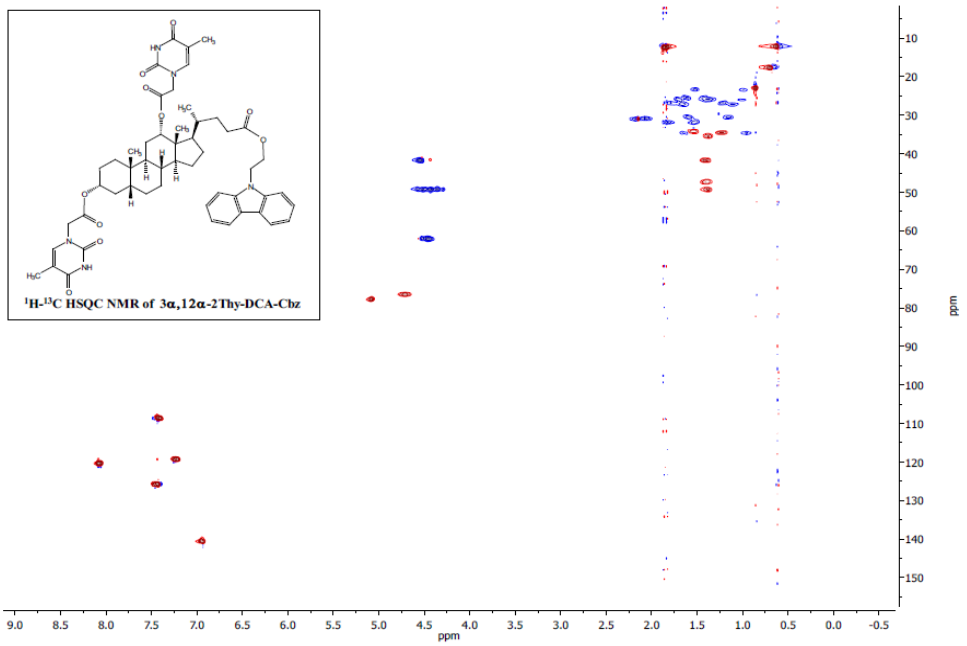

7.6.2.9. 3α-Cbz-DCA-Thy

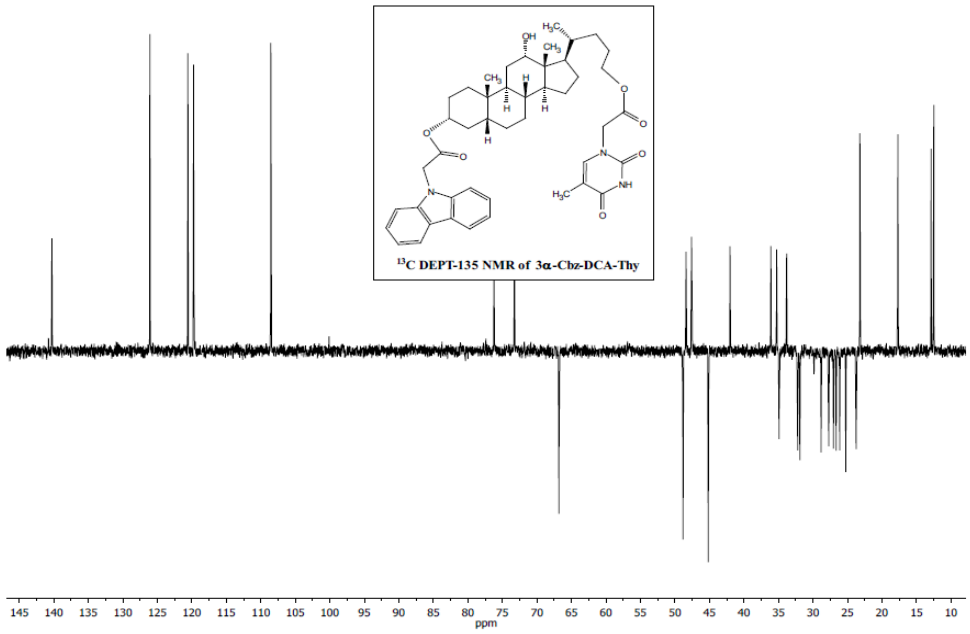

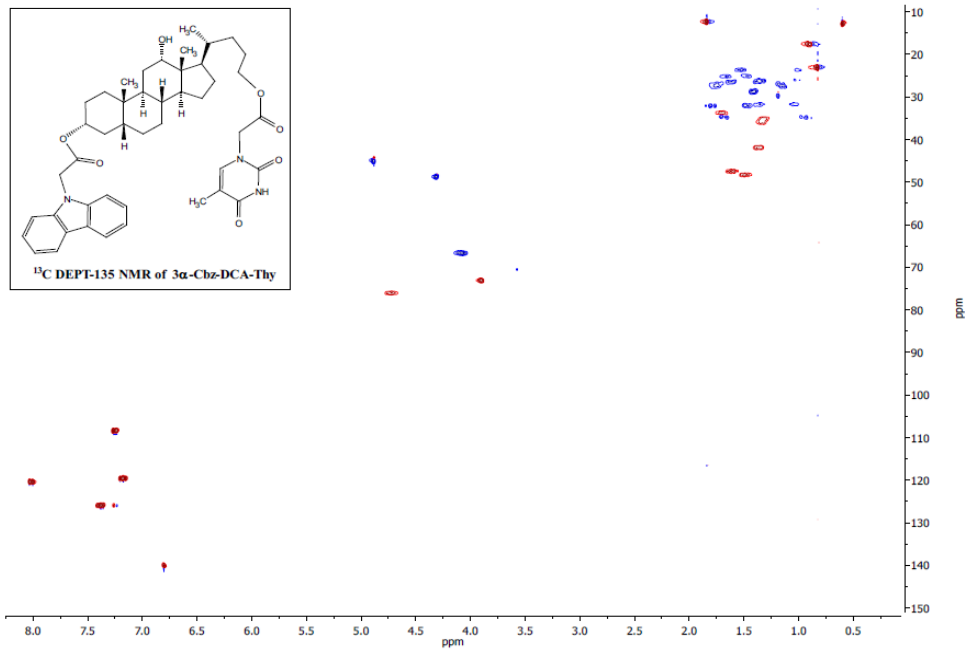

7.6.2.10. 3α-Cbz, 12α-Thy -DCA-Thy

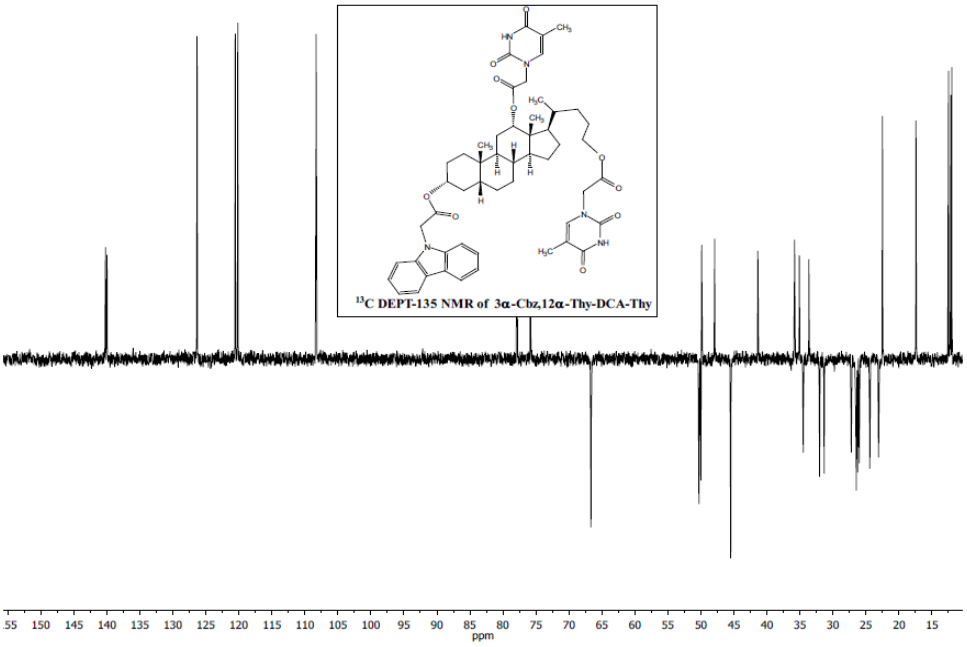

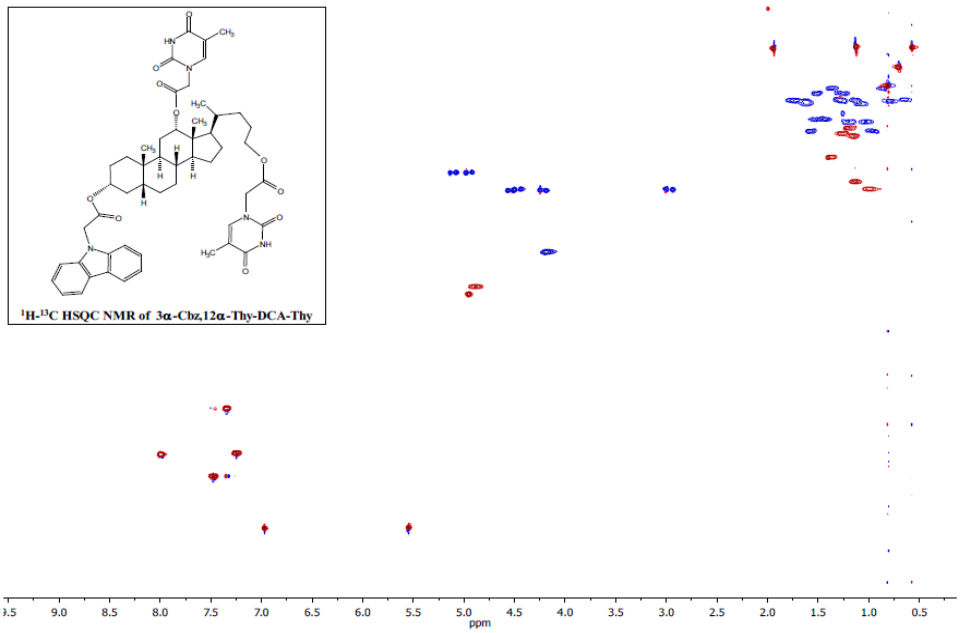

7.6.2.11. CDCA-Cbz

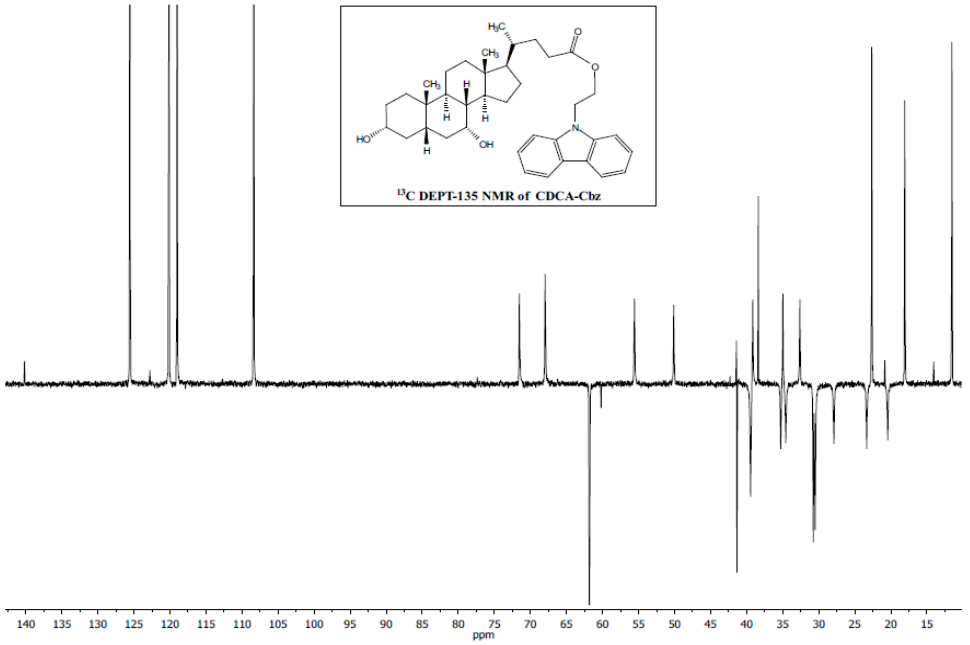

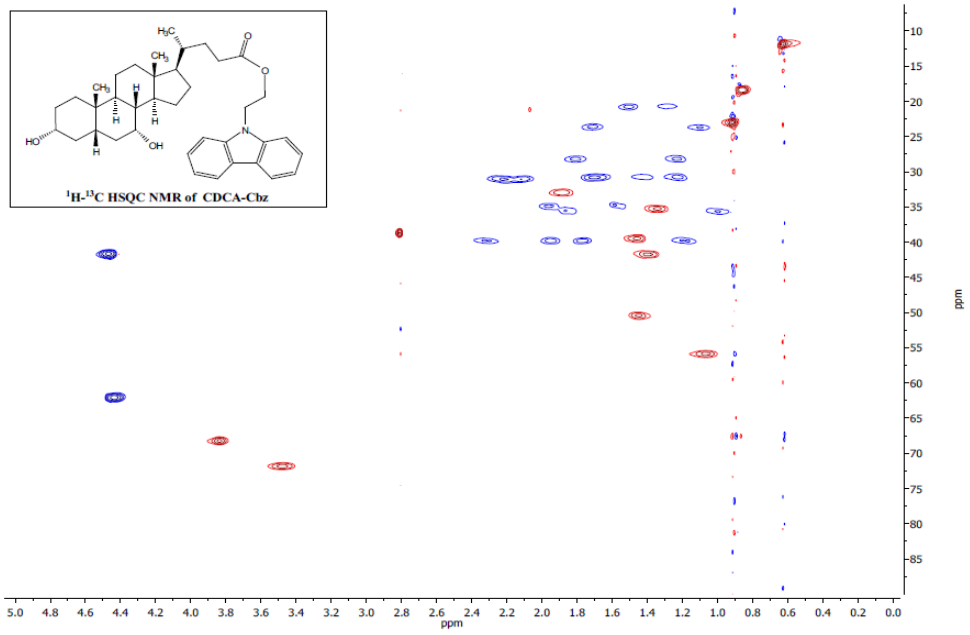

7.6.2.12. 3α, 7α-2Thy-CDCA-Cbz

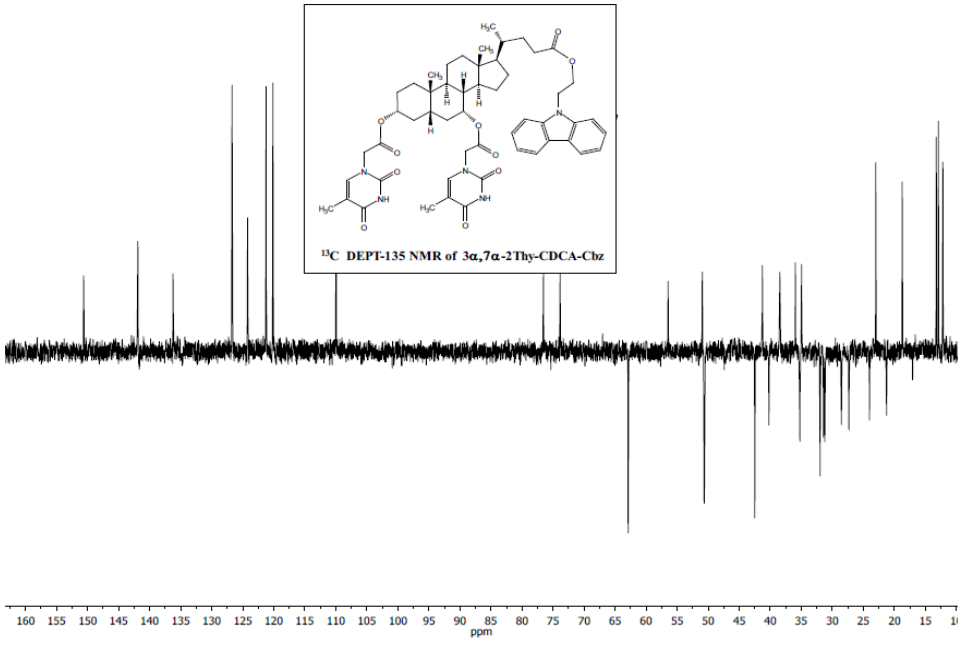

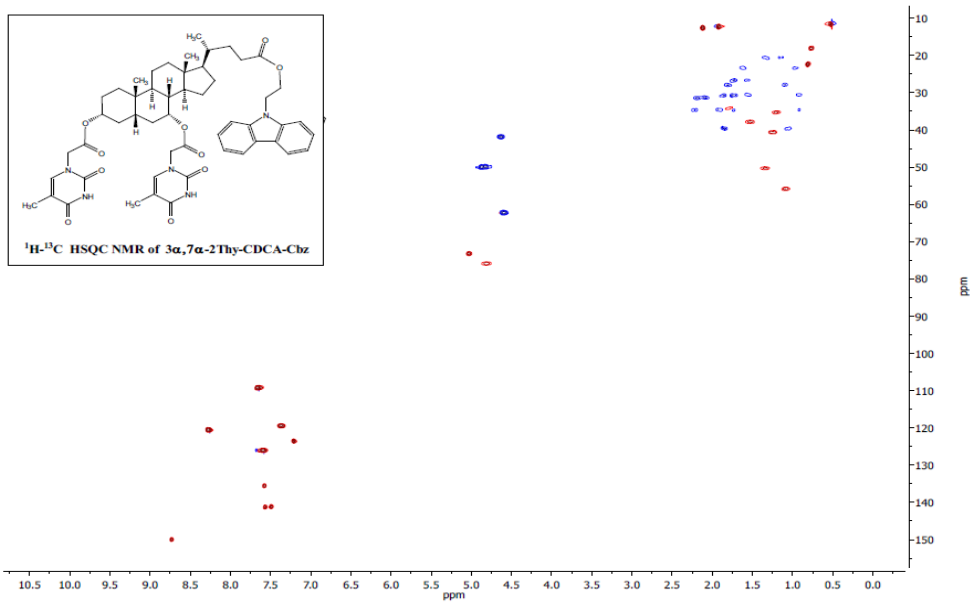

7.6.2.13. 3α-Cbz-CDCA-Thy

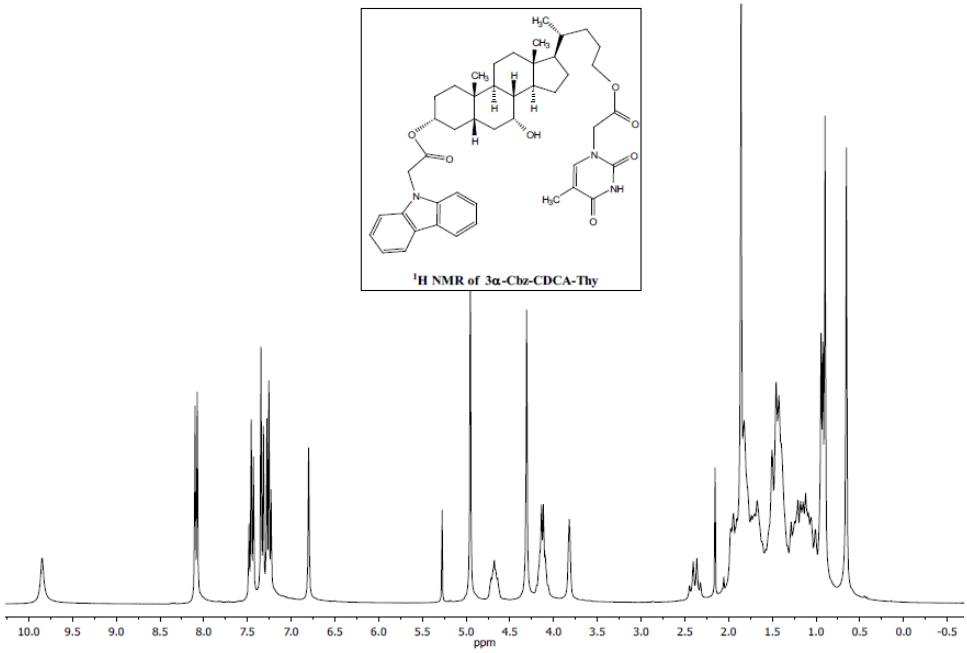

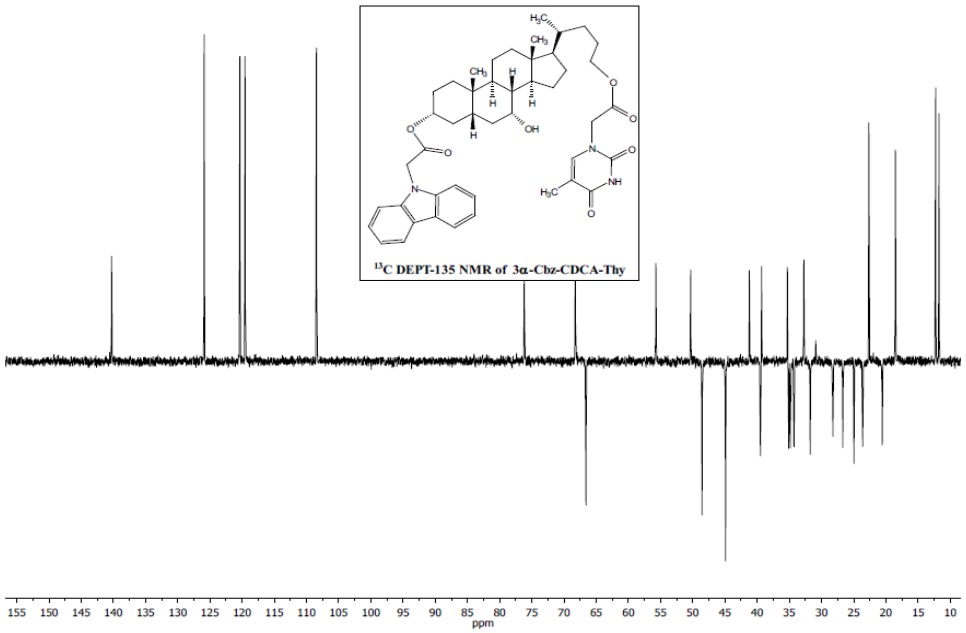

7.6.2.14. 3α-Cbz, 7α-Thy -CDCA-Thy

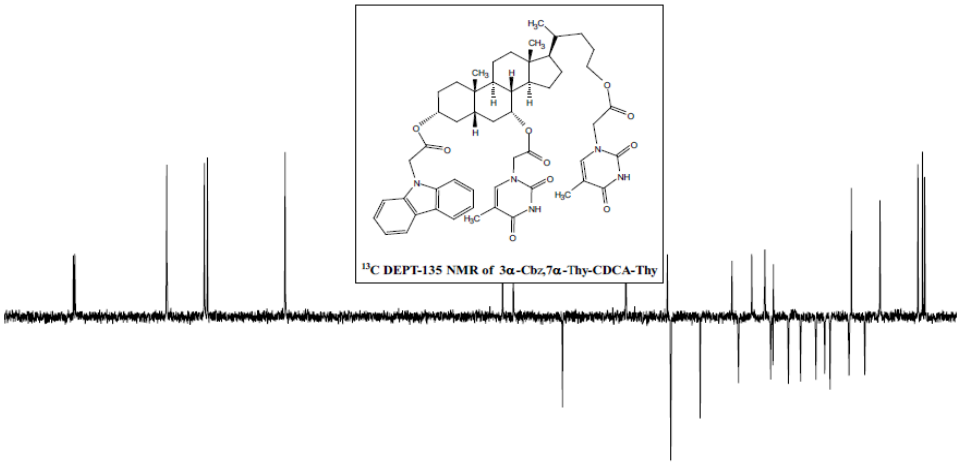

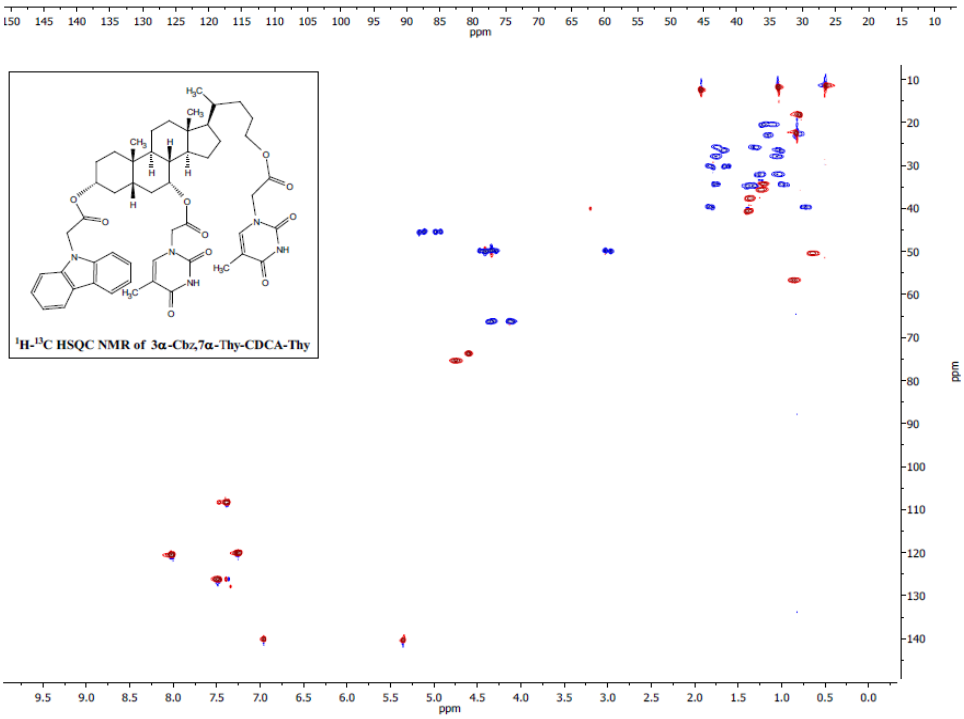

7.6.2.15. 3α,12α-Thy<>Thy-DCA-Cbz

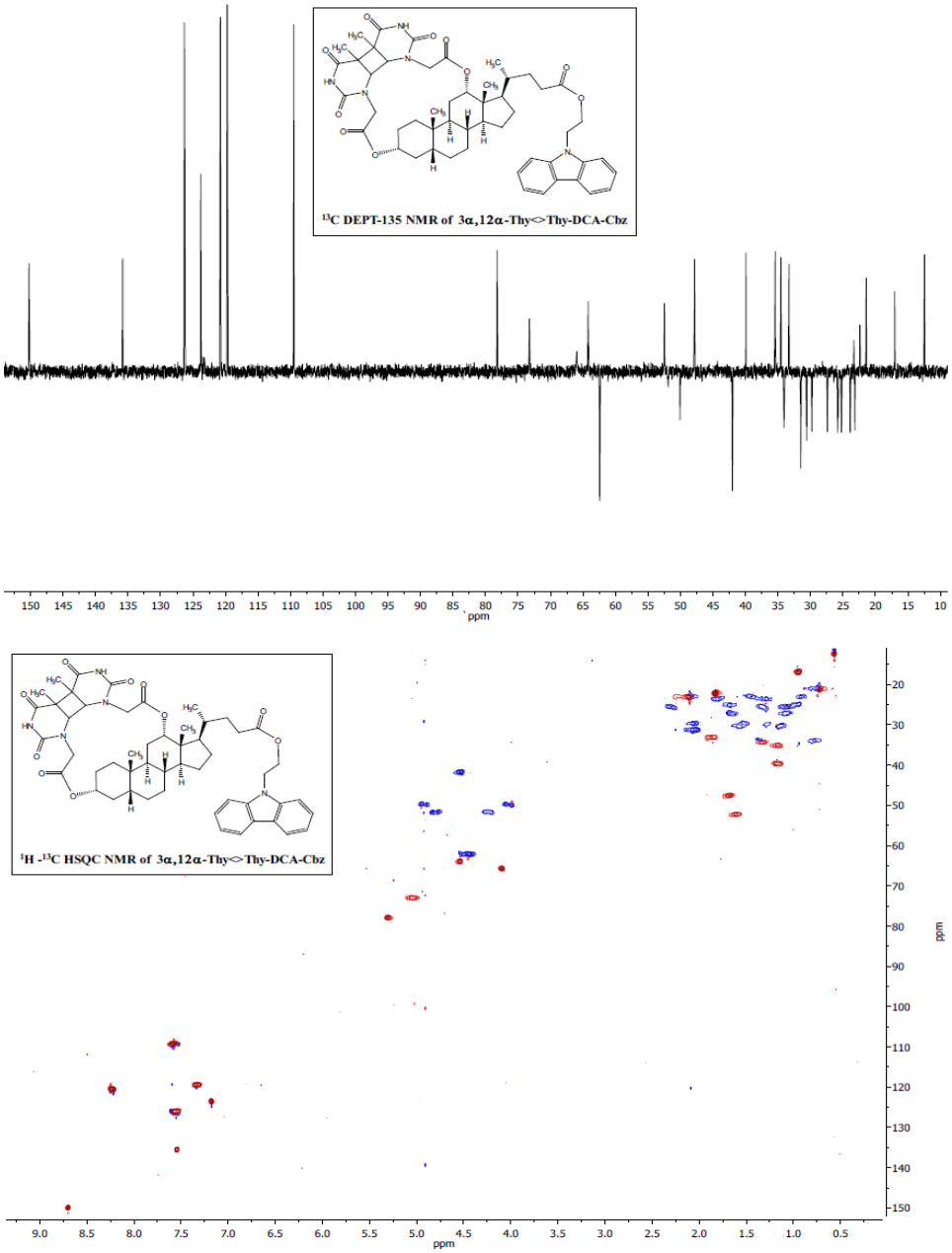

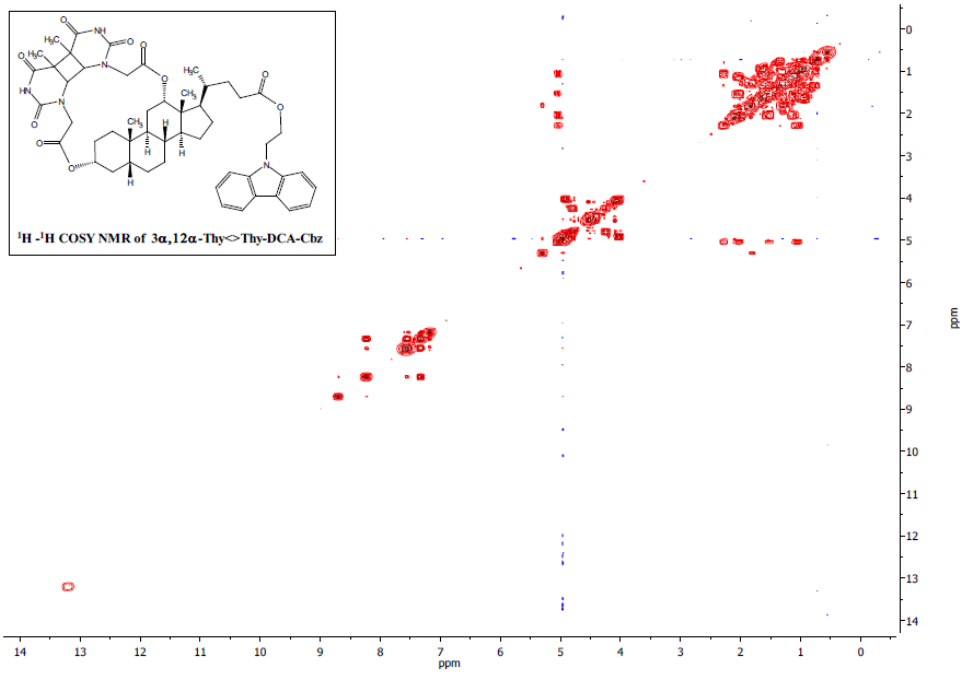
^{1}H -^{1}H COSY NMR of 3α,12α-Thy<>Thy-DCA-Cbz
ppm
ppm

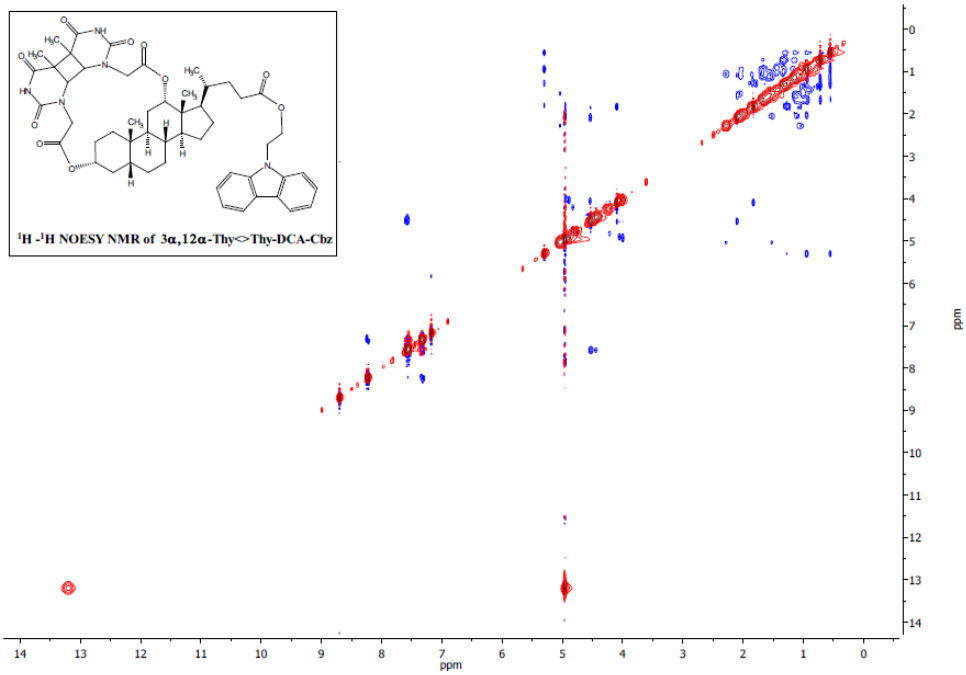
^{1}H -^{1}H NOESY NMR of 3α,12α-Thy<>Thy-DCA-Cbz
ppm
ppm

7.5.2.16. 3α-Cbz, -DCA-12α-Thy<>Thy

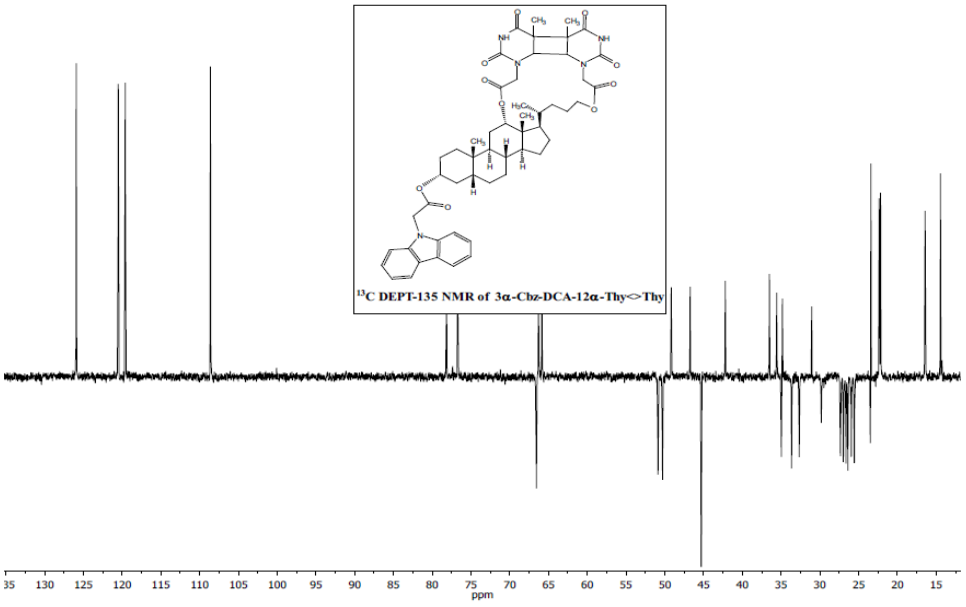

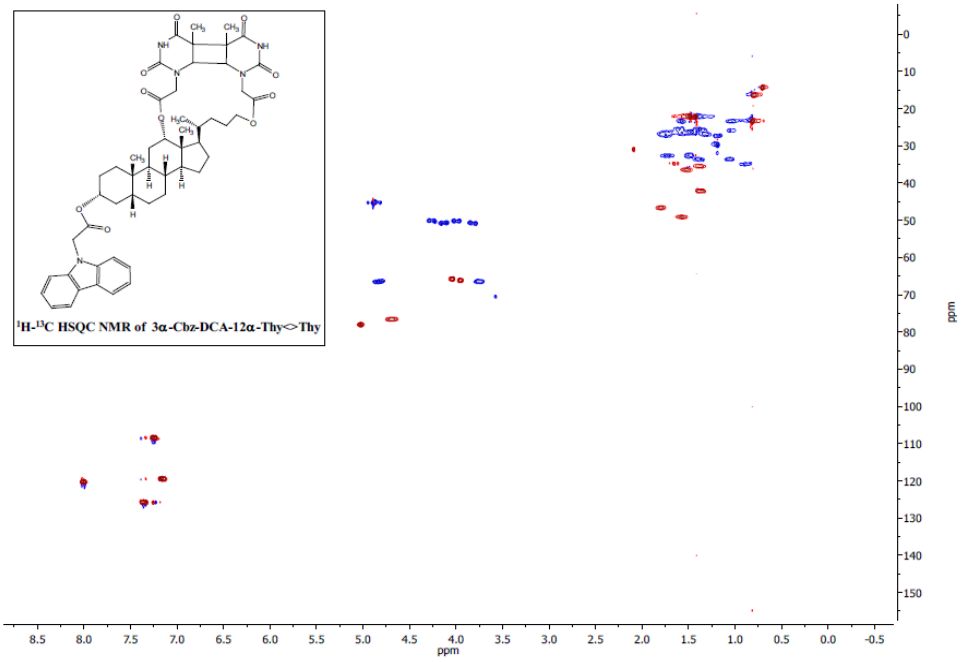

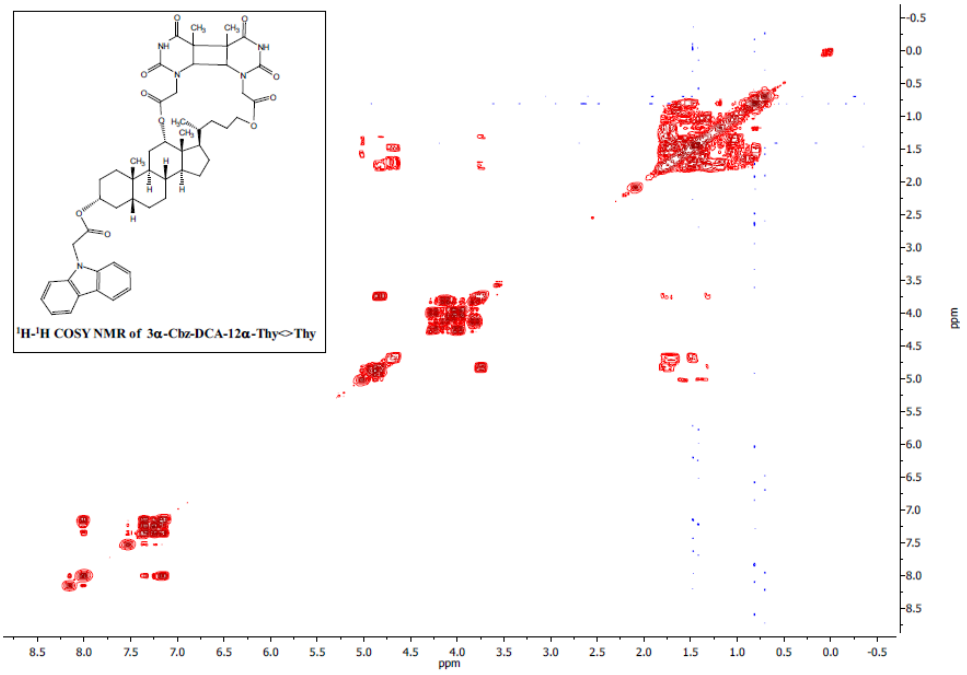
^{1}H-^{1}H COSY NMR of 3α-Cbz-DCA-12α-Thy<>Thy
ppm

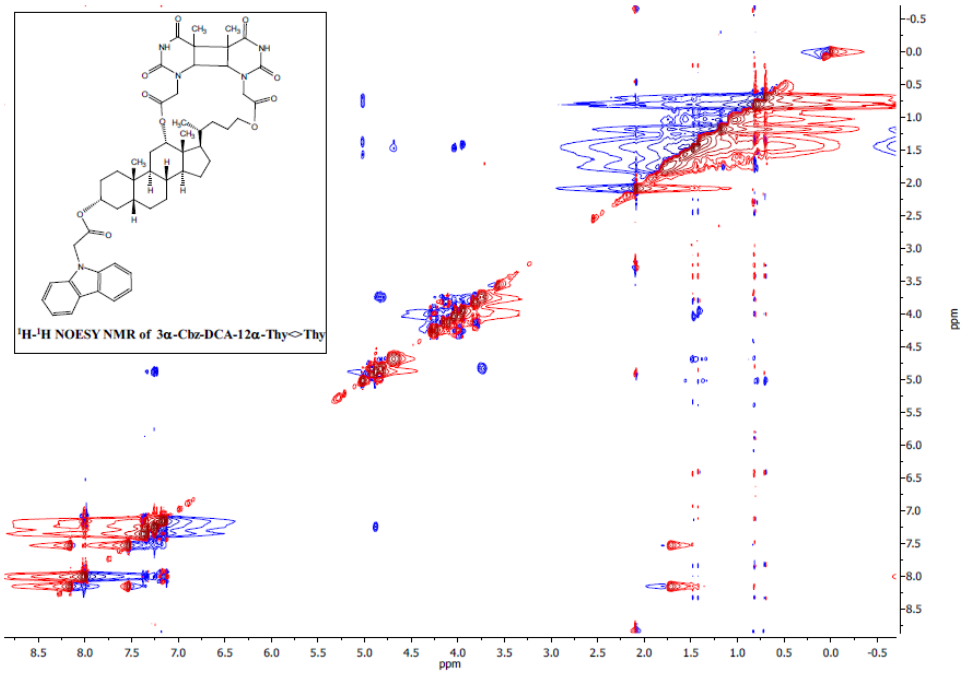
^{1}H-^{1}H NOESY NMR of 3α-Cbz-DCA-12α-Thy<>Thy
ppm

Chapter 8: Instrumentation

8.1. Chemicals

1,8-Diazabicyclo[5.4.0]undec-7-ene (DBU), 2,4,6-trichlorobenzoyl chloride, 4-dimethylaminopyridine (4-DMAP), 4-phenylbenzylalcohol (PBA), 9-carbazoleacetic acid (Cbz-CH_2-COOH), 9H-carbazol-9-ethanol (Cbz-$(CH_2)_2$-OH) , BAs (CA, CDCA, DCA, LA and UDCA), benzophenone (Bzp), benzyl bromide, borane-tetrahydrofuran complex solution, BSs (NaCA, NaCDCA and NaDCA), diethyl azodicarboxylate (DEAD), glacial acetic acid (CH_3COOH), KOH, lithium aluminum hydride ($LiAlH_4$), *N*-(3-dimethylaminopropyl)-*N′* -ethylcarbodiimide (EDC), *N,N′* -dicyclohexylcarbodiimide (DCC), *N,N*-diisopropylethylamine (DIEA), *O*-(benzotriazol-1-yl)-*N,N,N,N′* -tetramethyluronium tetrafluoroborate (TBTU), *(S)*-1-(1-naphtyhl)ethylamine (NEA), *S*-ketoprofen (KP), sodium chloride, sodium hydroxide, thymine 1-acetic acid (Thy-CH_2-CO_2H), triethylamine (Et_3N), triphenylphosphine (Ph_3P) and the solvents acetonitrile (CH_3CN), dichloromethane synthetic grade (CH_2Cl_2), dimethylformamide (DMF), ethylacetate (EtOAc), hexane, methanol (MeOH), pyridine (C_5H_5N) and tetrahydrofuran

(THF) were purchased from Sigma-Aldrich. Dichloromethane (HPLC grade) was from Scharlab.

8.2. Equipment

Nuclear Magnetic Resonance (NMR). Both Bruker 400 MHz and a Bruker 300 MHz spectrometers were used for the NMR experiments. The signal of the solvent, chloroform or methanol, was used as a reference for the determination of the chemical shifts (δ) in ppm.

UPLC-MS-MS. Chromatography was performed on an ACQUITY UPLC system (Waters Corp.) containing a conditioned autosampler at 4 °C. The separation was carried out on an ACQUITY UPLC BEH C18 column (50 mm × 2.1 mm i.d., 1.7 μm) at the temperature of 40 °C. The analysis was performed with isocratic elution of 70% MeOH and 30% water (containing 0.01% formic acid) as the mobile phase during 12 minutes followed by a gradient to reach 100% of MeOH. The injection volume was 1 μL. The Waters ACQUITY™ XevoQToF Spectrometer (Waters Corp.) was connected to the UPLC system via an electrospray ionization (ESI) interface. The ESI source was operated in positive or negative ionization mode depending on the experiment with the capillary voltage at 3.0 kV. The temperature of the source and desolvation was set at 120 °C and 500 °C, respectively. All data collected in Centroid mode were acquired using Masslynx™ software (Waters Corp.). Leucine-enkephalin was used as the lock mass generating an $[M+H]^+$ ion (m/z 556.2771) at a concentration of 500 pg/mL and flow rate of 20 μL/min to ensure accuracy during the MS analysis.

Absorption Measurements. UV spectra were recorded on a Cary 300 (Varian) spectrophotometer.

Photoreactor. Irradiations were performed in a Luzchem photoreactor (model LZC-4V) with lamps centred at 350 nm in quartz cuvettes or Pyrex vessels purged with N_2, using CH_3CN as solvent.

Laser Flash Photolysis at 266 or 355 nm and 308 nm. A pulsed Nd: YAG L52137 V LOTIS TII and an excimer laser of XeCl (LEXTRA 50 Lambda Physik Laser Technik) were employed for the measurements at the excitation wavelength of 355 or 266 nm and 308, respectively. The equipment consists of a pulsed laser, a 77250 Oriel monochromator and an oscilloscope DP04054 Tektronix. The output signal from the oscilloscope was transferred to a personal computer. The single pulses were *ca.* 10 ns duration, and the energy was 15 mg/pulse. Transient spectra were recorded using quartz cells of 1 cm path length.

Chapter 9: Conclusions

This Doctoral Thesis consists of the use of the rigid scaffold of bile acids to modulate the separation distances between chromophores to investigate different photophysical processes. The conclusions of each process can be sumarized as follows:

Related to the hydrogen atom transfer reaction from bile acids to benzophenone-derived triplet carbonyls:

- The triplet excited states of benzophenone derivatives, generated upon UVA excitation, are radical precursors in the hydrogen atom transfer from the methyne CH-OH groups of bile acids.
- Dehydrogenation of bile acids at positions C-3 and/or C-7 by a radical mediated mechanism gives the corresponding oxo derivatives.

Related to the synthesized donor/acceptor pairs separated by the rigid bridge of the bile acid scaffold for the study of through-bond processes:

- Through-bond energy transfer from benzophenone to naphthalene or biphenyl, followed by through-bond triplet exciplex formation as a deactivation channel of

the triplet acceptor in benzophenone/naphthalene and benzophenone/biphenyl linked systems, has been demonstrated by means of laser flash photolysis in solution at room temperature.

- Through-bond triplet-triplet energy transfer is dependent on the medium: in frozen matrix it does not play any role, while in solution it is very efficient.
- The energy gap between the donor and acceptor pairs is in agreement with the differences in the kinetic behavior.
- Both through-bond processes are strongly dependent on the relative spatial arrangement of the chromophores. Through-bond triplet-triplet energy transfer is faster in systems with benzophenone linked to the $3\alpha-$ position of the bile acid, whereas through-bond triplet exciplex deactivation is faster in systems with benzophenone linked to the $3\beta-$ one.

Related to the bile acid derivatives containing two linked thymine units and the benzophenone chromophore either linked or separated:

- A new mechanistic pathway leading to photosensitized formation of cyclobutane pyrimidine dimers, in which the key step is the generation of a triplet triplex has been evidenced.
- In the intermolecular systems containing two linked thymine units and a free intermolecular benzophenone, formation of a triplet triplex leads to cyclobutane pyrimidine dimers; conversely in the fully intramolecular systems, formation of the triplet triplexes is prevented due to geometrical strain.
- The photoreactivity of all the synthesized systems can be switched from a Paternò-Büchi, when the benzophenone and the two thymines are all linked to the skeleton, to a fully chemo-, regio-, and stereoselective [2+2] thymine dimerization when the two thymine units are attached to the bile acid skeleton being the benzophenone chromophore intermolecular.

Related to the cholic and lithocholic acid derivatives where one thimine unit and one benzophenone unit have been linked at non-bonding distances:

- Formation of thymine triplet by energy transfer from the triplet state of benzophenone has been proved by locating the chromophores at non-bonding distances, thus avoiding the Paternò-Büchi reaction.
- Slightly endergonic through-bond triplet-triplet energy transfer from benzophenone to thymine has been demonstrated.

Related to the bile acid derivatives where two thimine units and a protecting group or a carbazole unit have been linked at different positions:

- Deoxycholic and chenodeoxycholic acid derivatives containing two thymine units at positions 3α+12α, 12α+lateral chain, 3α+7α and 7α+lateral chain submitted to direct irradiation gave the corresponding thymine dimers in all cases.
- Deoxycholic acid derivatives containing two thymine units at positions 3α+12α and12α+lateral chain with an intramolecular carbazole unit gave the corresponding thymine dimers by sensitization from carbazole. Analogous chenodeoxycholic acid derivatives containing two thymine units at positions 3α+7α and 7α+lateral chain with an intramolecular carbazole unit did not give photoproducts.

Chapter 10: References

1 A. F. Hofmann and L. R. Hagey, *Cell. Mol. Life Sci.*, 2008, **65**, 2461-2483.

2 A. F. Hofmann, L. R. Hagey and M. D. Krasowski, *J. Lipid Res.*, 2010, **51**, 226-246.

3 E. Kolehmainen, *Angew. Chem., Int. Ed.*, 2009, **48**, 258-259.

4 S. Nishiyama, S. Yamamura, K. Kato and T. Takita, *Tetrahedron Lett.*, 1988, **29**, 4743-4746.

5 D. M. Small, S. A. Penkett and D. Chapman, *Biochim. Biophys. Acta*, 1969, **176**, 178-189.

6 M. Gomez-Mendoza, M. L. Marin and M. A. Miranda, *J. Phys. Chem. B*, 2012, **116**, 14776-14780.

7 M. Gomez-Mendoza, M. L. Marin and M. A. Miranda, *J. Phys. Chem. Lett.*, 2011, **2**, 782-785.

8 M. J. Armstrong and M. C. Carey, *J. Lipid Res.*, 1982, **23**, 70-80.

9 A. F. Attili, M. Angelico, A. Cantafora, D. Alvaro and L. Capocaccia, *Med. Hypotheses*, 1986, **19**, 57-69.

10 K. Solaas, A. Ulvestad, O. Soreide and B. F. Kase, *J. Lipid Res.*, 2000, **41**, 1154-1162.

11 D. W. Russell, *Annu. Rev. Biochem.*, 2003, **72**, 137-174.

12 J. Y. L. Chiang, *J. Lipid Res.*, 2009, **50**, 1955-1966.

13 A. F. Hofmann, *Arch. Intern. Med.*, 1999, **159**, 2647-2658.

14 A. V. LeBouton, *Molecular and Cell Biology of the Liver*, CRC, USA, 1993.

15 I. M. Arias, *The Liver: Biology and Pathobiology*, John Wiley & Sons Ltd., UK, 2009.

16 S. E. Gilliland and M. L. Speck, *Appl. Environ. Microbiol.*, 1977, **33**, 15-18.
17 H. S. Mita, H. Akita, H. Hayashi, R. Onuki, A. F. Hofmann and Y. Sugiyama, *Drug Metab. Dispos.*, 2006, ***34***, 1575-1581.
18 M. Trauner, P. J. Meier and J. L. Boyer, *N. Engl. J. Med.*, 1998, ***339***, 1217-1227.
19 M. Wagner, G. Zollner and M. Trauner, *J. Hepatol.*, 2009, ***51***, 565-580.
20 A. A. Gossard and K. D. Lindor, *Can. J. Gastroenterol.*, 2000, **14**, 93D-98D.
21 N. J. Turro, V. Ramamurthy and J. C. Scaiano, *Principles of Molecular Photochemistry: An Introduccion*, University Science Books, USA, 2008.
22 S. L. Murov, I. Carmichael and G. L. Hug, eds., *Handbook of Photochemistry*, USA, 2009.
23 J. D. Coyle, *Introduction to Organic Photochemistry*, John Wiley & Sons Can. Ltd., Canada, 1986.
24 P. Slavicek, *Chem. Listy*, 2010, **104**, 209-473.
25 A. Jablonski, *Z. Phys.*, 1935, **94**, 38-46.
26 W. M. Horspool, *Handbook of Organic Photochemistry and Photobiology*, CRC, USA, 1995.
27 M. Montalti, A. Credi, L. Prodi, M. T. Gandolfi and Editors, *Handbook of Photochemistry*, CRC Press LLC, USA, 2006.
28 I. Tinoco, Jr., K. Sauer and J. C. Wang, *Physical Chemistry: Principles and Applications in Biological Sciences*, Prentice Hall, USA, 1995.
29 D. L. Dexter, *J. Chem. Phys.*, 1953, **21**, 836-850.
30 I. R. Gould, R. H. Young, L. J. Mueller and S. Farid, *J. Am. Chem. Soc.*, 1994, **116**, 8176-8187.
31 T. Förster, *Annalen der Physik*, 1948, **437**, 55-75.
32 J. C. Scaiano, *J. Photochem.*, 1973, **2**, 81-118.
33 S. G. Cohen and H. M. Chao, *J. Am. Chem. Soc.*, 1968, **90**, 165-173.
34 I. Andreu, D. Neshchadin, E. Rico, M. Griesser, A. Samadi, I. M. Morera, G. Gescheidt and M. A. Miranda, *Chem. Eur. J.*, 2011, **17**, 10089-10096.
35 I. Andreu, I. M. Morera, F. Bosca, L. Sanchez, P. Camps and M. A. Miranda, *Org. Biomol. Chem.*, 2008, **6**, 860-867.
36 D. Neshchadin, F. Palumbo, M. S. Sinicropi, I. Andreu, G. Gescheidt and M. A. Miranda, *Chem. Sci.*, 2013, **4**, 1608-1614.
37 T. Bach, *Synthesis*, 1998, 683-703.
38 K. S. Peters, B. Li and J. Lee, *J. Am. Chem. Soc.*, 1993, **115**, 11119-11122.
39 D. I. Schuster, G. Lem and N. A. Kaprinidis, *Chem. Rev.*, 1993, **93**, 3-22.
40 M. C. Cuquerella, V. Lhiaubet-Vallet, F. Bosca and M. A. Miranda, *Chem. Sci.*, 2011, **2**, 1219-1232.
41 P. E. Eaton and T. W. Cole, *J. Am. Chem. Soc.*, 1964, **86**, 3157-3158.

42 R. Costalat, J. Blais, J. P. Ballini, A. Moysan, J. Cadet, O. Chalvet and P. Vigny, *Photochem. Photobiol.*, 1990, **51**, 255-262.

43 L. O. Essen and T. Klar, *Cell. Mol. Life Sci.*, 2006, **63**, 1266-1277.

44 G. Buchi, C. G. Inman and E. S. Lipinsky, *J. Am. Chem. Soc.*, 1954, **76**, 4327-4331.

45 E. Paterno, *Gazz. Chim. Ital.*, 1909, **39**, 237-250.

46 S. C. Freilich and K. S. Peters, *J. Am. Chem. Soc.*, 1981, **103**, 6255-6257.

47 R. M. Wilson, S. W. Wunderly, T. F. Walsh, A. K. Musser, R. Outcalt, F. Geiser, S. K. Gee, W. Brabender, L. J. Yerino, T. T. Conrad and G. A. Tharp, *J. Am. Chem. Soc.*, 1982, **104**, 4429-4446.

48 M. C. Cuquerella, V. Lhiaubet-Vallet, J. Cadet and M. A. Miranda, *Acc. Chem. Res.*, 2012, **45**, 1558-1570.

49 S. Encinas, N. Belmadoui, M. J. Climent, S. Gil and M. A. Miranda, *Chem. Res. Toxicol.*, 2004, **17**, 857-862.

50 A. Joseph, G. Prakash and D. E. Falvey, *J. Am. Chem. Soc.*, 2000, **122**, 11219-11225.

51 F. Bosca, I. Andreu, I. M. Morera, A. Samadi and M. A. Miranda, *Chem. Commun.*, 2003, 1592-1593.

52 J. Trzcionka, V. Lhiaubet-Vallet, C. Paris, N. Belmadoui, M. J. Climent and M. A. Miranda, *ChemBioChem*, 2007, **8**, 402-407.

53 L. A. Booth, I. T. Gilmore and R. F. Bilton, *Free Rad. Res.*, 1997, **26**, 135-144.

54 V. Labet, N. Jorge, C. Morell, T. Douki, A. Grand, J. Cadet and L. A. Eriksson, *Photochem. Photobiol. Sci.*, 2013, **12**, 1509-1516.

55 N. A. Petasis and M. A. Patane, *Tetrahedron*, 1992, **48**, 5757-5821.

56 D. H. Grayson and J. R. H. Wilson, *J. Chem. Soc., Chem. Commun.*, 1984, 1695-1696.

57 R. Ninomiya, K. Matsuoka and Y. Moroi, *BBA-Mol. Cell Biol. L.*, 2003, **1634**, 116-125.

58 J. Rohacova, M. L. Marin, A. Martinez-Romero, J. E. O'Connor, M. J. Gomez-Lechon, M. T. Donato, J. V. Castell and M. A. Miranda, *Org. Biomol. Chem.*, 2009, **7**, 4973-4980.

59 E. Nuin, M. Gómez-Mendoza, I. Andreu, M. L. Marin and M. A. Miranda, *Org. Lett.*, 2013, **15**, 298-301.

60 D. E. Cohen, M. Angelico and M. C. Carey, *J. Lipid Res.*, 1990, **31**, 55-70.

61 D. Lichtenberg, S. Ragimova, A. Bor, S. Almog, C. Vinkler, M. Kalina, Y. Peled and Z. Halpern, *Biophys. J.*, 1988, **54**, 1013-1025.

62 S. Mukhopadhyay and U. Maitra, *Curr. Sci.*, 2004, **87**, 1666-1683.

63 J. Rohacova, M. L. Marin, A. Martinez-Romero, L. Diaz, J. E. O'Connor, M. J. Gomez-Lechon, M. T. Donato, J. V. Castell and M. A. Miranda, *ChemMedChem*, 2009, **4**, 466-472.

64 J. Rohacova, M. L. Marin, A. Martinez-Romero, J. E. O'Connor, M. J. Gomez-Lechon, M. T. Donato, J. V. Castell and M. A. Miranda, *Photochem. Photobiol. Sci.*, 2008, **7**, 860-866.

65 J. Rohacova, M. L. Marin and M. A. Miranda, *J. Phys. Chem. B*, 2010, **114**, 4710-4716.

66 A. L. Lehninger, D. L. Nelson and M. M. Cox, *Principles of Biochemistry*, Hirokawa Publishing Co., USA, 1993.

67 J. M. Ridlon, D.-J. Kang and P. B. Hylemon, *J. Lipid Res.*, 2006, **47**, 241-259.

68 F. Secundo, G. Carrea, M. De Amici, S. Joppolo di Ventimiglia and J. S. Dordick, *Biotechnol. Bioeng.*, 2003, **81**, 391-396.

69 V. Prabha and M. Ohri, *World J. Microbiol. Biotechnol.*, 2006, **22**, 191-196.

70 A. K. Agarwal and R. J. Auchus, *Endocrinology*, 2005, **146**, 2531-2538.

71 P. P. Giovannini, A. Grandini, D. Perrone, P. Pedrini, G. Fantin and M. Fogagnolo, *Steroids*, 2008, **73**, 1385-1390.

72 D. Monti, E. E. Ferrandi, I. Zanellato, L. Hua, F. Polentini, G. Carrea and S. Riva, *Adv. Synth. Catal.*, 2009, **351**, 1303-1311.

73 G. Salen, A. Colalillo, D. Verga, E. Bagan, G. S. Tint and S. Shefer, *Gastroenterology*, 1980, **78**, 1412-1418.

74 M. V. Encinas and J. C. Scaiano, *J. Am. Chem. Soc.*, 1981, **103**, 6393-6397.

75 D. Z. Markovic, T. Durand and L. K. Patterson, *Photochem. Photobiol.*, 1990, **51**, 389-394.

76 S. Kamijo, K. Tao, G. Takao, H. Tonoda and T. Murafuji, *Org. Lett.*, 2015, **17**, 3326-3329.

77 P.-Y. Wang, Y.-J. Chen, A.-C. Wu, Y.-S. Lin, M.-F. Kao, J.-R. Chen, J.-F. Ciou and S.-W. Tsai, *Adv. Synth. Catal.*, 2009, **351**, 2333-2341.

78 K.-Y. Tserng, *J. Lipid Res.*, 1978, **19**, 501-504.

79 J. R. Miller, L. T. Calcaterra and G. L. Closs, *J. Am. Chem. Soc.*, 1984, **106**, 3047-3049.

80 G. L. Closs, P. Piotrowiak, J. M. Macinnis and G. R. Fleming, *J. Am. Chem. Soc.*, 1988, **110**, 2652-2653.

81 G. L. Closs and J. R. Miller, *Science*, 1988, **240**, 440-447.

82 G. L. Closs, L. T. Calcaterra, N. J. Green, K. W. Penfield and J. R. Miller, *J. Phys. Chem.*, 1986, **90**, 3673-3683.

83 G. L. Closs, M. D. Johnson, J. R. Miller and P. Piotrowiak, *J. Am. Chem. Soc.*, 1989, **111**, 3751-3753.

84 M. N. Paddon-Row, *Acc. Chem. Res.*, 1982, **15**, 245-251.

85 M. R. Wasielewski, *Chem. Rev.*, 1992, **92**, 435-461.

86 M. N. Paddon-Row, *Acc. Chem. Res.*, 1994, **27**, 18-25.
87 W. G. McGimpsey, W. N. Samaniego, L. Chen and F. Wang, *J. Phys. Chem. A*, 1998, **102**, 8679-8689.
88 J. K. Agyin, H. Morrison and A. Siemiarczuk, *J. Am. Chem. Soc.*, 1995, **117**, 3875-3876.
89 J. K. Agyin, L. D. Timberlake and H. Morrison, *J. Am. Chem. Soc.*, 1997, **119**, 7945-7953.
90 W. S. Li and H. Morrison, *Org. Lett.*, 2000, **2**, 15-18.
91 Z. Z. Wu, J. Nash and H. Morrison, *J. Am. Chem. Soc.*, 1992, **114**, 6640-6648.
92 Y. Zhu and G. B. Schuster, *J. Am. Chem. Soc.*, 1990, **112**, 8583-8585.
93 Y. Zhu and G. B. Schuster, *J. Am. Chem. Soc.*, 1993, **115**, 2190-2199.
94 C. H. Tung, L. P. Zhang, Y. Li, H. Cao and Y. Tanimoto, *J. Phys. Chem.*, 1996, **100**, 4480-4484.
95 C. H. Tung, L. P. Zhang, Y. Li, H. Cao and Y. Tanimoto, *J. Am. Chem. Soc.*, 1997, **119**, 5348-5354.
96 L. P. Zhang, B. Chen, L. Z. Wu, C. H. Tung, H. Cao and Y. Tanimoto, *Chem. A Eur. J.*, 2003, **9**, 2763-2769.
97 X.-H. Xu, X.-G. Fu, L.-Z. Wu, B. Chen, L.-P. Zhang, C.-H. Tung, H.-F. Ji, K. S. Schanze and R.-Q. Zhang, *Chem. A Eur. J.*, 2006, **12**, 5238-5245.
98 S. L. Zhang, M. J. Lang, S. Goodman, C. Durnell, V. Fidlar, G. R. Fleming and N. C. C. Yang, *J. Am. Chem. Soc.*, 1996, **118**, 9042-9051.
99 B. Paulson, K. Pramod, P. Eaton, G. Closs and J. R. Miller, *J. Phys. Chem.*, 1993, **97**, 13042-13045.
100 B. P. Paulson, L. A. Curtiss, B. Bal, G. L. Closs and J. R. Miller, *J. Am. Chem. Soc.*, 1996, **118**, 378-387.
101 M. E. Sigman and G. L. Closs, *J. Phys. Chem.*, 1991, **95**, 5012-5017.
102 K. Ohta, G. L. Closs, K. Morokuma and N. J. Green, *J. Am. Chem. Soc.*, 1986, **108**, 1319-1320.
103 M. D. E. Forbes, G. L. Closs, P. Calle and P. Gautam, *J. Phys. Chem.*, 1993, **97**, 3384-3389.
104 J. Jortner, M. Bixon, B. Wegewijs, J. W. Verhoeven and R. P. H. Rettschnick, *Chem. Phys. Lett.*, 1993, **205**, 451-455.
105 S.-M. Wang, M.-L. Yu, J. Ding, C.-H. Tung and L.-Z. Wu, *J. Phys. Chem. A*, 2008, **112**, 3865-3869.
106 L. Han, H. X. Wei, S. Y. Li, J. P. Chen, Y. Zeng, Y. Y. Li, Y. B. Han, Y. Li, S. Q. Wang and G. Q. Yang, *ChemPhysChem*, 2010, **11**, 229-235.
107 Z. Tan, R. Kote, W. N. Samaniego, S. J. Weininger and W. G. McGimpsey, *J. Phys. Chem. A*, 1999, **103**, 7612-7620.
108 D. Gust, T. A. Moore and A. L. Moore, *Acc. Chem. Res.*, 1993, **26**, 198-205.

109 D. Gust, T. A. Moore, A. L. Moore, C. Devadoss, P. A. Liddell, R. Hermant, R. A. Nieman, L. J. Demanche, J. M. Degraziano and I. Gouni, *J. Am. Chem. Soc.*, 1992, **114**, 3590-3603.

110 R. Hoffmann, *Acc. Chem. Res.*, 1971, **4**, 1-9.

111 J. Kroon, A. M. Oliver, M. N. Paddon-Row and J. W. Verhoeven, *J. Am. Chem. Soc.*, 1990, **112**, 4868-4873.

112 K. D. Jordan and M. N. Paddon-Row, *Chem. Rev.*, 1992, **92**, 395-410.

113 K. Kilsa, J. Kajanus, J. Martensson and B. Albinsson, *J. Phys. Chem. B*, 1999, **103**, 7329-7339.

114 M. R. Roest, A. M. Oliver, M. N. Paddon-Row and J. W. Verhoeven, *J. Phys. Chem. A*, 1997, **101**, 4867-4871.

115 J. W. Verhoeven, *Pure Appl. Chem.*, 1990, **62**, 1585-1596.

116 J. W. Verhoeven, B. Wegewijs, T. Scherer, R. P. H. Rettschnick, J. M. Warman, W. Jager and S. Schneider, *J. Phys. Org. Chem.*, 1996, **9**, 387-397.

117 X. Y. Lauteslager, I. H. M. van Stokkum, H. J. van Ramesdonk, D. Bebelaar, J. Fraanje, K. Goubitz, H. Schenk, A. M. Brouwer and J. W. Verhoeven, *Eur. J. Org. Chem.*, 2001, 3105-3118.

118 E. A. Khramtsova, V. F. Plyusnin, I. M. Magin, A. I. Kruppa, N. E. Polyakov, T. V. Leshina, E. Nuin, M. L. Marin and M. A. Miranda, *J. Phys. Chem. B*, 2013, **117**, 16206-16211.

119 I. M. Magin, N. E. Polyakov, E. A. Khramtsova, A. I. Kruppa, Y. P. Tsentalovich, T. V. Leshina, M. A. Miranda, E. Nuin and M. L. Marin, *Chem. Phys. Lett.*, 2011, **516**, 51-55.

120 I. Vaya, M. C. Jimenez and M. A. Miranda, *J. Phys. Chem. B*, 2007, **111**, 9363-9371.

121 H. Oevering, J. W. Verhoeven, M. N. Paddon-Row and J. M. Warman, *Tetrahedron*, 1989, **45**, 4751-4766.

122 B. Wegewijs, R. M. Hermant, J. W. Verhoeven, M. P. Dehaas and J. M. Warman, *Chem. Phys. Lett.*, 1990, **168**, 185-190.

123 B. Wegewijs, R. P. H. Rettschnick and J. W. Verhoeven, *Chem. Phys. Lett.*, 1992, **200**, 357-363.

124 J. W. Verhoeven, in *From close contact to long-range intramolecular electron transfer*, John Willey & Sons INC, 1999, vol. 106, pp. 603-644.

125 J. W. Verhoeven, T. Scherer and R. J. Willemse, *Pure Appl. Chem.*, 1993, **65**, 1717-1722.

126 H. Nagakubo, G. Kubota, K. Kubo, T. Kaneko, T. Sakurai and H. Inoue, *Bull. Chem. Soc. Jpn.*, 1996, **69**, 2603-2611.

127 M. C. Jimenez, S. E. Stiriba, R. Tormos, J. Perez-Prieto and M. A. Miranda, *Photochem. Photobiol. Sci.*, 2004, **3**, 36-38.

128 H. Shizuka, *Pure Appl. Chem.*, 1997, **69**, 825-830.

129 M. Yamaji, K. Okada, B. Marciniak and H. Shizuka, *Chem. Phys. Lett.*, 1997, **277**, 375–380.

130 O. Mitsunobu, *Synthesis*, 1980, 1–28.

131 P. D. Wood and R. W. Redmond, *J. Am. Chem. Soc.*, 1996, **118**, 4256–4263.

132 A. K. Rappe, C. J. Casewit, K. S. Colwell, W. A. Goddard, III and W. M. Skiff, *J. Am. Chem. Soc.*, 1992, **114**, 10024–10035.

133 S. Grimme, *J. Comput. Chem.*, 2006, **27**, 1787–1799.

134 J. D. Gale, *J. Chem. Soc., Faraday Trans.*, 1997, **93**, 629–637.

135 J. D. Gale and A. L. Rohl, *Mol. Simul.*, 2003, **29**, 291–341.

136 S. Mouret, C. Baudouin, M. Charveron, A. Favier, J. Cadet and T. Douki, *Proc. Natl. Acad. Sci. U. S. A.*, 2006, **103**, 13765–13770.

137 R. B. Setlow, E. Grist, K. Thompson and A. D. Woodhead, *Proc. Natl. Acad. Sci. U. S. A.*, 1993, **90**, 6666–6670.

138 P. J. Rochette, J.-P. Therrien, R. Drouin, D. Perdiz, N. Bastien, E. A. Drobetsky and E. Sage, *Nucleic Acids Res.*, 2003, **31**, 2786–2794.

139 C. A. Smith, M. Wang, N. Jiang, L. Che, X. Zhao and J.-S. Taylor, *Biochemistry*, 1996, **35**, 4146–4154.

140 A. Gentil, F. Le Page, A. Borden and A. Sarasin, *Nucleic Acids Res.*, 1996, **24**, 1837–1840.

141 K. Heil, D. Pearson and T. Carell, *Chem. Soc. Rev.*, 2011, **40**, 4271–4278.

142 T. Delatour, T. Douki, C. D'Ham and J. Cadet, *J. Photochem. Photobiol., B*, 1998, **44**, 191–198.

143 F. Bosca, V. Lhiaubet-Vallet, M. C. Cuquerella, J. V. Castell and M. A. Miranda, *J. Am. Chem. Soc.*, 2006, **128**, 6318–6319.

144 K. Sandros, *Acta Chem. Scand.*, 1964, **18**, 2355–2374.

145 I. G. Gut, P. D. Wood and R. W. Redmond, *J. Am. Chem. Soc.*, 1996, **118**, 2366–2373.

146 V. Lhiaubet-Vallet, S. Encinas and M. A. Miranda, *J. Am. Chem. Soc.*, 2005, **127**, 12774–12775.

147 N. Belmadoui, S. Encinas, M. J. Climent, S. Gil and M. A. Miranda, *Chem. Eur. J.*, 2006, **12**, 553–561.

148 X.-L. Liu, J.-B. Wang, Y. Tong and Q.-H. Song, *Chem. Eur. J.*, 2013, **19**, 13216–13223.

149 J. Cadet, L. Voituriez, F. E. Hruska, L. S. Kan, F. A. A. M. De Leeuw and C. Altona, *Can. J. Chem.*, 1985, **63**, 2861–2868.

150 J. I. Kim and G. B. Schuster, *J. Am. Chem. Soc.*, 1992, **114**, 9309–9317.

151 P. J. Wagner and D. J. Bucheck, *J. Am. Chem. Soc.*, 1970, **92**, 181–185.

152 M. González-Béjar, A. Bentama, M. A. Miranda, S.-E. Stiriba and J. Pérez-Prieto, *Org. Lett.*, 2007, **9**, 2067–2070.

153 K. Nakatani, T. Yoshida and I. Saito, *J. Am. Chem. Soc.*, 2002, **124**, 2118-2119.
154 J. P. Bays, M. V. Encinas and J. C. Scaiano, *Macromolecules*, 1980, **13**, 815-820.
155 G. Beck, G. Dobrowolski, J. Kiwi and W. Schnabel, *Macromolecules*, 1975, **8**, 9-11.
156 J. C. Scaiano, W. G. McGimpsey, W. J. Leigh and S. Jakobs, *J. Org. Chem.*, 1987, **52**, 4540-4544.
157 J. Perez-Prieto, R. E. Galian, M. C. Morant-Minana and M. A. Miranda, *Chem. Commun.*, 2005, 3180-3182.
158 S. Mouret, C. Baudouin, M. Charveron, A. Favier, J. Cadet and T. Douki, *Proc. Natl. Acad. Sci.*, 2006, **103**, 13765-13770.
159 R. B. Setlow, E. Grist, K. Thompson and A. D. Woodhead, *Proc. Natl. Acad. Sci.*, 1993, **90**, 6666-6670.
160 H. Gorner, *J Photochem Photobiol B*, 1990, **5**, 359-377.
161 A. A. Lamola and J. Eisinger, *Biochim. Biophys. Acta, Nucleic Acids Protein Synth.*, 1971, **240**, 313-325.
162 M. C. Cuquerella, V. Lhiaubet-Vallet, F. Bosca and M. A. Miranda, *Chem. Sci.*, 2011, **2**, 1219-1232.
163 T. Douki, I. Berard, A. Wack and S. Andrae, *Chem. Eur. J.*, 2014, **20**, 5787-5794.
164 I. G. Gut, P. D. Wood and R. W. Redmond, *J. Am. Chem. Soc.*, 1996, **118**, 2366-2373.
165 P. Miro, V. Lhiaubet-Vallet, M. L. Marin and M. A. Miranda, *Chem. Eur. J.*, 2015, **21**, 17051-17056.
166 Z. Zuo, S. Yao, J. Luo, W. Wang and J. Zhang, *J Photochem Photobiol B*, 1992, **15**, 215-222.
167 P. Miro, I. Vaya, G. Sastre, M. C. Jimenez, M. L. Marin and M. A. Miranda, *Chem. Commun.*, 2016, **52**, 713-716.
168 F. P. Noonan, M. R. Zaidi, A. Wolnicka-Glubisz, M. R. Anver, J. Bahn, A. Wielgus, J. Cadet, T. Douki, S. Mouret, M. A. Tucker, A. Popratiloff, G. Merlino and E. C. De Fabo, *Nat. Commun.*, 2012, **3**, 884.
169 T. Douki, A. Reynaud-Angelin, J. Cadet and E. Sage, *Biochemistry*, 2003, **42**, 9221-9226.
170 T. Douki and J. Cadet, *Biochemistry*, 2001, **40**, 2495-2501.
171 W. J. Schreier, T. E. Schrader, F. O. Koller, P. Gilch, C. E. Crespo-Hernandez, V. N. Swaminathan, T. Carell, W. Zinth and B. Kohler, *Science*, 2007, **315**, 625-629.
172 P. Miro, V. Lhiaubet-Vallet, M. L. Marin and M. A. Miranda, *Chem. Eur. J.*, 2015, **21**, 17051-17056.

173 S. Sauvaigo, T. Douki, F. Odin, S. Caillat, J.-L. Ravanat and J. Cadet, *Photochem. Photobiol.*, 2001, **73**, 230-237.

174 P. J. Rochette, J.-P. Therrien, R. Drouin, D. Perdiz, N. Bastien, E. A. Drobetsky and E. Sage, *Nucleic Acids Res.*, 2003, **31**, 2786-2794.

175 Z. Kuluncsics, D. Perdiz, E. Brulay, B. Muel and E. Sage, *J. Photochem. Photobiol., B*, 1999, **49**, 71-80.

176 A. Sancar, *Chem. Rev.*, 2003, **103**, 2203-2237.

177 S. Weber, *Biochim. Biophys. Acta, Bioenerg.*, 2005, **1707**, 1-23.

178 Y.-T. Kao, C. Saxena, L. Wang, A. Sancar and D. Zhong, *Proc. Natl. Acad. Sci. U. S. A.*, 2005, **102**, 16128-16132.

179 S. T. Kim, R. F. Hartman and S. D. Rose, *Photochem. Photobiol.*, 1990, **52**, 789-794.

180 S. T. Kim and S. D. Rose, *J. Phys. Org. Chem.*, 1990, **3**, 581-586.

181 R. Epple, E.-U. Wallenborn and T. Carell, *J. Am. Chem. Soc.*, 1997, **119**, 7440-7451.

182 T. Carell and R. Epple, *Eur. J. Org. Chem.*, 1998, 1245-1258.

183 W.-J. Tang, Q.-H. Song, H.-B. Wang, J.-Y. Yu and Q.-X. Guo, *Org. Biomol. Chem.*, 2006, **4**, 2575-2580.

184 B. Zelent and G. Durocher, *J. Org. Chem.*, 1981, **46**, 1496-1499.

185 Y. Yoshimura and K. Fujimoto, *Chem. Lett.*, 2006, **35**, 386-387.

186 Q.-Q. Wu and Q.-H. Song, *J. Phys. Chem. B*, 2010, **114**, 9827-9832.

187 F. Bosca, S. Encinas, P. F. Heelis and M. A. Miranda, *Chem. Res. Toxicol.*, 1997, **10**, 820-827.

Summary

Bile acids are a family of amphiphilic steroids that play a pivotal role in physiological functions such as elimination of cholesterol or solubilization of lipids. Chemically, they share a steroidal skeleton with an unusual *cis* fusion between rings A and B, a short lateral chain ending in a carboxylic acid moiety and different number of hydroxyl groups on the α-face. Hence, bile acids offer a versatile architecture that can be used to investigate photophysical processes of interest such as hydrogen atom transfer, through-bond energy trasfer, through-bond exciplex formation and DNA photodamage-related reactions.

First, unmodified bile acids have been used to evaluate hydrogen atom trasfer to benzophenone-like triplet carbonyls. Dehydrogenation of bile acids at positions C-3 and/or C-7 by a radical-mediated mechanism from the excited state of benzophenone has been demonstrated. Moreover, synthesized lithocholic acid derivatives including benzophenone or carbazole as donors and a naphthalene, biphenyl or thymine as acceptors have been employed to investigate through-bond energy transfer and exciplex formation processes. Thus, energy transfer from benzophenone to naphthalene or biphenyl and extended through-bond exciplex formation in benzophenone/naphthalene and benzophenone/biphenyl linked systems has been demostrated by laser flash photolysis. Moreover, bile acid derivatives incorporating one benzophenone and two thymine units with different degrees of freedom have been prepared to investigate the photochemical formation of oxetanes or thymine dimers. Photosensitized formation of cyclobutane pyrimidine dimers through the generation of a delocalized triplet excited state has been demonstrated in intermolecular systems, while oxetane formation is observed when the degrees of freedom are reduced. In additon, it has been possible to prove the generation of the thymine triplet by through-bond energy transfer from the triplet excited state of benzophenone using a bile acid derivative containing benzophenone and thymine chromophores placed at non bonding distance. Finally the

synthesis of direct or carbazole photosensitized thymine dimers susceptible to be inter- and intramolecular photorrepaired by carbazole has been accomplished.

Resumen

Los ácidos biliares son una familia de esteroides anfifílicos que juegan un papel clave en diferentes funciones fisiológicas tales como la eliminación del colesterol o la solubilización de lípidos. Su estructura química está constituida por un esqueleto esteroideo con una fusión *cis* poco común entre los anillos A y B, una cadena lateral corta que termina con una función ácida y un número variable de grupos hidroxilo en la cara α. Por tanto, los ácidos biliares ofrecen una estructura versátil que puede ser utilizada para investigar procesos fotofisicos de interés como abstracción de hidrógeno, transferencia de energía y formación de exciplejos a larga distancia o reacciones relacionadas con el daño fotoinducido al ADN.

En esta Tesis, en primer lugar, los ácidos biliares naturales se han utilizado para evaluar la abstracción de hidrógeno a carbonilos triplete en compuestos derivados de la benzofenona, demostrándose la deshidrogenación de los ácidos biliares en las posiciones C-3 y/o C-7 por un mecanismo radicalario desde el mencionado triplete de la benzofenona. En segundo lugar, se han preparado derivados de ácido litocólico que incluyen los dadores benzofenona o carbazol y los aceptores naftaleno, bifenilo o timina, que a continuación se han utilizado para investigar los procesos de transferencia de energía y formación de exciplejo intramolecular a larga distancia. De hecho, en los sistemas benzofenona/naftaleno y benzofenona/bifenilo, se demostró por fotólisis de destello láser la transferencia de energía desde benzofenona a naftaleno o bifenilo y la formación de exciplejo a larga distancia. También se han preparado derivados de ácidos bliares que incorporan una unidad de benzofenona y dos de timina en diferentes posiciones del esqueleto para investigar la influencia de los diferentes grados de libertad en la formación fotosensibilizada de oxetanos o dímeros de timina. Gracias a ellos, se ha demostrado la formación fotosensibilizada de dímeros ciclobutánicos pirimidínicos a través de la generación de estados excitados triplete deslocalizados en sistemas en los que la benzofenona es intermolecular, mientras que se observa formación de oxetanos cuando los grados de libertad se ven reducidos. Además, también ha sido posible probar

la generación del triplete de timina por transferencia de energía intramolecular a larga distancia desde el estado excitado triplete de la benzofenona en un ácido biliar donde tanto la timina como la benzofenona han sido unidos covalentemente y no se encuentran a distancia de enlace. Por último, se sintetizaron dímeros de timina directos o fotosensibilizados por carbazol susceptibles de ser fotorreparados intermolecular o intramolecularmente.

Resum

Els àcids biliars són una família d'esteroides anfifílics que juguen un paper clau en funcions fisiològiques com l'eliminació del colesterol o la solubilització de lípids. La seua estructura química està constituïda per un esquelet esteroïdal amb una fusió *cis* entre els anells A i B poc comuna, una cadena lateral curta que acaba amb una funció àcida i un nombre diferent de grups hidroxil en la cara α. D'aquesta manera, els àcids biliars ofereixen una estructura versàtil que pot ser utilitzada per investigar processos fotofísics d'interès com abstracció d'hidrogen, transferència d'energia i formació de exciplexes a llarga distància o reaccions relacionades amb el dany a l'ADN induït per llum.

En primer lloc, els àcids biliars naturals s'han utilitzat per avaluar la abstracció d'hidrogen a carbonils triplets derivats de la benzofenona, demostrant-se la deshidrogenació dels àcids biliars en les posicions C-3 i/o C-7 per un mecanisme radicalari des de l'estat excitat de la benzofenona. A més, derivats d'àcid litocòlic que inclouen els donadors benzofenona o carbazol i els acceptors naftalé, bifenil o timina s'han utilitzat per investigar els processos de transferència d'energia i formació de exciplexe a llarga distància. En els sistemes benzofenona /naftalé i benzofenona/bifenil la fotòlisis làser va demostrar la transferència d'energia des de benzofenona a naftalé o bifenil i la formació d'exciplexe a llarga distància. Per investigar la formació fotosensibilitzada d'oxetans o dímers de timina, s'han preparat derivats d'àcids bliars que incorporen una unitat de benzofenona i dues de timina amb diferents graus de llibertat. La formació fotosensibilitzada de dímers ciclobutànics pirimidínics mitjançant la generació d'estats excitats triplet deslocalitzats ha estat demostrada en sistemes intermoleculars, mentre que la formació d'oxetans s'observa quan els graus de llibertat es veuen reduïts. A més, també ha estat possible provar la generació del triplet de timina per transferència d'energia intramolecular a llarga distància des de l'estat triplet de la benzofenona en un àcid biliar on tant la timina com la benzofenona es troben units covalentment però no a distància d'enllaç. Finalment, es van sintetitzar dímers de timina

directes o fotosensibilitzats per carbazol susceptibles de ser fotorreparats intermolecular o intramolecularment .

Publications Related to this Doctoral Thesis

Generation of Thymine Triplet State by Through-Bond Energy Transfer

P. Miro, V. Lhiaubet-Vallet, M. L. Marin and M. A. Miranda, *Chem. Eur. J.*, 2016, under revision.

Radical-Mediated Dehydrogenation of Bile Acids by Means of Hydrogen Atom Transfer to Triplet Carbonyls

P. Miro, M. L. Marin and M. A. Miranda, *Org. Biomol. Chem.*, 2016, 14, 2679-2683.

Triplet Energy Management between Two Signaling Units through Cooperative Rigid Scaffolds

P. Miro, I. Vaya, G. Sastre, M. C. Jimenez, M. L. Marin and M. A. Miranda, *Chem. Commun.*, 2016, 52, 713-716.

Photosensitized Thymine Dimerization *via* Delocalized Triplet Excited States

P. Miro, V. Lhiaubet-Vallet, M. L. Marin and M. A. Miranda, *Chem. Eur. J.*, 2015, 21, 17051-17056.

Other Publications

Photocatalytic Treatment of Cork Wastewater Pollutants. Degradation of Gallic Acid and Trichloroanisole using Triphenyl(thia)pyrylium salts

R. Martinez-Haya, M. H. Barecka, P. Miro, M. L. Marin and M. A. Miranda, *Appl. Catal. B*, 2015, 179, 433-438.

A Mechanistic Study on the Oxidative Photodegradation of 2,6-Dichlorodiphenylamine-derived Drugs: Photo-Fenton *versus* Photocatalysis with a Triphenylpyrylium Salt

P. Miró, A. Arques, A. M. Amat, M. L. Marin and M. A. Miranda, *Appl. Catal. B*, 2013, 140-141, 412-418.

Singlet Oxygen Production by Pyrano and Furano 1,4-Naphthoquinones in Non-Aqueous Medium

N. C. de Lucas, R. J. Correa, S. J. Garden, G. Santos, R. Rodrigues, C. E. M. Carvalho, S. B. Ferreira, J. C. Netto-Ferreira, V. F. Ferreira, P. Miro, M. L. Marin and M. A. Miranda, *Photochem. Photobiol. Sci.*, 2012, 11, 1201-1209.